The Sedimentology and Dynamics of Mega-Dunes, Jamuna River, Bangladesh.

by

Julie Elizabeth Roden

Submitted in accordance with the requirements
for the degree of Doctor of Philosophy

School of Earth Sciences and School of Geography
University of Leeds

August 1998

The candidate confirms that the work submitted is her own and that appropriate credit has been given where reference has been made to the work of others.

ABSTRACT

This thesis quantifies the occurrence, morphology and flow dynamics of dune bedforms in the main rivers of Bangladesh: the Jamuna, Meghna and Ganges. Field work was conducted as part of the River Survey Project (Bangladesh Flood Action Plan 24) between November 1993 and March 1996, hence encompassing two flood hydrographs. River surveying was accomplished using a differential global positioning system to obtain vessel position and high resolution echo sounders and side scan sonar to monitor bed morphology. Flow, turbulence and suspended sediment transport were investigated using an Acoustic Doppler Current Profiler (ADCP) which measured both the instantaneous three-dimensional velocity structure and the relative suspended sediment concentration for the entire flow column beneath the survey vessel.

Dunes are ubiquitous in the Jamuna and range in height from 0.15 to over 6 m and in wavelength from 3 to 300 m. Both dune height and wavelength alter systematically with flow stage, increasing by factors of 6 and 8 respectively between low and high flow conditions. Lee side angle, which effects flow separation downstream of the dune crest and hence turbulence production and flow resistance, ranges from 2° to 58° and steepens with flow stage. There is little evidence of dune flattening with increasing flow stage, indicating that flow conditions do not reach the transition to upper-stage plane beds. An important corollary of this is that dunes are the dominant bedform at all flow stages and hence will dominate the preserved sediments of such alluvial channels. Existing models of dune morphology and occurrence are poor predictors at high flow stage in the Jamuna, most likely because of the low Froude numbers associated with such deep channels.

Mean flow and turbulence fields, obtained from at-a-point profiling during different flow stages, have been examined for dunes with steep (>20°) and low (<10°) lee side angles. No flow separation was detected over dunes with low lee face angles. Over dunes with steep lee face angles, mean negative downstream velocities do not occur downstream of dune crests, although intermittent flow separation (flow reversals) has been measured at both low and high flow stages, with instantaneous velocity reversals reaching -60% of the depth averaged mean. The free shear layer of the flow separation zone is temporally and spatially unstable, the growth and decay of high velocity gradients acting across the shear zone controlling both eddy shedding of quadrant-2 type 'ejections' and also movement of the shear layer within the water column. These 'ejections' from the shear layer are associated with substantially higher suspended sediment concentrations than the background ambient value and are therefore responsible for increasing suspended sediment transport over dunes. Near the flow reattachment zone, quadrant-4 type 'sweep' events are most important in terms of event occurrence, contribution to Reynolds stress and suspended sediment transport and hence are responsible for scour in the dune trough. These results show that dune stability is controlled by the spatial variation in sediment transport, which in turn is dependent on the turbulence structure that is a consequence of flow expansion and separation downstream of the dune crest.

ACKNOWLEDGEMENTS

There are many, many people that I must thank for their help, guidance, expertise, time, company and support through the four years it has taken to complete this thesis. The first vote of thanks goes to the staff and survey crews of the River Survey Project, Flood Action Plan 24. The assistance of RSP management and technical staff from Delft Hydraulics is gratefully acknowledged, in particular Johan Greissen, Pieter van Groen, Gerrit Klaassen and Maarten van der Wal, who were invariably both patient and helpful throughout my long stays in Bangladesh. I also thank all of the staff of the Danish Hydraulics Institute for their guidance. In particular, Hans Høyer (RSP survey manager) deserves an award for his invaluable instruction in hydraulic surveying methodology, equipment operation and gadget ownership, and Kim Kyhl Jensen, for continuing my education in river surveying after Hans' departure. Claus Iversen is duly thanked for his enthusiasm and good humour, and also for sun-downer procedures and aircraft identification. Many thanks also go to Dale Kerper for valuable lessons in survey databasing, data processing, how not to ride rickshaws, haki-sak technique and cheery company on the wetter monsoon days. Valuable discussions with Palle Mikkelsen and Mr Haque on data processing are also much appreciated. Dilip Barua and Zahirul Haque Khan also deserve many thanks for their help in data collection and collation, enthusiasm for river research and camaraderie. Thanks must also go to Roy Richardson, Angus Jackson and Jeffrey Peakall for their agreeable company in the field. I am also indebted to the crew of the RSP survey vessels, Captain Monjour, Chief, Bennedict, Saleem and Anese, who are the true specialists in the Bangladeshi rivers. Their expertise, diligence, attention to detail, interest, curiosity and company has been much valued.

Back in Leeds, all of the past and present members of Club Sed need a mention for their friendship, help and enthusiasm for all things sedimentological: Mark Trout, Shona Keogh, Jeffrey Peakall, Lawrence Amy, Rufus Brunt, Karen Braithwaite, Stuart McLellend, Bill McCaffrey and Ben Kneller. Especial thanks must go to Clare Buckee for turbulence talks, proof reading the entire thesis and keeping me sane for the last year or so. Sue Bowler also helped in proof reading and pasta making duties, and Alison Manson produced a number of the illustrations; both are gratefully thanked. Charlie Bristow is thanked for his occasional supervision, expertise in the field and general encouragement.

Tore Dimmestøl, aka Foggy Mountain Sheep Hut, deserves more thanks than I could give in an entire thesis for putting up with me and my many research-linked mood swings for the past few years. I am indebted to his support, bad jokes and washing-up capabilities. My parents and family are also thanked for their encouragement and support, both financial and emotional, during the writing of this thesis.

Finally, my greatest thanks must go to Jim Best and Phil Ashworth, my ever-enthusiastic, patient and mildly-hyperactive supervisors. Their expertise, skill, occasional prodding and boundless energy towards anything watery have benefited this research enormously.

CONTENTS

LIST OF FIGURES

Chapter 4. Dune Morphology

Figure 5.34, Normalised vertical time-averaged at-a-point velocity profiles from both low flow surveys. Dune wavelengths were also normalised so relative position along the bed form is illustrated above. The normalised velocity data of Bennett and Best (1995) are plotted to compare the field and flume measurements.(a) downstream velocity (U/u_{max}) where u_{max} is the maximum downstream transect velocity and (b) vertical velocity (V/v_{max}) where v_{max} is the maximum vertical velocity.

Figure 5.35, Vertical profiles of the mean Reynolds stress for the low flow February 1996 and March 1995 surveys.

Figure 5.36, vertical profiles of the at-a-point vertical and downstream time series skewness for the March 1995 and February 1996 low flow surveys over high angled dunes.

Figure 5.37, At-a-depth time series of the instantaneous values of the downstream and vertical velocity collected for the low flow surveys over (a) L/96/S, stoss side dune, (b) L/96/T, trough of a primary dune and (c) L/96/TS, trough of a secondary dune.

Figure 5.38, Contour maps of temporal variations in at-a-point downstream velocity for the low flow survey at (a) P7, trough of a secondary dune, and (b) P6, primary dune trough and (c) P5, stoss side of the subsequent dune. Flow is from top to bottom and a scale colour bar is given for each map. Flow depth bin sizes are 0.5 m. Each time series has been split to fit to page size and successive profiles are from left to right.

Figure 5.39, Intermittency in flow reversal variation with flow depth through the separation zone and shear layer for profiles L/96/TS and L/96/T collected at low flow stage.

Figure 5.40, Contour maps of temporal variations in at-a-point downstream velocity gradient for the low flow survey at (a) L/96/TS, trough of a secondary dune, and (b) L/96/T, primary dune trough and (c) L/96/S, stoss side of the subsequent dune. Flow is from top to bottom and a scale colour bar is given for each map. Flow depth bin sizes are 0.5 m. Each time series has been split to fit to page size and successive profiles are from left to right.

LIST OF TABLES

Chapter 3

Chapter 4

Chapter 5

NOTATION

Symbol	*Description*
C	Suspended sand fraction concentration
C'	Chezy coefficient
c'	Instantaneous suspended sand fraction concentration fluctuation about a zero mean
C_{sd}	Speed of sound
$C_{sd,w}$	Speed of sound in water
c	Constant
d	Flow depth
d_a	Distance from the ADCP to the river bed
d_c	Depth cell size
$d_{c,u}$	Depth cell size, uncorrected
d_{max}	Maximum flow depth
D_{50}	The 50th percentile of the grain size
D_{84}	The 84th percentile of the grain size
D_{90}	The 90th percentile of the grain size
D*	Dimensionless particle diameter
e	Absorption coefficient
E	Dune height parameter
EA	Echo amplitude
F_D	Doppler frequency shift
Fr	Froude number; $Fr^2 = U/gH$
f	frequency
G	Particle specific gravity
g	Gravitational acceleration
h	Dune height
H	Step height
I	Intermittency factor in flow separation
L	Length
n	Number of measurements
P	Power
R	Distance from ADCP tranducer to depth cell
R_{max}	Maximum depth of good data

SW	Spectral width
SV	Water mass volume backscattering strength
St	Strouhal number
T	Van Rijn's transport stage parameter
t	Time
U	Time-averaged mean downstream velocity
U_0	Mean downstream velocity upstream of flow separation
U_{RMS}	Root-mean-square of the downstream velocity distribution
U_{SKEW}	Skewness of the downstream velocity distribution
V	Time-averaged mean vertical velocity
V_r	Relative velocity between an observer and source
V_{RMS}	Root-mean-square of the vertical velocity distribution
V_{SKEW}	Skewness of the vertical velocity distribution
u	Instantaneous downstream velocity
u_c	Downstream velocity at flow separation point
u_{max}	Maximum downstream velocity
v	Instantaneous vertical velocity
v_{max}	Maximum vertical velocity
u'	Instantaneous downstream velocity fluctuation about a zero mean
v'	Instantaneous vertical velocity fluctuation about a zero mean
x_r	Length of flow separation zone
β	Shape factor
λ	Wavelength
λ_S	Length of lee side
λ_L	Length of stoss side
φ	ADCP beam angle from the vertical
ρ	Density
σ	Standard deviation
τ_r	Reynolds stress
ν	Kinematic viscosity

ABBREVIATIONS

ADCP	Acoustic Doppler current profiler
AGC	Automatic gain control
AWLR	Automatic water level recording
BIWTA	Bangladesh Inland Water Transport Authority
BTM	Bangladesh Transverse Mercator
BWDB	Bangladesh Waterways Development Board
DGPS	Differential global positioning system
EMF	Electromagnetic flow meter
DAS	Data acquisition system
DHI	Danish Hydraulics Institute
DoD	USA Department of Defence
EMF	Electro-magnetic flow meter
FAP24	Flood Action Plan 24
FI	Form index
GPR	Ground penetrating radar
GPS	Global positioning system
HFI	Horizontal form index
MBM	Moving boat method
PWD	Public Works Department
RSP	River Survey Project
SLW	Standard low water
SPS	Standard Positioning Service
SSS	Side scan sonar
USPB	Upper stage plane bed
WGS 84	World Geodetic System of 1984 (WGS 84).

Watching clouds is not time wasted for students of turbulence.
(Tennekes, I.T. and Lumley, J.L., 1994).

Everything changes and nothing stays the same.
You can never step into the same river twice.
(Plato).

Chapter 1. Introduction and Background to Study

1.1 The Significance of Dunes

The complex interrelations between flow, sediment transport and bed morphology govern channel configuration and stability in rivers with erodible beds. In sand bed rivers, the temporal and spatial variation in flow strength and turbulent fluctuation creates a wide range of sediment accumulations known as bedforms. Changes in sediment transport rate over sand beds cause the evolution of different bedform configurations, from lower stage plane bed to ripples, dunes, upper stage plane beds and antidunes, of which ripples and dunes are the most widespread. It is now widely accepted that most bedforms generated by sediment transport are produced by turbulence (Jackson, 1976; Yalin, 1977,1992; Müller and Gyr, 1982, 1986; McLean *et al.*, 1994; Bennett and Best, 1995). More specifically, dune bedforms are generally thought to be produced by turbulence which effects the entire flow column, and hence dunes may be defined as bedforms that scale with flow depth and have an associated turbulence structure that interacts with the flow surface. Dunes are therefore created and altered by the turbulent flow field which, in turn, controls the local sediment transport rate (the bedform 'trinity', Figure 1.1). Conversely, the flow is itself influenced by dune bedforms produced by sediment transport through the production of form drag and significant changes in the local mean flow and turbulence fields. The consequence of these complex interactions is that neither the local, nor spatially-averaged, flow can be predicted without a detailed knowledge of the bed geometry, which in turn is dependant on the detailed characteristics of the near-bed flow field. Many authors have noted the complex links and feedbacks between flow, sediment transport and dune morphology and that these processes should not be studied in isolation (e.g. Allen, 1968; Leeder, 1983; McLean *et al.*, 1984). However, many numerical studies using linear stability analysis to investigate the dynamics of dunes (e.g. Richards, 1980; Engelund and Fredsøe, 1982), have partially or fully ignored the interdependency between the elements of the bedform trinity and are therefore limited in their applicability to understanding the hydraulics and stability of bedforms. Furthermore, many flume studies of dune dynamics have neglected the effect of sediment transport which will influence both bedform morphology and fluid turbulence (e.g. Lyn, 1992; Nelson *et al.*, 1993; Bennett and Best, 1995).

Dune bedforms have been studied for many years as they play a key role in many aspects of engineering hydraulics and fluvial sedimentology, consequently dunes have been studied by workers from various different disciplines. Sedimentologists' interest in modern dunes stems

from the requirement of using ancient bedforms to reconstruct palaeo-environments and hence enable them to infer, for example, directions of river channels, channel depths, current speeds, temporal variation in currents and enable prediction of the architecture of ancient fluvial deposits which may form hydrocarbon and water reservoirs. Dunes also play a pivotal role in causing flow resistance, influencing local scour depths, and altering bedload transport rates. Hence, to the hydraulic engineer, prediction of dune occurrence and morphology is of great importance when planning well constrained sampling and measurement programmes (e.g. Klaassen *et al.*, 1988; Lukanda *et al.*, 1992; Peters, 1993) when determining, for example, locations for bridge building or in evaluating navigation routes. To the geomorphologist, the role of dunes in the growth of larger channel-scale features such as bars is of particular interest. River bed morphology, channel change, bank erosion and channel incision may all be affected by the growth and migration of dunes. In developing countries such as Bangladesh, understanding alluvial channel behaviour is of especial importance as rivers are one of the major transport routes and hence have a great effect on commerce. Further development of Bangladesh is involving the establishment of an extended infrastructure system including the implementation of large schemes such as bridge construction over the Jamuna river, bank protection schemes and land reclamation projects. Dunes bedforms are therefore a widely studied phenomenon which may have great impact not only on the form of the natural environment but also in humans terms due to their influence on large river systems and the dynamics of flooding. An understanding of dune bedform occurrence, morphology and interaction with flow structure will therefore aid precise prediction of scour, bank erosion and channel depth.

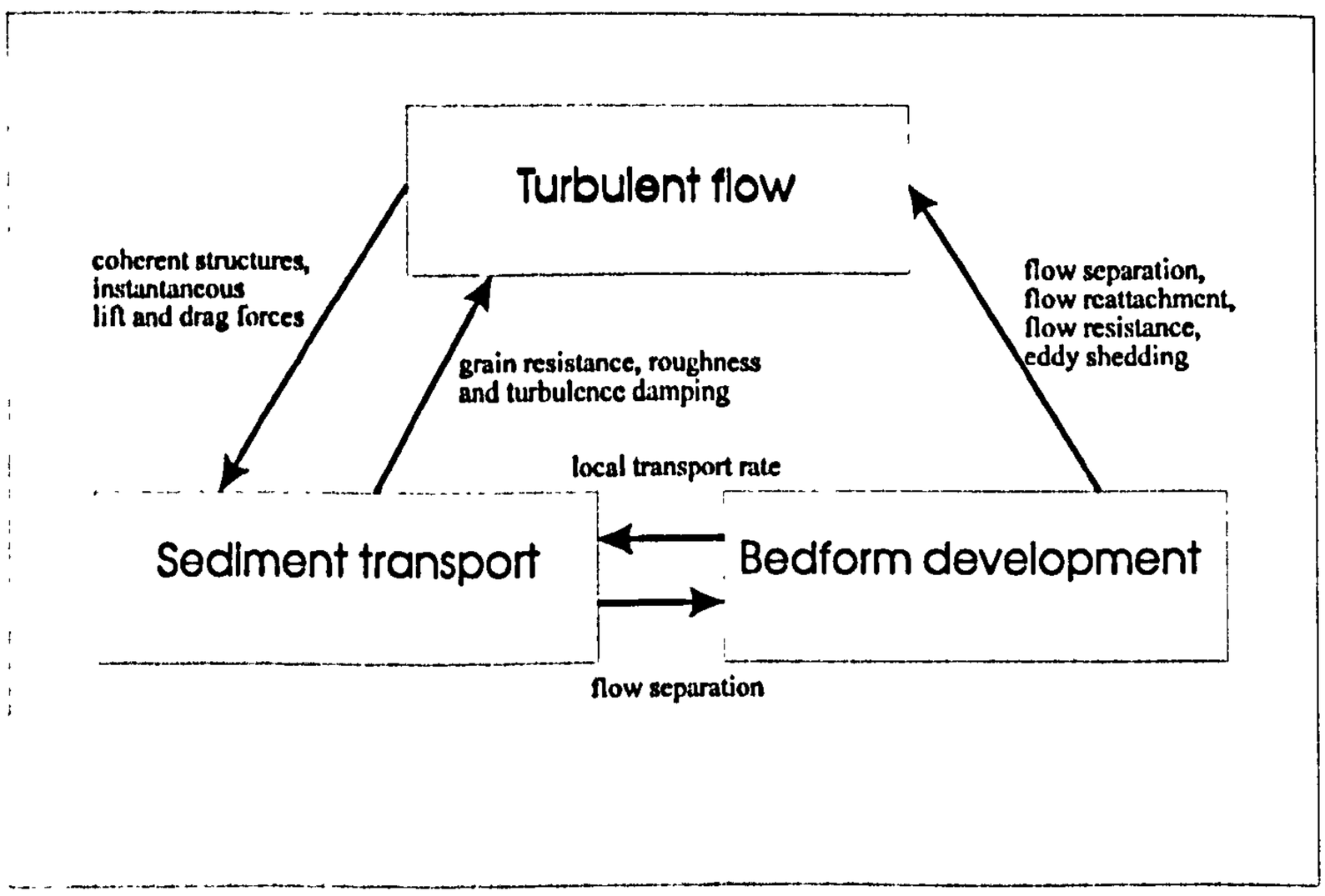

Figure 1.1, The bedform 'trinity' diagram showing the interactions and feedbacks between flow, sediment transport and bedform development. (modified after Leeder, 1983; Best, 1993).

1.2 The Stability of Dunes

The role of turbulence structure in dune development and stability has been noted for many years (e.g. Znamenskaya, 1964; Jackson, 1976; Yalin, 1977). Macro-turbulent structures which are visable at the flow surface representing slowly rotating, upward tilting vortices are termed 'kolks' (Mathes, 1947) or boils (Jackson, 1976) and have been suggested to play an important function in entraining and transporting sediment (Rood and Hickin, 1989; Kostaschuk and Church, 1993). The origin of these coherent turbulent structures was thought to be related to the processes of turbulence generation over flat beds (Jackson, 1976; Yalin, 1977). However, more recent work has suggested that the origin of these turbulent structures may be related to eddy shedding from the shear layer created by the process of flow separation at the dune crest (Müller and Gyr, 1982; Bennett and Best, 1995). The process of flow reattachment downstream of the dune crest has also been suggested to play a fundamental role in dune stability (Nelson *et al.*, 1995). However, several field studies have documented an absence of flow separation in the lee side of dunes where the lee face angle is low (Smith and McLean, 1977; Kostaschuk and Ilersich, 1995), so the mechanisms of eddy shedding in the absence of a shear layer is still a matter of some contention. Although these studies, and many others, have led to important advances in the theory of the hydraulic stability of dunes, many big questions remain unanswered: (i) the nature of the links between turbulence structure and sediment suspension mechanisms, (ii) the effects on dune stability of changes in scale between laboratory experiments (e.g. McLean *et al.*, 1994; Bennett and Best, 1995; Nelson *et al.*, 1995) and alluvial dunes which form in deep flows and may reach over 10 m in height (Ashley, 1990), (iii) the effects of non-uniformity in dune geometry on flow and turbulence over dunes. Although much research investigating dune morphology and dynamics has been conducted under laboratory conditions (e.g. Mendoza and Shen, 1990; Nelson *et al.*, 1993; McLean *et al.*, 1994; Bennett and Best, 1995; Nelson *et al.*, 1995), there is a paucity of data from alluvial environments which is primarily a result of difficulties in monitoring bedforms in alluvial channels. Previous studies detailing dune occurrence have stated that dunes are ubiquitous (e.g. Ashley, 1990) while others have stated that at high flow stages dunes may wash out as upper stage plane bed conditions become increasingly common (e.g. Klaassen, 1988). Although variation in dune morphology with flow stage has frequently been referred to in the literature, very little data exists that quantifies the change in dune morphology with respect to mean hydraulic conditions. It is clear that further work is needed to characterise the nature of dune related turbulence and also to quantify dune morphology at different flow stages in large rivers. Moreover, the complex linkages between dune morphology, flow and sediment transport in a field situation require much additional study.

1.3 Aims and Objectives of Research

The aims of this thesis are to describe the occurrence, distribution and morphology of dune bedforms in large, dynamic sand-bed braided rivers and quantify the mean flow and turbulence structure present over large alluvial dunes. The mechanisms that control alluvial dune dynamics and stability will also be characterised. More specifically, four research objectives will be addressed:

1. To assess the spatial and temporal variation in dune occurrence in the main rivers of Bangladesh in order to examine the significance of dune bedforms in a large sand bed river.

2. To quantify dune morphology in terms of height, wavelength, shape and lee slope and to appraise the variation in morphology with changes in mean hydraulic conditions. These data can then be utilised to test the model of van Rijn (1984b, 1993) that predicts dune morphology as a function of flow conditions.

3. To quantify the mean flow and turbulence fields present over dunes in order to assess the effect of changes in scale in the flow processes acting over large alluvial dunes compared to flow over dune bedforms in laboratory flumes.

4. To compare the flow field present over dunes with high and low-angled lee faces in order to test whether flow separation occurs over dunes with different morphology.

1.4 The Jamuna river

The Jamuna river is one of the three major rivers that drain the low-lying deltaic floodplain of Bangladesh (Figure 1.2). The source of the Jamuna river is in the Tibetan plateau on the north slope of the Himalayas, it then flows through China, Bhutan and India before entering Bangladesh and continuing south before joining the Ganges after which it becomes the Padma. The Padma then flows south east for about 100 km before meeting the Meghna River and eventually discharging into the Bay of Bengal. The Jamuna, which is named the Brahmaputra upstream of an offtake called the Old Brahmaputra (Figure 1.2), has a total length of 2840 km although only 230 km of this flows within Bangladesh (Klaassen and Vermeer, 1988). The Old Brahmaputra runs south eastwards and was the main channel up to the late 18th century when a major avulsion caused the Brahmaputra to switch to its present day course (Coleman, 1969; Thorne *et al.*, 1993). The main Bangladeshi rivers have a total catchment area of 16 million km^2 and 93% of the Jamuna catchment area (of approximately 550 000 km^2) lies outside

Bangladesh (Sarker, 1996). The peak discharge of the Jamuna at Bahadurabad (see Figure 1.2) is approximately 69 000 m^3s^{-1}, with a maximum of 100 000 m^3s^{-1} (Delft Hydraulics and DHI, 1996a) recorded during the 1988 flood. Estimates of total sediment load in the Jamuna range between 500 and 725 million tons per year (Coleman, 1969; Thorne *et al.*, 1993; Schumm and Winkley, 1994). The main rivers of Bangladesh have a combined annual sediment load of 2000 million tons, which is the third highest alluvial sediment discharge in the world (Schumm and Winkley, 1994). Discharge in the Jamuna is highly variable with variations in one year ranging from 4000 m^3s^{-1} to 68 000 m^3s^{-1} associated with changes in flow stage related to the monsoonal climate combined with snow melt in the Himalayas. The large variable discharge and high sediment load cause the Bangladeshi rivers to be extremely unstable and hence rapid lateral channel migration is common (Coleman, 1969). Bank erosion rates of 1 km per year (Hossain, 1993) and bed scour of up to 40 m can occur (Best and Ashworth, 1997). The Jamuna is a multi channel system with an overall braided appearance (Coleman, 1969; Bristow, 1993) with braidbelt width varying both spatially and temporally from 6 km to 14 km. The channel pattern has previously been described as both braided and anastamosed as meta-stable vegetated islands are present (named 'chars' in Bangladesh), which are inundated only during the largest flood events (Bristow, 1987; Thorne *et al*, 1993; Ashworth *et al.*, in review). General descriptions of channel patterns and processes from the Bangladeshi rivers may be found in Coleman (1969); Bristow (1987); Klaassen and Vermeer (1988); Burger *et al.* (1988); Thorne *et al.* (1993). Average bed grain size (as measured at Bahadurabad, Figure 1.2) is fine sand (D_{50} = 0.14 mm) with less than 1 % clay (Delft Hydraulics and DHI, 1996c) and over 70 % of the grains either quartz or mica. Water surface slope in the Bahadurabad region ranges between 0.000055 and 0.000091.

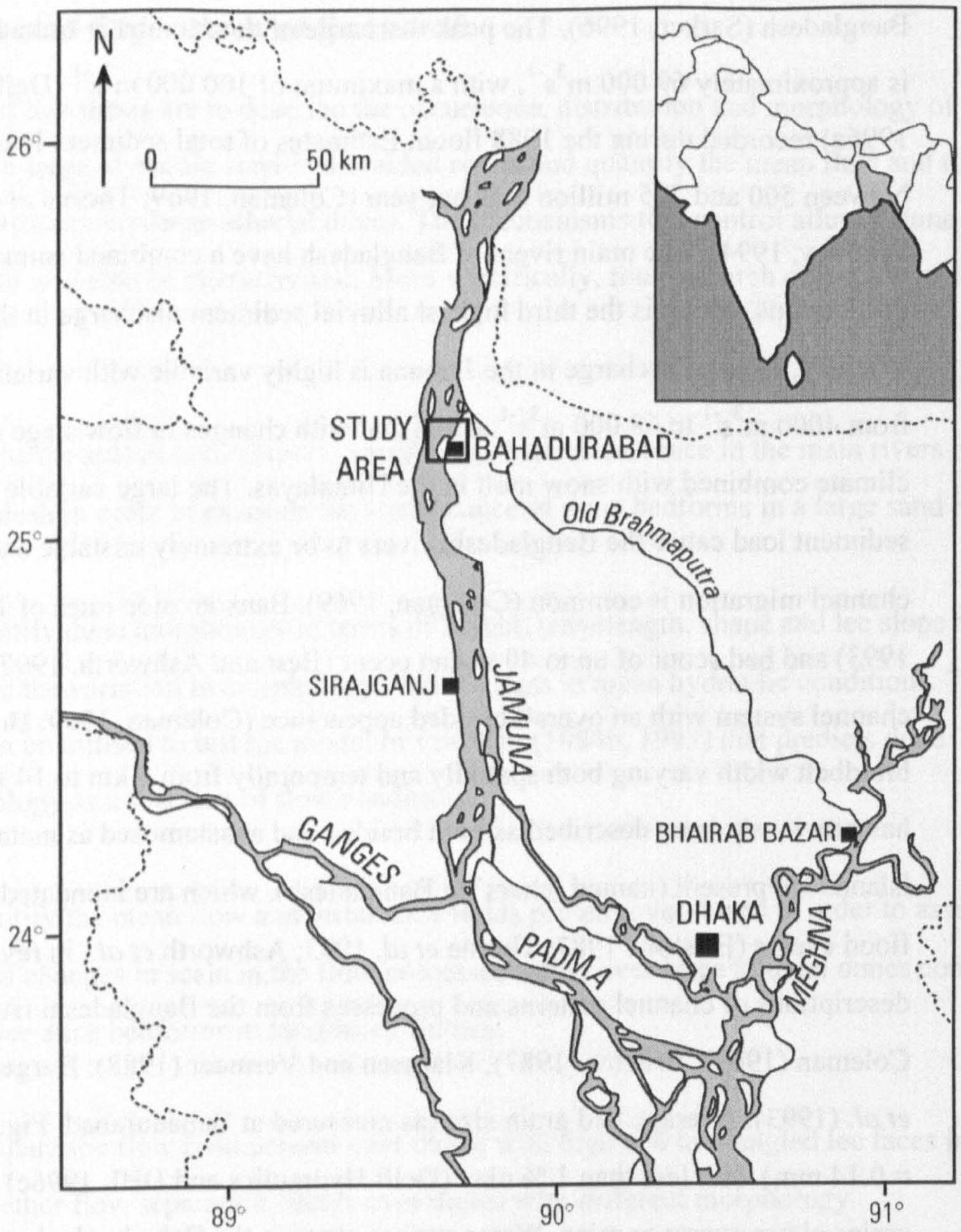

Figure 1.2, Location map showing the main rivers in Bangladesh and the location of survey areas Bahadurabad, Sirajganj and Bhairab Bazar.

1.5 Flooding in Bangladesh

The high sediment discharge of the main rivers of Bangladesh has created the largest sub-aerial delta in the world, as well as an even larger subaqueous delta and fan sequence in the Bay of Bengal (Curray and Moore, 1971), and hence the highest point in Bangladesh is a mere 60 m above sea level. The low lying topography and high monsoonal rainfall combine to make Bangladesh one of the most flood-prone areas worldwide. Flooding is therefore an annual event in Bangladesh with over 20 % of the land mass being inundated each year. Monsoonal rainfall occurs between May and September and the Jamuna river usually peaks in late July or early August which is somewhat earlier than the Ganges where maximum discharge occurs in late August to early September. However, on occasions when the Jamuna peaks later than usual and

coincides with the Ganges, catastrophic flooding may occur leading to much more extensive inundation and damage.

The two most severe flood events in Bangladesh in recent history occurred during 1987 and 1988, both causing chaos and devastation throughout the country. During 1987, flooding occurred from June to September, 40% of the country was submerged and the estimated cost to repair damage caused by the flood waters was £50 million. In the worst affected regions, flood waters remained for up to 58 days.

The flood of 1987 however was dwarfed by that occurring during 1988 which was the worst on record, flood waters exceeded maximum recordable water level measurements at 10 (out of 34) water level recording stations (Miah, 1988). An estimated 84% of the country was inundated and floods lasted from May to mid-September. Damage estimated at over £225 million occurred with 3000 km of roads, 630 km of railways, 46 railway bridges and 35 km of embankment being washed away and approximately 2700 schools destroyed (Miah, 1988). 4.93 million acres of crops were ruined and partial damage was caused to 6500 km of road, 8400 schools, and 680 km of embankment.

The suffering caused by flooding on this scale and in a developing country such as Bangladesh is amplified by the high population density and subsistence agricultural practices exercised by a large proportion of the population. An estimated one million lives were lost during the 1988 flood, most of which were associated with disease (such as typhoid, malaria, dysentery and cholera) which is a common consequence of flooding on this scale. To date (August) during the 1998 monsoon season, 368 people have died as a result of flooding which is minor compared to that occurring during 1987 and 1988.

1.6 Bangladesh Flood Action Plan

All field work in this thesis has been undertaken with the assistance of the River Survey Project (RSP), Bangladesh Flood Action Plan (FAP) number 24. FAP was set up in response to the 1987 and 1988 floods in Bangladesh which attracted much interest from the international community in supporting Bangladesh to find long-term solutions for the flooding problem. FAP24 RSP, which was financed by the European Union (formerly the European Community), and is one of 26 FAP projects implemented by the Flood Action Co-ordination Organisation (FPCO) under the Ministry of Irrigation, Water Development and Flood Protection. FPCO merged with the Water Resources Planning organisation (WARPO) in 1995 under the same

ministry at which time WARPO took over the project execution. FAP's remit is to co-ordinate a large scale study into river processes, flooding and response to flooding in the main rivers of Bangladesh. FAP projects include flood management modelling (FAP25), Jamuna river bank protection and river training (FAP21 and 22), flood forecasting and early warning (FAP10), Meghna river bank protection studies (FAP9b) and a management study of the southwest area water resources (FAP4).

The consultancy group of FAP24 RSP is headed by Delft Hydraulics and the Danish Hydraulics Institute, with Osiris as an expatriate contractor and Hydroland and Approtech as local contractors. Hydraulic surveying was conducted between November 1993 and February 1996, and final reports were completed in October 1996 (Delft Hydraulics and DHI, 1996b).

The River Survey Project's main objectives (from FPCO, RSP technical proposal, 1991) are listed below:

- to collect reliable all-season data on the hydrological, morphological and hydrographic processes at key locations on the country's main river systems with emphasis given to the collection of data during the monsoon season and to introduce improved or new technology where appropriate;
- to undertake special studies regarding the behaviour of the river system based on the new surveys that are carried out, and existing data and studies relevant to this objective;
- to provide specialised on-the-job training to Bangladeshi professional staff and employees of the Bangladesh Inland Water Transport Authority (BIWTA) and other local consultants in the fields of river surveys and river studies so that they can continue data collection programs in the long term and hence to upgrade the capability of Bangladesh for river hydrological and morphological data collection and study programs;
- to provide benchmarks against which to assess changes in the river morphology and hydrology.

Comprehensive data on the hydro-morphological characteristics of the main rivers of Bangladesh are scarce due to both the size of the rivers and their instability. The extremely high rates of bank erosion and channel change within the Bangladeshi rivers require a tremendous survey capacity to ensure accurate monitoring. A second problem in monitoring the Bangladeshi river system is the extreme climatic variation due to annual monsoonal wet season flooding which causes inherent difficulties in hydraulic surveying. Flood conditions render surveying more difficult due to large water depths, high current velocities and high sediment discharge, but also pose logistical constraints due to problems with communications, power

supply and transport. Finally, planning well constrained sampling and measurement programs in Bangladesh is problematic due to the inaccessibility of large parts of the country and lack of infrastructure. The data collection for this thesis would therefore have been impossible, in terms of both logistics and techniques, without the assistance and support of such a large, well equipped and organised project as the RSP (FAP24).

This thesis is based on field work undertaken as part of a subcontract between the University of Leeds and the RSP (FAP24) concerning bedform dynamics (special study topic 6). Four field seasons were completed covering a period of approximately 6 months. Additionally, a further joint project was conducted to study bar dynamics (special study topic 7), for further details see Ashworth *et al.* (in review) and Best *et al.* (in review). A main final report from the FAP24 RSP is available which contains a summary of the background to the project, a short overview of the activities within each survey component and overall recommendations of the study (Delft Hydraulics and DHI, 1996a). The joint University of Leeds and RSP study topics are detailed in Special Report no. 9. Details of RSP (FAP24) survey equipment and methodology are described in Chapter 3.

1.7 Thesis Structure

The aims of this thesis are to present data from the main Bangladeshi rivers detailing the occurrence, morphology and flow characteristics of alluvial dune bedforms. These data will be used to construct a conceptual model to interpret the processes and mechanisms governing dune stability in large sand bed rivers. An outline of the structure of this thesis and a synopsis of each chapter is presented below.

Chapter 2 describes the factors influencing dune stability, occurrence and morphology from previous studies. The chapter will broadly outline the current understanding of dune mechanics.

Chapter 3 provides details of the methodology of data collection used in this thesis. Techniques and instrumentation used during river surveying will be described along with data processing procedures and error analysis.

Chapter 4 quantifies dune occurrence and morphology from three survey sites in the Jamuna from November 1993 to November 1995. These data will be used to test previous models that predict bedform dimensions and flow resistance factors.

Chapter 5 describes the mean flow and turbulence fields acting over dunes at both high and low flow stage. The variations in the flow field over high and low lee face angled dunes will be examined. These data will be used to construct models of flow over dunes with steeply and gently dipping lee faces under varying mean flow conditions.

Chapter 6 investigates suspended sediment transport at low and high flow stages. Sediment suspension will be examined in relation to the mean flow and turbulence fields detailed in Chapter 5. This chapter aims to link quantitatively suspended sediment transport and turbulence structure and therefore explore the stability of dunes.

Chapter 7 will synthesise the findings from Chapters 4, 5 and 6 and discuss the processes which govern the stability of bedforms in large sand bed rivers. The scope for future research will also be outlined.

Chapter 2. The Morphology and Dynamics of Dunes

2.1 Introduction

Chapter one has introduced the concept that the development of dunes on an erodible bed involves the complex interactions between flow, sediment transport and bed morphology (the bedform 'trinity', Figure 1.1). This Chapter reviews previous work detailing the morphology and flow dynamics of dune bedforms and will discuss the factors which control dune stability. In particular, the processes which control the development of dunes, as opposed to other alluvial bed features such as ripples and upper stage plane bed, will be discussed. Firstly however, the term 'dune' will be defined along with the parameters widely used to classify and describe dune bedforms.

2.2 Dune Classification

Researchers from many different disciplines (e.g. engineers, physical geographers, geologists and oceanographers as well as many different environments (e.g. numerical and physical modelling, modern and ancient fluvial, intertidal and subtidal) have conducted studies on the morphology, hydrodynamic controls and internal structure of bedforms (see Chapter 1). This has lead to several different terms such as dune, megaripple (e.g. Coleman, 1969; Aliotta and Perillo, 1987) and sandwave (e.g. Karahan and Peterson, 1980) being used to describe bedforms that scale with flow depth and which have an associated turbulence structure that interacts with the water surface. However, as these bed perturbations are commonly believed to have a collective formative process distinct from those that form other bed configurations such as ripples (Yalin, 1964; Allen, 1968; Kennedy, 1969 and many others), the term dune is now widely accepted to describe a bedform that scales with flow depth (Ashley, 1990).

A schematic cross-section of a dune is given in Figure 2.1 which illustrates the parameters most commonly used to describe dune morphology, of which dune height (the vertical distance between the maximum and minimum elevation) and dune wavelength (the distance between the downstream end of the lee face and the upstream end of the stoss face) are the most two most widely used forms. The point of maximum elevation (crest, Figure 2.1) has been noted to frequently lie upstream of the top or brinkpoint of the lee face (Allen, 1968).

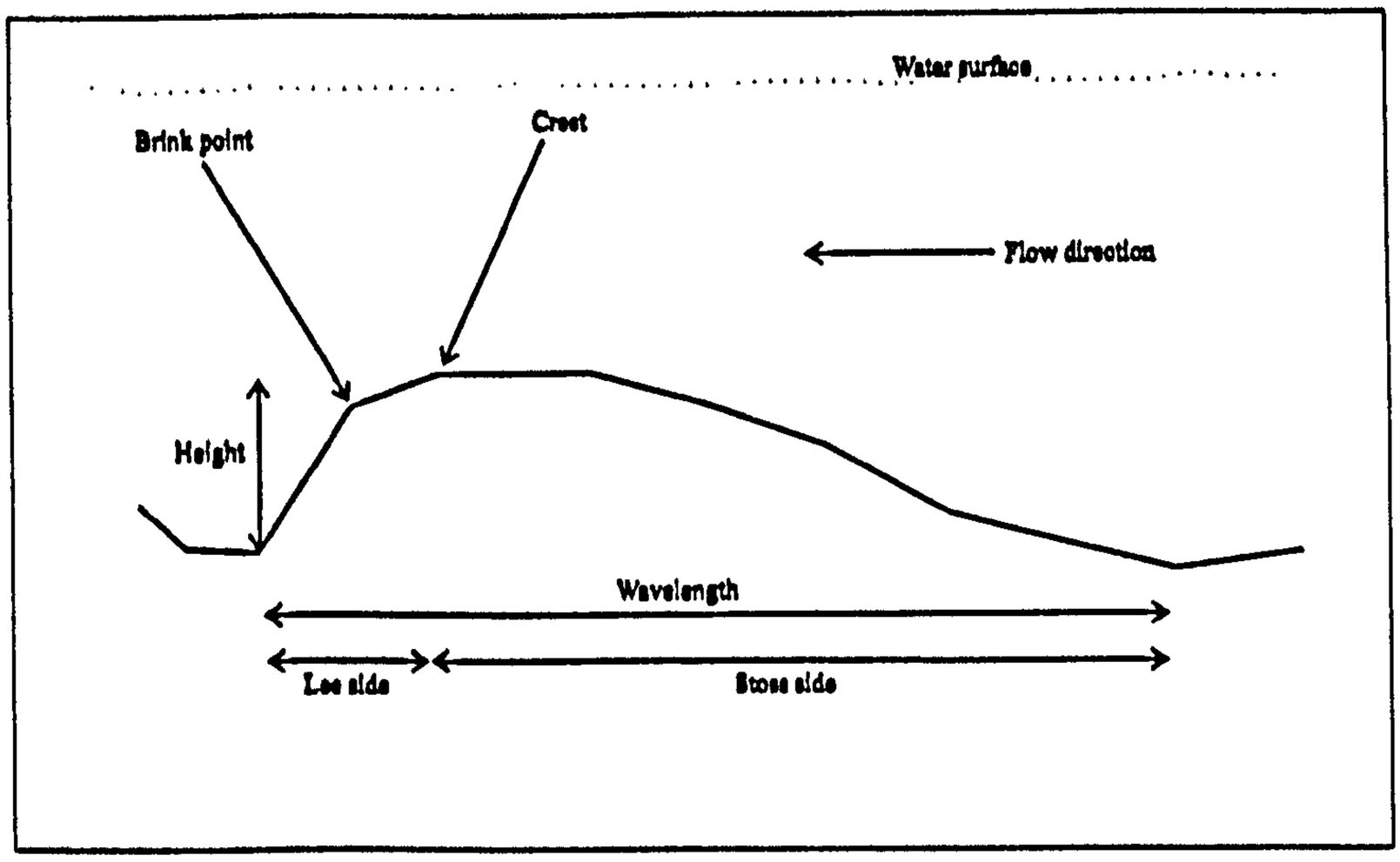

Figure 2.1, Schematic illustrating the descriptive morphological parameters of dunes in profile.

Extensive research has been undertaken to define existence fields of the types of bedforms which may result from sediment transport, namely: lower stage plane bed, ripples, dunes, upper stage plane beds and antidunes (e.g. Guy *et al.*, 1966; Allen, 1982; Leeder, 1983; Southard and Boguchwal, 1990). Many of these studies relate bedform type to flow force (boundary shear stress) or stream power to grain size or grain Reynolds number and an example of a bedform phase diagram is given in Figure 2.2. Although much earlier work concentrated on sand-grade material, more recent studies have examined bedform existence fields in gravel (Dinehart, 1989; Carling, 1998) and mixed sand-gravel sediments (Wilock and Southard, 1989; Wilock, 1992). The exclusion of gravel-sized sediment from earlier examples of bedform phase diagrams may have stemmed from the lack of laboratory and field data detailing the occurrence and stability of gravel dunes (Carling, 1998). However, as both flow processes and sediment transport characteristics have parallels between different grain sizes, the extension of bedform phase diagrams to encompass a greater range of grain sizes is appropriate (Best, 1996). The applicability of bedform phase diagrams to dunes forming in deep alluvial flows has recently been discussed by Kostaschuk and Villard (1996), where dune bedforms in the Fraser River are shown to fall into either upper stage plane bed or antidune stability fields using the phase diagrams of Ashley (1990), Leeder (1983) and Dingham (1984). The inapplicability of many bedform phase diagrams for predicting dune occurrence in deep natural flows may be because much of the data used to construct phase diagrams have commonly been recorded from flume studies where flow

depths are much lower (Kostaschuk and Villard, 1996; van den Berg and van Gelder, 1998). Although bedform phase diagrams may be a useful tool for predicting bedform stability in some environments, further work may be needed to extend their usage to greater variety of environments and grain sizes.

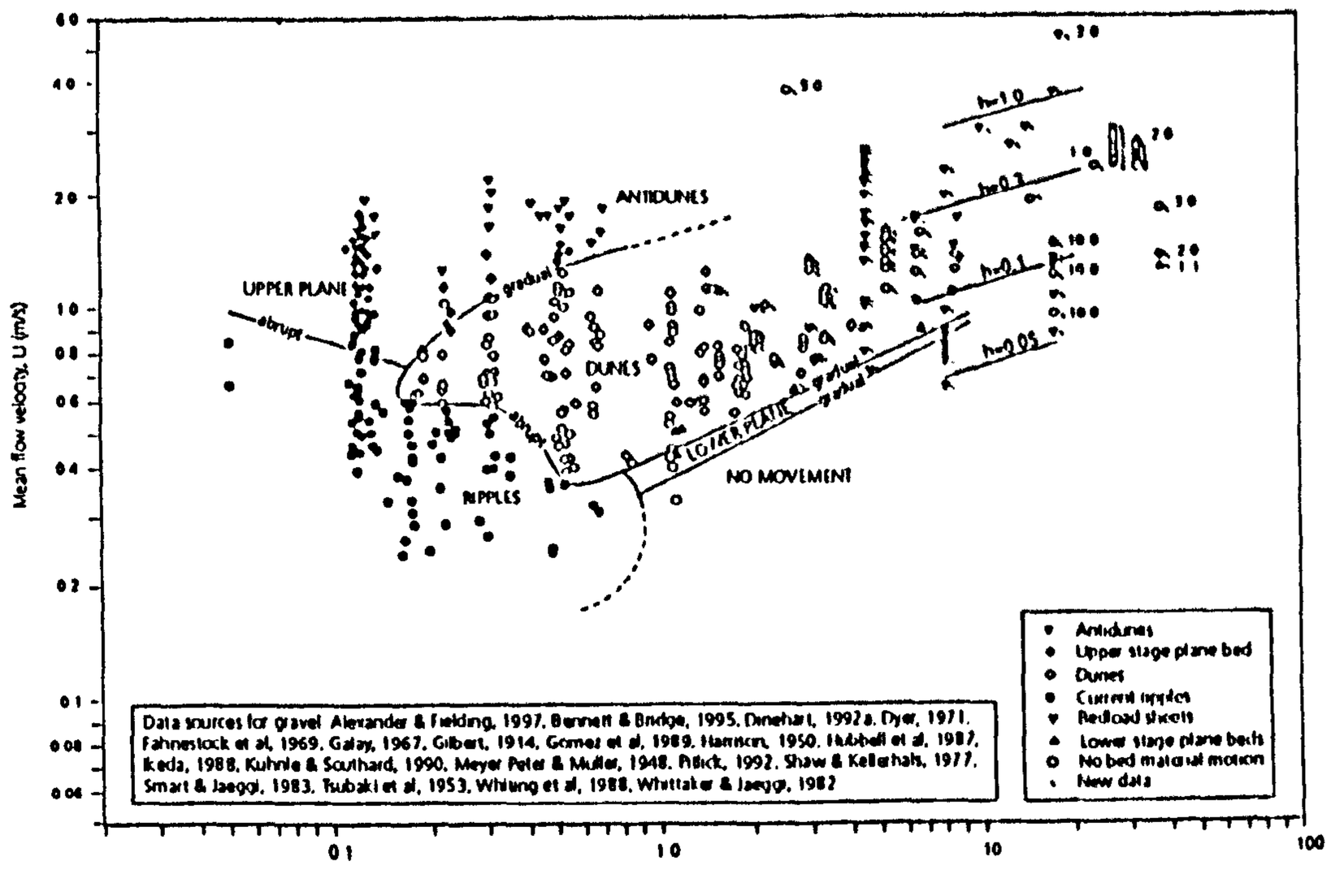

Figure 2.2, Bedform existence field defined by mean sediment size and mean flow velocity, extended to encompass grain sizes up to ~ 33 m. Southard and Boguchwal's original data were for mean flow depth of 0.25 to 0.4 m at a temperature of 10°c. The extended dataset of Carling (1998) are not temperature adjusted but are consistent with the proposed existence fields. Approximate depth isolines (e.g. h = 0.1) are for antidunes coarser than 6 mm and do not apply to dune data. (from Carling, 1998, extended from Southard and Boguchwal, 1990).

Unlike dune bedforms, ripples do not scale with flow depth and do not interact with the outer flow region. Ripples, which form in sediment of up to 0.7 mm in diameter, are widely believed to grow from turbulence-produced bed defects by the action of flow separation and reattachment (Raudkivi, 1963; Allen, 1968; Karahan and Peterson, 1980), for further reviews see Leeder (1983) and Best (1993, 1995). Ripples are termed 'micro' turbulent bedforms as flow separation over ripples, which is intrinsic for ripple stability, does not interact with the outer flow structure. Dune initiation is thought to occur when a bedform of sufficient size occurs that will trigger the development of macroturbulence and hence

significantly alter the entire flow field. The production of a bedform of a size large enough to effect the entire flow field has been postulated to involve the production of a 'rogue' ripple (Leeder, 1983) or ripple amalgamation (Costello, 1974). Thus, ripple amalgamation (or the production of a 'rogue' ripple) will act to increase turbulence associated with the bedform which may lead to an increase in scour in the dune trough thereby enhancing the sediment transport rate. In sediments coarser than 0.7 mm, increasing bed shear stress will cause transformation from lower plane bed to bedforms which are initially irregular in shape. These bedforms are two-dimensional dunes (originally termed bars by Costello, and
1974) have been interpreted to represent distinct bedforms (Costello, 1974) or transitional dunes (Allen, 1983; Ashley, 1990). Costello and Southard (1980) have shown that two-dimensional dunes are generally lower in height than three-dimensional dunes and are more irregular in wavelength. The smaller height of a two-dimensional dune will result in a less effective flow separation than that occurring over three-dimensional dunes and hence trough scour will be smaller for two-dimensional dunes. However, as dimensionality of small scale bedforms has been shown to increase with time, it may be that such two-dimensional bedforms are transitional dunes and will eventually evolve into three-dimensional dunes. At increasingly high bed shear stresses dunes progressively decrease in height due to intense sediment transport rates until upper stage plane bed results (e.g. Saunderson and Lockett, 1983; Figure 2.2). The sections that follow will discuss the morphological parameters used to describe dunes and fluid flow and turbulence over dunes.

2.3 Dune Morphology

2.3.1 Controls on Dune Morphology and Stability

The morphology and stability of dunes is a complex function of several variables including: applied bed shear stress and grain size (see Figure 2.2), flow depth, Froude number, occurrence of suspended sediment, generation time (maturity), flow unsteadiness and bedform response to changing flow conditions (e.g. Yalin, 1964; Allen, 1980). These topics will be described below and are further reviewed in Allen (1982), Southard and Boguchwal (1990) and Best (1996). Water temperature and sediment availability have also been suggested to influence dune morphology (Southard and Boguchwal, 1990; Dalrymple and Rhodes, 1995), although these effects may be minimal. In addition to these quasi deterministic controls on dune size, it should be noted that dunes exhibit appreciable stochastic variability even under steady equilibrium conditions. Nordin (1971), for example, found that the standard deviation of dune wavelength averaged 59% of the mean value while the standard deviation of the height averaged 52% of the mean. Several reasons exist for this variability:

1) the presence of both young and mature bedforms in an area

2) the inherent three dimensionally of dunes which causes variation in height and wavelength along a single crest line

3) the slightly different flow conditions an individual dune experiences because of the three dimensionality of its neighbours

Dune morphology may alter rapidly as it adjusts to variable flow conditions and processes of growth, attenuation and destruction (Gabel, 1993). This variability means that dune sizes, under given flow conditions, should be studied per population rather than per individual dune.

2.3.2 Dunes in Planform

Dunes have previously been described in terms of their planform and cross-sectional morphology, size and the presence (or absence) of superimposed bedforms. In planform, dunes have been frequently been split into two groups; two-dimensional forms which were conjectured to occur at low flow speeds and three-dimensional forms which were suggested to occur at higher speeds for a given grain size (Costello and Southward, 1981; Middleton and Southard, 1986) and hence the plan shape of dunes has been suggested to alter in a

predictable manner with flow speed (Southard and Boguchwal, 1990). However, more recent work has shown that the formation time of small scale bedforms may be a more important factor in governing dune geometry (e.g. Baas, 1994). The two forms are distinguished between by their geometry: two-dimensional forms can be described by one transect parallel to the mean flow direction whereas three-dimensional forms must also be described in a flow transverse direction. In addition, three-dimensional forms may also be characterised by scour pits and curved lee faces (Dalrymple *et al.*, 1978). Two-dimensional dunes have nearly straight crests and lee faces with a uniform height along their length as there are no scour pits present, whereas three-dimensional dunes are sinuous and irregularity of the troughline elevation is more pronounced (Ashley, 1990). As with any classification of this type, distinguishing between the two types of dunes in many cases can be difficult, as few dunes in nature are truly two-dimensional. The lee face of three-dimensional dunes consists of alternating lunate segments (lobes) up current of each scour pit and more sharply curved linguoid segments (saddles) which are fronted by a current parallel spur. These spurs may be parallel or oblique to the current direction depending on the relative bedform orientation. Even in strongly three-dimensional dunes, the elevation of the crest line is usually relatively uniform with almost all of the three-dimensionality occurring within the trough. Three-dimensional forms are the most widely developed types of dunes, especially in the small and medium classes. It has previously been indicated that as dune size increases, three-dimensional forms become increasingly uncommon (Fenster *et al.*, 1990; Dalrymple and Rhodes, 1995), however this seems unlikely as the more recent work of Baas (1994) has shown that generation time is a more important control on dune dimensionality. The studies of Dalrymple and Rhodes (1995) and Fenster *et al.* (1990) also indicated that current speeds may rarely be high enough in the deeper flows to generate three dimensional dunes, but it may also be that the complications which are inherent in monitoring deep flows have made observation of large three dimensional dunes more difficult.

The only quantitative attempt to relate dune morphology and flow characteristics was by Allen (1977). Allen (1977) found that the ratio of bedform wavelength (λ) to the flow-transverse spacing (S) of saddles and spurs was given by:

$$\lambda/S = 5.85\ (Fr\ h/d)0.412\ (1+d/w)1.71 \qquad \text{equation 2.1}$$

Where Fr is the Froude number ($Fr = \sqrt{Ug/h}$), h is the dune height, d is the flow depth and w is the flow width. This implies that more three-dimensional bedforms occur in flows with a higher Froude number. However, this relationship was formulated entirely on the basis of current ripple data and its application to dunes has not been tested. Also, bedform generation time, which has been shown to greatly effect bedform morphology, is not considered using equation 2.1.

The significance in distinguishing between two dimensional and three dimensional dunes is of great importance for dune classification and cross bedding geometry, but there has been little work to quantify the dividing line. Rhodes (1992) estimated the three dimensionality of dunes by measuring the variation in height of the trough line along the length of dunes n the Bay of Fundy and expressed this in terms of the coefficient of variation (standard deviation / mean), an increase in the height variability showing an increase in dimensionality. Another area that has been little studied is the lateral continuity of dunes. It is generally believed that the crestlines of 2D dunes are continuous for considerable distances, whereas 3D dune crests are less so (Dalrymple and Rhodes, 1995), but there is little quantitative data to support this belief. Dalrymple (1984) measured a mean horizontal form index (HFI, which is the flow transverse span divided by wavelength) of 10 (with a maximum of 18) for 2D estuarine dunes, and Langhorne (1973) reported 2D estuarine crest lines with continuous extent of 1700 m, but 3D estuarine dunes also show a strong continuity.

2.3.3 Dunes in Profile

One of the most frequently used terms to describe dune profile shape is the form index (FI) which is dune wavelength divided by dune height, and is also referred to as the ripple index and the steepness index. Dune height and wavelength have been shown by many authors to be positively correlated but with a wide scatter (Figure 2.3). This trend is not parallel to the lines of equal FI and dunes tend to become flatter as they become larger. Small to medium dunes (wavelength < 10 m) have a FI < 30 whereas very large dunes (wavelength > 100 m) have a FI > 30. As dune size alters with flow conditions so must the ripple index. It has been observed that dunes with higher FI characterise conditions near the limits of the dune stability field whereas steeper dunes (lower FI) characterise the core of the dune field. The minimum value of the FI decreases as water depth increases, a trend that appears to

contradict the observed tendency for larger dunes to have flatter profiles. This may be due to the fact that it becomes increasingly difficult to maintain flow velocities much above the lower limit of the dune stability field. Also, in environments where sediment supply is limited, large dunes may commonly be sediment starved and hence their height could be limited producing higher than expected form index values.

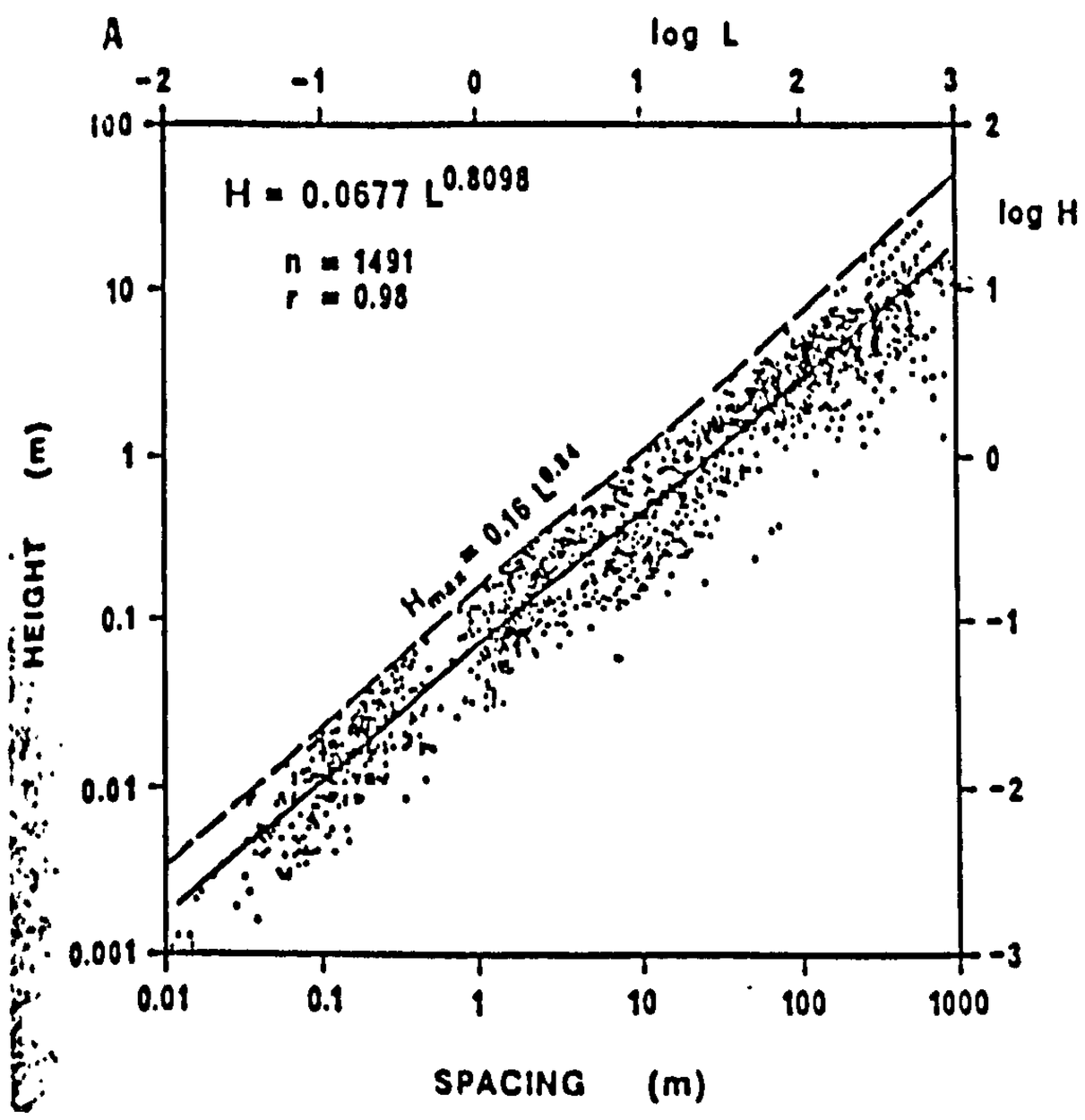

Figure 2.3, Plot of bedform height and wavelength for ripples and dunes. Both bedforms show a similar form but there is a gap between the two populations at approximately 0.8 m wavelength (from Ashley, 1990).

Dunes have most frequently been described as asymmetric in cross section with their shorter lee side being much steeper than their longer stoss. The exact shape and inclination depends on:

1) the size of the dune relative to the sediment transport rate

2) the orientation of the dune relative to the net transport direction (obliquity)

3) the presence or absence of superimposed dunes

4) dune maturity

The lee side slope angle is believed to reach a maximum near to or at the angle of repose (which is a function of grain size), however natural examples of dune lee face angle are often much less than this. The stoss side slope is commonly convex up and in the order of 2-

5°. If the flow approaches the upper limit of dune stability, the planing off of the crest produces a crestal platform which is either level or slopes gently downstream. However, more recent studies have shown that low lee face angled dune which are symmetric in cross-section may be common in some deep flows under high flow conditions where suspended sediment transport is dominant (Kostaschuk and Ilersich, 1995).

2.3.4 Current Speed

Flow strength, measured as either current speed or bed shear stress has a complex influence on bedform size. Other factors being constant, dune height increases as the mean current speed increases from the lower boundary of the dune stability field, reaching a maximum value in the central portion of the dune field before decreasing as the velocity or shear stress approaches the onset of the upper plane bed or antidune conditions (Figure 2.2; Allen, 1982). The initial increase in dune height is generally attributed to increased erosion in the trough due to an increase in the intensity of turbulence where separated flow reattaches to be bed (reattachment point) and also an increase in the strength of the flow reversals in the flow separation region increases (Costello and Southard, 1981). The decrease in height near the upper flow regime boundary is thought to be due to an increase in the amount of sediment in suspension and a washing out or planing off of the dune crest (Allen and Leeder, 1980). The effect of current speed on dune wavelength has not been systematically investigated, although it has been noted that wavelength decreases with increasing current velocity in the transition from two-dimensional to three-dimensional (Dalrymple *et al.*, 1978; Costello and Southard, 1981). The decrease in dune wavelength may be related to changes in the position of flow reattachment. However, the synthesis presented by Southard and Boguchwal (1990) indicates that wavelength increases steadily as velocity increases.

2.3.5 Flow Depth

Tabulations of height and wavelength clearly show that dune size increases with water depth (e.g. Allen, 1968; Ashley, 1990; Southard and Boguchwal, 1990). There is, however, a large scatter in the flow depth to dune height relationship which is attributable to other deterministic and stochastic factors which influence dune size. It has been suggested by Yalin (1964,1977) using theory and empirical observation, that (maximum) wavelength is approximately six times water depth while (maximum) height is approximately 17% of the water depth:

$$\lambda = 6d, h = 0.167d \qquad \textit{equation 2.2}$$

where λ is wavelength, h is height and d is flow depth. These approximations only apply to the largest dunes present in a given area and hence give an approximation to the upper bounds on dune height and wavelength (Yalin, 1964).

2.3.6 Other Factors Influencing Dune Formation and Size

As mentioned above, the correct combinations (within the dune stability field) of flow depth, current speed and sediment size are necessary for the formation of dunes but are not always sufficient as several other factors can influence dune occurrence.

1) Enough cohesionless sediment - the presence of a small amount of sand on the hard substrate may not permit formation of dunes (Aliotta and Perillo, 1987). Availability of sediment will also affect dune size: a rigid substrate will prevent erosion in troughs so decreasing effective height and such dunes are said to be starved.

2) The presence of a binding agent such as silt or clay-sized material may prevent dune formation. This is most important in areas of relatively low current speed (Bouma *et al.*, 1980).

3) Water temperature which may influence on viscosity can affect initial dune formation as well as dune height (Southard and Boguchwal, 1990). Decrease in water temperature leads to a corresponding decrease in dune height, although this effect is probably minimal.

4) the presence of suspended sediment in water has been shown to increase the current speed at which sediment begins to be transported (Best and Leeder, 1993). The affect of suspended sediment on the ripple dune boundary has not yet been investigated but may well also influence this threshold.

2.3.7 Dune Migration and Superimposition

Dune migration rates have been reported for both tidal (e.g. Dalrymple, 1984) and fluvial (e.g. Kostaschuk *et al.*, 1989) environments. Values of 40 m/day are not uncommon in fluvial environments. In tidal areas migration rates are much lower (100 m/year) due to periods of no motion near slack water and reversed migration during subordinate tides. A considerable variation in migration rates is common in areas with relatively uniform dune morphology (Aliotta and Perillo, 1987). This has been referred to as 'flexing' of the dune

crestline. Some of this variability is probably caused by the random behaviour but may also be related to changes in height along the crestline. Bedform orientation is also influenced by differences in forward migration speed in adjacent parts of the dune crest.

Dune migration rates have been frequently used to estimate bedload transport rates. However, if the bed material is composed of fine sands much of the load may be carried in suspension and hence using dune migration rates to calculate bedload sediment transport may be suspect (Van den Berg, 1987; Soulsby *et al.*, 1991; Kostaschuk and Ilersich, 1995; Mohrig and Smith, 1996). A percentage of the suspended load may be deposited in dune troughs and hence contribute to the lee side accumulation. Also, suspension of bedload in turbulent eddies has been frequently noted along with direct bedload transport measurements. Temporal variation in bedload transport rates at a variety of time scales may be associated with the migration of dunes (Gomez *et al.*, 1989).

The superimposition of smaller dunes on the stoss and lee side of larger ones is widespread in many environments. This is believed to represent a quasi-equilibrium superimposition related to the development of an internal boundary layer on the stoss side of larger dunes (Smith and McLean, 1977). For this process to operate, the larger form must be long enough to allow development of the internal boundary layer. The minimum length has been calculated by regarding the lower limit on compound dunes that the minimum wavelength is approximately 8-10 m (Dalrymple, 1984) but this of course in dependant on water depth and bed shear stress. Because the internal boundary layer thickens as the near bed current accelerates up the larger stoss side, a progressive change in the size and shape in the superimposed dunes should be expected between the trough and the crest of the main dune. Dalrymple (1984) for example has noted an increase in wavelength of the superimposed dunes towards the crest of the main dune, and a progression from 2d to 3d towards the crest, although the variation in dimensionality may in fact be related to the maturity of the superimposed bedforms rather than a change in current speed. A decreasing size of superimposed dunes towards the main dune crest has been noted by some authors. Possible reasons are:

1) very high current speeds at the crest may form dunes in to the upper half of the dune stability field where height, but not wavelength, is expected to decrease. However, the wavelength of the superimposed dunes decrease with height so this explanation is unlikely.

2) Sediment grain size commonly increases in size towards the crest of large dunes. This would mean that flow conditions at the crest may be closer to the lower limit of the dune stability field than in the finer sand below.

3) The smaller crestal dunes may have formed later and under slower flow conditions than that which the larger dunes superimposed lower on the stoss side of the main dune. Such a slower flow may only have been capable of remoulding the crestal part of the main dune, leaving the superimposed dunes in the trough largely unaltered. The lag between the smaller dunes and flow conditions would be smaller than that between the larger forms and flow conditions. Crestal superimposed dunes are observed to change their size, shape and distribution markedly over short time periods.

2.4 Flow over Dunes

2.4.1 Introduction to flow over dunes

The flow field over dunes has frequently been described in the literature (e.g. Raudkivi, 1966; Müller and Gyr, 1982; McLean and Smith, 1986) and has typically been divided into five sections. The greatest downstream velocities occur just before and at the dune crest where there is an area of topographically induced accelerated and converging flow (section one). Downstream of the crest there is a zone of flow separation and expansion with a characteristic recirculation pattern which occurs due to the asymmetry of the bedform (section two). Overlying the separation cell and its associated shear layer is a decelerated wake region (section three), and above the wake region is an outer, near-surface region (section four). Finally, there is the downstream growth of a new internal boundary layer originating at the flow reattachment (section five).

The formation of a flow reversal zone (section two) in the dune trough due to flow separation at the dune brink point, creates a zone of high shear (due to the different mean velocities of the bounding layers) with very high Reynolds stress which is located approximately at the level of the upstream crest. Consequently, high turbulence intensities and Reynolds stresses are associated with the separation zone free shear layer (Raudkivi, 1966; Rifai and Smith, 1971; Engelund and Fredsoe, 1982; Müller and Gyr, 1982; Mendoza and Shen, 1990; Nelson *et al.*, 1993 Bennett and Best, 1995). The extraction of momentum

from the flow due to turbulence production represents form drag exhorted on the flow by the bed morphology (and vice versa). Reattachment of the separated flow forces the development an the internal boundary layer (section five) on the stoss side of the bedform downstream of the point of flow reattachment (McLean and Smith, 1986). The mean boundary shear stress in the vicinity of flow reattachment is very small and increases rapidly with distance downstream because of acceleration in the outer part of the boundary layer due to the decay of the wake. The wake (section three) overlying the separation zone free shear layer also experiences high turbulence intensities and Reynolds stresses (Raudviki, 1966; Engelund and Fredsoe, 1982; McLean *et al.*, 1994; Bennett and Best, 1995). The wake region grows both vertically and horizontally in a downstream direction from the point of flow separation, increasing in size but decreasing in turbulent energy. McLean *et al.* (1994) have shown that the new internal boundary layer interacts with this wake zone and the two effectively merge by the next dune crest and hence approximates uniform boundary layer conditions. Such descriptions of the flow field over dunes have aided the formulation of numerical models and the quantitative partitioning of total boundary shear stress into skin friction and form drag.

Engel (1981) concluded that the length of the flow separation zone over dunes for flows with low Froude numbers is independent of flow depth when the average flow depth to dune height ratio is greater than 5. The length of the flow separation zone shows some dependence on sand grain roughness when the dunes have low form indices, with increasing form index the influence of grain roughness becomes negligible. As the length of the flow separation zone is greatest for a reverse rectangular step geometry, Engel (1981) concluded that it is not correct to compare flow separation lengths behind dunes with those behind reverse steps as had been assumed due to the lower angle of slope of the dune lee face. Engel (1981) and Nelson *et al.* (1993) found that, although variable, the separation length of steep dunes is approximately equal to four times the height. Negative velocities in this recirculation zone can reach -10% to -20% of the mean downstream velocity (Bennett and Best, 1995).

However, morphological studies have shown that a wide range of dune shapes occur in many alluvial and estuarine environments (Yalin, 1964; Allen, 1980) and hence descriptions of fluid flow over dunes based on flume studies over idealised asymmetric dunes may be misleading. For example, dunes with low lee slopes which do not exhibit flow separation

have been documented in the field (Smith and McLean, 1977; Kostaschuk and Villard, 1996).

2.4.2 The Structure of Turbulent Flow over a Flat Bed

Turbulent flows have been studied for well over a century and although no general solutions to problems in turbulence (such as turbulence prediction) exist, many advances have been made such as the characterisation of turbulent flow over a flat boundary. Turbulent boundary layers over flat beds may be considered to consist of different sections, each having distinctly different characteristics in terms of the vertical profiles of mean velocity and shear stress. The inner layer of a turbulent boundary layer extends from the wall to y/δ values ranging from 0.1 to 0.2, where y is the distance above the bed and δ is the depth of the boundary layer. The inner wall encompasses both the viscous sub layer and the log-law region where the mean velocity is logarithmically dependant on distance from the wall. The outer layer of a turbulent boundary layer lies above the inner layer, at depths of y/δ greater than 0.2. Extensive reviews of turbulent boundary layer structure can be found in Kline and Robinson (1989, 1990) and Robinson (1990a,b) and the four main turbulent components of a fully developed boundary layer structure over a smooth wall are described below:

1) Low speed streaks, which have a velocity of approximately half the mean flow velocity. These streaks have a dimensionless spanwise wavelength that scales with inner wall variables which increases with distance away from the boundary. They are one of the fundamental elements of the lower boundary layer and are responsible for feeding low speed fluid into uplifted ejections and bursts.
2) High speed sweeps. These are wall-directed inrushes of higher than average downstream velocity fluid. They are associated with the initiation of sediment transport as they contribute a large proportion of Reynolds stress.
3) Ejections of low speed fluid away from the wall. They have a characteristic low downstream velocity and positive vertical velocity and may act singly or in groups to give rise to boundary layer bursting.
4) Larger scale vortical coherent motions within the boundary layer, in the shape of hairpin or horseshoe vortices.

Many studies have tried to identify the nature of 'bursting' within flatbed turbulent boundary layers where bursting refers to the violent ejection of relatively slow moving bottom water towards the surface (e.g. Grass, 1971; Rao *et al.*, 1971; Bogard and Tiederman, 1986). The structure and spatial and temporal scales of ejection events has been investigated (e.g. Rao *et al.*, 1971) and a relationship between burst periodicity and outer wall variables was perceived such that

$$T_b = TU/\delta \approx 3 \text{ to } 7 \qquad \text{equation 2.3}$$

Where T_b is the dimensionless time between bursts, T is the actual burst period, U is the mean flow velocity and δ is the boundary layer thickness. However, more recent research (Luchik and Tiederman, 1987) has suggested that the relationship is incorrect and scaling with both inner and or inner-outer wall variables is more appropriate. These ejection events have been shown to greatly contribute to Reynolds stresses and have also been postulated to effect the formation of dune bedforms.

2.4.3 Turbulence over dunes

At larger scales, ejections or 'boils' have frequently been described on the surfaces of natural flows such as rivers and estuaries (e.g. Mathes, 1947; Coleman, 1969; Jackson, 1976; Rood and Hickin, 1989; Levi, 1991; Lapointe, 1992; Kostaschuk and Church, 1993). Jackson (1976) speculated that the turbulent bursting mechanism observed in laboratory turbulent boundary layer flows played a major role at this larger, geophysical scale in the formation of dune associated boils. Jackson reasoned that large scale bursting may also scale with outer flow variables and empirically derived the dimensionless periodicity of boils associated with dunes as:

$$T_b = TU/d \approx 3 \text{ to } 7 \qquad \textit{equation 2.4}$$

Where d is the flow depth. As this equation is equal in value to Rao's burst periodicity in the turbulent boundary layer, both Jackson (1967) and Yalin (1977), among others, assumed that the process controlling burst formation behind dunes and ejections from turbulent boundary layers is the same. Jackson reasoned that bursts were generated from within the

lee side separation zone of dunes (Figure 2.4). Hence dune formation was assumed to be related to microturbulent structures, and burst periodicity could be linked through to the scaling of dunes with flow depth. However, the change in scale between the two phenomena is huge and more recent flow visualisation studies (e.g. Itakura and Kishi, 1980; Müller and Gyr, 1982, 1986; Onslow *et al.*) have indicated that the origin of dune-related macro-turbulence may by due to eddy shedding from the separation zone shear layer (Figure 2.4). Levi (1983, 1991) also suggested that such macro turbulence is due to eddy shedding, where the frequency, f, can be determined from the Strouhal relationship:

$$St = fY/U \approx 0.16 \qquad \textit{equation 2.4}$$

Where St is the Strouhal number, Y is the upstream depth before separation and U is the mean downstream velocity.

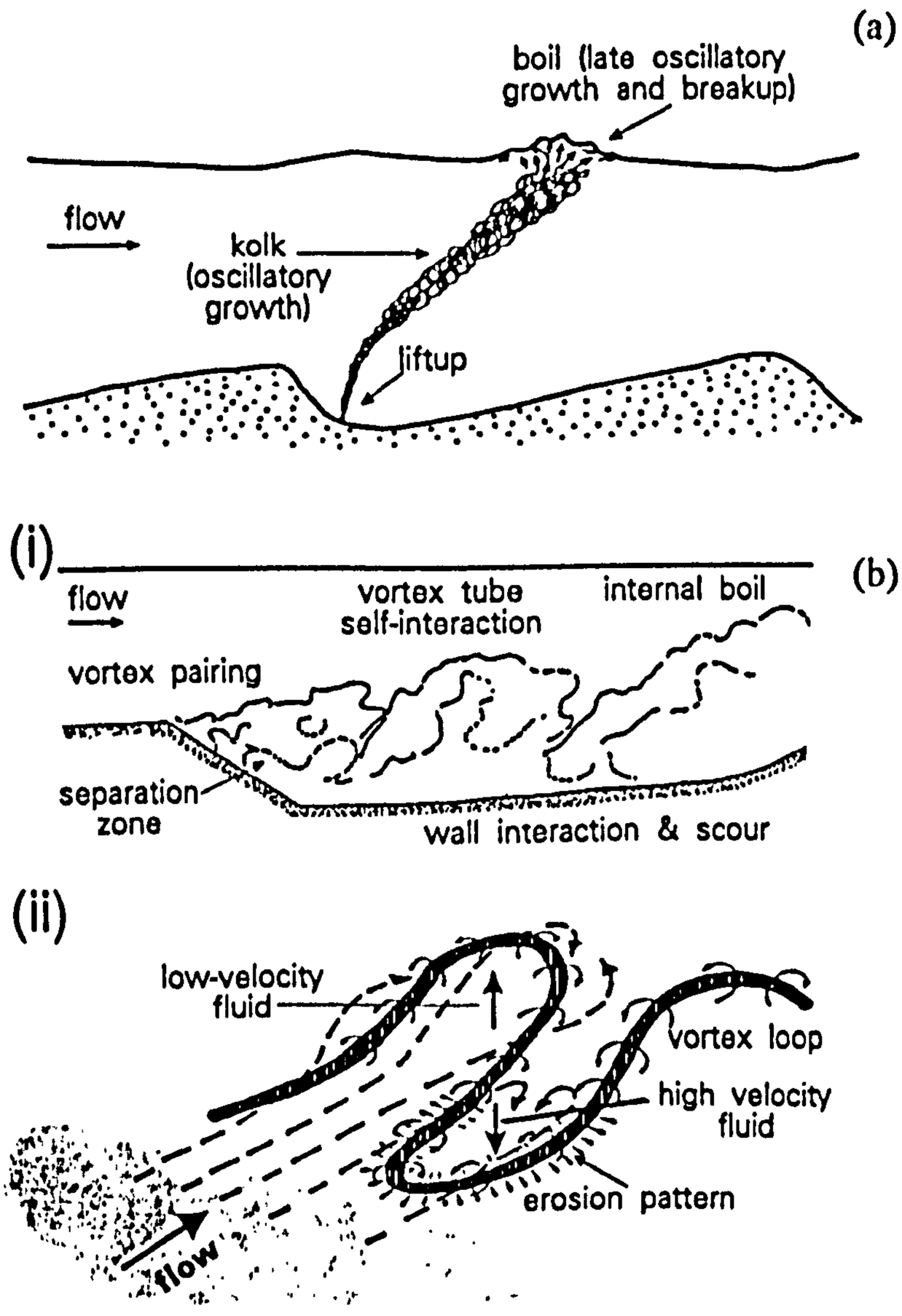

Figure 2.4, (a) Turbulence generation associated with dunes and the origins of kolks and surface boils (after Jackson, 1976), (b) Vortex generation associated with the free shear

layer of the dune flow separation zone (after Müller and Gyr, 1986): (i) vortex development and boil generation downstream of a dune; (ii) horseshoe shaped vortex originating on the free-shear layer of the flow separation zone. (from Best, 1996).

Eddy shedding from free (unattached to a boundary), unstable shear layers was first remarked upon by Helmholtz in 1868 and was formally posed by Kelvin in 1871, and hence is commonly referred to as Kelvin-Helmholtz instability (Drazin and Reid, 1981). Shear or vortex layers are unstable to disturbances of a wide range of wavelengths and break down into periodic vortices (Allen, 1968). Due to the different bounding velocities of the shear layer, the vorticity in the shear layer amplifies with time and feedbacks to further increase the range of wavelengths in the shear layer. The positive feedback mechanism of vorticity generation is a common physical explanation for the Kelvin-Helmholtz instability and further intensification of vorticity may eventually lead to the detachment or shedding of an eddy.

The structure of free shear layers downstream of a backward facing step has been extensively examined in the engineering and aeronautic literature (Figure 2.5). Such studies have found that a 'global' or large scale motion (or flapping) of the shear layer exists, with flapping correlating with change in the separation zone length (Driver *et al.*, 1987). An increase in the separation zone length is accompanied by an increase in shear stress within the shear layer which is interpreted by Driver *et al.* (1987) as the movement of coherent flow structures (Kelvin-Helmholtz instabilities) along the shear layer, which then impinge with the bed at flow reattachment. Flapping therefore displaces the instantaneous reattachment point of the shear layer, hence a flow reattachment zone is a more accurate description than a reattachment point. Another important point associated with shear layer flapping is that flow reversals within the downstream section of the reattachment zone will be intermittent, with a decrease in the frequency of reversals with distance away from the separation point (Figure 2.5). Further description of the structure of the flow separation zone can be found in Simpson (1981,1989).

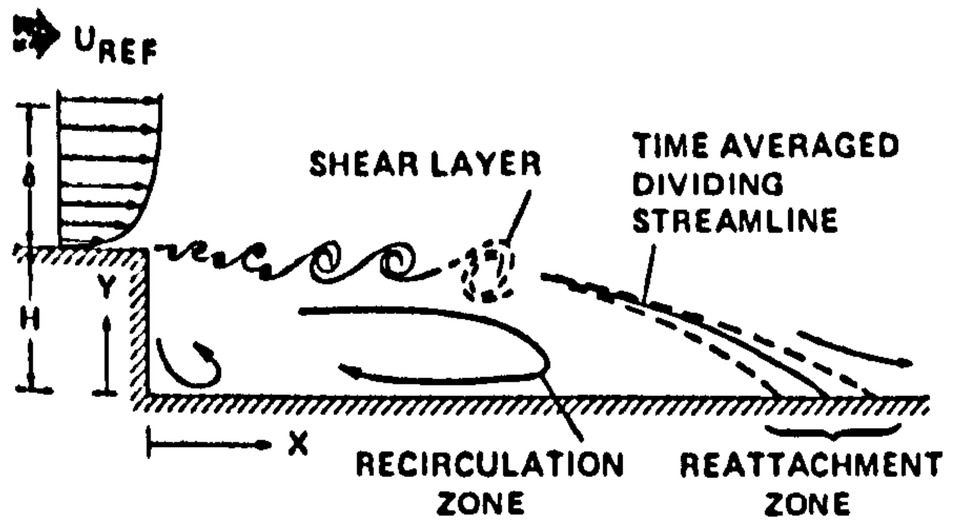

Figure 2.5, Features of flow over a backward facing step (Driver *et al.*, 1987)

Quadrant analysis has been frequently used to discriminate between different boundary layer turbulent motions and uses measurements of instantaneous deviations of velocity from the mean values (e.g. Bogard and Tiederman, 1986). Four quadrants can then be differentiated between when the horizontal and vertical fluctuations are plotted about a mean value of zero. Quadrants 2 (positive vertical and negative downstream instantaneous deviations from the mean velocity) and 4 (negative vertical and positive downstream instantaneous deviations from the mean velocity) then describe ejections and sweeps as outlined earlier in the classical boundary layer description. Quadrants 1 (positive vertical and downstream instantaneous deviations from the mean velocity) and 3 (negative vertical and downstream instantaneous deviations from the mean velocity) show 'outward' and 'inward' interactions of the flow. Quadrants 2 and 4 provide an extraction of energy from the mean flow field to generate turbulence, whereas the negative contributions to Reynolds stress in Quadrants 1 and 3 dissipate energy from turbulence structures back into the mean flow. The flume experiments of Bennett and Best (1995) examining flow over dunes showed that most quadrant 1 events occur within the flow separation zone and both at and downstream of reattachment and McLean *et al.* (1994) have suggested that these events may also be important for initiating sediment transport. Bennett and Best (1995) also quantified the magnitude of turbulence and delineated the morphology and downstream extent of the highly turbulent region along the shear layer produced by flow separation. Quadrant 2 events dominated in this region, and are responsible for a large part of the fractional contribution to Reynolds stress (Figure 2.6). The contribution of Quadrant 2 events to the Reynolds stress decreases away from the separation zone as the shear layer mixes and dissipates. Quadrant 2 events have therefore been postulated to be of great importance in the suspension of sediment from the separation zone shear layer towards the flow surface.

Quadrant 4 events are found to occur frequently within the separation zone and near flow reattachment and these inrushes of high velocity fluid have previously been linked to the entrainment and transportation of sediment (e.g. Thorne *et al.*, 1989), and are indicated by the flume study of Bennett and Best (1995) to be brought towards the bed along the shear layer. Flow reattachment, and the associated impingement of quadrant 4 events, at the bed is postulated to create high instantaneous shear stresses at reattachment and along the lower dune back, hence causing erosion and transport of sediment. McLean *et al.* (1994) show that the sediment transport rate at flow reattachment may not be predicted by the boundary shear stress, as is expected in uniform boundary layers. The measured sediment transport rate downstream of the reattachment point is significantly greater than that predicted using stresses from the near-bed velocity profile due to the high turbulence intensity (McLean *et al.*, 1994). It seems most likely that it is the combination of the turbulence structures (i.e. both sweeps and ejections) described above is the driving mechanism for sediment transport.

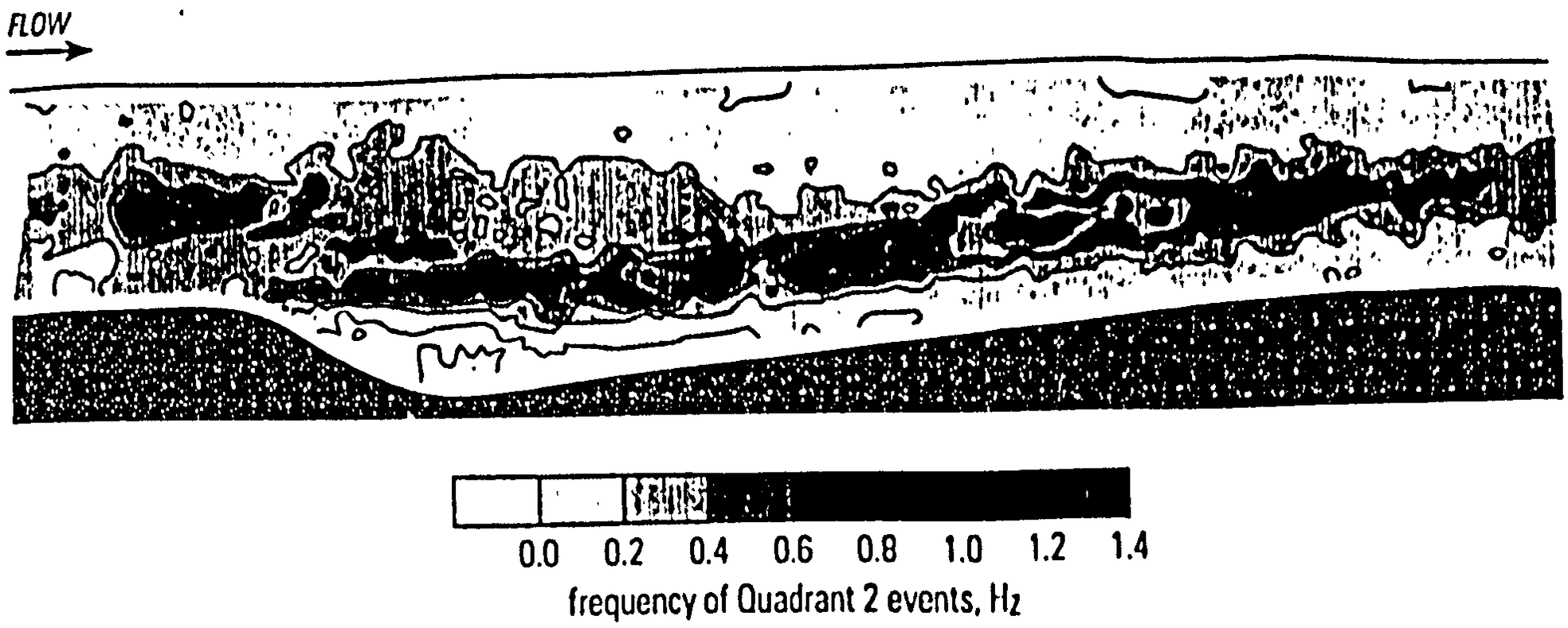

Figure 2.6, Summary diagram of the spatial distribution of the percentage number of each quadrant event using a threshold level of H = 2. For quadrant 2 (ejection) events, both the 2% and the 5% contours are shown (from Bennett and Best, 1995).

2.4.4 Sediment Transport Related to Dunes

Boils, the surface manifestation of large quadrant 2 ejections, have long been observed in the field to be associated with high concentrations of suspended sediment (e.g. Matthes, 1947; Coleman, 1969; Lapointe, 1992; Kostaschuk and Church, 1993; Rood and Hickin,

1989). Surface sampling of suspended sediment concentration has shown a great variation between boil and non-boil samples, with boils often containing five times higher sediment concentrations (Rood and Hickin, 1989). Additionally, Rood and Hickin indicate that the size (diameter) of sediment contained in boils is two times greater than the ambient or non-boil value. The visualisation studies of Kostaschuk and Church (1993) in the Fraser River, Canada, used acoustic techniques to identify variations in water density that are allied with changes in suspended sediment concentration. Localised increases in suspended sediment concentration are interpreted to represent turbulent boil events and were observed to originate over the lower stoss side of dunes (Figure 2.7). Kostaschuk and Church (1993) suggested that flow separation was unlikely to occur over their study dunes as the dune height to wavelength ratio was low (0.02 to 0.07) and proposed a Kelvin-Helmoholtz instability mechanism for boil generation due to flow expansion downstream of the dune crest even without flow separation.

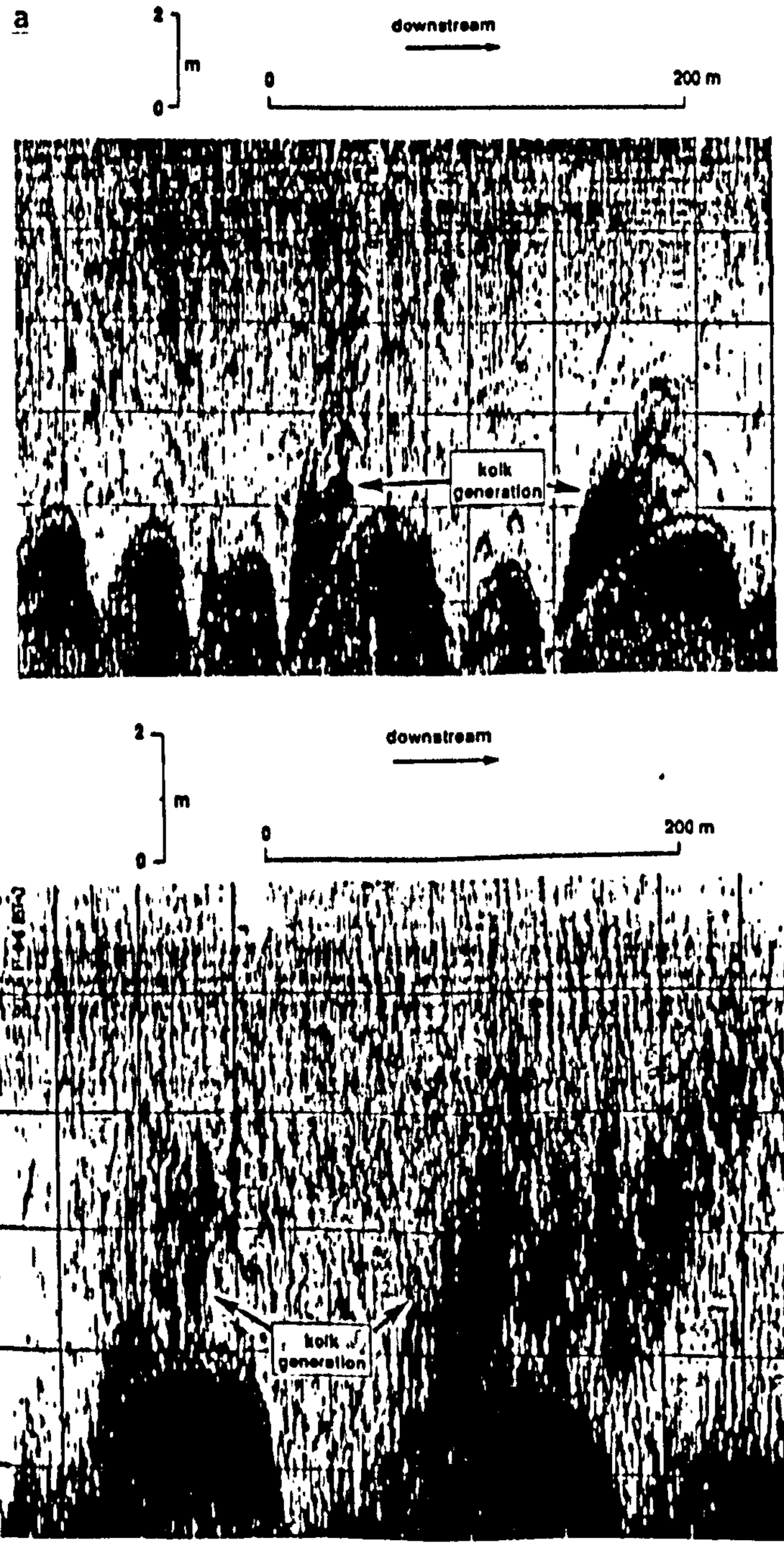

Figure 2.7, Suspension of sediment over dunes as visualised in the field using frequency acoustic profiling on the Fraser River, Canada (from Kostaschuk and Church, 1993). These suspension events have been linked with dune-associated macro-turbulence. (a) Two large kolks originating on the lower stoss side dunes. (b) Kolks generated over dunes with origin nearer the bedform crest. Downstream dune has two kolks inclined at 7.6° and 2.9° to the flow.

Soulsby *et al.* (1991) present field data of mean velocity and suspended sediment concentration profiles over large (h ~ 2m) dunes in the river Taw, U.K and suggest that sediment may be ejected from dune crests. The data of Soulsby *et al.* (1991) also shows that maximum values of both suspended sediment concentration and turbulent kinetic energy occur within the separation zone free shear layer, indicating that an eddy shedding mechanism may also be responsible for ejections of turbulent fluid. Boils may therefore be responsible for increasing suspended sediment transport although much further work is required to characterise dune-related macro-turbulence.

The links between turbulence structure and sediment transport is an area that has received little attention in the literature, but may ultimately control the stability and growth of dunes. The flume study of Nelson *et al.* (1995) however, has characterised the interactions between turbulence events and bedload sediment transport downstream of flow reattachment using a combination of laser-Doppler velocimetry to measure velocity and high speed cinematography to monitor sediment transport. Nelson *et al.* (1991) show that quadrant 4 sweep events (which contribute positively to the mean bed shear stress) are responsible for the majority of bedload sediment transport, although quadrant 1 events (which contribute negatively to the mean bed shear stress) individually transport as much as individual sweeps. Increasing the frequency of quadrant 1 events will therefore cause a decrease in the mean bed shear stress but will increase the bedload sediment transport and hence explaining the hypothesis of McLean *et al.* (1994) that prediction of sediment transport over dunes using bed shear stress is incorrect. The spatial variation in flow and turbulence over dunes is therefore accompanied by a spatial variability in sediment transport, with maximum sediment transport occurring downstream of flow reattachment.

Although extremely useful in determining mean flow fields and turbulence characteristics over bedforms, one of the main limitations with using flume experiments to investigate the fluid dynamics of dunes is that usually, the bedforms used are fixed and also, many studies

do not include sediment transport. Near bed velocities for mobile dunes would be smaller than for fixed dunes due to increased drag associated with a moving bed layer. Also, even though the flow field over two-dimensional dunes used in most studies is three dimensional, the effects of the three dimensional morphology which occurs in natural bedforms has not been investigated. The affect of suspended sediment transport has been neglected in many flume studies, although suspended sediment transport has been indicated in field studies to affect dune morphology and hence turbulence production (Smith and McLean, 1977; Kostaschuk and Villard, 1995).

2.4.5 Numerical studies dune stability

Linear stability analysis has been the approach most frequently applied by many researchers (e.g. Kennedy, 1963; Engelund, 1970; Fredsoe, 1974; Richards, 1980). In this approach, the equations of motion of fluid and sediment are linearised. Flow over an infinitesimally small bed defect is calculated to determine whether it will grow or decay, i.e. the stability of a perturbation is calculated. Kennedy (1963) was one of the first to show that a sinusoidal bed perturbation would grow if the maximum value of the sediment flux was found between the mid point of the upstream side of the feature and its crest. Kennedy therefore assumed that there was a phase lag between the near-bed flow velocity and the sediment flux. The magnitude of the phase lag then determined the type of bedform that would occur under a given flow regime. More recent work has shown that this phase difference can be separated into an upstream shift of the boundary shear stress relative to the velocity, which is entirely due to the mechanical response of the flow to the bedform, and a downstream shift of the sediment flux relative to the boundary stress, which is produced by sediment inertia effects (Smith, 1970), gravitational effects (Fredsoe, 1974) and suspended load transport (Engelund, 1970). While these analyses yield insight into the mechanisms causing the initiation of ripples and dunes, the extension of these results to the finite amplitude case is based on an assumption that the least stable wavelength identified in the small-amplitude theory is not altered by the introduction of finite amplitude phenomena. This is not the case for ripple and dune fields: bedforms sets tend to change in wavelength while growing to their fully developed form from an initial bed defect. Classical stability analyses indicate only if a bedform will form and give very little information about the geometric characteristics of features (Fredsoe, 1982). Most stability analyses do therefore not address the effects of bedform asymmetry, namely flow formation and the separation of a wake. It is

not physically correct to exclude these processes from small amplitude stability analysis. Fredsøe (1982) developed one of these first finite amplitude models to compute bed shear stress distribution downstream of a bedform, therefore including flow separation. However, Nelson *et al.* (1993) hypothesise that because of the nature of the turbulence field in a developing boundary layer, it is incorrect to characterise the sediment flux by boundary shear stress alone, which is the critical assumption made in all of the above stability analyses and in Fredsøe's model.

There have been several attempts to model flow in the finite amplitude situation. These can be split into fully computational models (e.g. van der Knaap *et al.*, 1991), and models that describe the flow field using a combination of piece wise flow solutions (e.g. McLean and Smith, 1986, Nelson and Smith, 1989). These solutions are based on the conservation of mass and momentum for a steady incompressible flow over two dimensional bedforms. This is expressed as the Reynolds equations which are solved numerically over the whole flow domain for the fully computational case. The main problem with this approach is in specifying the relationship between the Reynolds stresses and mean flow quantities that is applicable throughout the flow. As the flow field over dunes is spatially very variable (see above) this is, at present, very difficult. For piece wise solutions, simple models are developed for the different sections of the mean flow field. This partially overcomes the short comings of the fully computational case. The solutions for the different parts of the flow field are then coupled to give an integrated solution.

The main problem with these numerical methods of investigating dune dynamics is that they ignore, to some degree, the coupling between the processes acting in the different regions of the flow: neither the interaction between the wake and internal boundary layer turbulence or the connection between acceleration and the turbulence field is addressed. These methods disregard the process of flow separation which is intrinsic to mechanisms of dune formation and growth and hence are limited in their applicability to more fully comprehend the dynamics of dunes.

2.5 Discussion

The key element in dune initiation is the increase in bedform height (which may be caused by ripple amalgamation or the formation of a rogue ripple) which triggers an increase in the intensity of flow separation and hence turbulence production associated with the separation

zone shear layer (Costello, 1974; Leeder, 1983). The control on an increase in bedform height must be associated with an increase in sediment transport rate and hence sustaining dune bedforms requires a higher sediment transport rate than that acting over rippled beds. To maintain dune stability therefore requires the production of macroturbulence, but the mechanisms of how macroturbulence relates to dune morphology is still an area of some discussion. The emergence of boils at the water surface has lead some workers to surmise that macroturbulence may control both sediment suspension and the fallout of sediment from suspension, and hence may therefore control the wavelength of dunes (e.g. Yalin, 1977). There are, however, several problems associated with this hypothesis; (i) dunes have been shown to occur in gravels as well as sand-sized sediment and hence sediment suspension by boils does not control gravel dune wavelength, (ii) sediment fallout from boils will be dispersed over a large area and so the localised deposition required to form dunes seems unlikely. Detailed studies of the turbulence fields over dunes have shown that quadrant 4 'sweep' events occur most frequently in the flow reattachment zone and that these quadrant 4 events are very important in changing the bedload sediment transport rate. The impingement of turbulent flow on the bed due to flow separation and reattachment therefore causes a spatial variation in the sediment transport field along dunes, with erosion and scour occurring downstream of the dune crest where flow reattaches, and deposition of sediment occurring further downstream. The intensity of turbulence within the separation zone shear layer is a function of the velocity differential across the shear layer which is in turn is influenced by the height of the dune and the mean velocity prior to flow separation. The size and intensity of Kelvin-Helmholtz instabilities, which are produced by shear layer instability, scale with the height of the dunes, and may pair and coalesce as the advect downstream. The significance of other types of turbulent event (such as quadrant one events) has also been suggested to be of importance for sediment transport in the flow reattachment zone (Nelson *et al.*, 1995), although the role of quadrant one events is still an area of some controversy.

2.6 Summary

This chapter has described that if a turbulent flow acts upon a flat bed and is capable of producing significant sediment transport, the bed will be unstable to perturbations and may evolve into a train of bedforms (i.e., ripples and/or dunes, e.g. Nelson *et al.* 1993). The processes of sediment transport over the bed and bedform generation are governed by the

links and feedbacks between the structure and the turbulent flow and bed morphology (see Chapter 1, Figure 1.1). Dune bedforms are therefore created and altered by the flow and, conversely, the flow is acted upon by the bedforms through the production of form drag and significant changes in the local mean flow and turbulence fields. One consequence of these complex interactions is that neither the local nor spatially averaged flow can be predicted without a detailed knowledge of the bed geometry, which in turn is dependant on the detailed characteristics of the near-bed flow field. The flow field over dune bedforms is dominated by flow separation downstream of the dune crest. The separation zone shear layer is unstable and generates turbulence over dunes and hence alters local sediment transport rates, which may ultimately control the stability of dunes. Although great advances have been made regarding the stability of dunes in the last 20 years, since the influential study of Jackson (1976), there are still many areas, such as the links between turbulence and sediment transport, which require much further study.

Chapter 3. Survey Methodology and Instrumentation

3.1 Introduction

In order to address the issues outlined in Chapters 1 and 2, this research requires the measurement of bedform morphology, fluid flow and sediment transport under different flow regimes. The objectives of this chapter are to detail data acquisition methodology in terms of the instrumentation used, the survey locations, survey procedure and data reduction. The errors and reliability of data will also be examined along with post-collection data processing and calibration.

3.2 Acoustic Doppler Current Profilers

Acoustic Doppler current profilers (ADCP) measure instantaneous three dimensional velocity profiles from a transducer assembly that can be either mounted on the hull of a boat or on a river or sea bed. The ADCP transmits acoustic pulses from transducers along four beams, these transducers then receive sound that has been backscattered from sediment particles, or other impurities, that are transported by the water currents. Using the Doppler principle (see section 3.2.1), the ADCP converts the backscattered sound into components of water current velocity and therefore measures the speed and direction of the currents at multiple locations in the water column. The ADCP also records the intensity of the backscattered signal which is a relative measure of the suspended sediment concentration in the water. The ADCP produces a profile of these velocity and suspended sediment measurements for up to 128 designated locations called depth cells. Two RD Instruments ADCPs were used by the RSP (FAP24) which were mounted on the hull of the survey vessels and have operating frequencies of 300 kHz and 600 kHz. Routine FAP24 surveying was undertaken using both ADCPs, while special dune surveys, dedicated to this study of dune bedforms, were conducted only using the 300 kHz instrument.

3.2.1 The Doppler Effect

The Doppler effect is caused by relative radial motion between two objects and is observed as a change in sound pitch. It is commonly heard as a difference in sound as a siren moves past an observer. This is because an observer on a particle moving away from a fixed sound (or light)

source would hear the sound at a lower frequency than the source frequency, and, to a stationary observer, the sound emitted from the particle would also appear to have a different frequency. Since the exact change in frequency is directly proportional to the relative speed of the objects, the relative speed of the objects can therefore be calculated by measuring the change in sound or light frequency.

Sound consists of pressure waves in fluids, liquids or solids. The frequency (f), wavelength (λ) and speed of sound (C_{sd}) are related by the equation:

$$C_{sd} = f\lambda \qquad \textit{equation 3.1}$$

The Doppler shift is the difference between the emitted and the observed frequency and will only occur where the source and receiver are moving relative to each other. Hence, it is the velocity component in the direction of the line between the observer and the source which is important. The equation for the Doppler shift is:

$$F_D = F_S (V_r/C_{sd}) \cos A \qquad \textit{equation 3.2}$$

Where F_D is the Doppler frequency shift, F_S is the frequency of sound when there is no motion, V_r is the relative velocity between the sound source and the observer and A is the angle between the source and the observer.

ADCPs use the Doppler effect to calculate flow velocity by transmitting a pulse of sound at a fixed, known frequency and measuring echoes returning from sound scatterers moving in the water (RD Instruments, 1989). Scatterers are small sediment particles or plankton that reflect (or backscatter) sound towards the ADCP and which, on average, move with the same velocity as the water. The backscattered sound appears to the ADCP as if the scatterers were the sound source, hence the Doppler shift is doubled changing the original Doppler shift equation to:

$$F_D = 2F_S (V_r/C_{sd}) \cos A \qquad \textit{equation 3.3}$$

3.2.2 ADCP Beams

The ADCP uses multiple sound pulses or beams (Figure 3.1) to measure three velocity components. In order to use multiple beams it must be assumed that the water currents are

homogeneous over layers of constant depth since the beams are orientated in different directions to sense the different velocity components.

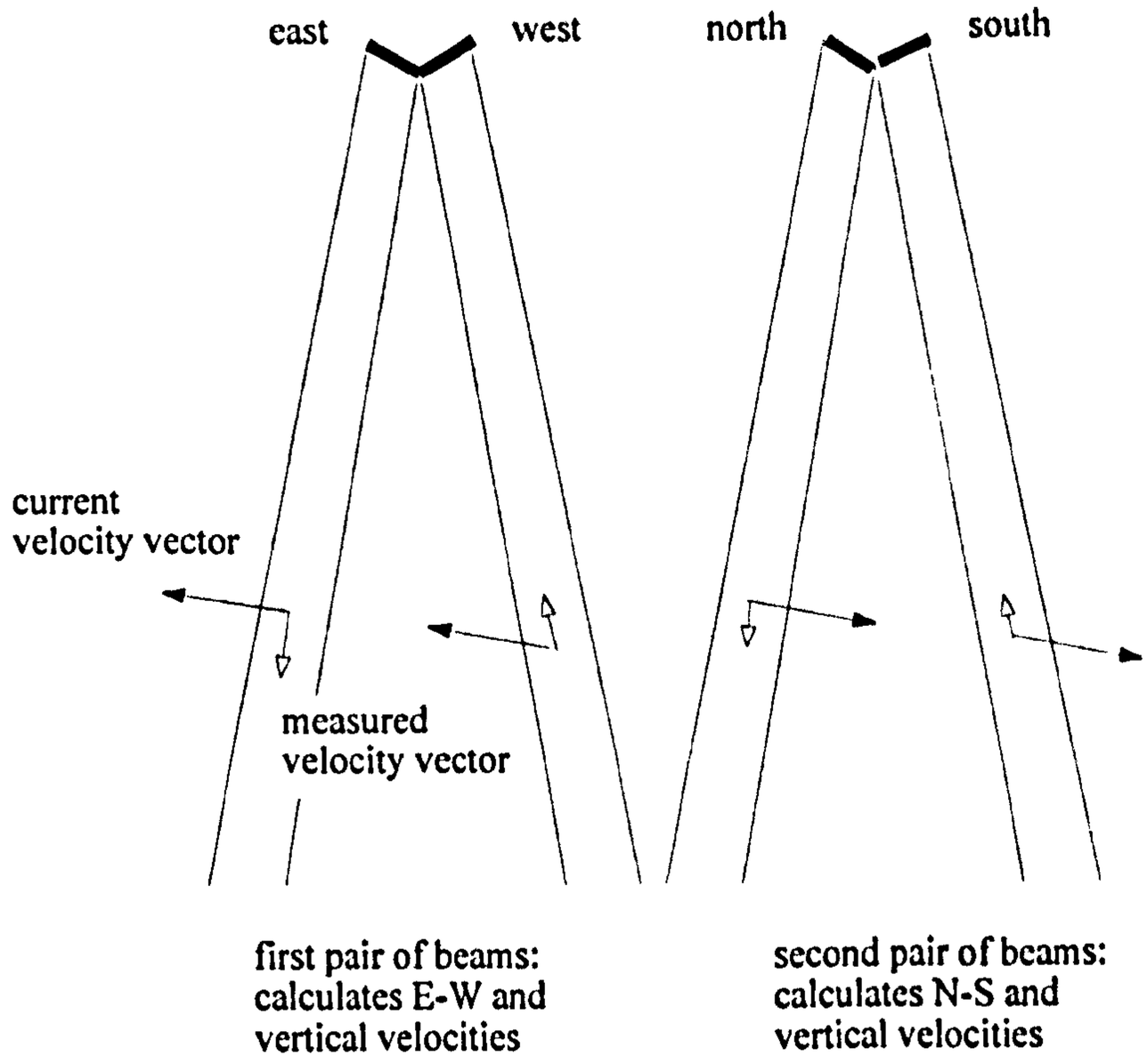

Figure 3.1, Four ADCP beams (shown here in 2-D) are used to calculate the 3 components of velocity, leaving one beam spare to take a second measurement of the vertical velocity which can be used to estimate errors where currents are homogeneous laterally (adapted from RD Instruments, 1989)

Each beam is orientated orthogonally and at 20° to the vertical. However, this means that measurements are being made in different places for the various velocity components (Figures 3.1 and 3.2). For example, for a beam direction setting of 20°, at a depth of 10 m there is a spacing of 11.6 m between each beam. As four beams are used by the ADCP to measure velocity, one is redundant, and is used to estimate errors by measuring the vertical velocity a second time. The error velocity is the difference between the two vertical components and allows evaluation of the assumption of horizontal homogeneity. Under homogeneous-layer flow conditions, errors caused by other factors (e.g. transducer quality) will also be quantified by this method. If flow conditions are turbulent however, a difference in the vertical velocities at different locations would be expected and so under turbulent flow conditions the redundant beam can give a measure of the correlation between the different beams.

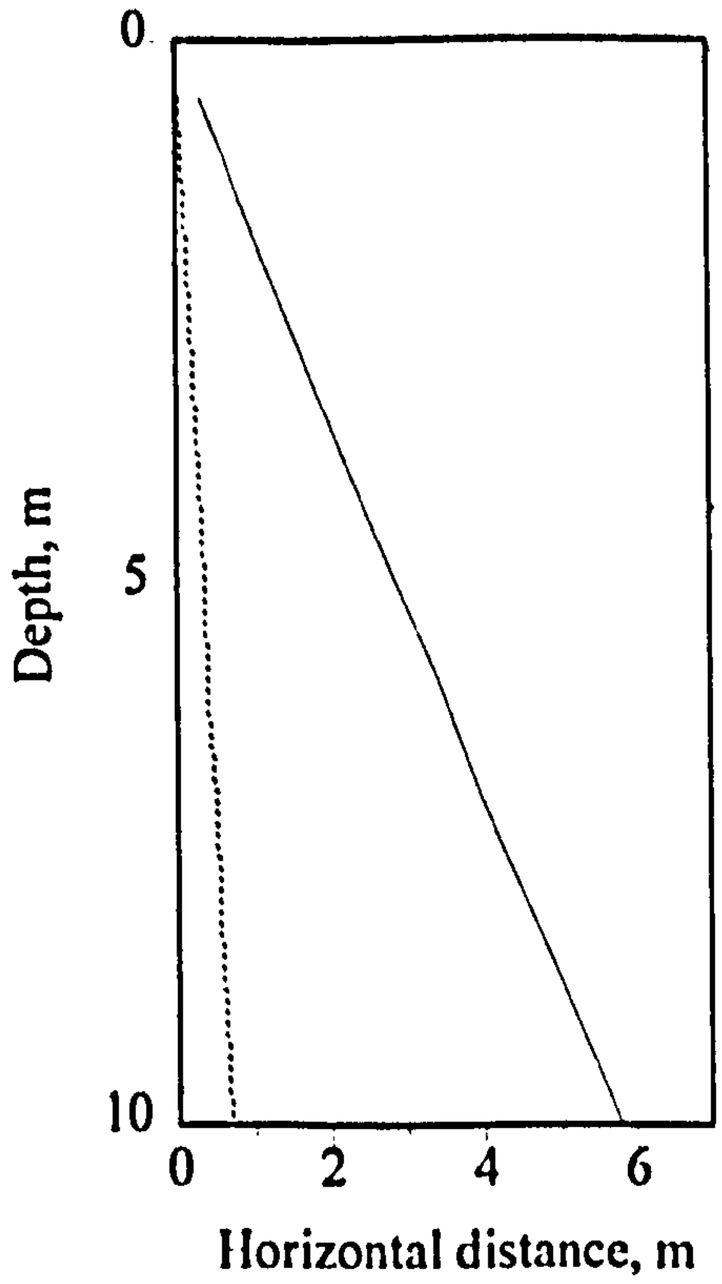

Figure 3.2, ADCP beam angle configuration is set at 20° to the vertical with beam location therefore increases with depth (solid line). Spreading of the beam main lobe also occurs due to attenuation of the transmitted signal causing an increase in bin width with depth (dotted line).

Beam configuration is such that tilt errors caused by roll and pitch are largely rejected because of two factors. Firstly, the two opposing beams allow the vertical velocity to cancel when computing horizontal velocity. Secondly, since tilt errors are proportional to the sine of the tilt rather than the sine of the main beam angle, errors associated with tilt calculated using the four beam configuration are an order of magnitude smaller than those occurring using a single beam.

3.2.3 Velocity Profiles

ADCPs measure entire velocity profiles which are split up into depth cells or bins. The depth cells are uniformly spaced and each reading for a depth cell is a weighted average of velocity measurements within that depth range. Averaging over a range of depths reduces the effect of spatial aliasing, which is a process where signals at frequencies higher than the instrument can

resolve are mistaken for low frequency signals. Eliminating aliasing effectively reduces the signal to noise ratio of the ADCP.

The ADCP receives a continuous echo signal which is then split up into successive segments. These segments, or ranges, correspond to increasing depth cells and each range gated signal is processed independently. Figure 3.3 illustrates the relationship between range gates (time) and depth (distance from the ADCP). A transmitted pulse of a set duration (left hand side of time axis) propagates through the water column and is reflected back to the ADCP as a continuous signal which can be split into time ranges which correspond to increasing depth ranges. After the pulse has been transmitted, the ADCP turns off for a set period to allow the transducer ringing to die down, then records the returning echo and processes the first gate and so on. Scatterers from the centre of a depth cell reflect more energy than scatterers in the top and bottom portions of the cell so each velocity recording is a weighted average. Depth cells overlap (Figure 3.3) giving a 15% correlation between cells.

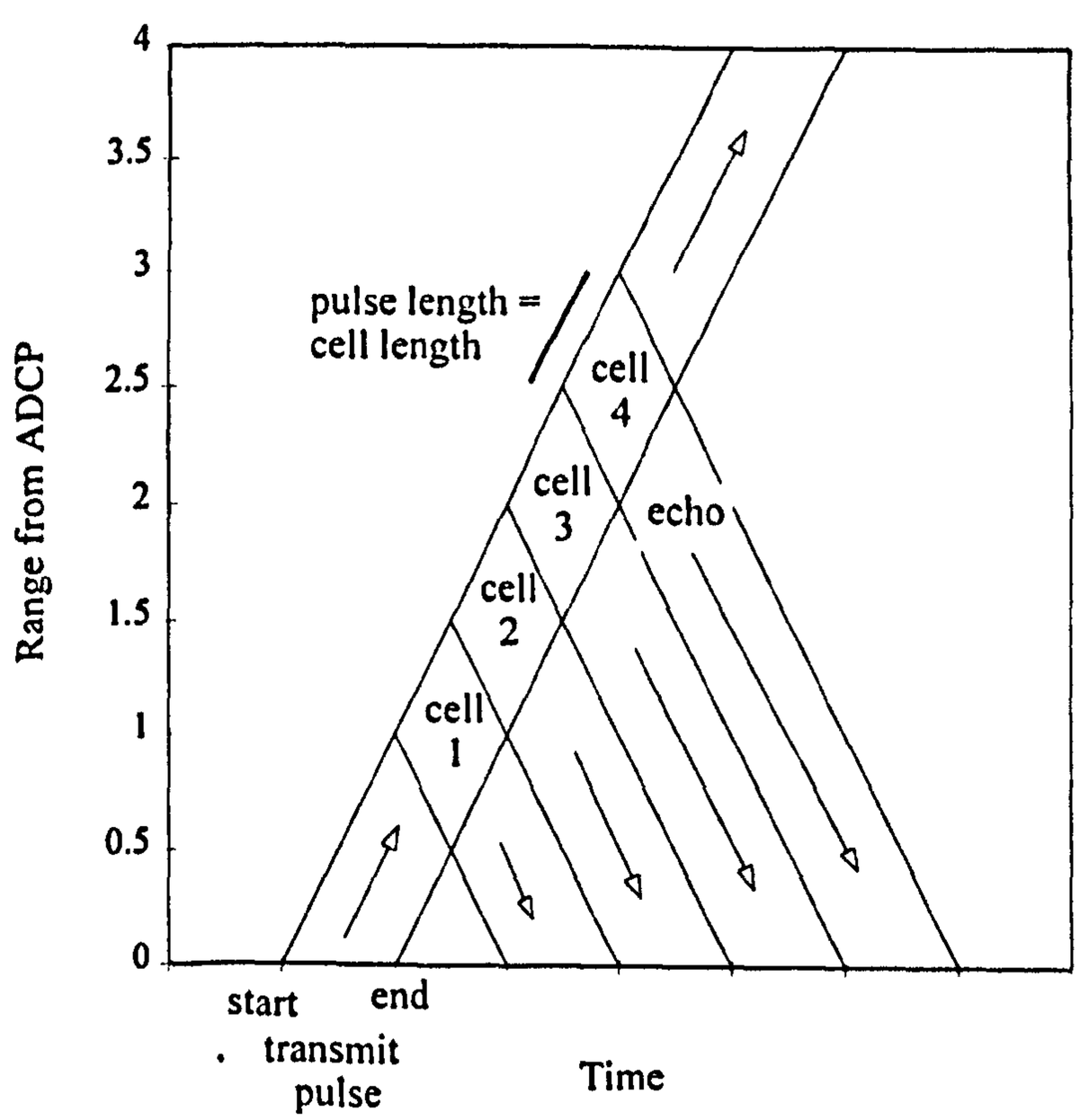

Figure 3.3, The relationship between range gates, depth cells and pulse timing. This is a 2D plot relating time and distance from the ADCP. At the left hand side of the time axis is the transmit pulse, its propagation being shown by the line sloping up and to the right. After the transducer ringing has died down, the ADCP listens for the returning echo and processes range gate 1 which incorporates the signals returned from the area labelled cell 1, (adapted from RD Instruments, 1989).

3.2.4 Transducers and the Echo Spectrum

Transducers are one of the most important factors influencing data quality. They consist of piezoelectric ceramic discs that expand or contract when an electric field is applied through a thin layer of silver which coats the discs. Ideally, narrow and directional acoustic beams are needed to reduce transducer-induced errors. Figure 3.4 illustrates an example of a beam pattern which shows the beam width and side lobes. Beamwidth is the width of the beam, expressed in degrees, at half the signal strength. The major lobe at the centre of the beam contains most of the power, but some power is also contained in the side lobes which effect data quality, especially at angles greater than 15° from the centre. The lobes are mainly a function of transducer size with large transducers generating thinner beams with fewer and smaller side lobes. The lobes can also be caused by vibrational modes in the piezoelectric ceramic which are prevalent at approximately 40° from the centre and can be dominant. The transducers are mounted on the hull of the survey vessel at a depth of 1.66 m below the water surface.

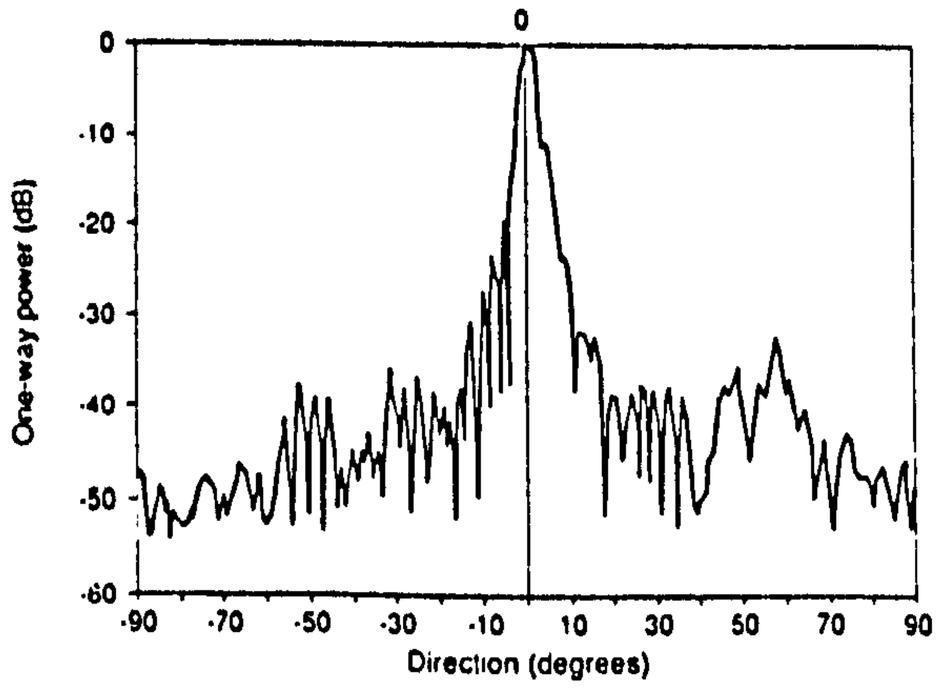

Figure 3.4, Acoustic beamwidth with side lobes (from RD Instruments, 1989)

The signal returned from river bed reflections is extremely strong and so can overcome side lobe repression of the transducer. This means that the last 6% of the profile nearest to the bed must be rejected as side lobe interference will occur and is calculated using the equation

$$R_{max} = d_a \cos(\varphi) \qquad \textit{equation 3.4}$$

where R_{max} is the maximum depth of good data, d_a is the distance from the ADCP to the river bed and φ is the angle of the beam relative to vertical. For example, in a water depth of 10 m, for a 20° beam angle, the bottom 0.6 m of the profile must be disregarded. This shows that decreasing the beam angle will increase the percentage of measurable flow depth, however, decreasing the angle from 30° to 20° also increases the standard deviation of the flow data by a factor of 1.5. A beam angle of 20° to the vertical has been used for all surveying undertaken by FAP24.

The emitted sound pulse is transmitted at a set single frequency which is controlled by a crystal oscillator. Before transmission, the signal is a line spectrum (i.e. a single frequency), however during transmission spectral broadening occurs due to attenuation caused mainly by the short duration of the transmit pulse. There is an inverse relationship between spectral broadening and transmit pulse length which can be set in the ADCP configuration file. Broadening is measured by the ADCP as a spectral width (Figure 3.5) and this is directly related to the uncertainty of the mean Doppler frequency and therefore uncertainty in the velocity measurement. Other secondary causes of spectral broadening are turbulence and acoustic beam width.

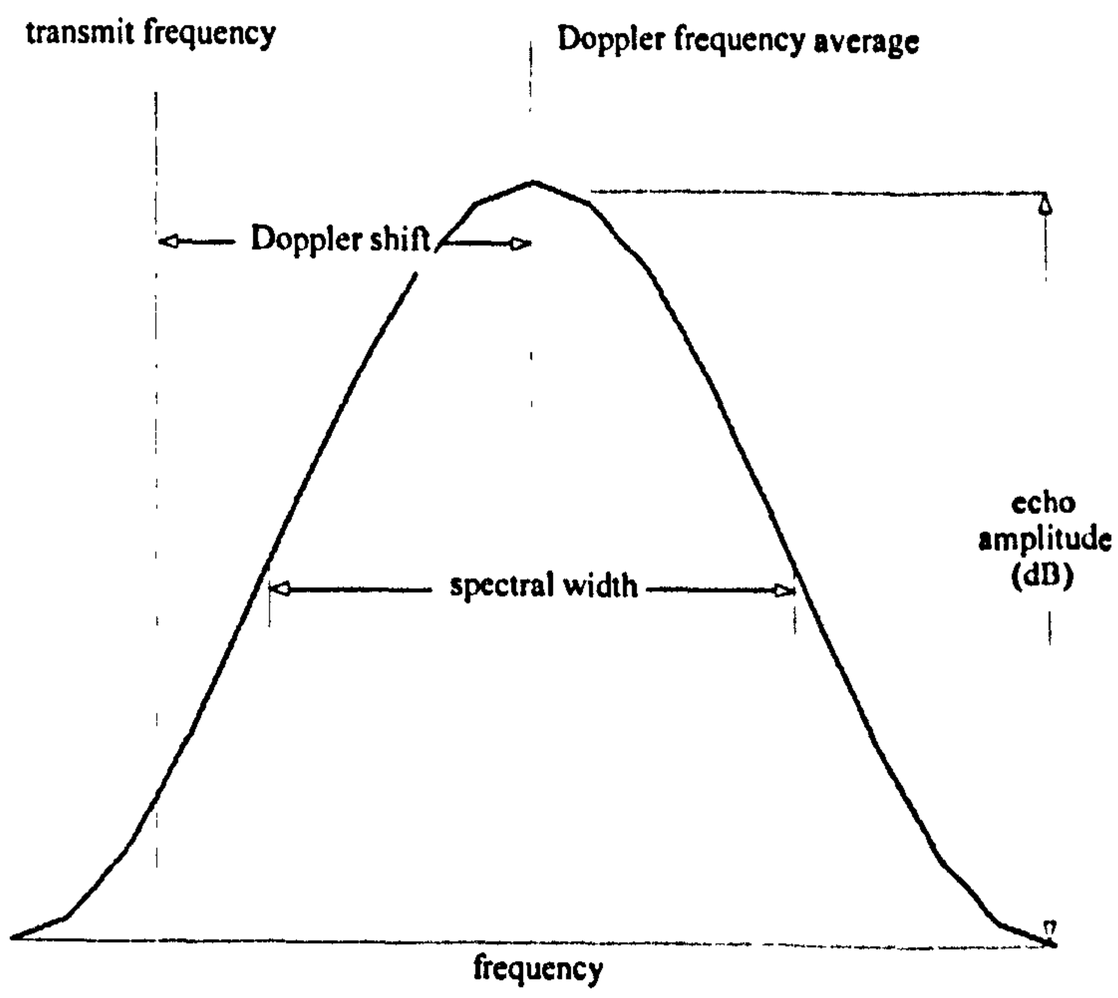

Figure 3.5, ADCP spectral broadening can be represented as a bell-curve of frequency against echo amplitude. Doubling the spectral width also doubles the uncertainty in the estimate of Doppler frequency

Data recorded by the ADCP are velocity, spectral width and echo amplitude. The velocity is a first moment of the echo spectrum which is the mean value of the Doppler shift. The echo spectral width is the second moment from the mean of the echo spectrum. The approximate expected value of the spectral width (SW, Hz) is proportional to the depth cell length (L, metres):

$$SW = 500/L \qquad \textit{equation 3.5}$$

The ADCP output also includes the standard deviation of the spectral width which is equal to SW/2.35. Echo amplitude is the zeroth moment of the spectrum and is a measure of the energy in the echo.

3.2.5 Echo Amplitude and Measurement Range

Echo amplitude (EA, dB) is the strength of the returning echo which is a relative measure of the suspended sediment concentration and is related to four factors:

- Sound absorption reduces echo strength as a result of both physical and chemical processes. It is much more rapid in salt water due to chemical reactions. Absorption causes an exponential reduction of returned energy with range when measured in dB.
- Source level depends on power transmission and transducer efficiency. Power transmission is solely dependant on the source which is either alternating current (AC) or batteries. An AC generator is used as the power source for all data collected for these studies.
- Beam spreading is a purely geometric cause of attenuation as a function of range: doubling the range to the scatterer quarters the amount of energy reflected (see Figure 3.2).
- Backscatterer concentration affects both echo amplitude and range. Higher concentrations of sediment particles radiate more sound back towards the transducers.

These four factors are related by the simple equation:

$$EA = P + SV + c - 20\log(R) - 2eR \qquad \textit{equation 3.6}$$

where SV (in dB) is the water mass volume backscattering strength, e is the absorption coefficient of water (dBm^{-1}), c is a constant, P is the transmitted power and R is the distance from the transducer to the depth cell (m). The constant is required as the measurements are

relative rather than absolute so the ADCP requires calibration. The term 2eR accounts for energy absorption and 20log(R) accounts for beam spreading (see Figure 3.2) which decreases the percentage of the signal which is reflected back to the transducer assembly. The calibration curve used to account for beam spreading and energy absorption is shown in Figure 3.6.

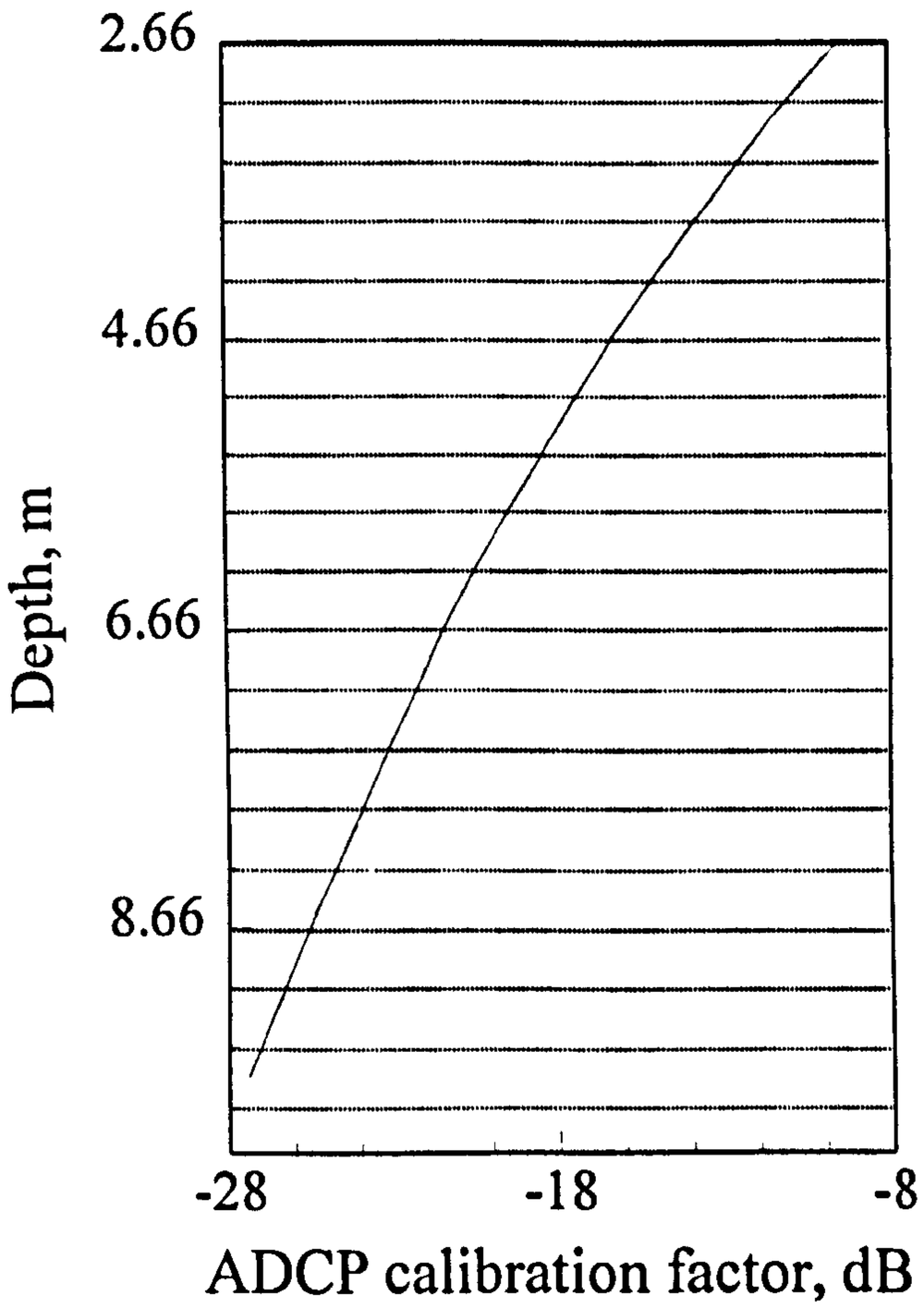

Figure 3.6, ADCP beam intensity calibration factor to account for loss of signal energy by beam spreading and absorption changes with depth.

3.2.6 Calibration of Backscatter Intensity to Suspended Sediment Concentration

Suspended sediment concentrations have conventionally been difficult to measure. Bottle sampling has been employed frequently but the temporal and spatial resolution of this technique is poor. Pump sampling provides improved temporal, although not spatial, resolution but is limited in some environments, such as oceanic boundary layers, due to the distances that the samples must be pumped. Additionally, these measurement techniques inherently average over the wave or turbulent processes which are the underlying driving forces of the dynamics

of sediment transport (Thorne *et al.*, 1994). The ADCP may therefore be a valuable tool when using the signal intensity to obtain suspended sediment concentrations. As the ADCP measures the relative suspended sediment concentration from the backscatter intensity in decibels (see above), a number of pump sampling surveys were undertaken by the RSP (FAP24) in order to calibrate the instrument. All the surveys used to calibrate the ADCP were conducted at Bahadurabad, the location used for all special dedicated dune surveys conducted for this research (see section 3.8.6). It is expected that anticipated variations in sediment size, shape and sorting will be lessened when sampling at the same location as variations in sediment size distributions would render calibration inaccurate. Increased ADCP error due to sediment size distributions occur because the backscattered signal recorded represents an integral signal for all scattering particles. If a mono-frequency ADCP is used, it is therefore not possible to distinguish between the section of the signal due to particle concentration and the section due to particle size (Reichel and Nachtnebel, 1994). The water mass volume backscattering strength (SV) is therefore a function of the particle size distribution of the suspended sediment.

Weiergang (1995) derived an expression relating the backscatter intensity signal (in dB) with the logarithm of sediment concentration. The value of silt concentration in each sample was shown to be important and indicated that calibration levels vary with the silt fraction present. Weiergang suggested that the signal intensity varies with the cube of particle diameter. Increasing the silt fraction will therefore decrease the intensity of the reflected signal. This indicates that for suspended sediment with a high silt:sand ratio, calibration of the ADCP is poor. The sand fraction of each sample can be related theoretically after Weiergang (1995) as:

$$EA = 58.2 + 0.96 * 10\log C \qquad \textit{equation 3.7}$$

where C is the concentration of the suspended sand fraction.

At high sediment concentrations (above approximately 90 dB, which corresponds to a suspended sediment concentration of about 2000 mgl^{-1}) the calibration equation underestimates the suspended sediment concentrations and this may be due to two factors:

1. Reflections from areas with high sediment concentration levels return stronger reflections which can overcome side lobe suppression in the transducer and therefore greatly increase errors (see section 3.2.4).

2. The grain size distribution may be expected to vary vertically with an increased D_{50} nearer the bed. This may cause over estimation of suspended sediment concentration at greater depths.

Acoustic attenuation varies with water temperature, although at the low operating frequency of the ADCP (300 kHz) there is only a 2% variation in backscatter value for a depth variation of 5 to 10 m at the average water temperature in the Jamuna (25° C, Sarker, 1996). Since it is not possible to calculate the acoustic properties of the sediment particles, the strength of the backscattered signal has been calibrated against known pump-sampled suspended sediment concentrations. The concentration of the sand fraction in the suspended sediment is given by the relationship (M^{c}Lelland *et al.*, 1998):

$$C^{0.5} = -68 + 1.04\ EA \qquad r^2 = 0.79, \qquad \text{sample size} = 73 \qquad \textit{equation 3.8}$$

The silt fraction is ignored in this calibration since particles in this size range have a negligible effect on the backscattered signal. However, it should be noted that although 74 % of the bed material in this study is sand, silt can constitute between 15 and 98% of the total suspended sediment concentration (Sarker, 1996). A minimum grain-size cannot be defined to give a threshold for ADCP response although backscatter intensity diminishes rapidly for smaller grain-sizes. Hence equation 3.8 is not resolved for backscatter intensities of less than 70 dB, which corresponds to a suspended sediment concentration of approximately 25 mgl^{-1} (M^{c}Lelland *et al.*, 1998).

3.2.7 Ensemble Averaging and ADCP Errors

The errors involved in a single recorded pulse or ping are too great for most uses. A number of pings are therefore averaged to reduce this uncertainty. There are two types of error associated with the ADCP: random error which is reduced by averaging and bias which is not. ADCP system bias errors are typically 0.5 to 1.0 cms^{-1} (Figure 3.7).

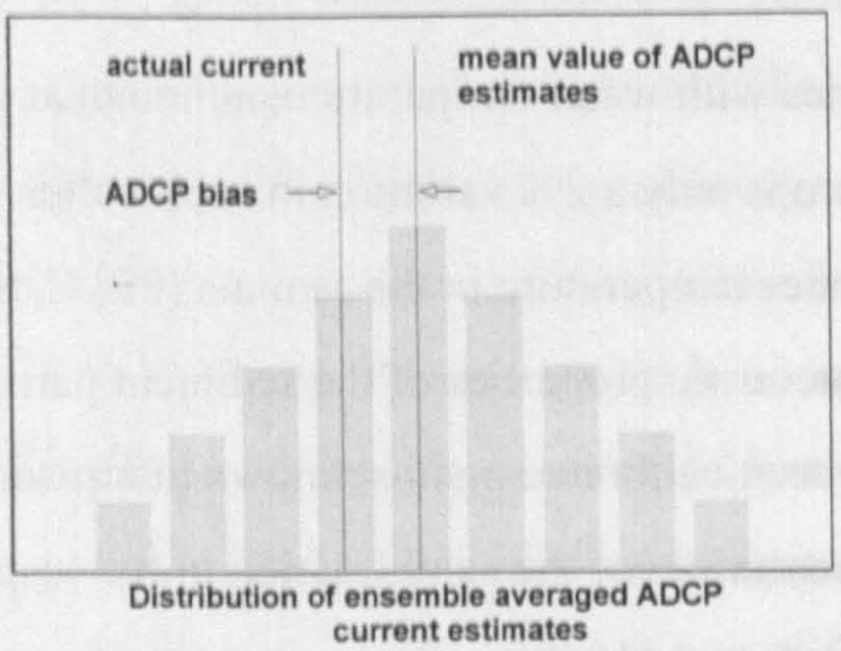

Figure 3.7, random error and ADCP system errors. **a)** shows a distribution of 20 000 measurements of exactly the same current. In this distribution, the measurements cluster around the actual value of the current, but there is a variation due to random error. **b)** shows what may happen if 200 ensembles were made of 100 pings each from the original 20 000 pings. Averaging the 100 pings in each ensemble reduces the random error of ensemble by a factor of about 1/10. Note that the average value here is still different from the true current. The difference that does not average out is ADCP system bias.

Bias depends on a number of factors including temperature, mean current speed, signal:noise ratio and beam geometry errors. It is not possible to measure bias or to calibrate for it during post processing. Random error is uncorrelated between pings so averaging will reduce the standard deviation (σ) as follows:

$$\sigma \propto n^{-0.5} \qquad \textit{equation 3.9}$$

where n is the number of pings averaged. After a certain amount of averaging the random error becomes smaller than errors due to bias. At this point further averaging is redundant as it will not reduce overall errors. Random errors in the horizontal velocity component are related to the standard deviation (σ, ms^{-1}), frequency (f, Hz), depth cell size (d_c, m) and number of pings averaged (n). For an ADCP using transducers orientated at 30° to the vertical, random errors are approximately:

$$\sigma = (1.6 \times 10^5) / (f\, d_c\, n^{0.5}) \qquad \textit{equation 3.10}$$

Total ADCP error (random and bias) have been estimated by FAP24 as 0.1 ms^{-1}.

3.2.8 Processing

Ensemble averaging can take place inside the ADCP or within its data acquisition system (DAS), or in both. Determination of which method to use depends on the conditions under which readings are taken as well as data requirements. For example, if attitude changes significantly during an ensemble interval, conversion from beam to earth co-ordinates should take place before averaging. The DAS is more flexible in converting co-ordinates and can correct each ping separately. Transmission time between the ADCP and the DAS is however longer if single pings are transmitted rather than ensembles, which uses up time when data could be collected. Averaging is limited by the ping rate, which is itself limited by how fast the ADCP can collect, process and transmit data. An example of ADCP file ASCII file format is shown in Figure 3.8 for a single ensemble. Several FORTRAN computer programmes have been written to reduce and reformat the ADCP file structure (Figure 3.8) to provide time series of downstream, vertical and error velocity, back scatter concentration, and the percentage of good data. These computer programs also remove the lowest 6% of the ADCP data (Section 3.2.4) by also extracting bed depth data from the separated bathymetric files.

date *easting* *northing* *ping no.*

start time *end time*

960228	15:54:30	+++50	15:54:31	00470025.6	00780072.3	3
960228	15:54:31	+++50	15:54:32	00470025.3	00780073.0	4
960228	15:54:32	+++50	15:54:33	00470025.0	00780073.8	5
960228	15:54:33	+++50	15:54:34	00470024.8	00780074.8	6
960228	15:54:34	+++50	15:54:35	00470024.5	00780075.5	7
960228	15:54:35	+++50	15:54:36	00470024.2	00780076.4	8

end of DGPS *morphology data file*

data *reference no.*

960228 15:54:36 +++30 1301283

ensemble 1 date and start time

0 1 96 2 28 15 54 29

no. of *no. of*

bins *beams*

1 20 4 1 20 0 0 0 0

c-w *n-s* *v1* *v2*

velocity, mms^{-1}

243	-1801	27	0	*depth cell 1 (2.66 m)*
130	-1666	31	21	*depth cell 2 (3.16 m)*
148	-1686	21	-37	*depth cell 3 (3.66 m, etc.)*
267	-1637	-8	-6	
326	-1557	49	37	
293	-1568	-12	-18	
-94	-1533	14	-8	
0	-1500	-8	9	
-32768	-32768	-32768	-32768	
54	-532	-24	8	
-129	-506	86	-315	
-32768	-32768	-32768	-32768	
-32768	-32768	-32768	-32768	
-32768	-32768	-32768	-32768	
-32768	-32768	-32768	-32768	
-32768	-32768	-32768	-32768	
-32768	-32768	-32768	-32768	
-32768	-32768	-32768	-32768	
-32768	-32768	-32768	-32768	
-32768	-32768	-32768	-32768	

echo intensity data, dB

3 20 4 1 20

beam 1 2 3 4

112	121	126	124	*depth cell 1 (2.66 m)*
101	113	119	117	
97	110	116	114	
97	107	114	112	
96	105	112	110	
96	105	112	108	
96	104	111	108	
95	103	111	109	
95	102	113	111	
120	136	131	155	
150	166	175	175	
148	158	182	154	
99	107	132	107	
77	91	102	94	
70	84	89	89	
69	82	84	91	
71	81	81	91	
67	83	80	89	
67	79	79	88	
67	76	77	85	

% good data

4	20	4	1	20

beam 1 2 3 4

90	100	100	100	*depth cell 1 (2.66 m)*
80	90	100	100	
100	100	100	90	
100	90	100	100	
100	100	100	100	
100	80	90	90	
100	100	90	80	
100	90	90	80	
0	0	0	40	
100	100	100	100	
90	90	100	50	
40	0	0	0	
0	50	60	0	
0	0	30	0	
0	0	0	0	
0	0	40	0	
0	0	0	0	
0	0	0	0	
0	0	0	0	
0	0	0	50	

end of ensemble 1 data

Figure 3.8, ADCP file structure for one ensemble (6 pings), descriptions of file contents are noted in ***bold italics***. Header information for each ensemble includes DGPS co-ordinates and time and a reference code to link the ADCP flow structure with morphological data from the echo sounder. Data for velocity, echo intensity and % good data are collated in 3 sections for each beam at successive depths in the flow column from 2.66m downwards in 0.5m cells, where -32768 is a default referring to bad or missing velocity data.

3.2.9 ADCP Motion Corrections

The velocities measured by the ADCP are relative to the ADCP and hence the boat. Velocities must therefore be corrected for this motion, and must be converted into an earth-referenced co-ordinate system. Three steps are necessary when converting from ADCP to earth referenced velocities:

1. Currents are primarily measured parallel to the four acoustic beams. These are converted into an orthogonal co-ordinate system of ADCP north, east and vertical. This correction requires pitch and roll data to account for ADCP attitude and corrections for beam tilt. An onboard gyrocompass in conjunction with a synchro interface is used to measure motion.
2. Data are rotated to true magnetic north and east co-ordinates.
3. The ADCP velocity (i.e. the boat velocity) is subtracted. There are two methods that can be used to calculate boat velocity: bottom tracking and navigation. Bottom tracking, which references velocity to a fixed river bed, is not applicable for the Bangladesh rivers as the river bed is in motion when flow rates are high. This means that accurate vessel positioning data is required from the onboard differential global positioning system (DGPS).

ADCP configuration for all FAP24 surveying is such that ADCP file data (see Figure 3.8) are referenced to DGPS co-ordinates rather than the boat. Velocity correction is undertaken after data acquisition using software developed by the Danish Hydraulics Institute (DHI).

Although attitude information can be obtained from a gyrocompass in many ways, most methods are limited due to ping frequency. Attitude data are needed at exact times for ping processing and synchro interfaces do not have such limitations. They consist of a pair of motors which rotate and when one rotates a given amount, the other rotates by the same amount and

they then output a voltage which depends on the rotation angle. Multiple turn synchros can be used, where the motors will rotate up to 360 times for a single ship rotation.

3.2.10 Signal Processing

Echo amplitude as measured by the ADCP is influenced by the Automatic Gain Control (AGC) circuitry. Echo signal strength typically varies over a range of 80 - 100 dB. An ADCP must use AGC to keep the signal level approximately constant in spite of large input signal strength variations. The input signal is converted to a logarithmic value, digitised and recorded as an echo amplitude. It is also fed into an amplifier with a voltage controlled gain and then continually adjusted to keep the output signal constant.

Frequency tracking is used to keep the recorded signal frequency in a band near zero frequency where it is digitised. This involves shifting the frequency by a variable frequency and filtering it twice. These successive filters allow the signal to noise ratio to be estimated.

An autocovariance method is used to estimate the frequency of the Doppler shift. The speed of sound may vary either with depth or near the transducers. This can be calibrated for post data collection. Velocity data are originally measured in units of frequency corresponding to the mean Doppler shift. The speed of sound is then assumed to be 1536 ms^{-1} so velocity can be converted to more useful units. If the speed of sound varies at the transducer, the velocity is corrected using the equation

$$V_c = V_u (C_{sd,w}/1536) \qquad \textit{equation 3.11}$$

where V_c is the corrected velocity, V_u is the uncorrected velocity and $C_{sd,w}$ is the speed of sound in water at the transducer which is dependant on salinity, temperature and depth. If the speed of sound alters with depth, depth cell depth may be corrected for in the same manner. For 20° transducers:

$$d_c = d_{c,u} (C_{sd,w}/1536) \qquad \textit{equation 3.12}$$

Where d_c is the corrected depth cell length, $d_{c,u}$ is uncorrected depth cell length and $C_{sd,w}$ is the speed of sound in that depth cell. Each depth cell must be corrected for successively.

3.5 Morphological Measurements

Measurement of river bed and bar top morphology have been carried out using echo-sounders, side scan sonar and land surveying. A description of each of these techniques is given below.

3.5.1 Echo Sounder

The echo sounder transducer comprises of a number of transducer elements embedded in reinforced plastic and is mounted on the hull of the survey vessels at a depth of approximately 0.9 m. Signal transmission is at right angles to the radiating face so the transducer is installed horizontally on the hull bottom and is connected to the echo sounder by a screened cable by way of a hull 'stuffing tube'. The transducers consist of a number of cylindrical resonators built up around a ceramic disc which changes its dimensions slightly when a varying voltage is applied. In this way the signal voltage reaching the transducer during the transmission period is converted to mechanical vibrations, or sound pulses, which are transmitted down through the water column. When the returning signal echoes are received, the opposite action takes place and in this mode the transducer operates as a microphone. The reflected sound waves that strike the transducer face cause the ceramic discs to vibrate at the same frequency. Thus, a varying voltage is generated between the disc surfaces which is supplied through the transducer cable to the receiver which amplifies the echo signals so data can be presented in either analogue or digital format. The larger the radiating face, the narrower the beam angle so consequently the detection range is improved and so is the ability to pick up weak echoes. When the echo sounder is operating, the transducer emits sound pulses with a pulse duration of 0.3 or 1 millisecond (on the standard version of the EA300P portable ES). The operator may choose between these pulse lengths. The velocity of sound in water is approximately 1536 ms^{-1} which gives sound pulses an extent of 0.45 m or 1.5 m respectively. Single (210 kHz) and dual (30 kHz and 210 kHz) frequency echo sounders are used, with an vertical accuracy of 0.05 m.

3.5.2 Side Scan Sonar

Side scan sonar (SSS) derives an image of a river bed or sea floor from reflected acoustic energy. The SSS bears a marked similarity to radar in that it produces a continuous, coherent plan view of a broad scanned area. A set of transducers mounted in a compact fish (Figure 3.9) generate high powered short duration acoustic pulses.

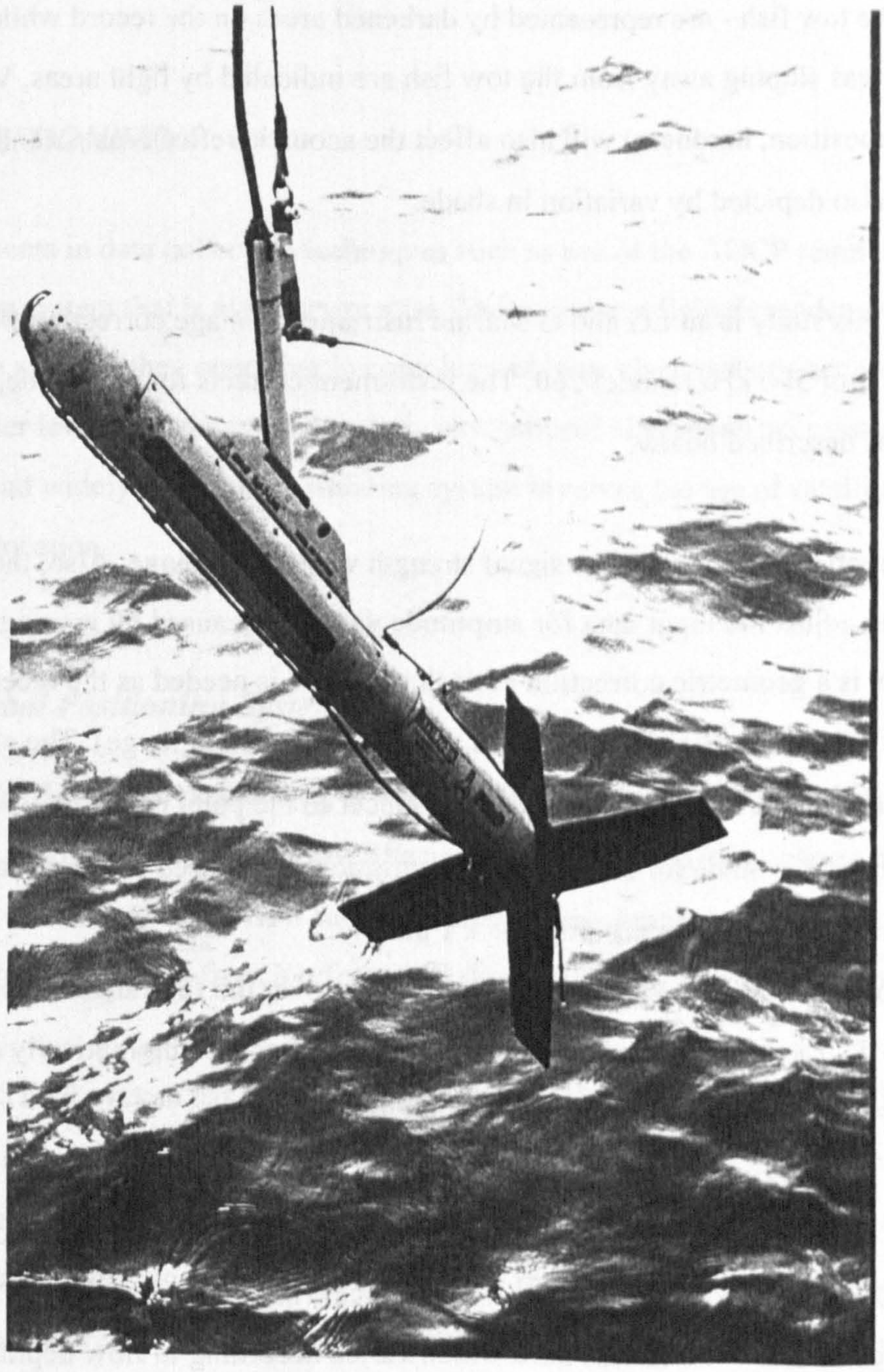

Figure 3.9, Side Scan Sonar fish.

The pulses are emitted in a thin, fan-shaped pattern that spread downward and outward to either side of the fish in a plane perpendicular to its path. As the fish follows the vessel's track, this beam scans a bottom segment ranging from the point directly beneath the fish outward as far as 600 m (if water depths are great enough) on each side. Acoustic energy reflected from the bottom and waterborne discontinuities is received by a set of transducers, amplified and transmitted digitally to the towing vessel. The signal is then amplified, processed and converted to hard copy by the side scan recorder. The resulting output is essentially a topographic map of the river bed in 3 dimensions. Good acoustic reflectors - rocks, metallic objects, bedforms sloping towards the tow fish - are represented by darkened areas on the record while depressions and areas sloping away from the tow fish are indicated by light areas. Variations in bed material (composition, hardness) will also affect the acoustic reflectiveness and consequently are also depicted by variation in shade.

The SSS used for this study is an EG and G Marine Instruments image correcting SSS, dual frequency (100 kHz or 500 kHz) model 260. The instrument corrects for amplitude, slant range and vessel speed as described below:

- Amplitude corrections are required as signal strength varies with range. Also, the tow fish height is used to adjust the input data for amplitude variations caused by grazing angle.
- Slant correction is a geometric correction of each pixel and is needed as the received signal is a measure of backscattering signal strength versus time (or slant range). The slant range is a function of the straight line range from the transducer to the point of interest. A new fish height determination is made for each sonar transmission and is used to locate each pixel at its true horizontal range with an accuracy of ± 1 pixel.
- Speed correction maintains a constant line print spacing over the full range of speed corrections (0 - 12.7 knots). Each pixel along the tow fish track is automatically displayed at its true position using the vessel speed which is inputted manually.

Graphic recording has 16 grey tones per pixel and 0.125 mm pixel size over a map display width of 20 cm (10 cm each side of the tow fish track). Scale markers are added at 25 m intervals and a range of 25 m - 50 m was used which varied according to flow depth. A vertical profile of the water column and river bed below the tow fish is plotted along with a planform map and positioning from the DGPS is also recorded on the output map.

Data quality is greatly affected by the concentration of suspended sediment in the water column. Since high suspended sediment concentrations reflect much of the energy back to the instrument, thereby decreasing the energy of the signal reflected from the bed and reducing data quality. At peak flow rates when suspended sediment concentrations are high, only large scale features (several metres or more) can be resolved. As turbulence from the survey vessel propellers may also interfere with the sonar reading, the SSS is deployed laterally from a winch mounted on the port side of the vessel. This may result in a 'shadow' on the sonar record where the hull of the boat reflects signals back, but produces better data resolution.

3.6 POSITIONING

Improvements in data collection techniques such as use of the ADCP require the use of a positioning system that is also very precise. There is also a field dependence on a reliable navigation system when operating in complex and large river systems such as the Jamuna, where water level changes can make daily navigational alterations necessary. The most accurate and widely available positioning system involves the use of satellite information to calculate location.

3.6.1 Global Positioning Systems

The NAVSTAR global positioning system (GPS) is a satellite based positioning system which came into service in the early 1990s. The use of differential GPS achieves higher accuracies by providing corrections to the GPS satellite ranging measurements. It is accomplished by broadcasting corrections from a reference station placed at a known location.

The NAVSTAR system has been developed by the USA Department of Defence (DoD) under Air Force Management through the GPS Joint Program Office to provide a worldwide radio navigation service with a precision which was previously only available over limited areas or limited time periods. It can give highly accurate position and velocity information in three dimensions, as well as precise time, to users around the globe 24 hours a day. Although its primary purpose is for military uses, it is a two tier system. The higher, and more accurate, tier is designed only for military objectives and so is not fully available to civilian users. Present policy is to provide an unrestricted Standard Positioning Service (SPS) at a 95% accuracy level to the international civilian user community. Its constellation consists of approximately

21 satellites in 6 orbital planes of 3 or more satellites each, plus a number of active spares. The orbital planes are orientated at about 55° from the equatorial and each satellite transmits at the same frequency, but employs a unique code. The frequency of operation is 1575.42 MHz for the SPS. In addition to this signal military sets will have access to the two frequency Precise Positioning Service (PPS) which employs very long encrypted sequences to ensure security of transmission. The satellites also transmit data at a 50 bps rate. The data message provides health status, identification, ephemeris (orbital) information, satellite clock correction and ionospheric coefficients. The ephemerides of the satellites are referenced to the DoD's World Geodetic System of 1984 (WGS 84).

A user receiver times the arrival of each satellite signal by synchronising an internal signal having that satellite's code with the satellite signal (code tracking). Information of the satellite's position is derived from the data transmission along with the time of arrival measurements from four or more satellites, and therefore enables the user to estimate the position and time. In addition to the code tracking measurements, it is also possible to phase-lock onto the carrier which allows a similar estimation of velocity. Advanced processing techniques use the carrier phase measurements to improve position estimates.

3.6.2 Differential GPS

Differential operation of GPS (DGPS) offers the possibility of accuracies of 2-10 m for dynamic navigation applications, and better than 2 m for stationary applications. The basic concept is to place a reference receiver at a known, surveyed point. By comparing the known location with that of the predicted by GPS, corrections can then be broadcast to the nearby users, who then use them to improve their position solutions.

The differential technique works if the preponderant errors are bias errors due to causes outside the receiver, which is the case for GPS. The main sources of error are the following:

1. Selective availability errors - artificial errors introduced at the satellites for security reasons. Psuedo-range errors of this type are about 30 m. PPS users have the key to these errors and can therefore eliminate them entirely.

2. Ionospheric delays - signal propagation group delay, which can be as much as 20-30 m during the day and 3-6 m at night. In the two-frequency mode of operation of the PPS, this effect is largely removed by applying the inverse square law dependence of delay on frequency.

3. Tropospheric delays - signal propagation delays caused by the lower atmosphere. While the delays are as much as 30 metres at low satellite elevation angles, they are quite consistent and modellable. Variations in the refractive index can cause differences (between reference station and user) in signal delays of 1-3 m for low-lying satellites.

4. Ephemeris error - differences between the actual satellite location and the location predicted by the satellite orbital data. Normally these are quite small, less than 3 m.

5. Satellite clock errors - differences between the satellite clock time and that predicted by the satellite data. The oscillator that times the satellite signal is free-running; the GPS ground control station monitors it and establishes corrections, which are sent up to the satellite to set the data message. The user reads the data and adjusts the signal timing accordingly.

Satellite clock errors are completely compensated by differential operation, as long as both reference and user receivers are employing the same satellite data. Ephemeris errors, unless they are quite large (30 m or more), are similarly compensated for by differential operation. Selective availability errors affecting the timing of the signals are also compensated by differential operation, except that the corrections loose their validity after a period of time. For users near the reference station, the respective signal paths to the satellites are sufficiently close so that compensation is almost complete. As the user-reference station separation is increased, the different ionospheric and tropospheric paths to the satellites may be sufficiently far apart that the atmospheric inhomogenities cause the delays to differ and the extent this difference constitutes an error in the differential measurement. This type of error will be greater at larger user-station separations. Separations of several hundred kilometres may cause a signal path divergences great enough that the respective group delays could differ by as much as a few metres.

3.6.3 GPS Testing

The FAP24 river survey project used a mobile reference station that may be installed in the individual survey areas as required. A Trimble 4000DL-II/IIR Differential locator then

continuously transmits the correction signals to the respective survey vessels. Known Bangladesh Transverse Mercator (BTM) co-ordinates of bench mark number GPS 764, approximately 1 km east of the left river bank at Bahadurabad, have been used to verify the system. The results, which were recorded in stationary mode are shown below:

GPS co-ordinates	Measured co-ordinates	discrepancy
BTM E 471086.158	BTM E 471084.4	E 1.8m
BTM N 778478.88	BTM N 778477.4	N 1.4m

Table 3.1, Variation in measured and GPS co-ordinates during GPS testing.

The deviation is within the 2m horizontal accuracy as claimed by the manufacturer for the DGPS operating in stationary mode. In dynamic mode the system is operating within a horizontal accuracy of 3m.

3.7 WATER LEVEL RECORDING

The RSP (FAP24) has installed automatic water level recording (AWLR) stations in the main rivers of Bangladesh to gauge river stage with the objectives of establishing stage-discharge relations, estimating local and regional hydraulic gradients and reducing bathymetric data to a reference level. These stations cover locations in the Ganges, Jamuna and Meghna rivers (see Table 3.2 and Figure 1.2) and also their tributaries and distributaries and conform to the discharge gauging and bathymetric sites. All of the water level data used in this study have been collected and processed by the RSP (FAP24).

River	Station	Sensor
Jamuna	Bahadurabad and Gabgachi	Pressure and Acoustic
Jamuna	Sirajganj and Bhuapur	Pressure
Upper Meghna	Bhairab Bazar R.B.	Acoustic

Table 3.2, Water level recording station locations.

Water level data are recorded every half an hour, both on- and off-line by both pressure cell and acoustic type water level recorders. A data logger is connected to the AWLRs which is equipped with either a removable memory or a communication interface for data retrieval.

Pressure sensor water level recorders require two pressure transducers to be installed. The lower transducer is fixed to a stable structure and placed below the lowest water level and the transducer measures the water pressure exerted by the water column plus atmospheric pressure. A second transducer measures atmospheric pressure only, so the real water pressure and therefore depth can be calculated. A correction may also be applied if the average water density in the column is not 1000 kg m^{-3}.

Ultrasonic depth gauges measure the time taken for a acoustic signal to reflect off the water surface and return to the sensor. The returning echo time is recorded along with transmission time so the distance to the surface can be calculated:

$$d = t\, C_{sd} / 2 \qquad \textit{equation 3.13}$$

where d is the water depth, t is the total travel time and C_{sd} is the velocity of sound in air.

The minimum range of the acoustic sensors is 0.6 m due to the change over time between transmitting and receiving signals. Signal range is inversely proportional to the magnitude of the reflection, so at longer sound paths resolution decreases. However, as no parts of acoustic sensors are submergent, they are less prone to structural damage by erosion and sedimentation and so exhibit fewer maintenance problems. Acoustic sensors are also not affected by changes in water density. At high sediment concentrations pressure readings may over estimate water levels. For example, at an immersion depth of 5 m and an average sediment concentration change of 2000 ppm, the indicated depth will be over-estimated by 0.1 m (RSP Special Report 2). Under extreme weather conditions, heavy rainfall may cause a decrease in accuracy of acoustic sensors due to reflections from raindrops.

The speed of sound in air, and to a lesser extent water, is temperature dependant and so both types of sensor require independent temperature measurements which are corrected for on-line. Temperature-induced error for acoustic sensors is 1.7 mm $°c^{-1}m^{-1}$, an over estimation of temperature leads to an under estimation of water level. Water temperature varies from approximately 26 °c to 30 °c annually and this is corrected for offline.

The two types of recorders have been extensively tested simultaneously and it has been concluded by the RSP (FAP24) that while acoustic sensors are less accurate, ~~and~~ pressure sensors are less reliable. An example of pressure sensor elevation for the Bahadurabad station is 12.35 m + PWD (Public Works Department geodetic datum) which is 0.32 m above standard low water (SLW, the datum water level used by FAP24) according to INTERCONSULT (1991), and 0.12 m above SLW according to NEDECO (1967). This sensor was installed as low as the actual water levels permitted

3.8 Survey Methodology

This section details survey procedures used by the RSP (FAP24) in terms of survey vessel deployment, bathymetric surveying and channel discharge measurement. RSP (FAP24) bathymetric and channel discharge survey data collected between November 1993 and November 1995 are used in this study to quantify the occurrence and morphology of dunes (Chapter 4) from three survey sites: Bahadurabad, Sirajganj and Bhairab Bazar (see Chapter 1, Figure 1.2). In addition to standard RSP surveys, special surveys were conducted which are dedicated solely to this study. These dedicated dune surveys, which were conducted at Bahadurbad, will also be briefly described in this chapter although more detailed discussion of the dedicated dune surveys follows in Chapter 5.

3.8.1 Survey Vessels

Five survey vessels are used by the RSP (FAP24) and these range in size and sophistication from the imaginatively named DHA (28 m long, draft of 1.5 m) to DHE (4 m long, draft of 1 m). A schematic diagram of DHA is shown in Figure 3.10 to display instrument deployment. Vessel DHC is a catamaran with a draft of 50 cm and so is extremely useful for surveying in very shallow waters e.g. distributary channels and across bar tops. Table 3.3 displays instrument deployment on board each boat. All special surveys dedicated to this present research were conducted using vessel DHA, while routine RSP (FAP24) survey data, which has also been used in this thesis for dune morphology measurement (Chapter 4), were collected using all of the survey boats. Although electro magnetic flow meters (EMF) were used by the RSP (FAP24), these data are not used in this study due to poor reliability.

	DHA	DHB	DHC	DHD	DHE
Flow					
DGPS	✓	✓	✓	p	p
ADCP	✓	✓	x	x	x
EMF	✓	✓	✓	p	x
Bathymetry					
Echo sounder:					
single frequency	x	✓	✓	p	p
dual frequency	✓	x	x	x	x
SSS	✓	x	x	x	x
Sediment					
bed load	✓	✓	✓	x	x
suspended load	✓	✓	✓	p	x

Table 3.3: *Survey equipment deployment on FAP24 vessels. p = portable.*

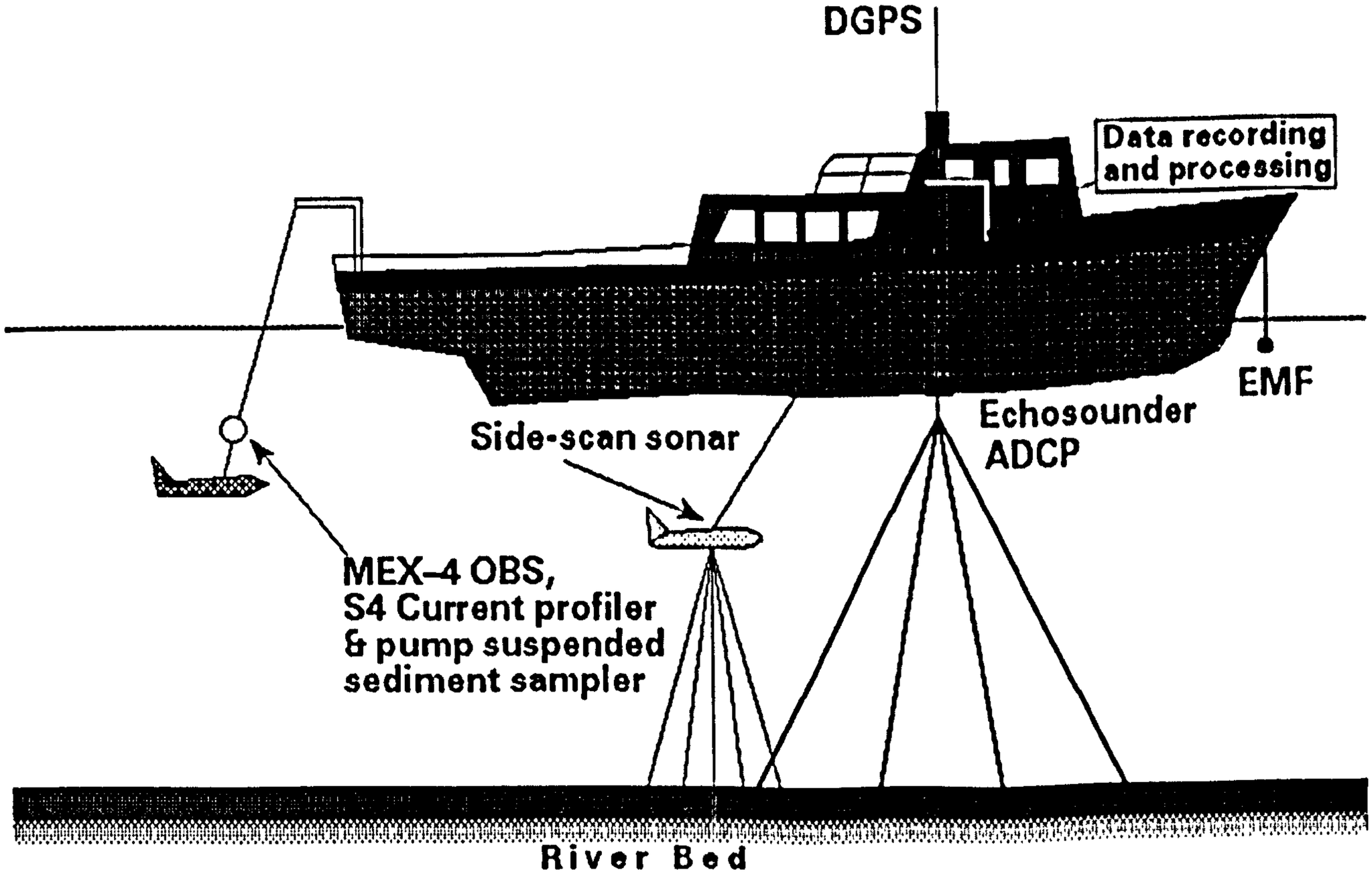

Figure 3.10, Schematic illustrating the survey vessel 'DHA' and instrumentation deployment.

3.8.2 RSP Surveying

A standard method (e.g. by the Bangladesh Waterways Development Board (BWDB)) for measuring channel discharge involves taking a series of velocity profiles across a channel using Electromagnetic flow meters (EMF). This velocity-area method is time consuming and may be inaccurate if flow conditions alter during the measurement period which is especially important in the Bangladeshi rivers due to the scale of the channels and rapid variations in flow stage. The RSP (FAP24) recommended survey method for measuring channel discharge is therefore the moving boat method (MBM) which uses data from both the ADCP and an EMF. Both instruments are required for the maximum water column coverage as the ADCP cannot measure the top 2.8 m of the water column, hence an EMF is mounted on the survey vessel hull at a distance of 0.5 m from the flow surface. Channel discharge is then calculated by the interpolation of numerous velocity profile measurements recorded in a cross section (Gordon, 1989) and hence discharge measurements for a channel are collected within a very short period. Results from the MBM are very consistent, with a standard deviation of discharge of 3.2%. When utilising the MBM to calculate discharge, the vessel does not have to move in a straight line which is of great importance in braided rivers where it is often impossible to conduct straight line transects due to the presence of mid channel bars and multiple channels. Standard RSP (FAP24) channel discharge surveying entailed conducting three downstream bathymetric profiles (of a minimum length of 1km) prior to conducting a cross-channel transect survey. These downstream bathymetric survey data have been used in this present study of dunes in order to quantify dune occurrence and morphology. Eight routine survey sites were selected by the RSP (FAP24) which were surveyed throughout the hydrograph, and data from three of these surveys sites have been selected for this dune study, namely Bahadurabed, Sirajganj and Bhairab Bazar (see Chapter 1, Figure 1.2). The RSP (FAP24) main survey sites were chosen to give good spatial coverage throughout the main Bangladeshi rivers concentrating on areas of key importance such as the Jamuna - Ganges confluence, and to correspond to pre-existing infrastructure such as railways, ferry terminals and roads. Historically, many of the survey sites, such as Bahadurabad and Hardinge Bridge, have been studied previously by the Bangladeshis due to the relative ease of access. FAP24 survey frequency is dependant on flow stage; under peak flow conditions bi-weekly surveys are undertaken and at low flow stages (December to March) survey frequency is decreased to monthly.

Additionally, long runlines from Bahadurabad to Aricha were surveyed during transit between routine surveys in order to permit assessment of bar and bedform occurrence within a large

area of the Jamuna, rather than at the specific survey sites noted above. The length of these surveys lines varies between 40 km and 65 km and surveys were conducted under low and high flow conditions. Due to the length of the survey lines, GPS could not be used in differential mode hence positioning errors are greater than for surveys located at one site. These longline surveys cover not only deep channel thalwegs but also cross bar tops and margins.

3.8.6 Special Surveys Dedicated to Dune Research

In addition to the routine FAP24 survey data which are used in this thesis to quantify dune occurrence and morphology, five special surveys over dunes occurring at Bahadurabad were conducted over the period August 1994 - March 1996 (Table 3.4).

Downstream bathymetric survey lines have been conducted for each study period at a spacing of 50 m across the channel, these survey lines are a minimum of 1000 m long, several cross-stream runlines were also surveyed for each study date. Each survey site was chosen due to the occurrence of large (> 1 m) dunes and the presence of large scale turbulence structures which are visible on the water surface as boils. Survey runlines were always conducted in an upstream direction to aid navigation and speed control and help avoid the problem of running aground, this is especially important when flow stage is decreasing as boats can become stranded. Runlines were directed as close to the main flow direction as possible, this was accomplished by carrying out several reconnaissance surveys to check both the main flow direction and the extent of the dune field at the beginning of each survey period. During each survey, repeat downstream survey lines were conducted in order to examine dune morphology, dune migration and mean flow structure as revealed by ADCP. When conducting these transect surveys, ADCP configuration was set to 6 s ensemble averaging and boat speed was kept to approximately 1 m s^{-1} which results in a horizontal echo sounder resolution of 1 m. Side scan sonar surveys were also executed as part of three of the surveys (Table 3.4) to detail dune planform morphology, to improve data resolution boat speed during these measurements was kept to approximately 0.5 ms^{-1}.

Special survey date	*Equipment deployed*	*water level, m*	*ADCP averaging time, s*
10-14 August 1994	standard surveying equipment: DGPS, ADCP, EMF, echosounder, MEX3, suspended sediment sampler and bed grab samples	17.86	5.5, 10.5
19-20 September 1994	standard surveying equipment	17.56	5.5
7-13 March 1995	standard surveying equipment and SSS	13.18	55
11-17 September 1995	standard surveying equipment and SSS	17.86	55
26 February - 4 March 1996	standard surveying equipment	13.31	5.5

Table 3.4, Special surveys conducted at Bahadurabad: equipment used, ADCP configuration and water levels.

At-a-point profiling surveys were also conducted during each survey period in order to collect velocity time series data, these profiles were carried out while the boat was on anchor at various locations over dunes. During the high flow season when dune migration rates are high, the length of studies carried out on anchor are limited to approximately one and one half hours due to problems caused by the anchor becoming buried in sediment. ADCP ensemble averaging times were varied during the profile surveys conducted, in order to investigate the effect of averaging times on data quality, these are shown in table 3.4. More details of these at-a-point velocity profiling surveys are given in Chapter 5, Section 5.1.

Examination of dunes exposed on bar tops during March 1995 and February 1996 also aided the study of dune morphology. During low flow conditions, additional land surveying was conducted on exposed bar tops to assess and quantify bar morphology. This entailed continuing bathymetric transects that had been partially surveyed by boat, using a portable DGPS to survey in the line position.

3.9 Morphological Data Processing

Dune bedforms have been defined from the bathymetric profiles according to the number of echo-sounder data pointson the dune lee and stoss side, where at least two points are required on a dune downstream-sloping lee face and three data points are required on the upstream-dipping stoss face in order to accurately define the dune shape. The number of data points along a dune bedform is a function of vessel speed in relation to the dune length, hence the minimum dune wavelength resolvable is 3m assuming a vessel velocity of $1ms^{-1}$. The minimum dune height resolvable during these surveys is 0.15 m (and the echo-sounder vertical resolution is 0.05 m).

The superimposition of smaller (secondary) bedforms on larger (primary) dunes is common in alluvial channels (e.g. Carey and Keller, 1957; Collinson, 1970; Jackson, 1976; Julien and Klaassen, 1995) and has previously been noted to occur in the Bangladeshi rivers (Coleman, 1969; Bristow, 1987). Superimposition of bedforms has been treated by dissimilar methods in previous studies, for example Julien (1992) did not include superimposed dunes when measuring dune geometry in large rivers whereas Gomez (1989) included both primary and secondary dunes when measuring dune morphology while investigating bedload transport. In this study of dune morphology, both primary and secondary dune morphological parameters are measured separately. A superimposed dune is defined as a bedform which has both a height and wavelength of less than half of the larger, primary bedform over which it is migrating and may be situated on either the stoss or lee side of the primary dune.

In order to aid investigation of variation in dune morphology with flow stage, the bathymetric survey data have been divided to encompass low, rising, high and falling flow stages. Division of the data requires use of the channel discharge measurements to obtain and depth-averaged channel mean velocity. Channel discharge is not used to divide data by flow stage due to the wide range in channel width (from approximately 500 to 6000 m) between survey sites. Rising and falling stage data are further divided according to whether the mean hydraulic conditions (water levels, velocity and total discharge) are increasing (rising stage) or decreasing (falling stage) and flow stage, as defined by mean velocity, is shown in Table 3.5.

Flow Stage	Depth-averaged mean velocity, ms^{-1}
Low	< 0.8
Rising and Falling	0.81 < velocity < 1.5
High	> 1.5

Table 3.5, Division of morphological survey data by flow stage using depth-averaged mean velocity.

3.10 Summary

This chapter has described survey procedures and instrumentation used for collection of positioning, bathymetric, flow and suspended sediment concentration data from the main rivers of Bangladesh. The use of an ADCP to monitor flow provides a unique dataset as instantaneous, three-dimensional velocity profiles are measured for the entire flow column beneath the survey vessel. Previous field and laboratory experiments detailing fluid flow over dunes have relied on at-a-point measurements and so simultaneous determination of three-dimensional velocity throughout an entire flow column may provide further information on the spatial variation in flow structure. Additionally, precision location measurement using DGPS in conjunction with the usage of multi-frequency echo-sounders enables reliable assessment of river bed configuration. The use of the RSP (FAP24) Bangladeshi river data, which has been regularly collected throughout two flood hydrographs, in conjunction with five surveys dedicated to dune research for this thesis, provides an unrivalled dataset with which to examine dune occurrence, morphology and dynamics in a large sand-bed river.

Chapter 4. Dune Morphology

4.1 Introduction

The complexity of bedform morphology in alluvial environments has been noted by many researchers for well over one hundred years (e.g. Sorby, 1859; Carey, 1957; Neill, 1965; Allen, 1968). All bedforms within any assemblage are to some extent three-dimensional and irregular in shape when described by their height, length and steepness and the description of the average geometries of the group as a whole and the deviations within that group are of great importance for the estimation of such factors as flow resistance, sediment transport and flow structure. Even under steady, equilibrium flow conditions bedform dimensions exhibit appreciable stochastic variability (Allen, 1976) as each individual dune experiences a unique set of flow and sediment transport conditions controlled by the corresponding upstream environment.

Most data detailing the morphology of unidirectional bedforms under different hydraulic regimes have been obtained from laboratory flume studies (e.g. Guy et al., 1966; Allen, 1976; Wibenga and Klaassen, 1981; Southard and Boguchwal, 1990) due to the relative ease of measurement of key parameters in flumes such as depth, water surface slope, discharge, velocity and sediment concentration. Field data from within any section of the physical sciences is invaluable for the verification of theoretical models and for substantiating datasets collected in the laboratory as, by its very nature, it will suffer from complications and intricacies which may not be inherent under experimental conditions. Additional complications of data collection by monitoring natural channels compared to flume analysis have been much discussed in the literature and some points from Simons et al. (1965) further modified by Allen (1968) are illustrated below:

- Large range of depth and discharges
- Slope over measurement reaches is relatively constant
- Velocity variations are temporally highly variable
- Variation in shear stress and streampower is principally a result of depth variation as opposed to slope variation as in flume studies
- Bank erosion rates are high and channel width is variable
- Non-uniformity in velocity and depth result in complicated bed configuration within any study reach
- Temporal and spatial sorting of sediment is variable

There is therefore a paucity of reliable, comprehensive data monitoring alluvial bedform configuration at different flow stages. This chapter aims to presents the most capacious characterisation of dune morphology ever conducted in a large natural fluvial system and seeks to describe the variations in bedform morphology with respect to flow stage. Factors controlling dune geometry such as water depth, bedform temporal history and response to changing flow conditions will also be investigated. These data will also be used to verify and test previously constructed models that predict bedform morphology and their resistance to flow under varying hydraulic conditions.

Not only is the data set one of the most extensive ever collected, it is also one of the most precise; the use of modern navigation techniques (DGPS, see Chapter 3) has allowed for measurement of bedform phase within an accuracy of centimetres which has only infrequently been available before. Previous datasets detailing bedforms in the Jamuna River (e.g. Coleman, 1969; van Rijn, 1993; Julien and Klaassen, 1995) have relied on location measurements which are unsuitable when used in such an environment. The size of channels yields many techniques untenable, such as using bankline markers for location. Other factors causing limitations in early data quality have previously been noted, for example, Neill (1965) reported the problem of beam spreading when measuring flow depth which led to errors in measuring bed morphological parameters where the river bed is not consistently level.

4.2 Bed Coverage

This section aims to quantify the fraction of the river bed occupied by dunes (termed fullbeddedness by Ashley (1990)) during different flow stages and at different locations. Bed coverage by dunes at three survey locations (Bahadurabad, Sirajganj and Bhairab Bazar; see Chapter 1, Figure 1.2 for locations) between the period of November 1993 to November 1995 is shown in Figure 4.1. Each data point in Figure 4.1 gives the percentage of bed covered by dunes over two downstream survey lines covering a minimum distance of 1 km each from main channel thalwegs. Bathymetric surveys were conducted by the RSP at regular intervals during the survey period (see Chapter 3), survey frequency is governed by the flow stage and survey location hence the greater number of data points measured detailing surveys at Bahadurabad which was the primary survey location (Figure 4.1). In addition to the regular standard surveys, bathymetric surveying was also carried out during specific surveys which were dedicated to this project (see Chapter 3 for dedicated survey dates), hence 'clusters' of data points (e.g.

March 1995) refer to periods where standard and specific surveys were conducted in close conjunction. Bed coverage by dunes at Bahadurabad varies from a maximum of 100% to a minimum of 76 % (Figure 4.1); the variation in dune occurrence does not follow changes in flow stage as maximum flow discharge, which occurs from July to September, does not coincide with maximum dune occurrence. Similarly at Sirajganj and Bhairab Bazar, where dune occurrence ranges between 41 % and 100 %, changes in bed coverage by dunes do not relate to change in flow stage. As multiple surveys were occasionally conducted during a short time frame (e.g. March 1995, over five days), the variation in dune occurrence within a particular channel reach is assessed with a variation in bed coverage of 15%. The variation in bed coverage within a short time period illustrates the spatial variability in bed configuration over any given channel reach. These data illustrate that dunes are the predominant bedform at all flow stages in the Jamuna river.

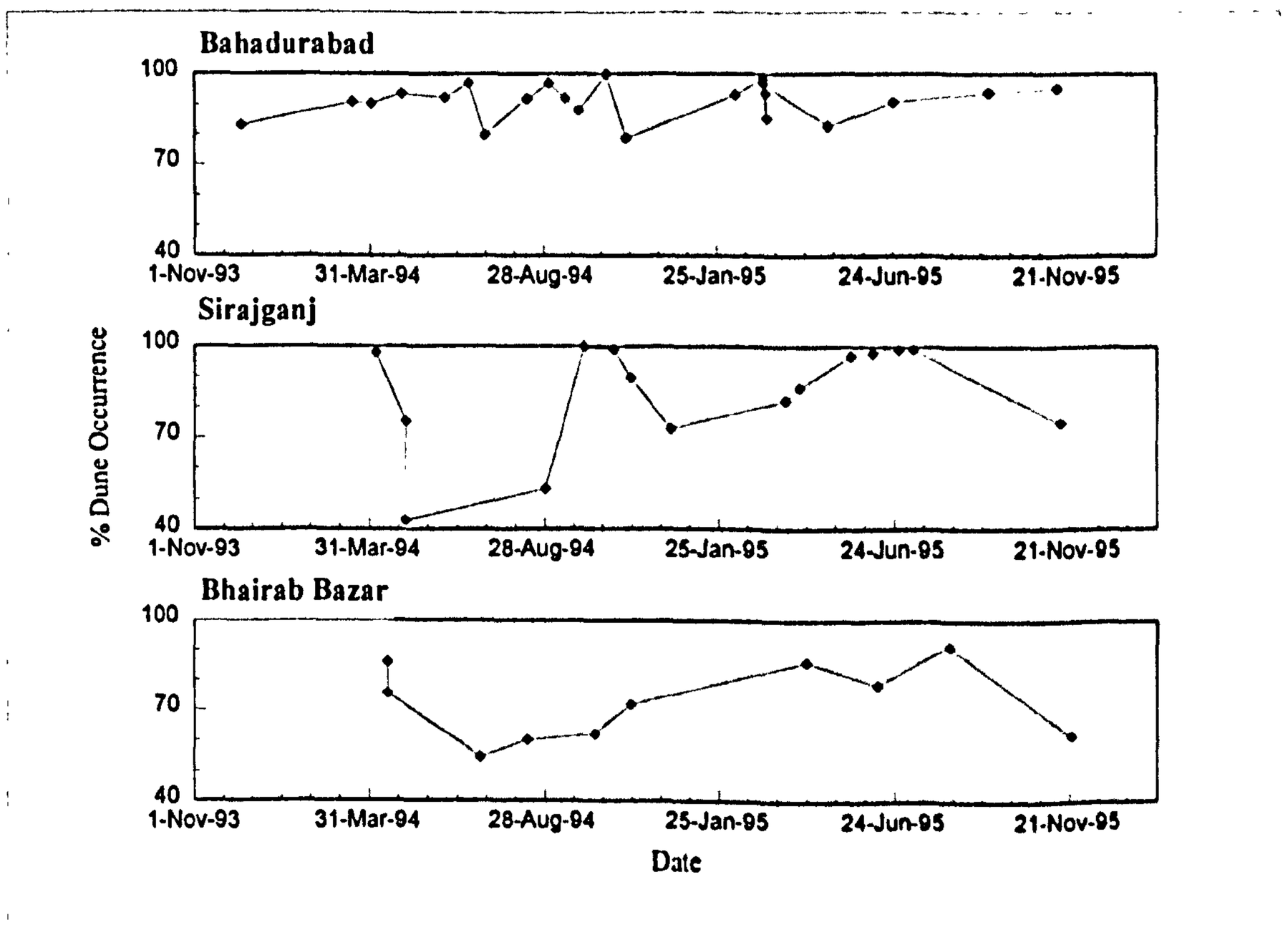

Figure 4.1, The percentage occurrence of dunes in the main channels at Bahadurabad, Sirajganj and Bhairab Bazar for the study period between November 1993 to December 1995. For survey site locations see Chapter 1, Figure 1.1.

Additionally, the percentage of bed coverage by dunes has been measured over much longer survey lines (Figure 4.2). Figure 4.2a illustrates a 65 km transect between Sirajganj and Aricha,

these 'longline' surveys being carried out by the RSP during journeys between their regular survey sites and so encompassing both channel thalweg and bar margins thereby providing a more comprehensive representation of dune coverage throughout the channel. Detailed cross-sectional channel morphology (e.g. the relative direction of the survey vessel to barform or bank and the direction of travel across dunes) is unknown so these data are solely used for relative bed coverage of dunes and plane bed, and not for more detailed measurement of dune geometry.

The percentage of bed coverage by dunes over a distance of 65 km shows that dune occurrence varies between 38% and 98% (Figure 4.2b), so agreeing well with the bed coverage rates from specific survey sites (41% to 100%). These data therefore substantiate the findings from specific survey sites (Figure 4.1) that dunes are the prevalent bed configuration in the Jamuna River, with large dunes (over 1 m in height) covering between 10% and 58% of the river bed. Smaller dune bedforms (less than 1 m in height) are more widespread, with bed coverage varying between 12% and 68% (Figure 4.2b).

It may be expected that ripples are superimposed on many of the dunes but these are below the horizontal resolution of the data due to the boat speed (and therefore the horizontal distance between echo-sounder data points) and echo sounder vertical resolution (0.05 m). Dunes are also commonly superimposed onto bars (Figure 4.2a,i), confirming that they are ubiquitous and not only found in deep channel thalwegs (Figure 4.1, Figure 4.2a, ii). There are common patterns of dune superimposition on bars which occur regularly within the channel reaches investigated: dune fields frequently migrate onto the upstream bar face and over the lower angle areas of the bar tops (Figure 4.ab, i). This wrapping of dune fields around the upstream face of a bar and over the bar top has also been observed during detailed bar surveys (Ashworth *et al.*, in review). Bedforms are only present on downstream bar faces when the angle of the slip face is low, hence no dunes are superimposed on steep bar faces (Figure 4.2a, iii) and this pattern is in accord with dune superimposition on dunes where secondary dunes are more commonly situated on the lower angle stoss faces of primary dunes (Dalrymple and Rhodes, 1995). Flat beds on bar tops are therefore unusual, where they do occur, they are probably associated with low flow rates and again these areas may be rippled.

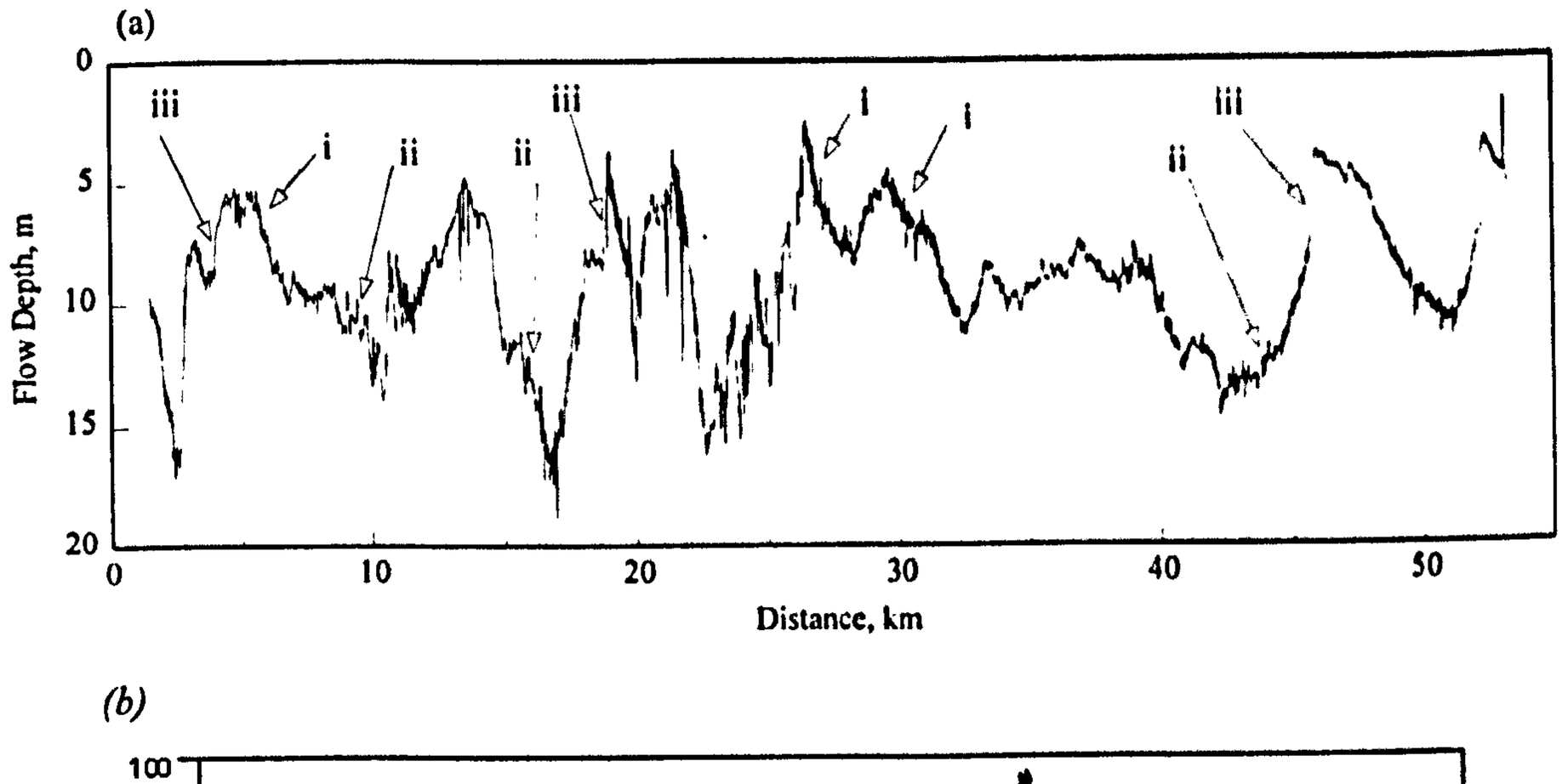

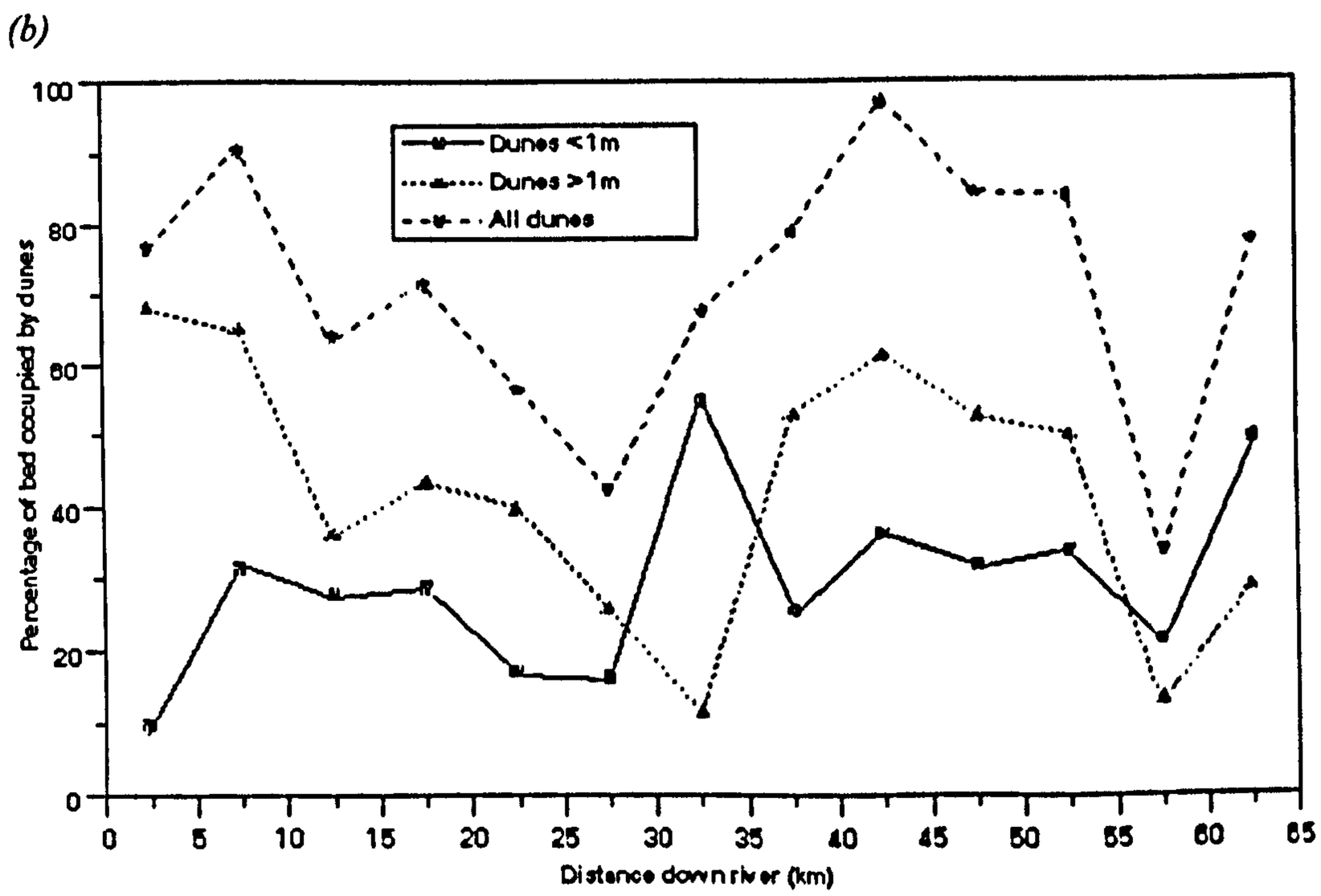

Figure 4.2, a, An example of downstream bathymetry from a longline survey between Sirajganj and Aricha used to quantify bed coverage of dunes. The survey reach is 55 km in length. i, superimposition of dunes on the upstream side of bars; ii, dunes are common in deep channel thalwegs; iii, dunes are not present on bar slip faces due to steep face angles. b, The percentage occurrence of dunes along the downstream transect.

These data detailing the bed coverage of dunes are consequential as they illustrate that dunes are important at all flow stages even though the effect of dunes on channel morphology and sediment transport will be maximised at high flow stage due to the increase in discharge and sediment transport. At low stage, dune occurrence rates are also high, depicting the ubiquity of bedforms in large sand bed rivers and the importance of dunes in terms of bed roughness, flow resistance, sediment transport and channel geometry.

The high dune occurrence rates from a minimum of 38 % to a maximum of 100 % at all flow stages in the Jamuna river illustrate that there is a requirement to precisely detail dune morphology, and any seasonal variations in morphology, to aid accurate prediction of sediment transport, flow resistance and channel geometry.

4.3 Dune Height and Wavelength

The variation of dune height as a function of flow depth is shown in Figure 4.3, the Jamuna bathymetric survey data have been split by flow stage using the mean depth averaged section velocity over each survey reach (see Chapter 3), the dune height prediction curves of Yalin, (1964), Allen (1968) and Julien and Klaassen (1995) are also shown. Dune height is shown to vary from 0.15 to 6 m, therefore varying from small to very large using the classification scheme of Ashley (1990), and flow depth ranges between 2 m and 20 m. Although there is wide scatter in the dune height to flow depth relationship, dunes at lower flow stages are generally smaller. One of the most significant implications of Figure 4.3 is the limitation on dune height produced by flow depth (or boundary layer thickness); although the spread in this relationship is great, the maximum dune height is never more than 0.37 times the flow depth. This relationship between flow depth and dune height agrees well much previous work (e.g. Yalin, 1964; Nordin and Algert, 1965; Allen, 1968). If the flow depth limit is taken as the principal factor affecting dune height (e.g., Rubin and McCulloch, 1979; Aliotta and Perillo, 1987) then dunes at all flow stages should approach a height of 0.37 times the flow depth; this is clearly not the case for bedforms at all flow stages in the Jamuna River. Lack of equilibrium between flow and bed configuration has previously been postulated to explain deviations in this relationship (e.g. Allen, 1964), but as the population deviations at low flow stage are only slightly smaller than at high flow stage (although sediment discharge will be smaller at low flow stage) this hypothesis may be limited as flow conditions are more stable during low stage. Disequilibrium between flow depth and dune height is no greater during the rising and falling flow stages.

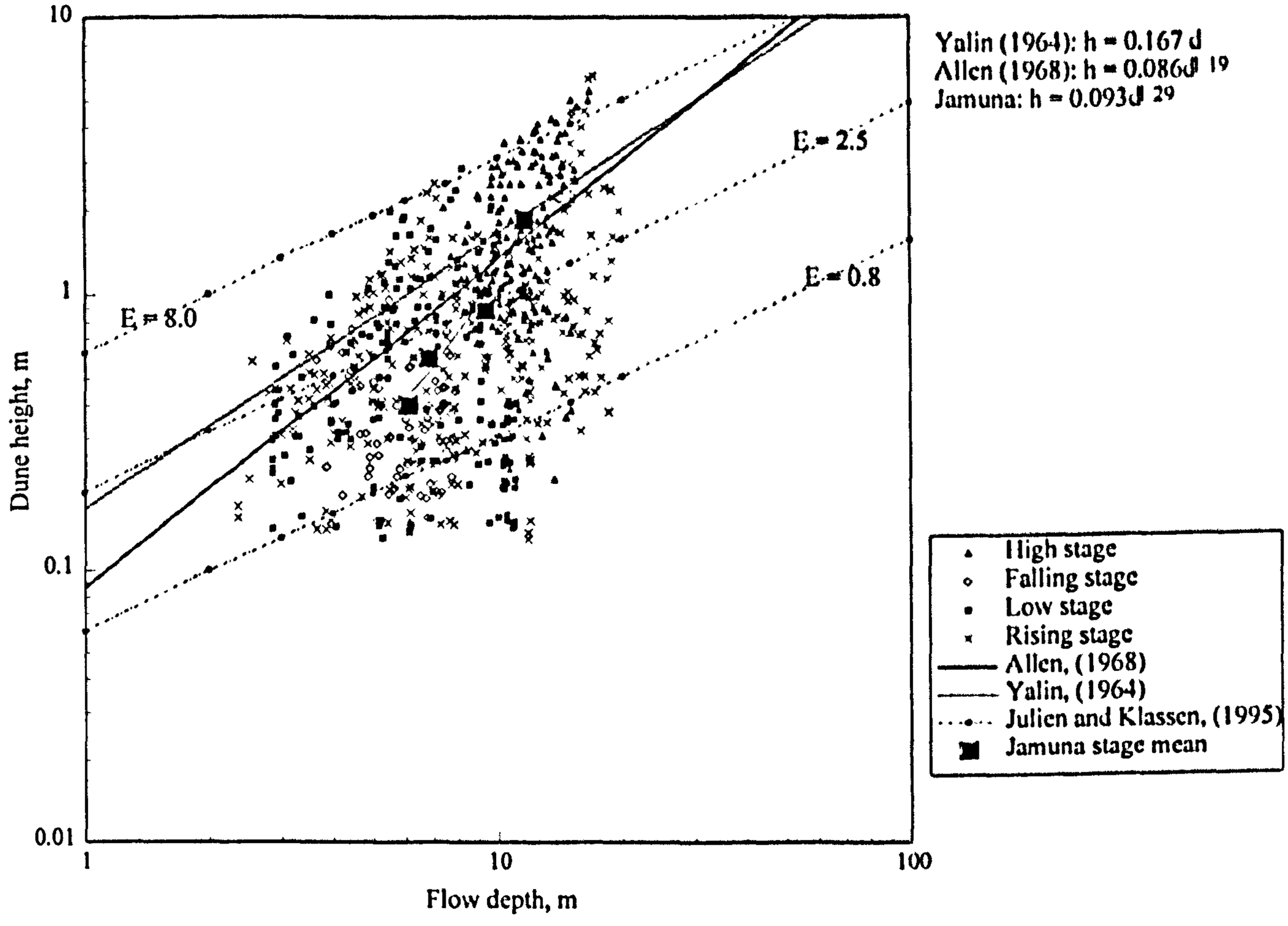

Figure 4.3, Dune height to flow depth relationships divided by flow stage. Prediction curves of Yalin (1964), Allen (1968) and Julien and Klaassen (1995) are also given.

Visual inspection of Figure 4.2a also displays this association between flow depth and dune height, larger dunes being most frequently found on the upstream face of bars (Figure 4.2a, i) and in deep channel thalwegs (Figure 4.2a, ii). This relationship between dune height and flow depth will of course be influenced and dispersed by the non-uniformity of channel configurations and flow conditions found in river systems. Even under steady, equilibrium conditions a characteristic variation in dune size is expected (Allen, 1976) due to the presence of both young and mature dunes, their inherent three dimensionality causing variation along a single crestline and the variation in flow conditions experienced by individual dunes (Dalrymple and Rhodes, 1995). Dune growth occurs by a combination of migration, superimposition and consolidation (Gabel, 1993), these readjustments of dune morphology being a consequence of response to changes in flow conditions. Both superimposition and lag effects may also cause dune geometries to deviate from equilibrium relationships. Other factors such as bedform maturity (i.e. the development time, Coleman and Melville, 1994), shear stress and suspended sediment concentration may also have a great affect on dune height, while flow depth limits the maximum height that can arise.

Many empirical relationships have previously been postulated to describe the relationship between dune height and flow depth, such as:

$$\text{Yalin, (1964)} : h = 0.167\, d \qquad \textit{equation 4.1}$$

$$\text{Allen, (1970)} : h = 0.086\, d^{1.19} \qquad \textit{equation 4.2}$$

$$\text{Julien and Klaassen, (1995)} : h = Ed\,(D_{50}/d)^{0.3} \qquad \textit{equation 4.3}$$

where h is the dune height and d is the flow depth, D_{50} is the median bed particle diameter (50% finer by weight) and E is van Rijn's dune height coefficient which varies between 0.8 and 8.0. These relationships are illustrated on Figure 4.3 and show that the dependency of dune height on flow depth (Yalin, 1964; Allen, 1970) refers to the limits or upper bounds of dune size and equilibrium dunes that are formed under steady flow conditions. The equations therefore cannot be used to predict alluvial dune height for entire populations at a given flow stage unless more details are given as to the expected deviations from the proposed relationship. A best fit line through the entire population for the Jamuna dataset yields the relationship:

$$h = 0.093\, d^{1.29} \qquad \textit{equation 4.4}$$

The deviation in dune height as a function of flow depth is 0.97, as given by

$$\text{deviation} = \{1/n \sum (h-h(d))^2\}^{1/2} / \{1/n \sum h\}^{-1} \qquad \textit{equation 4.5}$$

These data also illustrate that an increase in both flow depth and dune height occurs with increasing flow stage, with survey mean values of dune height increasing from 0.4 m at low flow stage to 1.86 m at high flow stage. This variation in dune morphology with flow stage is shown in more detail in Figure 4.4 where depth averaged velocity (Figure 4.4a) and dune minimum, maximum and mean height (Figure 4.4b, Table 4.1) are shown for each survey period from November 1993 to November 1995, hence covering two hydrographs. For both flood seasons, dune height increases considerably (by a factor of 5.8 during 1994 and 7.8 during 1995), for example during the 1994 hydrograph mean values vary between 0.43 m (January 1994) and 2.5 m (July 1994) and during the 1995 hydrograph the increase in dune mean height is from 0.39 m (February 1995) to 3.04 m (August 1995). On the temporal scale of the survey occurrence, dune height responds rapidly to changes in flow stage, and dune height is observed to increase with corresponding increases in depth averaged mean velocity. During the falling and rising limb of the hydrograph dune height, and all other morphological parameters, also alter rapidly.

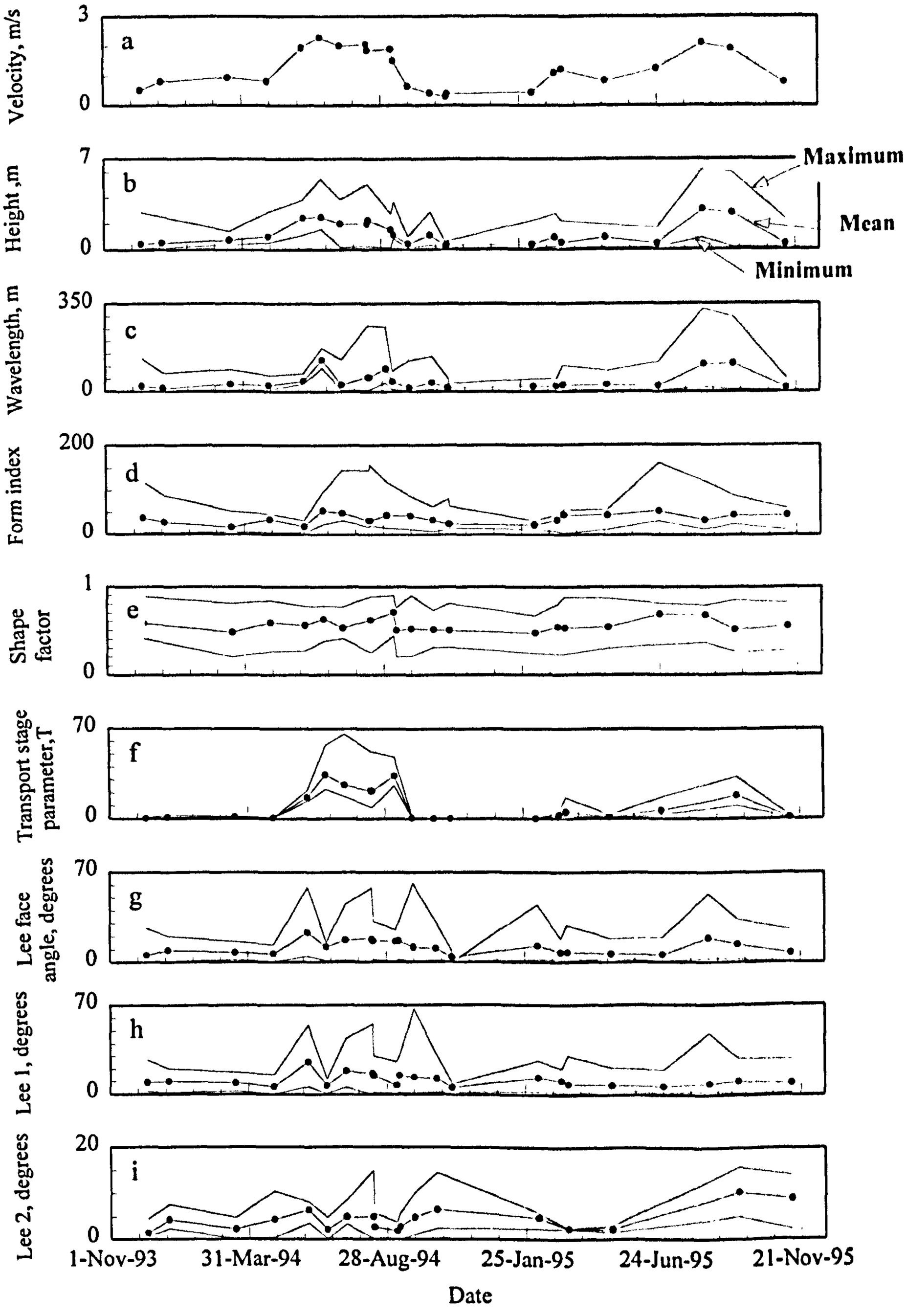

Figure 4.4, Temporal variation in the mean, maximum and minimum values of (a) depth averaged mean velocity, (b) dune height, (c) dune wavelength, (d) dune form index, (e) dune shape factor, (f) van Rijn's transport stage parameter, T, (g) lee face angle, (h) lee face angle 1 and (i) lee face angle 2, through the 1994 and 1995 flood hydrographs.

Date	*Velocity, ms⁻¹*	*Height, m*				*Wavelength, m*				*Lee face angle, °*				*Transport stage parameter, T*				*Shape Factor, β*			
		mean	*min*	*max*	*sd*	*mean*	*min*	*max*	*sd*	*mean*	*min*	*max*	*sd*	*mean*	*min*	*max*	*sd*	*mean*	*min*	*max*	*sd*
11.11.93	0.5	0.4	0.1	2.9	0.6	22.1	3.2	131.2	29.5	9.3	1.9	27.2	10.3	0.3	0.1	0.9	0.2	0.6	0.9	0.4	0.1
30.01.94	0.8	0.5	0.2	2.5	0.6	13.5	3.0	73	16	10.1	1.1	20.2	11.3	1.2	0.6	2.6	0.4	0.5	0.8	0.3	0.1
17.03.94	1.0	0.7	0.4	1.4	0.3	28.9	7.7	87.9	22.2	8.9	2.4	17.5	9.5	1.5	1.1	2.0	0.3	0.5	0.8	0.2	0.1
28.04.94	0.8	1.0	0.6	2.9	0.7	24.5	8.6	65.4	13.7	6.0	0.1	15.5	5.6	0.7	0.5	1.0	0.2	0.6	0.8	0.3	0.1
04.06.94	1.9	2.5	1.1	3.8	0.7	42.9	30.7	73.4	9.6	25.7	5.9	54.4	28.9	16.4	13.4	21.8	2.3	0.6	0.8	0.3	0.2
24.06.94	2.3	2.5	1.6	5.4	1.4	126.6	93.8	173	30.6	6.7	0.81	11.9	7.9	34.2	22.8	56.8	10.3	0.6	0.8	0.4	0.1
15.07.94	2.0	2.0	0.2	3.8	0.8	27.8	7.7	127.7	26.4	18.6	5.27	44.2	12.6	26	17.3	58.2	12.4	0.5	0.8	0.4	0.1
13.08.94	2.1	2.0	0.3	5.0	1.2	57.2	7.91	264.4	47.7	16.5	0.11	55.2	18.2	21.6	8.8	52	7.7	0.6	0.8	0.5	0.1
08.09.94	1.5	1.5	0.1	2.7	0.6	40.6	12.3	82.1	20.6	7.1	0.2	25.8	13.2	33.2	25.6	47.6	7.8	0.7	0.9	0.4	0.1
11.09.94	1.9	1.1	0.8	3.6	0.9	92.3	35.2	259.2	64.8	14.9	1.5	30.1	15.2	25.4	20.7	43.2	6.9	0.5	0.7	0.2	0.2
27.9.94	0.7	0.4	0.2	0.9	0.2	16.7	3.7	124.1	16.7	13.7	0.9	67.5	13.5	0.5	0.27	1.3	0.2	0.5	0.9	0.2	0.1
21.10.94	0.4	1.1	0.4	2.8	0.6	36.2	11.7	141.8	29.1	12.7	1.9	31.2	14.6	0.1	0.1	0.2	0.1	0.5	0.7	0.3	0.1
08.11.94	0.4	0.4	0.1	0.7	0.1	15.3	6.5	33.7	6.5	11.7	2.1	27.6	13.7	0.1	0.1	0.2	0.1	0.5	0.7	0.3	0.1
08.02.95	0.5	0.4	0.2	2.2	0.5	21.6	5.3	52.2	9.5	13.7	2.7	26.8	16.2	0.2	0.1	0.2	0.1	0.5	0.6	0.2	0.1
05.03.95	1.1	0.9	0.3	2.7	0.5	22.9	6.3	54.8	10.1	11.2	1.7	20.4	10.8	2.8	1.6	4.5	0.8	0.5	0.8	0.2	0.1
12.03.95	1.2	0.5	0.1	2.2	0.5	27.3	7.2	106.3	25	8.3	1.2	30.8	9.6	5.3	2.5	16.6	3.2	0.5	0.9	0.2	0.2
29.04.95	0.8	0.9	0.2	1.9	0.4	26.8	4.7	85.4	25.1	7.4	3.3	21.2	6.2	1.2	0.6	2.6	0.4	0.5	0.8	0.3	0.1
24.6.95	1.2	0.4	0.1	1.7	0.3	23.7	4.5	119.9	23.2	6.7	1.86	19.7	6.9	6.3	3.1	16.9	1.8	0.7	0.8	0.3	0.1
13.8.95	2.0	3.1	0.9	6.1	1.3	109.6	19.0	331.0	98.1	9.0	2.9	48.4	8.5	10.2	5.6	22.8	2.3	0.7	0.8	0.4	0.2
14.9.95	1.9	2.8	0.2	6.0	2.1	114.1	10.5	300.0	106.1	10.9	1.3	28.7	10.3	18.2	10.2	32.8	5.1	0.5	0.8	0.2	0.1
11.11.95	0.7	0.4	0.1	2.3	0.4	16.9	4.6	54.4	11.8	9.4	1.8	27.8	9.6	0.9	0.5	2.1	0.1	0.5	0.8	0.3	0.1

Table 4.1, Dune survey mean morphological parameters from November 1993 to November 1995.

Evidence of flattening at high flow stage is not obvious from the plots of dune height and flow depth (Figure 4.3) or dune height with flow stage (Figure 4.3). Julien and Klaassen (1995) defined the parameter E to define the relationship between dune height and flow stage (equation 4.4), with a mean value of E of approximately 2.5 (Figure 4.3). When applied to the Jamuna data, Julien and Klaassen's (1995) estimation of the factor 'E' under represents dune height for the largest dunes occurring at high and rising flow stages (Figure 4.3), since dune height continues to grow as flow depth increases. Even with the wide range in values of E proposed by Julien and Klaassen (1995), namely $0.8 < E < 8.0$, the 95% data point inclusion within that range as proposed by Julien and Klaassen (1995), is not confirmed by the Jamuna data where only 82% of the data fall into the suggested region. Since the high stage data in Figures 4.3 and 4.4 were collected near the peak of the hydrograph when the river was approaching overbank flow (see Chapter 3 for discharge hydrograph) and there is a consistent increase in dune height with flow depth, it may be concluded that upper stage plane bed (USPB) conditions are only infrequently reached in the Jamuna. Kennedy (1961), Znamenskaya (1964), Engelund and Hansen (1966) and Allen (1968) all invoke a variation in Froude number (Chapter 2) as a mechanism for the occurrence and stability of dunes, hence dunes forming under the low Froude number conditions found in such deep channels, like those that occur in the Jamuna River, will not reach the upper limits or transition area of the dune stability field and will correspondingly not flatten. Variation in Froude number will be discussed later in Section 4.6.

Empirical relationships have also been invoked to describe the variation in wavelength with flow depth. For example,

$$\text{Allen, (1970): } \lambda = 1.16\, d^{1.55} \qquad \textit{equation 4.6}$$

$$\text{Yalin, (1964, 1992): } \lambda = 6d \qquad \textit{equation 4.7}$$

$$\text{Julien and Klaassen, (1995): } \lambda = Nh\,(d/d_{50})^{0.3} \qquad \textit{equation 4.8}$$

where λ is dune wavelength, d is flow depth, D_{50} is the median bed particle diameter (50 % finer by weight) and N is a dune steepness parameter. The scatter in the relationship between dune wavelength and flow depth is large although generally dunes during high and rising flow stages have greater wavelengths and occur in deeper flow depths and minimum dune wavelengths occur during low flow stage (Figure 4.5). Dune wavelengths in the Jamuna river vary between 3 m and 300 m in water depths ranging from 2.5 m to 12 m. Although the wavelength to flow depth relationship shows great dispersion, stage mean values are also shown in Figure 4.5 and these correspond very well with the prediction curve of Allen (1970)

which was calculated from both experimental and field data (equation 4.5). This highlights the requirement that group mean values of dune morphological parameters should be examined rather than collating individual data points which correspond to dunes forming under differing hydraulic regimes and, as for the height to flow depth prediction estimates for a population, deviations must also be specified. A best fit line though the stage mean values yields the relationship:

$$\text{Jamuna data: } \lambda = 1.21\, d^{1.63} \qquad \textit{equation 4.8}$$

The deviation in dune height as a function of flow depth is 1.2, as given by

$$\{1/n \sum (\lambda - \lambda(d))^2\}^{1/2} \{1/n \sum \lambda\}^{1} \qquad \text{equation 4.9}$$

The prediction curves of Julien and Klaassen (1995) (equation 4.7) in the range of $0.8 < N < 8$ encompass most of the Jamuna wavelength to flow depth data, but cover a smaller range of the data (85%) than suggested by Julien and Klaassen (1995) where 95% of the data points were within the stated range. Dune wavelength is most frequently underestimated during high and rising flow stages.

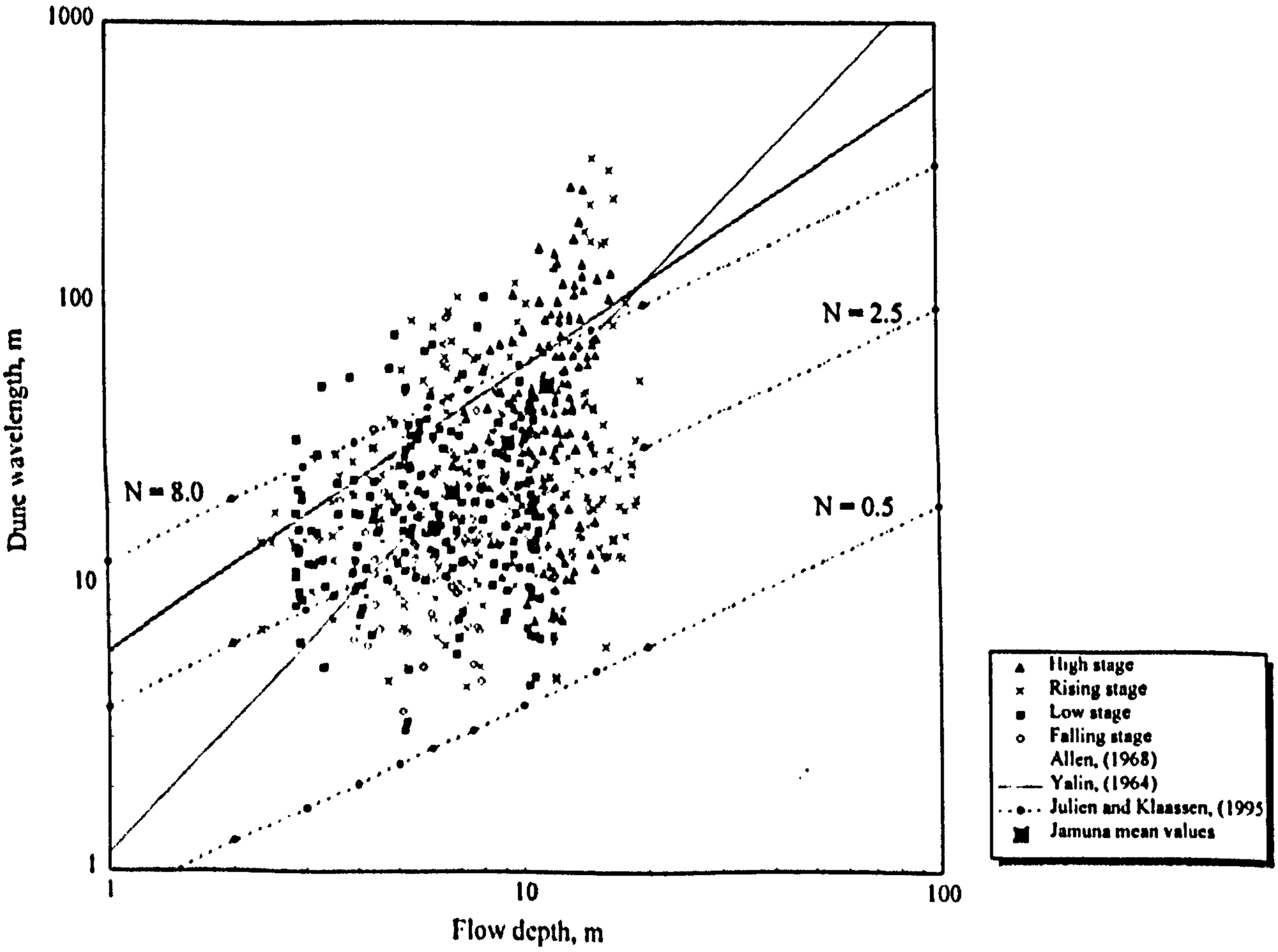

Figure 4.5, Dune wavelength to flow depth relationships split by flow stage. Prediction curves of Yalin (1964), Allen (1968) and Julien and Klaassen (1995) are also given.

Variation of group minimum, maximum and mean value of wavelength is given in Figure 4.4c and Table 4.1 for each survey period from November 1993 to November 1995. For both flood seasons, dune wavelength is seen to increase considerably (by a factor of 9.5 during 1994 and 7.5 during 1995), for example during the 1994 hydrograph mean values vary between 13.5 m (January 1994) and 128 m (July 1994) and during the 1995 hydrograph the increase in dune mean wavelength is from 15.3 m (January 1995) to 114.1 m (August 1995). On the temporal scale of the survey occurrence, dune height wavelength (like dune height) responds rapidly to changes in flow stage as dune wavelength increases and decreases with respective changes in depth averaged mean velocity (Figure 4.4a, Table 4.1). Periods of occurrence of maximum dune wavelength correspond to periods of peak discharge so if a lag between changes in flow conditions and dune wavelength occurs in the Jamuna river then it is not observable in this study due to the survey frequency.

4. 4 Dune Shape

An index of dune form is of fundamental importance when calculating bedload sediment transport rates using bedform morphology and when estimating flow resistance. Dune form index (FI), which has previously been termed ripple index and steepness index (Terwindt and Brouwer, 1986), is a measure of the ratio of dune wavelength to height. Figure 4.6 illustrates the variation in the relationship between height and wavelength measured at different flow stages in the Jamuna, and shows that these FI values corroborate well with previously measured estimates which range from 10 to 300 (e.g. Robinson, 1961; Jordan, 1962; Allen, 1963; Stride, 1963; Caston, 1965; Jones, 1965; Guy et al., 1966). Form index variations with flow stage are displayed in Figure 4.4d and show that form index increases with rising flow stage (Figure 4.4a). Between low and high flow stage during 1994 dune form index increases from 17.1 to 53.8 and during the 1995 hydrograph there is an increase from 22.8 to 54.1, hence showing that wavelength is increasing relatively faster than height (Figure 4.4d).

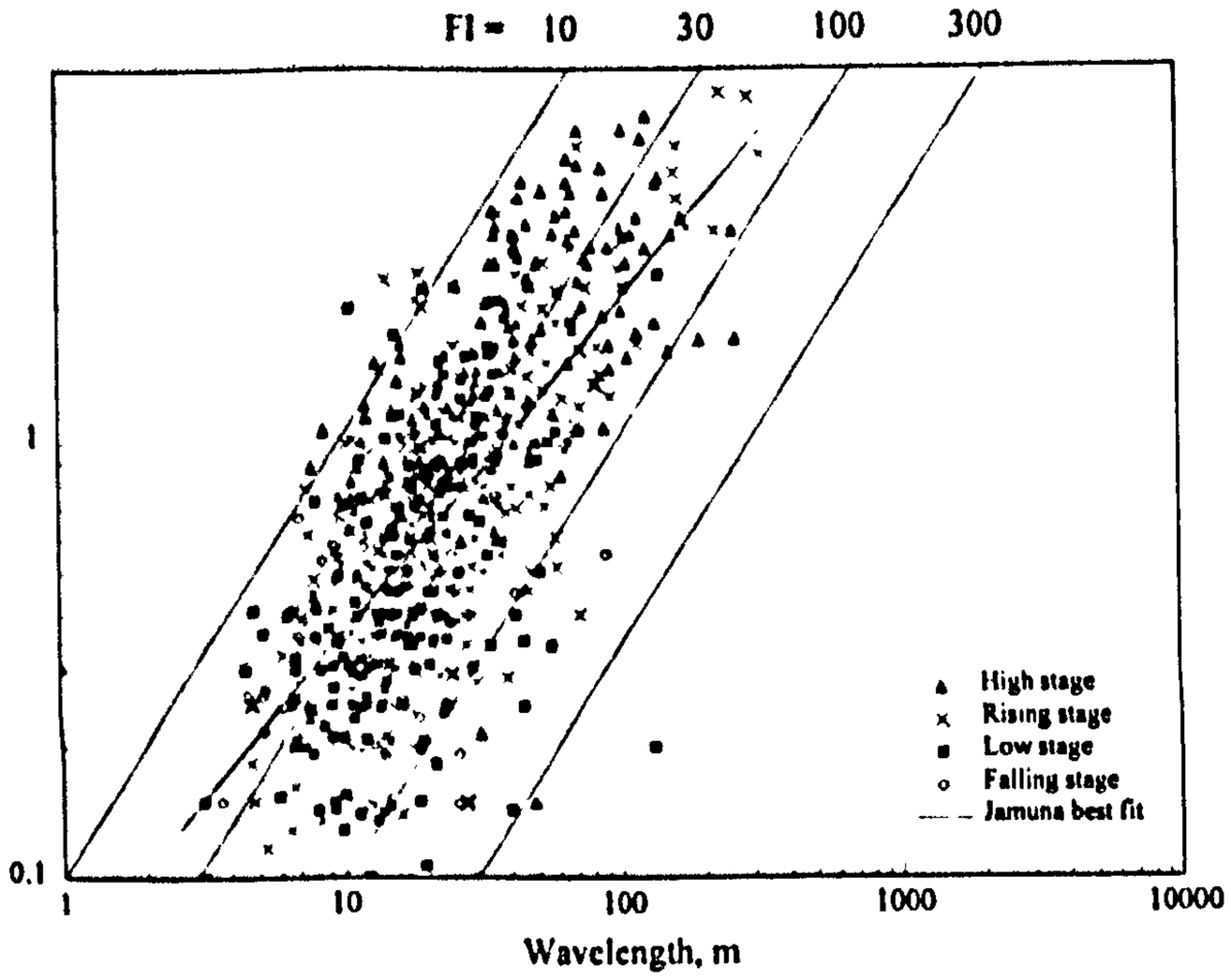

Figure 4.6, Dune height and wavelength relations divided by flow stage. Lines of equal form index (wavelength / height) are given for reference.

Although the FI as a measure of dune shape is of some interest for investigating changes in morphology and is simple to calculate, is does not truly characterise the form of a dune. Two dunes of radically different shapes can have the same FI (see Figure 4.7b) and so this measure may be of limited importance for classifying or describing dunes. Hence, its significance as a classification parameter should mainly be restricted to distinguishing between ripples and dunes.

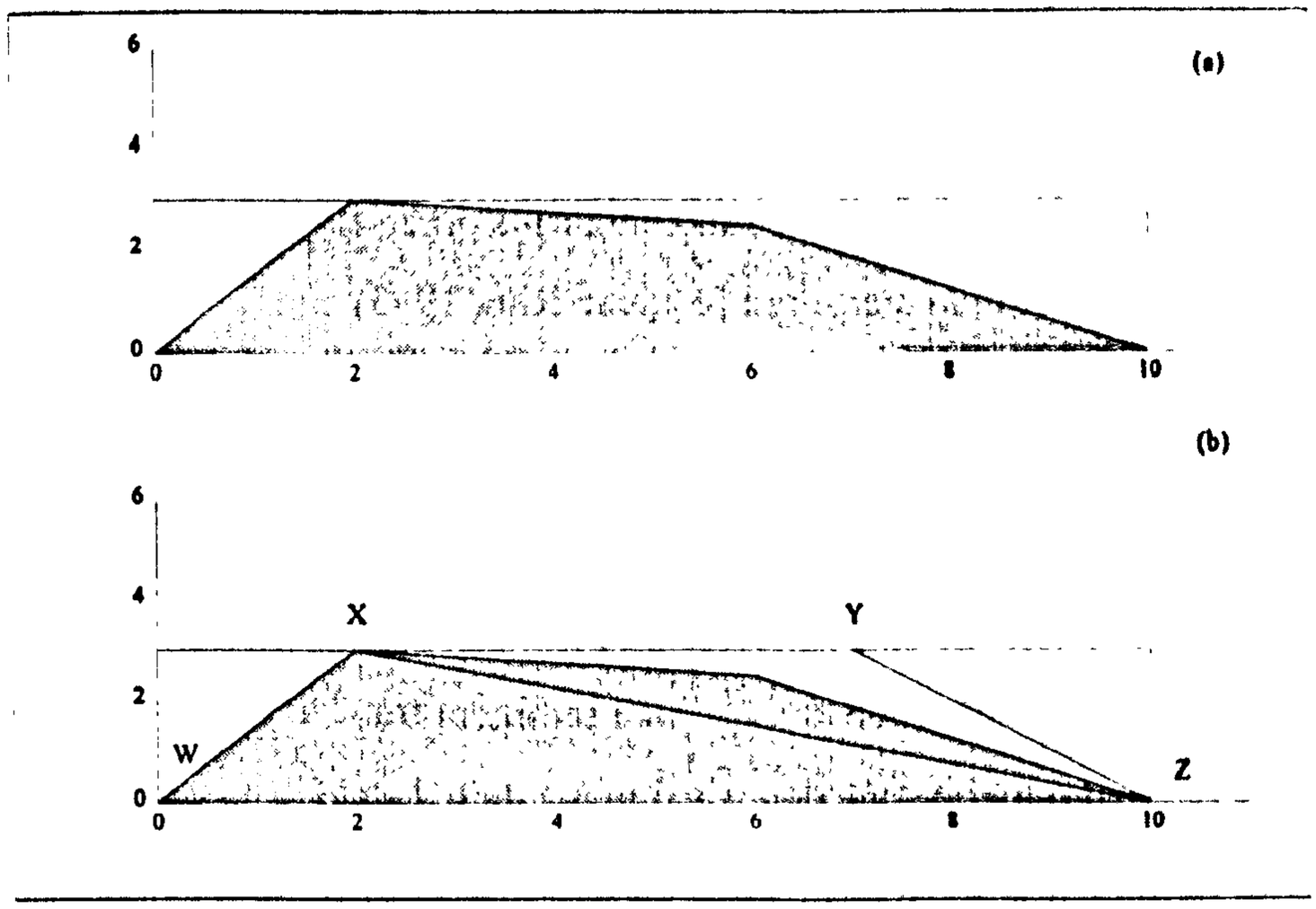

Figure 4.7, Schematic diagram defining dune shape factor. The shape factors is defined as the percentage of the rectangular area defined by the dune height and wavelength that is occupied by the bedform (shaded area), the shape factor in (a) is 0.58. (b) Variations in shape factor can be large for dunes with the same form index, in this case the shape factor varies from 0.5 (triangular dune, W-X-Z) to 0.67 (hump back dune, W-X-Y-Z).

Dune shape factor is a more detailed way of examining dune form or 'fullness' and is defined as the fraction occupied by the dune of the rectangle defined by the dune trough-to-trough wavelength and maximum height (see Figure 4.7 a and b). Shape factor has frequently been used to investigate sediment transport and form resistance (e.g. Gill, 1971; Allen, 1985; van Rijn, 1985) although there is little in the literature examining alluvial dune shape factors. The influence of using estimates of shape factor for a dune population or the variation in shape factor with flow stage have also received little attention. This may, of course, lead to inaccuracies in estimating flow and sediment properties. Mean shape factor in the Jamuna river varies from a minimum of 0.48 at low flow stage to a maximum of 0.71 at high flow stage (Figure 4.4e, Table 4.1), and hence 'humpbackness' of dunes is more common at high flow stage while a triangular cross-sectional shape is prevalent at low flow stages. Several studies have suggested that the migration and morphology of dunes may be used to yield estimates of bedload sediment transport rates (e.g. Simons et al., 1965; Williams, 1967; Crickmore, 1970; Engel and Lau, 1980; van Rijn, 1993) using the equation:

$$Q_b = \beta (1-p) \rho_s c h \qquad \textit{equation 4.10}$$

where Q_b is the bedload sediment transport rate, β is the shape factor, p is a porosity factor, ρ_s is the density of the sediment, c is the mean migration rate and h is the mean dune height. Morphological estimates of bedload sediment transport will only provide valid results if the morphology of the dune (the shape factor and height) is precisely defined, but the shape factor, β, is often estimated rather than measured (e.g. van Rijn, 1993) and no consideration is made concerning the change in shape factor with flow conditions. The discrepancy between estimated shape factors (usually approximated at 0.55) and measured mean shape factors (which vary between 0.48 and 0.71) at for dunes in the Jamuna river is great and may lead to an underestimate of bedload sediment transport by up to 30%. It should be noted however that equation 4.9, linking dune migration and bedload sediment transport, ignores partially or fully suspended material that may become deposited in the dune leeside and contribute to bedform migration (Kostaschuk and Illersich, 1995). Some past studies in large rivers have suggested that as little as 5% of dune migration may be accounted for by bedload transport (Kostaschuk and Illersich, 1995).

4.5 Lee Face Angle

The lee side angle of dunes is of considerable importance in relation to energy expenditure and flow resistance, as flow separation, which is responsible for increased energy loss, is expected to occur when the change in slope exceeds approximately 12° (e.g. Ogink, 1988; van Rijn, 1993). Flow separation may occur in the lee side of a dune if the change in pressure caused by the rapid variation in topography at the dune brink point is sufficiently great, thereby producing a free shear layer between the separated and unseparated flows. Such free shear layers are unstable and may break down into periodic vortices termed Kelvin Helmholtz instabilities (e.g. Prandtl, 1927), hence eddy shedding from the shear layer provides an extraction of energy from the mean flow.

Leeside angles in the Jamuna span a range from 2° to 58° (higher than the static angle of repose), with a mean angle of 8.6° and standard deviation of 7.9° (Fig. 4.8) and hence flow separation is not expected for most dunes in these channels. These mean leeside angle values correspond well with earlier studies in alluvial environments (e.g. Klaassen et al., 1988). The wide range of leeside angles present suggests that both leeside angle as well as bedform shape, which is commonly used, should be quantified when deriving bedform dimensions for use in resistance calculations.

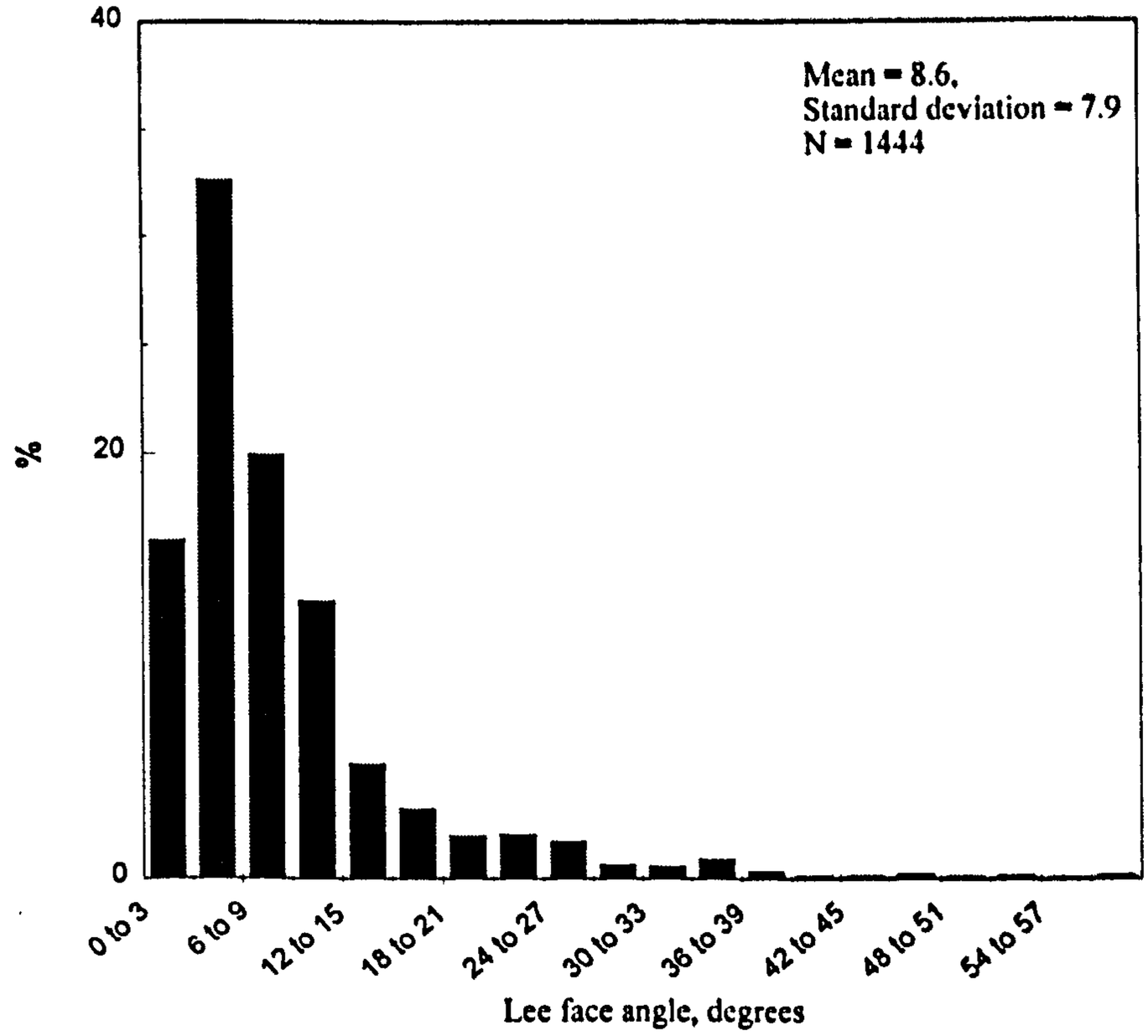

Figure 4.8, Histogram of dune lee face angle at all flow stages.

Variation in leeside angle with survey date is shown in Figure 4.4g (see also Table 4.1), during the 1994 hydrograph dune mean leeside angle increases from a minimum value of 5.6° (November 1994) to a maximum of 17.8° (August 1994) whilst for 1995, the leeside angle increases from 4.5° (January 1995) to 15.1° (August 1994), and hence lee side angle responds rapidly to a change in flow conditions (Figure 4.4a, Table 4.1). When split by flow stage (Figure 4.9) both the range in leeside slope and the fraction of dunes steeper than the critical angle for flow separation are found to vary: at high flow stage nearly half the dunes studied were capable of producing flow separation, while this figure drops to as low as 10 % for falling stage bedforms. This change in the percentage of dunes with lee side angles great than 12°, and therefore exhibiting flow separation, with flow stage may therefore be a function of the change of flow conditions. The increase in turbulence production at high flow stage caused by the enlargement of the fraction of dunes exhibiting flow separation may lead to additional sand suspension (e.g. Allen, 1968). Furthermore, as flow stage decreases, deposition of suspended sediment in bedform troughs may control the resulting change in shape and decrease in leeside angle. Hence, trough infilling caused by deposition of suspended sediment may be a factor in controlling lee side angle at falling flow stage.

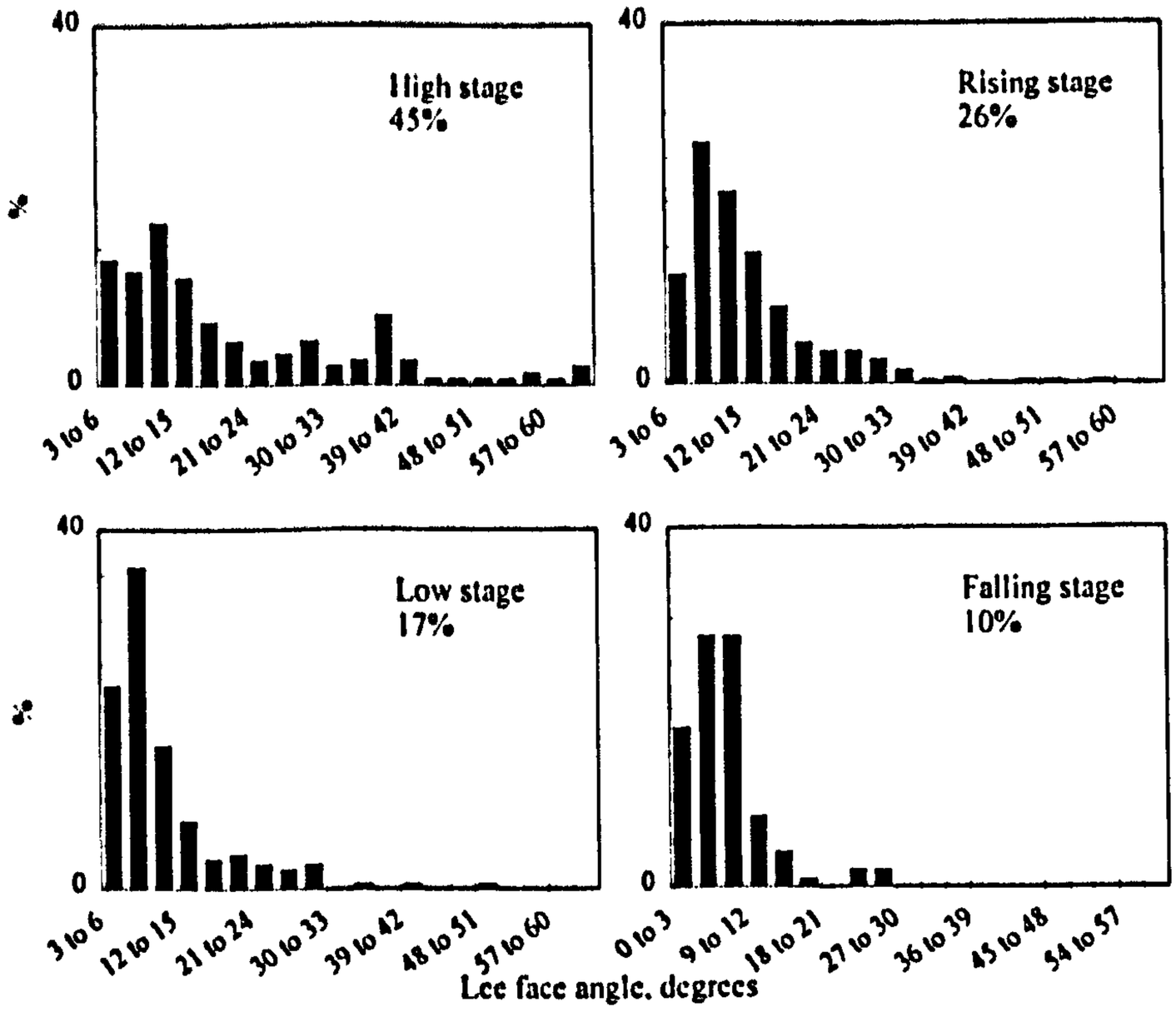

Figure 4.9, Histograms of dune lee face angle for high flow stage, N = 296, rising flow stage, N = 574, low flow stage, N = 360 and falling stage, N = 214. The number on each graph indicates the percentage of dunes that are steeper than the critical angle for flow separation.

It has been suggested that dunes in the transitional regime to upper stage plane bed (USPB) will flatten and wash out due to an increase in wavelength, a decrease in height and a change in form from asymmetrical to symmetrical (e.g. Termes, 1986; van Rijn, 1993), where asymmetrical dunes have lower lee-side length to stoss-side length ratios than symmetrical bedforms. This is obviously not the case for the population means in this study: increasing velocity accords with an increase in slip face angle, i.e. the dunes steepen with increasing flow stage indicating that most dunes may not be approaching upper stage plane bed (USPB) conditions (Figure 4.10).

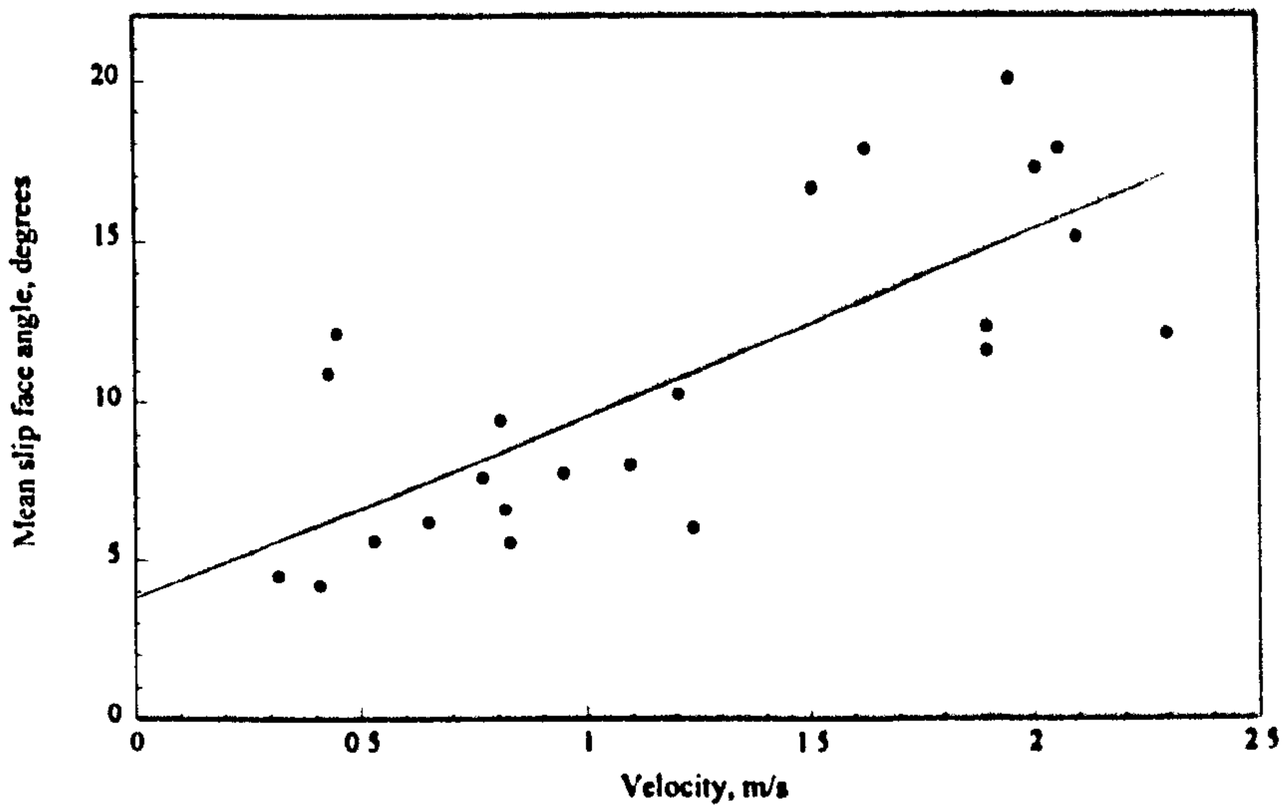

Figure 4.10, Leeside angle as a function of mean downstream velocity. Each point represents a group mean value of the lee face angle for a population of dunes during a given survey period.

Some studies have noted that low lee face angled dunes form at high flow stage and that a predominance of suspension transport results in an infilling of the dune trough (e.g. Smith and McLean, 1977; Kostaschuk and Villard, 1996). However, at high flow stage in the Jamuna river, asymmetric steep angled dunes are the most widespread bedform while suspended sediment concentrations are very high. As both dune height and lee face angle are increasing with flow velocity it seems likely that trough infilling is not occurring at high flow stage. Indeed, trough infilling in the Jamuna river may only occur when shear velocity decreases rapidly due to a drop in flow stage, hence at falling flow stage lee face angles are seen to decrease rapidly (Figures 4.9).

These data detailing dune lee side angle suggest that steep-angled dunes exhibiting flow separation are just part of a spectrum of bedforms that are continually changing in morphology in response to varying flow and sediment transport conditions. This range in dune shape accounts for the variation in morphology that has been frequently described for any particular population of dunes. Within this spectrum many subsets can be formulated, these transitional bedform features can then be explained by the differing flow and sediment transport conditions exerted on them. It may therefore not be applicable to classify dunes purely on account of their morphology as the processes, such as flow separation, which may control them are not acting in isolation. It is the complex feedback between flow, sediment transport and morphology which ultimately governs bed configuration (Leeder, 1983).

Recent work by Kornman (1995) has suggested that leeside angle may be better expressed through local slope changes at the crest and brinkpoint rather than the crest-trough slope (see Figure 4.11). Many dunes within the Jamuna possess complex downstream profiles, with the highest point on the crestal shoulder often being upstream of the brinkpoint of the main slipface. Derivation of the leeside angle at the point of slope change at the brinkpoint (lee2, Figure 4.11) and at the point of flow expansion at the crestal shoulder (lee1, Figure 4.11) allows two alternative measures of leeside slope to be derived. The mean value of angle lee2 (11.7°, Figure 4.12) is larger than that of crest-trough lee slope (8.6°, Figure 4.8). However, angle lee1 has a mean value of 4.1°, demonstrating the more gentle break of slope at the crestal shoulder as compared to the brinkpoint (Figure 4.12).

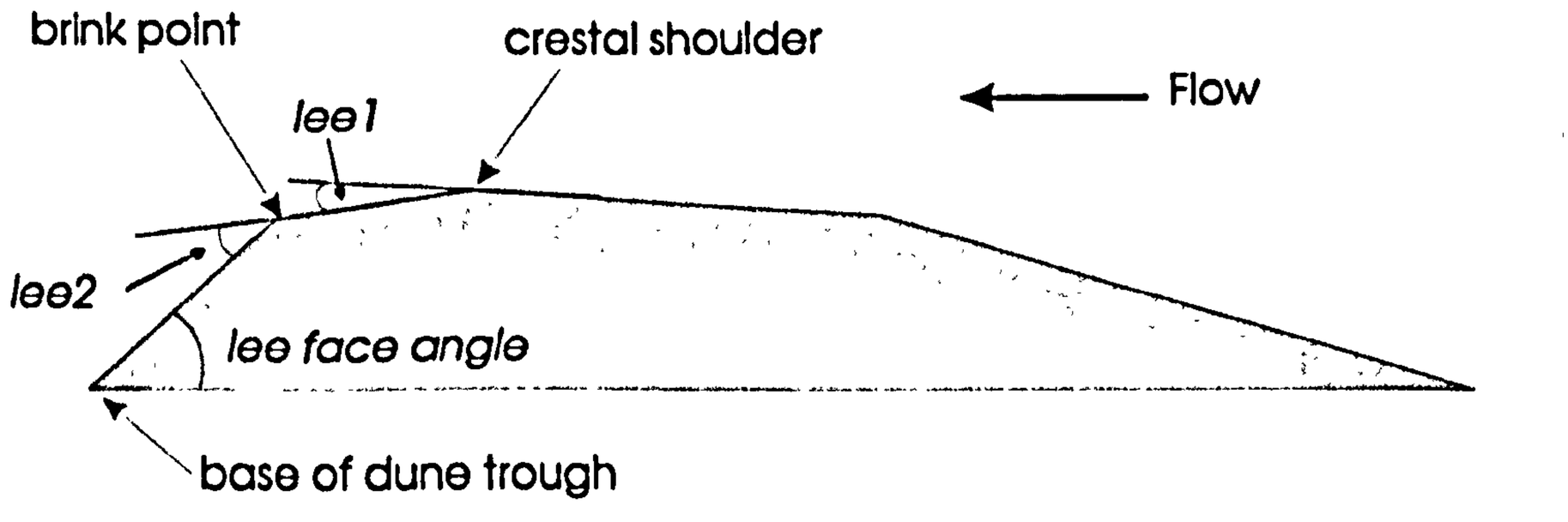

Figure 4.11, Leeside angle can be defined by the angle of the brinkpoint, the angle of the crestal shoulder or the mean leeside angle.

The complexities induced by this compound dune shape are several. First, the influence of flow separation in the leeside of the dune may be expected to lessen where a gentle crestal shoulder break of slope is present, thus producing smaller separation zones with a lower velocity gradient across the shear layer. However, a second point is that this effect may not act in just one way to diminish turbulence generation, since the additional turbulence generated along the shear layer at this first separation zone may feedback to produce enhanced local velocity gradients at the point of separation of the brinkpoint separation zone. It is clear that more detailed laboratory and field work is required to address the issues of hydraulic resistance, turbulence generation and sediment suspension over these complex dunes. The addition of superimposed dunes to already intricate dune morphologies will add further complexity to the flow separation process. Additional turbulence may also be generated by the presence of

smaller dunes that are stacked on top of a larger primary one. Superimposition is very common within all the rivers of Bangladesh with smaller dunes generated within evolving internal boundary layers upon the stoss sides of the primary bedforms. The sizes of superimposed dunes generally increase as the size of the primary dune upon which they are stacked increases. Superimposed dunes occur on all parts of primary dunes but are mainly generated on the stoss side of primary dunes. They are only detected on the lee side of primary dunes when the lee face angle is low. This highlights the need for consideration of bedform superimposition in resistance calculations.

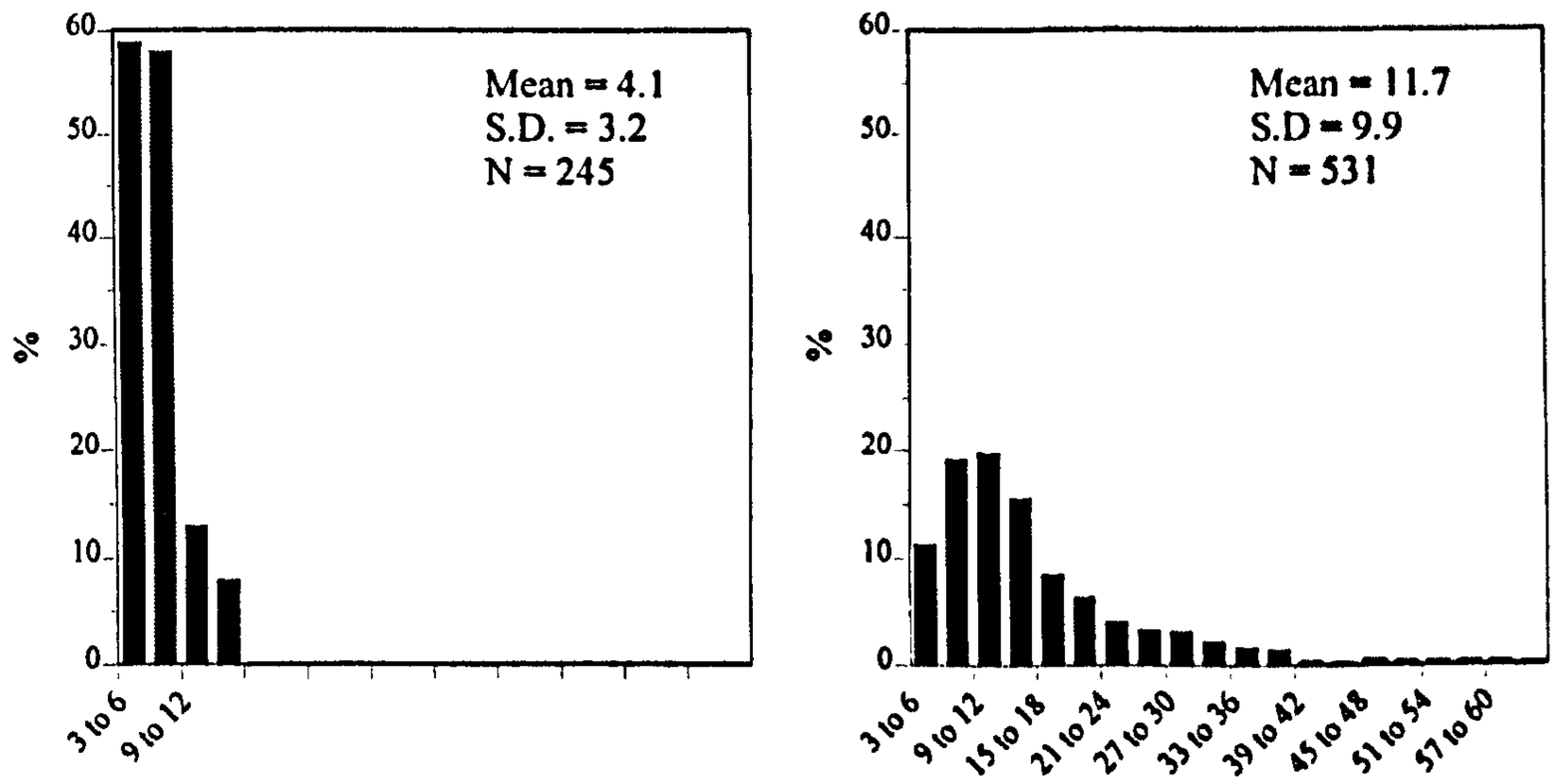

Figure 4.12, Histograms describing lee face angles defined by the angle of the brinkpoint and the angle of the crestal shoulder.

4.6 Models Predicting Dune Morphology

Many previous models have been proposed to predict dune morphology (e.g. Gill, 1971; Yalin, 1972; Allen, 1968; Fredsoe, 1980, 1982; Van Rijn, 1984, 1989, 1993; Julien and Klaassen, 1995). Van Rijn (1984, 1989, 1993) proposed that bedform occurrence and dimensions could be estimated by defining a transport stage parameter which is a measure of the relative excess shear stress acting on the bed. This transport stage parameter, T, is calculated using the applied grain shear stress on bed particles, and the critical shear stress corresponding to the onset of motion of bed particles.

$$T = ((u'_*)^2 - (u_{*c})^2) / (u_{*c})^2 \qquad \textit{equation 4.11}$$

van Rijn (1984) also defined a dimensionless particle diameter d_* as

$$D_* = D_{50} ((G-1)g/\nu^2)^{0.3} \qquad \textit{equation 4.12}$$

where D_{50} is the median bed particle diameter (50 % passing by weight), G is the particle specific gravity, ν is the kinematic viscosity, u_{*c} is the critical grain shear velocity which is obtained from the Shields' diagram, u'_* is the grain shear velocity which is given by $u(g/C')0.5$, where u is the depth averaged velocity, g is gravitational acceleration and C' is the grain Chezy coefficient which is defined by $C' = 18\log(12d/3D_{90})$ where d is the flow depth and D_{90} is bed particle diameter, 90% passing by weight.

Van Rijn (1984) then analysed flume and limited field data in terms of bedform dimensions under certain restrictions, namely 1) dune bed forms, 2) channel width to depth ratios larger than 3, 3) flow depth greater than 0.1 m, and 4) transport stage parameter T less than 25. He furthermore performed regression analysis on these data and defined fields of stability for bedforms and a bedform classification scheme. An amended version of this classification scheme is shown in Table 1 below.

Transport Regime		Particle size	
		$1 < D_* < 10$	$D_* > 10$
Lower	$0 \leq T \leq 3$	mini-ripples	dunes
	$3 < T \leq 10$	mega-ripples & dunes	dunes
	$10 < T \leq 15$	dunes	dunes
Transition	$15 < T, 25$	washed out dunes, sand waves	
Upper	$T \geq 25$, $Fr < 0.8$	symmetrical sand waves	
	$T \geq 25$, $Fr > 0.8$	plane bed and / or anti-dunes	

Table 1, van Rijn's classification of bedforms (after van Rijn, 1993)

According to van Rijn's scheme, asymmetric dunes with length scales much greater than water depth form at values of $T < 15$. Between T values of 3 and 10 these dominant bedforms may have ripples (termed 'mini ripples' by van Rijn) or secondary dunes (termed 'mega ripples' by van Rijn) superimposed which have length scales of the order of the scale of the near bed turbulence and water depth respectively. For T values of less than 3 and D_* less than 10, mini-ripples should be the dominant feature. For T values lying between 15 and 25, washed out transitional dunes should be the dominant feature, although van Rijn admits that "the type of bedforms in the transitional regime is somewhat obscure" as upper regime bedforms may also occur, depending on the preceding flow conditions. At T values greater than 25, van Rijn (1984) originally proposed that upper plane bed or antidunes would prevail and that suspended sediment transport would dominate. This proposal was modified (Van Rijn, 1993) to account for differences in Froude numbers; at $Fr < 0.8$, symmetrical bedforms would prevail with length scales much greater than water depth (Table 1). These bedforms are probably dynamically analogous to the symmetric bedforms reported by Smith and McLean (1977) and Kostaschuk and Villard (1996).

Prediction of bedform dimensions in terms of height, h and wavelength, λ as a function of flow depth d, bed particle diameter, D_{50} and the transport stage parameter, T were calculated by van Rijn (1984) using best fit lines from regression analysis:

height parameter: $h/d = 0.11\,(D_{50}/d)^{0.3}\,(1-e^{-0.5T})(25-T)$ *equation 4.13*

steepness parameter: $h/\lambda = 0.015\,(D_{50}/d)^{0.3}\,(1-e^{-0.5T})(25-T)$ *equation 4.14*

The data of van Rijn accorded very well with the predicted morphologies and an expression was derived for the relationship between dune height and wavelength

$$\lambda = 7.3\ h \qquad \textit{equation 4.15}$$

Julien and Klaassen (1995) however reported a more extensive field dataset concerning dune dimensions and van Rijn's transport stage parameter T. They showed that dunes occur at T values of up to 50 for sections of the data they investigated, namely dune bedforms from the Mississippi river. Their data also show that van Rijn's height prediction curve underestimates both the height of dunes during floods, and dune steepness for most of the data presented. However, an investigation of changes in geometry with flow stage for any particular dataset was neglected so the effect of increasing flow stage on values of T and dune height and steepness cannot be studied using these data. This renders it difficult to elucidate how changes in flow stage will effect dune occurrence and geometry, and also whether prediction methods are accurate when rivers are under flood conditions. The Jamuna dataset may therefore be very valuable when considering changes in flow stage with respect to prediction of dune geometry. Accordingly, the transport stage and morphological parameters were calculated for the Jamuna data and these are presented in Figure 4.13.

The first important point illustrated by Figure 4.13 is that dunes in the Jamuna do occur at values of T greater than 25. The maximum value of T calculated is 58 which occurs at high flow stage where T values vary between 10 and 58. During rising flow stage T varies between 3 and 33 whereas at low and falling flow stage T values are much smaller (1-3). There is a large range in values of the dune height and steepness parameter at all flow stages (Figure 4.13) again indicating the large scatter in dune height, dune wavelength and flow depth relationships that have been discussed above. There is a decrease in both the dune steepness and dune height parameters at $T > 40$ (Figure 4.13), but this decrease occurs for only a very small number of bedforms, so indicating that only a minor percentage (< 3 %) of dunes in the Jamuna river at high flow stage are transitional bedforms which are approaching upper stage plane bed conditions.

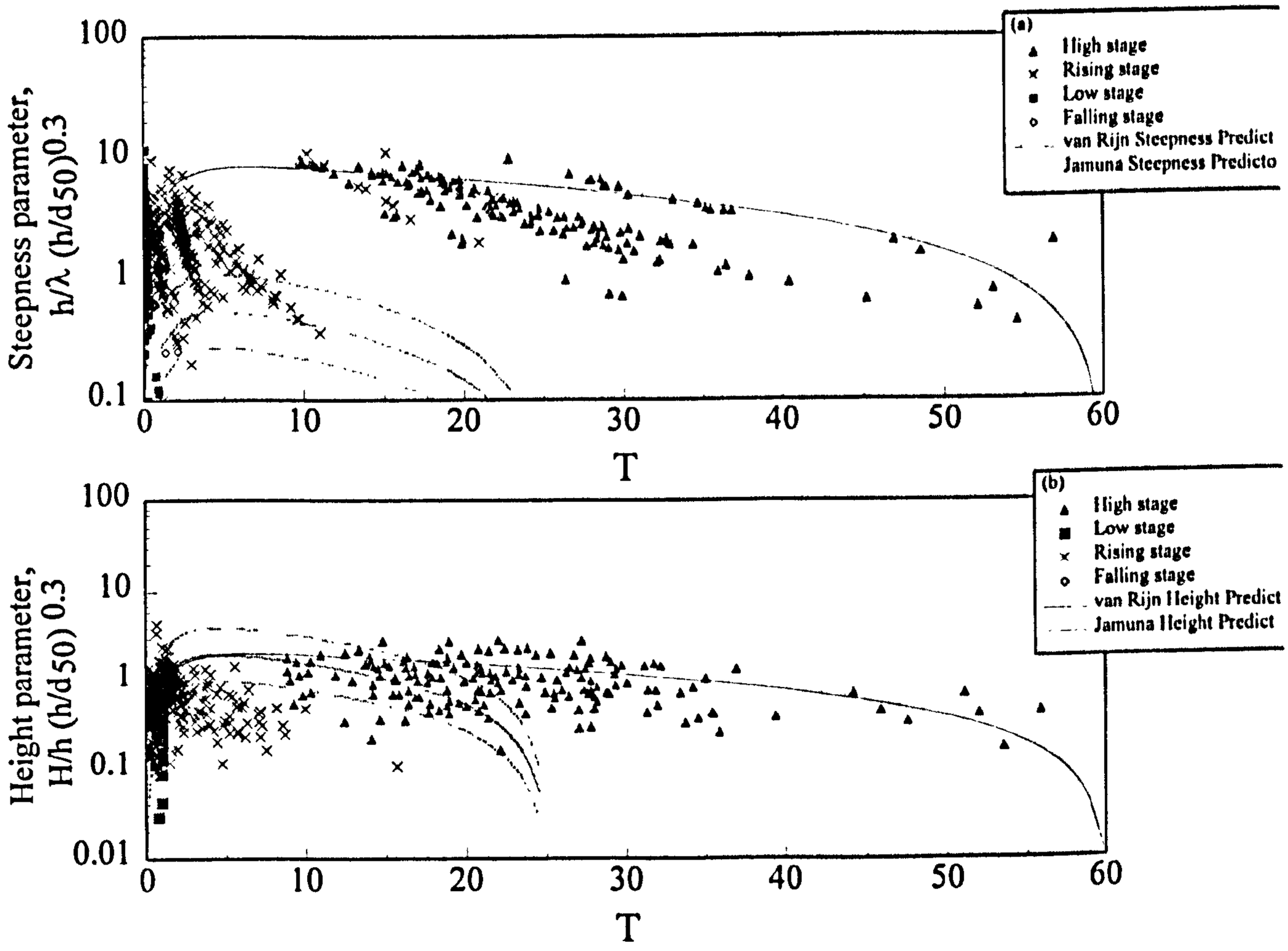

Figure 14.13, van Rijn's sediment mobility parameter T as a predictor of bedform (a) height and (b) steepness. Van Rijn's prediction curves are given together with the prediction curve based on the Jamuna dune morphology data.

Variation of T with van Rijn's height parameter (Figure 4.13b) indicates that van Rijn's prediction curve during low and falling flow stages is reasonably accurate, but at both rising and high flow stages there is some disagreement. Many of the T values calculated for rising stage overpredict dune height. This in good agreement with the results of Julien and Klaassen (1995) of dune bedforms from the Mississippi River (data from Raslan, 1991) where for low values of T (less than 10) the height parameter is commonly over predicted. The other datasets presented by Julien and Klaassen show in general an underprediction of the height parameter. At high flow stage in the Jamuna dune occurrence is not forecast by T, dunes occur at T values up to 58 and there is only a small decrease in the height parameter at these higher T values for a small number of bedforms. Under flood conditions, upper stage plane bed conditions are not reached and dune height does not decrease appreciably for most of the dunes. The same point is illustrated by Figure 4.13a as dunes are still occurring at high values of T and there is some decrease in the steepness parameter with increasing T indicating that there may be a decrease in dune height (and possibly an increase in dune wavelength) at very high T values. Van Rijn's

steepness parameter is however consistently under predicted for the Jamuna bedforms, this is true at all flow stages, so agreeing with the finding of Julien and Klaassen (1995).

Assuming that the maximum value of T obtainable is 60 (as no further information is available), best fit lines for the Jamuna data yield the relationships:

height parameter: $h/H = 0.165\,(D_{50}/H)^{0.3}\,(1-e^{-0.5T})(60-T)$ *equation 4.16*

steepness parameter: $h/\lambda = 0.04\,(D_{50}/h)^{0.3}\,(1-e^{-0.5T})(60-T)$ *equation 4.17*

In summary, the transport stage parameter increases with flow stage, maximum values of T occur at high flow stage during floods and dunes occur at higher values of T than predicted by van Rijn. Julien and Klaassen (1995) explained the values of T which were greater than those predicted by van Rijn for dune bedforms by re-writing the transport stage parameter T equation in terms of the Froude number. Under laboratory conditions a T value of 25 corresponds to critical flow conditions (Froude numbers equal to 1), under field conditions Julien and Klaassen (1995) estimate that this would result in a T value of approximately 325. Figure 4.14 shows Froude number and T; it illustrates that Froude numbers in the Jamuna do not approach critical conditions (the maximum Froude number is 0.3) and therefore USPB conditions may not be reached. A best fit line for the Froude number to T relationship is given by:

$$Fr = 0.0214\,\ln T + 0.125 \qquad \text{equation 4.17}$$

In large sand bed rivers under flood conditions, prediction of dune geometry using van Rijn's method is somewhat flawed. The trend in the Froude number shown in Figure 4.14 suggests that conditions may only rarely be achieved (at $T >> 20\,000$) which produce supercritical flow in the Jamuna River. This limiting effect of Froude number on bedform dimensions and occurrence has previously been noted by Kennedy (1961), Znamenskaya (1964), Engelund and Hansen (1966) and Allen (1968). It should be noted however that equation 4.17 indicates that Froude numbers approaching 1 will only very infrequently occur in the Jamuna river, and this may be imprecise. Although high Froude numbers will only very infrequently occur in main channel thalwegs, they may occur more often on bar margins where flow depths are shallower. Hence, the spatial variation in flow depth (Figure 4.2a) highlights the requirement that dunes forming in a variety of locations within a large sand bed river should be considered when modelling bedform occurrence and morphology.

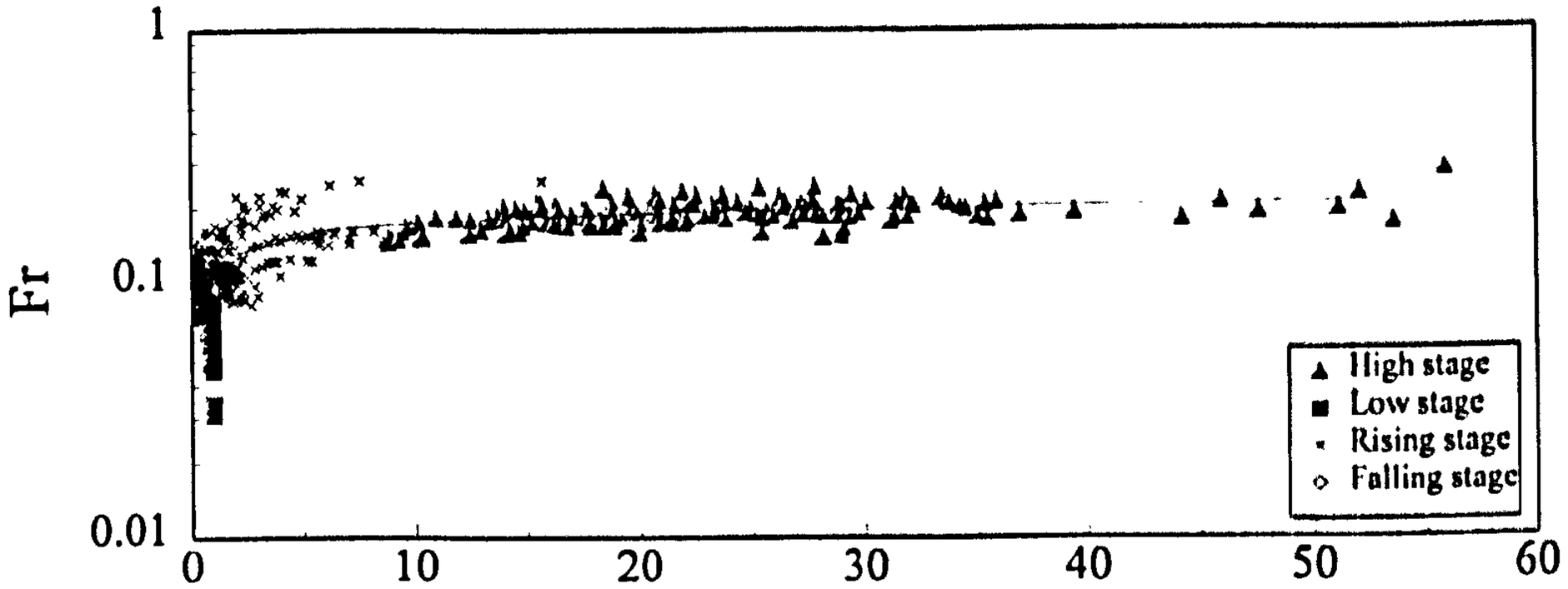

Figure 4.14, van Rijn's sediment mobility parameter T as a function of Froude number, Fr.

Figure 4.15a shows shape factor against T and illustrates that the dune shapes exhibit little variation at high flow stage hence the humpbackedness of dunes is not decreasing at very high values of T. However, at T values greater than 40 there is a decrease in the steepness of the leeside face (Figure 4.14b) which may be indicating an infilling of the dune trough caused by an increase in suspended sediment transport which may be expected at high shear stresses as the transition from dunes to upper stage plane bed occurs (Smith and McLean, 1977; Kostaschuk and Villard, 1996). However, the decrease in lee face angle at high values of T only occurs for a small number of dunes so indicating that low angled dune bedforms that have formed due to high shear stresses are very uncommon in the Jamuna river.

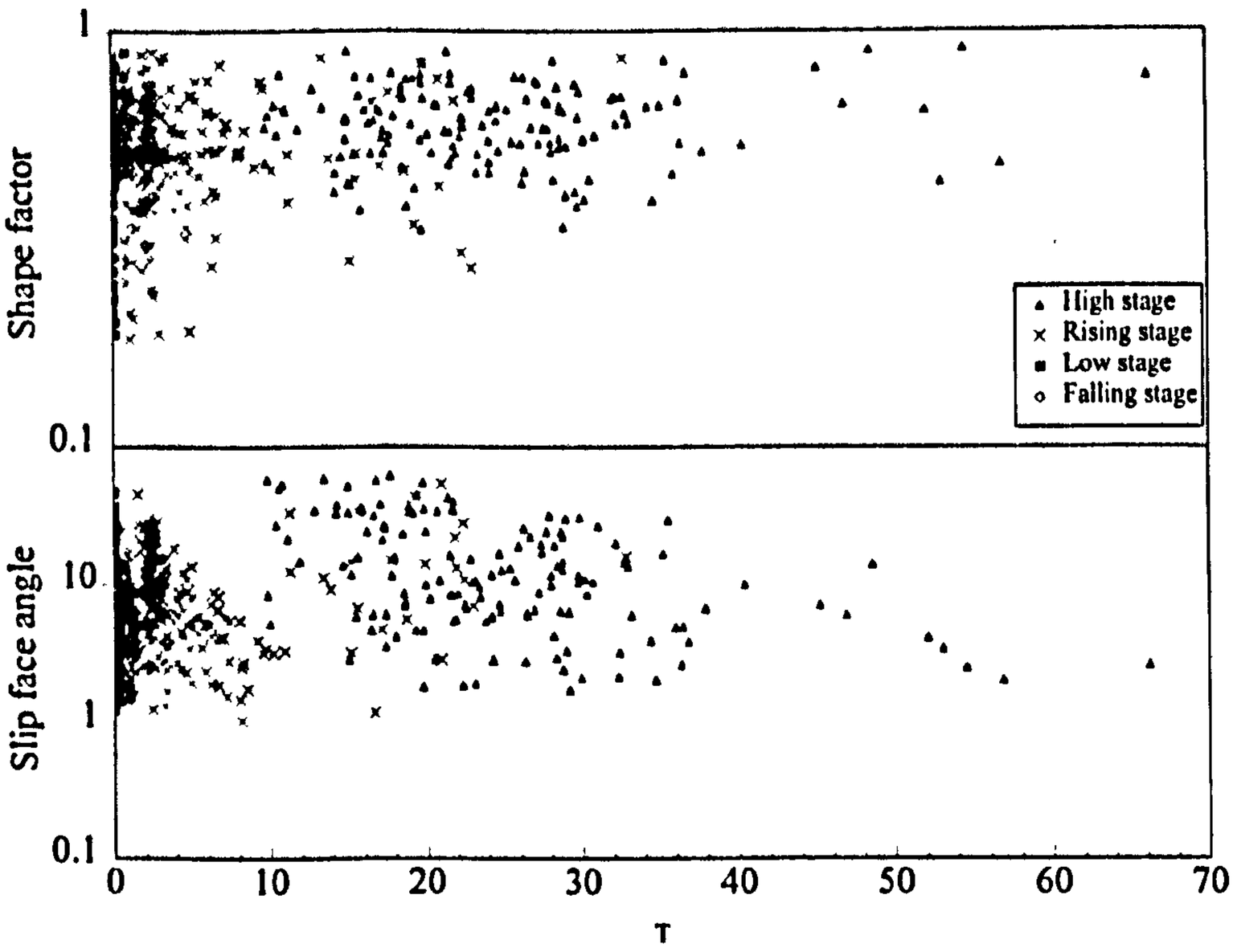

Figure 4.15, van Rijn's sediment mobility parameter T as a function of shape factor and lee face angle.

Amsler and Garcia (1997) suggested that the presence of superimposed bedforms (see Chapter 3) may be important when evaluating van Rijn's transport stage parameter. Their study of dune height and wavelength during a flood in the Parana river showed that the morphology of superimposed dunes responded differently to primary dune morphologies, with primary dune heights decreasing during and after the flood and superimposed dunes increasing and decreasing with rising and falling discharges respectively. This, however, is not the case for the Jamuna river as superimposed dunes increase and decrease in height and wavelength respectively in a similar manner as primary dunes as maximum dune height, wavelength, form index and slip face angle occur at high flow stage (Figure 4.16). This behaviour would be expected as hierarchical dunes are dynamically analogous to primary dunes, the processes which form both dunes are the same (Ashley, 1990; Chapter 5) although the flow fields of primary dunes control the stability and morphology of secondary dunes which are superimposed upon them. Superimposition is extremely common in both field and flume studies and is probably an equilibrium feature with superimposed dunes forming within the internal boundary layer generated by the primary bedform (Smith and McLean, 1977).

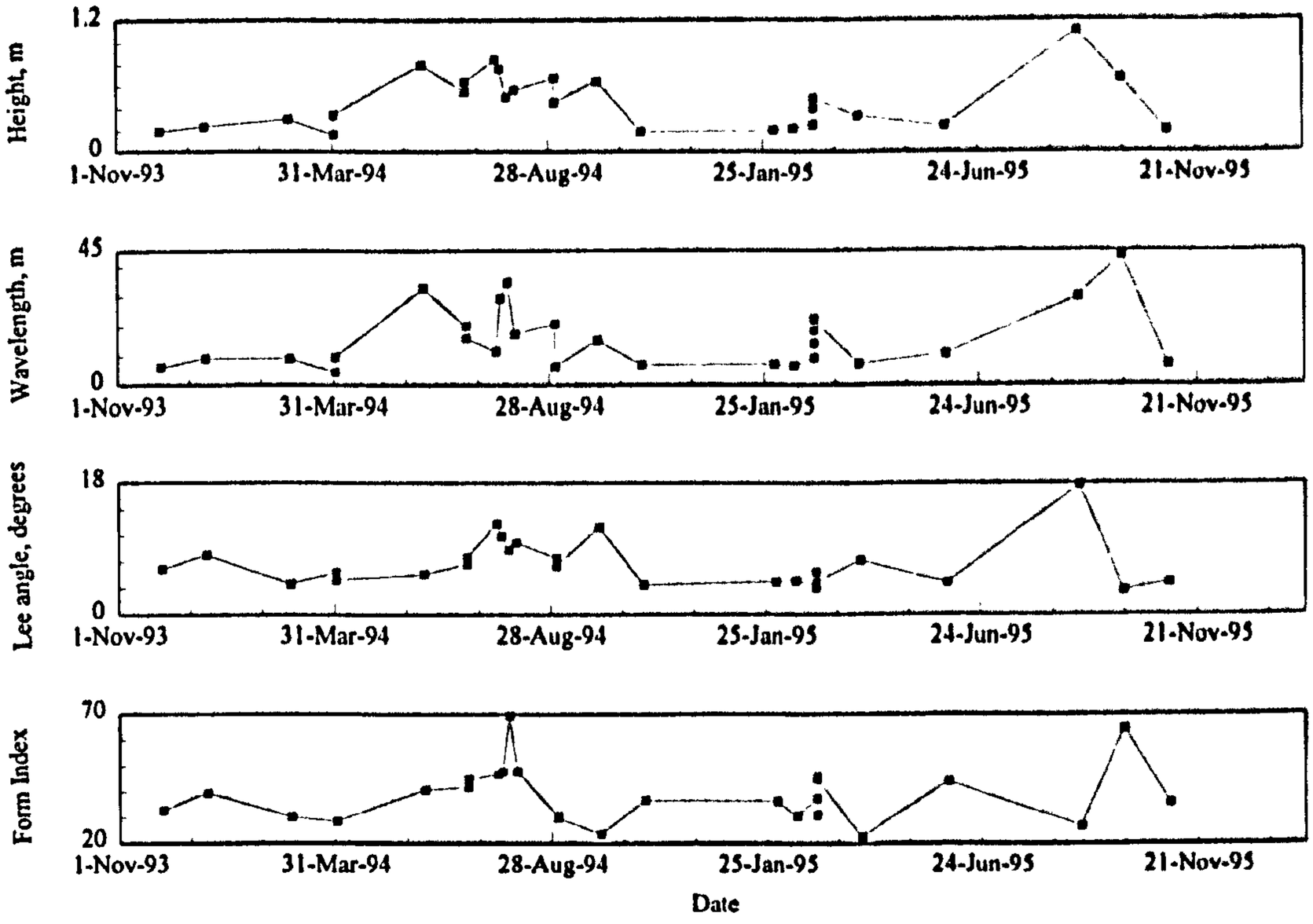

Figure 4.16, Temporal variation in the mean values of superimposed dune morphological parameters. Dune height, wavelength, lee face angle and form index are shown for the 1994 and 1995 hydrographs.

4.7 Flow Resistance

For a mobile sand bed the effective bed roughness may be divided into grain roughness generated by skin friction forces and form roughness generated by pressure forces acting on bedforms. Since bed roughness depends on both bed material size and flow conditions, a quantitative description of the evolution of bed configurations under changing hydraulic regimes is of fundamental importance when predicting flow resistance (e.g. Karim, 1995). Two approaches have been proposed in the literature to estimate bed roughness; the first relying on bedform and grain parameters (e.g. Engelund, 1977; van Rijn, 1993) whilst the second is based on integral parameters such as mean depth and velocity (e.g. Brownlie, 1983). This section will utilise the bedform morphology data described above to assess the validity of two methods based on bedform parameters to calculate form roughness.

The effective bedform roughness, $k_{s,c}$" is related to the bedform height, steepness and shape where:

$$k_{s,c}" = F(h, h/\lambda, \beta) \qquad \textit{equation 4.19}$$

For dunes, van Rijn (1993) proposes that

$$k_{s,d}'' = 1.1\,\beta\,h\,(1-e^{-25h/\lambda}) \qquad \text{equation 4.19}$$

where β is the shape factor, h is the dune height and λ is the wavelength. The shape factor is included to express the influence of dune form on the roughness height. Ogink (1988) showed that leeside slopes of river dunes are much smaller than those of laboratory dunes, having values in the range 1:5 to 1:7 (8° to 11°), yielding shape factors of about 0.7. However, this value is inconsistent with the measured shape factors for the Jamuna dunes where stage averaged values range from 0.48 to 0.71 (Section 4.4). Ogink's experiments also showed that the leeside angle of dunes influences flow resistance as the process of flow separation only occurs when dune lee face angles are steeper than the critical angle of separation (approximately 12° for a grain size of 0.2 mm). The relationship between shape factor and dune lee face angle is shown in Figure 4.17 and illustrates that the relationship is highly scattered and exhibits no obvious trend. Using the shape factor to account for the process of flow separation may therefore be very misleading as increases in shape factor do not always indicate increases in lee face angle (Figure 4.17).

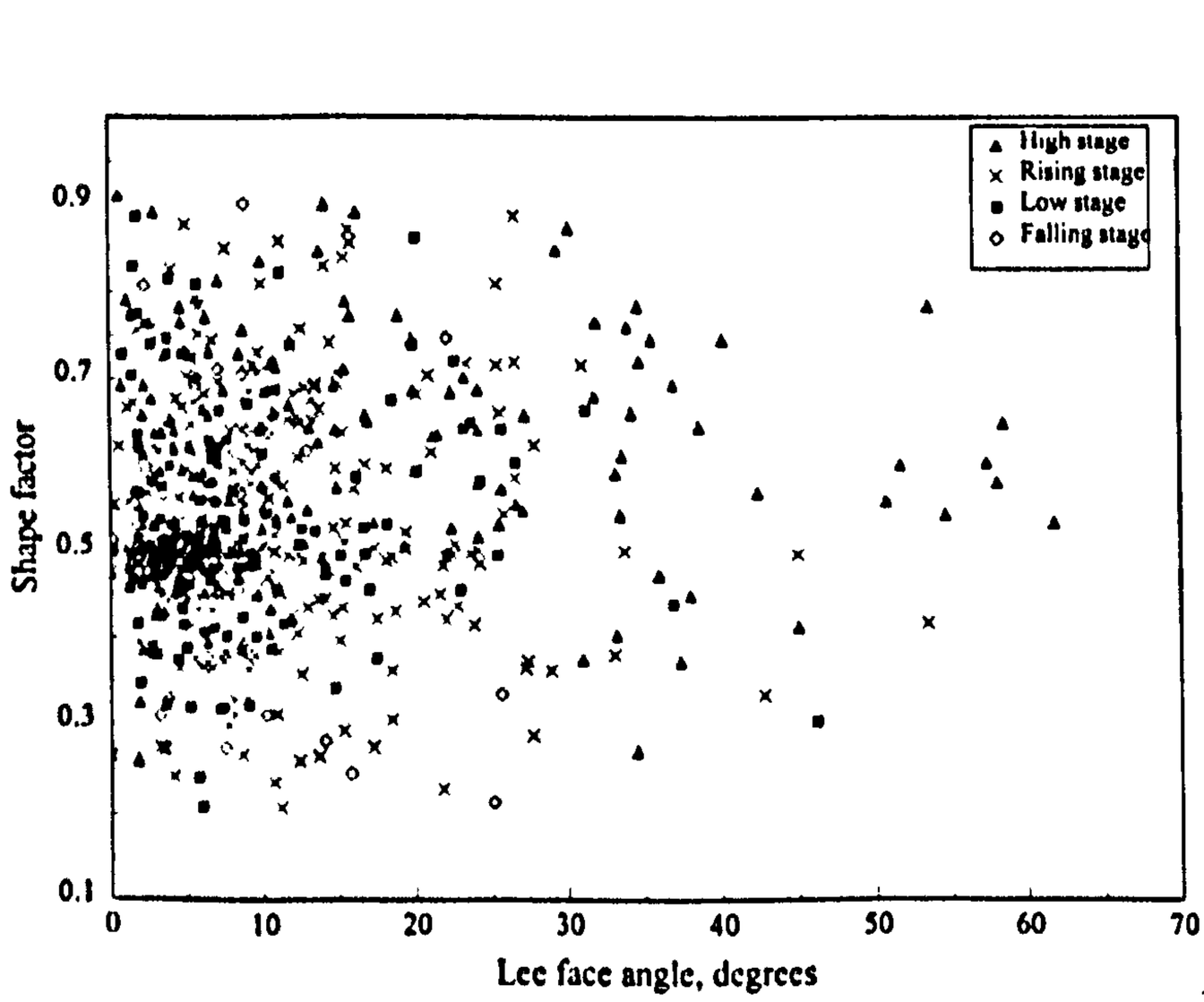

Figure 4.17, Dune shape factor and lee face angle split by flow stage.

Engelund (1977) proposed that the friction coefficient, f'' can be related to dune parameters by:

$$f'' = 10\,(h^2/d\lambda)(e^{-2.5h/d}) \qquad \text{equation 4.20}$$

A comparison of results of friction factors using the Engelund and van Rijn methods for calculating flow resistance is illustrated in Figure 4.18. The results, which are split by flow stage, show that although the results from applying both methods coincide at low and falling flow stage there is incongruity at high and rising flow stages. As high flow stages are the most significant times of year in terms of sediment transport, flow discharge and rate of channel change, it is important to investigate which parameters may lead to the discrepancies in the methods at higher flow stages. As turbulence production is of paramount importance due to the influence on flow resistance, the dune leeside angle must be elucidated when calculating flow resistance. Due to the paucity of information available detailing lee face angle, different parameters have been substituted such as the form index and shape factor. Figure 4.17 has shown that there is little correlation between shape factor and leeside angle at all flow stages.

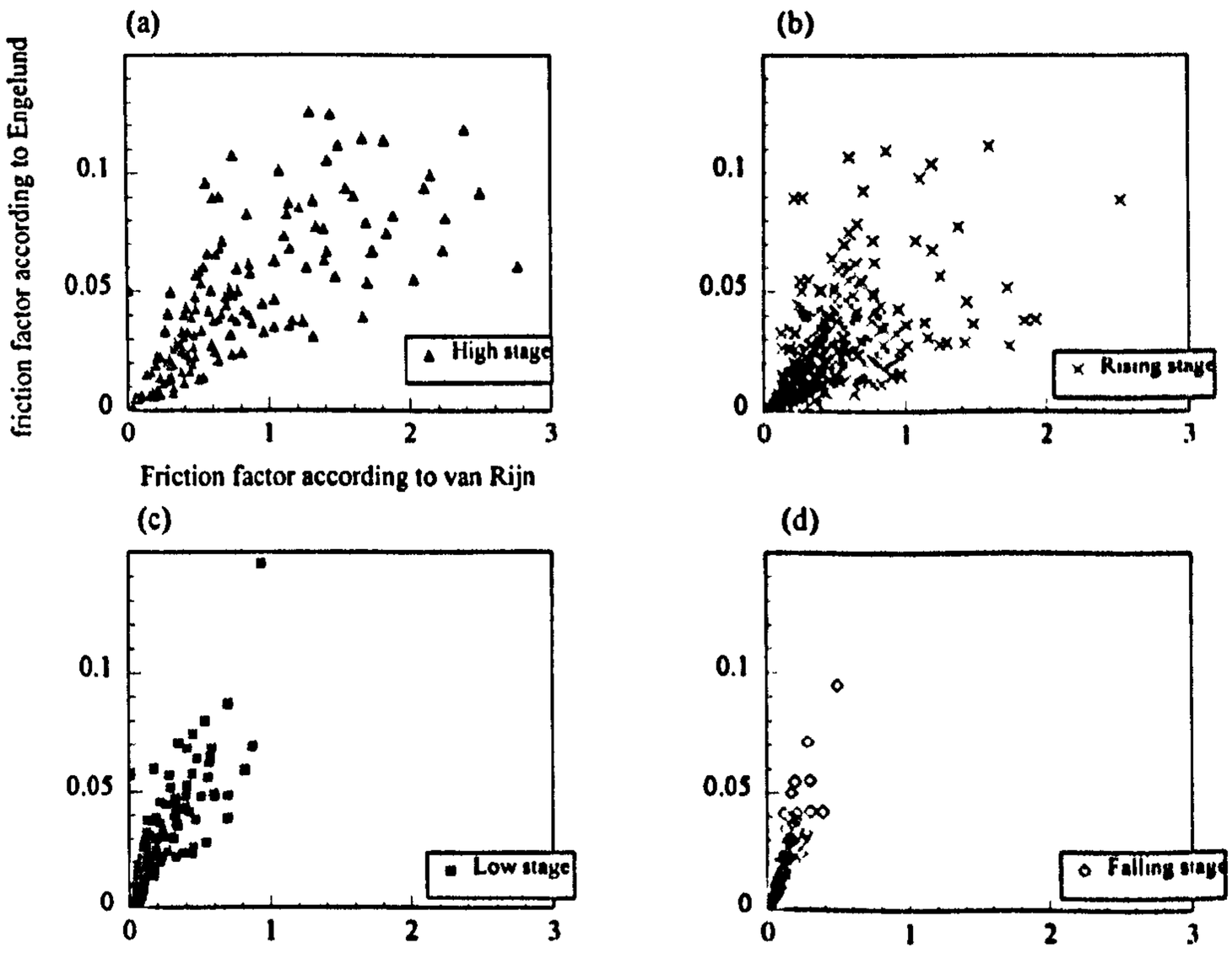

Figure 4.18, Friction factors calculated according to Engelund (1977) and van Rijn (1993) under (a) high stage, (b) rising stage, (c) low stage and (d) falling stage flow conditions.

The relationship between form index and lee side angle (Figure 4.19) shows that although there is a positive correlation between these parameters, there is still a wide discrepancy in the relationship ($r^2 = 0.09$) and so dune form index, like dune shape factor, does not adequately describe whether flow separation will occur. Hence, neither of the methods explored here therefore account for process changes that take place under varying flow conditions.

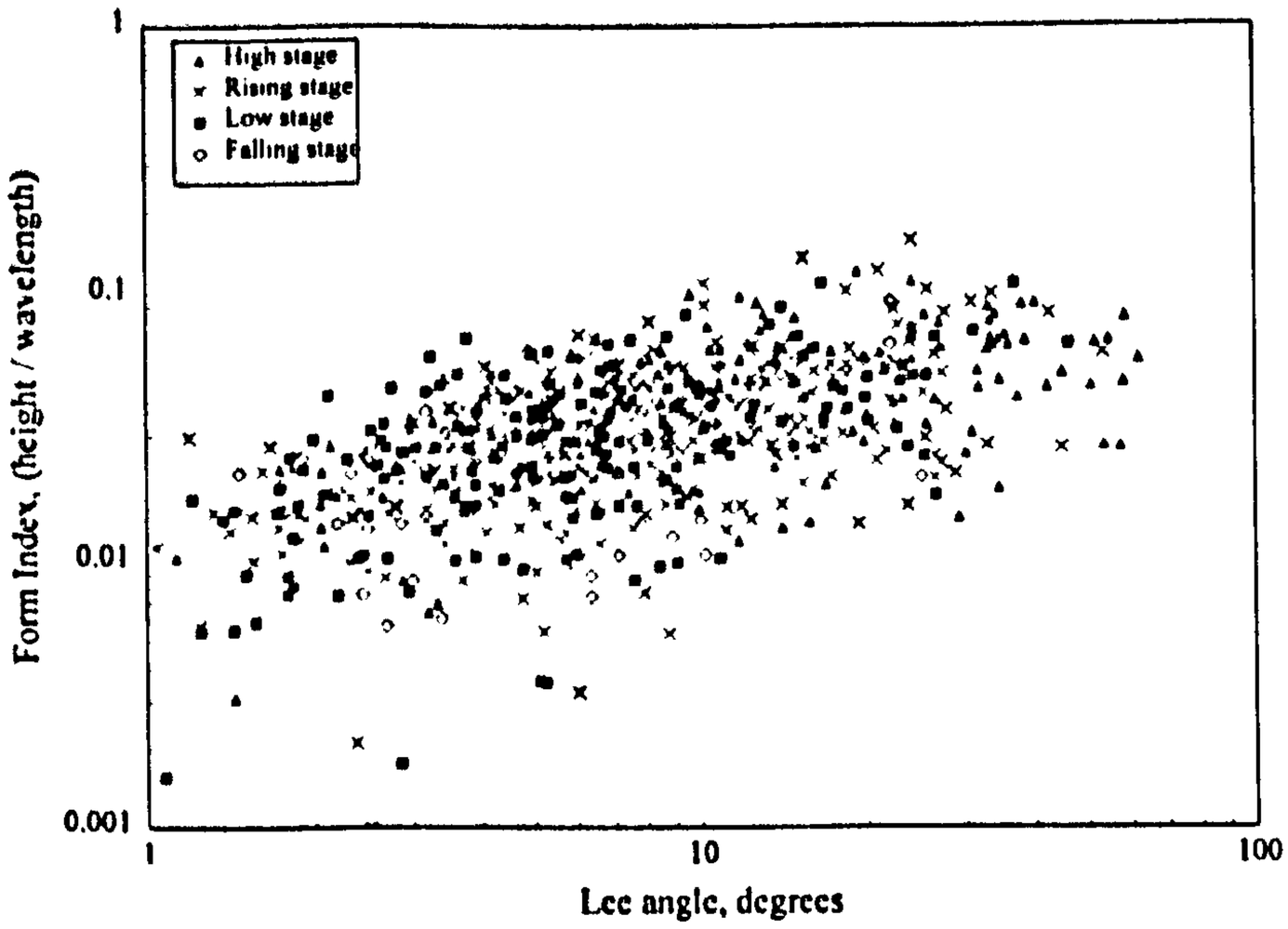

Figure 4.19, The relationship between form index and lee angle divided by flow stage.

Van Rijn (1993) reports that an average measure of dune shape factor can be used for these flow resistance calculations, and proposes a value of 0.55 (see Figure 4.20), however the use of such average values may be misleading as mean shape factor has been shown to vary with flow stage (Section 4.4, stage mean shape factor values range between 0.48 and 0.71). Van Rijn's (1993) estimate of the value of shape factor was measured under low flow conditions and from flume data. However, shape factors under high flow conditions may be more useful as this is when maximum channel change occurs. Van Rijn (1993) therefore consistently underestimates the shape factor; this underestimation is especially large when predicting flow resistance under rising and high flow regimes. The average values of dune shape factor detailed in Section 4.4 are more precise for dunes forming in the Jamuna river.

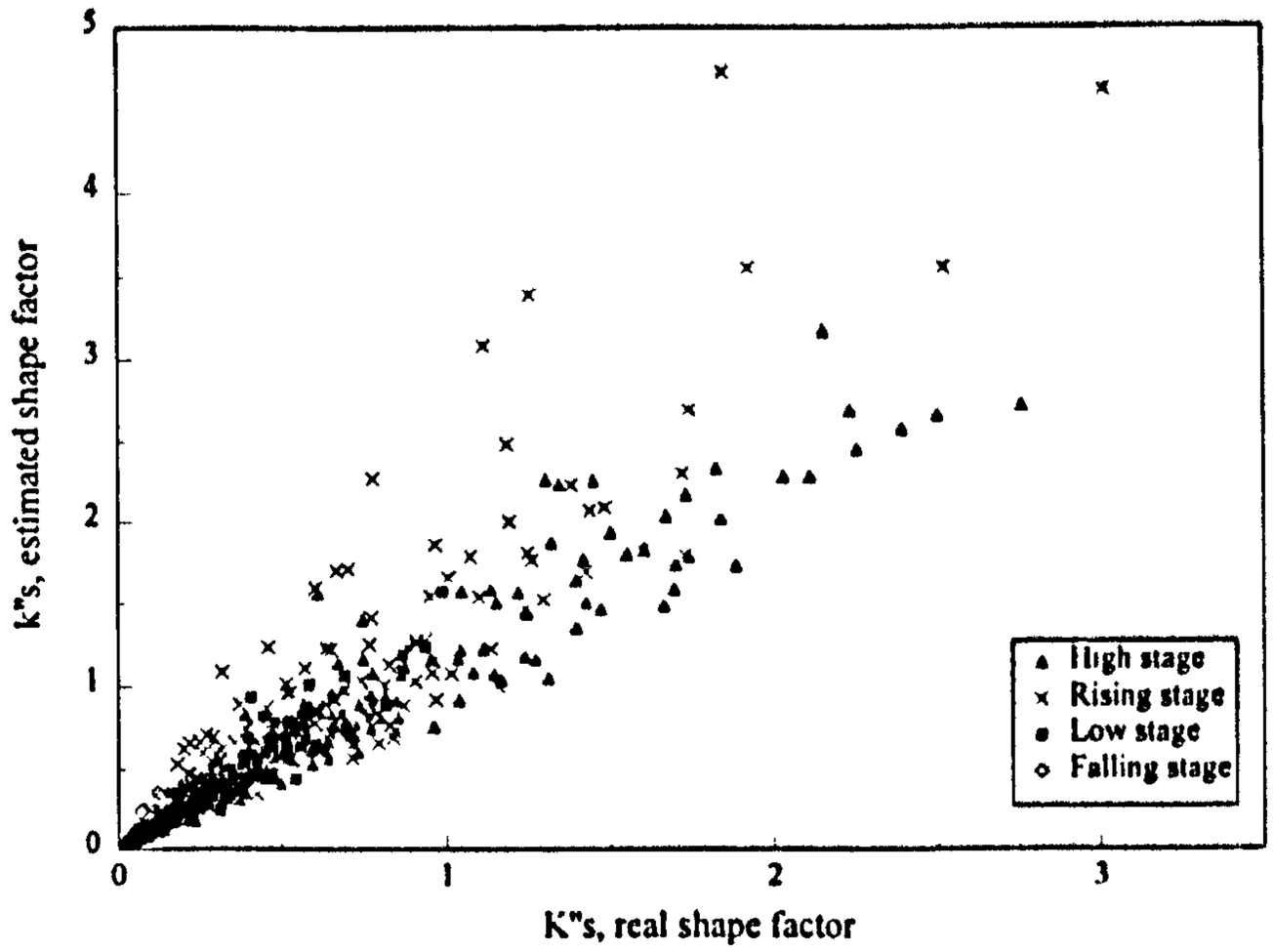

Figure 4.20, Friction factor calculated by van Rijn's (1993) method using measured and estimated dune shape factors

By ignoring shape factors, Engelund's method neglects the fullness of the dunes which will again alter resistance to flow. Many authors have described hump-backed dunes and superimposed bedforms which have a great effect on flow resistance in terms of fullbededness and morphological effects on flow structure. As shape factor has been seen to vary with flow stage it seems insufficient to ignore this term completely. Hence, dune geometry significantly influences resistance to flow in sand bed channels and many friction factor relationships do not take into account the role of bedform configuration in their formulations (Karim and Kennedy, 1990; Karim, 1995), which will lead to great inaccuracies in flow resistance calculations.

4.8 Dune Planform Morphology and Dimensionality

Bedform dimensionality has previously been proposed to reflect the strength of the flow (e.g. Allen, 1982), although recent work has suggested that bedform three-dimensionality more properly reflects the length of time available for bedform development, the amount of bedload transport and its spanwise variation (Baas, 1994). As bedform formation and migration occur throughout high and low flow, it is likely that all bedforms will display some degree of three-dimensionality and few dunes will remain two-dimensional. This section therefore aims to describe the dimensionality of bedforms in planform by studying dunes exposed on bar tops at

low flow stage and by using side scan sonar to image the river bed during both low and high flow stages.

4.8.1 Exposed Dunes

Examination of bar tops exposed during low flow showed a variety of dunes in terms of planform morphology, size and distribution (Figure 4.21). Dunes formed at both high and low flow rates were found to be well preserved after water levels have dropped, with mud drapes restraining aeolian transport. Ripples were often preserved in dune troughs indicting reverse flow sediment transport directions and flow expansion and fanning within the trough. A variety of planform features were observed including large scour holes and spurs showing preferential sediment transport pathways. Exposed bar top surveys were also conducted to detail directions of bedform migration as flow rates decreased. Several distinct dune morphologies were observed and these are described below.

Small dunes (Ashley, 1990) with superimposed linguoid ripples are exposed on bar tops that have formed under falling and low flow conditions (Figure 4.21a). The variation in dune height ranges from 0.1 m to 0.5 m, and crestlines are straight to gently sinuous. These dunes form on bar tops and margins in response to low flow rates and dropping water levels during the falling and low stage of the hydrograph and crestlines may be followed out from the bar edge into the channel when water level is still dropping.

Two types of dunes morphologies have been observed that have formed at high flow stage and are subsequently preserved on bar tops. First, highly three dimensional dunes with large scour holes along crestlines occur on bar tops, ranging in height between 1.5 m and 2.5 m (Figure 4.21b). Such three dimensional forms exhibit discontinuous crestlines, and are very irregular in both morphology and location, usually forming on the uppermost margin of the bar. These forms are probably produced due to very high flow velocities over a bar tops. Second, sinuous to straight crested dunes are present on bar tops with regular spurs interspaced between trough scour pits and ranging in height between 0.75 m and 1.5 m (Figure 4.21c).

(a)

(b)

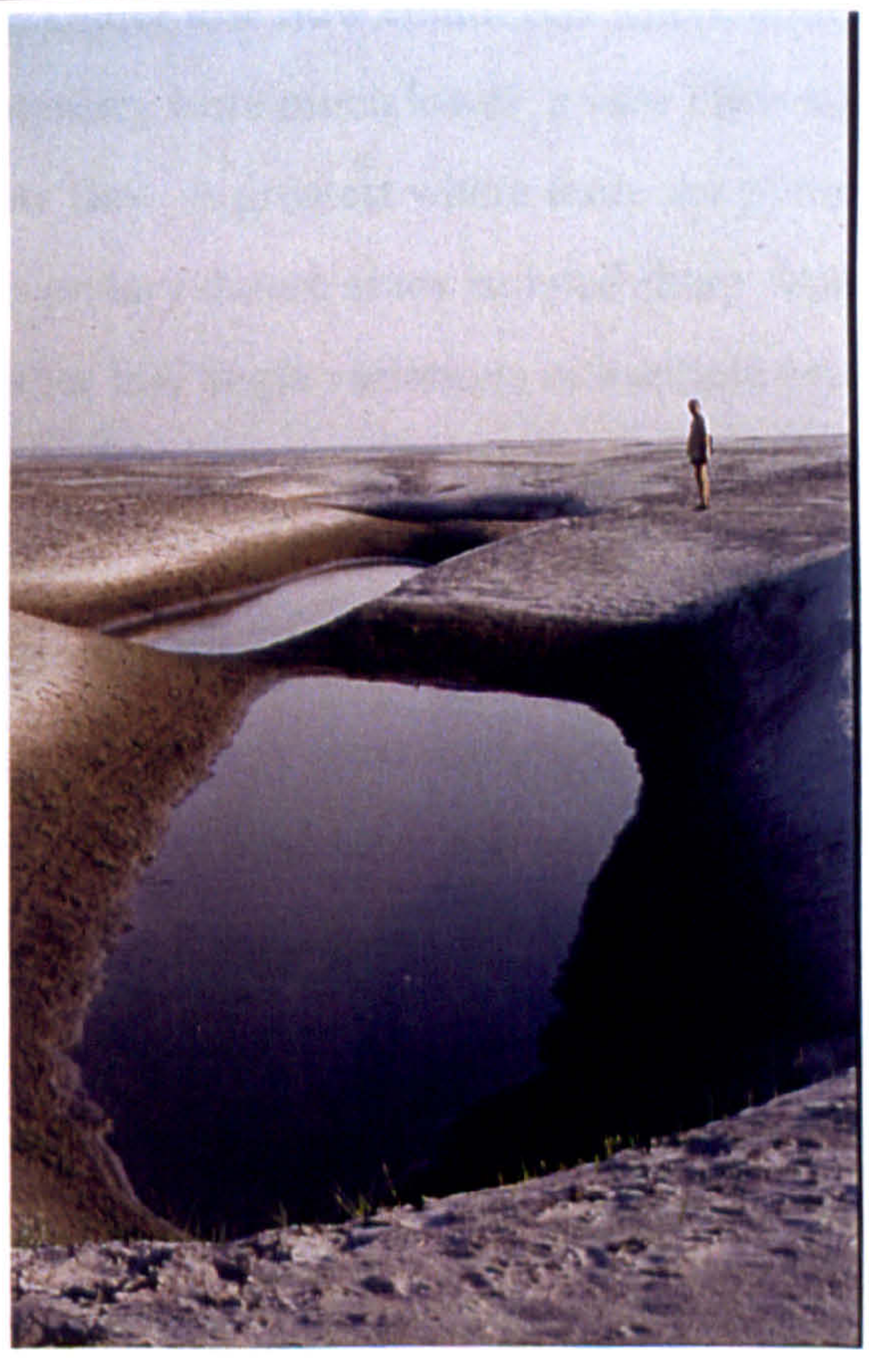

(c)

Figure 4.21, Photographs of dunes exposed on bar tops at low flow in March 1995. (a) large (h~ 1.5m) dunes with a sinuous crestline, distinct spurs and troughs. Flow is towards the bottom right, (b) large (h ~ 2.5m) highly three-dimensional dunes with pronounced scour holes. Flow is towards Jim Best and (c) small (h~ 0.15 - 0.35m) dunes with gently sinuous crestlines. Flow is towards the observer.

4.8.2 Side Scan Sonar Surveys

In conjunction with detailed surveying of the cross-sectional morphology of dunes using echo-sounders, side scan sonar surveys (SSS) were also carried out during two survey periods, namely March and September 1995, in order to monitor the river bed in planform. Although side scan surveys of alluvial and estuarine bedform morphology have previously been conducted where flow rates were low (e.g. Aliotta and Perillo, 1987; Boothroyd and Hubbard, 1975), there have been few attempts to monitor planform morphology under high flow conditions due to errors induced by high suspended sediment concentrations and the increased production of turbulence. Both high suspended sediment concentrations and vortices in the water column distort side scan sonar signals by reflecting and absorbing much of the signal energy, thereby masking river bed morphology. By careful adjustment of the gain, distance of the sonar fish from the river bed and boat speed, a reflected signal was obtained under high flow conditions which provided a signal adequate to produce a map of the river bed (Chapter 3). Under low flow conditions where both suspended sediment concentration and turbulence intensity were much lower, a very clear signal was recorded. Signal clarity, both at high and low flow, is greatest where there are primary bedforms present with no superimposed secondary dunes, since isolated sharp changes in bed topography show more distinctly than either low angle variations or multiple breaks in bed slope, i.e. single dunes with a high slip face angle are more easily identified and mapped than low angle superimposed dunes.

Side scan images show downstream and upstream dipping slopes in light and dark tones respectively. A cross-section of the flow column is also shown for each SSS planform image illustrating dune stoss and lee faces. SSS images collected at low flow (Figure 4.22) show three-dimensional dunes with heights of 0.6 - 1.75 m, wavelengths of 5 -30 m and crestline sinuosity ranging from 1.12 to 1.54. A composite mosaic (Figure 4.23) was produced from the SSS records covering an area of 200 m by 1000 m and show dune crestlines. Such composite mosaic tracings of these images allows the assessment of the laterally continuity of crestlines and also the dimensionality of the dune crestlines (Figure 4.23). At low flow rates dune crestlines were continuous for distances of up to 200 m across the survey line reach, although bifurcations are common throughout the survey area.

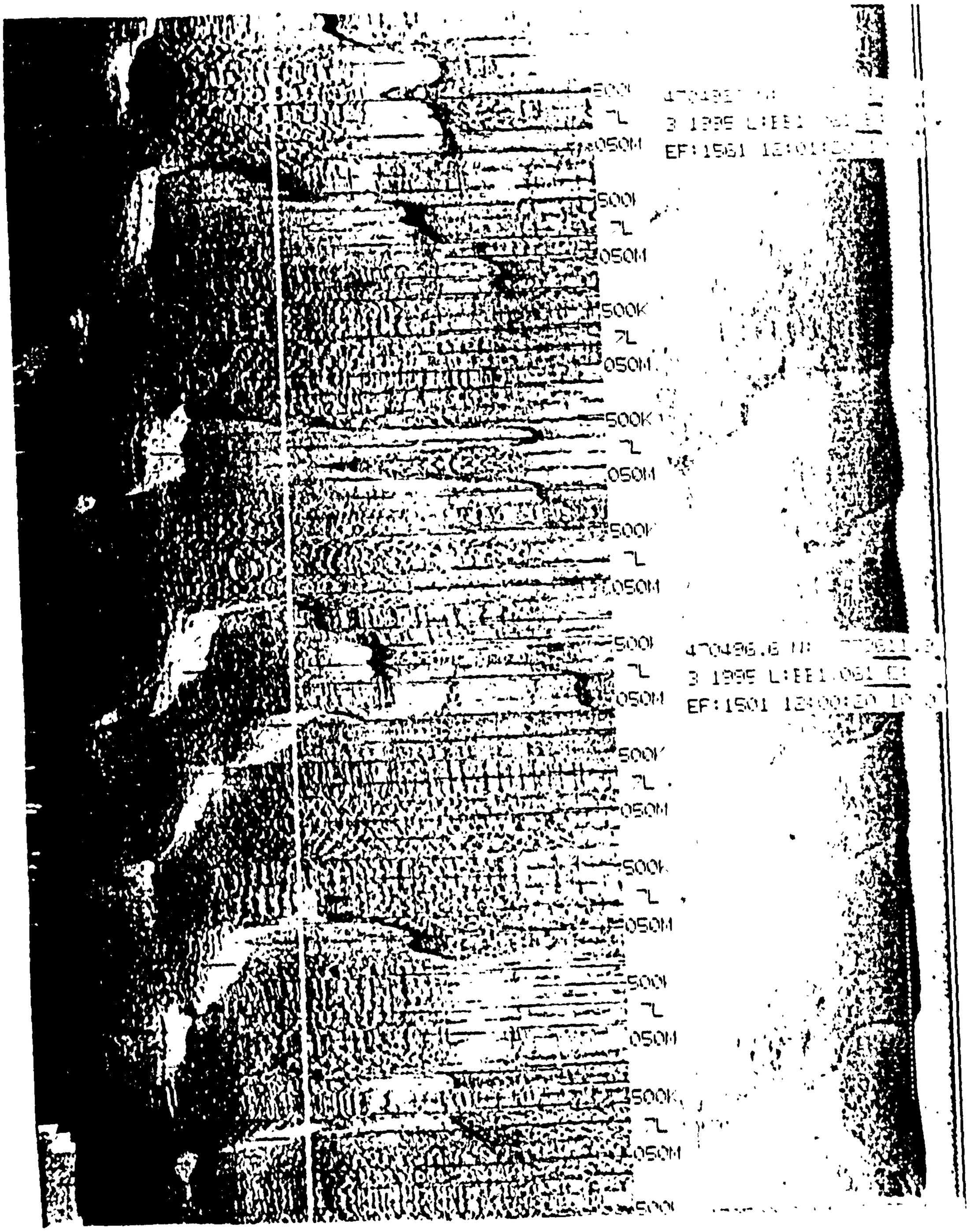

Figure 4.22, Side scan sonar image obtained at low flow (March 1995) illustrating clear dune crestlines, upstream dipping faces are shown in dark tones and downstream dipping faces (i.e. lee faces) are shown in light tones. Flow is from top to bottom. A cross-section of the flow column is given on the right hand side of the diagram illustrating that the dunes are asymmetric in profile.

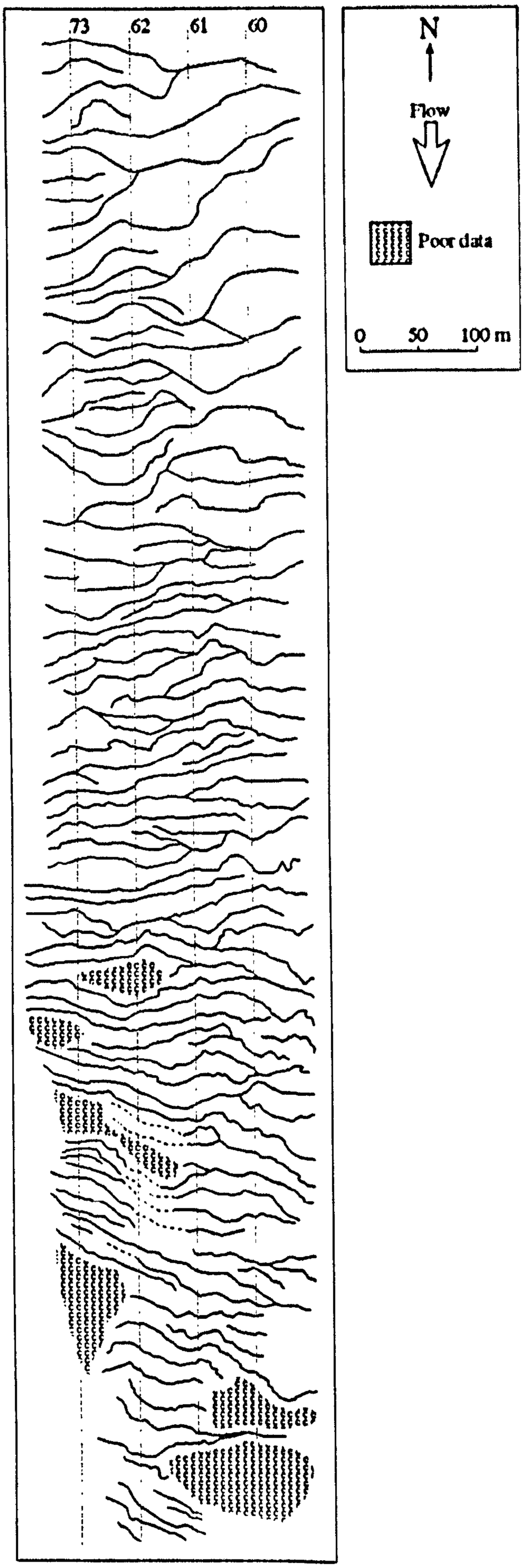

Figure 4.23, Composite mosaic tracing of dune crestline morphology derived from side scan image (March 1995) showing an area of approximately 1 km in length and 200 m in width. Note the sinuosity of both the larger and smaller wavelength dunes.

An example of SSS images collected under high flow conditions (September 1995) is given in Figure 4.24 and a composite mosaic tracing is shown in Figure 4.25, due to the large size of the bedforms at high flow, dune crestlines and also most troughlines are also shown. The echo-sounder cross-sectional bathymetry for each survey line (corresponding to Figure 4.25) is given in Figure 4.26, and shows that the dunes are asymmetric in cross section and have steeply dipping (> 15°) lee faces, larger dunes have been labelled A-F on both diagrams. Figure 4.24 shows two dune lee faces (in lighter tones) which are dipping at angles of 25° and 32°, the lightly shaded strip running from top to bottom is a shadow caused by reflection from the survey vessel hull and is not indicative of a change in bed slope.The SSS mosaic shows that three-dimensional dunes are occurring under high flow conditions, with heights ranging from 0.6 - 8.35 m, wavelengths of 10 - 192 m and crestline sinuosity ranging from 1.05 to 1.41. The dune bedforms are three-dimensional, have sinuous crests and display large scour holes in their troughs. The variability in dune height is much greater in dune troughs than crests (in terms of both width and slope) due to these intermittent scour holes, for example bedform A (Figure 4.25 and 4.26) shows variation in trough (scour) depth (1.5 m) across the channel and a variation in the length (3.2m) of the dune leeside. Bedform A therefore illustrates a variation in erosion and deposition laterally along a dune crestline. The phenomenon of lateral variation in height along the crestline has previously been reported by Dalrymple and Rhodes (1995). Although difficult to resolve using SSS, there are possible spurs bounding the scour holes which together are probably a reflection of preferential sediment transport pathways along any particular crestline caused by the lateral variation in flow conditions along a dune crestline. Lateral crestline continuity is shown to be high for these bedforms (Figure 4.25) which is contradictory to the widely held, but little tested, theory that only two-dimension dunes are laterally continuous. This adds support to the theory that dune dimensionality is a function of temporal history (Baas, 1994) rather than solely flow strength. Lateral continuity appears to be greater for larger dunes from these data but this may be an artefact as larger dunes are more easily recognisable from the original SSS output.

In addition to the planform map produced by the SSS, there is also a reproduction of the vertical flow column (Figure 4.24). The vertical depth section is recorded to ensure signal accuracy by indicating whether the SSS signal is efficiently tracking the river bed, but may also indicate boundaries of fluid marked by variations in water density. The SSS therefore records changes in suspended sediment concentration in the water column. As the sensitivity of the instrument to density variations in the water column is low, only density variations under high flow conditions could be visualised due to the larger variation in suspended sediment

concentration. The SSS records from high flow conditions show discrete increases in suspended sediment concentration originating from just downstream of dune crests and from the lower stoss side of dunes ((a), Figure 2.24), which is in accordance with previous studies using acoustic techniques to visualise variations in suspended sediment concentration associated with dunes (Kostaschuk and Church, 1993, see Chapter 2). Kostaschuk and Church (1993) interpreted the density disturbance features on their acoustic records to represent boil generation events. The appearance of boils on the water surface was also observed during this SSS survey, and boil eruption was noted to coincide with variation in sediment concentration in the water column, hence the discrete increases in suspended sediment concentration are interpreted as boil generation. The location of origin of the boils indicates that the production mechanism may be eddy shedding of Kelvin-Helmholtz instabilities from the flow separation zone free shear layer (Itakura and Kishi, 1980; Müller and Gyr, 1982, 1986). Mechanisms of boil generation will be further discussed in Chapters 5 and 6.

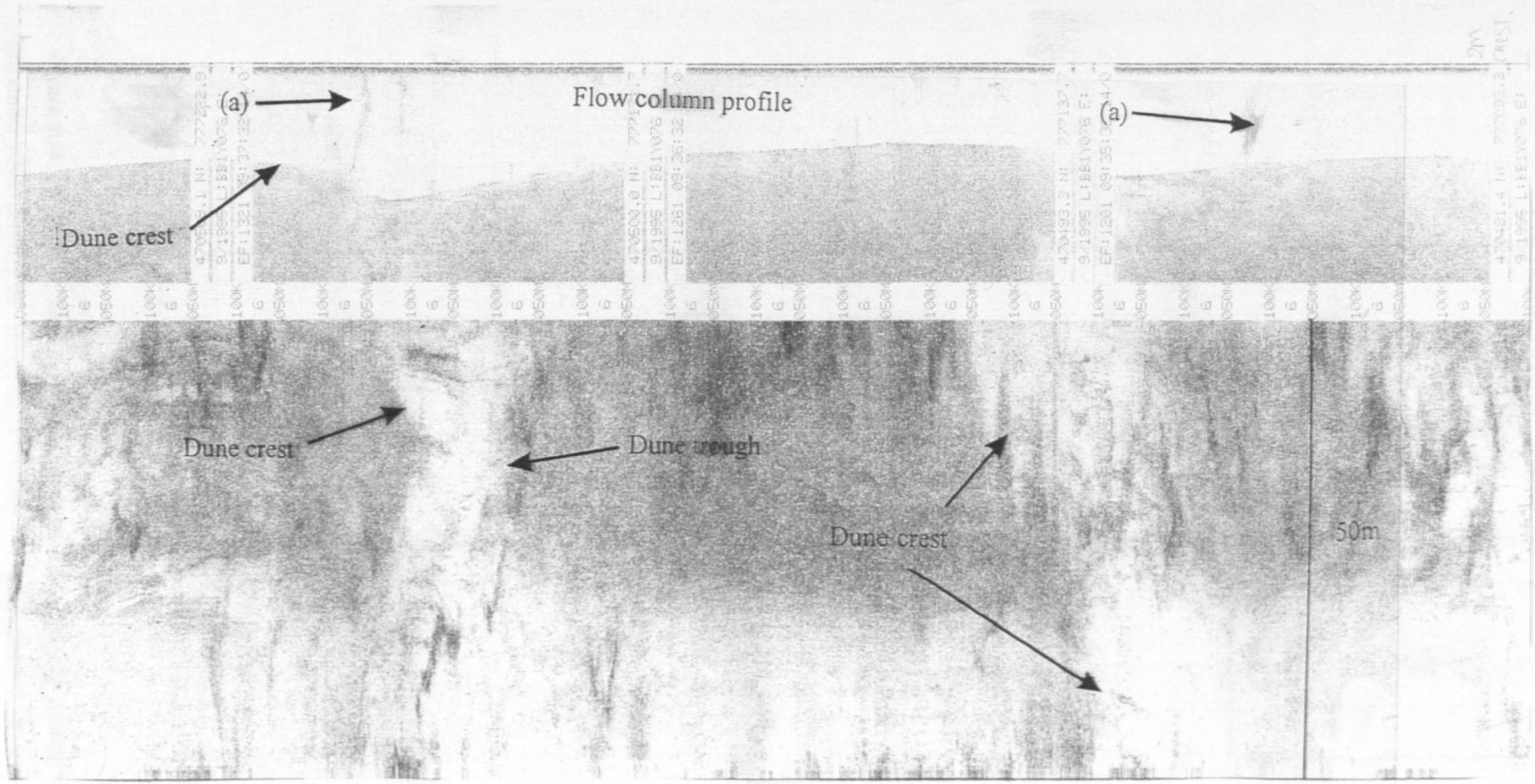

Figure 4.24, Side scan sonar image obtained at high flow (September 1995) illustrating two dune crestlines.
Upstream dipping faces are shown in dark tones and downstream dipping faces are shown in light tones.
Flow is from left to right and a cross-section of the flow column is given at the top indicating two steeply dipping lee faces.

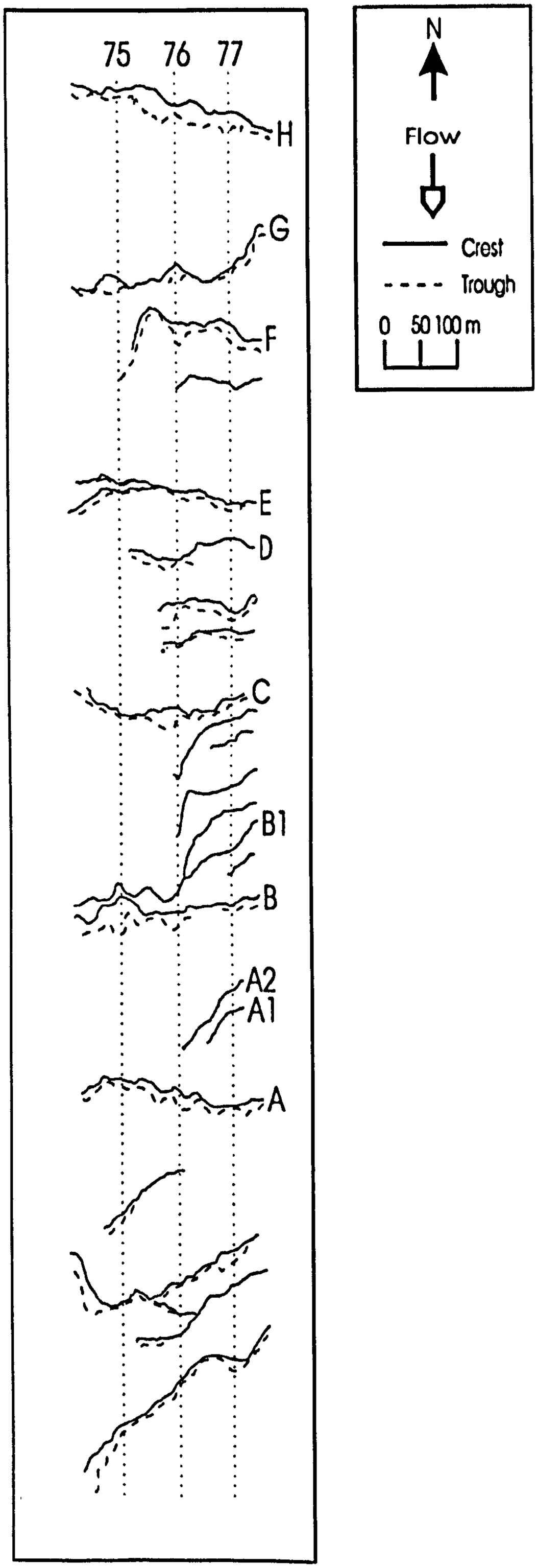

Figure 4.25, Composite mosaic tracing of dune crestline morphology derived from side scan image (September 1995) showing an area of approximately 1 km in length and 200 m in width. Labelled dunes (A-F) are also shown on Figure 4.26 in cross-section.

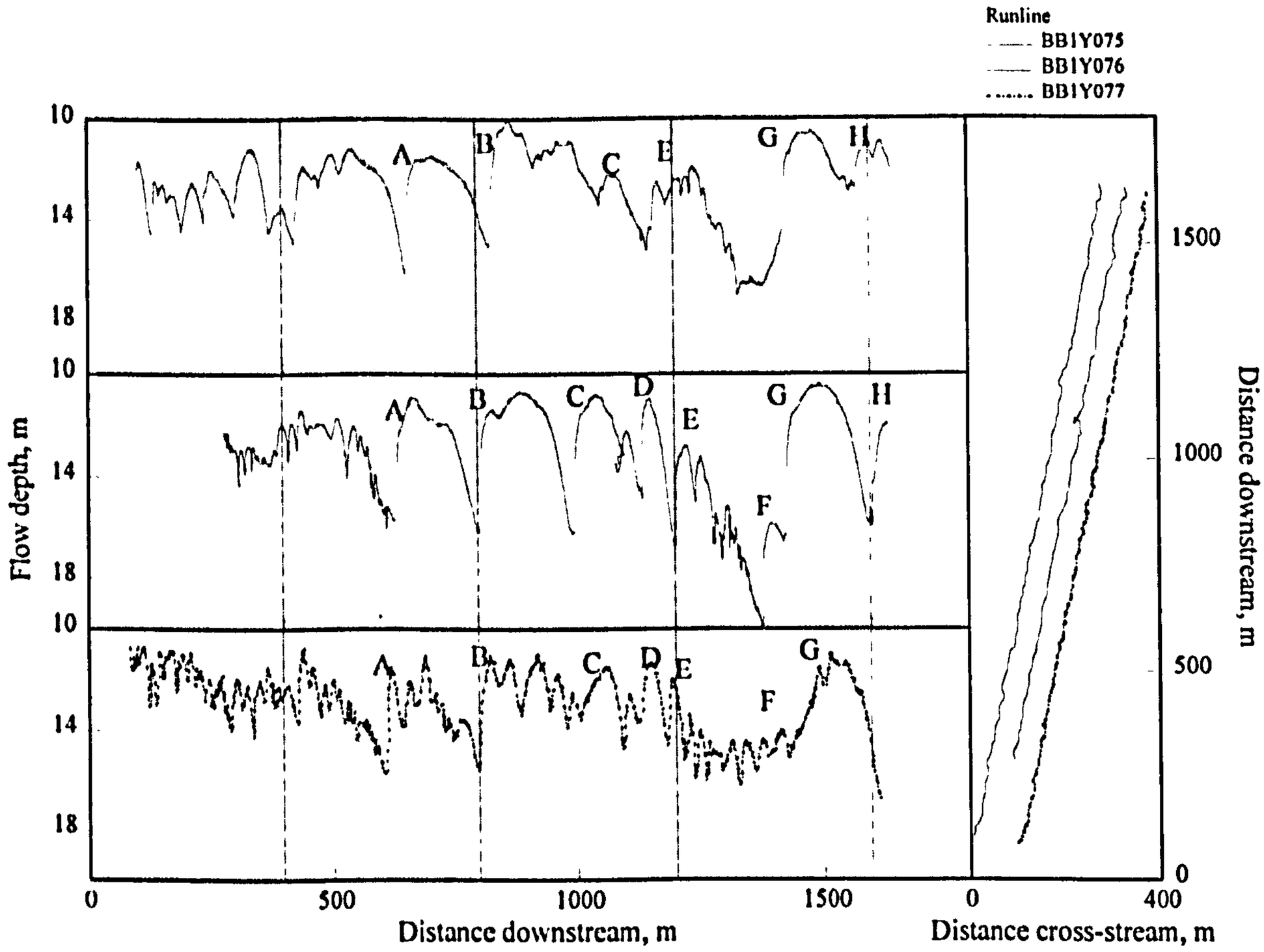

Figure 4.26, Bed morphology using an echo-sounder and survey line location during the SSS survey at high flow stage. Figure 4.25 shows the corresponding planform morphology of the dune field as a composite mosaic tracing.

4.9 Conclusions

This chapter has detailed an extensive survey of dune occurrence and morphology in the Jamuna river. The surveys have shown that dunes are ubiquitous in the Jamuna river at all flow stages and occupy between 38 and 100 % of the river bed. The use of 65 km 'longline' surveys together with morphological studies at three specific sites has provided increased surveillance of the river bed therefore adding credence to the results that dunes and the predominate bedform in both deep channel thalwegs and on bar margins.

Dunes range in height between 0.15 m and 6 m and in wavelength between 3 and 300 m and are therefore described as small to very large using the Ashley (1990) classification scheme. Dune shape has been shown to be complex with a wide scatter in the relationships between the height, wavelength and flow depth parameters. Although dune form index is commonly used to

describe dune steepness or morphology, shape factor is a more detailed way of describing dune shape. Estimates of the dune shape factor which have previously been used when estimating bedload sediment transport and flow resistance should be modified to encompass flow stage. Stage mean values of shape factor have been shown to vary from a minimum of 0.48 at low flow to a maximum of 0.71 at high flow stage.

Dune lee face angles have been shown to range from 2° to 58°, with the mean leeside increasing with flow stage. Flow separation is expected to occur for 45% of dunes at high flow stage with this figure lowering to just 10 % during the falling flow stage, this decrease in lee side angle may be a product of trough infilling by suspended sediment as flow stage decreases. Dune leeside shape is compound as multiple breaks in leeside slopes are common and may therefore produce a complex pattern of flow separation and turbulence generation.

Van Rijn's method of predicting height and steepness has been extended (after Julien and Klaassen, 1995) to encapsulate large sand bed rivers at varying flow stages. Values of the transport stage parameter T increase with flow stage to a maximum value of 58 and height and steepness parameters have been shown to decrease after a T value of approximately 40. The decrease in bedform height occurs for very few dunes and hence the transition from dunes to upper stage plane bed is shown to be uncommon in deep channel thalwegs.

One of the key factors of determining alluvial flow resistance depends on accurate formulation of bedform dimensions that occur at different flow stages and relating them to hydraulic resistance. Hence, flow resistance models which are based on imprecise bedform prediction models, may be inaccurate in calculating flow resistance and channel depth. The methods of van Rijn (1993) and Engelund (1977) have been shown to diverge at rising and high flow stages which is precisely when prediction of friction factors and channel depth is most important for flood prediction. Lee side angle has been shown to be inadequately described by either dune form index or shape factor and the process of flow separation is not accounted for by either of the methods predicting flow resistance. Hence the key process in controlling turbulence generation, dune stability and bed configuration is not taken into consideration when using the methods of Engelund (1977) or van Rijn (1993).

Visual inspection on exposed bar tops has confirmed findings of dune morphology using echo sounders, with both three-dimensional, high flow, large dunes and smaller, low flow dunes being observed on bar tops. Side scan sonar surveys at low and high flow rates have revealed

that dune crestlines are laterally continuous and vary in height. Large scour holes have also been identified along crestlines of large dunes under high flow conditions.

SSS surveys conducted under high and low flow conditions have detailed the planform morphology of dune fields and show that dunes are three-dimensional and have laterally continuous crestlines. Variation in suspended sediment concentration in the water column has been interpreted as boil generation and the location of these turbulent vortices indicates that they may form due to eddy shedding from the flow separation zone shear layer.

This extensive study of dune occurrence, size and shape has therefore quantified river bed configuration at differing flow stages in the Jamuna river. The variation in dune morphology with flow stage has been shown to be great with height increasing by a factor of 6.8 and wavelength increasing by a factor of 8.5 between low and high flow conditions.

Chapter 5. Mean Flow and Turbulence

5.1 Introduction

Morphological studies of bedforms have shown that a wide range of dune shapes, in both profile and planform, exist in large sand-bed rivers, contrary to the simplistic dune morphologies used for most laboratory and theoretical studies of flow over dunes (e.g. Coleman, 1969; Allen, 1983; Julien and Klaassen, 1995; Kostaschuk and Villard, 1996; Amsler and Garcia, 1997; Chapter 4). Although sand dunes vary in geometry, they have typically been characterised in many laboratory and theoretical studies by an asymmetric cross section with a steep leeside slope and a shallow stoss slope. This shape will from here be termed a 'classical' dune. Most numerical and theoretical experiments seeking to define the flow field over dunes have used such a classical dune morphology (e.g. Nelson *et al.*, 1993). Although use of this classical profile has been of great importance in the understanding of the flow field associated with dunes, it cannot be used to fully describe the flow processes acting over non-classically shaped dunes where morphology departs from this classical shape. The range in dune morphology is of great importance as it is the geometry of a dune slip face, and specifically the change in angle at the brink point, which governs whether separation of flow will occur (e.g. Müller and Gyr, 1986; Onslow *et al.*, 1993) and which will therefore influence the entire flow field. Kostaschuk and Ilersich (1995) illustrated that dunes with gently sloping lee faces do not exhibit flow separation and therefore that different flow and sediment transport processes must be acting.

The feedbacks between dune morphology, dune development, flow and sediment transport are extremely complex (Leeder, 1983) and the mechanisms which link them have been somewhat neglected in many previous studies (Müller and Gyr, 1986). The feedback mechanism is of prime importance for naturally occurring bedforms (Kennedy, 1969) as their shapes have been shown to be non-classical in most situations (Coleman, 1969; Kostaschuk and Villard, 1996; Chapter 4). Such non-uniformity of morphology will affect both the production of turbulence and sediment transport. An understanding of the mechanics of the various interactions between the flow and the bed is of prime importance for the development of predictive models for the flow field, sediment transport and bed geometry (Nelson *et al.*, 1993).

This chapter investigates the mean and turbulence characteristics of flow over a range of dunes with dissimilar morphologies that have formed under differing mean hydraulic conditions. A variety of dune shapes were therefore selected for this study over which to conduct at-a-point velocity time

series profiling in order to characterise flow conditions that occur over natural alluvial dunes for both classical and more complex shapes. The presence of superimposed smaller dunes, which migrate with a higher velocity over the stoss (and sometimes lee) side of the parent dune, adds a complexity to the form roughness, and hence the flow field and production of turbulence over the dune. Dunes were selected to provide a range of leeside angles, a range of geometries, in terms of both height and wavelength, and both smooth and rough cross-sectional profiles. The temporal and spatial evolution of turbulent flow structures associated with the dunes is also analysed.

5.2 Data Collection

This chapter presents the results of ADCP velocity profiling conducted while the survey vessel was on anchor during four survey periods, August 1994 (high flow), March 1995 (low flow), September 1995 (high flow) and February 1996 (low flow). Six, at-a-point, velocity time series are analysed from the high flow surveys, which profile the flow column beneath the survey vessel in an array of 0.5 m vertical bins. Additionally, six velocity time series from the low flow period are also detailed. Survey start times and data sample rates for all surveys are shown in Table 5.1, whilst survey site in relation to channel and bar margins is given in Figure 5.1a and survey line positions are shown in Figure 5.1b. Two further time series were collected during the August 1994 high flow survey but are unusable due to data corruption errors and partially incomplete data sets. The study reach for all surveys (Figure 5.1a) is in the eastern Jamuna channel north of Bahadurabad (Figure 1.2) and this site was chosen because it possesses a relatively simple channel configuration with a single thalweg.

To aid identification of each at-a-point velocity profile, individual data sets from hereon will be referred to in terms of the survey flow stage (where H signifies a profile conducted at high flow stage and L signifies low flow stage), the year the survey was conducted and the position of the profile with respect to the position along the bedform (where T signifies a profile conducted over a dune trough, C signifies crest, S signifies stoss and LOW signifies a profile collected over a gently dipping lee face). For example, H/94/T refers to a profiling survey conducted at high flow stage (H), during 1994 (94) over the dune trough (T).

high flow: 13.8.94

file name	*start time*	*end time*	*duration, s*	*ensemble averaging time, s*
H/94/C1	11:44:57	12:37:51	3174	5.5
H/94/C2	12:55:03	15:02:15	7668	10.5
H/94/T	16:04:35	16:56:45	3130	5.5

low flow: 12.4.95

file name	*start time*	*end time*	*duration, s*	*ensemble averaging time, s*
L/95/C	16:35:46	17:16:14	2428	55.5

high flow: 16-17.9.95

file name	*start time*	*end time*	*duration, s*	*ensemble averaging time, s*
H/95/S1	12:54:33	14:02:02	4049	55.5
H/95/C	14:36:43	15:21:45	2698	55.5
H/95/S2	08:57:51	09:59:30	3699	55.5

low flow: 27-28.2.96

file name	*start time*	*end time*	*duration, s*	*ensemble averaging time, s*
L/96/S	10:12:07	11:19:29	4042	5.5
L/96/T	11:46:12	12:56:19	4193	5.5
L/96/TS	14:29:12	15:32:55	3823	5.5
L/96/LOW1	11:27:41	12:21:41	3540	5.5
L/96/LOW2	16:41:05	17:17:42	2197	5.5

Table 5.1, Survey data collection dates, start times and end times. ADCP data averaging setting (ensemble averaging times) are also shown, indicating the collection duration of each outputted data point. One velocity data reading is taken each second.

Although the ADCP continually records one velocity measurement each second, a set or ensemble of data points are averaged (Table 5.1) to decrease errors (Chapter 3). The data recorded in the outputted data acquisition file are therefore an average of either 4 or 5, 10 or 11 or 55 or 56 ADCP measurement pings respectively. This variation in the averaged ensemble times for a specified number of pings is due to the listening time between the ship's onboard computers during data transfer from the ADCP, DGPS and,echo-sounder.

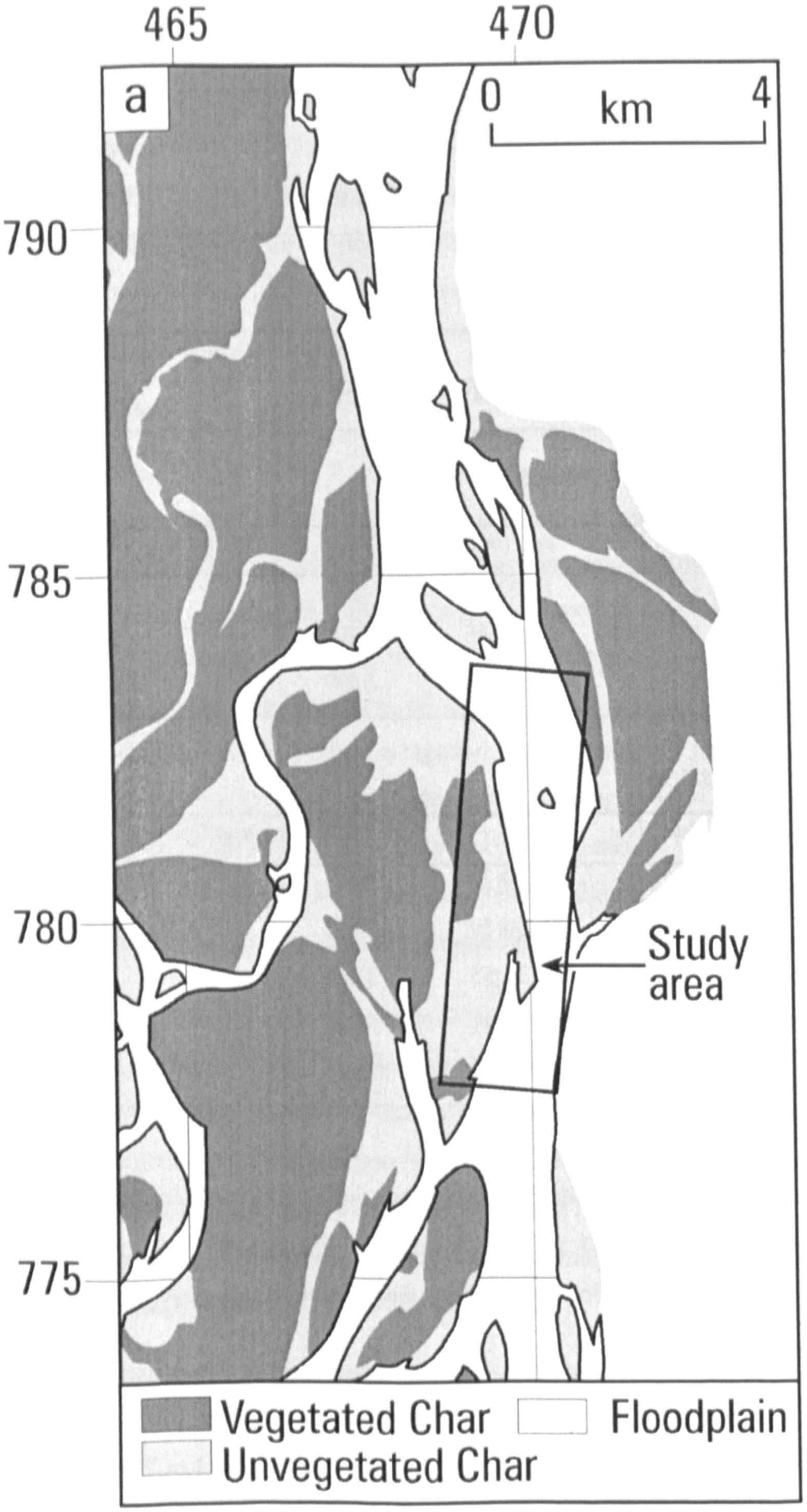

For Figure Caption see over.

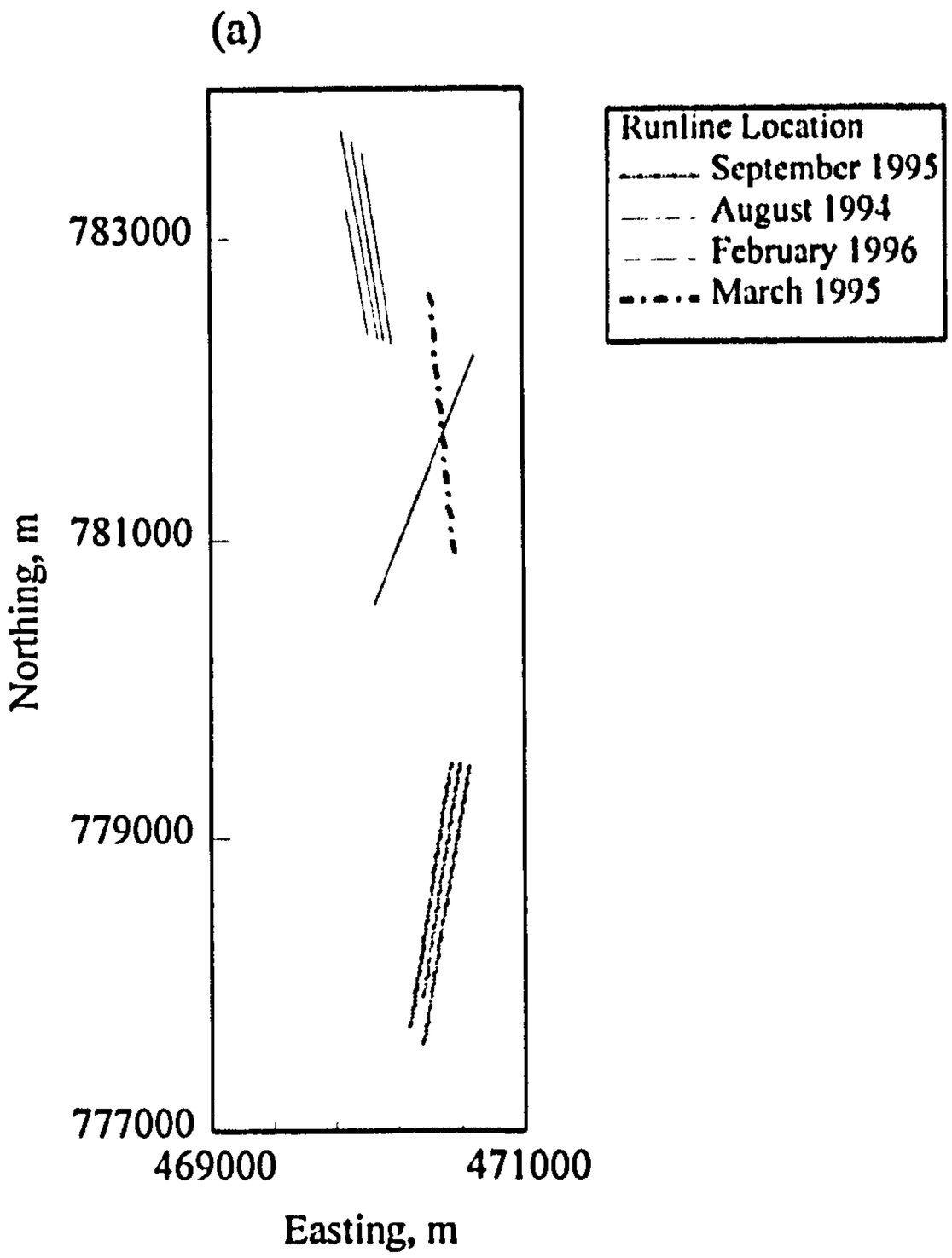

Figure 5.1, (a) survey study reach morphology traced from G12 SPOT image on 24/3/95 (low flow stage) illustrating the dune survey site location (in box) in relation to bank lines and bar margins, *(b)* Runline locations for surveys conducted during August 1994 (high flow), March 1995 (low flow), September 1995 (high flow) and February 1996 (low flow). All downstream transect lines that were repeatedly surveyed during each study period are shown.

5.2.1 Stage Hydrograph

The August 1994 high flow survey was conducted at close to the maximum annual flood discharge (Figure 5.2). Mean water level during the survey was 18.2 m compared to a maximum of 18.5 m during the flood peak of the 1994 hydrograph. During the March 1995 survey, mean water level was 13.2 m which was very close to the minimum water level recorded for the 1995 hydrograph (13 m). The 1995 flood season was more severe than 1994 with maximum water levels reaching over 20 m, which represents a 20 year flood (M^{c}Lelland *et al.*, 1998). No surveys were conducted during the peak flow interval due to difficulties in navigation and vessel manoeuvring in the channels, with maximum surface velocities exceeding 3 ms^{-1}. The 1995 September survey was conducted under

similar flow conditions to August 1994 and the February 1996 surveying was also executed under similar conditions to the previous low flow survey.

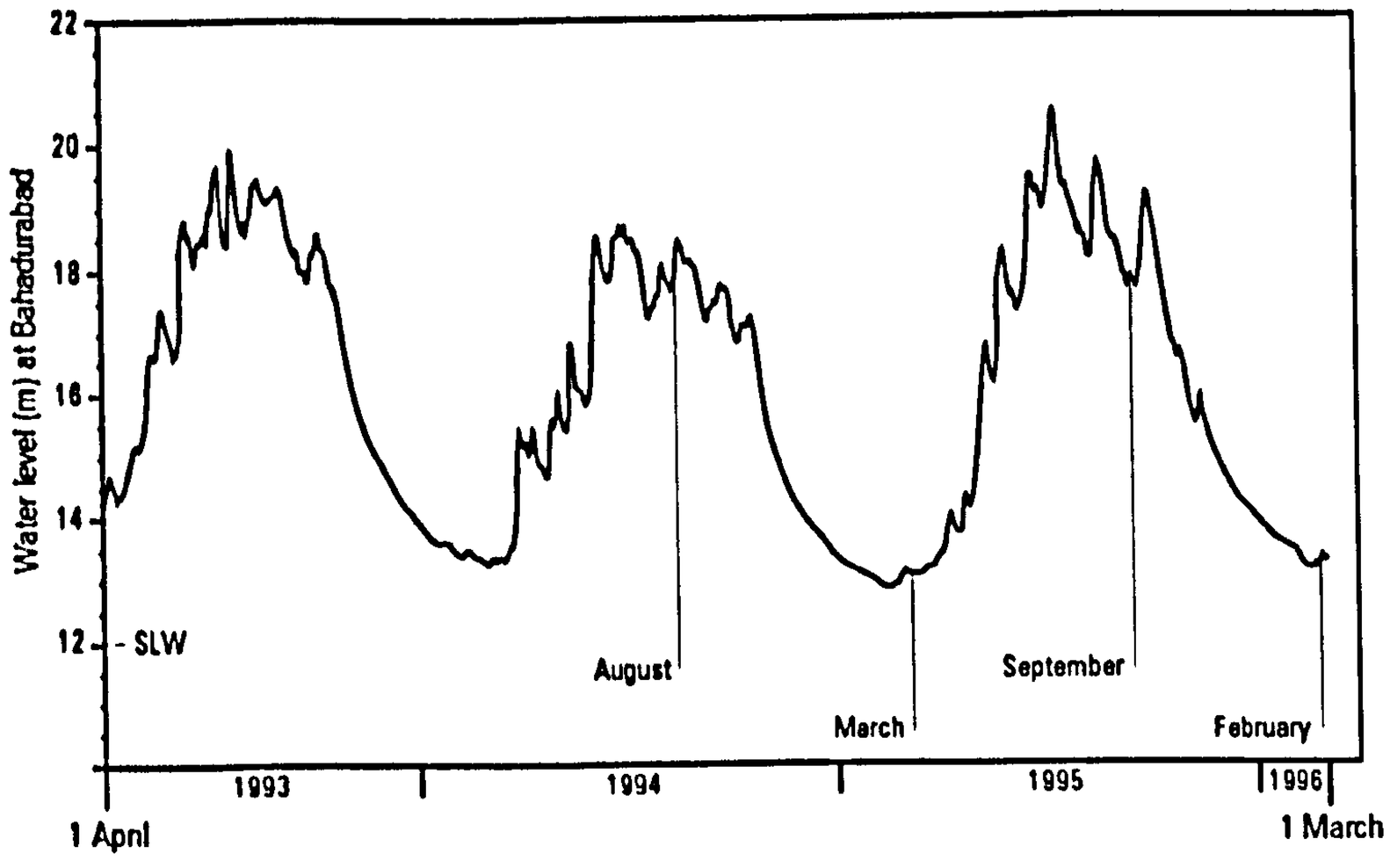

Figure 5.2, Stage hydrograph covering the period from 1994 to 1996 recorded at Bahadurabad. The mean date of each survey are superimposed on the hydrograph.

5.2.2 Bathymetric Profiling

In addition to the collection of time series data, repeat surveying of the transect runline on which the profile points are located was also carried out, both prior to and after the at-a-point velocity time series profiling. Bathymetric profiles of the runlines surveyed during all study periods are shown in Figure 5.3 in order to illustrate changes in the cross-sectional morphology across the whole dune field. For the August 1994 survey the bathymetric profiles (Figure 5.3a) indicate that the dune over which surveying was conducted was the second largest (in terms of height and wavelength) of the population, the dune was selected for surveying because of the classical asymmetric geometry and smooth profile. During the March 1995 survey the dune selected for at-a-point profiling was characteristic in cross-sectional shape of the dune population but was one of the largest bedforms present (Figure 5.3b). The profile dune from the September 1995 survey was the largest in the dune field surrounding it and, like the August 1994 survey, had a classical asymmetric shape (Figure 5.3c). Dune morphology was much more irregular during the February 1996 survey and the dunes selected for at-a-point profiling exhibit a range in geometry (Figure 5.3d). Repeat surveying of each transect line is important as it enables quantification of dune migration rates and any changes in morphology

that may occur during the survey period which may significantly influence the mean velocity and turbulence fields associated with the dunes.

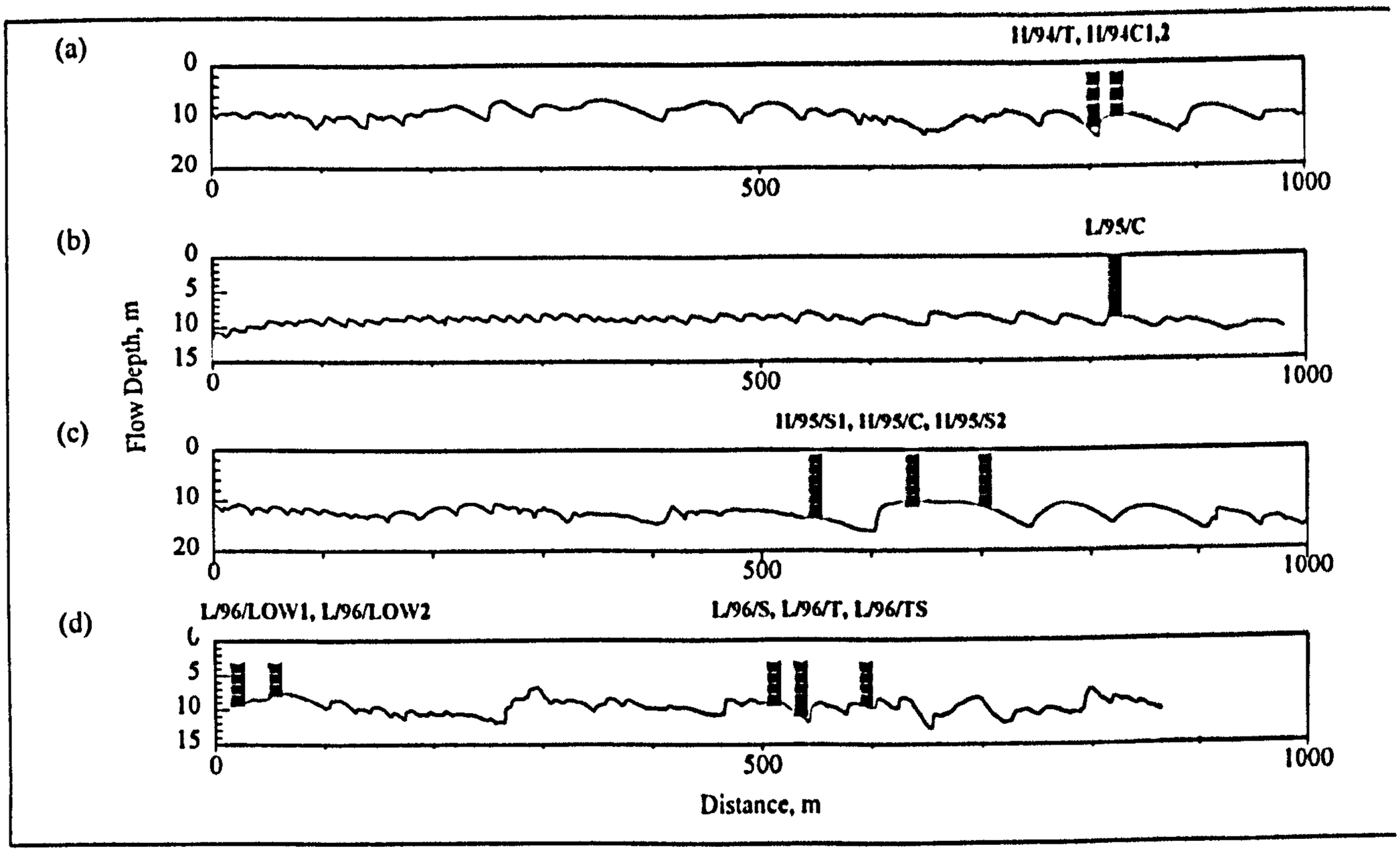

Figure 5.3, Downstream river bed bathymetric profiles showing cross-sectional morphology of dune fields for (a) August 1994, (b) March 1995, (c) September 1995 and (d) March 1995 surveys. At-a-point velocity profiling location and nomenclature are shown for each transect. Note that vertical exaggeration is different for the low and high flow survey periods.

5.3 Dune morphology

The dunes over which the velocity profiling was conducted were selected to provide a range of morphologies, thus enabling investigation of any changes in the associated flow characteristics. The selection process involved surveying several downstream transects using the echo-sounder to locate appropriate bedforms. When a desired bedform (e.g. steep leeside slope with a smooth shape for the high flow survey) was located, at-a-point profiling positions were chosen and the boat manoeuvred as close as possible to the required site. Velocity time series profiling locations for each survey period were selected from the bathymetric transects which are shown in Figure 5.3, and detailed

cross-sectional profiles of each dune over which surveying was conducted are given in Figure 5.4, with the time series profiling positions indicated.

During both surveys conducted under high flow conditions a steep, smooth, classical, asymmetric dune was selected over which to profile. For comparison, the low flow survey undertook to study flow over smaller, high and low lee face angled dunes with smaller dunes superimposed on both the lee and stoss sides. Profiles were carried out over the crest, trough and/or stoss side of the selected dunes. Details of the dune geometries, mean flow conditions and profiling location with respect to position over the dunes selected for profiling are given in Table 5.2a for the low flow surveys and 2b for the high flow surveys. These data illustrate the variation in mean hydraulic conditions between low and high flow conditions, with an increase in mean depth averaged velocity from 0.89 ms^{-1} to 2.26 ms^{-1} and an increase in mean Froude number from 0.09 to 0.21. Mean flow depth increases by 2 m between the survey periods from 9.4 m to 11.4 m and mean dune height more than doubles between low flow and high flow surveys. These variations in flow conditions and the response of mean dune geometries agree well with the detailed bedform morphological studies described in Chapter 4.

Low flow 1995 and 1996

(a)	L/96/TS	L/96/T	L/96/S	L/96/LOW2	L/96/LOW1	L/95/C
H, flow depth, m	9.85	9.9	9.6	9.7	8.85	8.7
h, height, m	1.4	2.85	1.3	2.15/09	2.15/15	1.4
lee angle ,°	35	40	-4.6	8.5/3.5	8.5 /4.9	12
λ, wavelength, m	20	143	102	140 /28	140/66	49.8
profile position	stoss/ lee	trough	stoss	lee / lee	lee / lee	crest
No. of secondaries	0	3	2	3	3	0
U, mean velocity ms^{-1}	0.87	0.87	0.87	0.87	0.87	0.99
Fr Number	0.09	0.09	0.09	0.09	0.09	0.11

high flow 1994 and 1995

(b)	H/94/T	H/94/C1	H/94/C2	H/95/S1	H/95/C	H/95/S2
H, flow depth, m	13.35	9.9	9.9	13.6	10.1	11.4
h, height, m	2.6	4.4	4.4	5.5	6	6
lee angle, °	30.2	55.2	55.2		42	42
λ, wavelength, m	51	74.3	74.3	123.2	123.2	123.2
profile position	trough	crest	crest	stoss	crest	stoss
no. of secondaries	0	0	0	0	0	0
U, mean velocity ms^{-1}	2.06	2.06	2.06	2.47	2.47	2.47
Fr Number	0.19	0.19	0.19	0.23	0.23	0.23

Table 5.2, Statistics detailing dune morphology and mean hydraulic conditions for the surveys conducted under: (a) low flow and (b) high flow conditions. x / y refers to the primary dune and secondary dune superimposed upon it where the profile location is above a superimposed secondary dune.

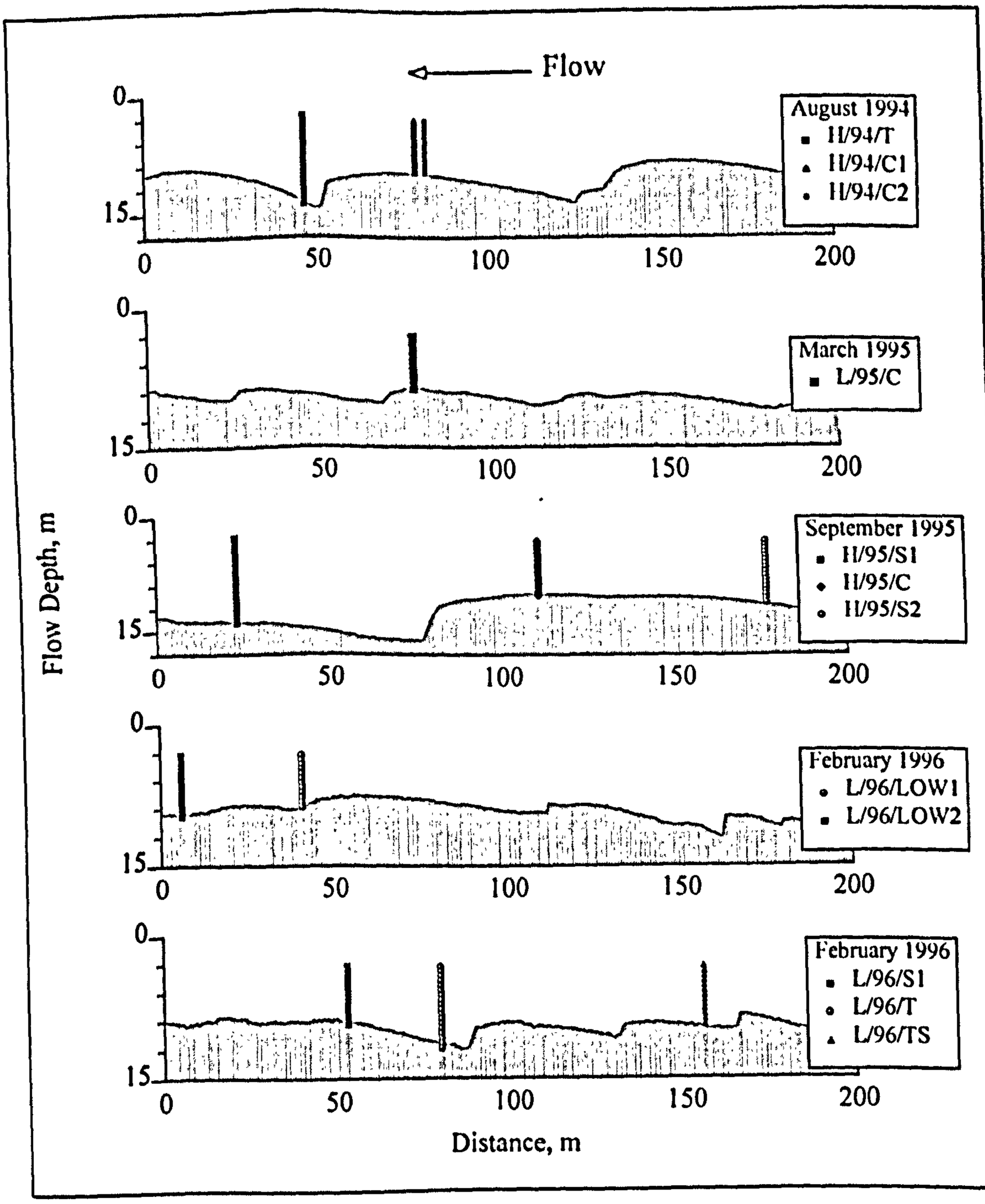

Figure 5.4, Detailed cross-sectional morphology of dunes for each survey period over which at-a-point velocity time series data were collected showing all profile locations and nomenclature.

5.3.1 High Flow Survey, 1994

The selected dune over which at-a-point profiling was conducted had a height of 4.5 m, wavelength of 74.3 m, steep leeside angle (35°), in a maximum flow depth of 14.2 m and was asymmetric in cross-section with a lee:stoss ratio of 1:3 (Figure 5.4). At the time of transect surveying, the dune had no secondary dunes superimposed on either the stoss or leeside. The profiling positions are located on the crest (H/94/C1, H/94/C2) and above the trough (H/94/T). For the high flow survey, two transect surveys were carried out at 09:00 and 17:10 during which time the dune migrated by approximately 12 m (a migration rate of 0.0004 ms^{-1}) and did not alter in cross-sectional morphology.

5.3.2 Low Flow Survey, 1995

One at-a-point velocity profile (L/95/C) was surveyed in March 1995. This profile was measured on the crest of a 1.4 m high dune with a wavelength of 50 m and in a flow depth of 9 m (Figure 5.4). The dune was asymmetric in shape (the lee:stoss ratio was 1:4) with a gentle leeside slope of 12°. There were no secondary dunes superimposed on this dune which was characteristic of all the dunes on the transect line surveyed (Figure 5.3b). Side scan sonar surveying was also conducted during this survey (see Chapter 4, Figure 4.23) which showed that the dune over which profiling was conducted had, in planform, a sinuous crest line with occasional scour holes located laterally along the trough.

5.3.3 High Flow Survey, 1995

High flow surveying for the 1995 flood season was conducted over a large (6 m high, 145 m wavelength) dune (Figure 4) which was asymmetrical in shape (lee:stoss ratio of 1:3) with a flow depth of 16.1 m, height of 4.45 m and slip face angle of 42°. The dune had no secondary bedforms superimposed on either the stoss or lee side. Profiles were collected from the crest (H/95/C) and stoss side (H/95/S2) of the dune and on the stoss side (H/95/S1) of the subsequent downstream dune. Repeat transect surveys were carried out over the profiling location at 08:54 on the day of surveying and 08:05 on the following day by which time it had moved 35.5 m giving a dune migration rate of 0.0004 ms^{-1}.

5.3.4 Low Flow Survey, 1996

Two dissimilarly shaped dunes were selected for at-a-point profiling over at low flow conditions (Figure 5.4). Firstly, a low angle (8.5°) slip face dune with secondary dunes superimposed on the lee and stoss side was chosen. Two profiles were carried out over this gently sloping dune, one just downstream of the crest (L/96/LOW1) and one in the trough (L/96/LOW2) of the primary and secondary dune. The dunes had a height of 2.15 m, a wavelength of 140 m, and showed lower cross-sectional asymmetry than all of the other dunes over which profiling was carried out, with a lee:stoss ratio of 1:1.5.

Secondly, a steeper angled (35°) slip faced dune with three secondary dunes migrating up its stoss side was monitored. Three vertical profiles were collected over this steeper dune, one in its trough (L/96/T), one on the stoss of the following bedform (L/96/S) and finally, in order to investigate the influence of secondary dunes on the flow field, a profile was collected on the stoss side of the primary dune but within the trough of the middle steep-faced secondary dune (L/96/TS). The primary bedform was asymmetric in cross section (lee:stoss of 1:6), had a height of 2.85 m, and wavelength of 143 m and a flow depth of 9.9 m. Repeat transect surveying showed that migration rates were much slower during the low flow survey with primary dune migration rates of 0.05 m hr-1 and secondary dune migration rates of 0.11 m hr^{-1}.

5.4 Profile Depth

Changes in profile depth occur during all at-a-point time series collection periods which may be caused by movement of the survey vessel or by changes in bed height due to bedform migration. This variation in profile depth is maximised during the high flow survey due to the relatively larger steeper dunes, higher flow rates and poor weather conditions which cause the boat location to oscillate about its anchor. An example of boat position tracking from the DGPS for the August 1994 high flow survey (profile H/94/T) is shown in Figure 5(a) with the positions of the repeat runline surveying displayed. The maximum boat oscillation distance is 12 m for profile H/94/C1, 25 m for H/94/C2 and 20 m for H/94/T. An echo sounder track of bed level for profile H/94/T is shown in Figure 5(b) and shows a variation in flow depth of 2.1 m.

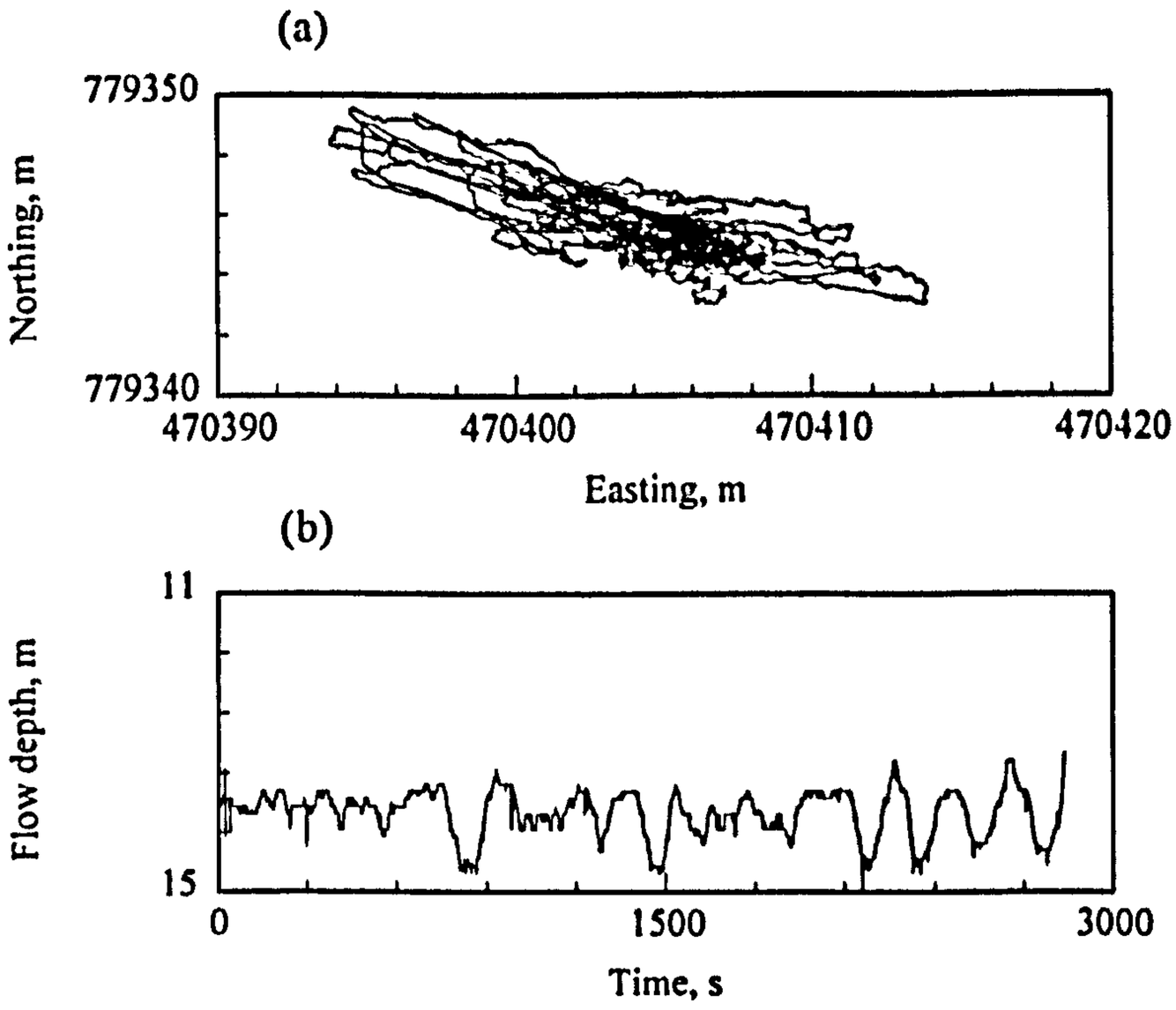

Figure 5.5, (a) Survey vessel location tracking by DGPS during at-a-point velocity time series profiling, showing boat movement during time series data collection. (b) Variation in bed level recorded using the echo-sounder for the 11/94/T at-a-point profile survey.

As variation in bed level (Figure 5.5b) increases and decreases in amplitude during the survey, it cannot be associated with the migration of the primary bedform alone as this would result in a consistent trend. The oscillation period is of the order of 200 to 300 s ' and there are two explanations for this variation:

1) a series of secondary dunes are migrating over the dune crest
2) the variation in height is solely due to the boat's oscillation

It seems unlikely that smaller dunes are superimposed on the primary bedform (Figure 5.3) since secondary dunes are not observed on the runline transect and they would not be expected to be a transient feature on the time scales involved. Fluctuations in flow depth at-a-point may therefore be associated with the boat's motion alone. The absolute boat drift from the start position of profiling is illustrated in Figure 5.6a and b in relation to flow depth. This shows that the variation in flow depth is predominantly caused by the movement of the survey vessel about its anchor and this phenomena is consistent for all three surveys. However, it is important to remove the motion of the boat from recorded at-a-point profile velocities. This was conducted off-line by calculating average boat speed for each ADCP velocity ensemble and deducting this from the collected velocity time series.

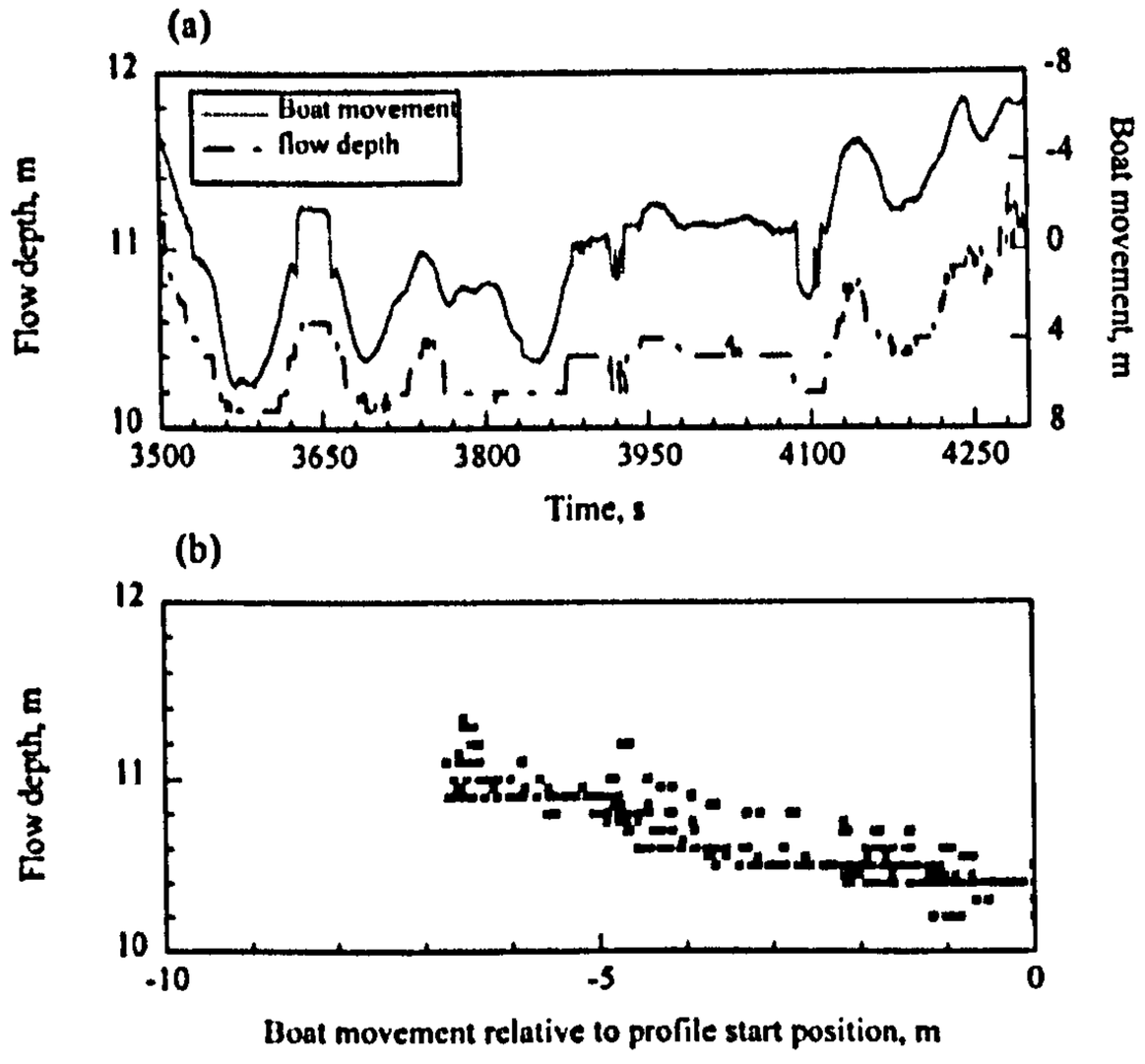

Figure 5.6, The relationship between bed level and boat motion, where the boat migration distance is relative to a common datum which is the boat location at the beginning of the at-a-point profile survey. (a) illustrates flow depth and boat movement for an 800 s extract of the time series (b) shows flow depth and vessel motion association for the entire time series.

Although the survey vessel motion will not greatly increase errors in processed velocity data, it will affect the position of the profile relative to the dune. However, the profile location is moving roughly perpendicular to the mean flow direction (because the vessel is moving about the anchor site) and therefore parallel to the dune crest. The survey vessel motion will therefore only increase errors significantly if the movement of the survey vessel is great in comparison to the dune size or if the planform dimensionality of the dune is high. During the low flow surveys when dune size was significantly smaller than during the high flow surveys, movement of the survey vessel when at-a-point profiling was decreased due to lower wind speed and lower flow velocity: the maximum oscillation distance was 14 m.

If the dune, and hence the flow over it, was purely 2-dimensional then movement of the profile perpendicular to the crest would have little effect on the relative location of position along the bedform and profile location. However, it seems unlikely that such dunes are purely 2-dimensional as

bedforms exposed on bar tops during the low flow season often exhibit 3-dimensional morphology, especially if steep angled scour holes are present in the dune trough. Such scour holes measured on bar tops generally had widths of less than 10 m and depths of up to 2.8 m. If such a scour hole was present at any of the at-a-point survey locations then a rapid and large variation in bed height would be expected during profiling. As such large gradients are not observed during any of the at-a-point surveys it can be assumed that the survey locations are not in close proximity to scour holes.

5.5 High Flow Surveys

5.5.1 Introduction

Many previous studies (e.g. Raudkivi, 1966; Engelund and Fredsoe, 1982; Müller and Gyr, 1982; McLean and Smith, 1986; Mendoza and Shen, 1990; Nelson *et al.*, 1993, McLean *et al.*, 1994; Bennett and Best, 1995) have described the mean flow field over classical, asymmetric, angle of repose dunes. Such flow fields can be divided in 5 regions, a brief summary of these is given below (for further discussion see Chapter 2) :

1) accelerated and converging flow over the dune crest,
2) a zone of flow separation on the crest leeside with a characteristic recirculation pattern,
3) a decelerated wake region overlying the separation cell and extending downstream,
4) an outer near surface region overlying this wake,
5) downstream growth of a new internal boundary region originating at reattachment.

The highest downstream velocities occur prior to and at the dune crest and are followed by a sudden expansion and separation of flow just downstream of the crest. Across this separation zone, downstream velocity profiles exhibit intense shear or drag and are overlain by a decelerated wake region where flow advection and diffusive mixing occur. The wake region increases in size from the point of separation but decreases in turbulent energy, so by the next crest, flow conditions approximate a uniform boundary layer (Bennett and Best, 1995). Such flow fields over dunes are therefore described as 'quasi-equilibrium' as they are symmetrical over successive crests.

Many studies have shown that flow separation, and its accompanying free shear layer, is the most dominant feature of flow over classical-shaped dunes and that flow separation affects the entire flow field (e.g. Nelson *et al.*, 1993). However, although the shape of the dune crest is known to be one of the most important factors influencing the onset of flow separation, there has been little work to date

studying the variation in flow field associated with changes in the slip face angle (Ogink, 1988). Low slip face angle dunes which lack flow separation in their lee side have been documented in the field by Smith and McLean (1979) and Kostaschuk and Ilersich (1995). These studies suggested that low slip face angle bedforms which lack flow separation originate when suspended sediment transport is dominant, although the same forms have also been observed in bedload transport dominated systems (Carling, pers. comm).

The following section will describe the mean flow profiles from several locations over dunes of different geometries (Figures 5.3 and 5.4), in order to compare these flow field profiles with those described in previous work and to investigate any differences in the profiles with respect to their morphology.

5.5.2 Mean velocity profiles at high flow

Six vertical profiles of downstream and vertical velocities collected during August 1994 and September 1995 are shown in Figures 5.7 and 5.8 respectively. As the flow conditions were similar for the two surveys, the profiles will be described together.

The vertical profile of mean downstream velocity collected over the dune trough (Figure 5.7a, H/94/T) illustrates a typical trough profile shape (e.g. Nelson *et al.*, 1993) with velocity decreasing with depth from a maximum 1.8 ms^{-1} at the ADCP minimum measuring depth to a minimum velocity of 0.01 ms^{-1} near the bed.

(a)

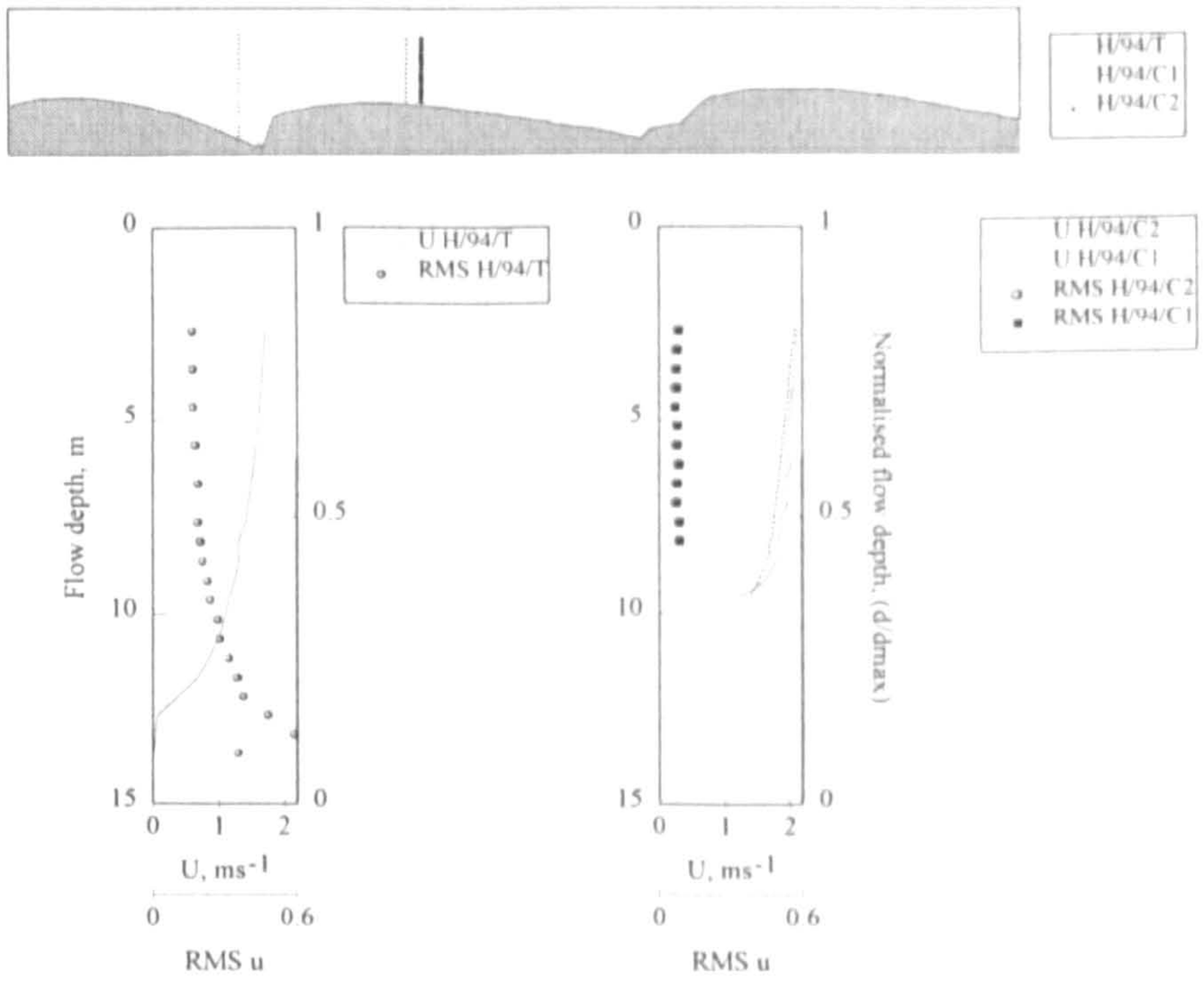
H/94/T
H/94/C1
H/94/C2
0
1
U H/94/T
RMS H/94/T
U H/94/C2
U H/94/C1
RMS H/94/C2
RMS H/94/C1
5
10
15
0.5
0
Flow depth, m
Normalised flow depth, (d/dmax)
0
1
2
U, ms-1
0
0.6
RMS u

(b)

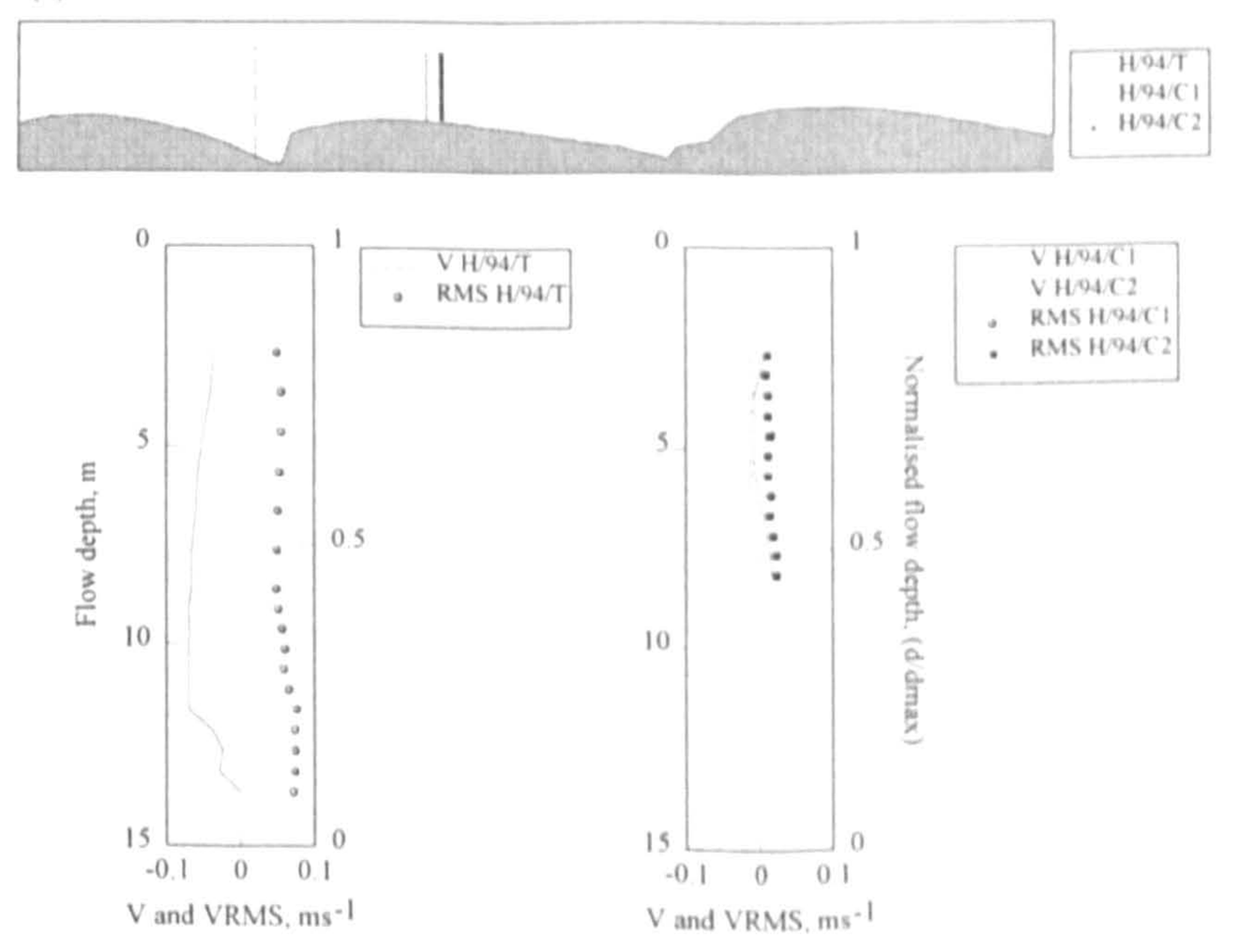
H/94/T
H/94/C1
H/94/C2
0
1
V H/94/T
RMS H/94/T
V H/94/C1
V H/94/C2
RMS H/94/C1
RMS H/94/C2
5
10
15
0.5
0
Flow depth, m
Normalised flow depth, (d/dmax)
-0.1
0
0.1
V and VRMS, ms-1

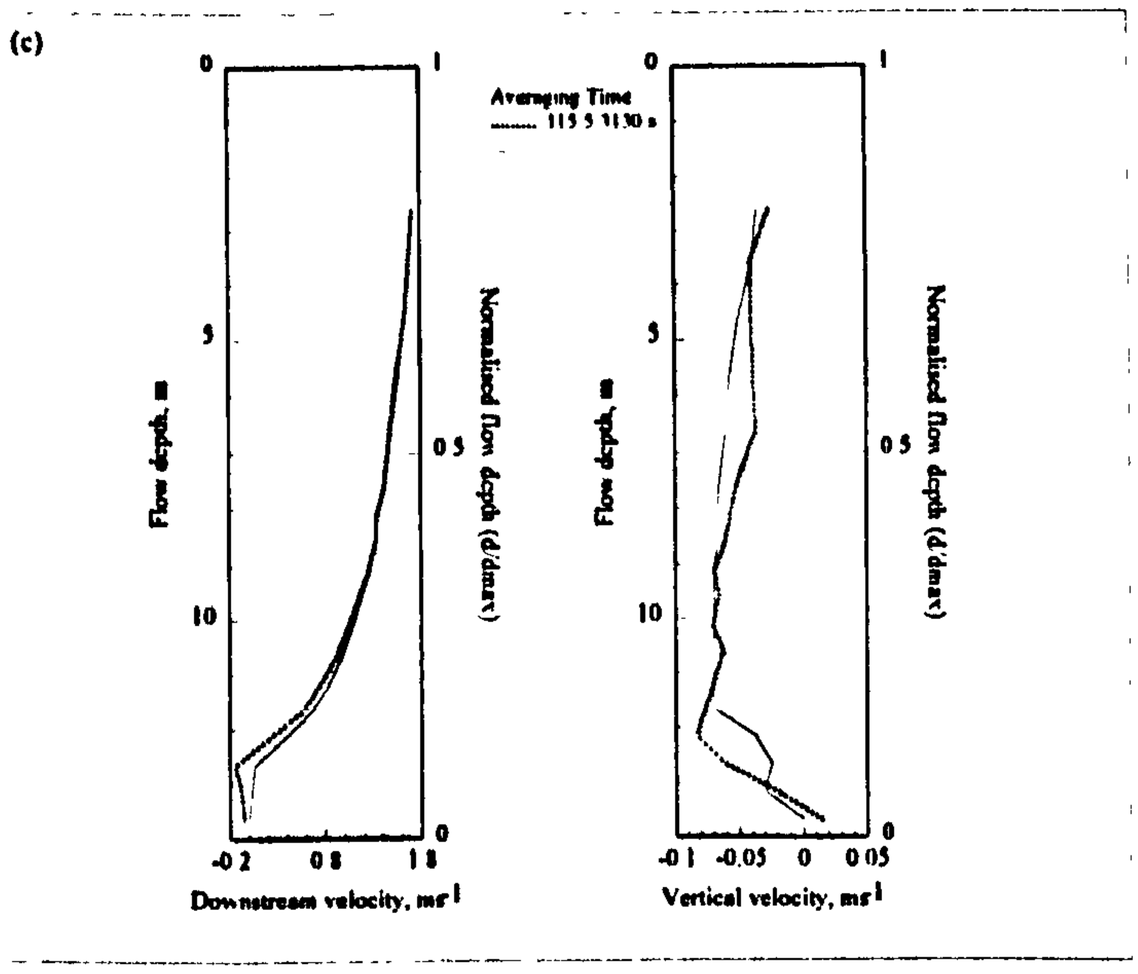

Figure 5.7, Vertical profiles of the mean at-a-point velocity and corresponding RMS values collected during the high flow August 1994 survey over the dune trough (H/94/T) and crest (H/94/C) showing (a) downstream velocity and (b) vertical velocity and (c) both vertical and downstream velocity over the dune trough averaged over the entire time series (3130 s) and over 115.5s.

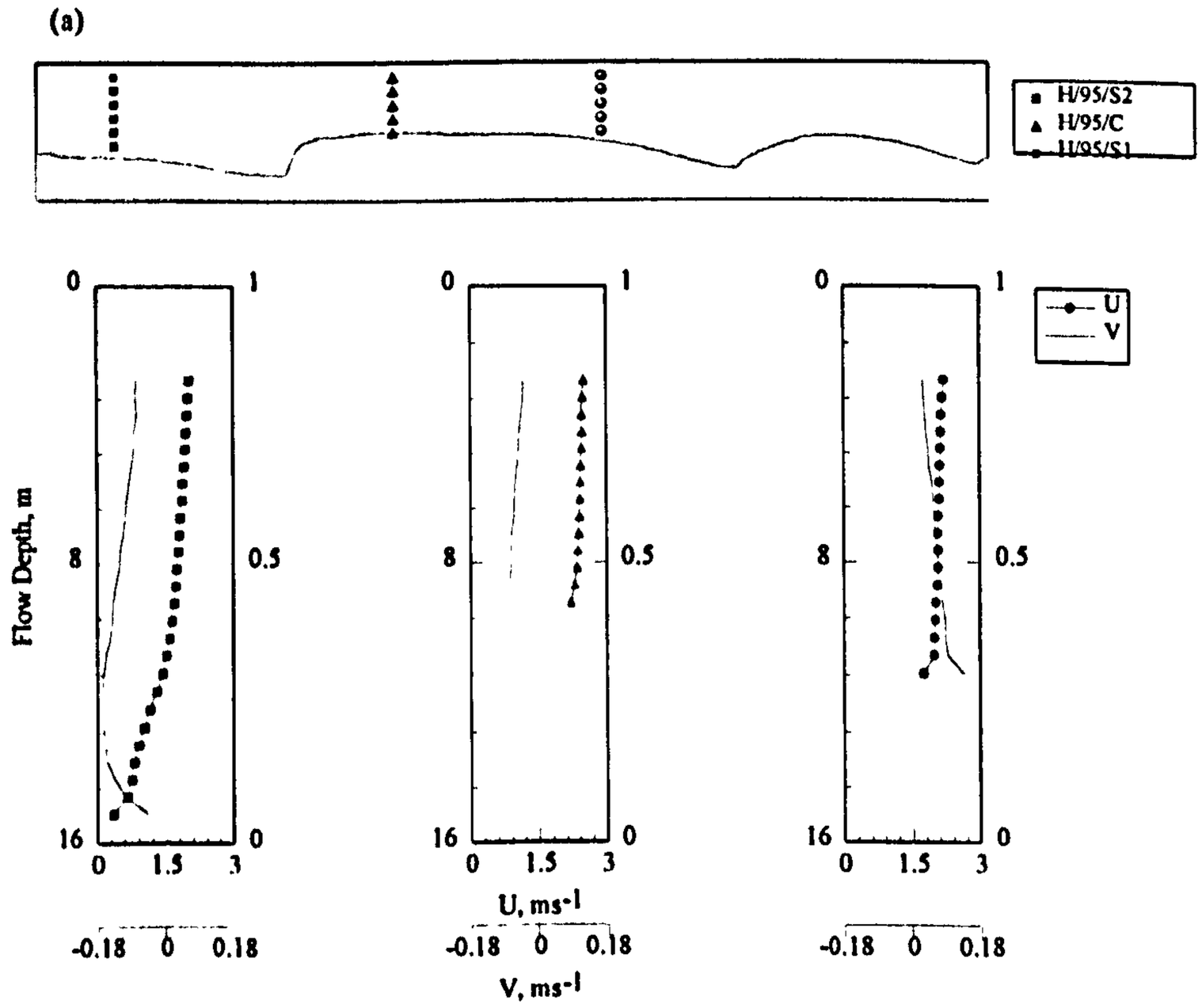

Figure 5.8, Vertical profiles of mean at-a-point downstream and vertical velocity collected during the high flow September 1995 survey over the dune stoss-side, crest and just downstream of reattachment.

The vertical flow column may be divided into 3 regions with a high flow zone extending from near the water surface down to 9.5 m where there is a zone exhibiting high velocity gradients, demonstrating intense shear or drag. The high velocity gradient zone reaches 12.5 m and is overlying a low flow region which extends down to the bed. Throughout the zone beneath the high velocity gradient region, mean downstream velocities are consistently very low, approaching zero at the bed. Simpson (1989) suggested that the definition of a separation cell does not have to encompass constant flow reversal as this condition will only consistently be found under steady, two-dimensional flow regimes. Therefore, although the mean downstream velocity within the low flow region for the entire survey duration is not negative, the occurrence of a zone of high shear above a low flow region indicates that a separation cell may exist. The presence of negative downstream velocity over an averaging time of 115.5 s is shown in Figure 5.7c, thereby confirming that flow separation does exist in the lower section of the dune trough profile. The zones described above are distinguished by their range in downstream velocity and hence by the vertical variation in velocity gradient or shear. In order to further distinguish between the zones, Figure 5.9 shows the vertical variation in the gradient of dimensionless downstream velocity. The mean velocity gradient for profile H/94/T shows a small increase with depth down to 9.5 m, from this depth the velocity gradient more than triples to a maximum gradient of 0.14 m^{-1} suggesting that this section may be termed a shear zone. Beneath the shear zone is a region of very low mean velocity gradient, there is no near-bed increase in velocity gradient, so indicating that bed shear stress is low. Figure 5.9 therefore highlights the vertical change in velocity gradient and therefore aids description of the outer high flow zone and the inner low flow zone which are separated by a region of intense shear. Soulsby (1991) noted the intermittency in flow reversals over estuarine dunes; in this present study of alluvial dunes, instantaneous velocities within the flow separation cell reach -0.5U, these negative velocities will be described and displayed later in Section 5.5.5. It may therefore now be postulated that flow separation does exist over the dune trough even though the mean downstream velocity near the bed is never negative, from hereon the near-bed low flow zone will be referred to as a separation cell. Above this flow separation cell, the downstream velocity is lower than at comparative heights on the other profiles collected, possibly due to flow expansion and deceleration in the wake area above the free shear layer. Towards the water surface, the outer layer of the flow is unaffected by the flow disturbance caused by the separation cell. This profile illustrates the dominant affect of flow separation on the local flow field which has been previously described by Bennett and Best (1995).

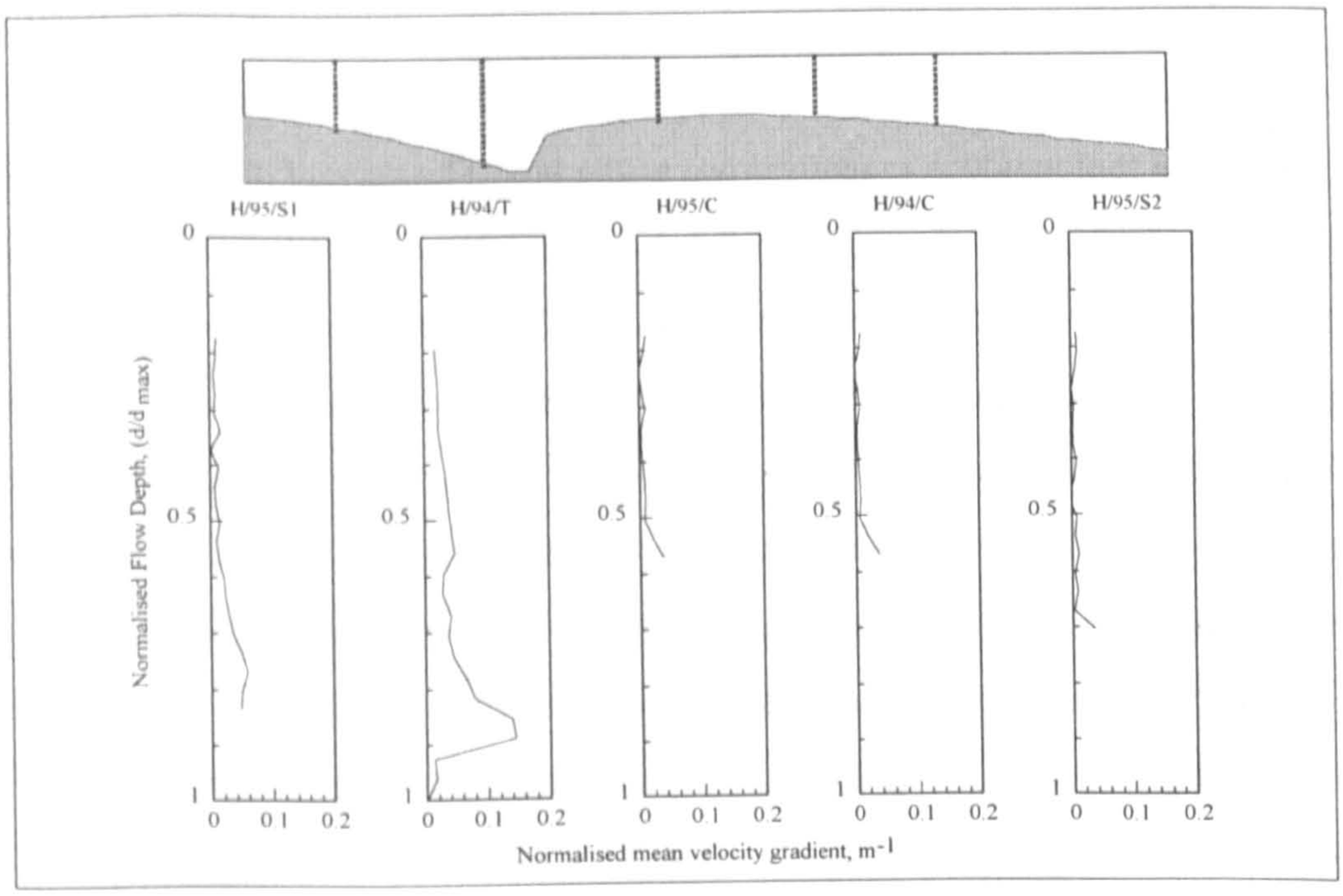

Figure 5.9, Vertical profiles of the time averaged at-a-point normalised velocity gradient collected during the August 1994 and September 1995 surveys. The relative location of each profile is indicated by the schematic above and each profile is labelled.

As flow expansion and separation begins, negative vertical velocities occur as flow is directed towards the bed (Figure 5.7b, H/94/T). Within the flow separation cell the mean vertical velocity is still negative (H/94/T), but the magnitude of the mean vertical velocity is smaller than higher in the flow which may be indicative of a flow circulation pattern. Nearer to the slip face it is expected that positive vertical velocities would occur as recirculation is likely to be stronger there (Nelson *et al.*, 1993).

The subsequent profile downstream (Figure 5.8, H/95/S1) again shows a decrease in velocity with depth with a maximum velocity of 1.7 ms^{-1} located near to the surface. Profile H/95/S1 also exhibits some shear in the downstream velocity from a depth of 10 m and towards the bed. The flow magnitude is lower here than for all of the other profile sections except the trough section, which must again be due to flow expansion and deceleration downstream of the crest. Profile H/95/S1 lacks the low flow zone which was apparent for profile H/94/T, and must therefore be located downstream of the flow reattachment point. The effect of flow expansion on section H/95/S1 is also depicted by the variation in mean velocity gradient (Figure 5.9), as this profile shows the second largest increase (of all the profiles recorded) in velocity gradient with maximum values of 0.055 m^{-1}. The increase in velocity gradient is associated with a zone of flow recovery and growth of a new internal boundary

layer downstream of flow reattachment, comparison with profile H/94/T indicates that the flow has accelerated from the minimum velocity values recorded over the trough, so the effect of flow separation at the dune crest and of the wake region depicted in the trough profile decreases downstream of the trough as diffusion and mixing with the main flow occurs.

On the upper dune stoss side and crest (H/95/S1, H/94/C1, H/95/C) the downstream velocity continues to increase (Figures 5.7 and 5.8) from the levels recorded at profiles H/94/T and H/95/S1. The maximum mean downstream velocity, of over 2.5 ms^{-1} is recorded near the flow surface at the crestal sections. This increase in velocity from the separation cell profile (H/94/T) illustrates that the flow is accelerating over the dune stoss side due to topographic forcing and therefore that maximum downstream velocities must occur at the dune crest. The mean downstream velocity gradient has consistently small values for all of these profiles (H/95/S1, H/94/C1, H/95/C) with only near-bed values showing an increase in velocity gradient above 0.04 m which is due to friction with the bed (Figure 5.9). This topographic forcing and flow acceleration also results in positive vertical velocities near the bed (H/95/C), so the time-averaged vertical velocity over the dune crest is close to zero.

The reliability and reproducibility of these results must be assessed due to the novel technology used to collect the data; to this end, two sets of at-a-point time series were collected from one location and these data are shown on Figure 7a, profiles H/94/C1 and H/94/C2. Both the downstream and vertical velocities deviate from each other by a maximum of 7%. The deviation in mean downstream velocity between the profiles H/94/C1 and C2 is extremely small and shows that the ADCP mean flow field results are reproducible so allowing further investigation of the data. The variation in the two data sets may be partially a consequence of boat movement leading to variation in profile location. However, differences in velocity may also be due to the inherent variation exhibited by field data: each set of velocity measurement collected at any one time and location are unique. The results must also, of course, be examined in relation to other data sets to review the reliability of the data and to investigate the differences in flow fields measured in a scaled experiment compared to a field situation. Before inferences can be drawn to link the processes illustrated by the separately collected at-a-point velocity profiles, the reliability of the data must be substantiated. The flume data of Bennett and Best (1995) are plotted along with all the high flow velocity data in Figure 5.10. To calculate the corresponding profile location, the experimental and field data dune wavelengths were normalised (profile location / total dune wavelength) so the relevant positional profiles could be compared, and flow velocities have also been normalised (velocity / maximum velocity per survey). The amalgamation of velocity profiles from different dunes into one ensemble over a more characteristic or general dune shape is a standard technique (e.g. McLean and Smith, 1979).

This comparison shows very good agreement between flume and field measured downstream velocities, especially for crestal and stoss profiles where the two sets of data are identical, indicating that not only are the ADCP data reproducible, they are also accurate. The shape (in terms of changes in velocity with depth) of the profiles conducted in the flume and field experiments corresponds well, and most differences occur mainly in the trough profile where lower downstream velocities occur in the outer flow zone and increases in velocity gradient occur at different depths. The maximum deviation of the two sets of data is 40% which occurs within the flow separation zone in the dune trough whilst the mean difference is 13.2 %. The final downstream profile (H/95/S1) also has lower downstream velocities for the field data compared to the flume experiments. Bennett and Best (1995) measured negative mean downstream velocity within the dune trough whereas this study did not encounter any mean negative downstream velocities; this may partially be explained by the better resolution of flume data (which was measured using Laser Doppler Anemometry at fixed locations) compared to field data but may also be due to differences in dune morphology.

The differences in the downstream velocity profiles can be partially explained by examining the shape of the crestal section on the field and flume dunes. For the September 1995 and August 1994 profiles there are a downstream-sloping section of bed, of lengths of 25 m and 13 m respectively, between the dune crest point and brink point which is the apex of the flow separation zone.

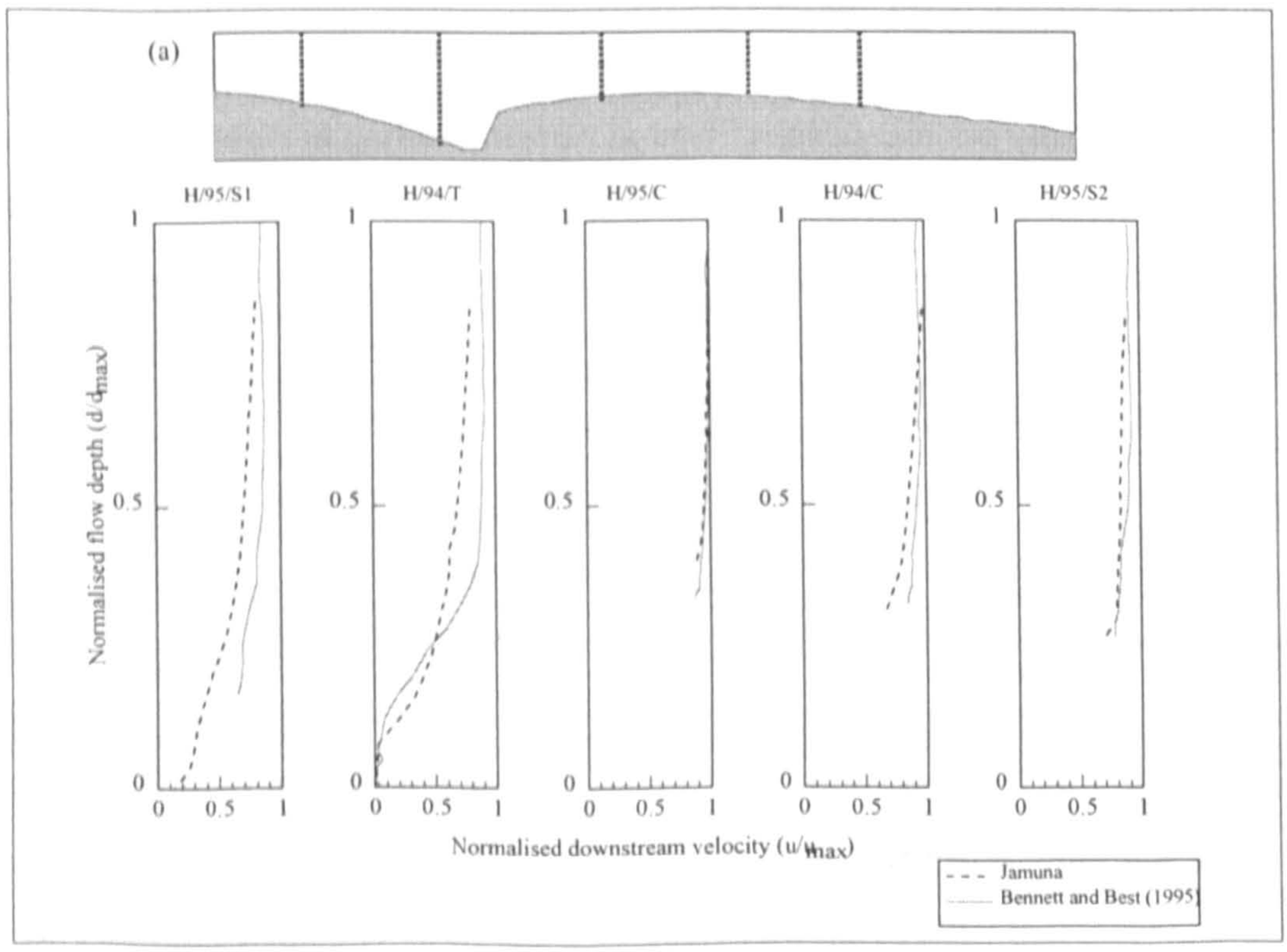

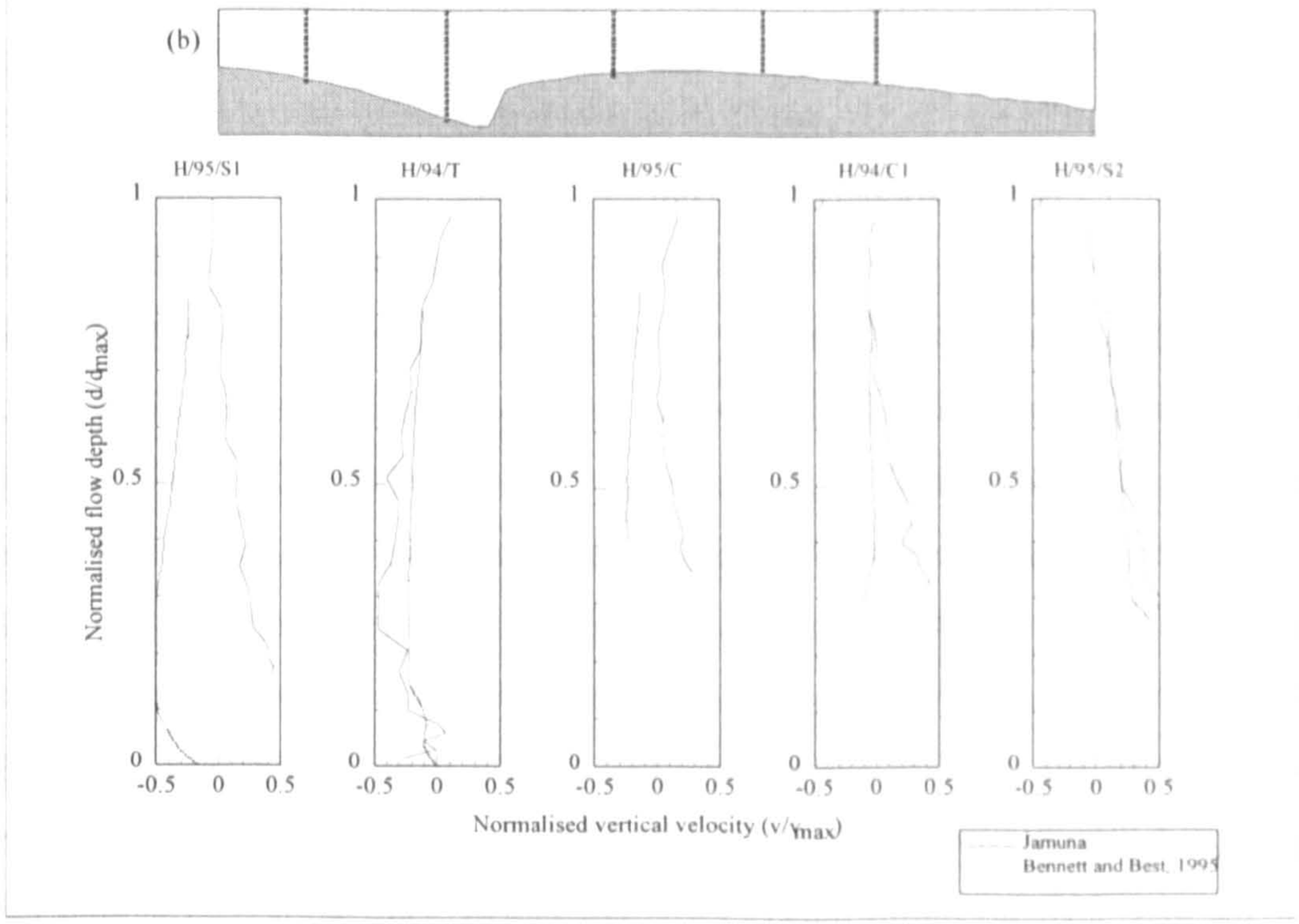

Figure 5.10, Normalised vertical time-averaged at-a-point velocity profiles from both high flow surveys. Dune wavelengths are also normalised so that the relative position along the bed form is illustrated above. The normalised velocity data of Bennett and Best (1995) are plotted to compare the field and flume measurements. (a) downstream velocity (U/u_{max}) where u_{max} is the maximum downstream transect velocity and (b) vertical velocity (V/v_{max}) where v_{max} is the maximum vertical velocity.

This downstream-sloping sloping length section between the crest and brink point is a common feature on field dunes and has a gradient of 3.4° for the September 1995 survey and 6.3° in August 1994. However, this complex lee side profile is usually absent in most laboratory or theoretical studies of flow over bedforms (e.g. Mendoza and Shen, 1992; Nelson *et al.*, 1993; Bennett and Best, 1995). As this area in the lee side slopes in a downstream direction, flow expansion must occur prior to separation. Since the structure of flow separation is dependant on both the bed geometry and the initial flow field (Simpson, 1989), the effect of the critical change in slope at the brink point will be reduced as flow deceleration begins before separation occurs due to the change in pressure gradient (Simpson *et al.*, 1981). The differences in the height and magnitude of the zone of intense changes in velocity gradient seen in the field data can again be attributed to the differences in morphology seen in both the high flow dune surveys compared to the flume dunes. Turbulent free shear flow has been described as highly directional (Wadock, 1980), so flow expansion between the crest and brink points will change the principal direction of shear that occurs as separation commences. This change

in direction of shear will cause the separation cell to be shortened compared to those caused by a classically shaped dune or a negative step perturbation (e.g. Engel, 1981).

Finally, much higher slip face gradients (45° and 37° degrees) were measured in both the high flow dune surveys compared to the angle of repose flume dunes. The dunes used in the experimental work are fixed and so their morphologies can not readjust to account for flow recirculation and reverse flow sediment transport which can be expected in steep angled bedforms to conserve the dune shape (Müller and Gyr, 1986). Hence the steep angled bedforms described in Chapter 4 may be attributed to the initial affect of flow separation and the feedback of reverse-flow transport which will occur once separation has been initialised.

Correspondence between vertical velocity measurements for the field and flume experiments is less convincing than for the downstream velocity. Although profiles H/94/T and H/95/S1 show good agreement, the discrepancies for profiles H/95/S1 and H/94/C1 are large, for example vertical velocities on the stoss side of a bedform are expected to be positive (e.g. Bennett and Best, 1995).

These profiles illustrate the dominant effect of flow separation on the local flow field over dunes. The development of an internal boundary layer which merges with the outer flow region by the next crest is also shown (by the variation in downstream velocity gradient) so indicating that quasi-equilibrium flow conditions do exist, as similar flow profiles are found from crest to crest. However, the profiles also illustrate the great effect that morphology has on the flow processes acting over bedforms, so changes in bed morphology will lead to a variation in the flow field compared to that forming over a classically shaped dune. An examination of mean dune morphology for any set of hydraulic and sedimentological conditions is therefore of primary importance when considering or predicting mean velocity fields over dunes. As these profiles are in good agreement with earlier field, flume and numerical studies (Soulsby, 1991; Nelson *et al.*, 1993; Bennett and Best, 1995), the velocity data measured using the ADCP may be further investigated with confidence.

5.5.3 Comparison of Mean Profiles with Transect Surveys

In addition to the mean flow profiles collected by at-a-point velocity profiling described above, the instantaneous profiles measured under transect surveys may also be collated. Primarily they may be compared to the mean profiles collected at anchor in order to verify their precision. If these profiles prove to be in reasonable agreement with the mean at-a-point profiles then the transect velocity fields may be used to examine the flow over dunes of different morphologies in order to gain a greater

understanding of the link between bed geometry and flow. It should be noted however that there will be greater variation in the measured flow field due to the motion of the boat; each profile is not only a temporal average due to ensemble averaging of the ADCP (see Chapter 3) but is also a spatial average due to the movement of the survey vessel along the survey runline. Average boat velocity was 1.5 ms^{-1} during transect surveying so each ADCP measurement covers a distance of approximately 9 m. Instantaneous velocity profiles were selected from the downstream transect surveys with regard to the position of the vessel in relation to dune morphology. The location of each ADCP ensemble average (5.5 second mean) was selected from the bathymetric data for positions which were situated above either a dune trough or a dune crest. The averaged data showing instantaneous downstream velocity profiles collected over the trough and crest of 24 dunes are shown in Figure 5.11 and the streamwise river bed transects showing the cross-sectional morphology of the dunes from which instantaneous profiles were measured is shown in Figure 5.3a and c.

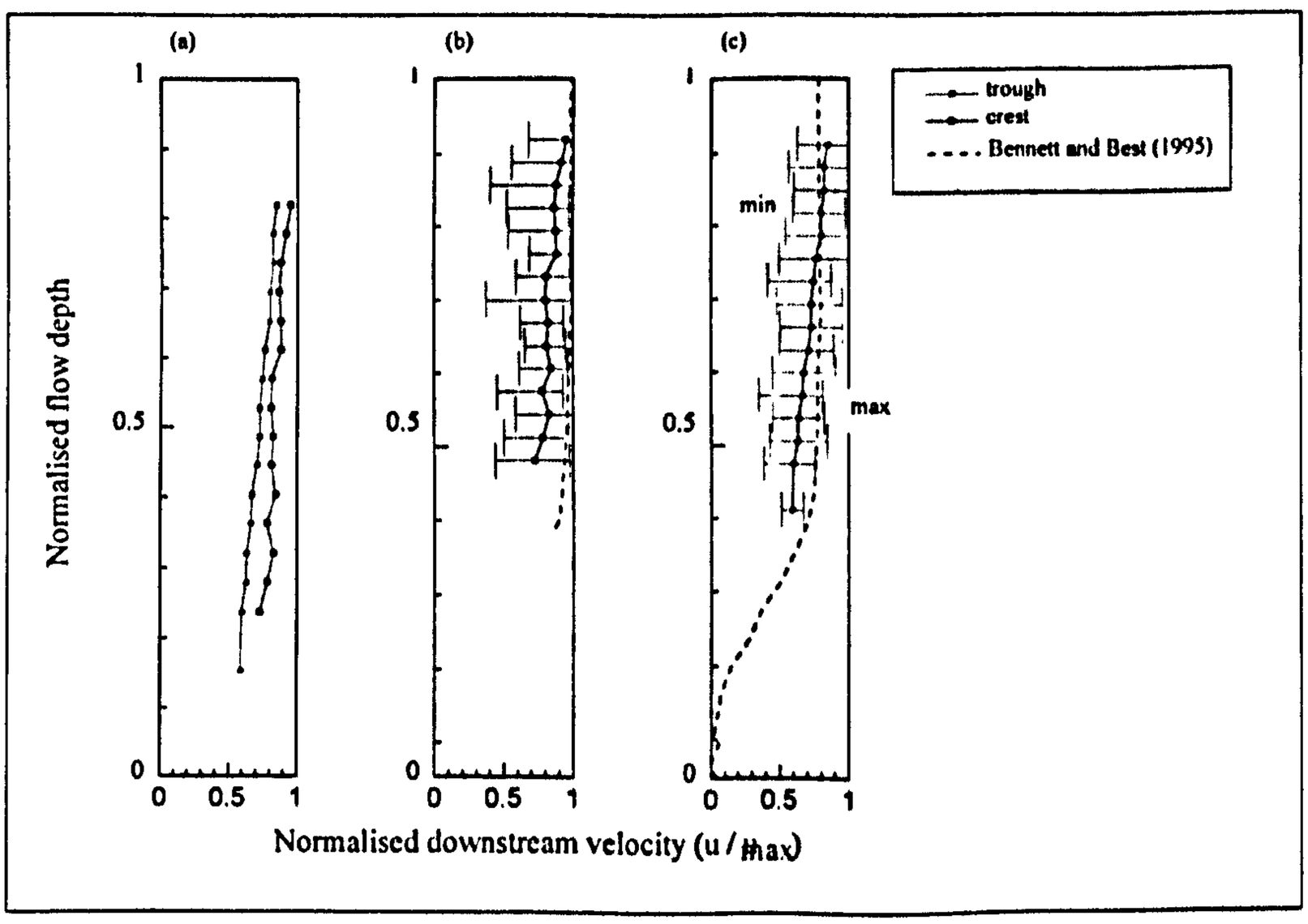

Figure 5.11, Spatial mean downstream velocity profiles measured from transect surveying from crest and trough positions across the dune field shown in Figures 3a and 3c. Each value is the mean of instantaneous profiles collected from above 24 individual dune crests and troughs. For comparison, the mean velocity from both trough and crestal positions is given in (a), and minimum, maximum and mean values of the downstream velocity are given in (b) for the crest and (c) for the trough. Spatial averages from trough and crestal locations of the data of Bennett and Best (1995) are also shown in (b) and (c).

In transect mode, spatial averaging caused by the motion of the survey vessel means that the ADCP cannot image the velocity profile within a dune trough, hence velocity profiles through the shear layer and separation zone are not measurable by this method of surveying.

Each instantaneous velocity profile from transect surveying is normalised to the maximum velocity value recorded for the section and each depth is normalised to the height of the bedform. These normalised instantaneous profiles were then averaged for both the crestal and the trough positions and are shown in Figure 5.11. Figure 5.11a shows the average values of downstream velocity measured over 24 dune troughs and crests, and illustrates that dune trough velocities are lower than those measured over crests. The downstream velocity profiles measured from transect surveys (Figure 5.11a) therefore again illustrate the affect of flow expansion and deceleration in dune troughs as downstream flow velocity is lower for the trough profiles than those measured over crests. The comparison of trough and crestal velocities from a multitude of dunes therefore shows that the description and interpretation of the mean flow field over two steep angled dunes from the August 1994 and September 1995 surveys are generic and may be applied to other bedforms of similar morphologies.

The minimum, maximum and mean values of all of the velocity profiles measured over the troughs and crests of bedforms and the data of Bennett and Best (1995) are also shown in Figure 5.11. The range of downstream velocities is high (Figures 5.11 b and c) for both the trough and crest profiles, and the mean values of both are consistently smaller than the flume data of Bennett and Best (1995). The range in velocity values encountered is partly a factor of the spatial averaging of the ADCP velocity data due to vessel speed and the range of morphologies over which transect surveying took place. Spatial averaging is especially illustrated by the crestal profile; as maximum downstream velocities along a dune wavelength are observed at the crest, an averaging of profiles measured before and after the crest region will record a lower downstream velocity value. The examination of multiple vertical velocity profiles is very useful as it shows that the processes described from the mean at-a-point velocity profiles above are common to all dunes in the survey area and so generalisations may be applied to a population of dunes as a whole rather than just a single isolated bedform.

5.5.4 Velocity Moments and Reynolds Stresses

The velocity data collected by at-a-point profiling were also used to calculate the second moments (root-mean-square) of the velocity component distributions and are shown in Figure 7 for the August

1994 survey. The root-mean-square (RMS) of the downstream and vertical velocity components are calculated as:

$$U_{RMS} = [\ 1/n \Sigma (u-U)^2\ ]^{0.5} \qquad \textit{equation 5.1}$$

$$V_{RMS} = [\ 1/n \Sigma (v-V)^2\ ]^{0.5} \qquad \textit{equation 5.2}$$

where U_{RMS} and V_{RMS} are the root-mean-square values of the mean downstream and vertical velocities respectively, u and v are the instantaneous velocities, U and V are the time-averaged downstream and vertical velocities and n is the number of observations. For the high flow profiles, only the data collected in August 1994 will be useful for examination of the velocity time series distributions due to the longer averaging time set for the ADCP during the September 1995 survey. The September 1995 velocity profiles are averaged over 55 s which is too long in order to enable an examination of the distribution of velocity times series in terms of the RMS or skewness values or to enable calculation of the Reynolds stresses. As an example of the low velocity moments for the September 1995 survey, the RMS values of profile H/95/C are shown in Figure 5.12, and are very close to zero for the entire profile. The H/95/C profile downstream RMS values are 200% smaller than the H/94/C values again illustrating that the long ADCP averaging time eliminates any useful study of the distribution of the instantaneous velocity measurements.

For the high flow profiles there is a large increase in the downstream RMS values over the dune trough (H/94/T) from a depth of 9.5 m down to the bed (Figure 5.7a). Near to the flow surface, downstream RMS values of 0.2 ms^{-1} were measured in comparison to the trough RMS values of 0.6 ms^{-1} which are the greatest that occur on either of the profiles. The increase in downstream RMS values seen in the trough profile begins at depths concurrent with the increases in velocity gradient described above (from 9.5 m). In conjunction with the high downstream RMS values there is a corresponding increase in RMS values of the vertical velocity component at equivalent depths from a near surface value of 0.06 ms^{-1} to 0.09 ms^{-1} at 12 m depth. This indicates that, as the area is detached from the bed and the mean velocity is removed in RMS calculations, the relatively higher RMS values are not caused by topographic forcing but are more likely a result of eddy shedding along the shear layer (Bennett and Best, 1995). Maximum exchange of fluid momentum occurs along the shear layer where maximum u' and v' values occur which is shown by the RMS vertical and distributions of the downstream velocity. Within the zone of flow separation the RMS values decrease (to 0.35) but are still higher than those found in the outer flow zone. This may be explained by a variation in the length of the flow separation zone with time suggesting that the shear layer is moving, or flapping, both vertically and horizontally in the flow column. This may mean that the main sites of turbulence

production are variable; this will be explored further in the subsequent section. Over the crest (profile H/94/C), the RMS signatures are markedly different as both vertical and downstream RMS values are lower than for the trough section (maximum 0.18) and show little variation with depth. This indicates that there is very little turbulence production over the crestal section of the bedform when compared to the trough section.

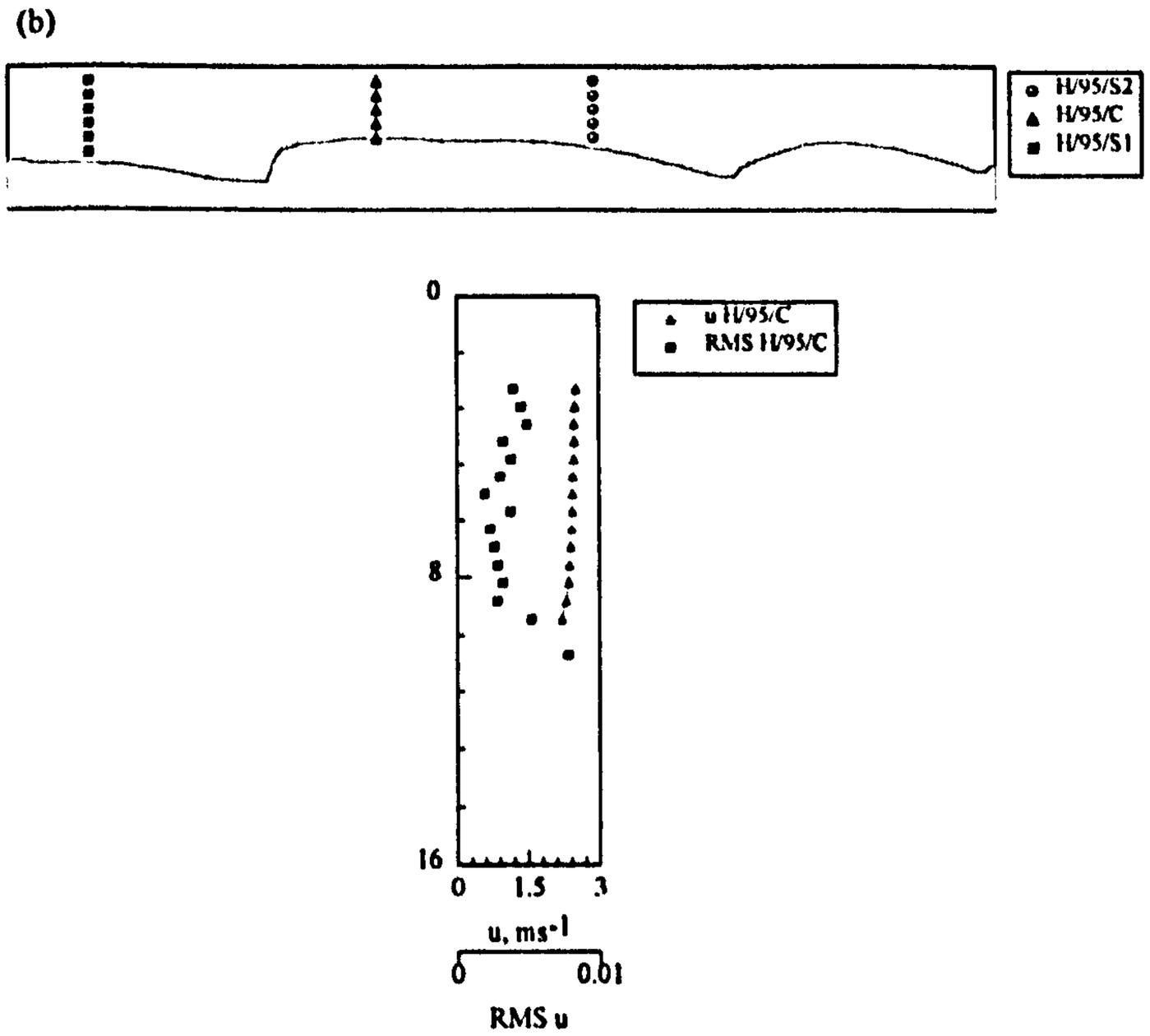

Figure 5.12, An example of the downstream velocity RMS values from the September 1995 survey. The very low RMS values are a function of the ADCP ensemble averaging time set (55.5 s) during this survey.

The time-averaged Reynolds stress for each profile depth cell for the August 1994 survey (shown in Figure 5.13) is calculated using:

$$\tau_r = - \rho u'v' \qquad \textit{equation 5.3}$$

where - $u'v' = 1/n \sum (u-U)(v-V)$ and ρ is the fluid density.

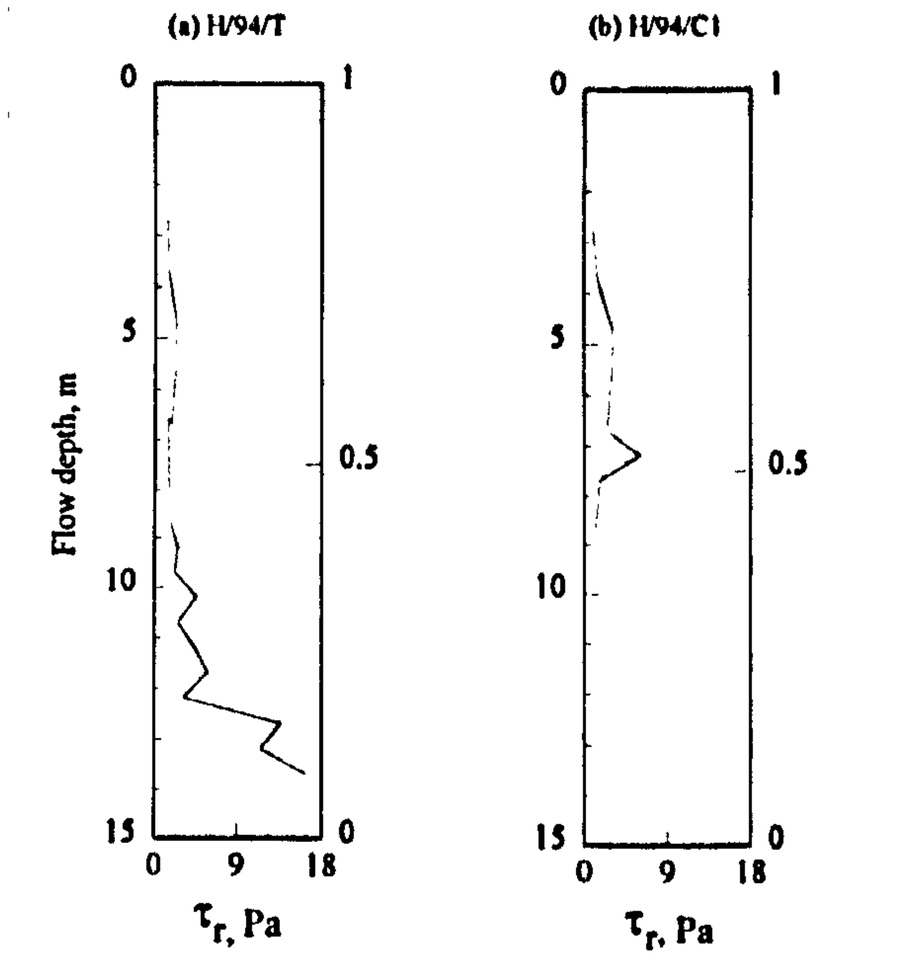

Figure 5.13, Vertical profiles of the mean Reynolds stress for the August 1994 high flow survey collected over the dune (a) trough and (b) crest.

Vertical profiles of the mean Reynolds stress from the August 1995 survey (Figure 5.13) illustrate the strong spatial variation of the stress field acting over the bedform. The crestal profile (H/94/C1) shows a slight increase in Reynolds stress with depth from a minimum of 1.5 Pa to a maximum value of 3 Pa at 7.2 m followed by a small decrease towards the bed, this pattern in Reynolds stresses over a dune crest compares very well with previous work (e.g. Bennett and Best, 1995). For the high flow survey, profile H/94/T over the dune trough also shows an increase in Reynolds stress towards the bed (Figure 5.13), with this increase occurring from a depth of 9.5 m, with maximum values of up to 16 Pa, located near the bed. Previous studies (e.g. Raudkivi, 1963; Nelson *et al.*, 1993) have shown that maximum Reynolds stress values are found along the separation zone and both at and just downstream of reattachment and that values of Reynolds stress within the separation are very low. As profile H/94/T is situated within the low flow zone, a decrease in shear stress would be expected within the low flow zone. The initial increase in Reynolds stress observed in profile H/94/T occurs through the shear zone identified by the mean velocity profiles described above so agreeing well with previous work. However, the increase in Reynolds stresses down to near the bed level may be a function of two factors; firstly the position of the profile with respect to the dune slip face and the measuring depth of the ADCP may mean that any near-bed decrease in Reynolds stresses may not be within the ADCP measurable depth range, and secondly a variable separation zone length would

show an increase in the temporal mean measured Reynolds stresses as they have been shown to be greatest near reattachment locations (Bennett and Best, 1995). Variation in reattachment zone position downstream of a negative step has previously been documented by Driver *et al.*, (1987) and Simpson, (1989), where flow visualisation studies behind a negative step have shown that the length of the separation zone fluctuates so that the instantaneous impingement location of the shear layer moves up and down. Driver *et al.* (1987) showed that the reattachment location may vary by 2H, where H is the step height and the mean reattachment location is 4H (see also Engel (1981)). This demonstrates that the location of profile H/94/T, which is at a distance of 3 dune heights from the lee face, is well within the range of possible flow reattachment locations. The time-averaged Reynolds stress values at a single location would therefore encompass the reattachment zone, separation zone and the area downstream of reattachment. The time-averaged near-bed Reynolds stress for profile H/94/T is therefore higher than would be expected upstream of the reattachment point for a stationary shear layer, but is lower than that expected at, or just downstream of, flow reattachment. The RMS and Reynolds stress values have therefore shown that turbulence production is maximised along the shear layer which develops due to flow separation, and that the length of the flow separation zone is variable.

The third moments of the velocity distributions at-a-point are defined as:

$$U_{skew} = 1/n \sum\{(u-U)/U_{RMS}\}^3 \qquad \textit{equation 5.4}$$

$$V_{skew} = 1/n \sum\{(v-V)/V_{RMS}\}^3 \qquad \textit{equation 5.5}$$

The crestal vertical profile (H/94/C1) shows very little variation in the skewness of the downstream and vertical velocity components with depth, with both U_{skew} and V_{skew} approaching zero at any distance from the bed (Figure 5.14). However, the spatial variation in U_{skew} and V_{skew} is markedly different over the dune trough (profile H/94/T). A zone of strongly positive downstream skewness is located just below the shear layer which is similar to that documented by Bennett and Best (1995) and reasoned to represent the mixing of higher velocity fluid above and within the shear layer with the lower velocity fluid of the separation zone. Beneath this zone there is an area of negative downstream skewness which may again be accounted for by movement of the shear layer and therefore the reattachment point. For a stationary shear layer downstream of a dune crest, positive downstream skewness value would be expected in the low flow zone down to near-bed levels (e.g. Bennett and Best, 1995). In this field situation the spatial averaging caused by motion of the shear layer relative to the profile may lead to a decrease in the time-averaged downstream skewness value. A small zone of weakly negative downstream skewness is located at the height of the shear layer

which is diagnostic of fluid ejection of lower than average velocity fluid along this layer into the outer flow (Itakura and Kishi, 1980). The trough profile (H/94/T) of skewness in the vertical velocity component shows a zone of positive values along the shear layer. Positive vertical skewness is symptomatic of fluid ejections along the shear layer into the outer flow. Relatively high values of negative skewness are found beneath shear zone heights and this is indicative of entrainment of low velocity fluid into this zone (Bennett and Best, 1995).

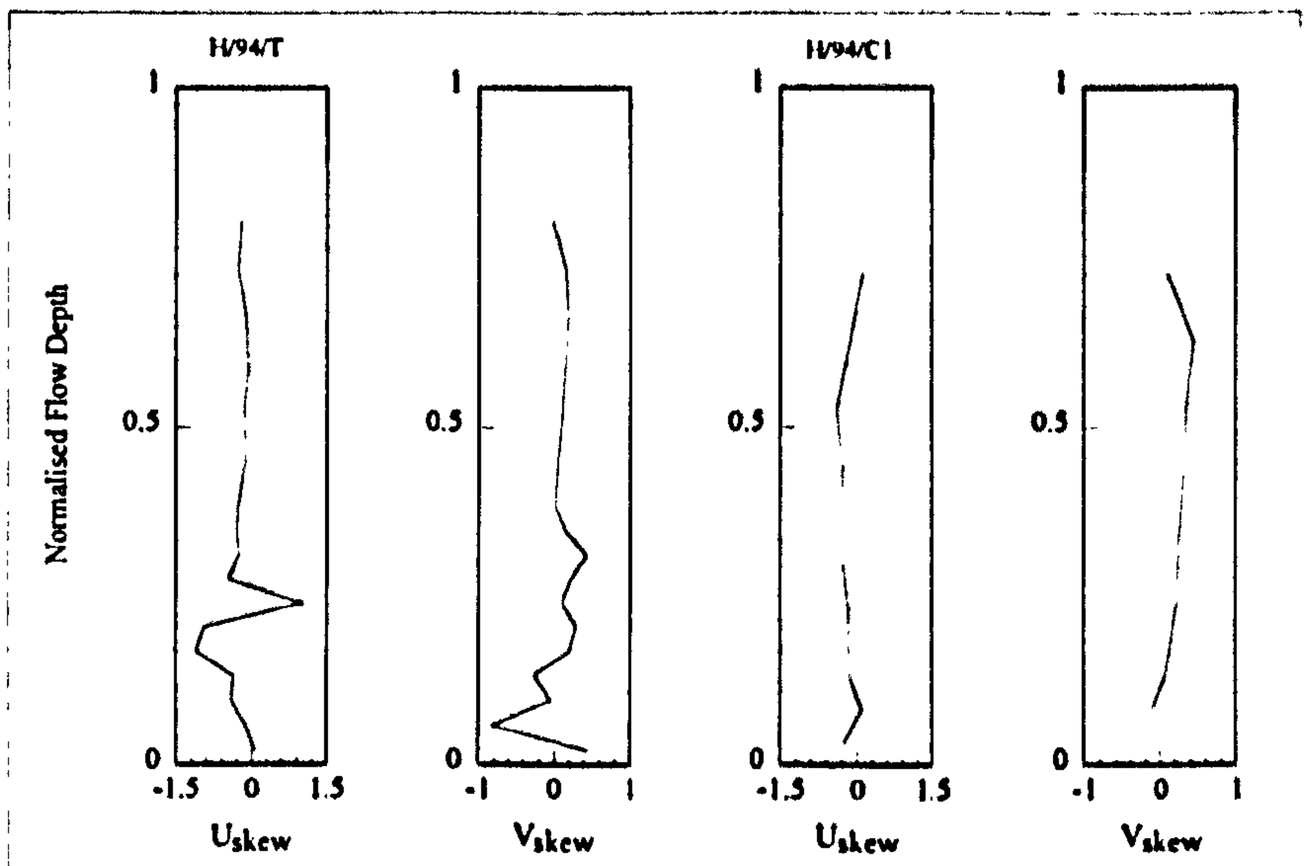

Figure 5.14, Vertical profiles of the skewness of the at-a-point vertical and downstream velocity time series for the August 1994 high flow survey collected over the dune crest (H/94/C1) and the dune trough (H/94/T).

5.5.5 Temporal Changes in Downstream Velocity

The time series of downstream velocities for profiles H/94/C and H/94/T are displayed for the vertical profile as at-a-point velocity time series for various flow depths (Figure 5.15 a and b) and as a contour plot for 0.5 m depth intervals through the entire flow column (Figure 16 a and b).

Contouring of all data in this thesis has been conducted using the data visualisation program Spyglass Transform®, with kriging used to interpolate unmeasured grid data. Kriging employed a spherical distribution model and a normalised variance of zero was applied to all velocity time series grid data. The at-a-point velocity time series (Figure 5.15) illustrate the dominant affect of flow separation on the flow field.

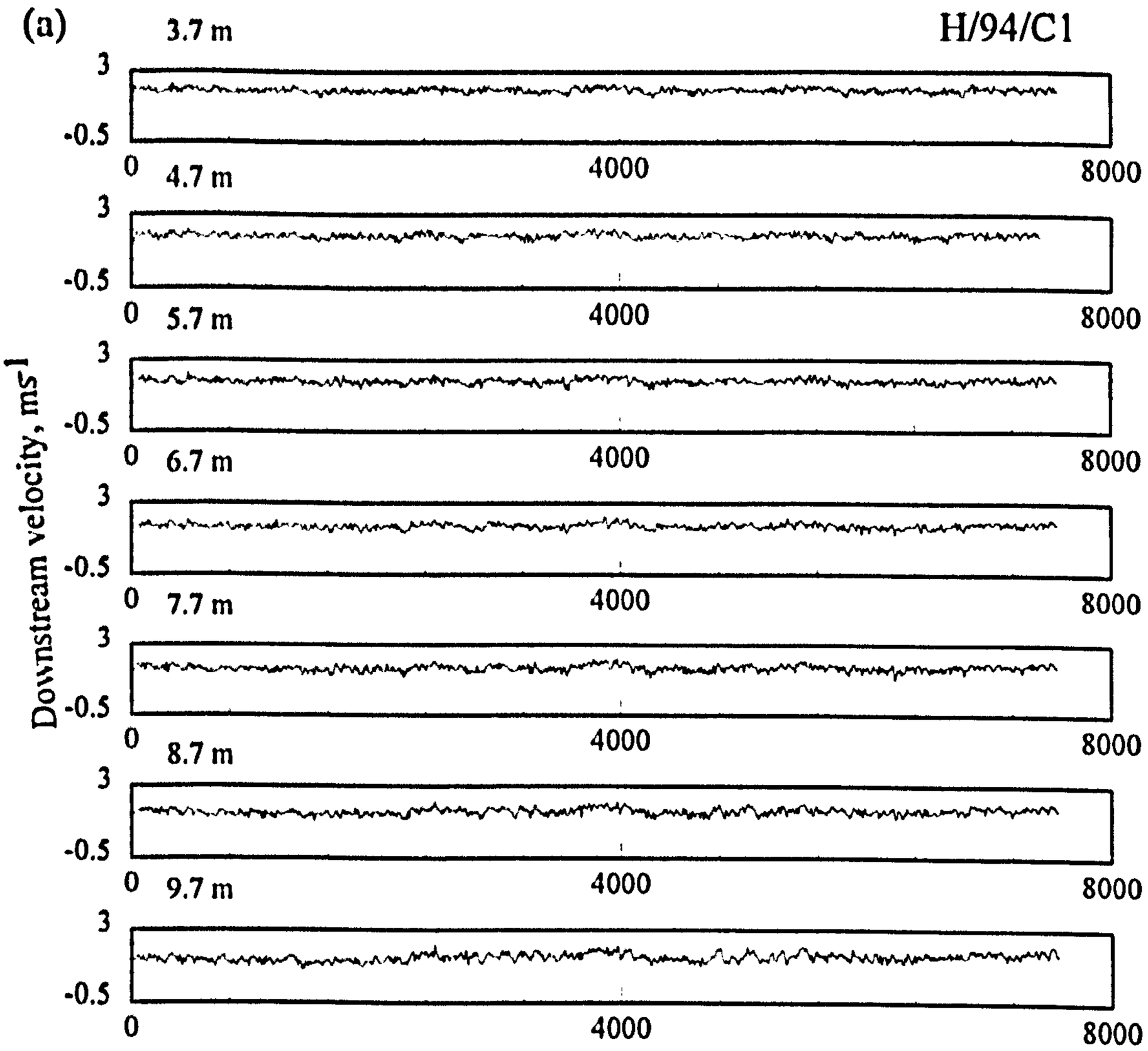
(a)
3.7 m
H/94/C1
4.7 m
5.7 m
6.7 m
7.7 m
8.7 m
9.7 m
3
-0.5
0
4000
8000
Downstream velocity, ms-1
Time, s

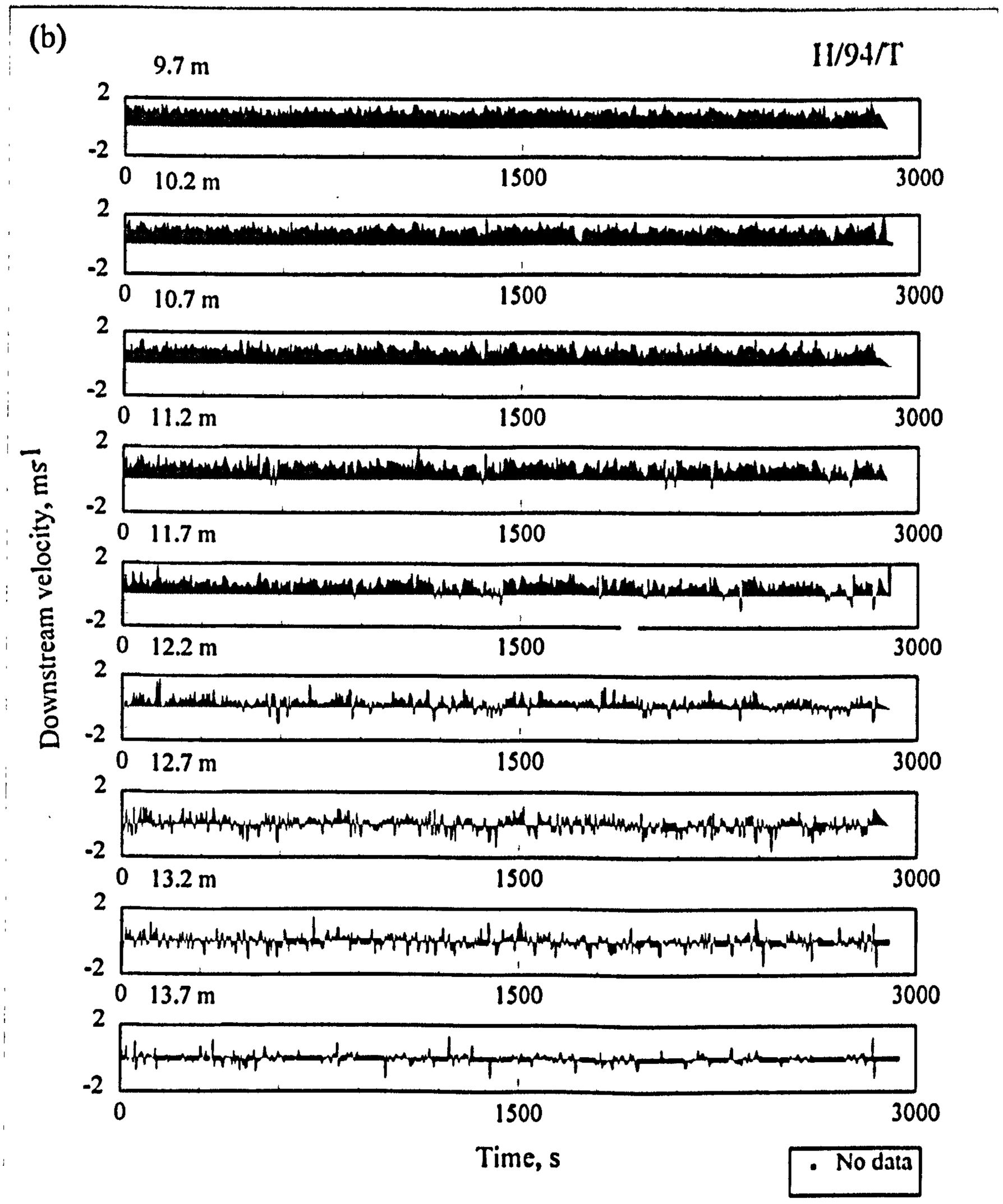

Figure 5.15, At-a-point time series of the instantaneous values of the downstream velocity collected at different heights above the dune (a) crest, H/94/C and (b) trough, H/94/T for the high flow August 1994 survey. The time series depth is marked above each plot.

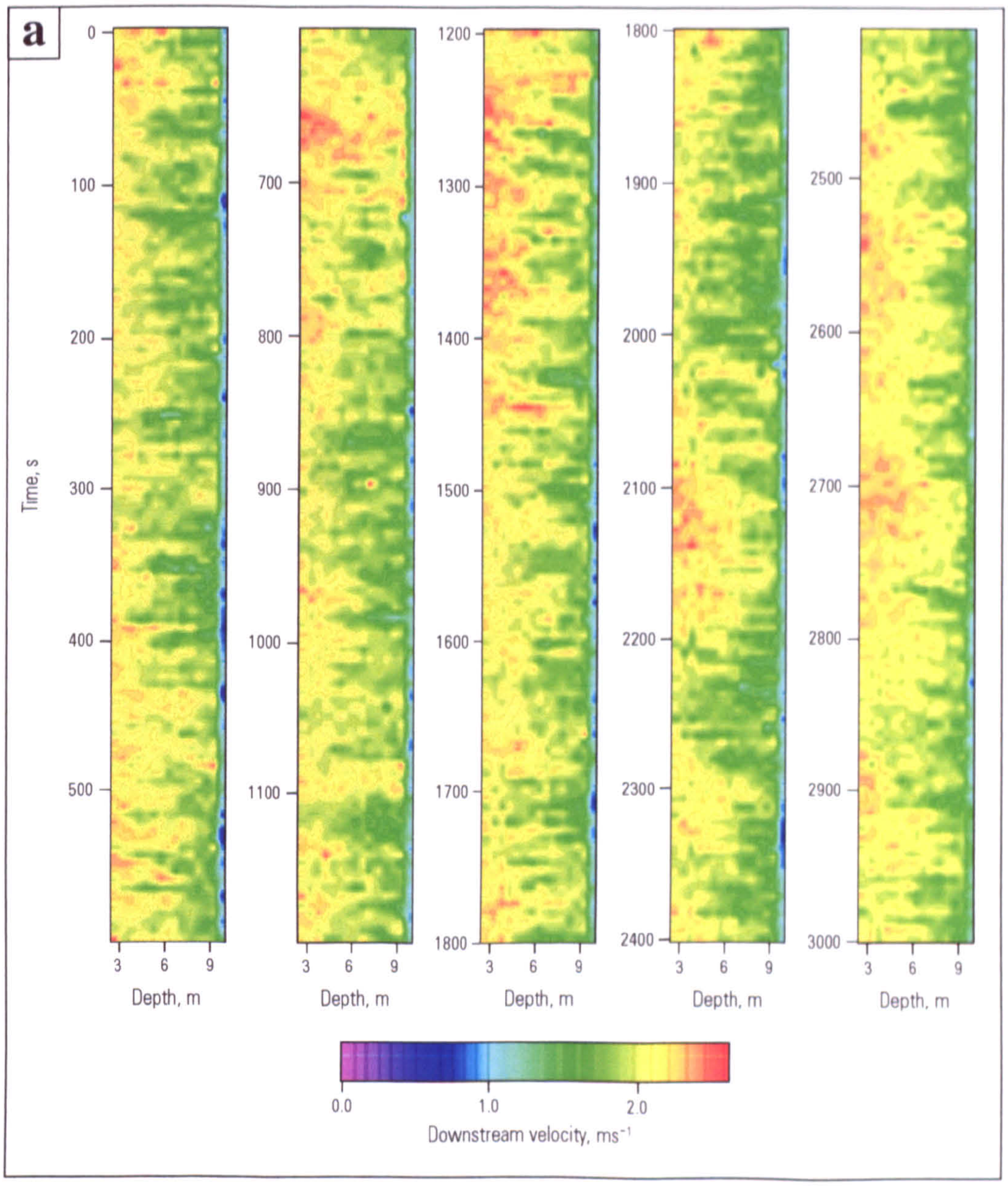

Figure 5.16: Contour maps of temporal variations in at-a-point downstream velocity for the high flow survey at (a) H/94/C, dune crest and (b) H/94/T, dune trough. Flow is from top to bottom and a scale colour bar is given for each map. Flow depth bin sizes are 0.5 m. Each time series has been split to fit to page size and successive profiles are from left to right.

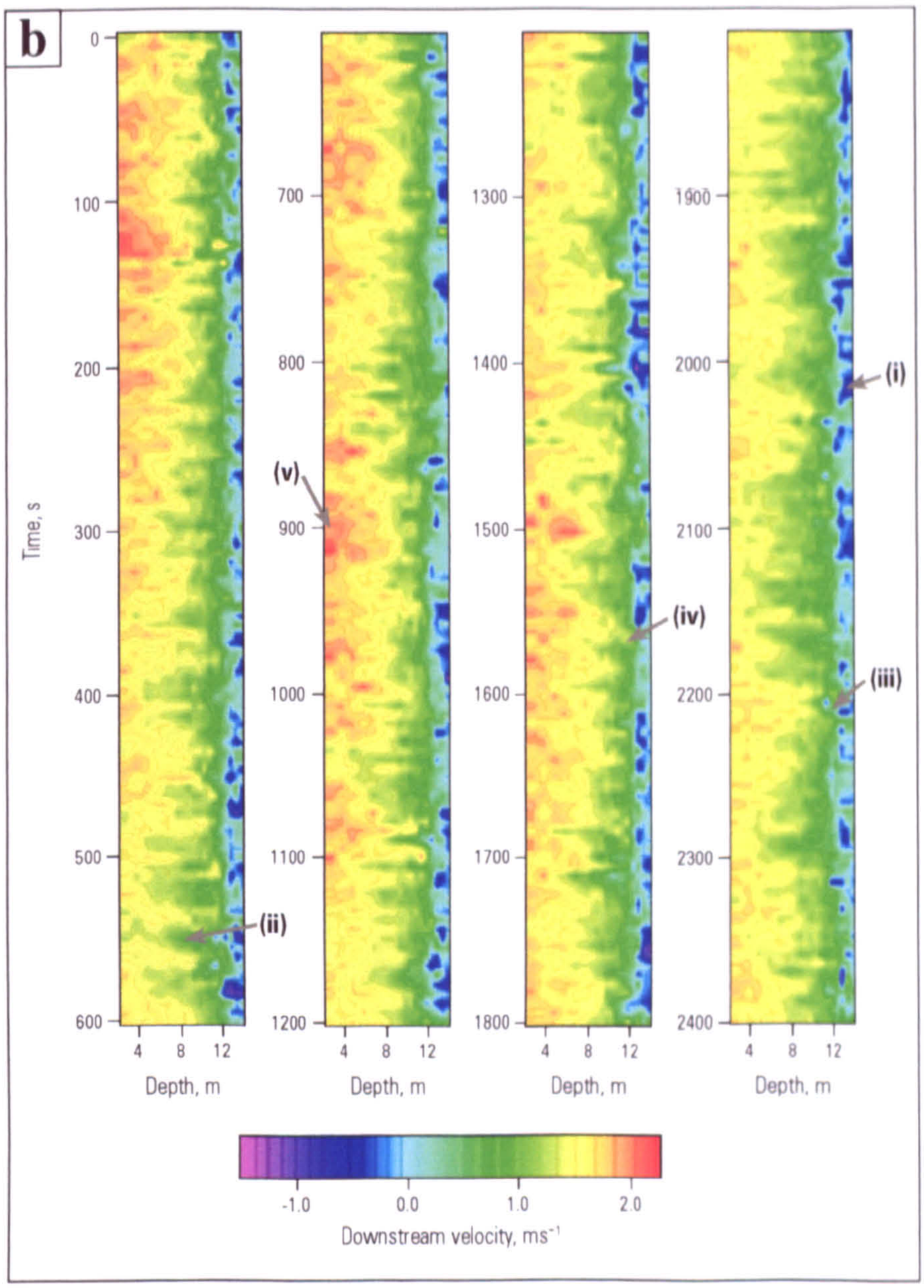

Figure 5.16: Contour maps of temporal variations in at-a-point downstream velocity for the high flow survey at (a) H/94/C1, dune crest and (b) H/94/T, dune trough. Flow is from top to bottom and a scale colour bar is given for each map. Flow depth bin sizes are 0.5 m. Each time series has been split to fit to page size and successive profiles are from left to right. (i) intermittent flow reversals, (ii) ascension of the shear zone after a period of flow reversal, (iii) the location of reversal varies vertically in the flow column, (iv) vertical drop in the shear zone height associated with period with no flow reversal and (v) intermittent variation in downstream velocity in the outer flow zone.

The outer flow zone of profile H/94/T exhibits high magnitude (up to 2 ms^{-1}) positive downstream velocities with a variation of the order of ±0.5 ms^{-1}. From a depth of 11.2 m down to the bed, negative downstream velocities occur (Figure 5.16b(i) and 5.15b), with the rate and duration of occurrences of these flow reversals increasing with depth. Sandborn and Kline (1961) and Sandborn and Liu (1968) noted intermittency in flow reversals at certain distances downstream of a negative step in wind tunnel experiments, they defined the limiting points of the region as the 'intermittent' and the 'fully developed' separation points. The former indicating the onset of separation by the appearance of intermittent flow reversals and the latter signifying the fully developed separation zone (accompanied by a rapid decrease in the mean bed shear stress). Intermittency in flow reversal in the leeside of dunes has previously been shown by Soulsby *et al.* (1991) in estuarine conditions. Soulsby suggested that the intermittency in reversal was a function of the variation in flow stage and dune morphology caused by tidal fluctuation but this is, of course, not the case here. Intermittency in flow reversal at a given distance from the brink point is a characteristic feature in both alluvial and estuarine bedforms as implied by the wind tunnel experiments of Sandborn and Kline (1961) and Sandborn and Liu (1968). The intermittent flow separation zone has also been documented in the wind tunnel experiments of Simpson (1976) and Simpson *et al.* (1981). Intermittency in flow reversal has also been linked to flapping of the shear layer (Driver *et al.*, 1987) which drives the variation in the instantaneous impingement location of the shear layer that was described above.

The change in at-a-depth downstream velocity through the flow column for profile H/94/T is apparent: from 9.5 m upwards to the minimum depth measurable by the ADCP (2.66 m from the water surface) there is a consistent increase in velocity with depth which ranges from 1.0 ms^{-1} to 2.5 ms^{-1}. At depths greater than 9.5 m the pattern of downstream velocity is markedly different: low downstream velocities (< 0.5 ms^{-1}) dominate and negative velocities occur depicting the presence of a recirculation of flow. Flow recirculation has never previously been illustrated over dunes of this size in the field. This recirculation pattern is temporally inconsistent and maximum periods of recirculation persist for up to 110 s (see Figure 5.15b), in this lower portion of the flow column beneath (> 9.5 m) the velocity fluctuation (of over 2 ms^{-1}) is twice that of the upper section. The experiments of Driver *et al.* (1987) examined flow reversals behind a negative step and found that flow reversals at a mean reattachment point of 4 times the step height had recurrence interval of between 50 and 300 *H/ U (where H is the step height and U is the mean velocity before flow separation) and that reversals have a relatively short life span of 14H/U. The corresponding values for this study are recurrence intervals of between 3.5 and 250 *H/U and a mean life span of 25H/U. The variation in these field study values from experimental conditions are influenced by several factors:

1. The difference in relative measurement location since the profile position is a distance of 3H from the slip face for the field study. This would suggest that recurrence intervals would be shorter which agrees with the measurements and that the longevity of the reversals would be greater which is also the case.
2. The variation in step angle between field and flume which will also cause a change in reattachment zone length, with higher step angles producing longer separation zone lengths. The further complexity of the crest to brink point region in this field situation will also affect flow recirculation as flow expansion occurs before the brink point.
3. The directional nature of a free shear layer will mean that upstream morphology again will influence reattachment location and flow expansion will begin before separation occurs in the field experiment.

The Froude number has also previously been postulated to affect the length of the separation zone (Engel, 1981). However, the affect of variation in separation length with Froude number is not relevant for this study as maximum Froude numbers measured are 0.3, and Engel (1981) showed that separation length is independent of Froude number when $Fr < 0.5$.

The magnitude of these flow reversals reaches 40% of the outer zone downstream velocities (-1.4 ms^{-1}) which are found in the upper 5 m of the flow column, the magnitude of the reverse velocities being slightly higher than previous experimental work where measured maximum reversed velocities are usually ~20% of the free stream velocity (Simpson, 1989). The degree of intermittency in flow reversals has been shown to be a factor of distance from the separation point (Sandborn and Kline, 1961; Sandborn and Liu, 1968; Simpson *et al.*, 1981; Driver *et al.*, 1987) and also of vertical distance from the bed (Soulsby *et al.*, 1991). Maximum intermittency values of 45% (Figure 5.17, where I is the percentage of time that flow is in a downstream direction hence I = 100% corresponds to a constant downstream flow direction) compare very well with the data of Soulsby *et al.* (1991) where the maximum intermittency values recorded were 40%, both of these maximum intermittency measurements being located close to the bed. This also indicates that the longer measuring period (5.5s) of the ADCP compared to the 1s measuring period used in the study of Soulsby *et al.* (1991) does not invalidate the measurements of mean reversal period. These high, intermittent velocity reversals can be utilised to explain the extremely steep (up to 55°) leeside angles documented in Chapter 4 as they will be responsible for transporting sediment back up the avalanche face of the dune and therefore steepening the slope to angles much greater than the static angle of repose. It is

likely that these high magnitude reversal events are localised laterally along the bedform (Kostaschuk and Villard, 1996; Williams, 1996).

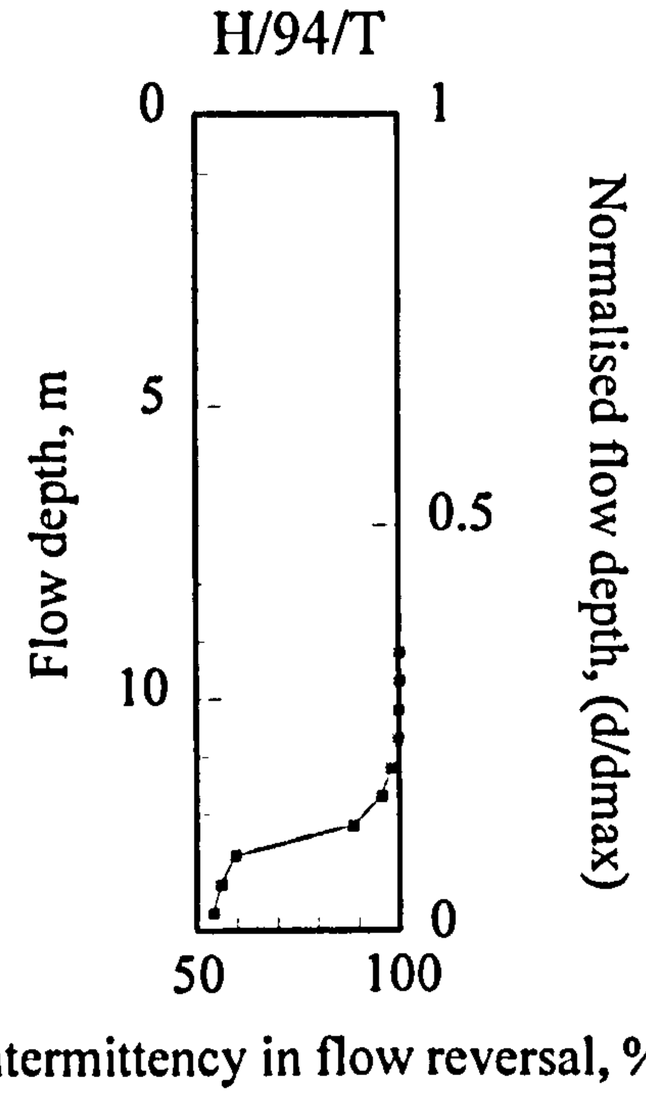

Figure 5.17, Intermittency in flow reversal variation with flow depth through the separation zone and shear layer for profile H/94/T collected during the high flow survey, August 1994.

The increase in slip face steepness caused by reverse flow sediment transport will cause a feedback to increase turbulence production (Müller and Gyr, 1986) as steeper slip face slopes will in turn cause higher magnitude velocity gradients to occur across the shear layer and will therefore be responsible for increasing the three-dimensionality of the dune. Dimensionality will increase because turbulence production (and therefore increases in sediment transport) is localised (e.g. Nelson *et al.*, 1995), so feedbacks between increasing slip face steepness and increased turbulence production will therefore lead to localised scouring. The pronounced scour holes and spurs observed on bedforms formed on bar tops, which are exposed during the dry season, may therefore be partly a function of this phenomenon. Further evidence of reverse flow transport in the opposing direction to the mean flow is seen in climbing ripples formed on exposed dune slip faces (Bristow, 1987).

The location of the reversals varies from an upper limiting depth of 11.7 m down to the river bed (Figure 5.16b(iii)) and is therefore situated beneath the shear layer previously identified by the mean and RMS velocity profiles. The studies of Sandborn and Kline (1961), Sandborn and Liu (1968), Simpson *et al.* (1981) and Driver *et al.* (1987) indicate that although separation is intermittent at the

profile location of this study, permanent flow reversal may occur closer to the dune slip face so producing negative mean velocities. It is well established that separation of a turbulent boundary layer at a negative step does not occur at a single streamwise location but is spread over a streamwise region and involves a spectrum of velocity states (in terms of downstream and reverse flows) (e.g. Simpson *et al.*, 1981). Müller and Gyr's (1986) visualisation studies show that a permanent recirculation cell ('vortex roller') may occur close to the slip face of a dune and be accompanied by an intermittent-reversal zone further downstream; therefore a velocity profiling location closer to the dune slip face may have revealed a permanent recirculation zone. The shifts recorded in the minimum reversal depth may again be related to a vertical motion or 'flapping' of the shear layer as illustrated in Figure 5.16b(ii), where an extensive period of negative downstream velocity is accompanied by an ascension of the shear zone to almost 2m above the background or mean shear layer height. This phenomena of correlation of high velocity gradients or shear layer flapping with strong flow reversals in the vicinity of the reattachment zone has previously been documented by Driver *et al.* (1987), who suggested that flapping is produced when a particularly high-momentum structure moves far downstream before reattaching. This would create a somewhat greater pressure gradient that would subsequently cause greater back flow (Simpson, 1989).

There is also a weak intermittent, although inconsistent, variation in the downstream velocity through the upper section of the flow field (see Figure 5.16b(v)) which may be linked to these variations that occur within the shear layer height. McLean and Smith (1986) for instance use far field wake theory in their numerical model of the flow field over dunes. Physically, variations in the wake produced due to flow separation may be produced by these variations in the velocity gradient across the shear layer. Nelson and Smith (1989) further developed far field wake theory by recognising that some wake structure is typically still present in the velocity profile when the flow separates over the next crest downstream. Hence, there is a 'stacking' of wakes and the outer flow region over successive upstream dunes is given by a series of suitably matched wake profiles created by the flow separation process acting at upstream crests (McLean, 1990). Nelson and Smith (1989) suggest that wakes from successive bedforms will interact as the momentum defects diffuse both outwards and upwards in the flow column. Hence, the influence of this translocation of the shear layer not only affects the zone of flow separation on the crest leeside, but also extends upwards in the flow column above the shear zone towards the next crest downstream (see Figure 5.16b(iii)) as lower downstream velocities occur in conjunction with the characteristic recirculation. This decrease in velocity continues for a period after an extended flow reversal has diminished.

During periods where there are no flow reversals it is evident that, on average, the position of the high velocity gradient or shear layer drops in the flow column (Figure 5.16b(iv)). During these intervals, much higher flow velocities occur closer to the river bed which has great implications for sediment transport. These periods may be due to the position of the profile H/94/T with respect to the dune: the profile is towards the downstream end of the recirculation zone, where flapping of the shear layer will cause a change in the length of the recirculation zone. Higher velocities near the bed may therefore be indicative of movement of the reattachment zone towards the profile position. It has previously been well documented that high turbulence intensities are associated with zone of flow reattachment (McLean *et al.*, 1993: Bennett and Best, 1995).

The main elements of this section describing the temporal variations in downstream velocity are summarised in Figure 5.18. The presence of intermittent flow reversals in the dune trough has been established which agrees well with previous air tunnel (Sandborn and Kline, 1961; Sandborn and Liu, 1968, Simpson *et al.*, 1981), field (Soulsby *et al.*,1991) and flume (Bennett and Best, 1995) studies. The dominant effect of flow separation over the trough has been quantified and the spatial variability in shear has been described. The presence of weaker intermittent variations in the upper flow column has also been recorded.

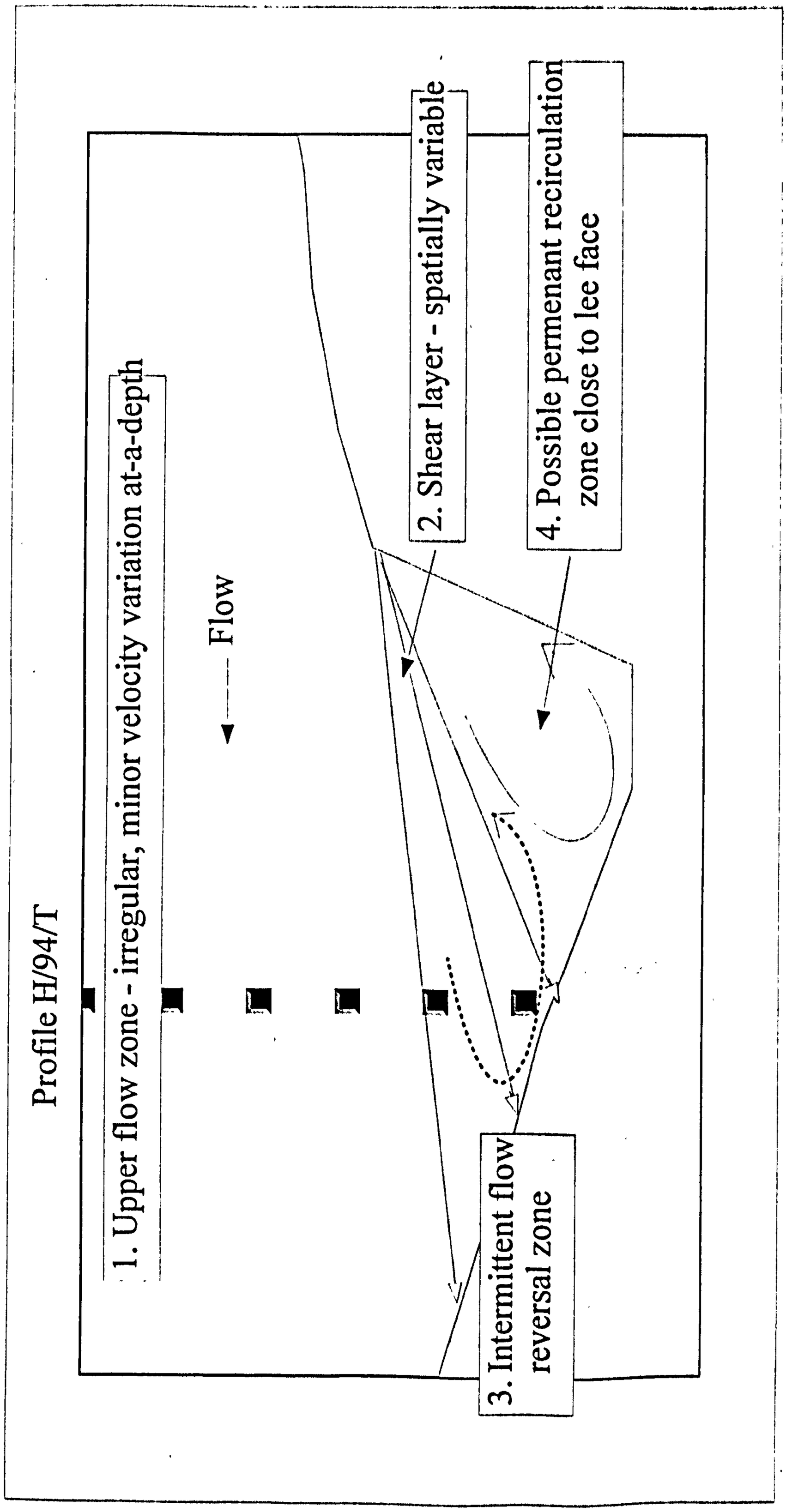

Figure 5.18, Schematic ilustrating the key features of the instantaneous downstream flow field.

5.5.6 Visualising the Shear Layer

Many studies have noted the association between the occurrence of dunes and the presence of large scale macroturbulence within alluvial channels (e.g. Coleman, 1969; Jackson, 1976). It was postulated (e.g. Jackson, 1976; Yalin, 1977) that the source of the boils was 'bursting events' within the turbulent boundary layer. However, more recent flume studies have suggested that such boils result from flow separation in the lee of dunes (e.g. McLean *et al.*, 1994, Bennett and Best, 1995). The origin of this turbulence has been postulated to be eddy shedding of Kelvin-Helmholtz instabilities along the separation zone shear layer (e.g. Müller and Gyr, 1982; Rood and Hickin, 1989, Bennett and Best, 1995). In field studies there are inherent difficulties in linking the generation of turbulence to either bedform or hydraulic parameters since the data associated with turbulence studies often lack the spatial and temporal resolution required to locate the production sites of turbulence or any periodicity inherent to ejections of turbulent fluid. The next section will therefore aim to investigate the link between variations in the velocity differential in the shear layer and the production of turbulence in lee side of dunes.

As the ADCP records velocities at multiple flow depths simultaneously, it is possible to calculate the vertical downstream velocity gradient between depth cells and to study its temporal variation. The transitory changes in velocity gradient or shear velocity over a dune have not been studied in detail before due to data limitations, but may be invaluable for investigating the relationship between growth of a shear layer and the ejection of turbulent flow structures away from it, thus providing a mechanism for the entrainment and suspension of sediment. The velocity differential through the shear layer will also govern the frequency and size of any coherent flow structures formed due to the instabilities of a shear layer, and hence high velocity gradients are indicative of the formation of these structures.

Each gradient measurement is calculated between two 0.5 m deep adjacent depth cells and so images large scale shear velocities with a time scale longer than 5.5 s and a length scale greater than the depth of a cell (0.5 m). It should be noted that as all ADCP measurements are temporal and spatial averages, the shear velocities given here are minimum values for each depth: it is possible that higher shear stresses occur on smaller time and length scales than the measuring period and volume.

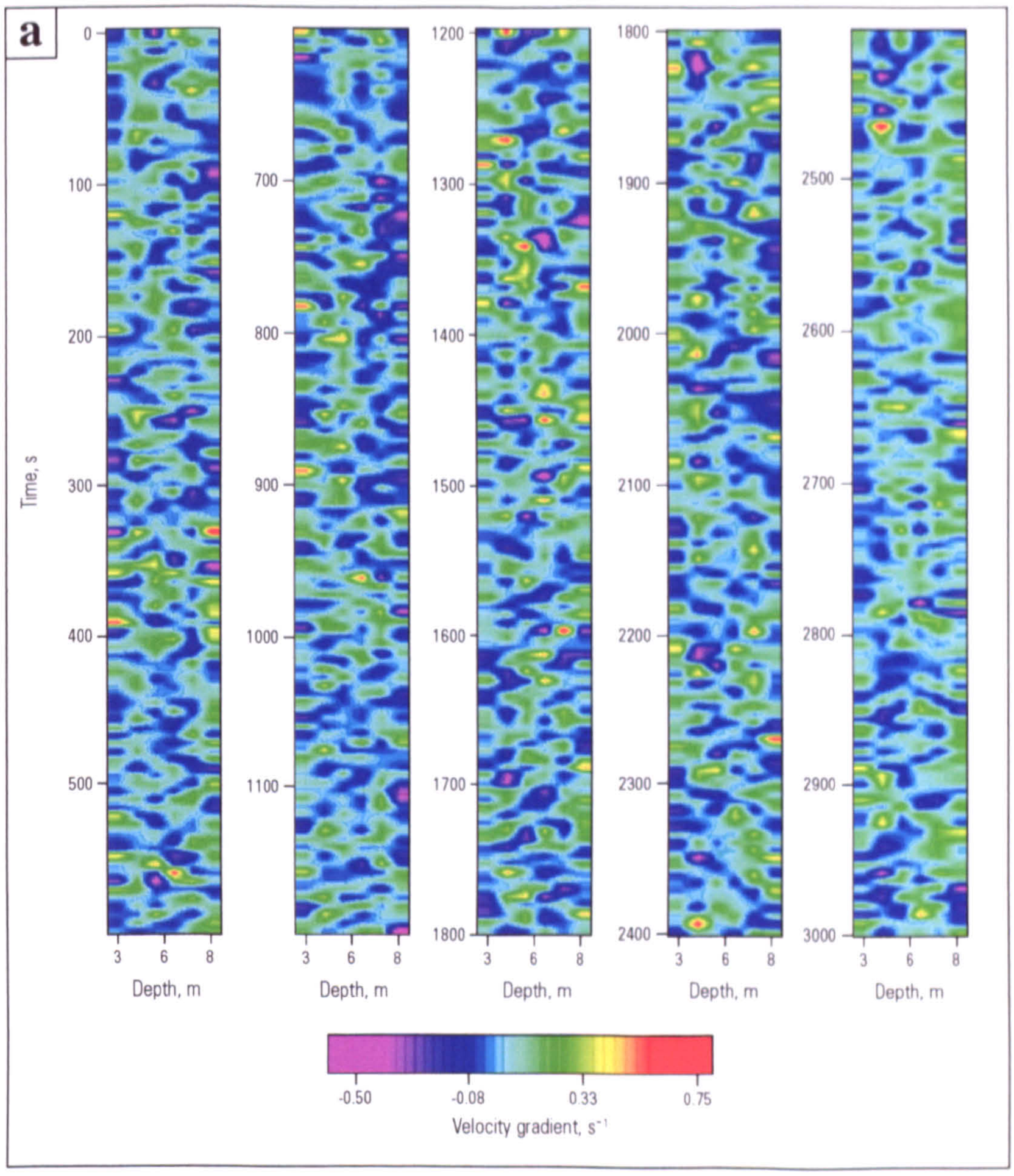

Figure 5.19: Contour maps of temporal variations in at-a-point downstream velocity gradient for the high flow survey at (a) H/94/C, dune crest and (b) H/94/T, dune trough. Flow is from top to bottom and a scale colour bar is given for each map. Flow depth bin sizes are 0.5 m. Each time series has been split to fit to page size and successive profiles are from left to right.

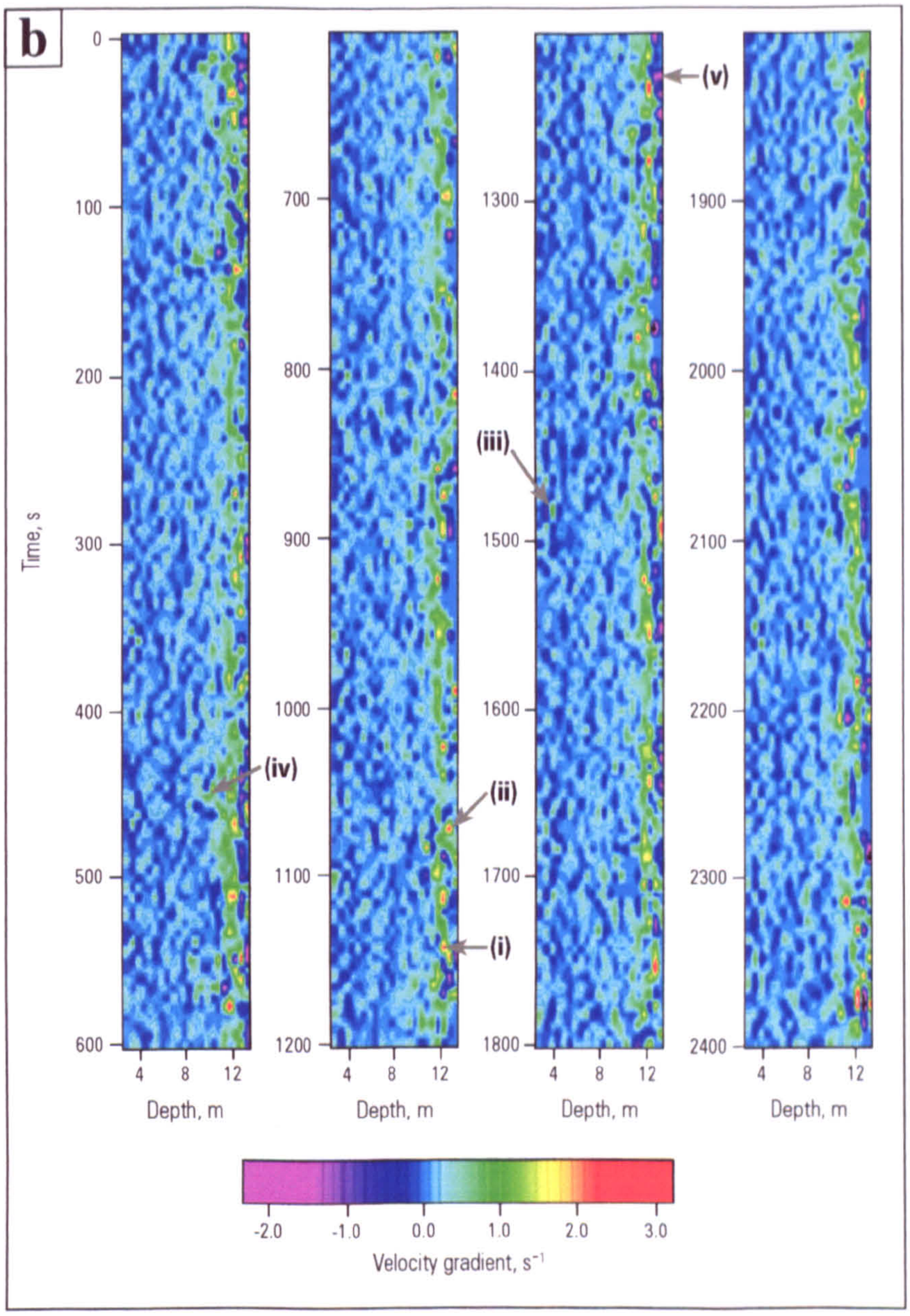

Figure 5.19: Contour maps of temporal variations in at-a-point downstream velocity gradient for the high flow survey at (a) H/94/C, dune crest and (b) H/94/T, dune trough. Flow is from top to bottom and a scale colour bar is given for each map. Flow depth bin sizes are 0.5 m. Each time series has been split to fit to page size and successive profiles are from left to right. (i) intermittent period of high velocity gradient, (ii) movement of high velocity gradient packages upwards in the flow column, (iii) occasional high velocity gradient packages in the outer zone of the flow column, (iv) high velocity gradient packages lifting in the flow column as they detach from the shear layer indicating an ejection of turbulent fluid. These may be linked with flow reversals shown in Figure 16b and (v) high negative velocity gradients near the bed.

The most obvious characteristic of the profile collected at high flow in the dune trough is periods of high intensity shear that occur in a zone at a depth of 10.5 -12.5 m (see Figure 5.19b(i), which is in agreement with the mean downstream velocity measurements (Figure 5.10) where maximum mean gradients also occur at this depth range. These events exhibit velocity gradients of up to 3.2 s^{-1} where as the ambient gradient varies between ±0.8 s^{-1}, these events appear to be unstable, occur intermittently and usually decay after approximately 20 s. No other shear events of such high magnitude are found at any other location in the flow column for this profile, or in any other position over the additional bedforms studied. The flow visualisation studies of Müller and Gyr (1982, 1986) give some insight into these findings. Müller and Gyr (1982, 1986) found that the velocity difference across the shear layer is much higher than for the rest of the flow and therefore contains the vorticity distribution of the up stream boundary layer. Since the shear layer is unstable, vertical deformations start to grow and the vorticity is transported into discrete vortices. Hence the spatial and temporal variation in velocity gradient shown in Figure 5.19 is indicative of the movement and growth of vortical structures in the shear layer. These vortices grow by viscous diffusion and entrainment, until they start a pairing cycle (Roshko, 1976) which will then create larger vortical structures. As velocity differentials may be viewed as being proportional to the turbulence intensity (Bennett and Best, 1995), these results show that turbulence production in the lee side of the dunes is dominated by eddy shedding caused by shear layer instability.

Although most of these events are distinct and temporally brief, a proportion of the higher magnitude shear events are seen to move upwards in the column (see Figure 5.19b (ii)) with time. The magnitude and frequency of turbulent ejection events is determined by the velocity gradient across the shear layer and hence the rotational velocity of the Kelvin-Helmholtz instabilities that are generated (Bennett and Best, 1995). The movement of spatially and temporally distinct packages seen in Figure 5.19b (ii) can therefore be postulated to be the growth and ejection of some of the high shear events away from the shear layer upwards into the flow column. As the profile is only a vertical time slice, the continued ejection and trajectories of these structure cannot be seen from one profile alone as ejected vortices will be convected downstream. There are, however, occasional higher shear (>0.5 s^{-1}) events which occur nearer to the water surface (see Figure 5.19b (iii)). These events could well be indicative of rotational vortices that were originally formed at a shear layer as described above (e.g. Nelson, 1989).

These velocity gradient plots can be linked with the downstream and vertical velocity results shown in Figure 5.16b. An extended period of lower than average downstream velocity and wake formation, together with higher than average vertical velocity (see Figure 5.16b (i)) is accompanied by lifting of

the shear layer (Figure 5.19b (iv)) which can be interpreted as a detachment of high shear, low downstream velocity fluid from the main shear layer. Müller and Gyr (1986) suggest that the evolution of an ejection begins with a strong flow reversal within the trough and this corresponds very well with the temporal variations in downstream velocity and velocity gradient data. This is therefore an ejection of a rotational vortex away from the unstable shear layer upwards into the flow column, if the eddy is large enough (especially if eddy amalgamation or pairing occurs) it may have enough rotational energy to move upwards and be ejected to the water surface where it will be visible as a boil or vortex. Nelson *et al.* (1993) also suggested that such high momentum coherent structures are advected downstream from the flow separation point thereby producing variations in the separation zone geometry. Periodic motions of this nature are associated with regular vortex shedding from the shear layer, and these events may then give rise to increased movement or flapping of the shear layer. These high positive shear intensity zones after often accompanied by high negative shear directly beneath them (see Figure 5.19b (v)), these negative shear zones are attached to the bed and illustrate the effect of flow reversals that have been shown to be concurrent with a highly developed shear layer.

It is apparent from this analysis that the origin of bursting behind steep angled dune bedforms is from eddy shedding by the provision of extremely high, intermittent, instantaneous velocity differentials across the shear layer and within the flow reattachment zone. The main points of this section are summarised schematically in Figure 5.20.

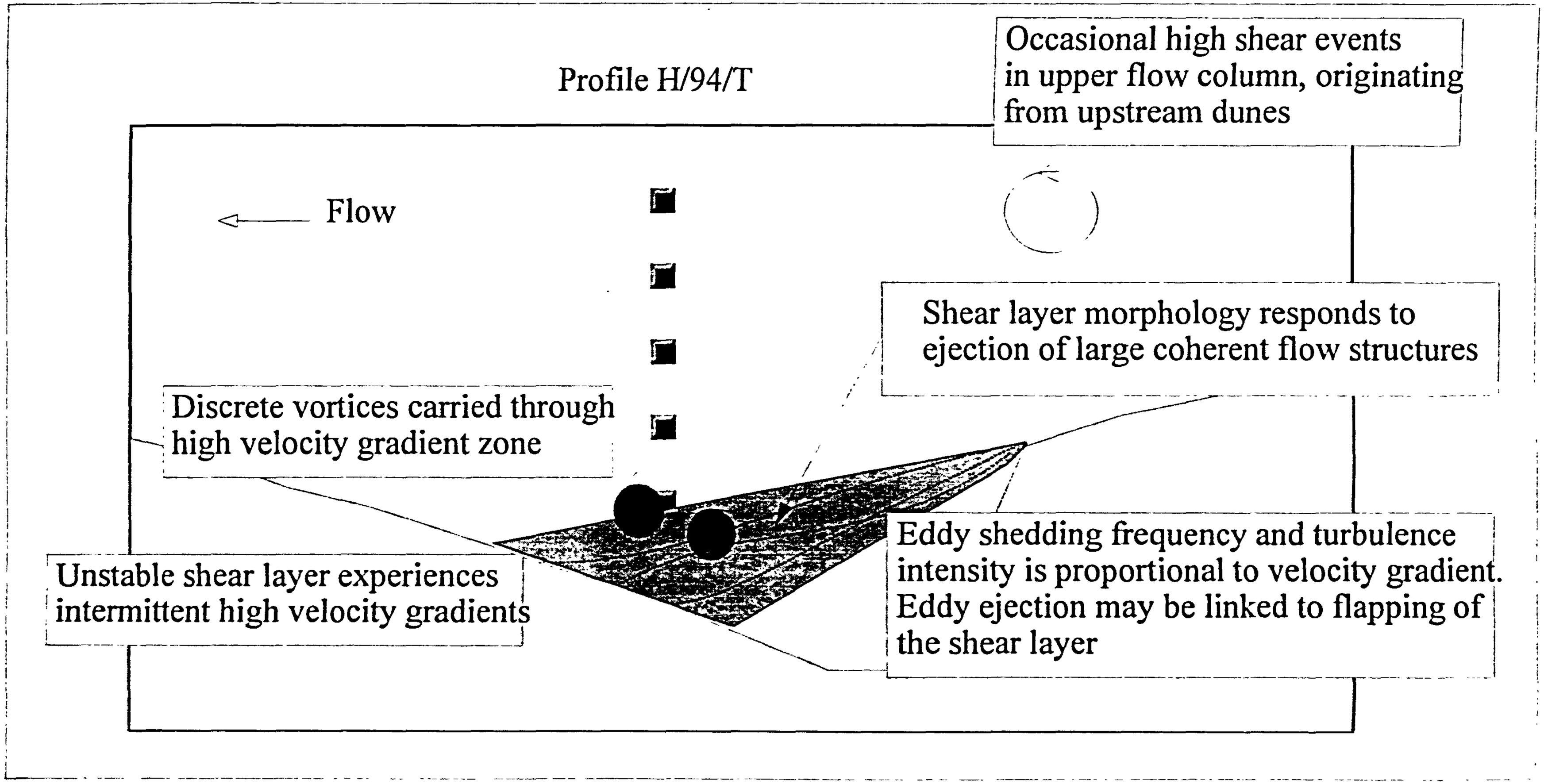

Figure 5.20, Schematic ilustrating the main features of the spatial and temporal variations in the downstream velocity gradient.

5.5.7 Quadrant Analysis

The use of quadrant analysis facilitates distinction of different types of turbulent event through examination of the signatures of the u' and v' records and has previously been used to discriminate boundary layer turbulent episodes by many workers (e.g. Lu and Willmarth, 1973; Bogard and Tiederman, 1986). Turbulence structure determined using quadrant analysis (Figure 5.21) defines the type of turbulent event by which quadrant in the u'v' plane each event falls into.

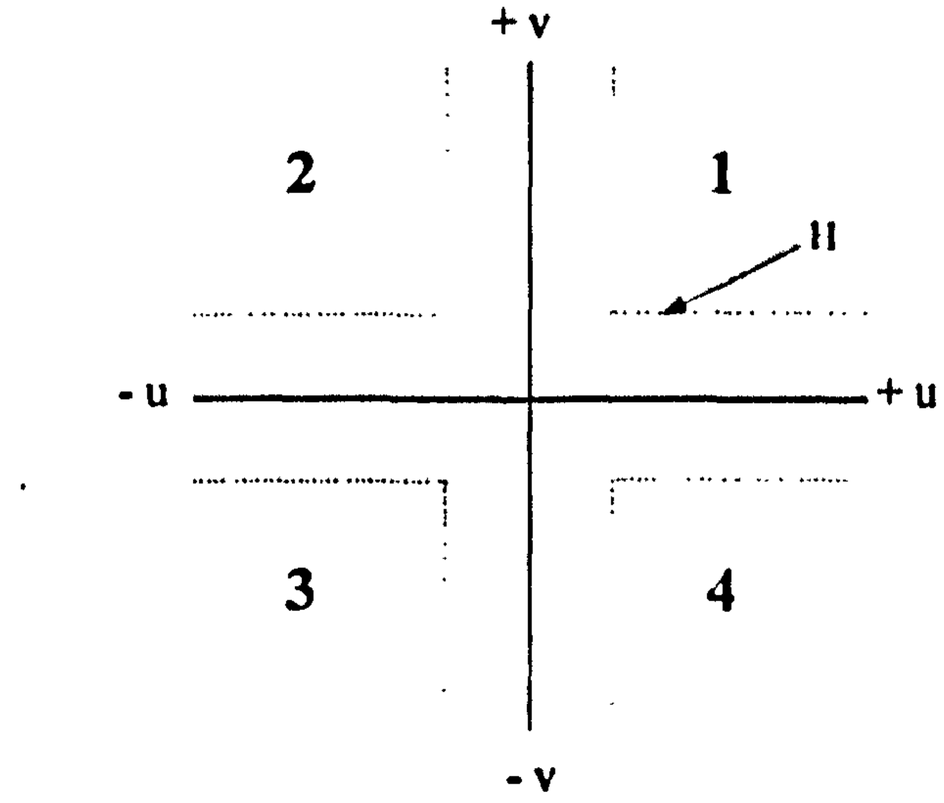

Figure 5.21, Quadrants of the instantaneous uv plane. Quadrants 2 and 4 denote 'ejections' and 'sweeps' of turbulent boundary layer studies, whereas quadrants 1 and 3 depict outward and inward interactions. Threshold values of H are determined from the variance of the u' and v' velocity distributions.

Plotting the horizontal and vertical velocity fluctuations about a zero mean defines four quadrants, with quadrants 2 and 4 events describing ejections and sweeps of boundary layer studies and quadrants 1 and 3 defining outward and inward interactions. Quadrant 2 and 4 events therefore provide an extraction of energy from the mean flow field to generate turbulence whereas events 1 and 3 provide an extraction of energy from turbulence back into the mean flow field. The contribution to -uv from each turbulent velocity pair may be investigated either through examination of the entire signal or only those events that lie above a certain threshold value of -uv. An example of the relationship of contributions to -uv from each turbulent velocity pair is illustrated in Figure 5.22 where at-a-point values of the downstream and vertical velocities are plotted with the corresponding -uv record for a 1500 second period at a depth of 12.7 m for profile H/94/T collected under high flow conditions over the dune trough.

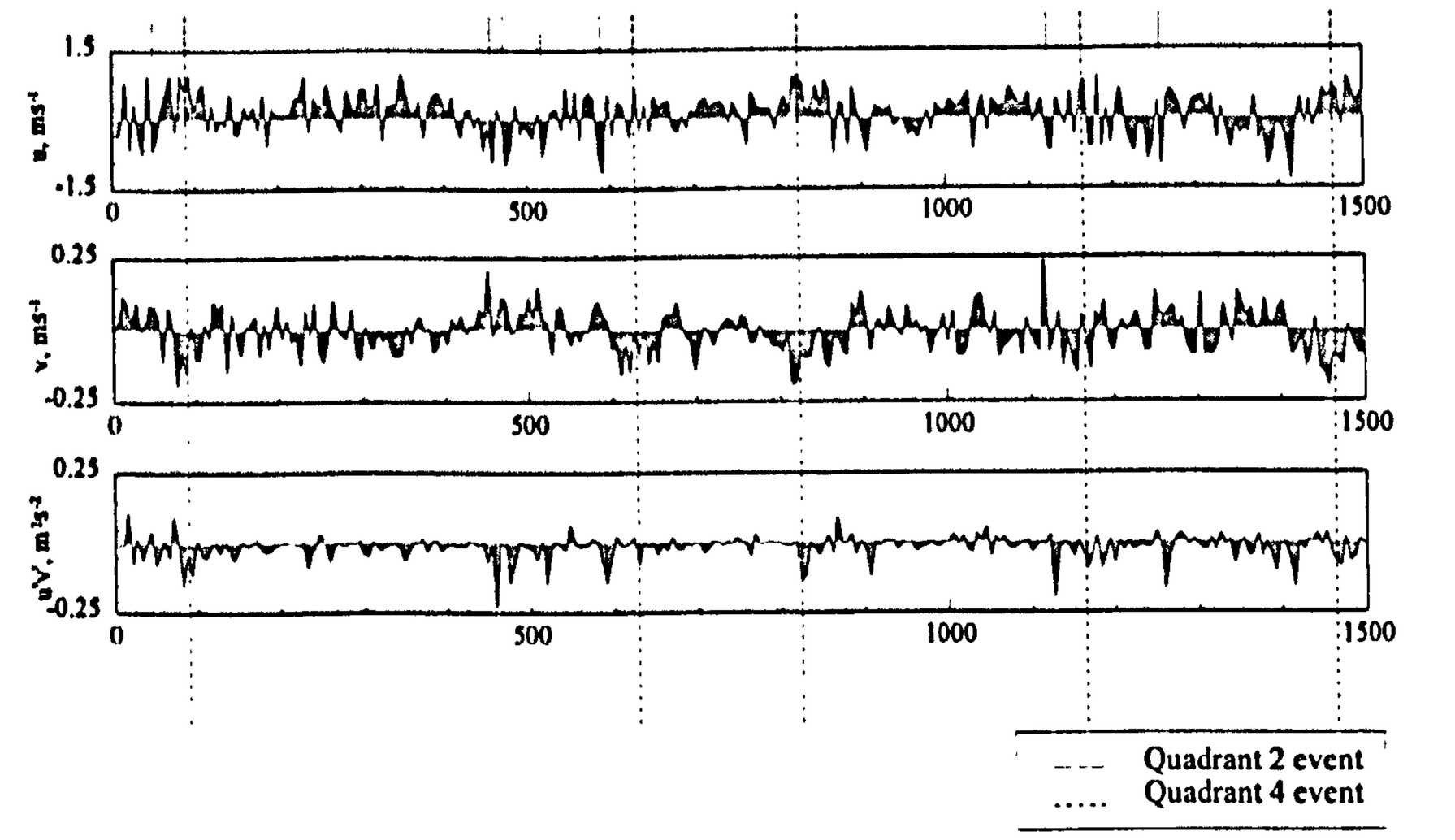

Figure 5.22, Downstream and vertical velocity fluctuations and uv time series for the first 1500s of a 3000s record from the high flow survey profile H/94/T. The flow depth at which the data were recorded was 12.7m and quadrant 2 and 4 events are labelled.

Quadrant 2 and 4 events have been identified and illustrate that excursions in u and v do in fact correspond to high contributions to the Reynolds stress; these events occur intermittently along the record, with some possible grouping of large quadrant 2 and 4 events. One difficulty in this approach for examining turbulence structure is to determine a threshold value to delineate true turbulent events from background noise (Lapointe, 1992). In earlier investigations using quadrant analysis, thresholding was conducted using a 'hole' size where the hole is defined as $H = u'v' / U_{RMS}V_{RMS}$, which delimited the turbulent events by removing those signals of magnitude less than the hole size. As the u'v' field data used in this study are less reliable, a simpler model is used to remove smaller events based simply on the standard deviation of the entire u' and v' signal. Increasing multiples of the standard deviations of the velocity population have been used to remove successively larger events. When thresholding values are set to zero, $-uv_Q$ for each quadrant Q is defined as:

$$-u'v'_Q = 1/n \sum S\,(u - U)(v - V) \qquad \text{equation 5.6}$$

where S is a sorting factor which is equal to 1 if u-U and v-V fall into quadrant Q, and equals 0 otherwise. For a threshold $T > 0$, $S = 1$ if $|\acute{u}\acute{v}| > T$, otherwise $S = 0$. A FORTRAN computer program was written to perform all quadrant analysis.

It should be noted that the sampling frequency of the ADCP in conjunction with relatively harsh filtering for the velocity distributions described above by thresholding in this fashion signifies that only the largest events may be observed.

The percentage occurrence of quadrant events at different depths in the trough of the steep angled high flow dune (H/94/T) are shown in Figure 5.23 as a percentage of the total event occurrence. These data were calculated using a threshold value of 1 standard deviation for the instantaneous deviations from the mean value for both the downstream and vertical flow components. In addition to the percentage occurrence of events, the fractional contributions of each quadrant to $-\acute{u}\acute{v}$ for increasing threshold values at three particular depths are also presented (Figure 5.24).

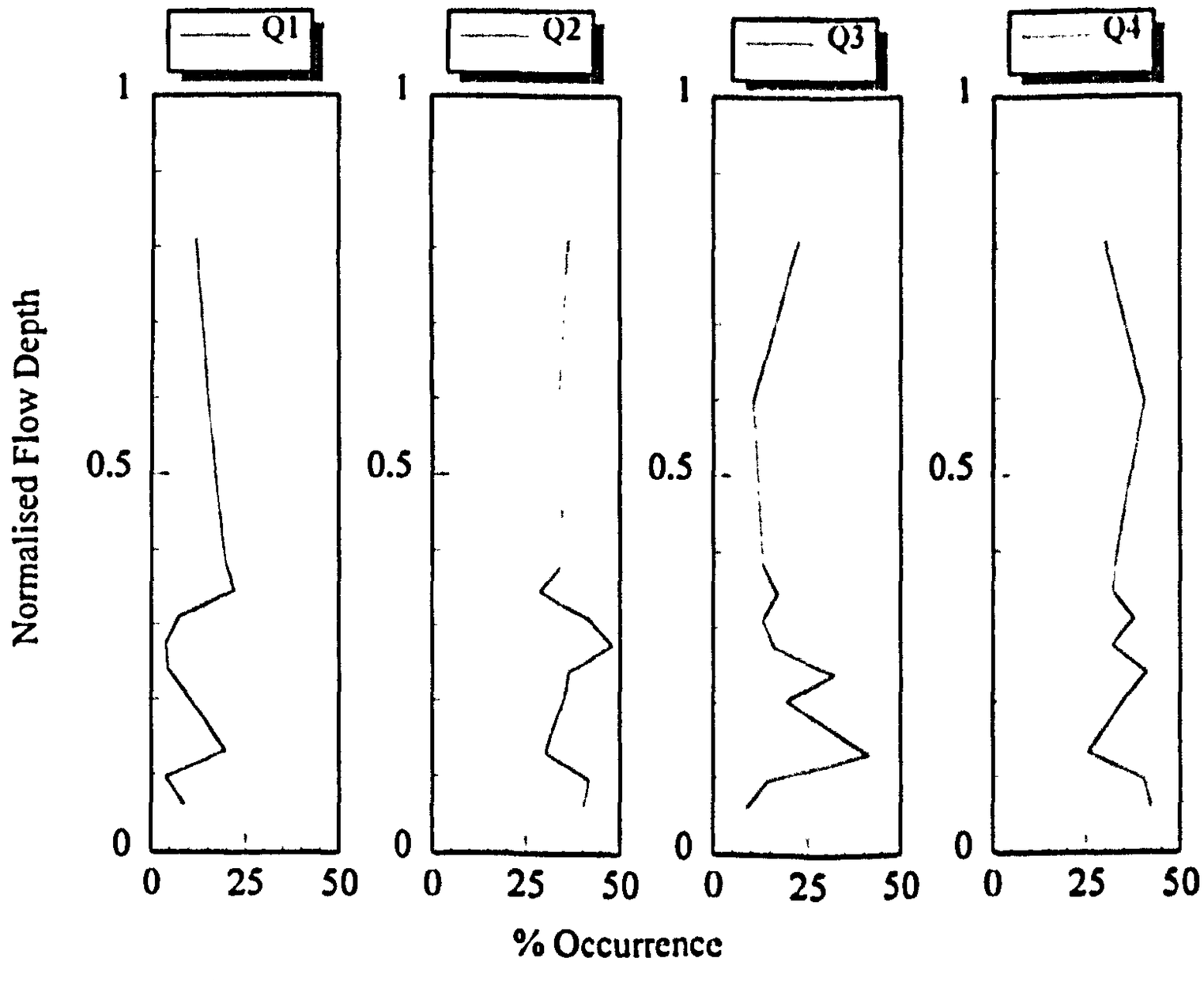

Figure 5.23, Vertical profile of percentage of occurrence of quadrant 1, 2, 3 and 4 events. Threshold value for u and v is 1 standard deviation.

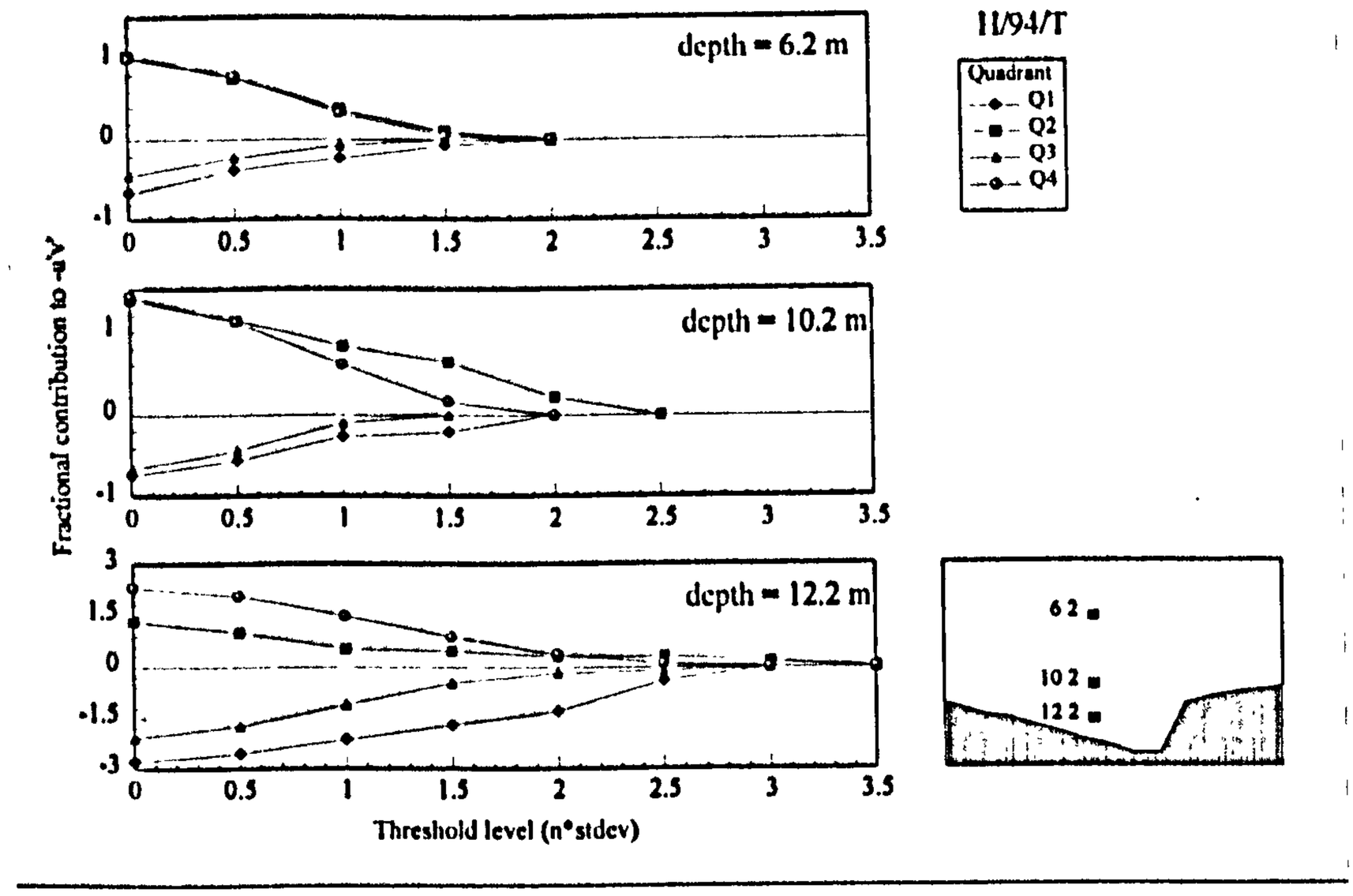

Figure 5.24, Fractional contribution to -uv of quadrants 1, 2, 3 and 4 for profile H/94/T. Flow depths of 6.2 m, 10.7 m and 12.2 m are shown for varying threshold values (0 to 3.5 standard deviations).

Quadrant 1 events show a decrease in occurrence through the shear layer followed by an increase in occurrence through the separation zone, principally near the bed. This has previously been explained as the ejection of fluid that has earlier been brought towards the bed within and along the separation zone shear layer (Bennett and Best, 1995). The magnitude of these quadrant 1 events is also at a maximum within the separation zone.

The percentage occurrence of quadrant 3 events is likewise at a peak within the separation zone, with most occurring just below the mean shear zone level. This may be due to entrainment of low velocity fluid from the lower part of the separation zone shear layer. The rate of decrease of the contribution of quadrant 3 events to -uv is higher than for those falling in the other quadrants, showing that quadrants 3 events do not occur at higher turbulence magnitudes.

Quadrant 2 events occur most regularly within and slightly above the shear layer: the peak in their distribution at this depth is pronounced. The values of percentage occurrence of quadrant 2 events are consistent through the flow column until the shear layer increase, this is followed by a decrease

within the separation zone and sudden increase at the bed. Although this second increase in events is smaller than that at the mean shear layer level, it is still considerable and can possibly be explained by the variations in shear zone height that were described above. This would lead to an increase in the ejections of fluid as the flow reattachment point is approached. Quadrant 2 events also dominate the fractional contribution to -u'v' over the dune crest (profile H/94/C, Figure 5.25) at all threshold levels, so agreeing well with previous work (Bennett and Best, 1995)

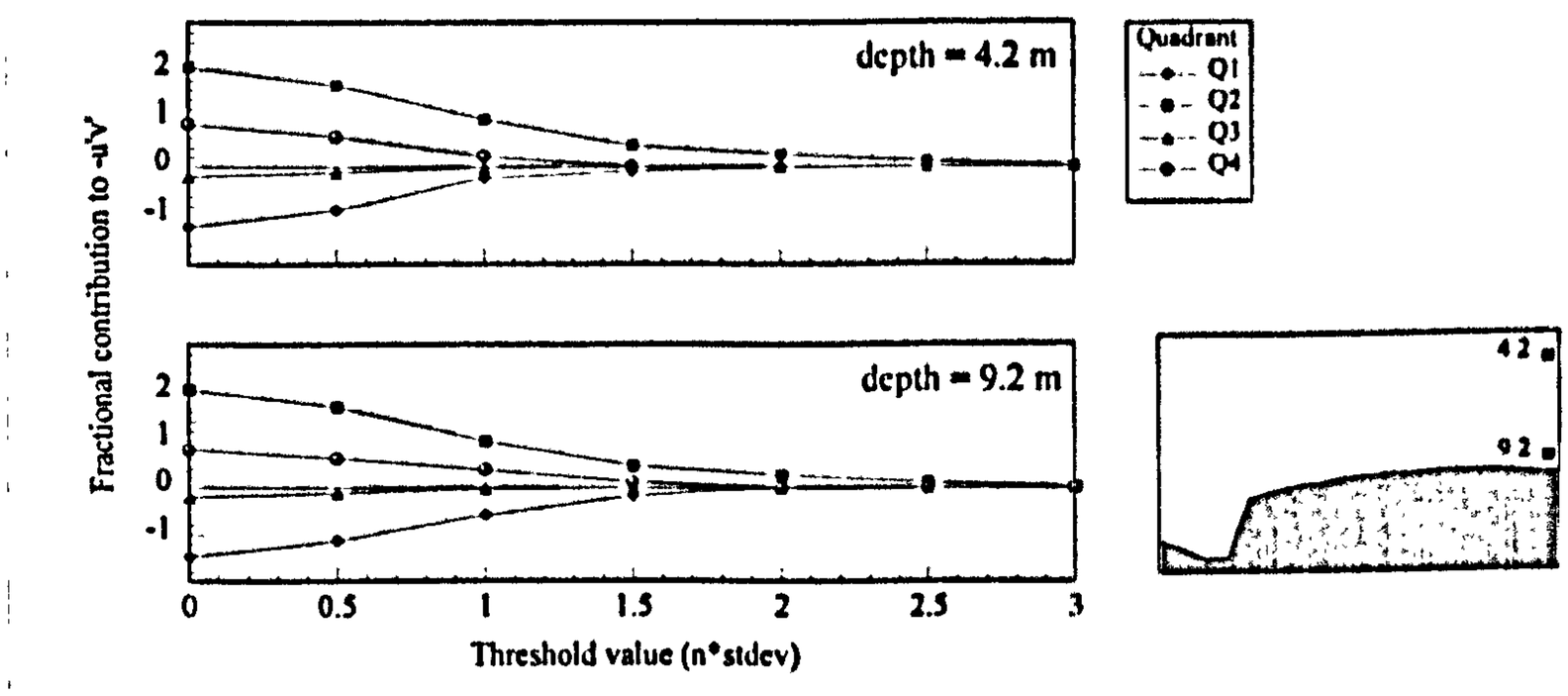

Figure 5.25, Fractional contribution to -u'v' of quadrants 1, 2, 3 and 4 for profile H/94/C1. Flow depths of 4.2 m and 9.2 m are shown for varying threshold values (0 to 3 standard deviations).

These results of quadrant analysis correspond well with the variations in velocity gradient described previously as they indicate that turbulence production in the leeside of dunes is generated by a Kelvin Helmholtz mechanism of eddy shedding of quadrant 2 'ejection' events from the unstable free shear layer created by flow separation at the dune crest. The fractional contribution of quadrant 2 events to -u'v' is at a greatest at the height of the shear layer. Domination of -uv by quadrant 2 events is primarily represented at higher threshold values (above 0.5) which may be a consequence of the ADCP data quality, as the effect of any background noise will be diminished at higher thresholding magnitudes. The dominance of quadrant 2 events at this height again highlights the linkage between the high shear or velocity gradients previously shown above and the mechanism of eddy shedding away from the shear layer into the main unseparated outer flow area. This is tested again in Figure 5.26 which shows both the temporal variation in velocity gradients and quadrant 2 and quadrant 4

event occurrence and illustrates that these two phenomena do mainly coincide temporally. The periodicity of these ejections will be examined in the subsequent section. The correspondence between quadrant 4 events and high velocity gradient is striking with 70.7% of quadrant 4 events occurring at a velocity gradient greater than $1s^{-1}$ and 27.4 % occurring at velocity gradients less than $-1\ s^{-1}$. There is greater variability in the occurrence of quadrant 2 events relative to high velocity gradients but even so 71.5% of quadrant 2 events occur at velocity gradient magnitudes greater than $1\ s^{-1}$. These results show that the velocity differential across the shear zone does in fact determine turbulence production.

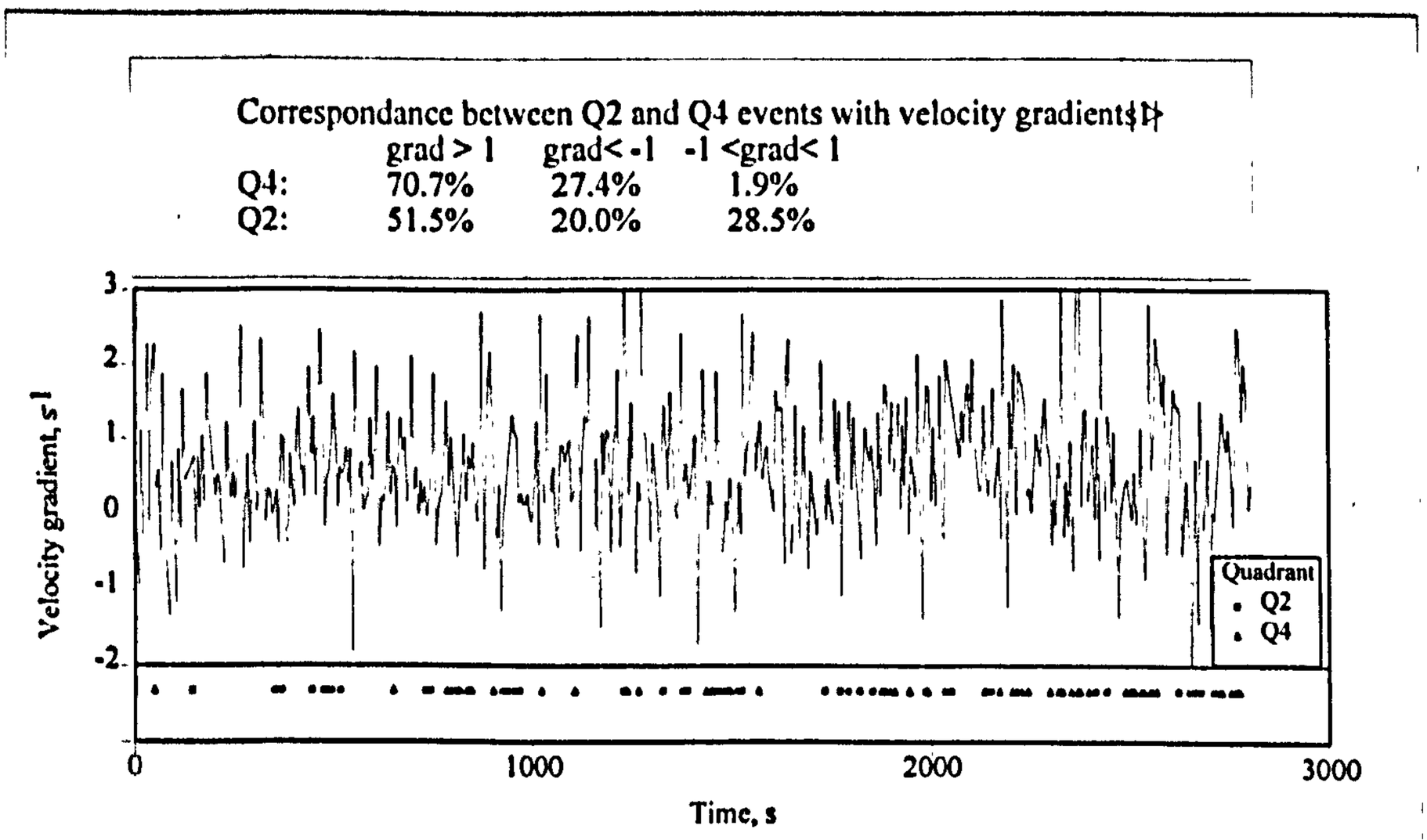

Figure 5.26, The temporal relationship between quadrant 2 and 4 (thresholded on 1 deviation of u' and v') events and high velocity gradients in the shear layer, profile H/94/T, depth 12.2 m.

The percentage occurrence of quadrant 4 events (Figure 5.24) shows small increases through the shear layer and at reattachment so exhibiting the same pattern of occurrence with depth as quadrant 2 events, although absolute event occurrence is much less for quadrant 4 than for quadrant 2. However, the fractional contribution of quadrant 4 to -u'v' is much greater than quadrant 2 within the separation zone itself which is in very good agreement with previous experimental work (Bennett and Best, 1995): although the events are less frequent they are relatively more energetic. This may be explained by the inrushes of high velocity fluid which are brought towards the bed from the outer

flow along the shear layer and which may therefore be very important for the entrainment and bedload transport of sediment.

5.5.8 Event Recurrence in Dune Related Macroturbulence

Results of quadrant analysis and the differences in temporal variation in velocity gradient along the separation zone shear layer when compared to the rest of the flow (Figure 5.19) have indicated that there are differences in turbulence structure downstream of flow separation. The variations in velocity gradient appear to exhibit intermittent or periodic development and these variations have been postulated to be linked to different sources; shear layer flapping and eddy ejection. Previous studies which used sonar to visualise turbulent ejections associated with dunes (Kostaschuk and Church, 1993) displayed an apparent repeated cyclicity on time scales of several minutes. Levi (1983, 1991) proposed a universal relationship between the frequency of oscillation induced in a body of fluid restrained by an external free flow described by the Strouhal number, $St=fD/U \sim 0.16$, where f is the shedding frequency, h is the height of the restrained body of fluid and U is the mean downstream velocity. If the Strouhal law is applicable for eddy shedding from the lee side of the high flow survey dune then expected frequencies should approximate 0.07 Hz.

Simpson (1989) proposed that the dominant frequency associated with vortex shedding downstream of flow separation is about 0.8 U_o/x_r and that associated with wake flapping is less than about 0.1 U_o/x_r where x_r is the reattachment length and U_o is the mean velocity upstream of the separation point. In their flume study of the flow downstream of a negative step, Nelson *et al.* (1995) observed spectral peaks at frequencies approximating those proposed by Simpson. For this present study the expected eddy shedding frequency according to Simpson (1989) is 0.13 Hz and the expected shear layer flapping frequency is 0.015 Hz. However, Simpson showed that reattachment length is variable on a scale of between 2 and 6 times the obstacle height, in which case eddy shedding frequencies would vary between 0.06 and 0.17 Hz, and shear layer flapping frequencies should vary between 0.02 and 0.007 Hz. This variation in postulated eddy shedding and flapping frequencies implies that quantifying the phenomena may be more complex than implied by Levi's universal Strouhal number studies.

It should be noted here that the sampling rate of the ADCP will severely limit investigations into periodicity in flow processes. For a time series sampled at an interval of dt, the Nyquist frequency, which is the shortest wavelength which can be resolved, is 2dt and the longest wavelength that can be filtered to a time series of length T is therefore T/2. Therefore the shortest period measurable for this

study is 0.09 Hz, which according to Simpson (1989) is too low a frequency to resolve all eddy ejection.

This section seeks to quantify any apparent periodicity in the variations in the velocity gradient, and the downstream and vertical velocities and also to test the assumption of a consistent value of the Strouhal number. This section will also seek to distinguish dominant frequencies which relate to different phenomena, namely eddy shedding and shear layer flapping. In addition, visual evidence of the recurrence time of fluid upwellings or boils on the water surface will be compared with the ADCP data. It should be noted that the measuring times of the ADCP limit the frequencies that can be observed: any fluctuations that are on a time scale smaller than the ADCP measuring time of 5.5 s will not be resolved.

The periodicity and temporal lag of turbulence structures may be examined using spectral analysis. Spectral analysis concerns the partitioning of the variation in a time series into components according to the duration or length of the intervals within which the variation occurs. Spectral decomposition is accomplished by considering the time series to be the sum of many simpler time series that have the form of regular sinusoids of differing amplitudes, wavelengths and starting points. Any time series, regardless of the complexity in its form, can be represented as the sum of a series of cosine and sine wave forms with the following provisos:

1) the time series must be continuous or without breaks

2) there must be only one value of Y for each value of X.

This means that velocity time series collected at depths greater than 10 m using the ADCP must be resampled before they can be used for spectral analysis due to the inconsistency of the record. The sinusoids are calculated so they are orthogonal, or statistically independent of one another. Since the sum of all the sinusoids is equal to the original time series, the sum of the variation in all the sinusoids must also be equal to the total variation in the series

To produce the spectrum of any time series the following protocol must be followed:

1. Filtering to remove all energy near and above the Nyquist frequency. This band limits the signal.
2. Tapering to smooth the ends of the time series to zero. This is necessary because the Fourier Transform recognises that the series is periodically continued. Unless the end of the points are equal there will be an apparent jump in the frequency series. Tapering involves multiplying the time series by a function that goes to zero at the ends; it is equivalent to convolution in the frequency domain which has the effect of smoothing the spectrum.

3. Removing the mean and trend (e.g. by fitting a polynomial) because this spreads energy to high frequency.
4. Pad with zeros, usually to make the number of samples a power of 2 for the FFT. This smoothes the spectrum by interpolation and also make it computationally more efficient.

These procedures have been carried out using the time series analysis software package PITSA. Firstly, traces are baseline corrected to remove any slowly varying component from the trace (i.e. detrend the signal). A linear regression is used to do this, which also subtracts the mean from the series. The signal is then filtered using a Butterworth low pass filter (a recursive time domain filter). This filter is applied backwards and forwards to give zero phase characteristics (i.e. the phase of the signal is not changed by the filtering process so correlation can later be carried out). The filter frequency chosen is slightly lower than the Nyquist frequency of each signal which has the effect of smoothing the signal in excess of the amount needed to allow spectral analysis to remove any obvious excess noise from the data. Finally a Bartlett taper (a linear taper of strength 0.1) is applied to smooth the signal ends to zero. The spectral amplitude of each series is output by PITSA after demultiplexing the Fourier transform which involves extracting the real and imaginary parts of the FFT. This amplitude is then converted to the line power spectrum (also known as the variance), which is simply half the square of the amplitude.

Possible problems concerned with spectral analysis on these data include:

- ADCP records could be too noisy to distinguish periodic turbulence structures
- If the data quality is viable for spectral analysis, turbulence could be intermittent (or homogeneous) and therefore no particular periods would be dominant and spectral analysis would not be useful.

Due to the noise component which is inherent in velocity measurements, it is important to test whether peaks in frequency spectra can be attributed to noise or show dominant frequencies. To test for significance in any peaks arising in the frequency-power spectrum the g statistic is used (see Swan and Sandilands, 1995). The g statistic is an interpretation of power as variance; it is based on the ratio of the maximum variance at a frequency (s^2max) to the total variance of the series (s^2), which is equivalent to the sum of the powers at all frequencies.

$$g = s^2max / 2s^2$$

H0 is the power at frequency attributable to randomness and H1 is cyclicity existing at that frequency.

The critical value of g is estimated by

$g = 1\text{-}e\ \{(lnp - lnm)/m\text{-}1\}$

where p is the level of significance and m is half the number of observations.

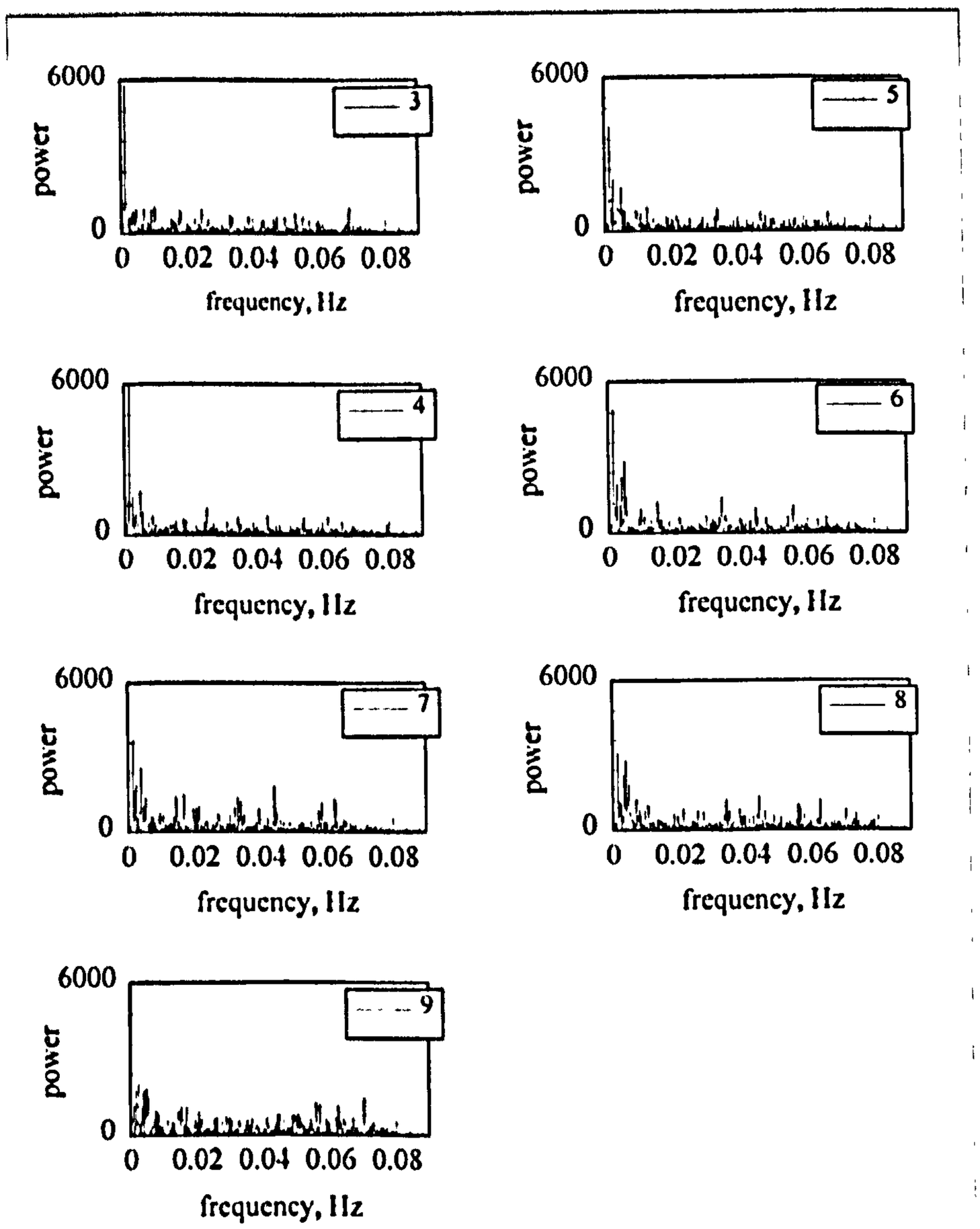

Figure 5.27, Power spectra of downstream velocity at the depths indicted from the high flow survey over the dune trough (H/94/T).

Results from spectral analysis for profile H/94/T are shown in Figure 5.27, the spectra have been calculated at 1m depth intervals and are plotted as spectral power vs. frequency. As some of the signals are rather noisy, an attempt to quantify which peaks are significant has firstly been accomplished by imposing the limit of spectral powers greater than 3 standard

deviations of the population for the power of each potential significant peak (to avoid computing statistics for small peaks) and secondly calculating the critical value of the g statistic values as described above. All peaks with values greater than 3 standard deviations from the mean have been tabulated in Table 5.3 for both the downstream and vertical velocity components.

	Period (s)								
u-component									
H/94/T	227	135	*62.7*		*29*		17.5	15.3	
v-component									
H/94/T			*71*	34	*27*	22.9	19	16	14
mean			*67.0*		*27.2*				

Table 5.3: Dominant FFT peak periods for profile H/94/T (time in s)

None of the peaks in the FFT power spectrum for any of the data analysed were statistically significant when examined in relation to the variance of the whole signal. All values of g calculated for the larger spectral peaks were a minimum of 1 standard deviation smaller than the critical values required for significance. This implies that the visible peaks are either a result of background noise and there are no dominant frequencies or periodicities in the signal (eddy ejection or shear layer flapping are intermittent) or that any dominant frequency is weak and is masked by background noise due to the inherent variability in data of this nature compounded by the measurement precision of the ADCP. However, as the period of shear layer flapping proposed by Simpson (1989) of 66.7 s is in agreement with the largest peak occurrences for u and v, it may be postulated that this variation is caused by this phenomenon.

The second largest peak frequency in downstream and vertical velocity is 27 s (Table 3) which may be caused by noise in the signal or may be a real period related to eddy ejection. To try to distinguish which of the hypotheses is correct a comparison with visual observations of the occurrence of boils on the water surface can also be made and also a comparison with the recurrence interval of high velocity gradient packages within the shear layer. Visual observations of periodicities of boils erupting at the water surface show a range from 5 - 50 s with a mean of approximately 22.5 s (Figure 5.28), a standard deviation of 10.3 s and a positive skewness of 0.73. The positive skewness in the frequency distribution compares well with previous studies in the field (Jackson, 1976; Kostaschuk and Church, 1993) and flume work (Kim *et al.*, 1971; Fukuorka and Fukushima, 1980). The mean

periodicity of boil occurrence on the water surface of 22.5 s is close to the second highest peak frequency in downstream and vertical velocity from spectral analysis, indicating that this second peak may be relating to shedding of large eddies upwards into the flow column away from the shear layer.

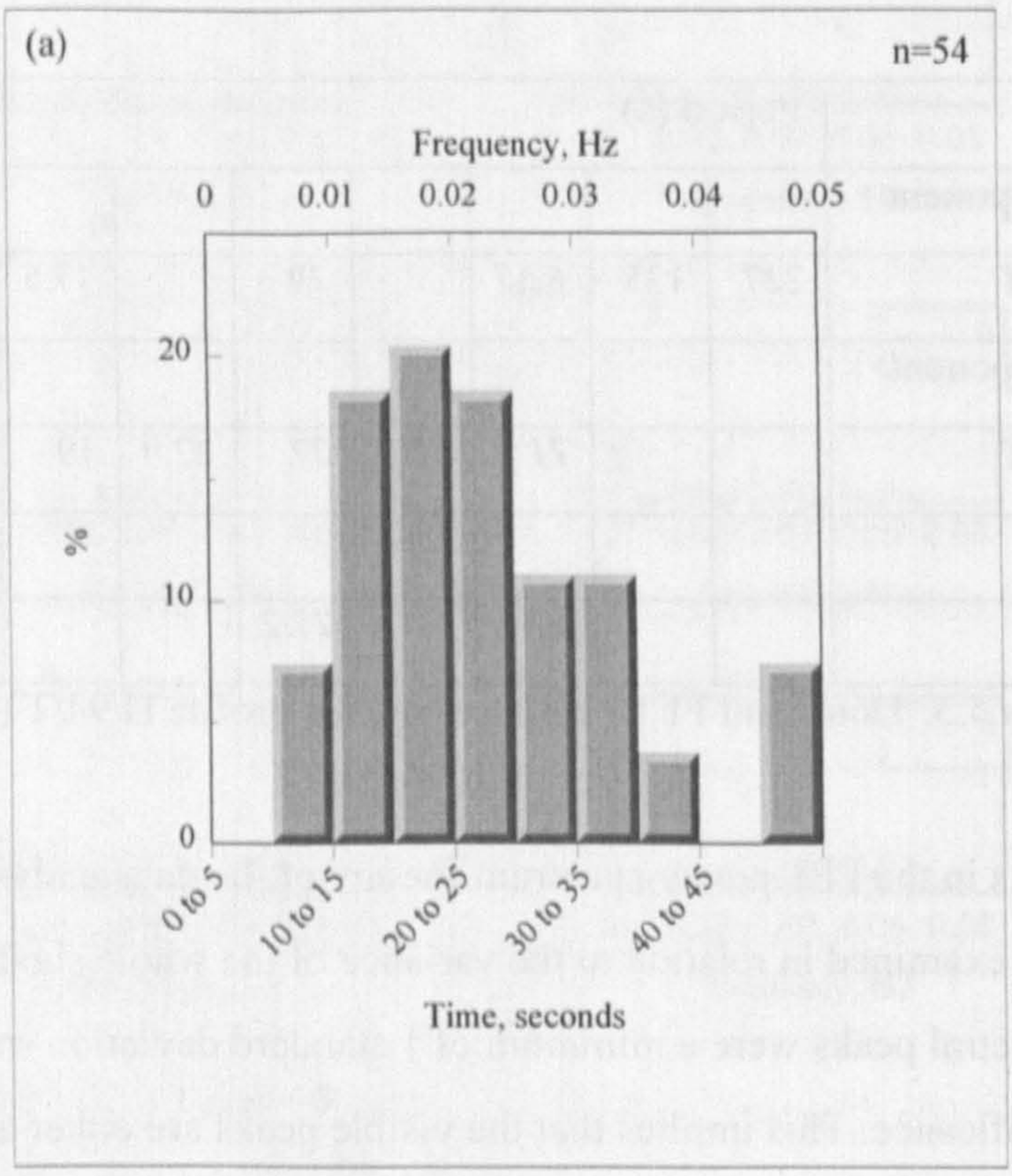

(b)

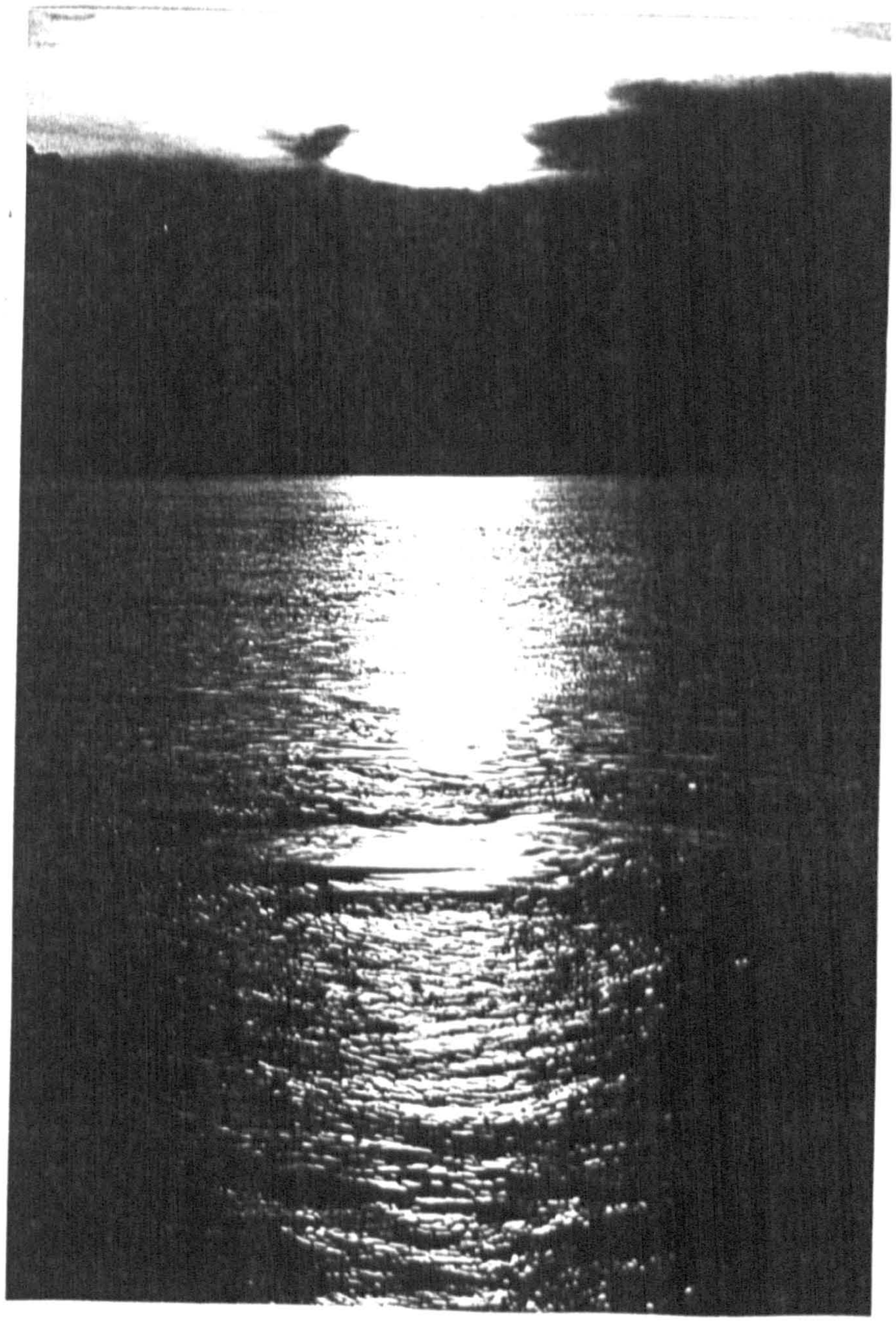

Figure 5.28, (a) Histogram describing visual observations of boil eruption at the water surface and (b) photograph of a boil of 10 m in diameter erupting at the water surface.

It should be noted that the results of such visual observations of turbulence structures on the water surface may be circumspect since the generation location of the boils is unknown, and hence the interval time between boil eruption may be erroneous. The range in surface boil size was between 1 m and 15 m in diameter. In planform, the shapes of the surface boils ranged from circular to elongate, depending on the length of time the eddy had been at the surface due to propagation of the structures downstream, the eddies increasing in elongation with increasing surface exposure. An example of a circular boil erupting at the water surface is given in Figure 5.28(b). The internal structure of all boils displayed a strong upward and outward movement of fluid (Kostaschuk and

Church, 1993) and many boils displayed multiple point sources of turbulent upwellings indicating that they consisted of amalgamations of a number of smaller vortices (Itakura and Kishi, 1980). Boils with multiple upwellings have been termed to have a 'cauliflower' morphology (Babakaiff and Hickin, 1996).

The variation in velocity gradient through the shear layer has been shown above to be intermittent with high velocity gradient packages being possibly linked to a combination of shear layer flapping and turbulent ejections away from the shear layer. As the high velocity gradient data signal is discontinuous at higher flow depths, spectral analysis cannot be used to calculate periodicites in the data using the entire time series. The longest time period with a continuous signal is 850 s and the spectral power of this record is given in Figure 5.29.

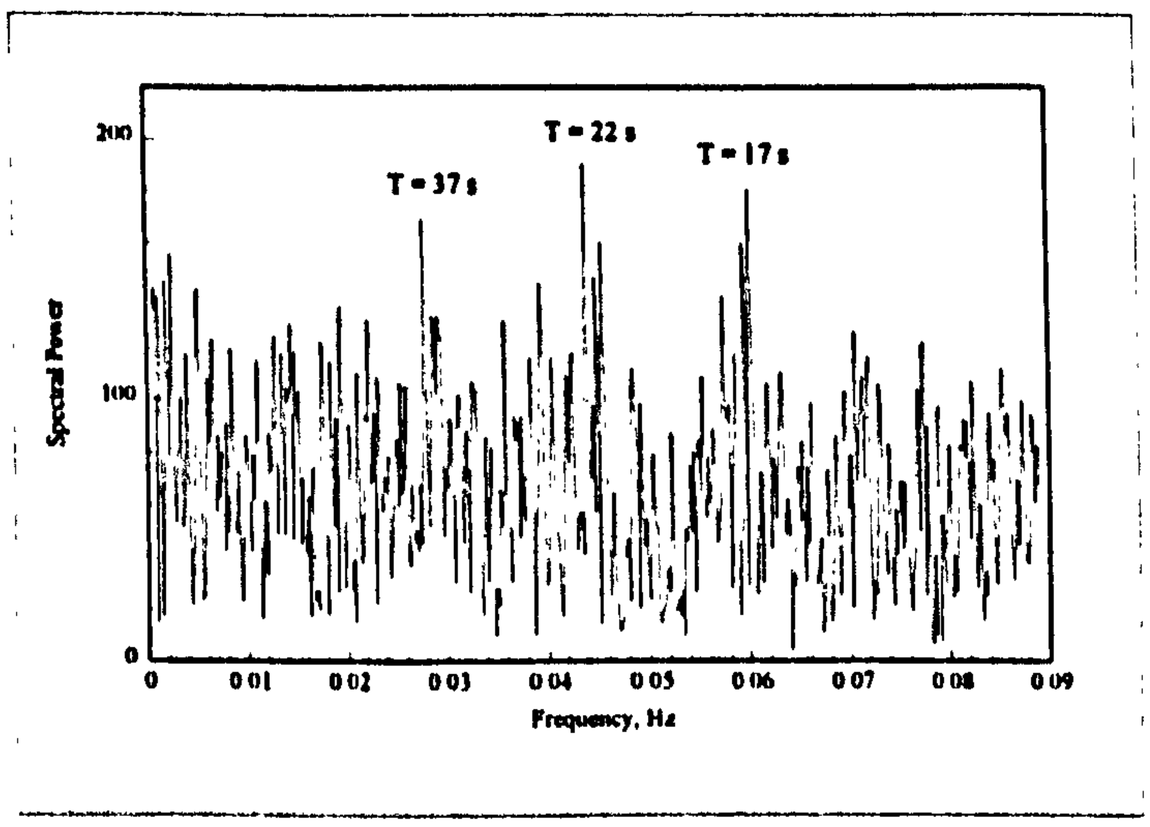

Figure 5.29, Power spectra of the velocity gradient through the separation zone shear layer from profile H/94/T. The height of profile is 12 .2 m.

As for the velocity data, any apparent peaks (e.g. 37 s, 22.7 s and 17 s) in the frequency distribution of the velocity gradient time series are not statistically significant and may therefore be an artefact of the low signal to noise level. However, visual observation of these records has also been used to examine the frequency of their occurrence with the mean event period of 22.5 s, so the peak identified using spectral analysis may well be real rather than apparent periodicity. The maximum recurrence time of high velocity gradient packages is 65 s with a mean duration of 11 s. The recurrence periods noted through visual observation of boils at the water surface and spectral analysis of the downstream and vertical velocity compare remarkably well with the periodicity of high

velocity gradient packages within the shear layer which have been postulated to be linked to eddy ejection.

The mean period of Quadrant 2 events in the shear layer is 22.8 s (Figure 5.30) which agrees well with estimates of the mean period of high velocity gradients occurrences (22.7 s), visual observations of boil eruption on the water surface(22.5 s) and peaks in the FFT spectra of the downstream velocity (27 s). There is, however, a high variance in all of the recurrence intervals observed and no single result is in itself statistically significant. However, the weight of evidence from different sources points to a mean recurrence period of around 22 s for ejection of eddies from the free shear layer. Although the mean values correspond well, any periodicity is rather weak in eddy ejection from the shear layer.

One problem with comparing results on periodicity in ejection using current meter records and boil occurrence at the flow surface is that only the largest structures ejected will succeed to the flow surface. The magnitude of turbulent events should therefore also be taken into consideration when examining their frequency: events of different sizes may well occur at different frequencies. To this end the recurrence time of events from different quadrants has been calculated. Quadrant 2 event recurrence period increases with event magnitude, larger quadrant 2 events in the shear layer, which have higher a contribution to the Reynolds stress, are relatively infrequent and occur at progressively longer time periods (Figure 5.30c). It may also be that the long ensemble averaging time of the ADCP means that the measured recurrence periods will only refer to larger ejections from the shear layer; there may well be higher frequency eddy shedding occurring that cannot be resolved by the ADCP.

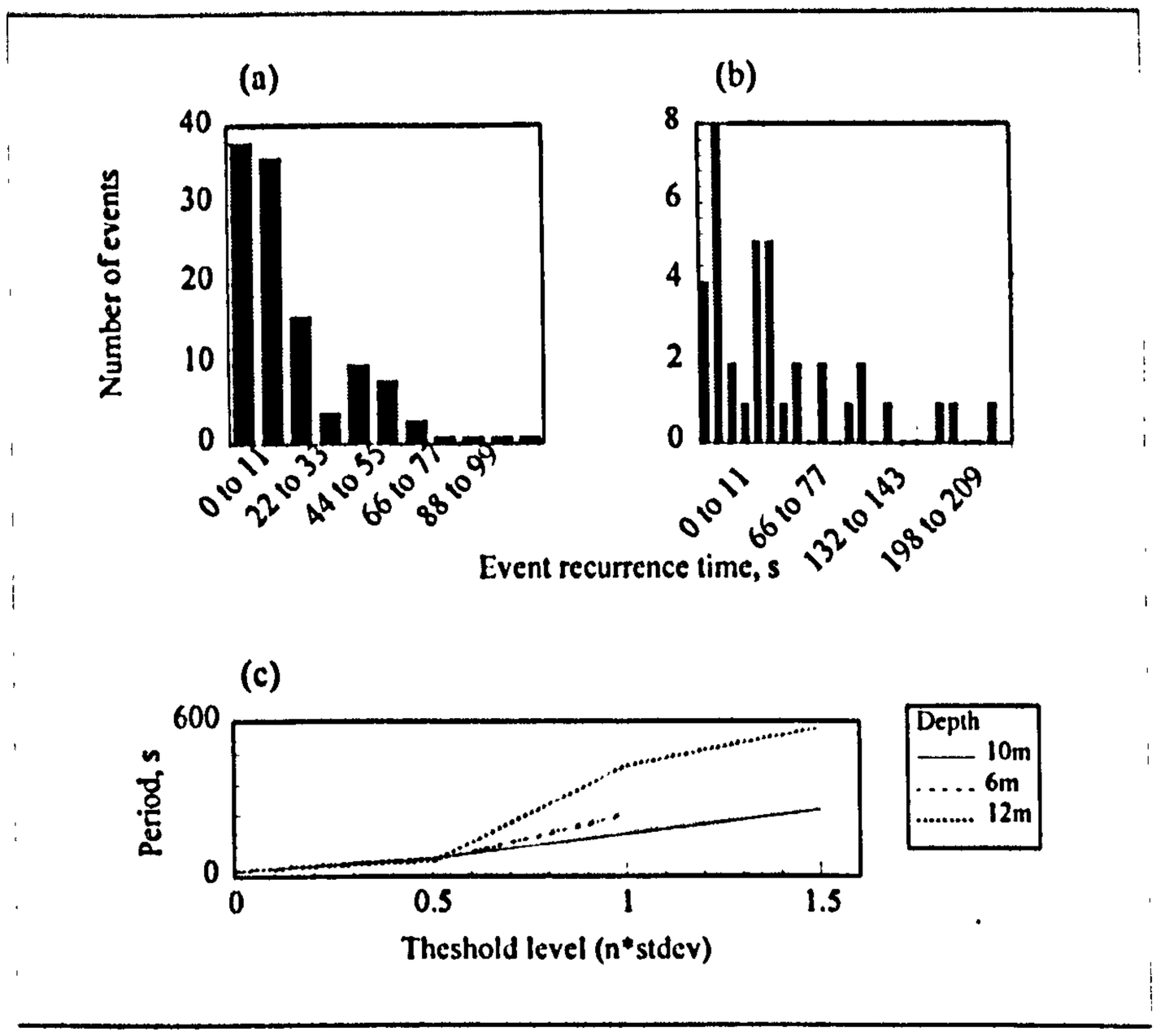

Figure 5.30, Histogram describing quadrant 2 events recurrence distributions with thresholding levels set at (a) 0 and (b) 0.5 standard deviations and (c) Recurrence period for quadrant 2 events at increasing threshold levels at depths of 6m, 10m and 12 m.

5.5.10 Summary of High Flow

The results of at-a-point velocity time series surveying at high flow rates have shown that the ADCP is a very useful instrument for studying mean flow and turbulence over dune bedforms in a field situation. Time-averaged mean velocity profiles agree very well with previously published work and show that the mean velocity is highly spatially variable along a dune. The formation of a flow separation zone and the corresponding production of a free shear layer dominates the flow field, and is controlled by dune morphology, probably being determined principally by the brink point angle of the bedform but is also a function of pre-separation crestal morphology and velocity.

Although the time averaged mean downstream velocity within the separation zone is not negative, intermittent flow reversals occur at the profile location for 45 % of the survey

duration and a more permanent separation cell may occur closer to the dune lee face. The magnitude and period of flow reversals decreases with increasing distance from the bed.

The free shear layer produced by flow separation has been shown to be temporally unstable, growth and decay of the velocity gradient through the shear layer has been linked to both turbulence generation and shear layer flapping. Turbulence generation associated with steep angled bedforms has been shown to be dominated by eddy shedding of Kelvin Helmholtz instabilities from the free shear layer, whereas quadrant 4 inrush-type events dominate turbulence production within the separation zone. Both quadrant 2 and 4 events are linked to high unstable velocity gradients acting across the separation zone free shear layer. The velocity differential through the shear layer may therefore control the erosion of sediment and hence the formation, growth and stability of high slip face angled bedforms.

{

5.6 Low Flow Surveys

5.6.1 Introduction

Both the results of surveying at high flow stage and previous studies (e.g. Kostaschuk and Villard, 1996) have shown that morphology has a great effect on the flow field over dunes. This next section presents results of two further at-a-point velocity time series surveys which were carried out at low flow stage. The surveys were conducted during March 1995 and February 1996, and the mean flow conditions and bed morphology have been described in sections 5.5.2 and 5.5.3. Under low flow discharges, surveying was conducted over both high lee face angle and low lee face angle bedforms and these results are described separately in the sections that follow. The aims of this section are to describe the mean and turbulence flow field over dunes of different morphology which have formed under a lower hydraulic regime. More specifically, several key questions must be addressed when comparing the flow fields:

1) Are the primary features of flow described above, such as flow separation and the growth of a free shear layer, present over high slip face angled dunes that formed under low flow rates?
2) If the features are present, how do processes such as the growth and decay of the shear zone and the formation of a flow separation zone scale with the change in mean hydraulic parameters and different bedform geometries?
3) How do any differences in the mean flow field and turbulence production processes link with the differing bedform morphology of the low and high slip face angled dunes?
4) Do flow reversals occur over low angled bedforms and if flow reversals are absent in the lee side of low angled bedforms (such as those described by Smith and McLean (1977) and Kostaschuk and Villard (1996)) then what processes govern sediment transport and bedform morphology?

During the low flow survey it should be noted that the increased bed roughness caused by the superimposition of secondary bedforms (Figure 3d) will induce an increase in flow complexity which is manifested as an increase in variation in at-a-point velocity information (McLean and Smith, 1979).

5.6.2 Mean Velocity Profiles over Steep Angled Dunes

Four at-a-point profiles of downstream and vertical velocity are presented which were collected during March 1995 and February 1996. These profiles were collected over bedforms with steeply dipping slip faces and will be described together as the flow conditions during both survey periods were similar.

The time-averaged at-a-point velocity profiles (L/96/S1, L/96/T, L/96/TS) conducted in February 1996 under low flow conditions are shown in Figure 5.31, whilst the profile conducted during the March 1995 low flow stage survey (profile L/95/C) is given in Figure 5.32. All of the at-a-point profiles show a decrease in downstream velocity with depth, with a near-surface maximum of 1.05 ms^{-1} over the March 1995 survey dune crest (Figure 5.32a). During the February 1996 survey the maximum downstream velocity of 0.75 ms^{-1} was measured over profile L/96/S1 which is located on the lower stoss side of the bedform (Figure 5.31a). The minimum mean downstream velocity measurements (0.15 ms^{-1}) were situated near the bed of the trough profile over the primary bedform (L/96/T) during the February 1996 survey. The rate of decrease of downstream velocity with depth is markedly different between profiles, for example profiles L/96/T and L/96/TS, which are located over the trough of a primary and a secondary bedform respectively, display a much greater vertical rate of change of the velocity with depth than the other two profiles. The change in velocity gradient is quantified in Figure 5.33 which shows vertical profiles of the gradient of the normalised velocity for all of the profiles and indicates that maximum velocity gradient occurs in the leeside trough of the primary bedform. The maximum velocity gradient acting in the trough of the primary bedform (L/96/T, 0.15 m^{-1}) is more than twice as large as that acting in the trough of the secondary bedform (L/96/TS, 0.07 m^{-1}). Velocity gradients occurring over the dune crest (L/95/C) and stoss side (L/96/S) profiles are very low and show a small increase near the bed which is probably due to friction between the bed and flow. As described during the high flow surveys, a high velocity gradient is indicative of the production of a shear zone which forms due to flow expansion, and possibly separation, downstream of a dune crest. However, the high flow velocity profile over the dune trough demonstrated the development of a distinct low flow zone beneath the shear layer and this feature is not present for any of the profiles collected during the low flow survey data. This may be a function of several factors:

(1) The difference in data quality between the high and low flow surveys which is caused by a combination of the lower resolution of the ADCP data at lower velocity magnitudes and the relative movement between the profile location and the dune. As the size of the dunes being surveyed is small in comparison to the high flow survey then the vessel motion will have a more pronounced effect on the relative location of the profile and dune. A decrease in the data resolution may mean that a low flow zone, if present, is unrecognisable.

(2) The low flow zone is too small to be imaged using an ADCP. The ADCP cannot measure the lowest 7% of the flow column due to signal interference (see Chapter 3) and therefore a shallow near-bed low velocity zone would not be measurable. As the height of a shear layer downstream of flow separation, and therefore the height of a low flow zone, is proportional to the height of the bedform, it seems reasonable to expect a low flow zone downstream of these relatively smaller bedforms to be short.

(3) The mean relative position of profile and slip face: profile L/96/T is located at three dune heights from the slip face and profile L/96/TS is at 3.9 dune heights. If a recirculation zone length of four times the step height is assumed (e.g. Engel, 1981) then the profile locations for both trough sections are towards the end of the recirculation zone.

(4) There is no low flow zone.

As for the high flow survey over a dune trough, the mean downstream velocity measured under low flow conditions is never negative although flow reversals do occur for profiles L/96T and L/96/TS. It is therefore likely that a low flow zone will exist and intermittency in flow reversals will be described later in this section. The most plausible explanation of the lack of a distinct low flow zone on the velocity profiles may be a combination of some of the above, most likely a small near-bed low flow zone does exist but due to the position of the profile relative to the lee face and the expected depth of the low flow zone, it is not measurable using the ADCP. However, although there is no distinct low flow zone visible which is obviously separate from the high shear region, the mean near-bed downstream velocity for both of the low flow profiles located above dune troughs is small relative to the near bed velocities of the other profiles conducted during the low flow survey.

The magnitude of the vertical velocities measured for both of the low flow surveys is very small with a maximum range of 0.08 ms^{-1}. The vertical velocity measurements are below the resolution of the ADCP but as some of the trends in the mean vertical velocity are consistent with the high flow surveys they will be described briefly here. The mean vertical velocity at-a-point profiles show negative vertical velocities within and above the dune troughs (Figure 5.31b, profiles L/96/T and L/96/TS) which increase to above zero in the outer flow area. Further downstream of the trough, the mean vertical velocity becomes weakly positive as flow lines are directed upwards due to topographic forcing (L/96/S). The mean vertical velocity over the dune crest is close to zero and shows little variation with flow depth (Figure 5.32b, L/95/C).

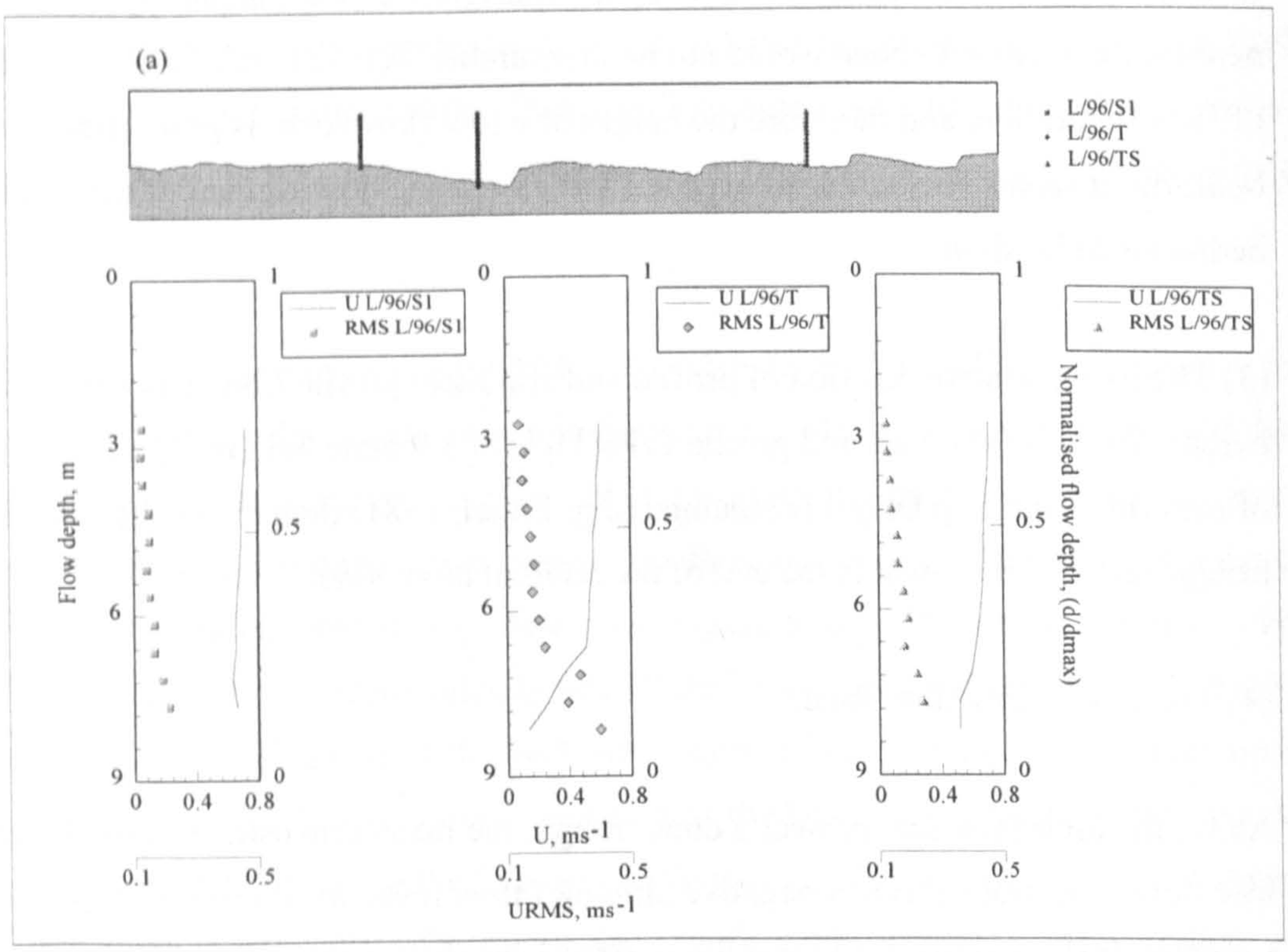

Figure 5.31, Vertical profiles of the mean at-a-point velocity and corresponding RMS values collected during the February 1996 survey over the primary dune stoss side, primary dune trough and secondary dune trough showing (a) downstream velocity and (b) vertical velocity.

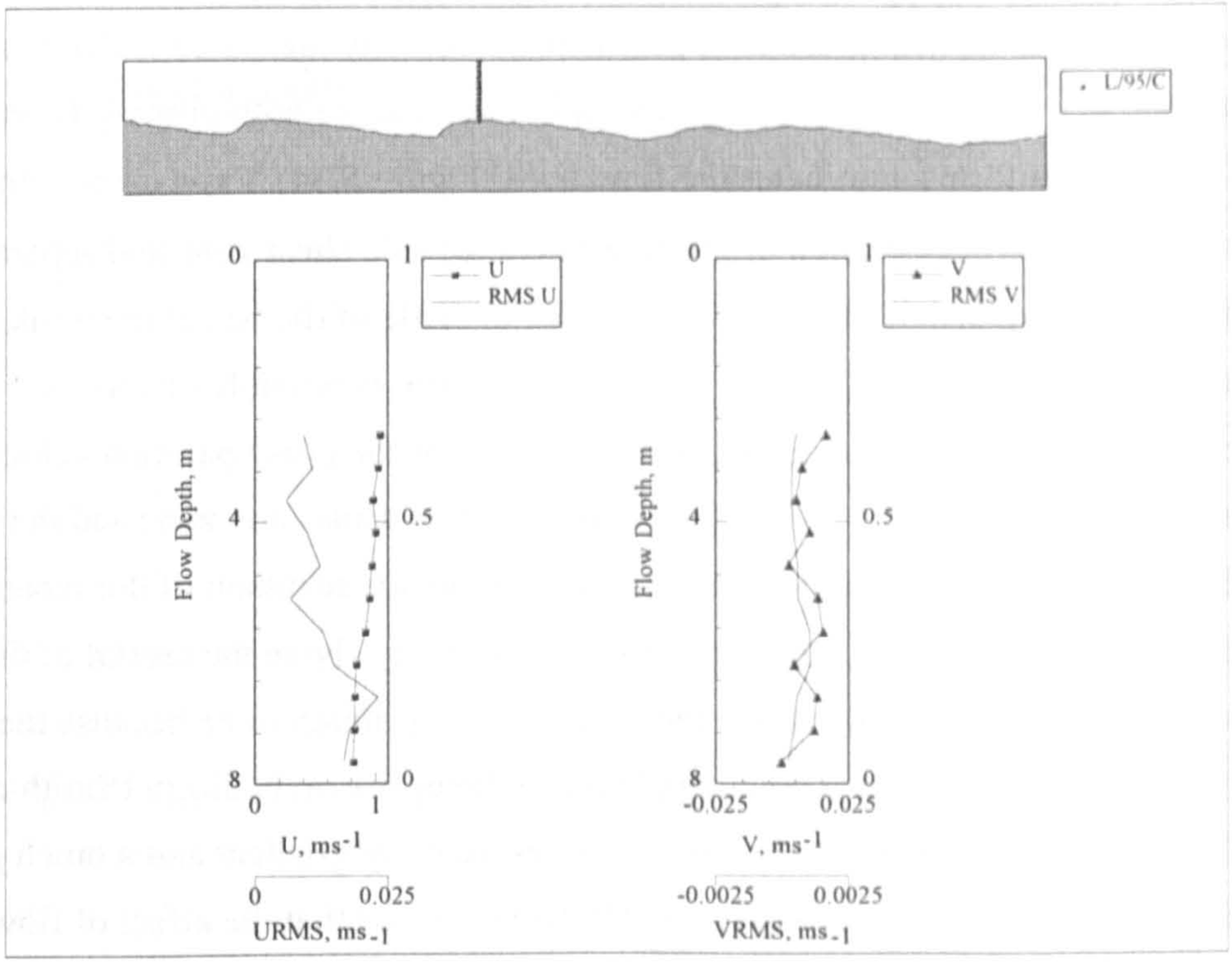

Figure 5.32, Vertical profiles of the mean at-a-point downstream and vertical velocity and corresponding RMS values collected during the March 1995 survey over the dune crest.

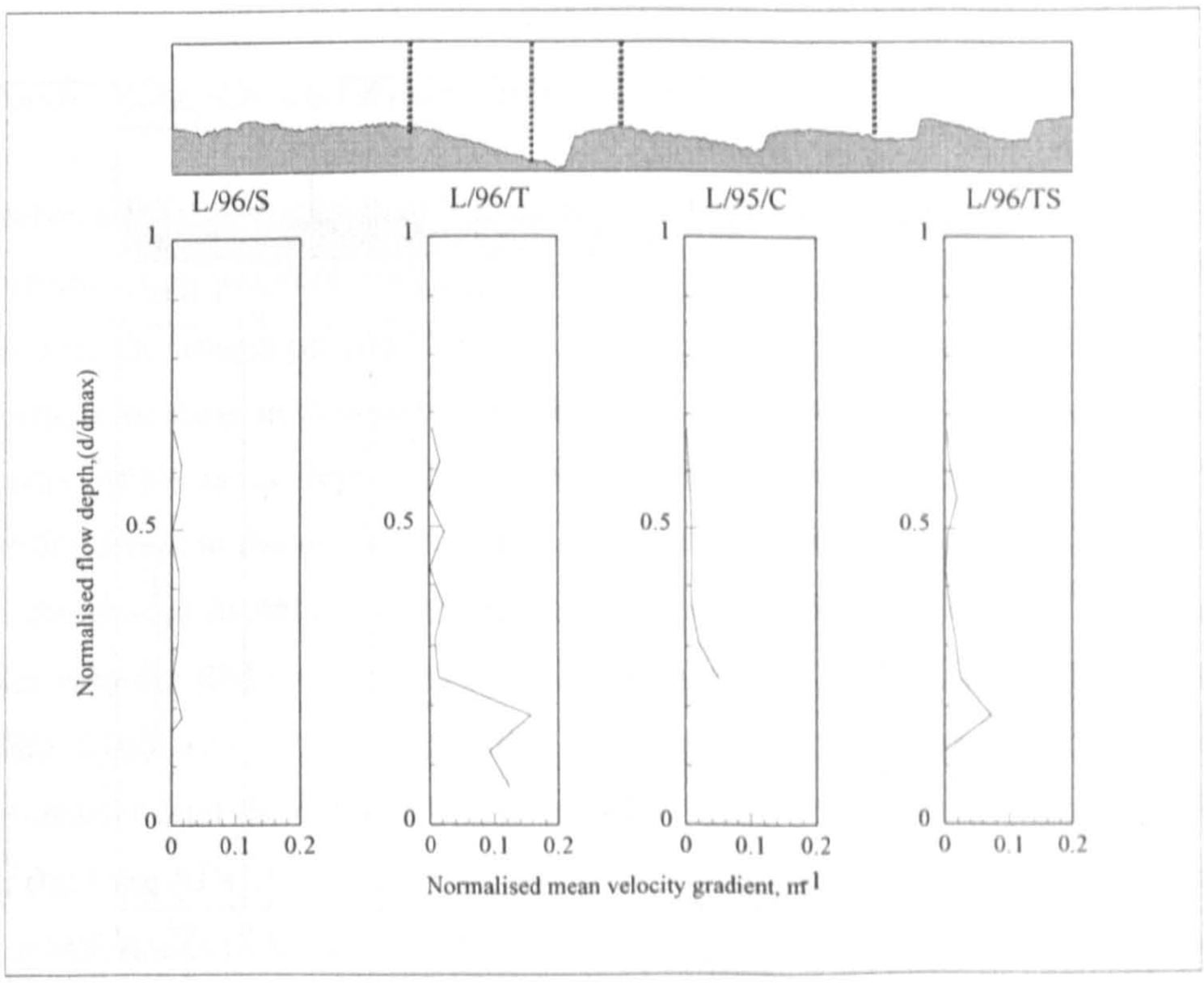

Figure 5.33, Vertical profiles of the time averaged at-a-point normalised velocity gradient collected during the March 1995 and February 1996 low flow survey over high slip face angled dunes. The relative location of each profile is indicated by the schematic above and each profile is labelled.

In general, the vertical profiles of downstream velocity measured under low flow conditions indicate that flow expansion downstream of the crests of both primary (L/96/T) and secondary (L/96/TS) bedforms dominates the flow field (Figure 5.34). Flow expansion at the dune crest leads to a rapid deceleration of the flow and a lee side shear zone and separation cell are produced due to flow expansion caused by the change in angle of the bed at the brink point. The lower flow deceleration in the trough of the secondary bedform is possibly due to the profile location with respect to the slip face but is also a consequence of the pre-separation velocity and the height of the bedform (Simpson, 1981). The length of a flow separation zone and the magnitude of the corresponding shear zone is a function of the velocity upstream of the separation point and the height of the dune (Driver *et al.*., 1987). The velocity above the crest of the secondary dune will be lower than the velocity above the crestal of the primary dune because the secondary dune has formed within the internal boundary layer of the upstream bedform (Smith and McLean, 1979). The stoss-side profile (L/96/S) exhibits a low velocity gradient and a much greater mean downstream velocity than profile L/96/T which shows that the effect of flow expansion has rapidly decreased downstream of flow reattachment, and that flow is accelerating up the dune stoss side.

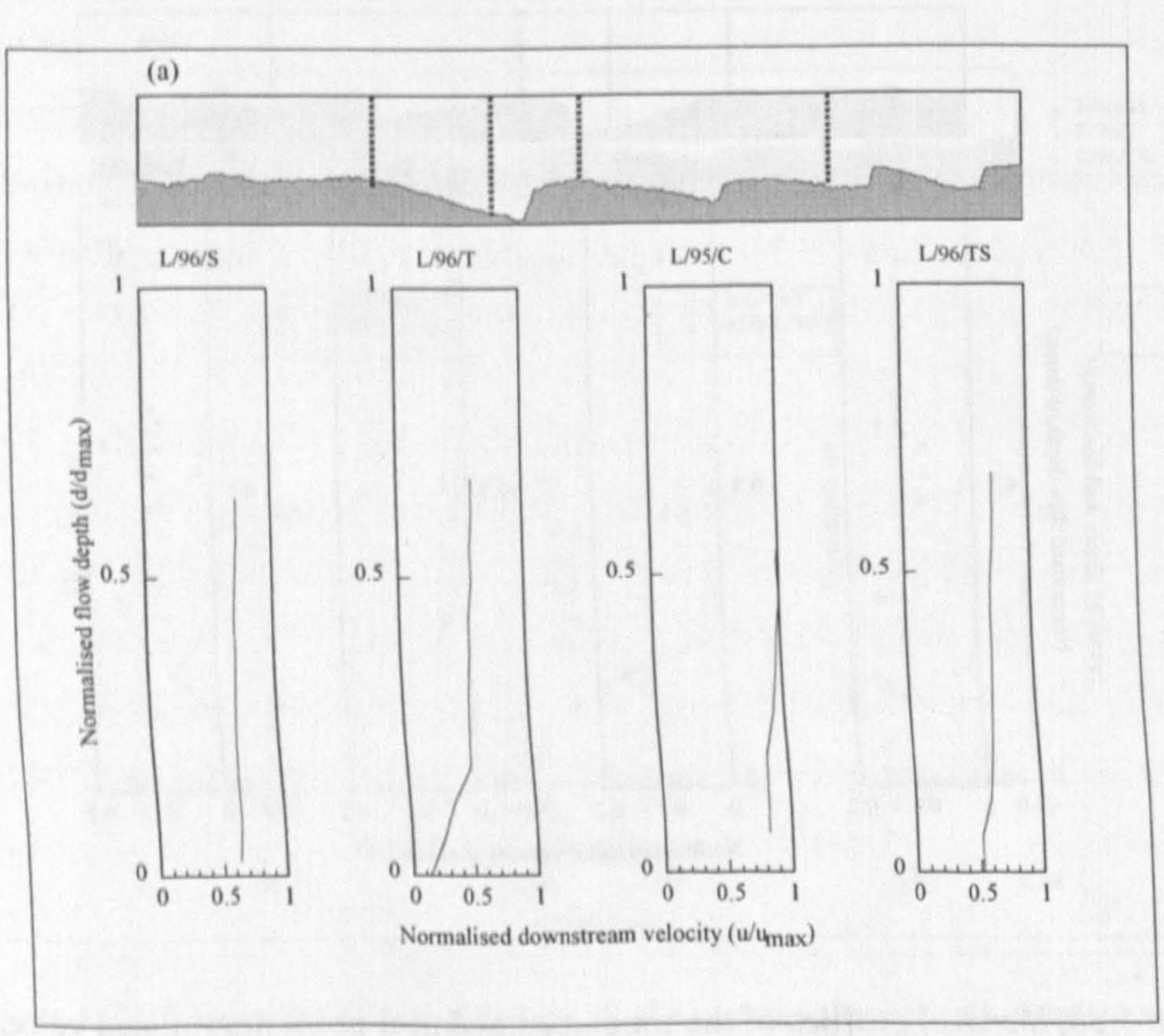

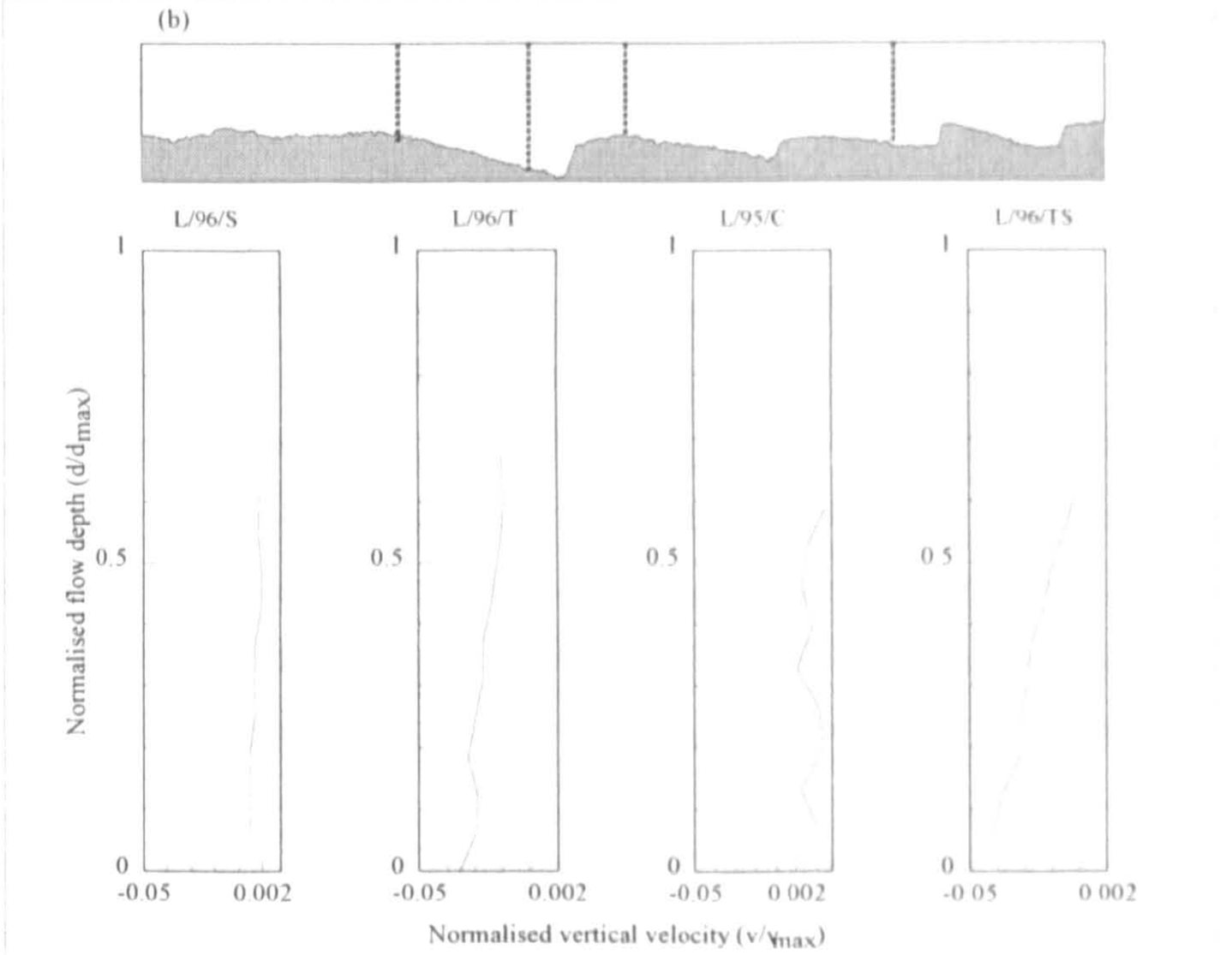

Figure 5.34, Normalised time averaged at-a-point velocity profiles from both low flow surveys showing (a) downstream velocity and (b) vertical velocity.

5.6.3 Velocity Moments and Reynolds Stresses

The downstream RMS velocity distribution for all of the profiles collected during the February 1996 survey shows an increase with depth (Figure 5.31). The greatest downstream RMS values are located over the trough profile (L/96/T) and reach a maximum of 0.48 ms^{-1} near the bed. The greatest vertical increase in downstream RMS also occurs over profile L/96/T from a depth of 7.2 m downwards, which is the depth corresponding to the brink point height and the onset of the shear layer described in the previous section. Downstream RMS values from profiles L/96/S and L/96/TS show similar distributions although the L/96/TS RMS values are slightly higher. The downstream velocity RMS values from the crestal profile (L/95/C) also show a very small increase with depth although the maximum magnitude of the RMS values is an order of magnitude smaller than those located over the dune troughs during the February 1996 survey because of the long ADCP averaging time period during the March 1995 survey (Figure 5.32). The small RMS values indicate that the ADCP averaging time for the March 1995 survey is too long to assess the at-a-depth variation in the downstream or vertical velocity distribution. The distribution of the vertical velocity RMS values again shows an increase with depth although the magnitude of the vertical RMS values is very small (maximum 0.065 ms^{-1}). Maximum vertical velocity RMS values are located above profile L/96/T and the rate of increase of RMS with depth

increases from a depth of 7.2 m downwards, although the nearest measurement to the bed shows a decrease.

The maximum RMS values for the low flow survey are therefore situated on the primary high angle-dune trough profile at depths equivalent to the height of the shear layer shown in the mean velocity and velocity gradient profiles. The increase in RMS values over the dune trough is therefore associated with a zone of high shear which may indicate a consequential increase in turbulence production. The magnitude of RMS values over the secondary dune trough is much lower than those measured over the primary dune, which is related to the lower velocity gradients over the secondary dune trough, due to the position of the profile with respect to the dune slip face, the lower pre-separation crestal velocity and the smaller dune height.

The vertical profiles of Reynolds stress for the low flow surveys have a range from -1.1 Pa to 2.1 Pa (Figure 5.35), although the profile collected over the stoss side (L/96/S) of dune has little variation in Reynolds stress with flow depth and has consistently low values of Reynolds stress (maximum 0.7 Pa). However, both of the profiles situated over dune troughs do show some increase in Reynolds stress with depth, Reynolds stresses for profile L/96/T increase from a depth of 5.2 m with a maximum value of 2.1 Pa at a depth of 7.2 m. Both profile L/96/T and L/96/TS show an above-bed Reynolds stress maximum value with a sharp decrease at the bed.

Previous studies have shown that the maximum Reynolds stress values are found along the separation zone shear layer and both at and just downstream of flow reattachment and that values of Reynolds stress within the separation zone are very low (e.g. Raudkivi, 1963; Nelson *et al.*, 1993). The spatial distribution of Reynolds stresses for this low flow survey therefore corresponds well to the pattern of Reynolds stress distribution previously described from flume and theoretical studies. The high Reynolds stress values found over dune troughs are related to the onset of the shear layer which was described with respect to the mean velocity distribution, the decrease in stress values towards the bed is caused by a decrease in the velocity gradient and hence fluid shear or drag. The magnitude of Reynolds stresses found over profile L/96/TS is much smaller than those over the primary dune trough and is again related to the lower velocity gradient acting over the trough of the secondary dunes. The lower velocity gradient is in turn a factor of the upstream velocity above the dune crestal prior to flow separation, the height of the secondary dune and the position of the profile relative to the separation point (Simpson, 1981, 1989).

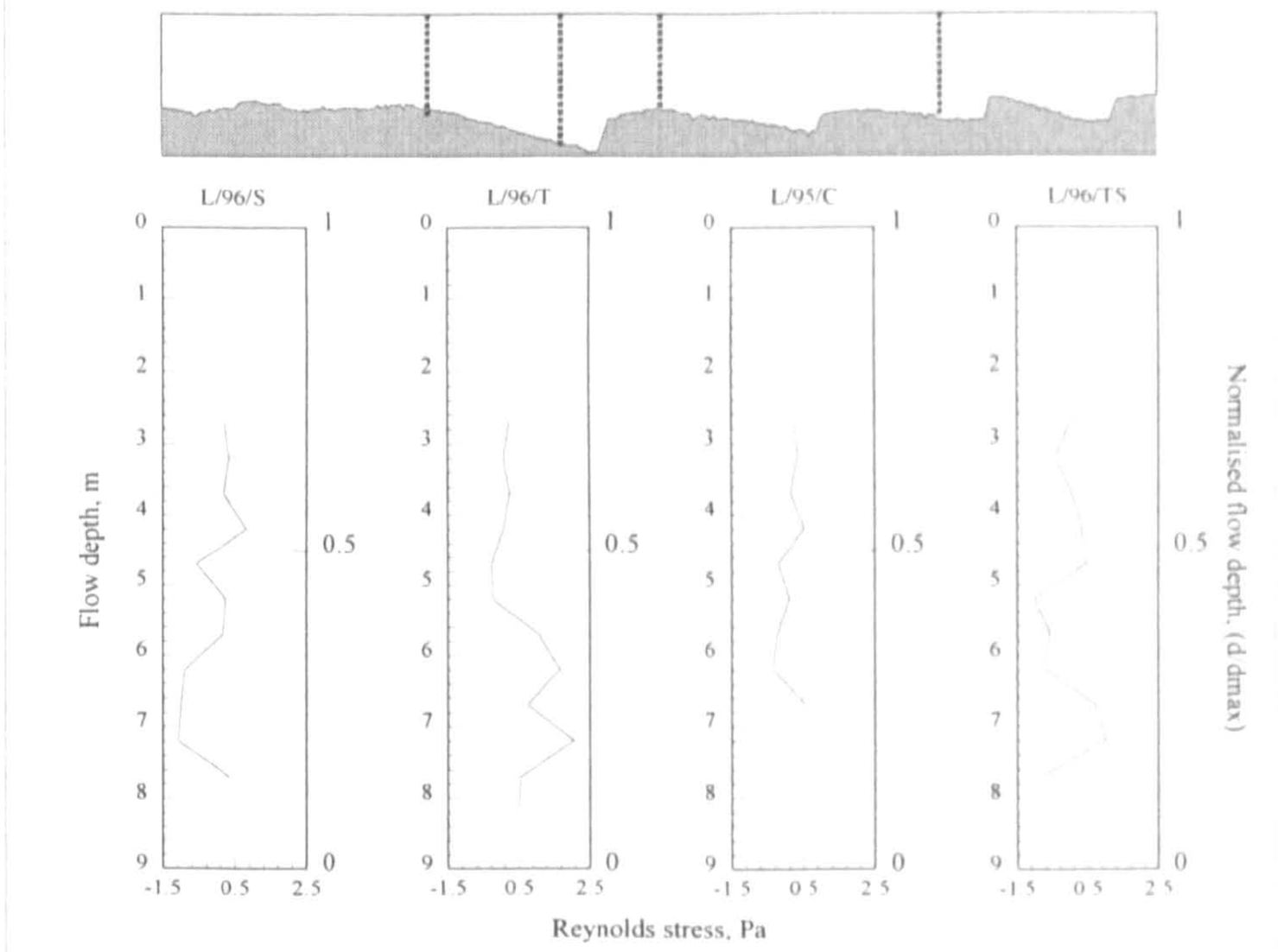

Figure 5.35, Vertical profiles of the mean Reynolds stress for the low flow February 1996 and March 1995 surveys.

The crestal and stoss side profiles show very little variation in the skewness of the downstream and vertical velocity component with depth, with both Uskew and Vskew approaching zero at any distance from the bed (Figure 5.36). The stoss side profile shows greater fluctuation than the crestal profile in the Uskew distribution but there is no consistent spatial trend. There is a similar lack of trend in Uskew and Vskew for the profile collected in the trough of the secondary bedform and again skewness is very low. However, profile L/96/T does exhibit spatial variation in the skewness distribution, with a zone of weakly positive (0.6) vertical velocity skewness from 5.2 m to 6.7 m with a corresponding zone of weakly negative downstream skewness. This pattern of skewness distribution is diagnostic of fluid ejection of lower than average velocity fluid along this layer and in to the outer flow (Itakura and Kishi, 1980). Below this zone there is a region of strongly positive (2.7) downstream velocity skewness near the bed and such strongly positive downstream skewness has been shown by Bennett and Best (1995) to indicate mixing of higher velocity fluid above and within the shear layer with the lower velocity fluid of the separation zone. The positive downstream skewness extends down towards the bed and therefore indicates that the shear layer may be less mobile than during the high flow survey as positive near-bed skewness is expected for a stationary shear layer downstream of a dune crest (Bennett and Best, 1995).

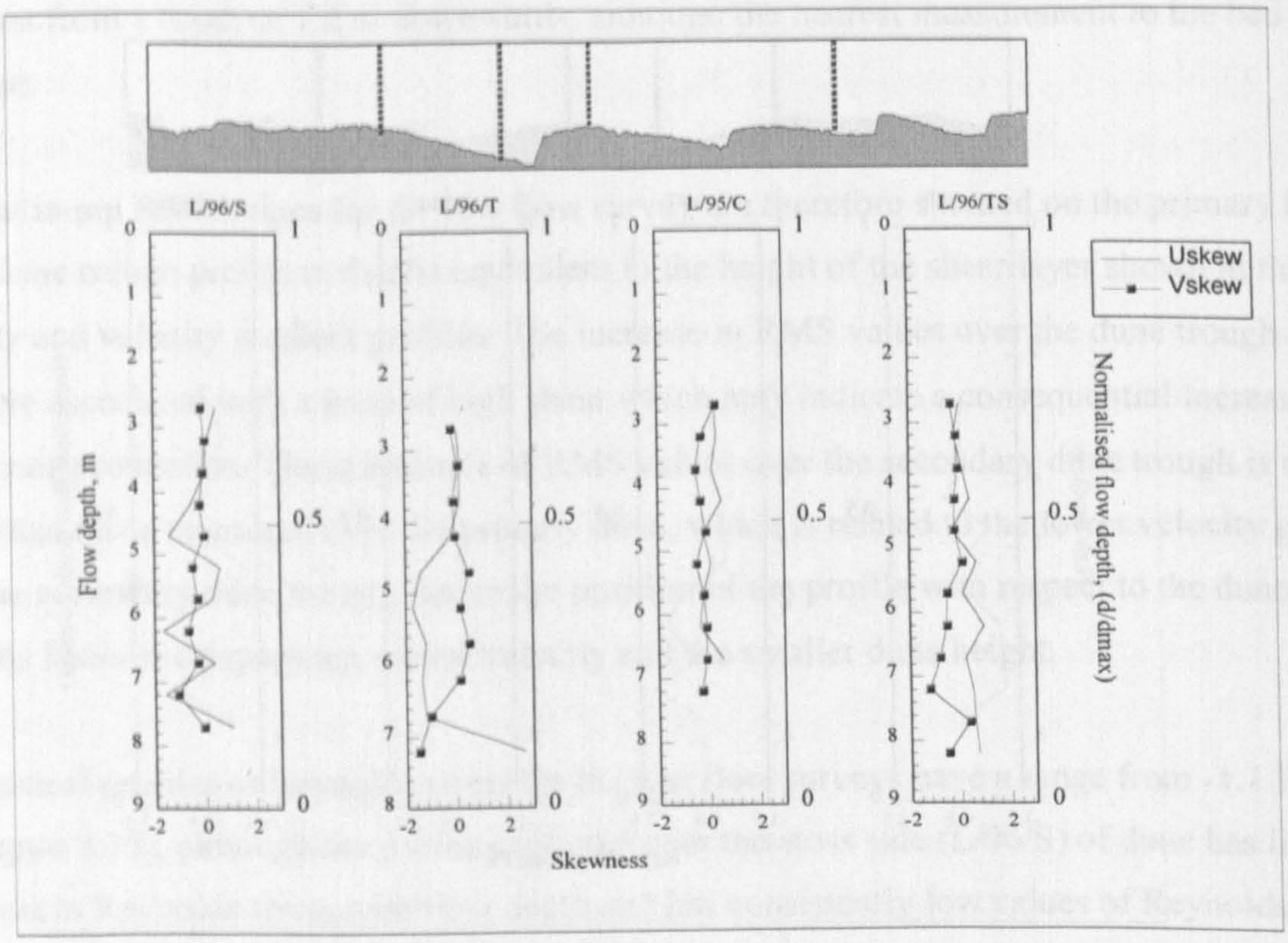

Figure 5.36, Vertical profiles of the at-a-point vertical and downstream time series skewness for the March 1995 and February 1996 low flow surveys over high angled dunes.

5.6.4 Temporal Changes in Downstream Velocity

This section will examine temporal changes in the downstream velocity of the profiles collected over high slip face angle bedforms under low flow conditions. At-a-point velocity time series for profiles L/96/T, L/96S and L/96/TS are shown in Figure 5.37 for various depths in the flow column and contour maps of the entire flow field for 0.5 m depth intervals are shown in Figure 5.38.

The effect of flow separation on the flow field over dunes is highlighted by comparison of velocity time series collected on the dune stoss side (L/96/S) and downstream of dune crests (L/96/T and L/96/TS) (Figure 5.37). The outer flow zone of all of the profiles exhibits high magnitude positive downstream velocities (up to 1.4 ms^{-1}) with a variation in the order of ±0.5 ms^{-1}. Both of the profiles which are located just downstream of a crest exhibit temporally inconsistent flow reversals from depths of 7.2 m down towards the bed, showing that flow separation occurs over both primary and secondary bedforms. There is a consistent decrease in velocity downwards through the flow column for the trough profiles, with minimum velocities situated close to the bed, although throughout the flow separation zone fluctuations in downstream velocity (up to 1.5 ms^{-1}) are higher than in the outer flow regions (up to 0.5 ms-^{1}). There are no flow reversals over the dune stoss side which illustrates the dominant effect on the

flow field caused by the change in bed slope at the dune brink point (Figure 5.37a). The stoss side profile (L/96/S) also exhibits a decrease in velocity with depth and increase in velocity fluctuation closer to the bed although the magnitude of both of these phenomena is smaller than over the trough profiles.

Flow reversals have been shown to be intermittent during the high flow survey, in wind tunnel experiments (Driver *et al.*, 1987) and over the trough of estuarine dunes (Soulsby, 1991) and this is also the case under low flow conditions (Figures 5.37 and 5.38). The larger mean downstream velocity gradients (Figure 5.33) present over profile L/96/T compared to L/96/TS suggest that flow separation should be greater (in terms of the extent of the reversal zone and the magnitude and duration of reversals) for the larger primary dune. The velocity time series show that maximum reverse flow velocities (-0.6 ms^{-1}) are higher within the recirculation cell of the primary dune than the secondary dune (-0.35 ms^{-1}), with the rate and duration of reversals increasing for each profile with depth. To test for flow reversal intermittency variation with profile depth and profile location, the intermittency factor, I, for subsequent depth cells above the bed is illustrated in Figure 5.39. Intermittency in flow reversal is greater for the primary bedform, with maximum percentage of time that flow reversals occur (39 %) situated at the closest measuring depth to the bed, whereas flow reversal over the secondary dune reaches a maximum of 19 % of the survey duration. The vertical extent of the reversal zone in the water column is greater for the primary dune, with reversals occurring to a depth of 7.2 m, than the secondary dune (where the minimum depth of flow reversal is 8.7 m). Profile L/96/T has a greater fraction of time that reversals occur at all flow depths compared to profile H/96/TS and this is the result of the higher velocity gradients acting through the shear zone and the relative profile location for profile L/96/T. Perturbations in the shear layer have been shown to have different magnitudes which are related to the height of the discontinuity with flow depth (Bradshaw and Wong, 1972). Bradshaw and Wong (1972) showed that decreasing the flow depth to dune height ratio increases the velocity gradient across the shear layer and the turbulence intensity near reattachment. Variation in the flow depth to dune height ratio will alter the pressure gradient acting over bedforms (Raudkivi, 1963; Mendoza and Shen, 1990) and thus will change the rate of flow expansion downstream of the crest. Flow depth to dune height ratios for the primary and secondary bedforms are 3.5 and 7.0 respectively, showing that the affect of flow separation will be greater for the primary bedform. The magnitude and lifespan of flow reversals in the trough of a bedform are therefore partially a consequence of the height of the bedform with respect to the flow depth. The period between flow reversals for the primary bedform is between 2.5 and 114 *H/U (where H is the step height and U is the mean velocity at the crest), and the reversal life span is 3.2*H/U. For the secondary bedform the period between flow reversals is between 3.8 and 192 *H/U, and the reversal life span is 2.1*H/U. The recurrence period of reversals is therefore shorter for the larger primary bedform and the duration of reversal is also greater. It must also be noted

that the angle of the dune slip face will also effect the degree of separation of the flow, although for this low flow survey, the lee angles of the primary and secondary dunes are similar (40° and 35° respectively).

Lastly, there is a weak, inconsistent variation in the downstream velocity in the upper layer of the flow (Figure 5.38). Similar to the high flow survey, this may be linked to stacking of wakes from successive bedforms upstream. The increased bed roughness during the low flow survey caused by the superimposition of secondary bedforms will induce an increase in turbulence production. An increase in production of turbulence will be manifest as increased variation in the resulting velocity field.

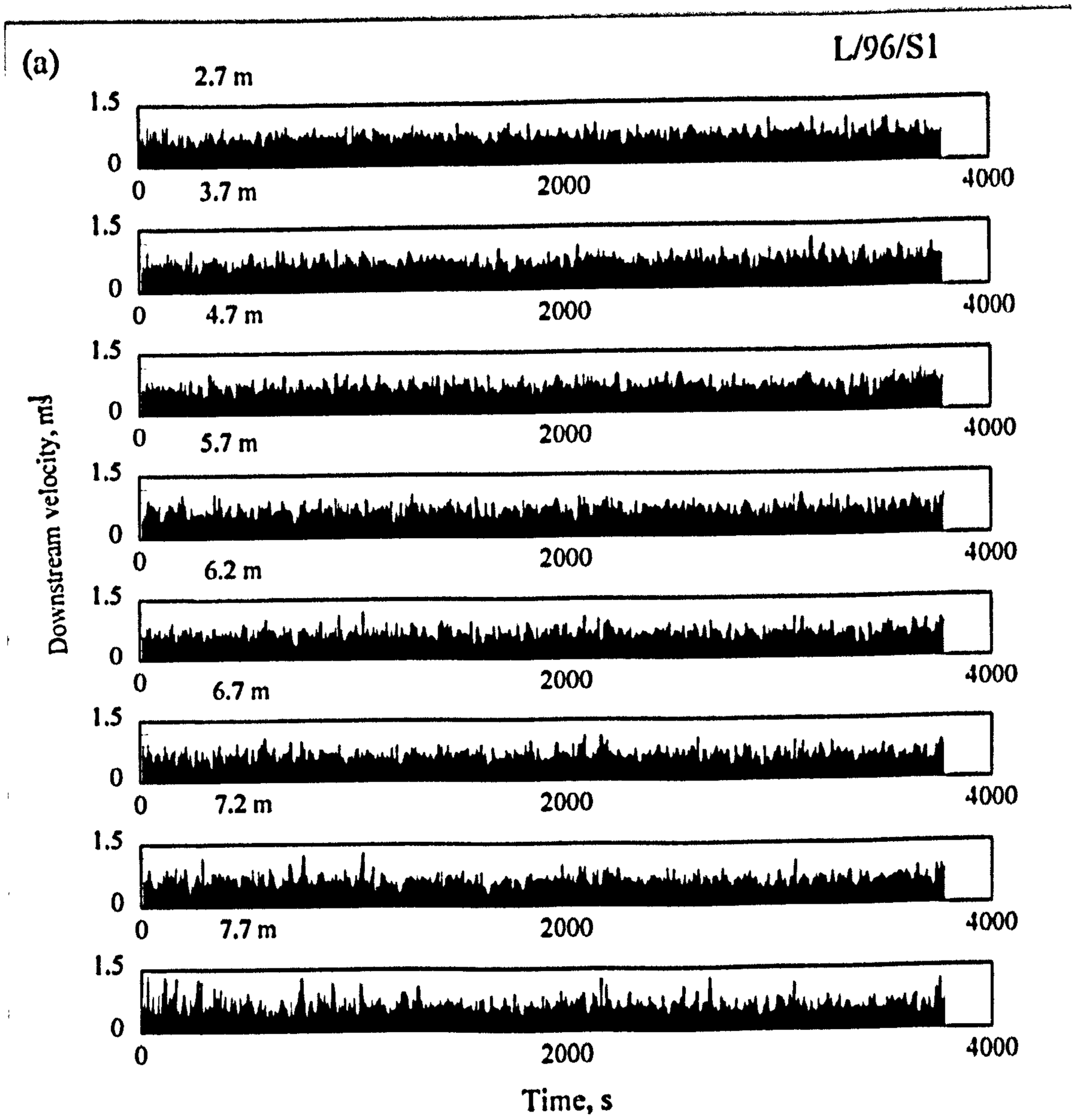
(a)
L/96/S1
2.7 m
3.7 m
4.7 m
5.7 m
6.2 m
6.7 m
7.2 m
7.7 m
1.5
0
2000
4000
Downstream velocity, m/s
Time, s

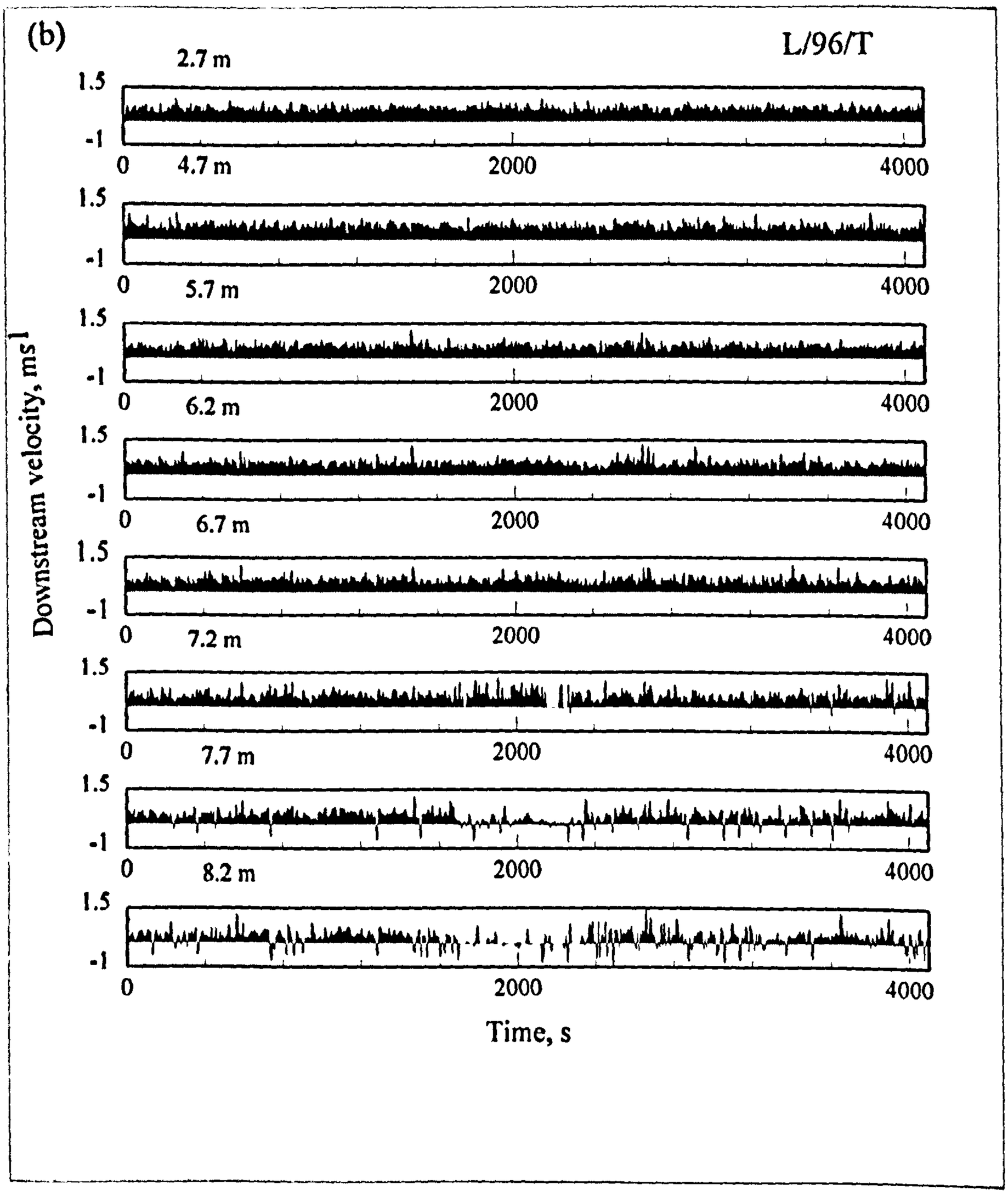
(b)
L/96/T
2.7 m
4.7 m
5.7 m
6.2 m
6.7 m
7.2 m
7.7 m
8.2 m
1.5
-1
0
2000
4000
Downstream velocity, ms-1
Time, s

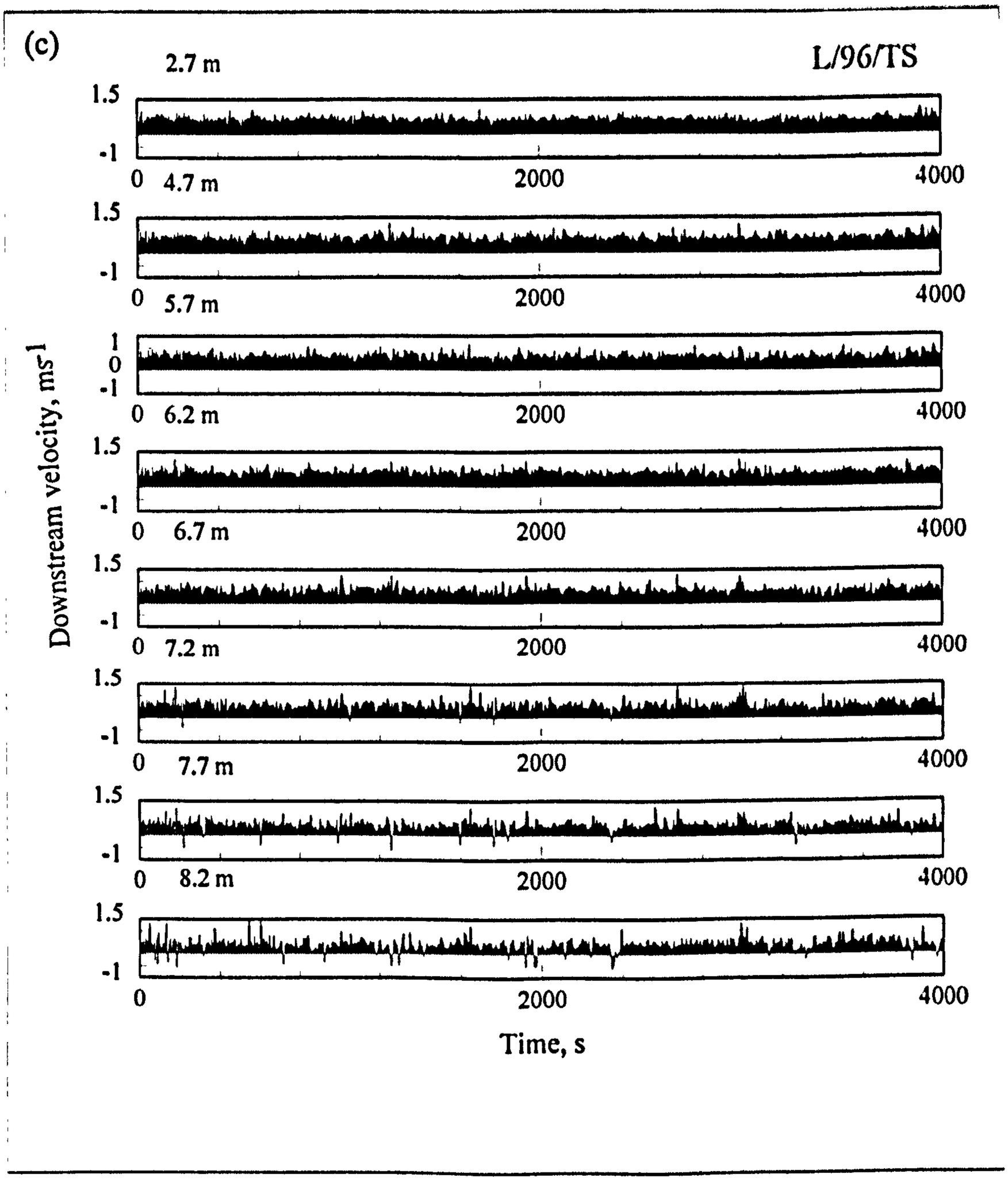

Figure 5.37, At-a-depth time series of the instantaneous values of the downstream velocity collected over the (a) primary dune stoss side (L/96/S), (b) primary dune trough (L/96/T) and (c) secondary dune trough (L/95/TS).

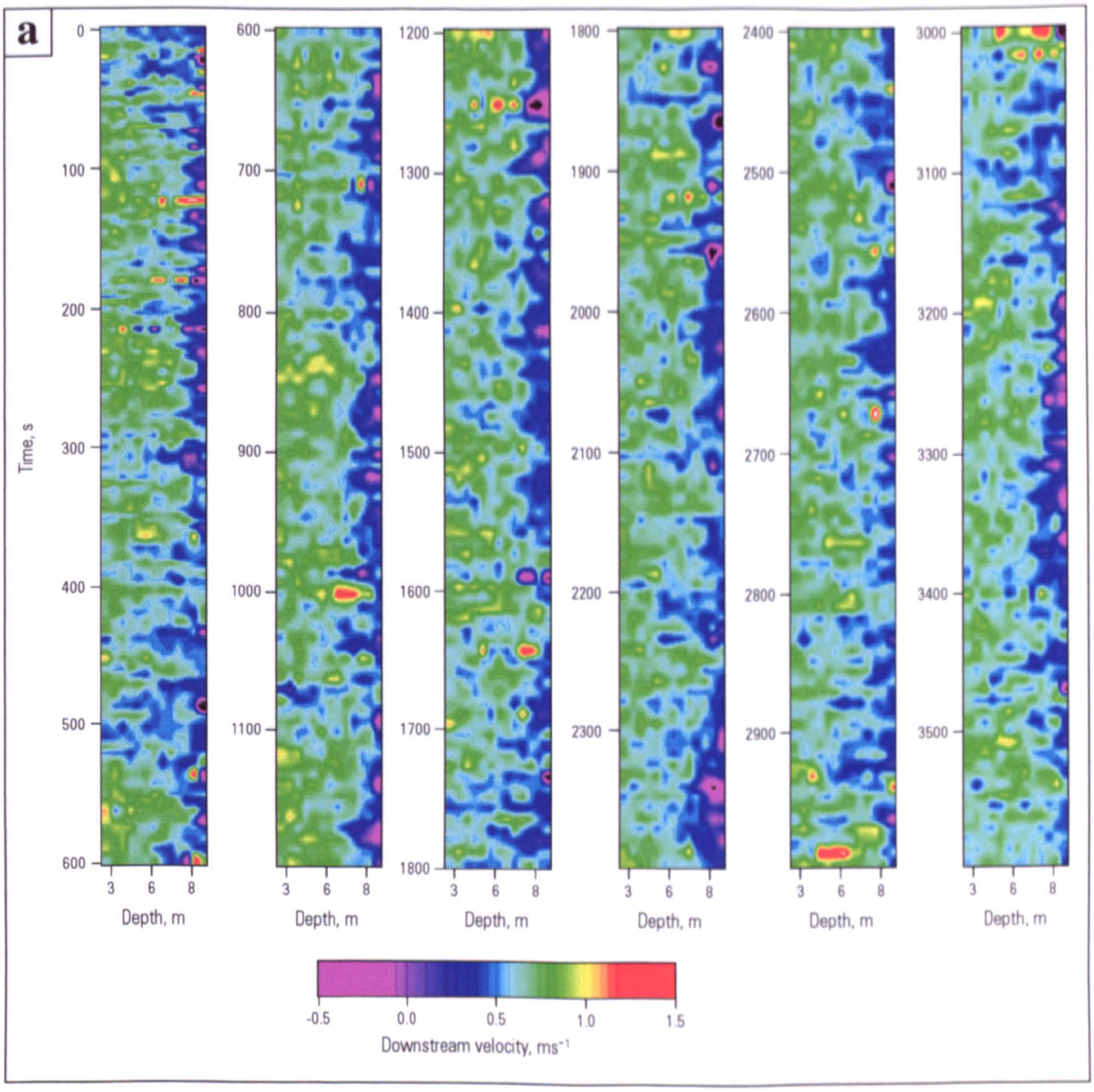

Figure 5.38: Contour maps of temporal variations in at-a-point downstream velocity for the low flow survey at (a) L/96/TS, trough of a secondary dune, (b) L/96/T, primary dune trough and (c)L/96/S, stoss side of the subsequent dune. Flow is from top to bottom and a scale colour bar is given for each map. Flow depth bin sizes are 0.5 m. Each time series has been split to fit to page size and successive profiles are from left to right.

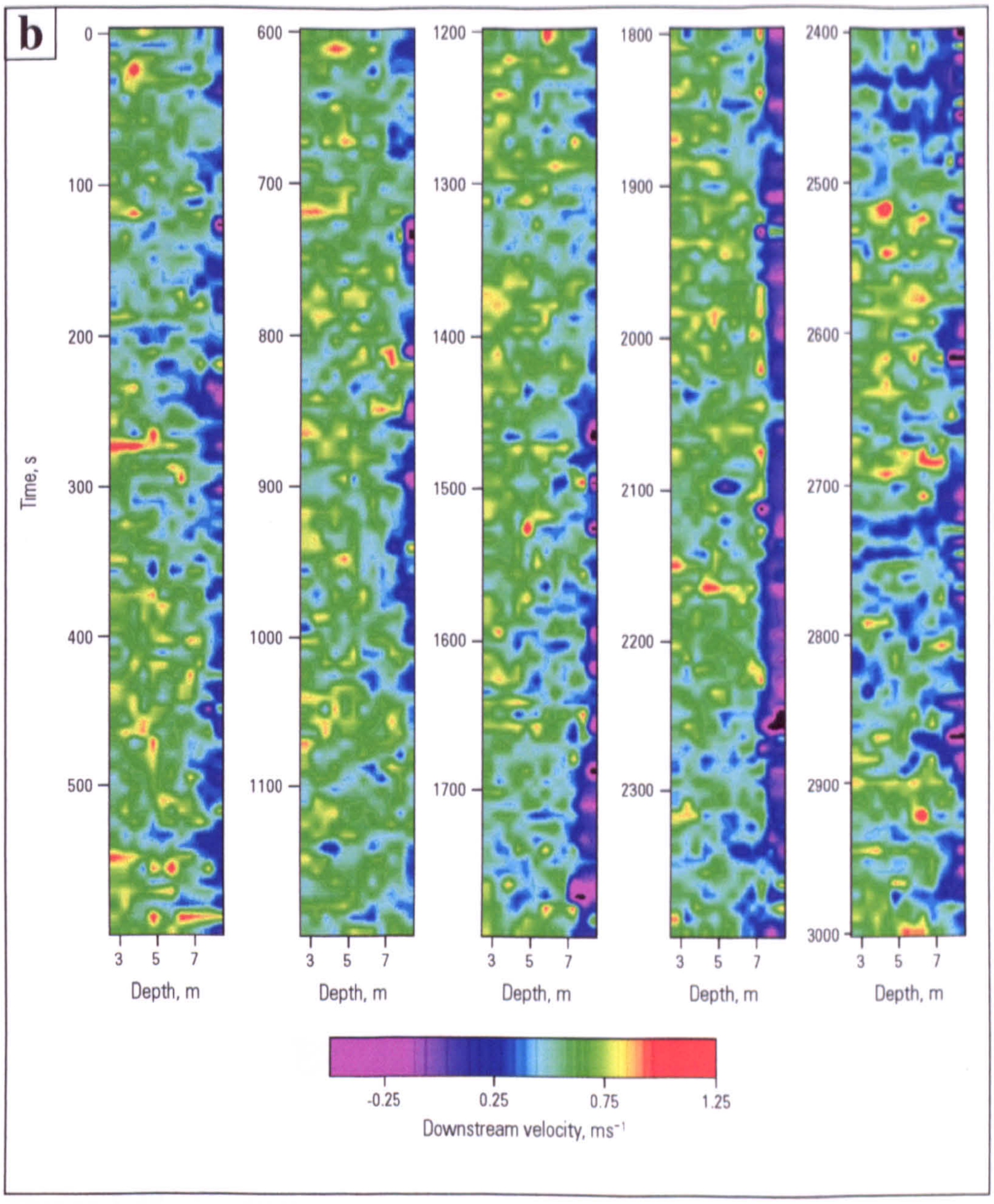

Figure 5.38: Contour maps of temporal variations in at-a-point downstream velocity for the low flow survey at (a) L/96/TS, trough of a secondary dune, (b) L/96/T, primary dune trough and (c) L/96/S, stoss side of the subsequent dune. Flow is from top to bottom and a scale colour bar is given for each map. Flow depth bin sizes are 0.5 m. Each time series has been split to fit to page size and successive profiles are from left to right.

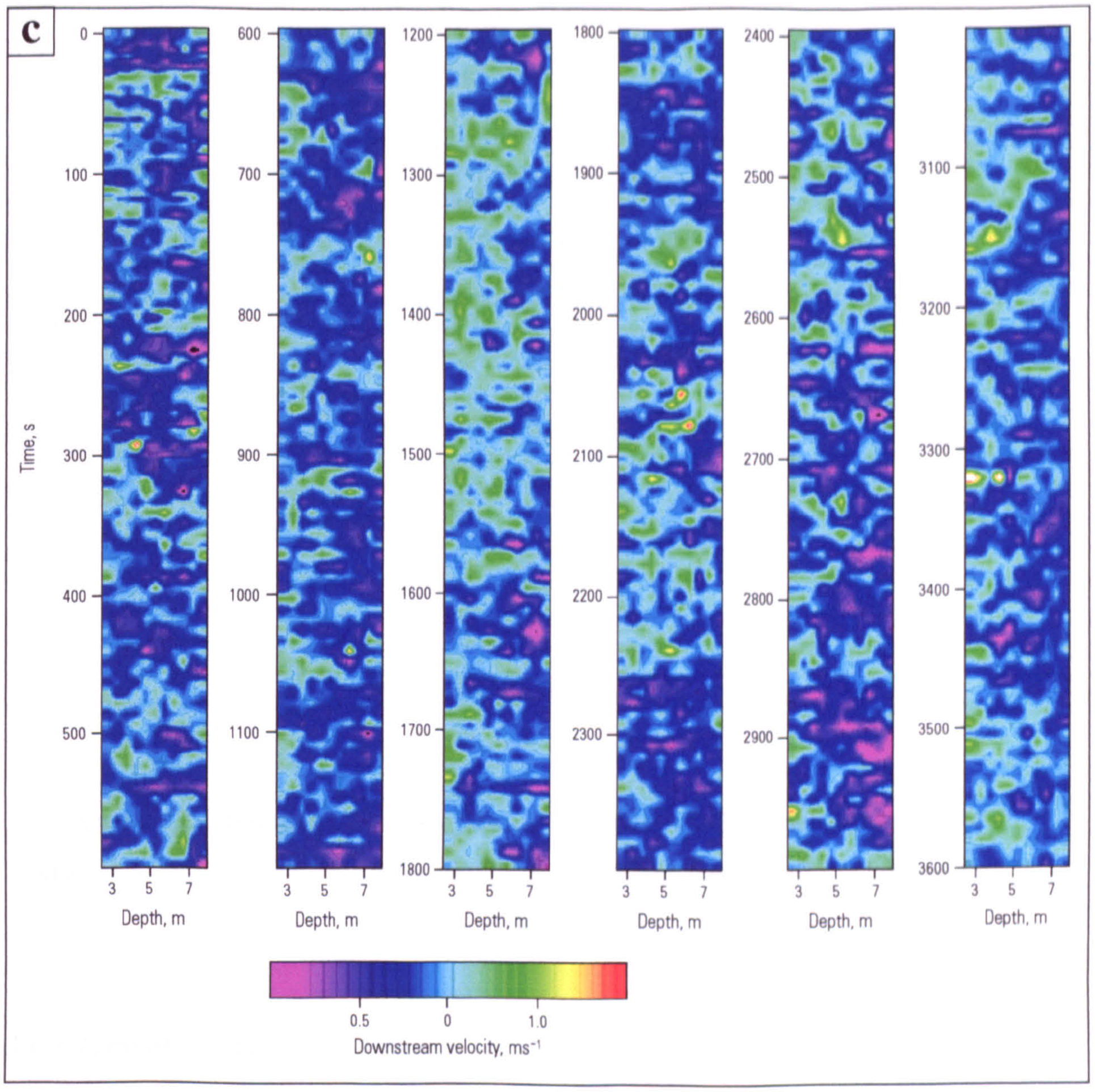

Figure 5.38: Contour maps of temporal variations in at-a-point downstream velocity for the low flow survey at (a) L/96/TS, trough of a secondary dune, (b) L/96/T, primary dune trough and (c) L/96/S, stoss side of the subsequent dune. Flow is from top to bottom and a scale colour bar is given for each map. Flow depth bin sizes are 0.5 m. Each time series has been split to fit to page size and successive profiles are from left to right.

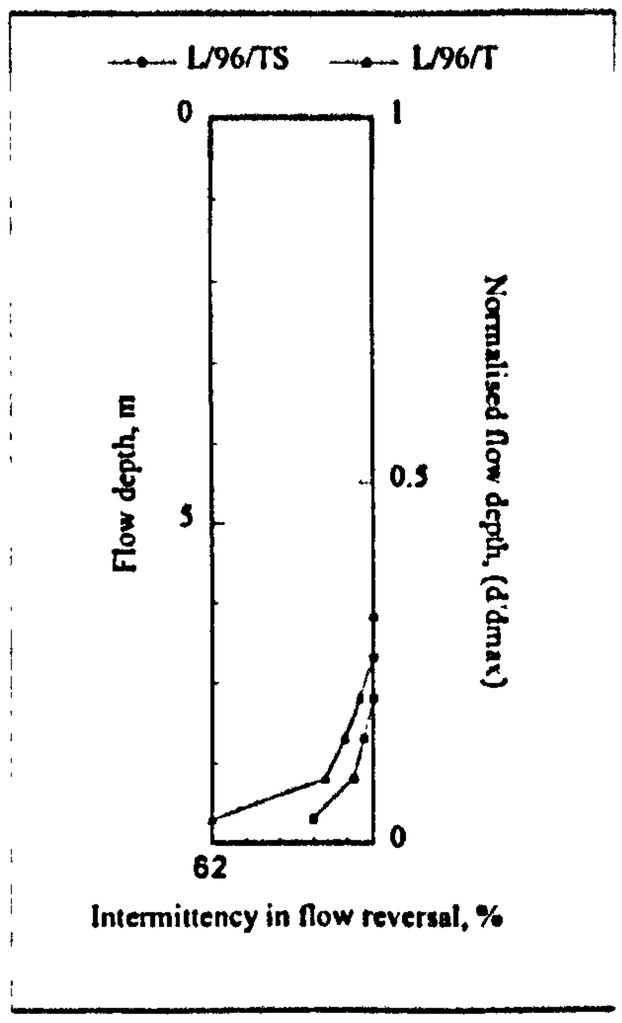

Figure 5.39, Intermittency in flow reversal variation with flow depth through the separation zone and shear layer for profiles L/96/TS and L/96/T collected at low flow stage.

5.6.5 Temporal Changes in Velocity Gradients

This section will examine temporal variations in instantaneous velocity gradients measured during the low flow survey. The production of a shear layer in the lee side of steep angled dunes is again illustrated by variations in velocity gradients (Figure 5.40) for both the primary (L/96/T) and secondary (L/96/TS) dunes. The high velocity gradient zone occurs at depths equivalent to the dune brink point, maximum gradients over profile L/96/T are 1.45 s^{-1} and over profile L/96/TS are 1.25 s^{-1} , which are of a lower magnitude than that encountered in the leeside of dunes during the high flow survey (maximum 3.1 s^{-1}). The lower velocity gradient forming downstream of the brink point of the secondary bedform compared to the primary is due to the variation in H/U ratio (3.2 primary to 1.6 secondary), leeside angle (40° primary and 35° secondary), location relative to the separation point of the two profile dunes and the different pre-separation crestal velocity.

No similar increase in velocity gradient is seen near the bed for profile H/96/S, which is located further downstream from flow reattachment, indicating that the growth of a shear layer, and therefore the allied increase in turbulence production, is associated with the process of flow separation alone.

Many of the types of structures similar to those visible for the high flow survey are also present for the low flow measurements, such as the movement of high velocity gradient packages moving upwards in the water column from the shear layer (see Figure 40(a)). These structures are more difficult to discern for the February survey, as the magnitude of the high shear zone is much smaller relative to the ambient conditions when compared to the high flow survey. However, the distinction between high shear events in the water column and the high velocity gradient produced due to the shear layer growth is lessened for the low flow survey as the gradients measured though the shear layer are not as great as for the high flow survey. This decreased distinction of the velocity gradient through the shear layer is partially a consequence of the lower mean flow velocity but will also be linked to the increase in bed roughness caused by the superimposition of secondary bedforms. An increase in bed roughness will induce an increase in flow turbulence which is exhibited as increased variation and complexity in the resulting velocity and velocity gradient information (McLean and Smith, 1979).

The variation in velocity gradient magnitude is also highlighted by comparison of the profiles collected in the trough of the primary (L/96/T) and the secondary (L/96/TS) bedforms. There are lower velocity gradients across the shear layer produced by the secondary bedform so although flow separation does exist, it will be relatively less effective in enhancing the downstream sediment transport rate and producing reattachment scour, as the velocity gradient and hence turbulence intensity across the separation zone is lower. The length of flow reattachment, which is linked to both step height and angle and the shear zone velocity gradient will also be smaller for the secondary bedform. The spatial pattern of sediment entrainment, transport, suspension and deposition is controlled by the formation and downstream extent of the separation zone shear layer (Bennett and Best, 1995). The lower velocity gradients present across the secondary dune shear layer may lead to less active scouring at reattachment as the magnitude and frequency of ejection events is determined by the velocity gradient across the shear layer and hence the rotational velocity of the Kelvin-Helmholtz instabilities that are generated. Hence, turbulence production along a shear layer will be less active under low flow conditions than high and also less active for secondary dunes relative to larger primary bedforms. As flow separation is less intense at low flow rates, the irregularities in wavelength for a dune population may be greater than at high flow as the flow separation process is less efficient in promoting regularly spaced bedforms.

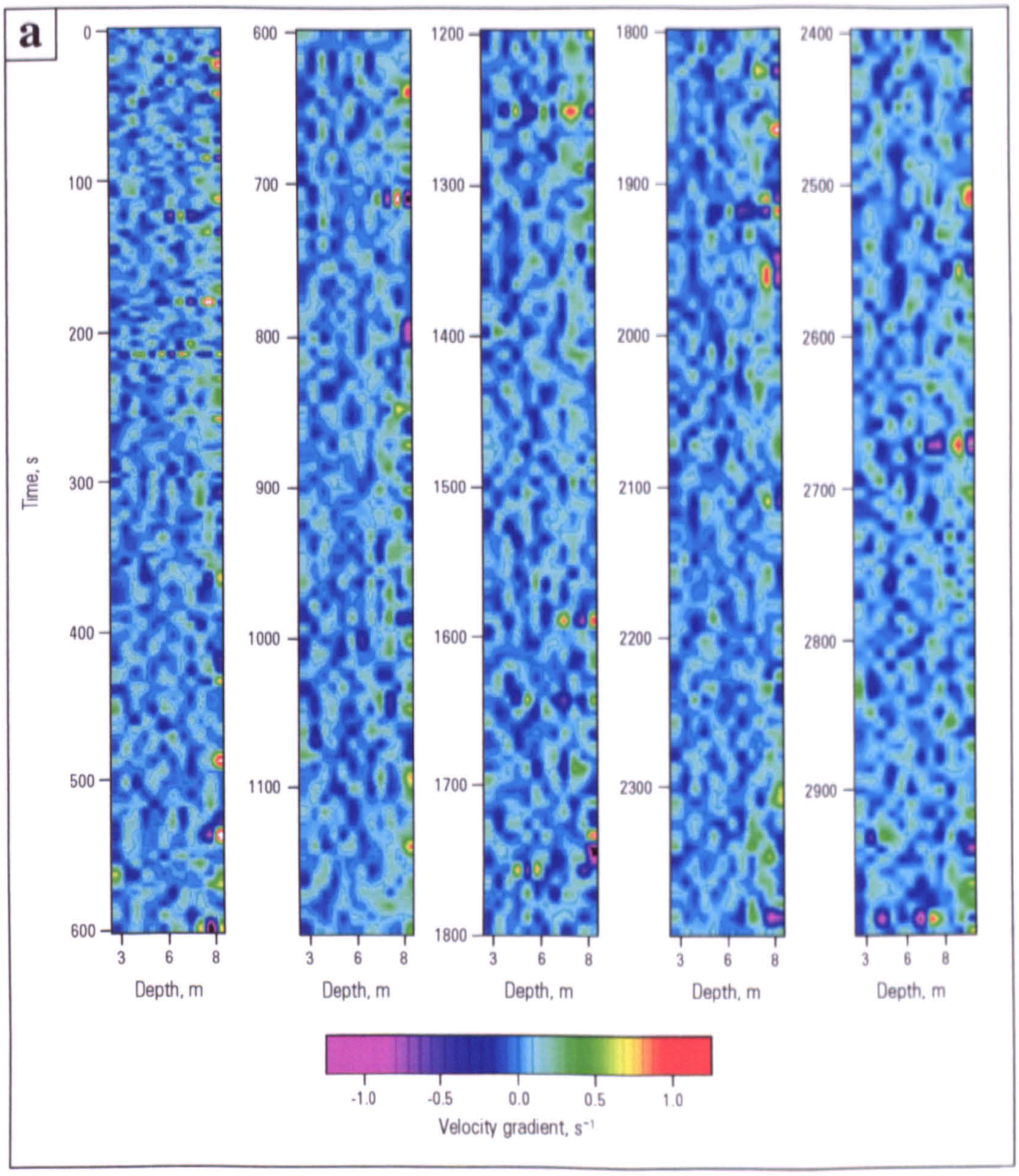

Figure 5.40: Contour maps of temporal variations in at-a-point downstream velocity gradient for the low flow survey at (a) L/96/TS, trough of a secondary dune, (b) L/96/T, primary dune trough and (c) L/96/S, stoss side of the subsequent dune. Flow is from top to bottom and a scale colour bar is given for each map. Flow depth bin sizes are 0.5 m. Each time series has been split to fit to page size and successive profiles are from left to right.

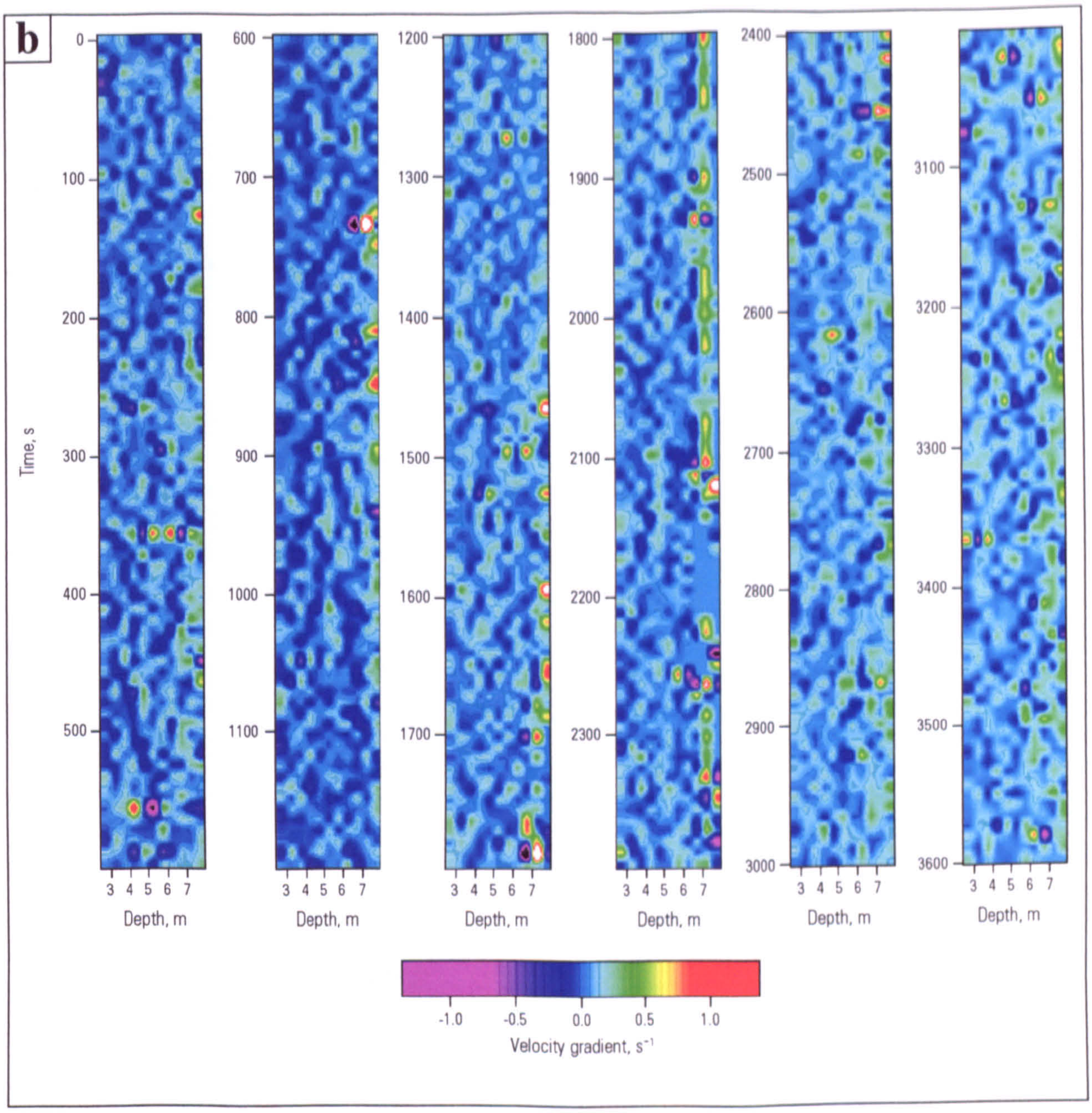

Figure 5.40: Contour maps of temporal variations in at-a-point downstream velocity gradient for the low flow survey at (a) L/96/TS, trough of a secondary dune, (b) L/96/T, primary dune trough and (c) L/96/S, stoss side of the subsequent dune. Flow is from top to bottom and a scale colour bar is given for each map. Flow depth bin sizes are 0.5 m. Each time series has been split to fit to page size and successive profiles are from left to right.

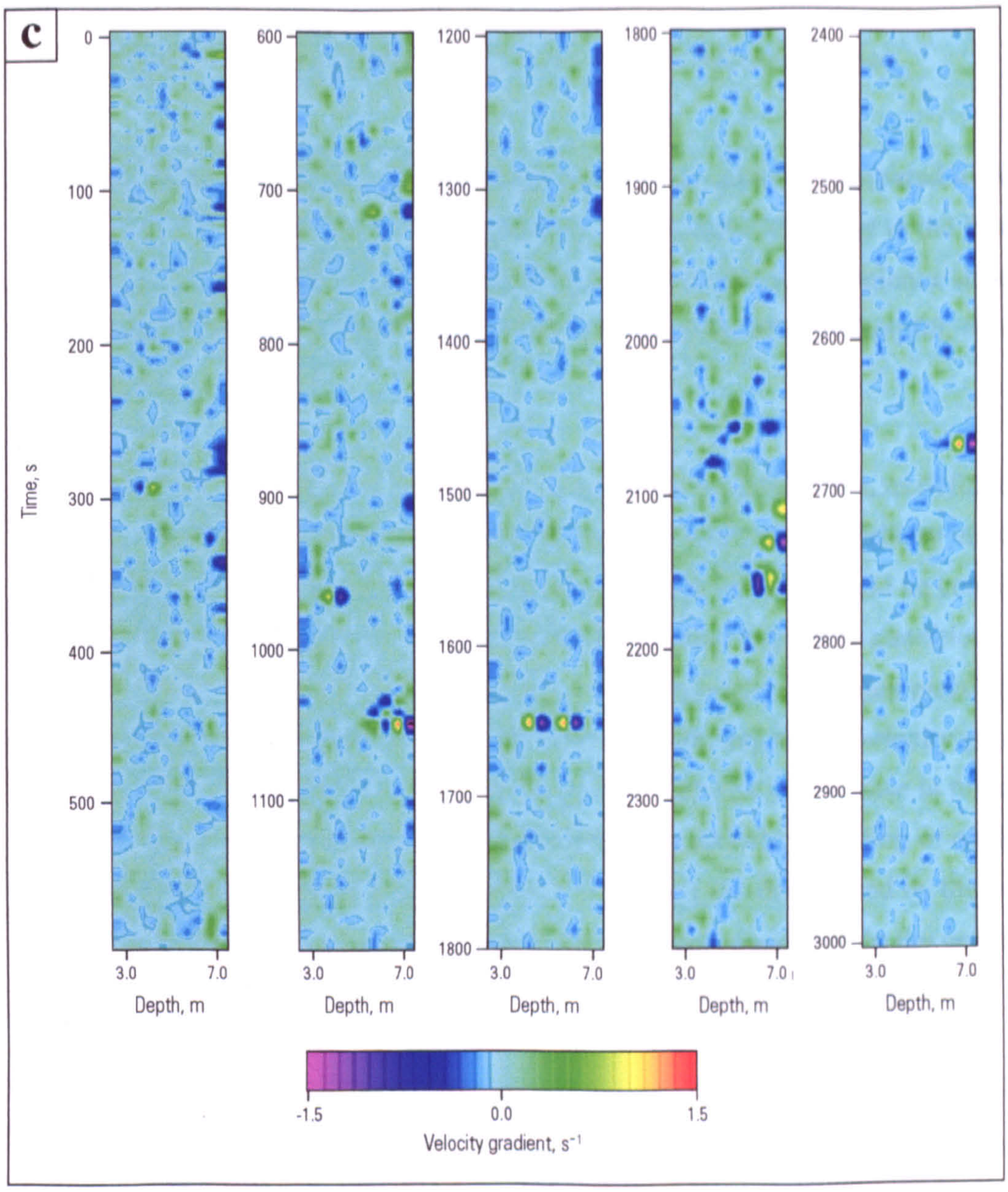

Figure 5.40: Contour maps of temporal variations in at-a-point downstream velocity gradient for the low flow survey at (a) L/96/TS, trough of a secondary dune, (b) L/96/T, primary dune trough and (c)L/96/S, stoss side of the subsequent dune. Flow is from top to bottom and a scale colour bar is given for each map. Flow depth bin sizes are 0.5 m. Each time series has been split to fit to page size and successive profiles are from left to right.

5.6.6 Event Classification and Recurrence in Dune Related Macroturbulence

The lower resolution of the ADCP during the low flow surveys compared to the high flow surveys indicates that the vertical velocity component will be inaccurate due to the low magnitude of the excursions. The usefulness of quadrant analysis for examining turbulence structures seems limited and results of quadrant analysis were inconsistent and therefore unhelpful, these are shown in Appendix 1.

Although the frequency of occurrence of particular turbulent events, as defined by quadrant analysis, may therefore not be examined at low flow rates, the periodicity in both the downstream velocity and in the vertical gradient of the downstream velocity could be considered using spectral analysis. Temporal variations in velocity gradients under high flow conditions above a dune trough have been linked to instabilities in the shear layer due to vortex ejection and shear layer motion. It seems likely therefore that the frequent high magnitude velocity gradients downstream of a dune crest during the low flow survey are indicative of an increase in turbulence intensity and therefore may also be associated with intermittent or periodic shedding of eddies and shear layer flapping. As the magnitude and frequency of ejections are determined by the velocity gradient (Bennett and Best, 1995), investigation of the frequency variations in the velocity gradient time series may therefore be used to quantify frequency in turbulence production.

Power spectra of the downstream velocity for profiles L/96/T and L/96/TS show an increase in spectral power with depth (Figure 5.41 a and b) across a broad range of frequencies with maximum values occurring at depths of 7.7 m. Spectral power in the downstream velocity frequency over the stoss side of the dune (Figure 5.41c) show little variation with depth indicating that there is no variation in velocity periodicity and therefore no change in turbulence production with depth. There is an increase in spectral power with depth for the trough profiles which may be associated with shear layer instability downstream of the dune crest. Such instability in the shear layer is associated with vortex shedding and amalgamation away from the shear layer and also flapping in the shear layer location. Simpson (1981) suggested shear layer flapping frequencies to approximate 0.8 *U/H and eddy shedding frequency to approximate 0.1 * (U/H), hence the expected frequencies for the primary dune are 0.03 Hz and 0.24 Hz respectively and for the secondary bedform are 0.06 Hz and 0.49 Hz respectively. It therefore seems likely that the ADCP records will not be able to resolve periodic eddy shedding from the shear layer due to the sampling rate (0.18 Hz). The increase in spectral power with depth for the trough profiles may therefore represent increased velocity variation due to shear layer flapping. The intermittent variation in velocity gradient described above may also reflect a combination of processes acting at different frequencies, the spectral power shows a peak at a frequency of 0.036 Hz which is very

close to the theoretical value of the frequency of shear layer flapping (0.03Hz) proposed by Simpson (1981) (Figure 5.42).

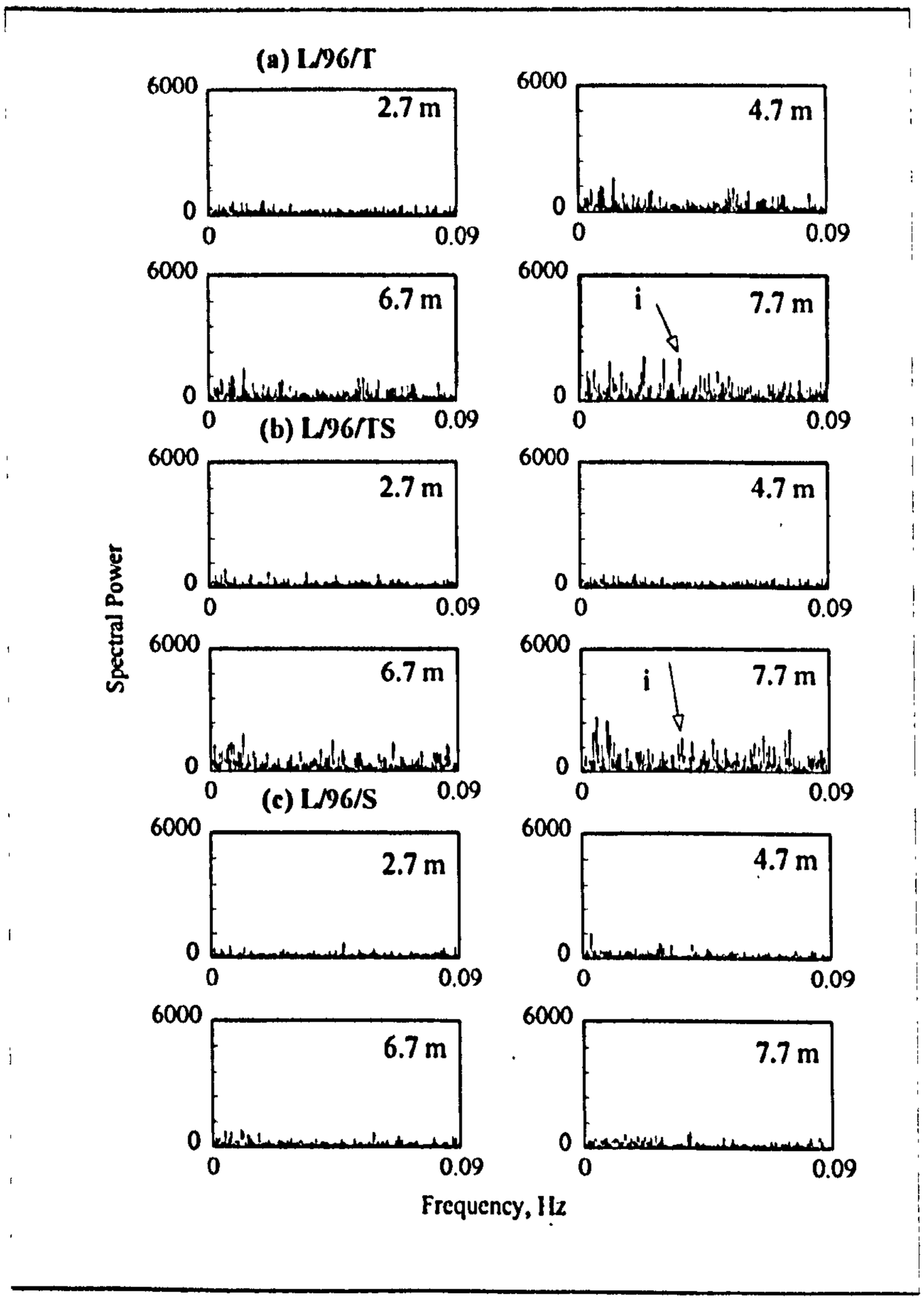

Figure 5.41, Power spectra of downstream velocity for profiles L/96/T, L/96/TS and L/96/S. The depth of each time series is shown on each graph. Label i refers to a spectral peak at a frequency of 0.036 Hz (27.8s).

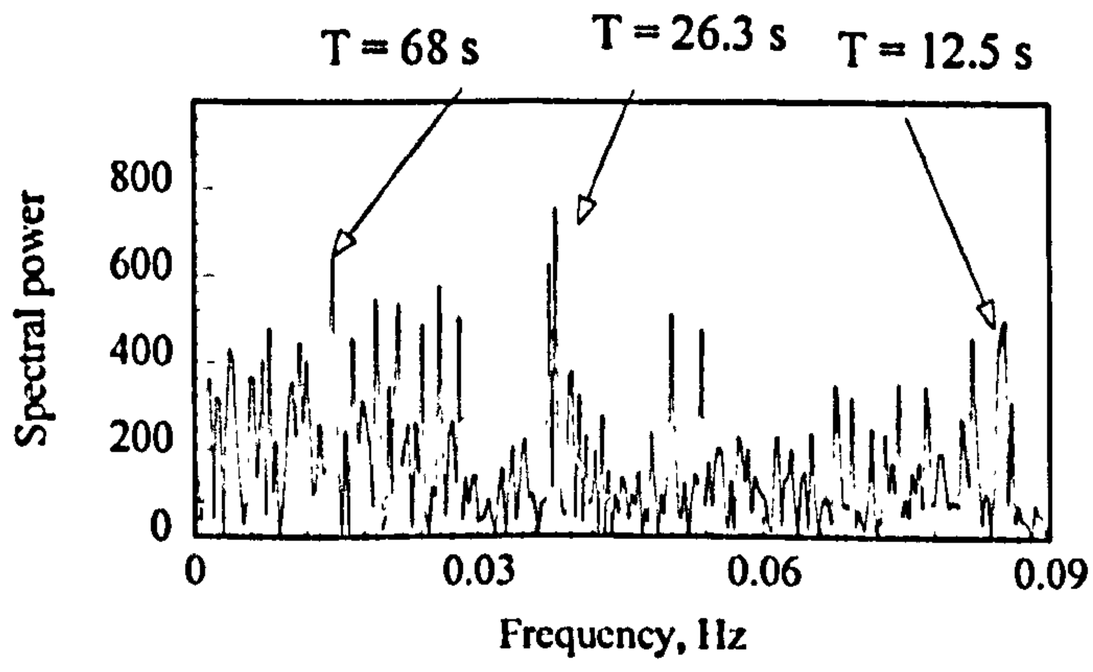

Figure 5.42, Power spectra of downstream velocity gradient for profile L/96/T at a depth of 7.7 m.

5.6.7 Summary of Low Flow Surveying over High Angled Bedforms

The flow field over high angled dunes at low flow stage has been shown to be dominated by the process of flow separation at the dune crest. Flow separation occurs over both primary and secondary dune bedforms although the magnitude of the separation zone velocity gradient is lower for the secondary bedform which is related mainly to its smaller height. The variation in dune height (and slip face angle) will alter the expansion ratio of the flow field and therefore flow deceleration and hence the velocity gradient through the separation zone shear layer. The development of a boundary layer downstream of the primary dune crest has been illustrated by the mean vertical velocity gradient on the stoss side of the downstream bedform. The effect on the magnitude and duration flow separation caused by the differences in the height and pre-separation velocity for the primary (H/U = 3.2) and secondary (H/U = 1.55) bedforms has been illustrated. A greater H/U ratio leads to an increase in the velocity gradient acting across the shear layer and therefore to higher magnitude and more frequent flow reversals and an increase in the turbulence intensity. In turn, increasing the H/U ratio may precipitate greater scouring in the trough and therefore increased entrainment and suspension of sediment. It therefore appears that the velocity gradient acting across the free shear layer produced by flow separation and the accompanying variation in the turbulence structure is a key element in determining dune height and therefore in governing dune stability.

5.6.8 Mean Velocity Profiles over Low Angled Dunes

The mean at-a-point velocity profiles L/96/LOW1 and L/96/LOW2 are located on the lee side of a low (2.5°) lee-face angled dune (Figure 5.43). The downstream velocity profiles show a decrease in velocity with depth from a maximum of 0.95 ms^{-1} at the ADCP minimum measuring depth of 2.7 m, to a minimum velocity of 0.6 ms^{-1} near to the bed. The downstream velocity over profile L/96/LOW2 is slightly higher than L/96/LOW1 and this is most probably because of flow expansion and deceleration between the two profiles.

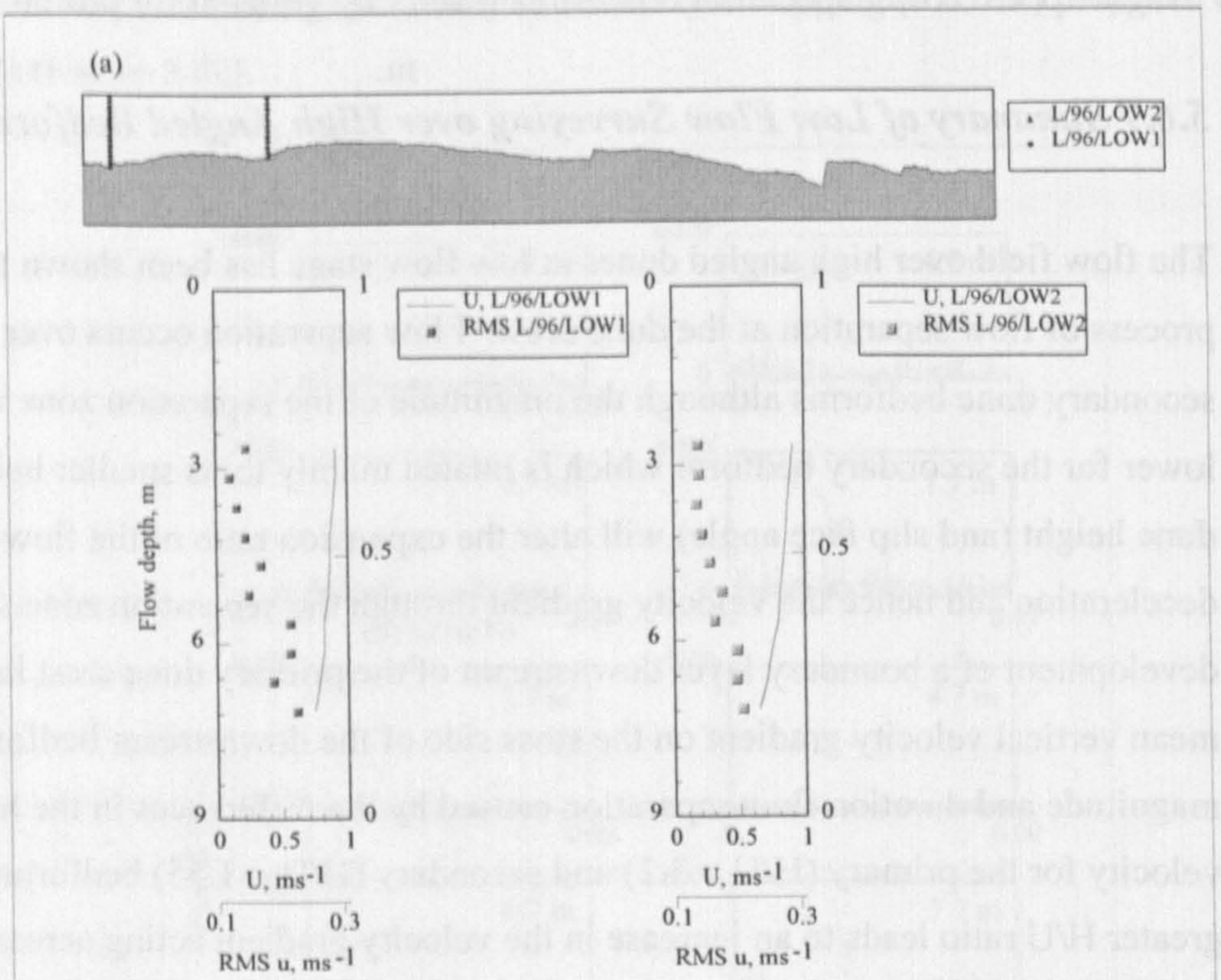

Figure 5.43, Vertical profiles of the time-averaged at-a-point velocity and corresponding RMS values collected during the low flow February 1996 survey over a low lee faced angle dune showing (a) downstream velocity and (b) vertical velocity.

The vertical rate of change of velocity with depth is illustrated by the profiles of gradient of the normalised mean velocity (Figure 5.44) and shows a small, although inconsistent, increase with depth, with a maximum gradient of 0.06 s^{-1} which is located close to the bed of profile L/96/LOW2. The maximum gradient in mean velocity measured over the low lee-face angled bedform is therefore less than half the maximum value recorded during the low flow survey over high angled bedforms. The greater velocity gradients over the upstream profile are representative of the higher rate of flow expansion over profile L/96/LOW2 as this profile is located closer to the dune crest. The profiles of velocity gradient therefore indicate that there is no development of a distinct high shear zone downstream of the dune crest.

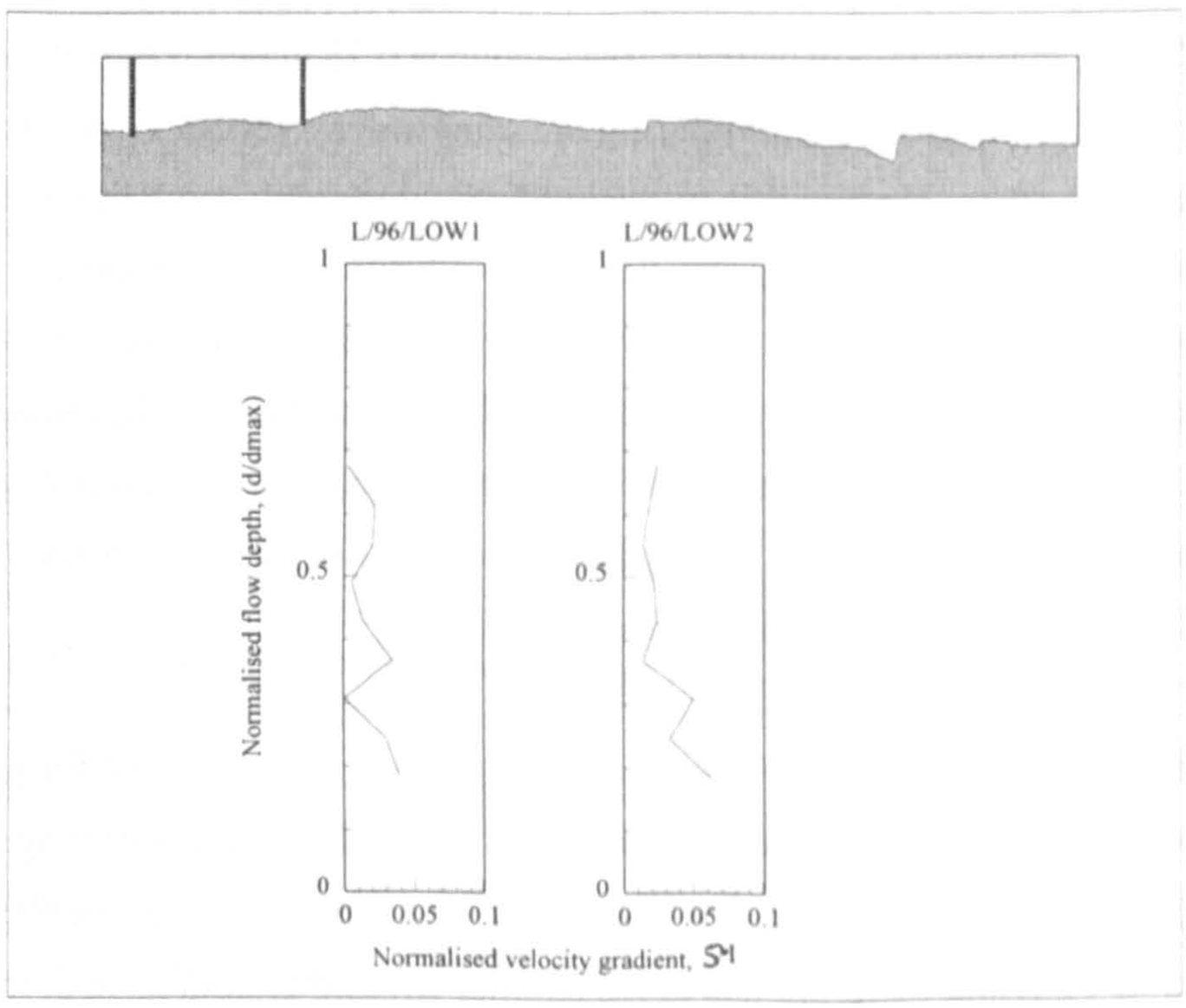

Figure 5.44, Vertical profiles of the time averaged at-a-point normalised downstream velocity gradient collected during the February 1996 low flow survey over a low lee face angled dune. The relative location of the profiles is indicated by the schematic above.

The mean vertical velocity for both profiles is very low with a maximum value of 0.01 ms^{-1} and a minimum of -0.07 ms^{-1}, which is below the resolution of the ADCP (Figure 5.43b). Mean vertical velocity over profile L/96/LOW2 is lower than that measured over the downstream profile and this may be due to flow expansion and therefore deceleration between the two profiles.

The mean downstream velocity profiles therefore demonstrate no evidence of the flow separation process which was documented on the leeside profiles of high slip face angled dunes at both low and high flow stage (L/96/T and H/94/T). The vertical profiles of velocity gradient show a small increase with depth which is indicative of flow expansion downstream of the dune crest.

However, the rate of expansion is much smaller than for the high or low flow profiles in the leeside of dunes where mean velocity gradients were twice as high as those measured over the low angle bedform. The absence of the development of a distinct shear zone and a low flow region is in good agreement with previous work on the flow field over low angled dunes where no flow separation was detected (e.g. Smith and McLean, 1977; Kostaschuk and Ilersich, 1995; Kostaschuk and Villard, 1996).

5.6.9 Velocity Moments and Reynolds Stress

The vertical and downstream RMS values over the low lee-face angled dune both show a small increase with depth although there are no rapid or distinct changes in the distribution (Figure 5.42). The maximum downstream RMS value is 0.25 which is half the maximum value recorded over the steep angled bedform during the same survey period. In general, therefore for the low angled dune there is a small increase in RMS values with depth but with no evidence of increased turbulence production at any specific depth indicating no development of a turbulence-producing shear layer. The mechanisms of flow and sediment transport over flat dunes must be radically different to those acting over steep dunes which were described previously. The dominant feature of the flow field over steep angled dunes is separation of the flow at the dune brink point and there is no evidence of flow separation from the mean velocity profiles described above, acting over the low angled dunes in this survey.

Variation in Reynolds stress with depth shows no consistent trend for profile L/96/LOW1 with fluctuations in Reynolds stresss between -1.3 Pa and 0.72 Pa occurring through the flow depth (Figure 5.45). Profile L/96/LOW2 has consistently weakly negative Reynolds stress values (-1.11 Pa to -0.4 Pa) and therefore has much smaller stress fluctuations than the upstream profile.

The vertical profiles of downstream velocity skewness show no consistent trend with depth, Uskew values fluctuate between -1.6 and 0.95 and are therefore lower than the Uskew values over steep angled bedform troughs (Figure 5.44). The vertical skewness profiles over both of the low angled bedforms are weakly negative from a depth of 4m, with profile L/96/LOW1 (minimum -0.3) exhibiting lower Vskew than L/96/LOW2 (minimum -0.95). Above 4.2 m, Vskew values increase slightly for both profiles.

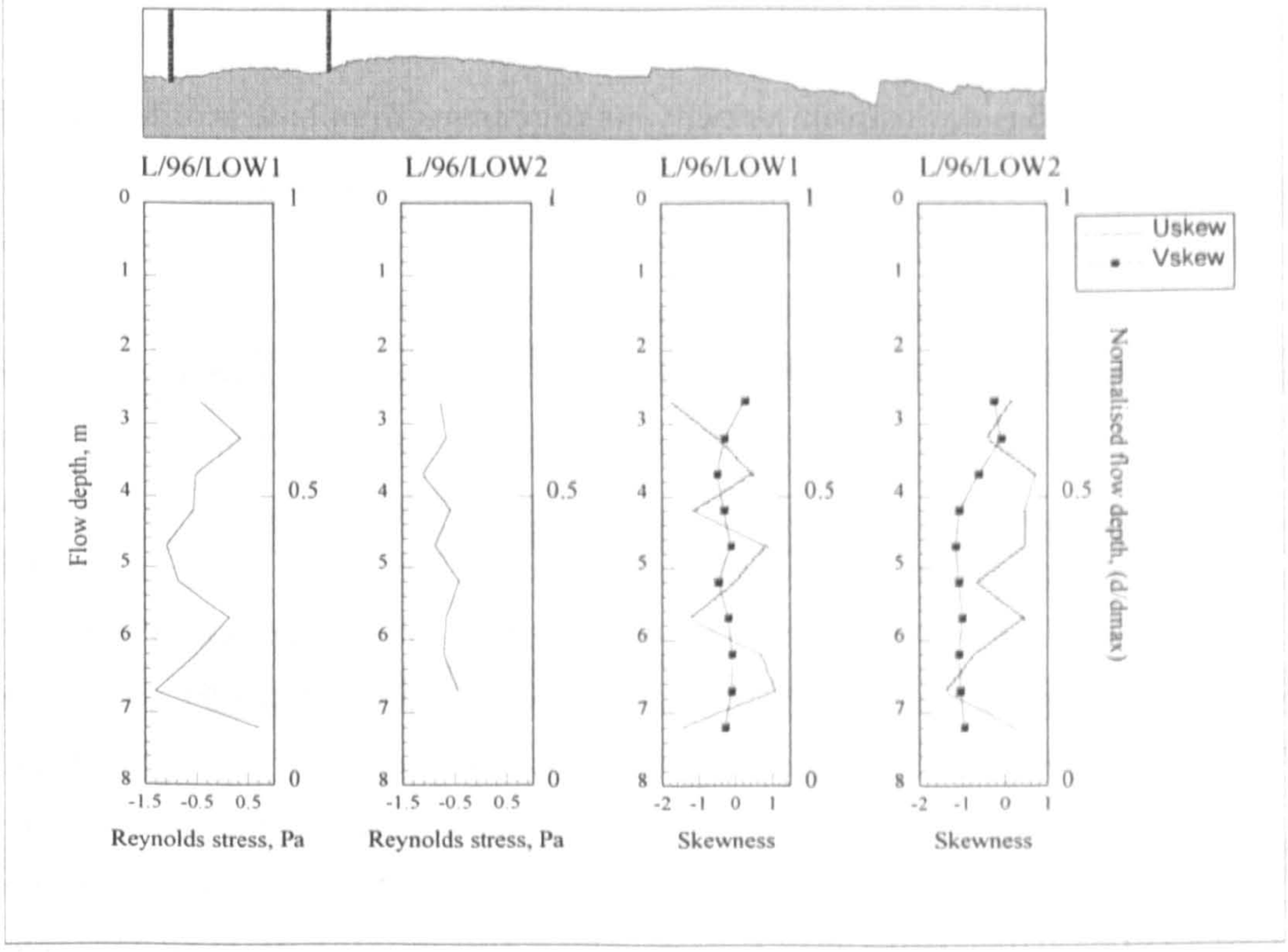

Figure 5.45, Vertical profiles of the mean Reynolds stress and downstream and vertical velocity skewness for the February 1996 survey over a low lee face angled bedform.

5.6.10 Temporal Variation in Downstream Velocity

This section will describe the temporal variations in downstream velocity on the lee side of the low angled bedform. At-a-point velocity time series are shown in Figure 5.46 for profiles L/96/LOW1 and L/96/LOW2 at various depths and colour contour maps for the entire flow field for 0.5 m depth intervals are shown in Figure 5.47.

Maximum downstream velocities measured over the low angle dunes are 1.41 ms^{-1} for the upstream profile and 1.36 ms^{-1} further downstream (Figure 5.46 and 5.47). The slightly lower velocity measured over profile L/96/LOW1 represents the expansion and deceleration in flow that was recognised from the mean profiles. The minimum downstream velocities measured over profiles L/96/LOW1 and L/96/LOW2 are 0.12 ms^{-1} and 0.25 ms^{-1} respectively.

The presence of flow separation has been shown to be a key factor influencing the flow field over steep angled dunes in some field situations (Soulsby *et al.*, 1991; Chapter 5) and in flume studies (Nelson *et al.*, 1993; Bennett and Best, 1995). However, other field studies (Smith and McLean, 1977; Kostaschuk and Villard, 1996) have noted the absence of flow separation over bedforms with lower lee face angles. There are three possible cases regarding flow separation for this study:
1) Flow separation exists

2) Flow separation is intermittent

3) There is no flow separation

The instantaneous downstream velocity measurements from both profiles have shown no evidence of flow reversals at the location of profiles L/96/LOW1 and L/96/LOW2 over the leeside of the dune. Flow reversals have been shown to be a function of pre-separation velocity, dune height (Driver *et al.*, 1987; Simpson, 1981), dune lee face angle and the morphology of the brink point (Ogink, 1981). Profiles L/96/LOW1 and 2 are located over a bedform with lower lee face angle (8.5° compared to 40°), lower pre-separation velocity (1 ms^{-1} compared to 1.2 ms^{-1}) and smaller height (2.15 m compared to 2.85 m) than profile L/96/T. Hence, if flow reversals are present over the lower angle bedform, they would be expected to exhibit lower flow magnitude and lower reversal frequency compared to those occurring over the steeper angled dune. Driver *et al.* (1987) showed that the life span of flow reversals is a function of step height and pre-separation velocity, it may be that if low magnitude reversals are occurring over the low angled bedform then the sampling frequency of the ADCP is too short to measure them. The shape of the brink point for the two bedforms is also quite different, the concave profile will inhibit separation over L/96/LOW2 relative to the sharply convex boundary over the steeper profile (Ogink, 1981; Hand and Bartberger, 1987). If any flow reversals do occur over the low angled bedform they would also be expected to arise at lower flow depths closer to the bed. As the ADCP cannot measure velocity in the lower 7% of the flow column it may be that any possible flow reversals are missed. Flow separation may also be expected to be discontinuous laterally along the bedform crest. For example, studies of the dimensionality of dunes in the Fraser river (Kostaschuk and MacDonald, 1988) showed that scour holes are present inconsistently along trough lines which may be local foci of flow separation zones. The locations of any flow reversals may also be limited in the downstream direction which means that profile location would be critical in detecting them.

The mean velocity gradients measured over profile L/96/LOW1 have shown an increase with depth to a maximum value of 0.06 m^{-1} (Figure 5.44) which is comparable to those over the secondary bedform which did exhibit intermittent separation. It is therefore possible that low frequency, low magnitude flow reversals do occur over low angled bedforms but that they are not quantifiable in the present field study. Further detailed study of the flow field over low angled bedforms is needed in a flume to resolve this problem.

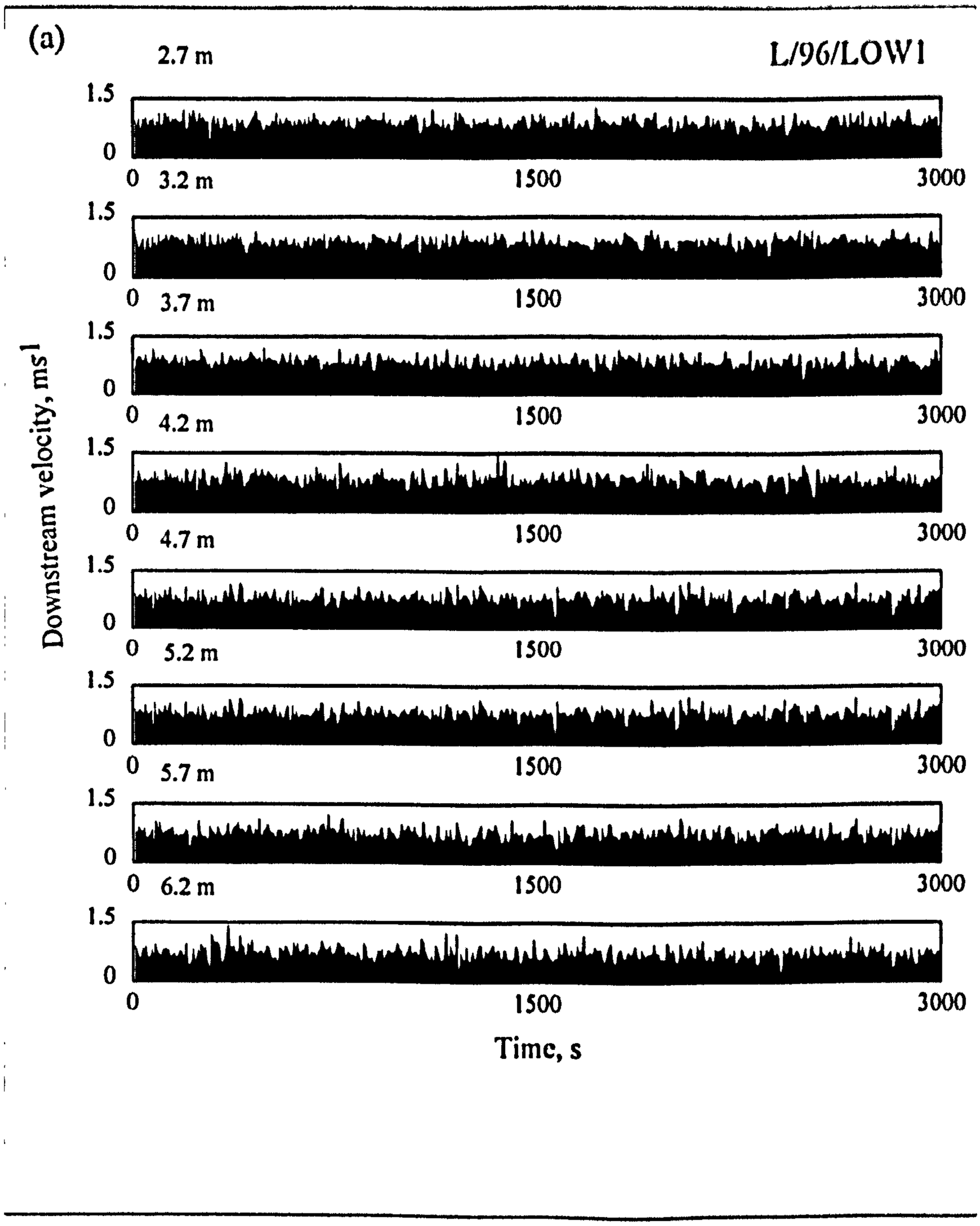
(a)
L/96/LOW1
2.7 m
3.2 m
3.7 m
4.2 m
4.7 m
5.2 m
5.7 m
6.2 m
1.5
0
0
1500
3000
Downstream velocity, ms-1
Time, s

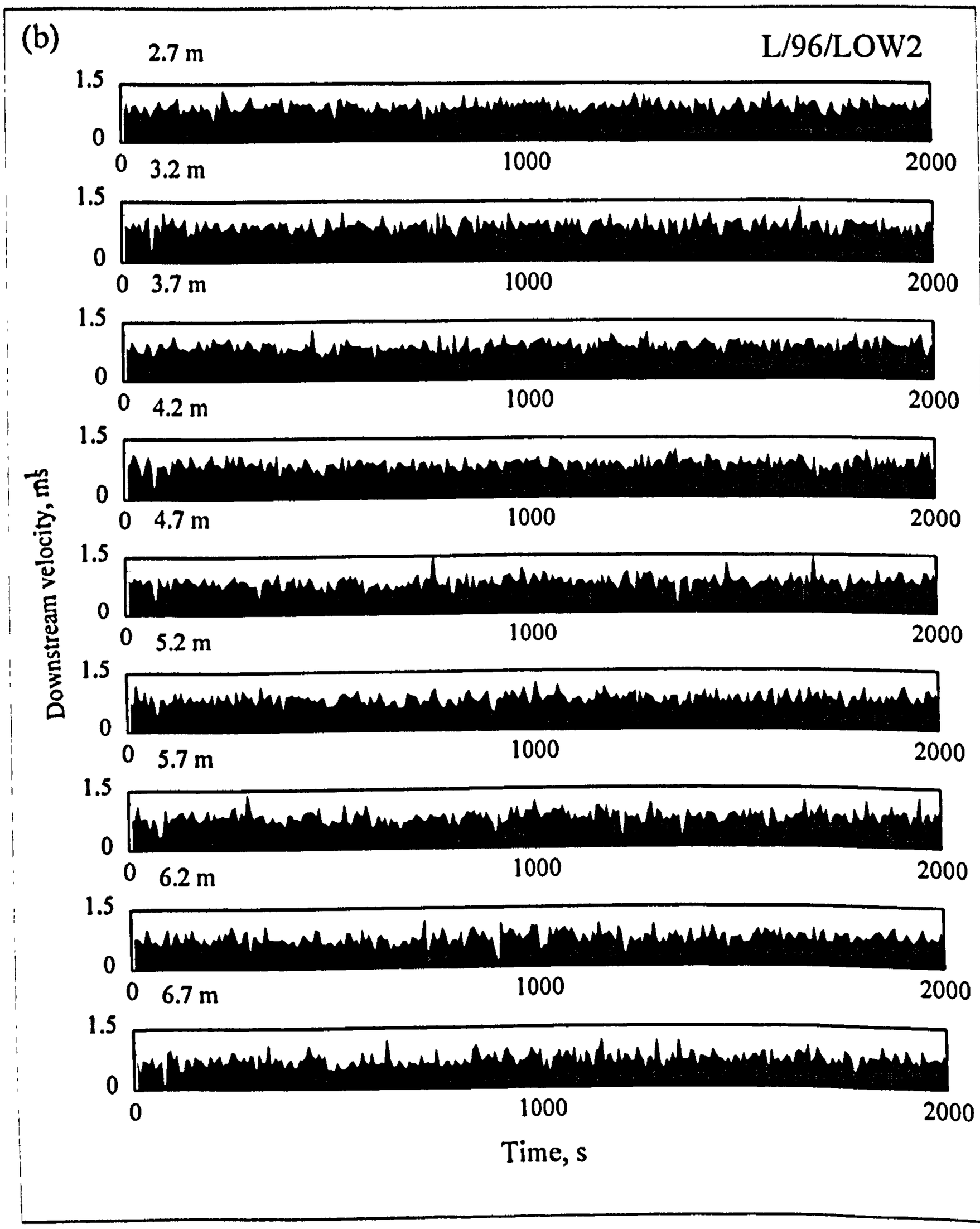

Figure 5.46, At-a-depth time series of the instantaneous values of the downstream velocity collected on the lee side of a low angled dune for profile (a) L/96/LOW1 and (b) L/96/LOW2.

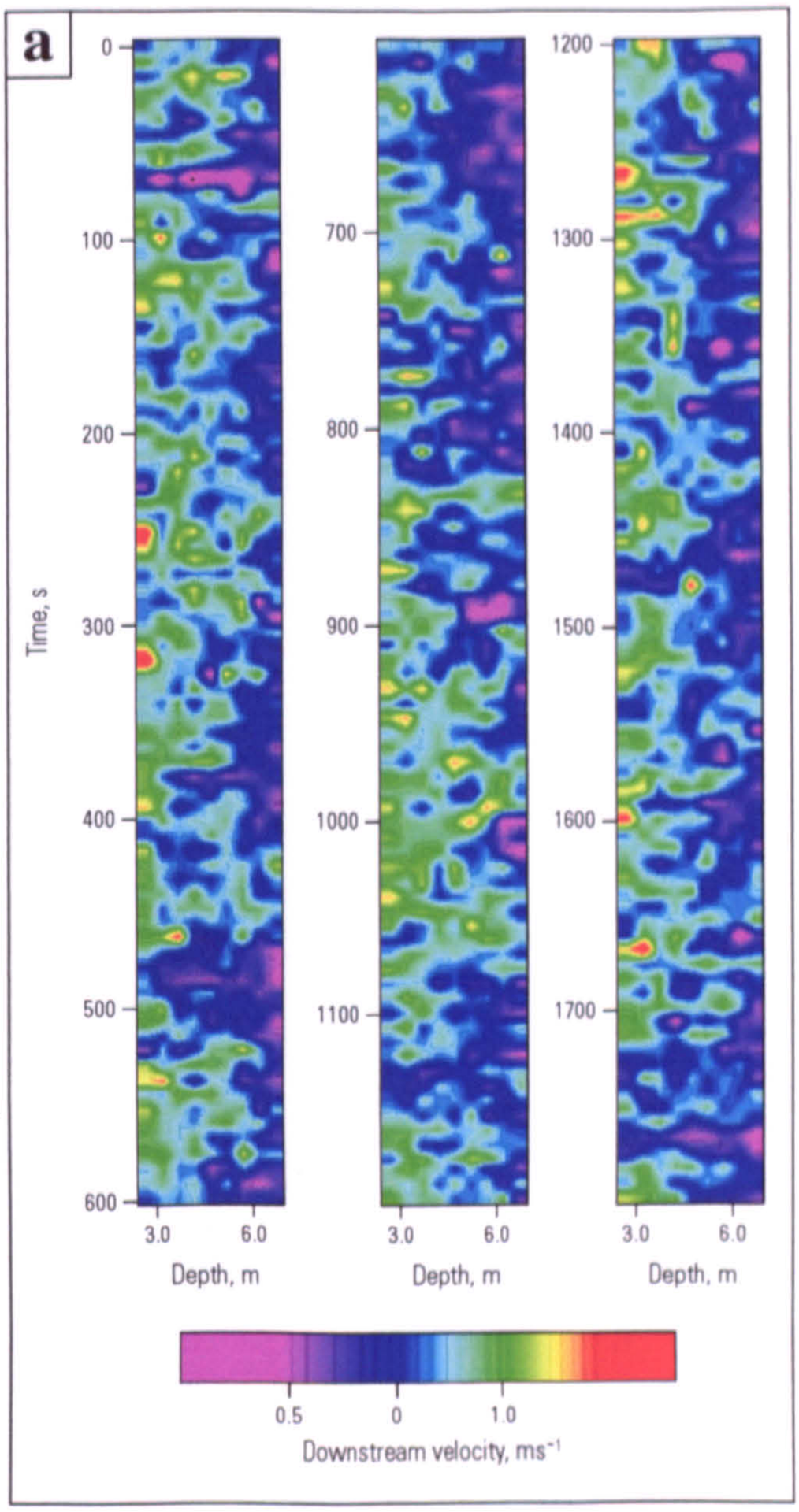

Figure 5.47: Contour maps of temporal variations in at-a-point downstream velocity for the low flow survey over a low-angled dune at (a) L/96/LOW2, just downstream of the dune crest and (b) L/96/LOW1, dune lee side. Flow is from top to bottom and a scale colour bar is given for each map. Flow depth bin sizes are 0.5 m. Each time series has been split to fit to page size and successive profiles are from left to right.

226

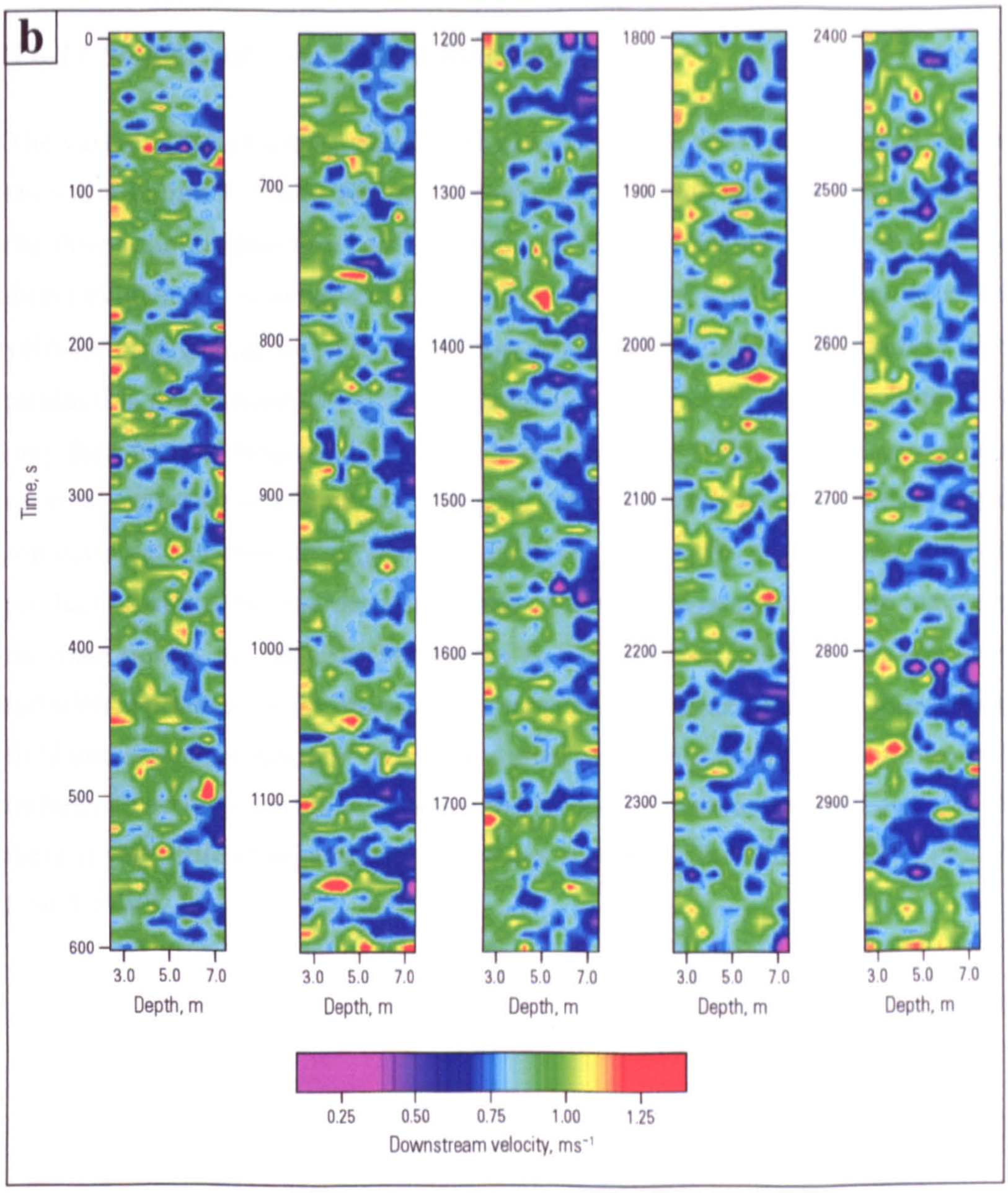

Figure 5.47: Contour maps of temporal variations in at-a-point downstream velocity for the low flow survey over a low-angled dune at (a) L/96/LOW1, just downstream of the dune crest and (b) L/96/LOW2, dune lee side. Flow is from top to bottom and a scale colour bar is given for each map. Flow depth bin sizes are 0.5 m. Each time series has been split to fit to page size and successive profiles are from left to right.

5.6.11 Stability of Low Angled Bedforms

The variation in velocity gradient with time and depth above this low lee face angled bedform is shown in Figure 5.48 and shows no production of a high velocity gradient zone at any height in the flow column, therefore confirming the findings of the mean velocity profiles that there is no direct evidence of flow separation or the production of a corresponding free shear layer. As velocity gradient can be taken to be proportional to the turbulence intensity, the turbulence production mechanism described for steep angled dunes is not in operation. Low angled dunes may therefore be dynamically distinct from steep angled dunes. The amount and rate of flow reversal occurring over a negative step has been shown to increase with the velocity pre-flow separation at the dune crest crestal (e.g. Driver, 1987), this has the effect of increasing turbulence production along the free shear layer and at reattachment and therefore increasing erosion from the dune trough. As eddy shedding from an unstable free shear layer is not the mechanism of turbulence production for dunes of this morphology, other processes must be influencing the flow field and sediment transport over low angled dunes. Further evidence of the lack of coherent turbulence acting over the low angled bedforms is shown by spectral analysis (Figure 5.49) as there is very little change in spectral power with depth for either profile L/96/LOW1 or L/96/LOW2.

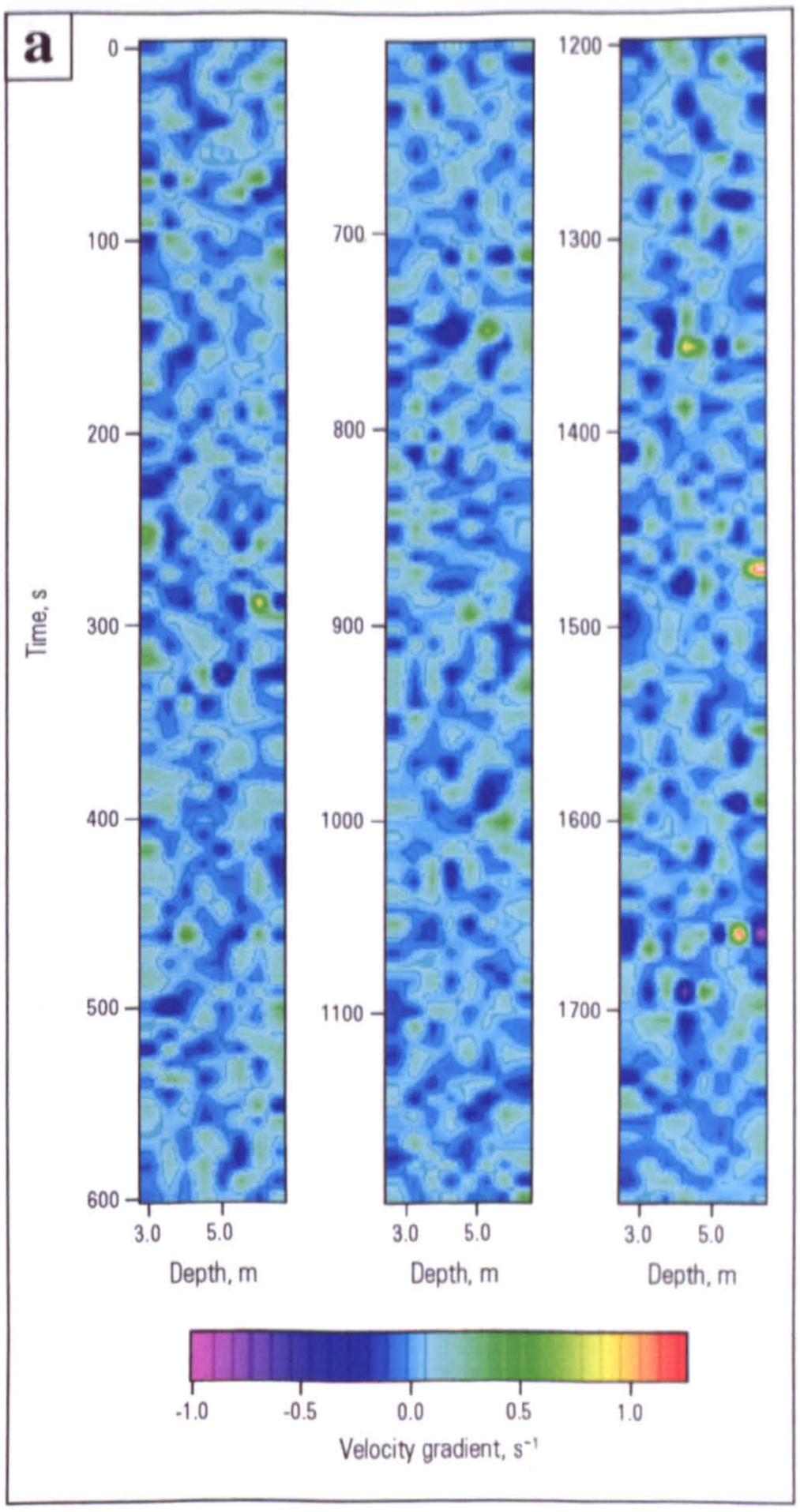

Figure 5.48: Contour maps of temporal variations in at-a-point downstream velocity gradient for the low flow survey over a low-angled dune at (a) L/96/LOW2, just downstream of the dune crest and (b) L/96/LOW1, dune lee side. Flow is from top to bottom and a scale colour bar is given for each map. Flow depth bin sizes are 0.5 m. Each time series has been split to fit to page size and successive profiles are from left to right.

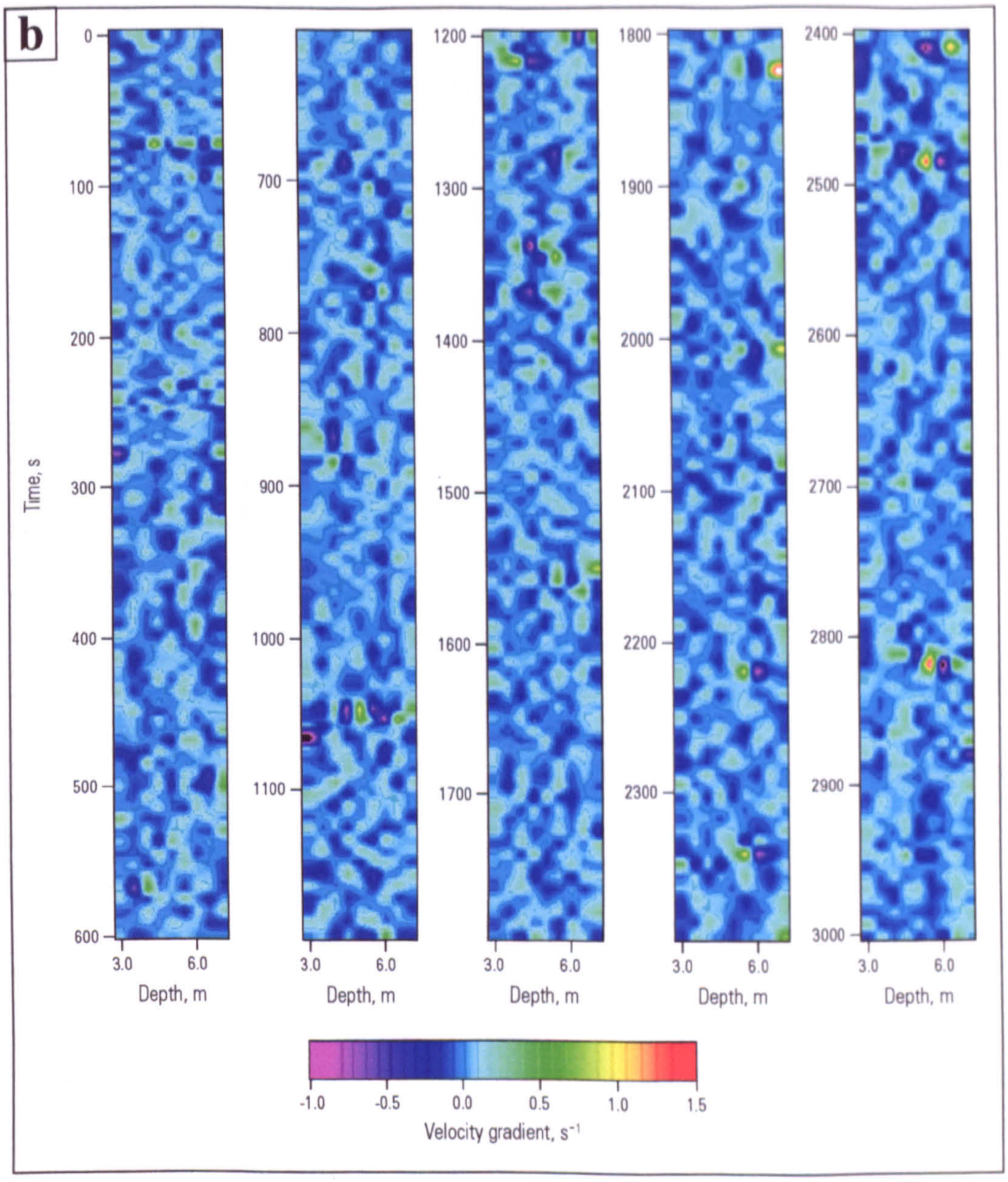

Figure 5.48: Contour maps of temporal variations in at-a-point downstream velocity gradient for the low flow survey over a low-angled dune at (a) L/96/LOW2, just downstream of the dune crest and (b) L/96/LOW1, dune lee side. Flow is from top to bottom and a scale colour bar is given for each map. Flow depth bin sizes are 0.5 m. Each time series has been split to fit to page size and successive profiles are from left to right.

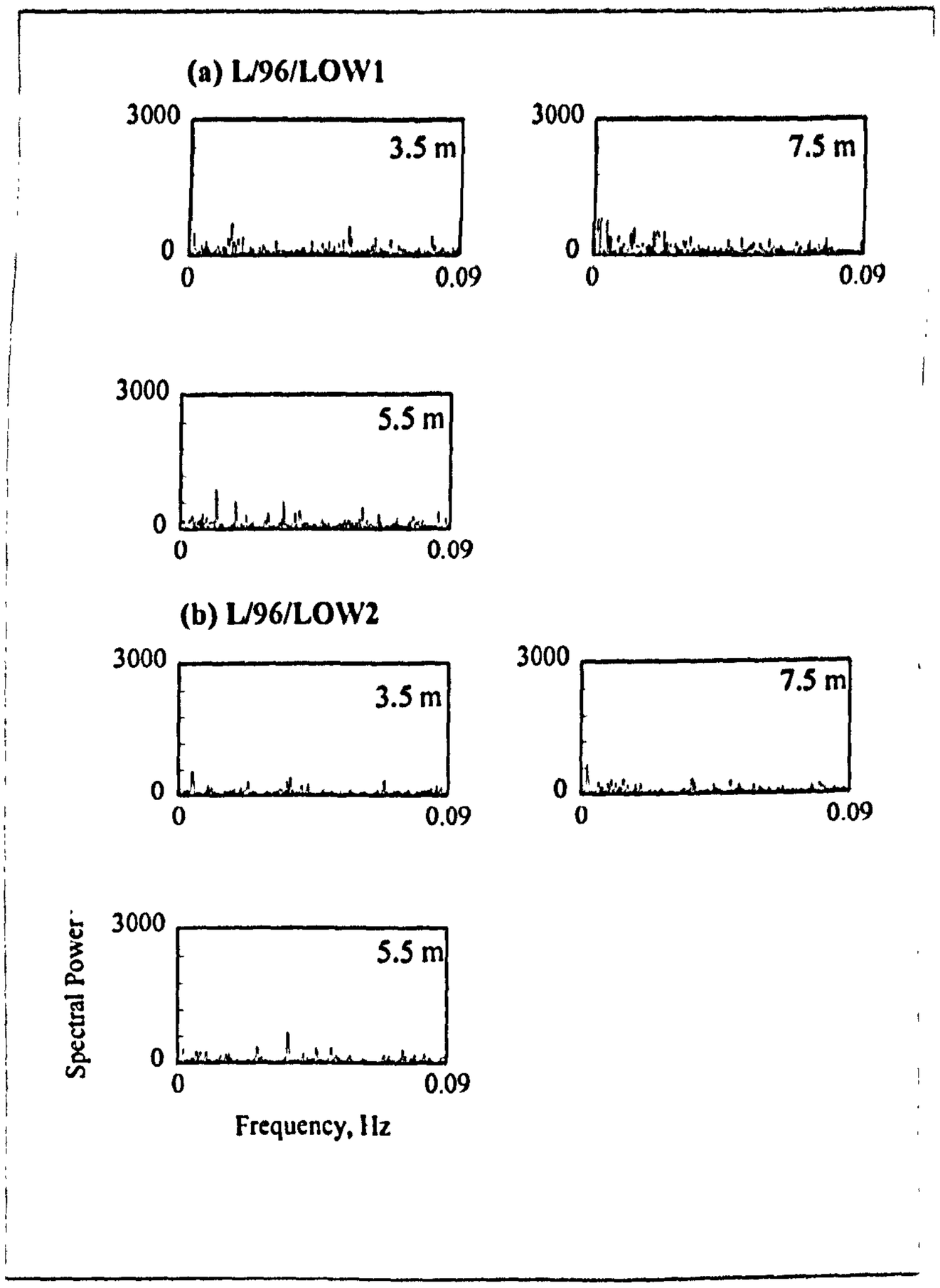

Figure 5.49, Power spectra of the downstream velocity for profile L/96/LOW1 and L/96/LOW2. The depth of each profile is given on each graph.

Studies of the transition from dune to upper stage plane bed (e.g. Saunderson and Lockett, 1983) have shown that although the morphology of the dune alters (wavelength: height ratio increases), a distinct (although small) steep slip face will still occur until the bedform has been washed out. No such high-angle slip face is present on the low angled bedforms studies here, so the morphology of the dune therefore indicates that they may not be a result of increasing bed shear stress leading to transitional bedforms.

A variation in the magnitude of suspended sediment concentration has been proposed previously to explain decreases in the lee face angle of a bedform (Smith and McLean, 1977; McLean and Smith, 1979; Kostaschuk and Ilersich, 1995; Kostaschuk and Villard, 1996). These studies noted that dominant sediment transport mechanisms change with flow stage in the Colombia and Fraser rivers, from bedload dominated at low flow stage to suspension dominated at high flow stage. The morphology of the bedforms was seen to alter with changes in sediment transport mechanisms from asymmetric dunes with steep lee sides (bedload dominated transport) to more symmetric bedforms with shallow-dipping lee sides (suspension dominated transport). The change in morphology was postulated to be caused by suspended sediment deposition in-filling in the leeside of the bedforms. Experiments of sediment fallout patterns in the leeside of dunes (Hand and Bartberger, 1987) have shown that the angle of the brink point is critical in governing whether flow separation will occur. Variation in brink point morphology from angular to smooth will cause a variation in sediment fallout patterns: convex brink points are formed when enough of the sediment load is transported high enough to cause the position of the maximum sediment outfall to shift downstream away from the brinkpoint.

Increasing sediment suspension load at higher discharges cannot be the cause of low-angled dunes forming in the Jamuna river as low lee face angled dunes are more common under low flow rates (see Chapter 4) when suspended sediment concentrations are much lower than during high stage (approximately two orders of magnitude, see Chapter 6) and much less variable. The morphological studies of bedforms in the Jamuna have also shown that lee-side deposition (and therefore a decrease in lee-face angle) mainly occurs during the falling stage of the hydrograph, not at high flow stage when suspended sediment concentrations are at a peak (Chapter 4).

Previous studies have shown that dune morphology changes rapidly and that dunes undergo complex processes of growth, attenuation and destruction (Gabel, 1993). Secondary dunes are extremely common during this low flow survey (Figure 5.3), possibly indicating that the bedforms are not in equilibrium with the flow conditions (Allen, 1976). Secondary dunes are not present on lee faces of primary dunes where the lee angle is high enough to cause flow separation as secondary dunes will be incorporated into the primary dune at the brink point if this is the case. However, if the lee angle of the primary dunes is too low to cause flow separation, a migrating secondary bedform may not be incorporated at the crest, the ensuing migration of a secondary dune down the leeside of a primary will act to further decrease the lee angle and may lead to permanent non-separation of the flow. Migration rates for all the bedforms along the survey transect line vary, with secondary dunes migrating faster than the primary bedforms (Figure 5.50). Dune amalgamation will therefore occur as upstream, faster-migrating bedforms combine with slower migrating downstream dunes. The slower downstream bedform may often become sediment starved through the influence of the upstream bedform.

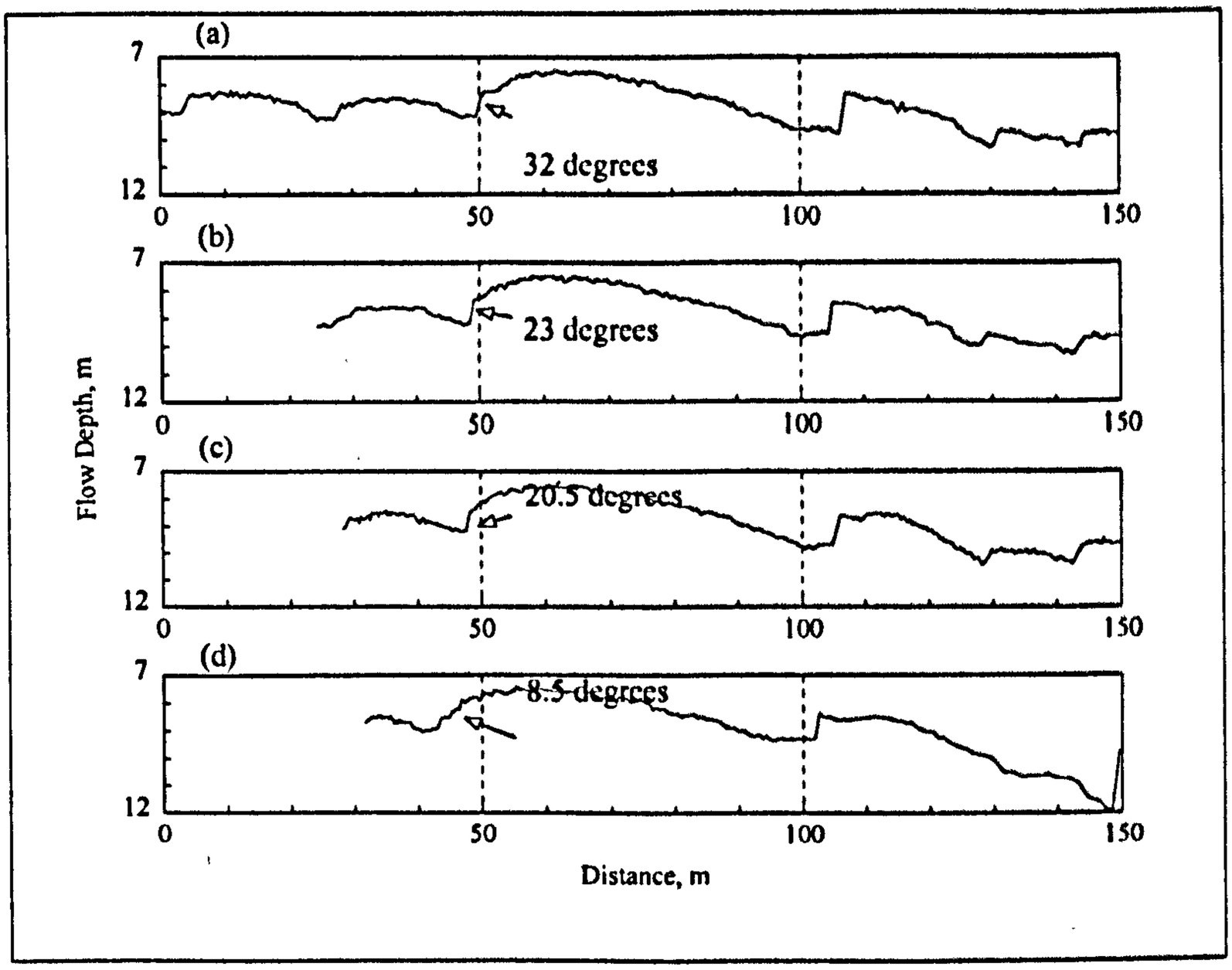

Figure 5.50, Bathymetric profiles over the February 1996 survey low flow dune conducted over a 4 day period. (a) 25/2/96, 16:12:22, (b) 26/2/96, 15:15:42, (c) 27/2/96, 17:06:23 and (d) 28/2/96, 15:17:15.

For example, Figure 5.50 shows a succession (over four days) of bathymetric profiles over the at-a-point velocity profiling location. The upstream bedforms initially has a high slip face angle (of 30°, Figure 5.48a) which decreases over the four day survey period to 8.5°. The decrease in lee face angle may partially be linked to the migration of the secondary dune up the stoss side of the primary bedform, as the influence of an upstream separation zone may decrease the sediment supply to the downstream bedform (Best, 1996), so stalling the primary dune. Sediment starvation due to the proximity of a secondary dune to the primary crest may also lead to a decrease in the primary dune height (Ditchfield and Best, 1992). An initial decrease in lee side angle will also cause feedbacks to further decrease the steepness of the lee face as a rounded or convex brink point will inhibit flow separation (Hand and Bartberger, 1987). Therefore, as the lee face changes in steepness, the flow processes acting over the dune will alter and so will the sediment fallout patterns. As lee face angle begins to flatten the velocity differential acting across the shear layer will decrease, since the velocity gradient is proportional to the turbulence intensity then turbulence production relating to the free shear layer and flow reattachment also will decrease (Bennett and Best, 1995). Additionally, if the turbulence intensity through the shear layer and at flow reattachment control the spatial pattern of sediment entrainment, suspension and deposition, then decreasing the lee face angle will change the sediment transport characteristics of a bedform.

The decrease in lee face angle will result in a decrease in scouring in the dune trough and also an increase in deposition on the lee face.

The low lee face angle bedform is not in equilibrium with the flow depth with a flow depth:height ratio of 5 compared 3.4 and 2.25 for the low-flow, high angled dune and the high flow at-a-point profiling dune respectively. This lack of equilibrium with the present flow regime may indicate firstly that sediment starvation has occurred causing a decrease in height and secondly that the present morphology is ephemeral and the geometry of the dune is transitional between a stalled primary dune amalgamating with secondary dunes and a more equilibrated feature. Low angled dunes in the Jamuna river formed at low flow rates are probably disequilibrated, amalgatory, transitional features that form due to a combination of sediment starvation, preferential migration rates and a possible decrease in the lee face angle so leading to less pronounced flow separation, fewer flow reversals and a decrease in scour in the dune trough, and eventually no flow separation. It may therefore be more correct to term these hydraulically distinct, non-flow-separating bedforms as transitional, non-equilibrium dunes.

5.7 Comparison of High and Low Flow Surveys

The data presented in this chapter are the first detailed measurements of three-dimensional flow columns over dunes in a large, dynamic braided sand-bed river.The results of velocity profiling using an ADCP compare very well with previous laboratory and theoretical work showing that the ADCP is a very useful implement for studying flow over bedforms in a field situation. Although acoustic techniques have been used to describe flow fields in alluvial and estuarine environments before (e.g. Thorne *et al.*, 1996), this is one of first studies to quantify both the mean flow and turbulence structures associated with dune bedforms.

The mean velocity profiles measured over high angled dunes have been shown to be highly spatially variable at both high and low flow discharges. Over high slip face angled dunes, flow separation at the dune brink point has been shown to dominate the flow field. Rapid flow expansion and deceleration downstream of the crest forces the production of a shear layer, the normalised velocity gradient acting through the shear layer being very similar under high and low flow conditions (0.141 s^{-1} and 0.135 s^{-1} for the high and low flow surveys respectively). There is little evidence of a low flow zone beneath the shear layer under low flow conditions although this may be due to the measuring depth of the ADCP and the position of the profile. Downstream of flow reattachment the mean profiles illustrate that flow accelerates up the stoss side of the dune and that maximum downstream velocities occur over the crest.

The impact of dune morphology on the mean velocity field has been highlighted during the high flow survey where flow expansion occurs before separation due to multiple breaks in the lee side face. Decreasing crestal velocity before separation occur will lessen the effect of the break in slope at the brink point as the velocity gradient acting through the shear layer is a function of the pre-separation velocity.

Flow reversals have been quantified in the trough of dunes under both high and low flow conditions. These flow reversals have also been shown to be intermittent and this may be affected by the position of the profile with respect to the slip face; permanent reversal zones may occur closer to the dune lee side. The magnitude and length of flow reversals has been linked to flow conditions and the morphology of the bedform. Intermittency in flow reversal is therefore controlled by the slip face angle of the dune, the height of the slip face and the upstream flow velocity

Temporal variations in the velocity gradient are linked to turbulence production with 90% of quadrant 4 events and 70% of quadrant 2 events occurring at velocity gradients greater than 1 or less than -1. Thus, the turbulence intensity both within the shear layer and near the reattachment point may be viewed as being proportional to the velocity differential across the shear layer. The utilisation of temporal variations in velocity gradients is a valuable tool for studying turbulence production over a bedform and gives an insight into the movement of an unstable free shear layer within the flow column. Previous work on negative steps has demonstrated that the shear layer exerts a significantly greater influence on the entire flow field when the step height becomes a substantial fraction of the flow depth and hence it appears that it is the velocity gradient produced by the flow separation process that controls bedform stability. An increase in turbulence production caused by higher velocity differentials through the shear layer will in turn increase the sediment flux at flow reattachment (by quadrant 4 events) and also increase suspension of sediment from the shear layer (by quadrant 2 events). Thus the spatial variation in turbulence structure, which is regulated by flow separation, controls the downstream sediment flux which is the fundamental control on bedform development (Figure 5.51). The key controls on turbulence production and hence sediment flux are therefore the ratio of dune height to crestal velocity, the ratio of dune height to flow depth and lee face angle. The growth and decay of an unstable shear layer formed by flow separation and the subsequent changes in reattachment location control the formation and growth of high slip face angled dunes. The local controls on turbulence production for the low and high flow surveys over steep angled dunes are shown in table 5.4.

	H/94/T	L/96/T	L/96/TS
H/U	3.4*	3.2	1.6
H/d	0.4	0.28	0.14
profile location	3H	3.5H	3.9H
lee angle	55	40	35

*possible flow expansion between crest and brink point due to downstream dipping length section may increase H/U

Table 5.4, Summary of hydraulic conditions and bedform morphology for surveys at high and low flow discharges over steep angled dunes.

These results of flow over dunes at high and low flow rates have therefore shown that the processes acting under differing hydraulic regimes are identical although the magnitude of the processes (such as the intensity of the velocity gradient acting through the shear layer and hence

turbulence production is lower under low flow rates) and hence the size of the bedforms is smaller.

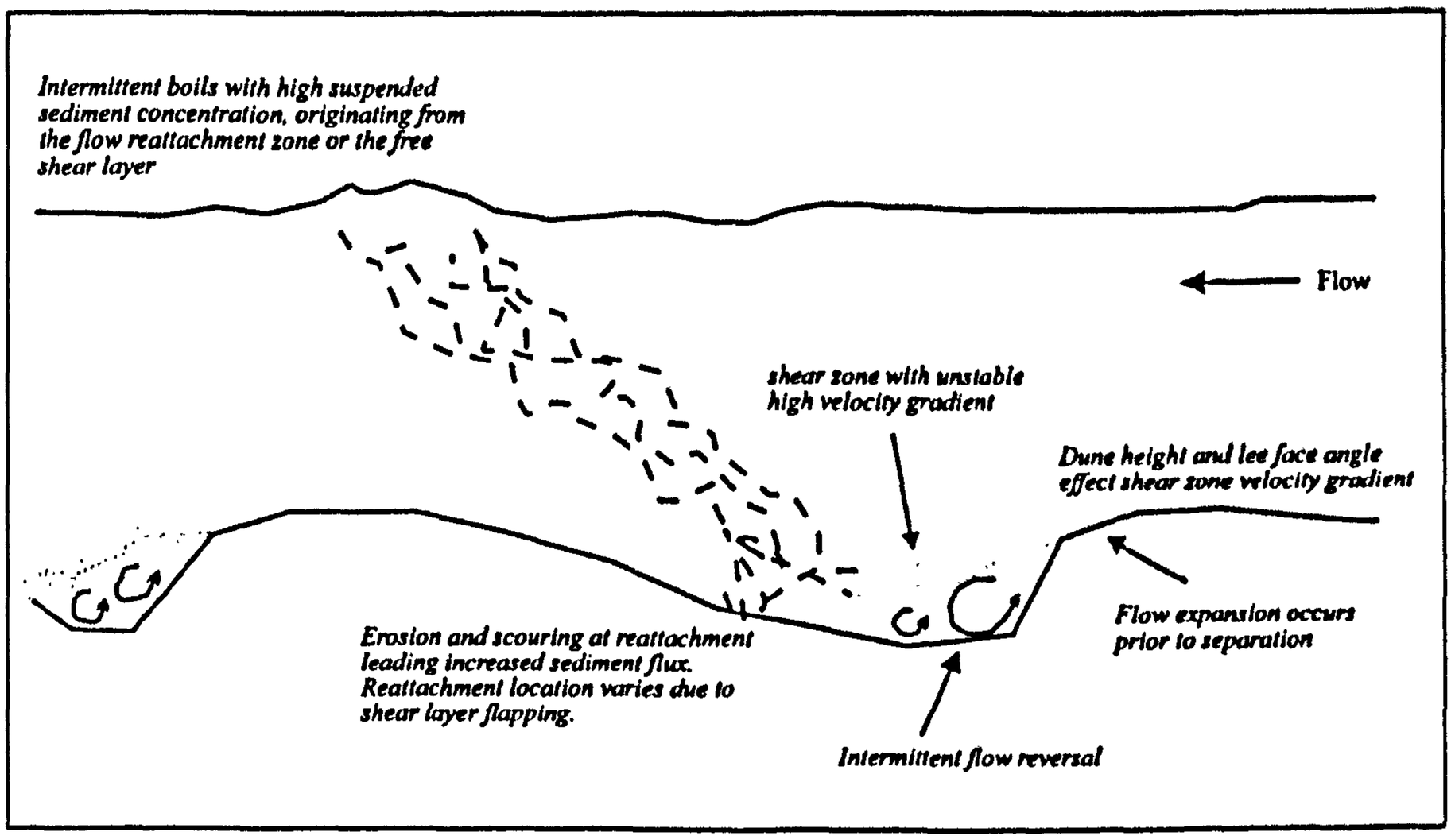

Figure 5.51, Summary diagram of flow over high angled dunes.

Mechanisms of flow and sediment transport over low lee face angled bedforms at low flow stage in the Jamuna river are very different to those acting over high angled bedforms. Low lee faced angles do not generate flow separation and have lower rates of flow expansion and deceleration downstream of the crest (Figure 5.52). Mechanisms of turbulence production are therefore different for high and low angled dunes, the key morphological elements controlling flow expansion and the production of a shear layer described above are shown in Table 5.5. There is little evidence of turbulence production over low angled dunes formed at low flow stage in the Jamuna river. If turbulence is produced then it is not caused by the shear layer eddy shedding mechanisms proposed previously and may be linked to classical turbulent boundary layer bursting. Low angled dunes in the Jamuna river formed at low flow rates are disequilibrated, amalgatory, transitional features that form due to a combination of the complex processes of dune growth, aggregation, attenuation and destruction which are related to the unique flow conditions over each dune, preferential migration rates and a possible original lower-than-average slip face angle so leading to less marked flow separation, fewer flow reversals and a decrease in scour in the dune trough.

	L/96/LOW1	L/96/LOW2
H/U	2.47	2.47
H/d	0.22	0.22
profile location	0.5H	1.2H
lee angle	8.5	8.5

Table 5.5, Summary of hydraulic conditions and bedform morphology for surveys under low flow conditions over low lee faced angled dunes.

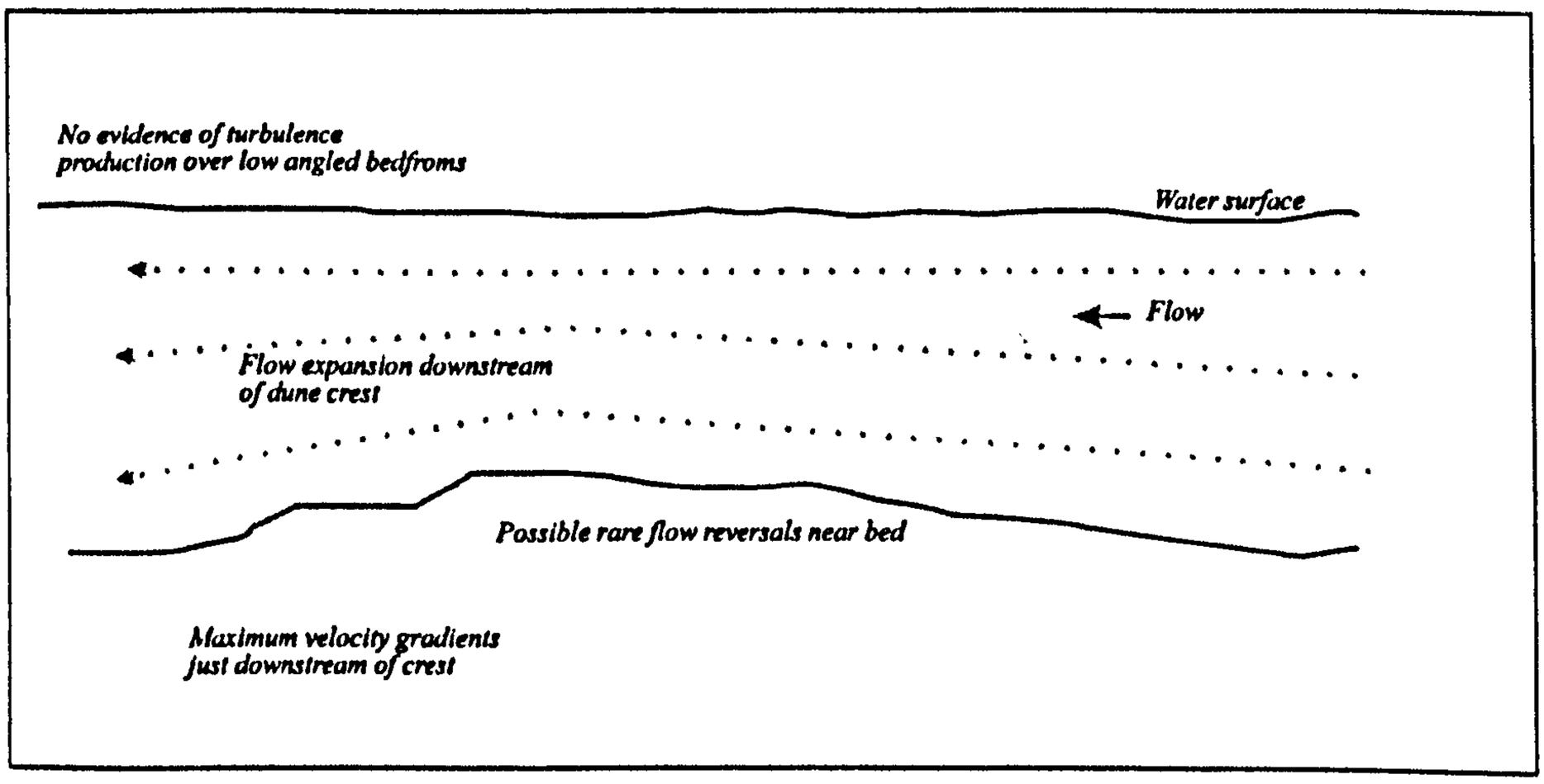

Figure 5.52, Summary diagram of flow over low angled bedforms

Chapter 6. Suspended Sediment Transport

6.1 Introduction

The previous chapter has described and quantified both the spatial and temporal variations in mean flow and turbulence over dunes of differing morphology. This chapter will investigate mean suspended sediment concentrations and their temporal and spatial variation in relation to the features of the flow field identified and described in Chapter 5. An understanding of sediment transport in relation to fluid flow over dunes is a principal objective in any study of dunes, as it will influence both their morphology and dynamics. Many workers have suggested that macro-turbulence associated with dune bedforms is important for both entrainment and transport of sediment and therefore in controlling the formation and hydraulic stability of dunes (e.g. Jackson, 1976; Yalin, 1977; Allen, 1980; McLean *et al.*, 1994; Bennett and Best, 1995). The occurrence of large eddies downstream from dune crests associated with high concentrations of suspended sediment has previously been documented by Jackson (1976), Yalin (1977), Rood and Hickin (1989), Lapointe (1992) and Kostaschuk and Church (1993). The acoustic profiles of Kostaschuk and Church (1993, see Chapter 2, Figure 2.7) and surface 'grab' sampling of Rood and Hickin (1989) revealed substantial increases in suspended sediment associated with the entrainment of bed material by boils (named 'kolks' by Kostaschuk and Church (1993) after Matthes (1947)), which were conjected to originate from the lower stoss side of dunes.

However, the role of coherent turbulent structures, such as those described in Chapter 5, in suspending sediment is still poorly understood (Nelson *et al.*, 1995). The coupling between flow and sediment transport, and in particular the significance of shear layer eddies, in the entrainment and movement of sediment grains is of great importance to the formation and stability of dunes (Kostaschuk and Church, 1993). This chapter will therefore aim to examine the links between turbulence structure and sediment transport in the spatially non-uniform flow conditions present over dunes.

Firstly, the time averaged mean suspended sediment concentration profiles will be described for both low and high flow survey conditions corresponding to the at-a-point velocity profiles from Chapter 5. Suspended sediment concentrations over both high and low slip faced angled dunes will be examined. Secondly, spatial variations in instantaneous

suspended sediment concentrations from the entire flow fields associated with dunes will be described for the high and low survey periods, in order to allow for more generalised hypotheses to be made as to sediment transport processes associated with dunes. Thirdly, variations in the suspended sediment concentration at-a-point will be investigated and examined in relation to the turbulence structures elucidated in Chapter 5.

6.2 Mean Suspended Sediment Concentration Profiles

Vertical profiles of time-averaged mean suspended sediment concentrations measured at locations corresponding to the velocity profiling detailed in Chapter 5 for the low and high flow surveys are examined below. These profiles will be compared in order to assess any spatial variation in mean sediment concentrations at different points downstream along low and high slip face angled dunes and to quantify the variation in suspended sediment concentration at different flow stages. Calculation of suspended sediment concentration from the ADCP acoustic backscattered signal is detailed in Chapter 3.

6.2.1 Mean suspended sediment concentration at high flow stage

Suspended sediment profiles from the August 1994 and September 1995 surveys are shown in Figure 6.1a, the concentration profiles have been amalgamated into an ensemble over one bedform to aid comparison. All of the vertical profiles show an increase in suspended sediment concentration with depth towards the bed, with the exception of profile H/94/T. Profile H/94/T was collected above the dune trough and shows a slight decrease in suspended sediment concentration within the flow recirculation zone (identified in Section 5.5.2). Maximum suspended sediment concentration is over 1100 mgl^{-1} and this maximum is associated with the lower part of the separation zone free shear layer which was identified from the downstream and vertical velocity measurements above the trough (Chapter 5, Figure 5.7a). A very similar pattern in vertical profiles of suspended sediment concentration was also shown by Soulsby *et al.* (1991) where maximum mean suspended sediment concentrations of 1800 mgl^{-1} were located over the dune trough with a decrease in sediment concentration into the flow separation zone and down to bed level (Figure 1b). None of the vertical mean suspended sediment profiles approximate to an equilibrium flat-bed Rouse profile (Soulsby, 1991), illustrating the dominating affect of dune bedforms on sediment

transport. Minimum levels of suspended sediment concentration (200 mgl^{-1}) are found in the outer flow column at the minimum depth measurable by the ADCP (2.7 m).

However, the mean sediment concentration profiles for the Jamuna are dissimilar to those shown by Kostaschuk and Villard (1996) which were collected over both symmetrical and asymmetrical dunes in the Fraser river. The asymmetrical dunes of Kostaschuk and Villard (1996) are similar in morphology to those examined here unlike the symmetrical forms as they exhibit steeper lee slopes of up to 18.9°, and higher lee:stoss ratios (Section 5.3). Kostachuk and Villard (1996) showed that sediment concentration (and sediment transport rate) generally increased up stoss sides and decreased down lee sides with maximum values usually on the upper stoss sides, or on lee sides just downstream of the crest. Over asymmetric dunes, Kostachuk and Villard (1996) found little or no increase in suspended sediment concentrations in dune lee sides, contrary to this study where maximum sediment concentrations are located at heights equivalent to the separation zone shear layer downstream of the dune crest (Figure 1a, H/94/T). The variation between the profiles of Kostaschuk and Villard (1996) and those presented here may be related to two factors: firstly, the absolute sediment concentrations measured in this study are one fifth of those of Kostaschuk and Villard (1996), and secondly, the morphology and therefore mean flow fields of the dunes over which surveying was conducted is very different for the two studies. Kostaschuk and Villard (1996) did not detect the presence of flow reversals or the production of a shear layer in the lee side of either the asymmetric and symmetric bedforms studied, hence the shear layer-associated high suspended sediment concentrations which have been found in this study are absent. Thus the effect of flow separation is shown to increase suspended sediment concentration downstream of the dune crest as suspended sediment passing the crest is convected away from the bed (e.g. Zyserman and Fredsoe, 1994). Also, if flow separation is not present then the effects of eddy shedding from the separation zone shear layer will be absent and the resulting reduction in turbulence intensity may lead to decreased scouring in the dune trough.

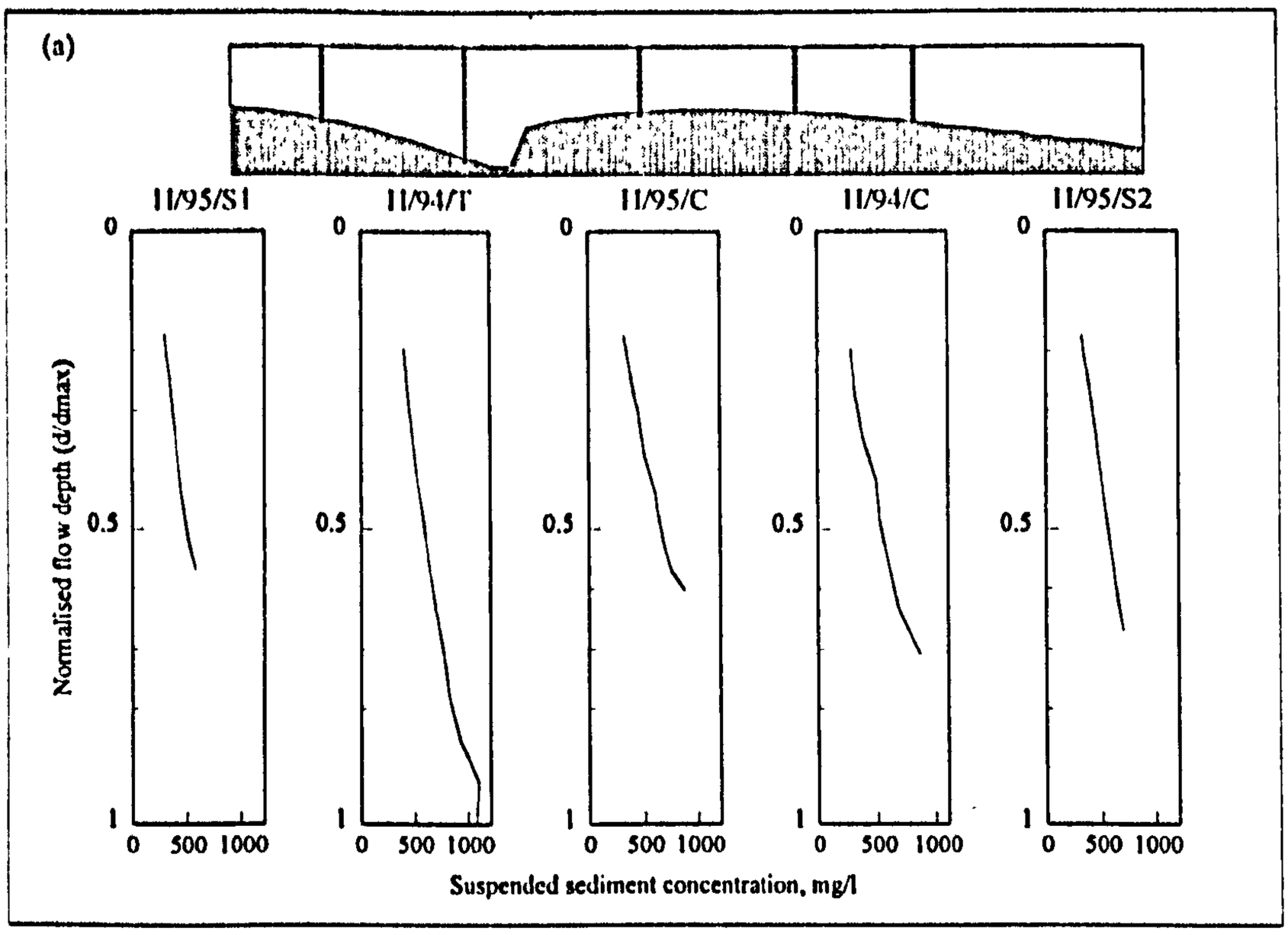

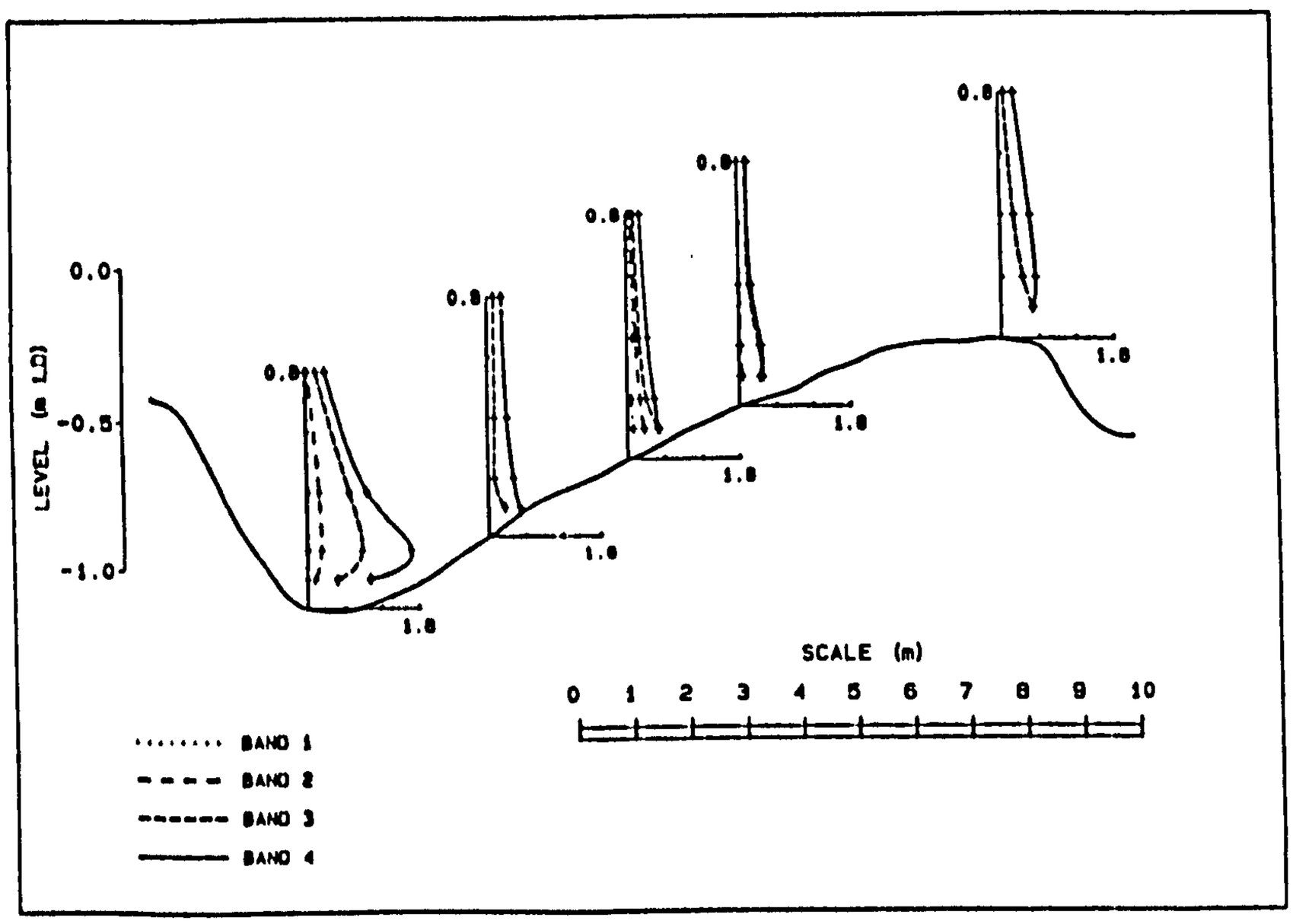

Figure 6.1, Vertical profiles of the mean time averaged at-a-point suspended sediment concentration from (a) the August 1994 and September 1995 surveys conducted at high flow rates and (b) Soulsby *et al.* (1991). Position along the bedform of each profiles is indicated.

The RMS values of suspended sediment concentration over the dune trough (H/94/T, Figure 6.2a) have a maximum value of 113 mgl^{-1} which is located near the bed, maximum RMS values for the crestal profile are also located near the bed and are much smaller (83 mgl^{-1}, Figure 6.2a). The vertical profile of RMS values shows that there is a slight increase in the sediment concentration RMS with depth for the crest profile from 70 to 83 mgl^{-1}, whereas the trough profile RMS values decrease to a depth of 11.7m and then increase down towards the bed (Figure 6.2a). The greater near-bed variation in sediment concentration may partially be a result of variations in downstream and reverse flow transport due to intermittent flow reversals (Section 5.5.5) but will also be affected by occasional flow reattachment at the profiling location due to flapping of the shear layer. The relative magnitude of the suspended sediment concentration fluctuations are larger closer to the bed which implies that the suspension of particles near to the bed may be driven by coherent events with discrete vortices carrying substantially higher particle concentrations than the surrounding fluid upwards away from the boundary. The much smaller crestal profile RMS values may reflect the lower turbulence intensity over the dune crest (Section 5.5.4) which may lead to a decreased variation in sediment concentration variation.

The skewness of the suspended sediment concentration distribution shows a large increase with depth for the trough profile, from values approximating zero for the outer flow region to over one at the bed (Figure 6.2b). If fluctuations in sediment concentration were purely Gaussian then the skewness of the distribution would be zero, hence positive skewness indicates that sediment suspension near the bed is event driven (e.g. Thorne, 1996). Positive skewness values occur from a depth of 11.2 m down towards the bed for profile H/94/T whereas skewness values over the crest (H/94/C) approach zero at all distances from the bed (Figure 6.2b). This may indicate that episodicity in sediment transport is associated with the process of flow separation and subsequent reattachment. Higher in the flow column at heights where the shear layer is more pronounced and velocity gradients are higher (Section 5.5.2), negative skewness in the sediment concentration distribution shows that sediment transport may be related to turbulent ejections of quadrant 2 type eddies away from the shear layer. Previous studies (e.g. Lapointe, 1992, 1993; Nelson *et al.*, 1995) have documented intermittency in both sediment transport and momentum exchange over dunes and have shown that relatively few, but large, suspension events produce a considerable fraction of the total sediment suspension. Intermittency in near-bed sediment transport in the dune trough in this study may be caused by flapping of the shear layer which will lead to intermittent reattachment at the profiling location.

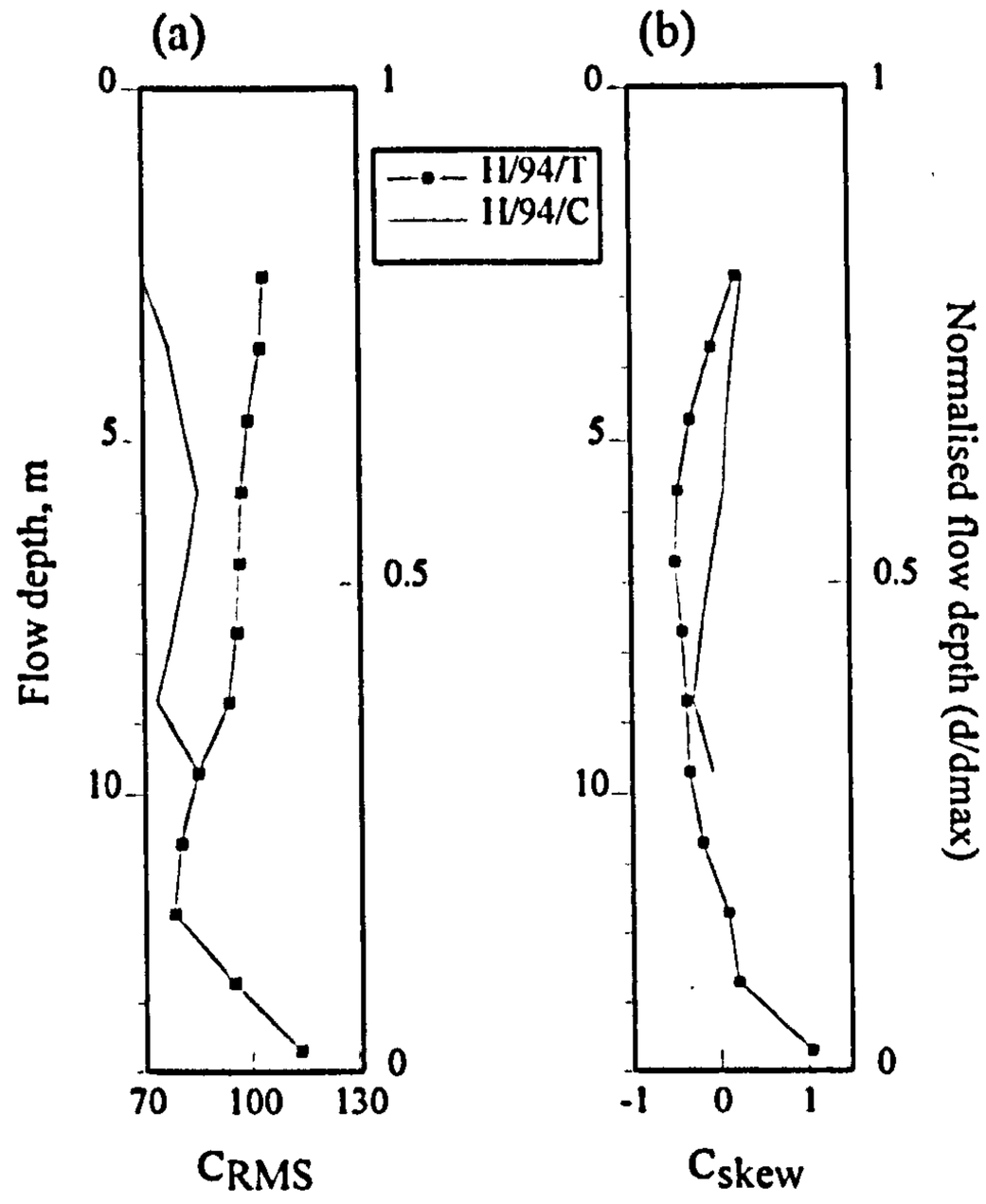

Figure 6.2, Vertical profiles of the at-a-point (a) RMS and (b) skewness of the suspended sediment concentration distributions for the August 1994 high flow survey over the dune trough (H/94/T) and crest (H/94/C).

6.2.2 Mean suspended sediment concentration at low flow stage

Suspended sediment concentrations under low flow condition are, as expected, much smaller than those measured at high flow rates, with maximum mean concentrations of 450 mgl^{-1} at low flow compared to over 1100 mgl^{-1} at high flow (Figure 6.3). The lower population of suspended sediment concentrations measured under low flow conditions are not resolvable due to the calibration between ADCP backscatter intensity and absolute sediment concentration. The lowest backscattered sound intensity resolvable by the ADCP is 70 dB which corresponds to a sediment concentration of 25 mgl^{-1} (see discussion in Chapter 3). However, although the calibration is inaccurate when backscattered sound intensity is below 70 dB, the reflected signal is still useful as it does indicate that total suspended sediment concentration is less than 25 mgl^{-1}. However, as sediment concentrations through the upper flow column for all profiles conducted under low flow conditions are below 25 mgl^{-1}, the low flow profiles may be subject to greater errors due to the poor calibration between backscatter intensity and sediment concentration. This section

will therefore only briefly describe spatial variations in mean sediment transport conditions and will not discuss the distributions of the sediment concentration time series.

Mean suspended sediment concentrations measured over high angle dunes at low flow rates show a rapid increase in concentration at greater depths (Figure 6.3). The maximum time-averaged mean concentration measured of 450 mgl^{-1} is located at the maximum near-bed ADCP measurement depth over the primary dune trough. Results from the high flow survey showed a small but consistent decrease in sediment concentration within the flow reversal zone (Figure 6.1a) but there is no corresponding decrease over the primary or secondary bedform trough during the low flow survey. This may be related to a decrease in shear zone turbulence intensity compared to that measured during the high flow survey, thus causing an associated decrease in sediment suspension. The near-bed increase in sediment concentration over the dune trough may also be related to the factors described and discussed in Section 5.6.2 (Figure 5.31a) which are briefly: the decrease in resolution between high and low flow surveys, the anticipated smaller size of the flow separation zone, the measuring depth of the ADCP (only the upper 93 % of the flow column may be measured) and the relative position of the profiles during the high and low flow surveys, which may all result in the differences of near-bed sediment concentration.

More generally, the downstream variation in sediment concentration over the high angle slip-face bedform compares well with that measured during the high flow survey, as maximum sediment concentrations are located over the trough (L/96/T) with decreasing concentrations occur at greater distances downstream of the flow reattachment zone (L/96/S).

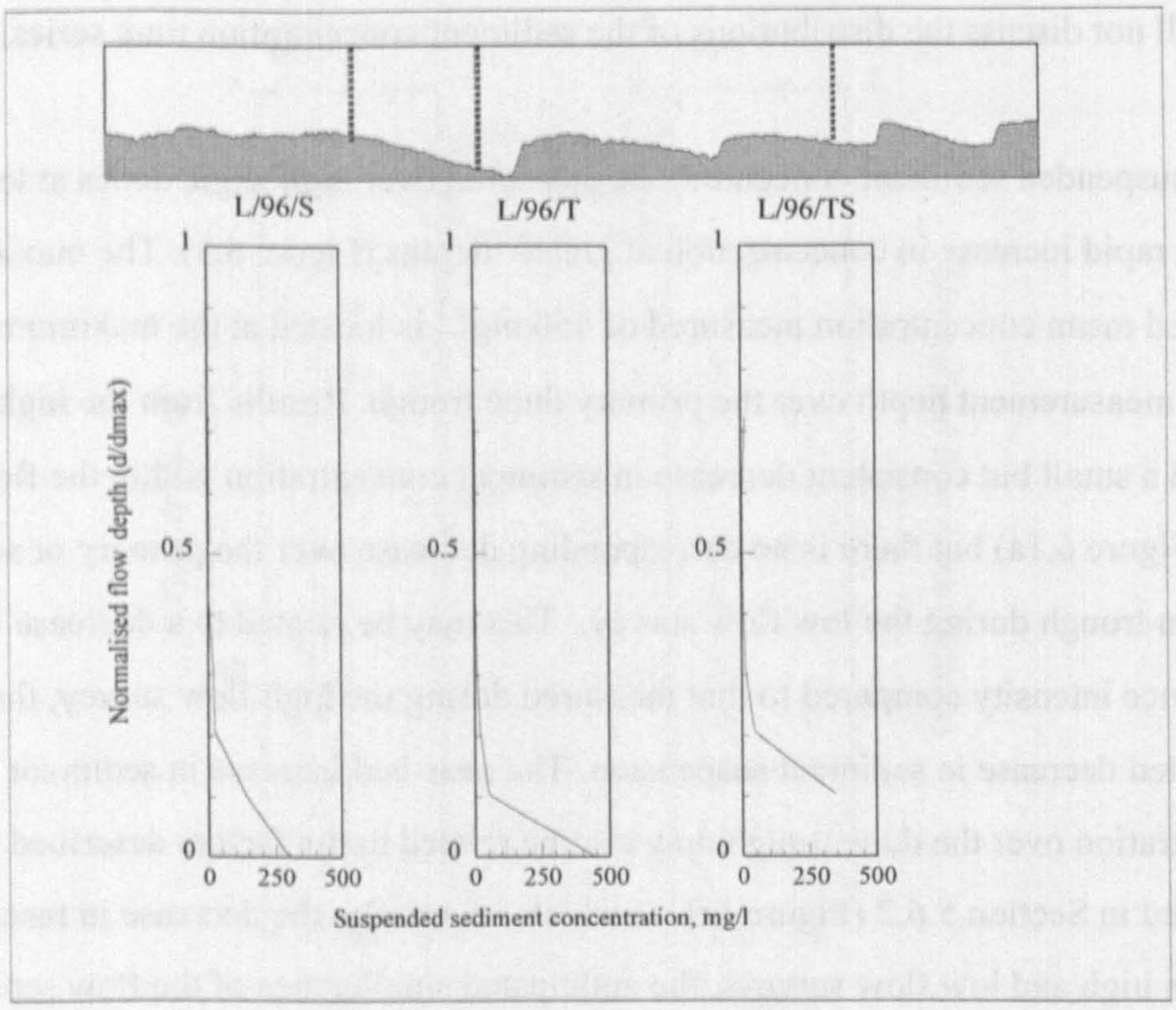

Figure 6.3, Vertical profiles of the mean, time-averaged, at-a-point suspended sediment concentration conducted at low flow over a high angled dune. Position along the bedform for each profile is indicated.

Suspended sediment concentrations measured over the low angled bedform are extremely low with a maximum time-averaged mean value of 35 mgl^{-1} occurring close to the bed (Figure 6.4). These low suspended sediment concentrations confirm the earlier hypothesis (Section 5.6.6) that low angled lee face dunes forming under low flow conditions in the Jamuna may not be related to high suspended sediment concentrations, such as those described by McLean and Smith (1979) and Kostaschuk and Villard (1996).

The mean suspended sediment profiles also indicate that dune related turbulence, produced due to the process of flow separation at the dune brink point and the resultant formation of a free shear layer, may be absent over low angled bedforms. As macroturbulence may be responsible for increased suspension of sediment (e.g. Rood and Hickin, 1989), low angled lee face bedforms forming under low flow conditions may be expected to have correspondingly low suspended sediment concentrations associated with them.

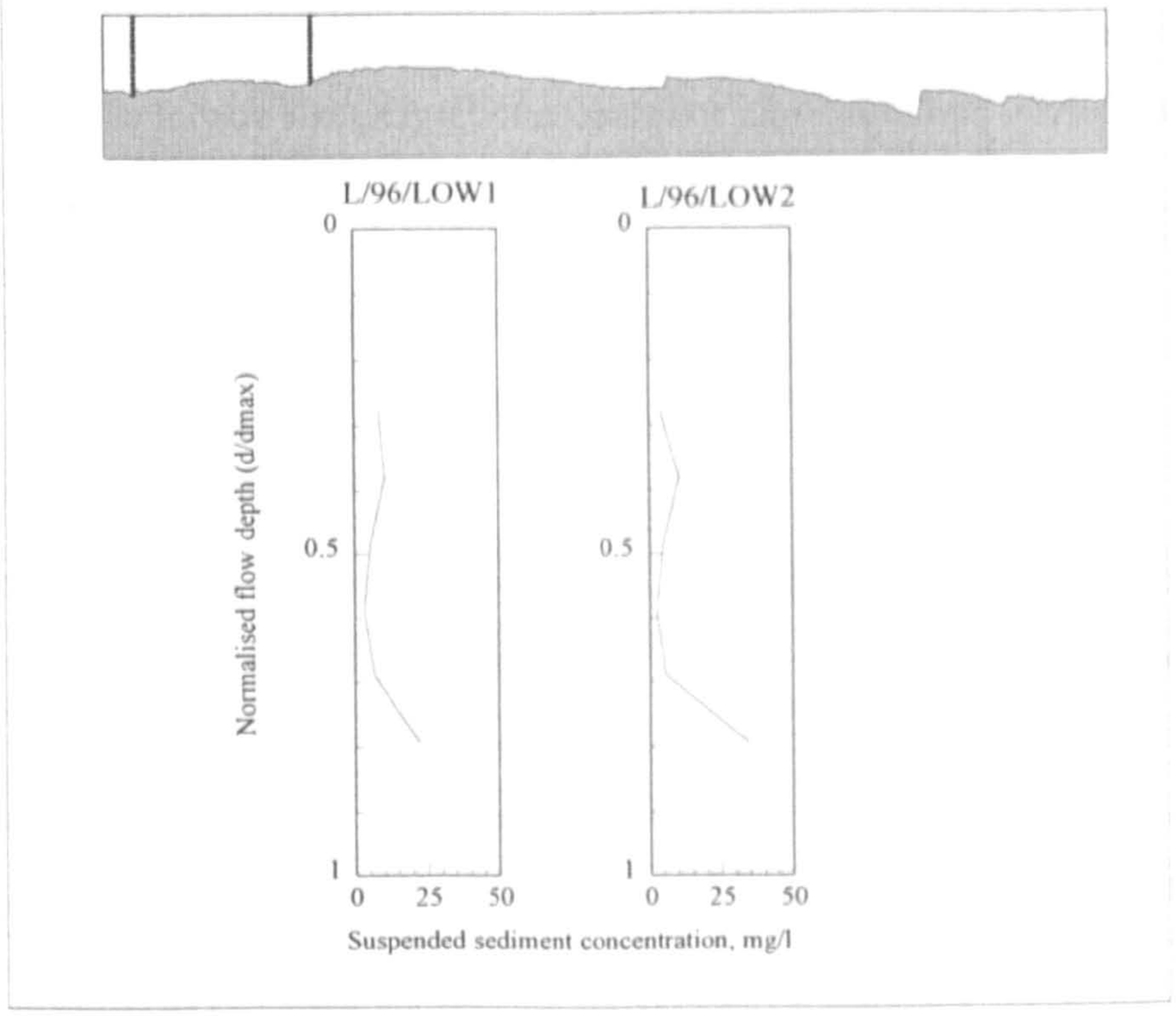

Figure 6.4, Vertical profiles of the mean, time-averaged, at-a-point suspended sediment concentration conducted at low flow over a low lee face angled dune. The position along the bedform of each profile is indicated.

6.2.3 Mean suspended sediment profiles

The profiles from both the high and low flow surveys highlight the fact that mean suspended sediment profiles along a high angled slip face dune bedform are highly spatially variable, and that maximum suspended sediment concentrations are associated with the production of a shear layer downstream of the dune crest. Sediment concentrations are shown to more than double from low to high flow stage, indicating that most sediment transport and therefore channel change will occur under high flow conditions. This increase in sediment transport is partially due to an increase in bed shear stress as flow stage rises but is also a product of increased turbulence production by dunes (see Chapter 5), as indicated by the high skewness of the suspended sediment distribution over the dune trough under high flow conditions (H/94/T, Figure 6.2a). As flow stage rises, dune slip faces have been shown to steepen (see Chapter 4), hence producing an increase in the velocity gradient associated with flow separation. Increasing the velocity gradient will lead to an increase in the shear-zone turbulence intensity and may therefore increase both scour at and around flow reattachment and also sediment suspension related to ejections of turbulent fluid (quadrant 2 events) from the shear layer.

6.3 Downstream Instantaneous Suspended Sediment

A series of profiles were undertaken while the survey vessel was moving downstream during each survey period in order to investigate larger scale spatial changes in suspended sediment concentrations to assess the effect of multiple bedforms on suspended sediment transport. The downstream profiles cover a distance of 1500 m for the August 1994 survey (Figure 6.5a) and 1200 m for the February 1996 survey (Figure 6.5b): maximum suspended sediment concentrations for the surveys are 1050 mgl^{-1} and 178 mgl^{-1} respectively. The lower 'blocky' structure shown in Figure 5 indicates the lowest measurement depth resolvable by the ADCP, with actual bed level being approximately 2-3 m below this and block length being a function of the ADCP ensemble averaging time and therefore vessel velocity (see Chapter 3). Due to the rapid variation in bed level on dune lee faces, and the spatial averaging of the ADCP measurements caused by the motion of the survey vessel, the relative measurement depth of the ADCP is decreased in transect mode compared to at-a-point profiling mode. Visualisation of the flow separation zone is therefore not possible when conducting downstream profiles. This accounts for the lower maximum sediment concentrations measured during the two transect surveys (Figure 6.5) compared to the mean at-a-point vertical profiles (Figures 6.3 and 6.4) as maximum sediment concentration occurs too near to the bed to be measured.

Suspended sediment concentration is contoured for the August 1994 survey period in Figure 6.5a and shows that the greatest suspended sediment concentrations, of up to 1030 mgl^{-1}, are located over the largest and steepest (slip face angles up to 58°) bedforms (A, Figure 5a). Highest instantaneous sediment concentrations are on the lower stoss side of dunes around the flow reattachment location and at depths approximating the estimated height of the free shear layer (A, Figure 5a) which agrees well with the time-averaged mean vertical profiles described above (Figure 6.1a). Increased sediment suspension concentration on the dune stoss side is a result of flow contraction, convergence and acceleration, whereas increased suspension in the flow expansion zone downstream of the dune crest is associated with turbulence production resulting from the flow separation process.

The highest suspended sediment concentration in outer flow regions is also associated with larger steep bedforms, indicating that dune-associated suspension of sediment affects the entire vertical flow column (B, Figure 6.5a). It is also notable that there is a great spatial variation in sediment suspension relating to individual primary and secondary bedforms, especially in the vertical extent of higher sediment concentrations which is again related to

spatial variation in the mean flow and turbulence field over dunes (Itakura and Kishi, 1980) (B, Figure 5a).

During the February 1996 low flow survey (Figure 6.5b) there is also an increase in sediment suspension concentration (up to 162 mgl^{-1}) over the dune field in areas where dunes are larger and steeper (C, Figure 6.5b), whereas suspended sediment concentration is much lower (up to 52 mgl^{-1}) above the flatter, smaller at-a-point profiling dunes (D, Figure 6.5b). This variation in instantaneous suspended sediment concentration with differing dune morphology is important as it reiterates that low slip-faced angled dunes in the Jamuna river at low flow periods do not form as a consequence of increasing suspended sediment concentration as has previously been demonstrated by Smith and McLean (1977) and Kostaschuk and Villard (1996) under high flow conditions. Maximum sediment concentrations during the low flow period are generally less than 25 % of those occurring during the high flow surveys, which again agrees well with results of the time-averaged values described above (Sections 6.2.1 and 6.2.2). Increased sediment concentrations during the low flow survey are again located on dune stoss sides and downstream of crests and are therefore associated with flow convergence (see Section 5.6.2) and flow separation (See Section 5.6.4) respectively. However, there are several examples of high suspended sediment concentrations in the upper part of the flow column in Figure 5b (E). These distinct increases in suspended sediment concentration occur downstream of steeply-dipping (up to 42°) lee faced dunes. The individual packages have suspended sediment concentrations of up to 170 mgl^{-1} and may well be the acoustic manifestations of rotational vortices shed off an upstream free shear layer which have been advected upwards in the flow column and may therefore be analogous to the high suspended sediment structures visualised by Kostaschuk and Church (1993). Such vortex structures or boils, with visibly higher suspended sediment concentrations than the ambient flow, were intermittently present at the water surface during the survey period.

The downstream surveys (Figure 6.5) show that dune related turbulence may be responsible for increasing suspended sediment transport in sand bed rivers, that the effect of turbulence extends through the entire flow depth and that sediment suspension varies spatially over dunes.

Figure 6.5, (right) Contour maps of downstream variation in suspended sediment concentration at (a) high flow, August 1994 and (b) low flow, February 1996. Flow is from right to left and a colour scale bar is given for each map. The labels indicate: (A) the highest suspended sediment concentrations are associated with larger, steeper dunes; (B) the highest suspended sediment concentrations in the outer flow column are located near larger, steeper dunes and the effect of individual bedforms on the spatial variation in sediment concentration is visible; (C) increased suspended sediment concentration usually occurs over larger and/or steeper dunes; (D) lower suspended sediment concentrations are associated with smaller, less steep dunes; (E) occasional individual packages of high suspended sediment fluid occur in the upper flow column.

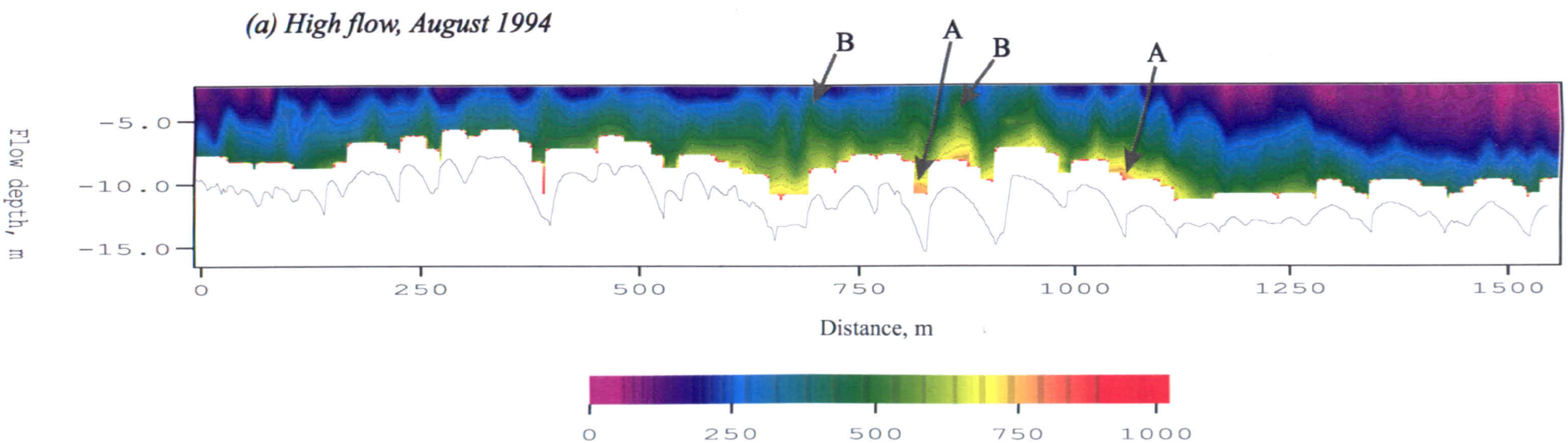
(a) High flow, August 1994
B
A
B
A
-5.0
-10.0
-15.0
0
250
500
750
1000
1250
1500
Flow depth, m
Distance, m
0
250
500
750
1000
Suspended sediment concentration, mg/l
(b) Low flow, February 1996
D
C
C
E
C
-5.0
-10.0
0
250
500
750
1000
Flow depth, m
Distance, m
0
50
100
150
Suspended sediment concentration, mg/l

6.4 Turbulence-Associated Sediment Suspension

6.4.1 Temporal variations in sediment concentration

Comparison of variations in the at-a-point suspended sediment concentrations with the mean flow and turbulence processes described in the previous chapter may be very useful as many studies have shown that suspended sediment concentrations in boils are higher than the background value. Many studies (e.g. Heathershaw, 1974; Lapointe, 1992; Thorne *et al.*, 1996) have noted that high magnitude turbulent events often have a short duration but are responsible for a large proportion of the Reynolds shear stress production. Observation of the surface activity of boils with high suspended sediment concentrations have been noted to exhibit intermittency in occurrence (Jackson, 1976; Kostaschuk and Church, 1993). Turbulent boils may therefore play a dominant role in transporting sand-sized sediment (Rood and Hickin, 1989) but little work has been carried out to explicitly link turbulence and sediment transport or to quantify the role of turbulence in entraining and transporting sediment. The previous chapter postulated that eddy shedding is controlled by the velocity gradient across the shear layer and it may therefore follow that an increase in sediment flux will occur with an increasing velocity differential across the shear layer.

The following section will firstly qualitatively relate the deviation in sediment flux to the turbulence structure by comparing temporal variations in sediment flux with the temporal variations in velocity gradients that were described in the previous chapter. Sediment flux in this thesis is defined as the concentration of suspended sediment passing a point in a given time ($u_i * c_i$), negative fluxes therefore depict upstream sediment transport. The use of images of suspended sediment fluxes to illustrate the dynamic nature of suspension processes will aid insight into links between the two and begin to quantify sediment concentrations in boils compared to the 'background' ambient value. Secondly, this section will investigate whether variations in sediment concentration are linked with the turbulent quadrant events described in the previous chapter. This may permit identification of the complex mechanisms of the processes of sand suspension and transport which have been shown to vary over periods of seconds (Thorne *et al.*, 1996).

6.4.1.1 Temporal variation in sediment flux over a dune trough

The at-a-point downstream sediment flux over the dune trough (profile H/94/T) is shown as a colour contour map in Figure 6.6b, (page 259) for reference the corresponding velocity gradient measurements are shown in Figure 6.6c. The most striking feature of Figure 6.6b is that the variation in sediment flux is larger closer to the bed with maximum upstream sediment flux transport rates at a depth of 13.7 m reaching -1500 mg $ml^{-1}s^{-1}$ (A, Figure 6.6b) and downstream transport rates of over 1000 mg $ml^{-1}s^{-1}$ (C, Figure 6.6b). An increase in instantaneous maximum sediment flux is expected near the bed for this profile conducted over the dune trough, as intermittent high-intensity turbulence production has been shown by many authors to be greatest at and around flow reattachment locations (e.g. Nelson *et al.*, 1993; Bennett and Best, 1995). There are sporadic, very high downstream sediment transport fluxes near the bed of up to 1280 mg $ml^{-1}s^{-1}$ which may be associated with temporary reattachment of the shear layer at the profiling location, and therefore high near-bed instantaneous velocity gradients (Figure C, 6.6b and H, 6.6c). The very high near-bed sediment flux packages often occur after a period of intense reverse flow sediment transport (Section 5.5.5) and may be linked to shear layer flapping which may be associated with changes in velocity gradient (H, Figure 6c) and the ejection of high suspended sediment turbulent eddies away from the shear layer upon reattachment (see Section 5.5.7). High near-bed sediment flux values may therefore be indicative of macroturbulent bursting which is also evident at the water surface. These results show that although the mean near-bed velocity is very low (below the critical velocity for incipient motion) at and around the location of profile H/94/T (Section 5.5.2), there are intermittent events which are capable of entraining and suspending sediment, a phenomenon also described by McLean *et al.* (1996).

Intermittent coherent events are apparent which carry clouds with substantially higher (up to 1400 mg $ml^{-1}s^{-1}$) suspended sediment concentrations upwards away from the boundary (D, Figure 6.6b). The individual packages of high suspended sediment concentration fluid are sometimes seen to coalesce, the linking of multiple packages may occasionally result in movement of larger packages upwards in the flow column. These packages are associated with periods of high velocity gradient through the separation zone shear layer (G, Figure 6c). The distinct zones of high velocity gradient fluid were shown to occasionally move upwards in the flow column and have been interpreted as ejections of turbulent vortices away from the shear layer (see Section 5.5.6). The packages of high sediment flux may therefore be associated with high velocity gradients, shear layer flapping and eddy shedding

away from the shear layer; a link may therefore be postulated between high suspended sediment concentrations and vortex shedding.

Flow reversals and upstream sediment transport occur at depths greater than 10.7 m (A, Figure 6b) which may result in deposition from ripples climbing up the lee face of the bedform. Such reverse flow transport and deposition sediment on the lee face may cause steepening of the dune slip face to slopes greater than the static angle of repose (Müller and Gyr, 1982). At the maximum ADCP near-bed measurement point, 46 % of sediment transport is in a reverse flow direction (Figure 6.7), indicating the significance of upstream sediment transport in the dune trough and lee side. Although high upstream transport rates give credence to the extremely high slip face angles measured, the upstream flux may be too great to be accounted for purely by incorporation with the dune face. A mechanism may therefore exist for re-incorporation of proportion of the high upstream sediment flux into the main flow.

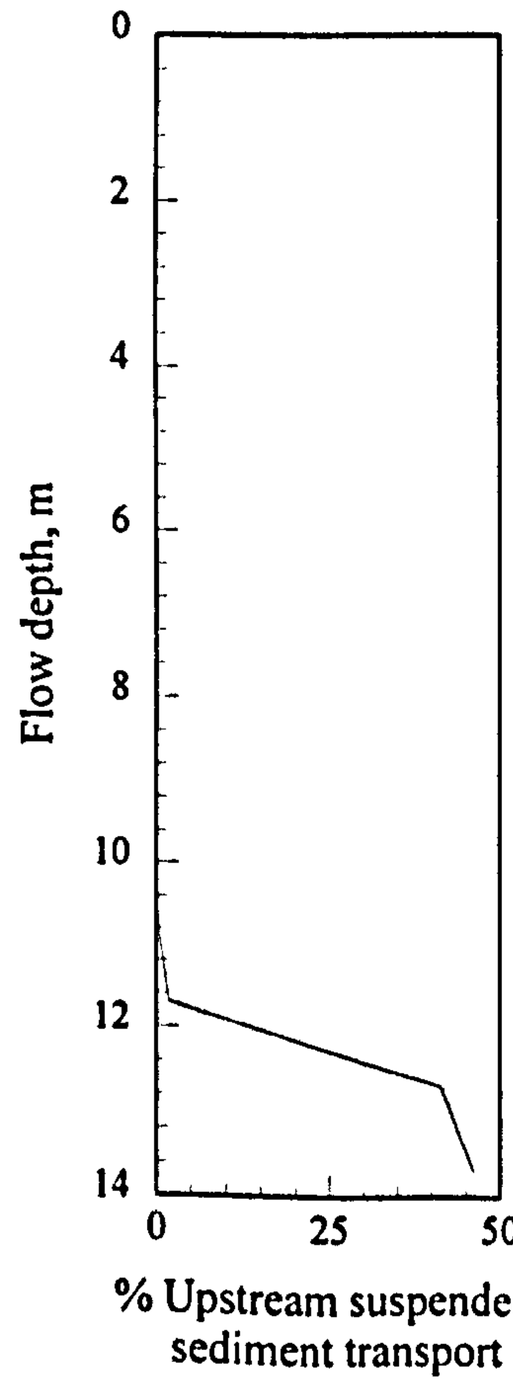

Figure 6.7, Variation in the percentage of total reverse flow (upstream) suspended sediment transport with depth for profile H/94/T.

6.4.1.2 Temporal variation in sediment flux over a dune crest

The at-a-point downstream sediment flux over the dune crest (profile H/94/C) is shown as a colour contour map in Figure 6.6a. It is noticeable that the sediment flux profiles from the trough and crest are very different: as expected, there is no reverse flow transport over the dune crest and the large at-a-depth temporal variation in sediment concentration in the outer flow column, which is linked to intermittent ejections away from the shear layer, is not present. Variation in high values of the sediment flux (above 1000 mg $ml^{-1}s^{-1}$) in the upper flow column above the crest is on a much shorter time period than for similar high flux rates above the trough. On average, downstream sediment flux is greater above the crest than above the trough with fluxes of over 1500 mg $ml^{-1}s^{-1}$ (E, Figure 6.6a) commonly occurring at depths up to 6 m. This increase in sediment flux above the crest is most likely due to flow convergence and acceleration (Section 5.5.2).

The greatest sediment fluxes are located above the bed and the maximum fluxes occur at a depth of 9.2 m (F, Figure 6a; there is a decrease in sediment flux at a depth of 9.7 m. Although the time-averaged mean vertical profiles of sediment concentration show an increase down to the bed level, flow constriction and bed friction at the crest are high due to flow convergences caused by the change in topography. Hence the mean near bed downstream velocity shows a rapid decrease and the sediment flux decreases close to the bed.

Figure 6.6, (right) Contour map of the temporal variation in downstream sediment flux over the dune (a) crest, H/94/C and (b) trough, H/94/T and (c) the velocity gradient over the dune trough. Flow is from top to bottom and a colour scale bar is given for each map. Flow depth bin sizes are 0.5 m. (A) intermittent periods of reverse (negative) sediment flux transport; (B) intermittent downstream (positive sediment flux in the outer flow column; (C) occasional high downstream flux close to the bed; (D) clouds of high sediment flux above and within the shear layer; (E) maximum fluxes are located above the bed over the dune crest (F) near-bed decrease in sediment flux and (G) high velocity gradient packages.

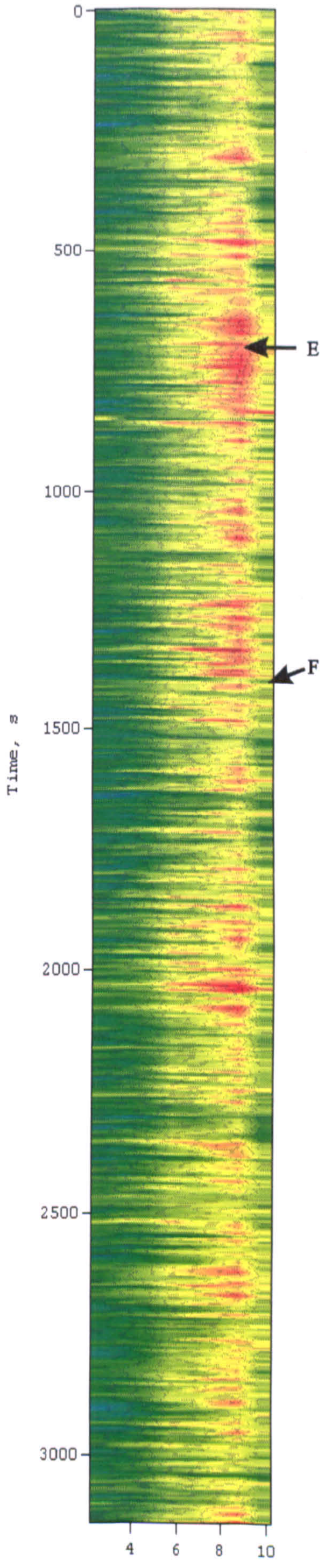
0
500
1000
1500
2000
2500
3000
Time, s
E
F
4
6
8
10
Depth, m
-1500
-500
500
1500
Downstream sediment flux, mg m/l/s

(a)

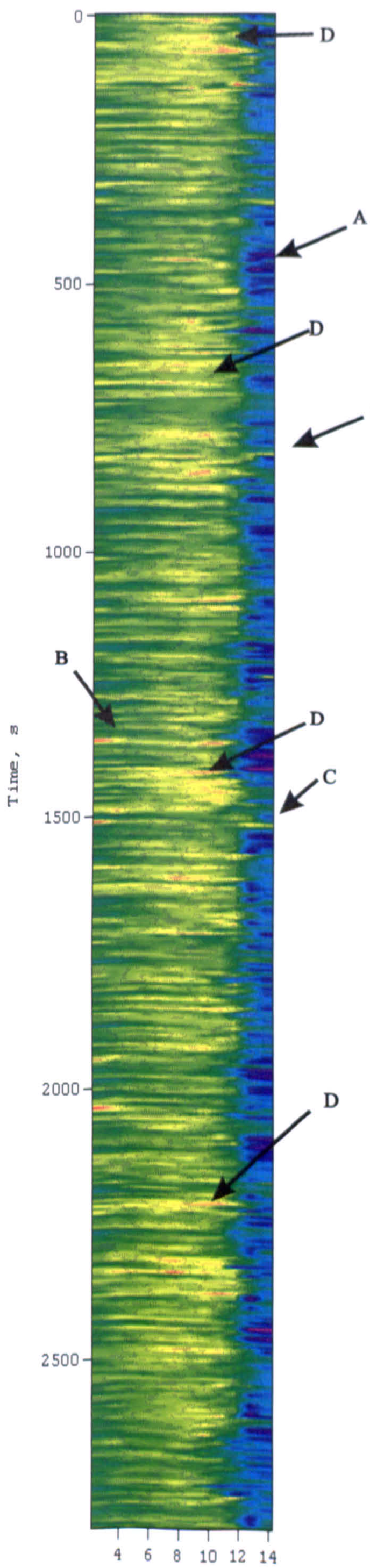
0
500
1000
1500
2000
2500
Time, s
D
A
D
C
B
D
C
D
4
6
8
10
12
14
Depth, m
-1500
-500
500
1500
Downstream sediment flux, mg m/l/s

(b)

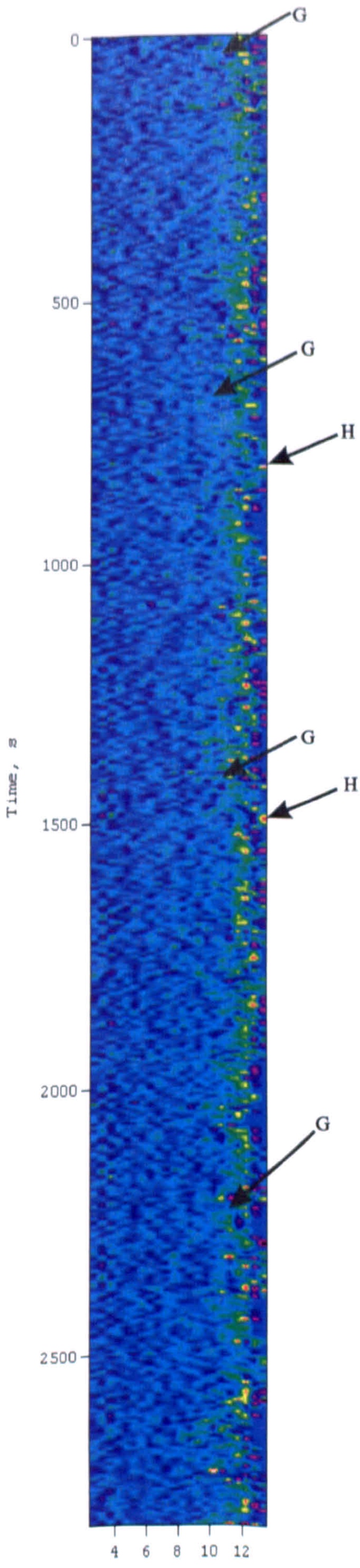
0
500
1000
1500
2000
2500
Time, s
G
H
G
H
G
4
6
8
10
12
Depth, m
-2
-1
0
1
2
3
Velocity gradient, /s

(c)

6.4.2 The relationship between suspended sediment concentration and turbulence.

Many studies have detailed that there are significant changes in the instantaneous fluctuations in downstream and vertical velocity and sediment concentration at different distances from a dune crest or negative step in terms of turbulence structure and mode of sediment transport (e.g. Soulsby *et al.*, 1991; Nelson *et al.*, 1995; McLean *et al.*, 1996). Both turbulence intensity and mean sediment transport rate are much greater downstream of a negative step near the flow reattachment zone and the associated instantaneous sediment transport rate shows greater variation. Nelson *et al.* (1995) investigated sediment transport in relation to turbulence structure at increasing distances from the reattachment point downstream of a negative step and illustrated that quadrant 4 events (sweeps) and quadrant 1 events (outward interactions) are responsible for the majority of near-bed sediment transport. Comparison of experiments conducted with and without the presence of a negative step showed significant differences in both turbulence structure and sediment transport (Nelson *et al.*, 1995). Sediment transport downstream (at a distance of 10 step heights) of flow reattachment is strongly episodic with short periods of transport interspersed with long periods of low or zero transport (Nelson *et al.*, 1995). This variability in transport rate downstream of a negative step can partly be attributed to low excess shear stress but must largely be driven by differences in the turbulence structure of the flow which are produced by flow separation. However, Nelson *et al.* (1995) did not investigate variations in sediment transport through the free shear layer even though turbulence generation on the lee-side of dunes has frequently been shown to be associated with eddy shedding from the shear layer (e.g. Bennett and Best, 1995). As suspended sediment concentration is highest within the shear layer (Soulsby *et al.*, 1991; Zyserman and Fredsoe, 1994; Figure 6.1), it may be important to examine turbulence-related sediment suspension at greater distances from the bed.

Although the investigation of different turbulent events by quadrant analysis provides a useful way of quantifying the nature of turbulence structure over dunes (see Chapter 5), it does not improve our knowledge of the coupling between turbulent events and sediment transport. To accomplish a better understanding of the links between sediment transport and turbulence, the variations in sediment concentration associated with turbulence must be investigated. Instantaneous suspended sediment concentration variation from the time-averaged mean value at-a-point have therefore been plotted in relation to quadrant event in Figures 6.8 and 6.10 for profiles H/94/T and H/94/C respectively at 2 m depth intervals

through the flow column. The positions of depth intervals from Figures 6.8 and 6.10 are shown in Figure 6.9 to locate them within the flow column with respect to dune morphology. These diagrams (Figures 6.8 and 6.10) are constructed by plotting each individual u' and v' pair for the at-a-point profile depth for the entire time series (see Table 5.1 for profiling duration) and contouring the associated suspended sediment concentration. The objective of the following section is therefore to try to explicitly link the variations in suspended sediment concentration to the turbulence structure that has already been defined. Specifically, this section will attempt to relate sediment concentration fluctuations to individual turbulent events and therefore will describe the spatial changes in sediment transport processes in relation to changes in turbulence production along a bedform.

6.4.2.1 Turbulence-related sediment transport over a dune trough

The greatest positive sediment fluctuations at depths associated with the shear layer (section 5.5.2), of over 250 mgl^{-1}, are associated with quadrant 2 type ejection events at values of u' greater than 1 ms^{-1} (Figure 6.8b). This is an extremely important finding at it confirms the earlier hypotheses that quadrant 2 events, which arise due to eddy shedding from the shear layer and at flow reattachment (Rood and Hickin, 1989; Kostaschuk and Church, 1993; Bennett and Best, 1995), are responsible for transporting and suspending sediment. Previously, the observation of high suspended sediment concentrations associated with boils (Coleman, 1969; Jackson, 1976; Rood and Hickin, 1989; Kostaschuk and Church, 1993) has not been categorically linked with sub-surface turbulence structure. These data shown here demonstrate a direct physical relationship between discrete quadrant 2 type ejections moving upwards away from the shear layer and distinct packages conveying substantially higher sediment concentrations than the surrounding fluid. The affect of these high suspended sediment bearing vortices will be to increase sediment suspension over the lee and lower stoss side of dunes. Hence, the increase in suspended sediment concentration over entire dune fields (Figure 6.5) and also larger channel scale features such as bars which commonly have dunes superimposed on them (Ashworth *et al.*, in review) may be partially a result of such quadrant 2 type ejections from the separation zone shear layer.

As implied by descriptions of the turbulence field (Sections 5.5.5, 5.5.6, 5.5.7), quadrant 2 events are intermittent with generally larger sediment suspension occurring at larger u' values (Figure 6.8b). It is apparent that relatively rare, high magnitude ejection events are

influential in Reynolds stress production and also in the suspension of sediment (Grass, 1974; Sumer and Oguz, 1978; Bennett and Best, 1995).

The role of quadrant 3 events ('inward interactions') within the shear layer however has not previously been thought to be important for sediment transport (e.g. Bennett and Best, 1995; Nelson *et al.*, 1995). Quadrant 3 event occurrence is extremely frequent in the shear layer (Section 5.5.7), but the magnitude of these events is small, with only small contributions to u'v' over a threshold level of 1 standard deviation. Figure 6.8b shows that quadrant 3 events are indeed associated with variations in sediment transport within the shear layer, with maximum sediment variation attributed to quadrant 3 events being between 100 and 150 mgl^{-1} over a threshold of u' less than -1 ms^{-1}. Quadrant 3 events occurring in the shear layer and at reattachment have been previously described as reflecting movement towards the bed of entrained low-velocity fluid from the separation zone (Bennett and Best, 1995). The mean suspended sediment concentration within a separation zone has been shown to be higher (over 1000 mgl^{-1} compared to 800 mgl^{-1}) than at the crest both in this study and in previous studies (e.g. Soulsby, 1991), so entrainment of fluid from the separation zone into the shear layer may be a mechanism for transporting sediment into the shear layer from below. The possible movement of sediment-laden fluid from the flow reversal zone into the shear layer is extremely important in lieu of the findings on reverse flow sediment transport near the bed. As up to 46 % of near-bed transport at the at-a-point profiling location is being transported in an upstream direction, it is apparent that a large percentage of sediment must be re-introduced into the shear layer closer to the dune slip face. This re-introduction of suspended sediment into the shear layer is highlighted by the quadrant 3 type events bearing high suspended sediment concentrations reflecting re-entrainment of low velocity fluid and sediment from the flow separation zone in to the shear layer.

This re-entrainment of sediment into the shear layer from the low flow zone has important consequences for the ejection of turbulent eddies (quadrant 2 events) away from the separation zone as described in Chapter 5, as sediment entrainment into the shear layer from the separation zone will result in higher sediment concentrations in ejected vortices. The high sediment flux levels attributed to quadrant 2 events from the shear layer will intermittently increase sediment suspension in the wake zone and in the outer flow. Quadrant 3 events are therefore extremely important for sediment suspension processes, and this highlights the requirement that turbulent events must be examined in terms of both their

magnitude and frequency distribution and also that turbulent events, as defined by quadrant analysis should not be examined independently.

The high positive sediment fluctuations of up to 180 mgl^{-1} occur in the upper section of the shear layer at 9.7 m (Section 5.5.2) and are again associated with quadrant 2 events (Figure 6.8c). The dominance of quadrant 2 events at this flow depth is related to eddy shedding from the shear layer which has previously been documented by Bennett and Best (1995). Mean velocity gradients (Section 5.5.2, Figure 5.9), and therefore eddy shedding frequencies (Section 5.5.7), are relatively lower at this depth (9.7 m) than closer to the bed, hence the high suspended sediment concentrations related to quadrant 2 events may also reflect advected eddies shed from upstream parts of the shear layer closer to the dune crest and flow separation point. There is no occurrence of high suspended sediment concentrations associated with quadrant 3 events which was shown in the 11.7 m depth cell (Figure 6.8b) which indicates that entrainment of low velocity fluid and sediment from the low flow zone into the shear layer is much less prevalent in the upper part of the shear zone.

The near-bed relationship between quadrant event and sediment fluctuation (Figure 6.8a) indicates that different turbulent processes are acting at this location compared to higher in the flow. Positive contributions to the sediment fluctuation of up to 300 mgl^{-1} are mainly related to quadrant 4 (sweep) events, with smaller additions associated with occasional quadrant 1 events. It should be noted that high positive fluctuations in sediment concentration at this depth are episodic, and this may be related to the pre-identified flapping of the shear layer which will lead to intermittent flow reattachment at the profiling location. Hence quadrant 4 events, and to some extent quadrant 1 events, at the reattachment location are extremely important in the process of sediment suspension from the bed. A previous study by Nelson *et al.* (1995) also illustrated that quadrant 4 and quadrant 1 events are responsible for the majority of near-bed sediment transport and established that quadrant 1 events (outward interactions) were increasingly important in the process of sediment transport at decreasing distances downstream of the flow reattachment point. Both quadrant 1 and quadrant 4 events represent positive streamwise velocity fluctuations and therefore conditions that are conducive to sediment suspension from the bed (McLean *et al.*, 1994). Quadrant 1 events have also been suggested to be important for sediment entrainment in the reattachment region and add to the downstream sediment flux (Bennett and Best (1995)).

Sediment variation in the outer flow area above the dune trough (up to 160 mgl^{-1}) is much smaller than near the bed (Figure 6.8 d,e,f). Generally, a positive contribution to the sediment fluctuation is supplied by quadrant 2 and 3, events whereas a negative contribution is afforded by quadrants 1 and 4. This spatial pattern of turbulence-related sediment transport agrees well with the flume study of Bennett and Best (1995) where the most widespread turbulent occurrences in the flow field in the outer flow zone above a dune trough are lower magnitude quadrant 2 and quadrant 3 events.

Figure 6.8, (right and overleaf), Fluctuations in suspended sediment concentration in relation to turbulent fluctuations in the instantaneous deviations from the downstream and vertical velocity above a dune trough, at a depth of (a) 13.7 m, (b) 11.7 m, (c) 9.7 m, (d) 7.7 m, (e) 5.7 m and (f) 3.7 m.

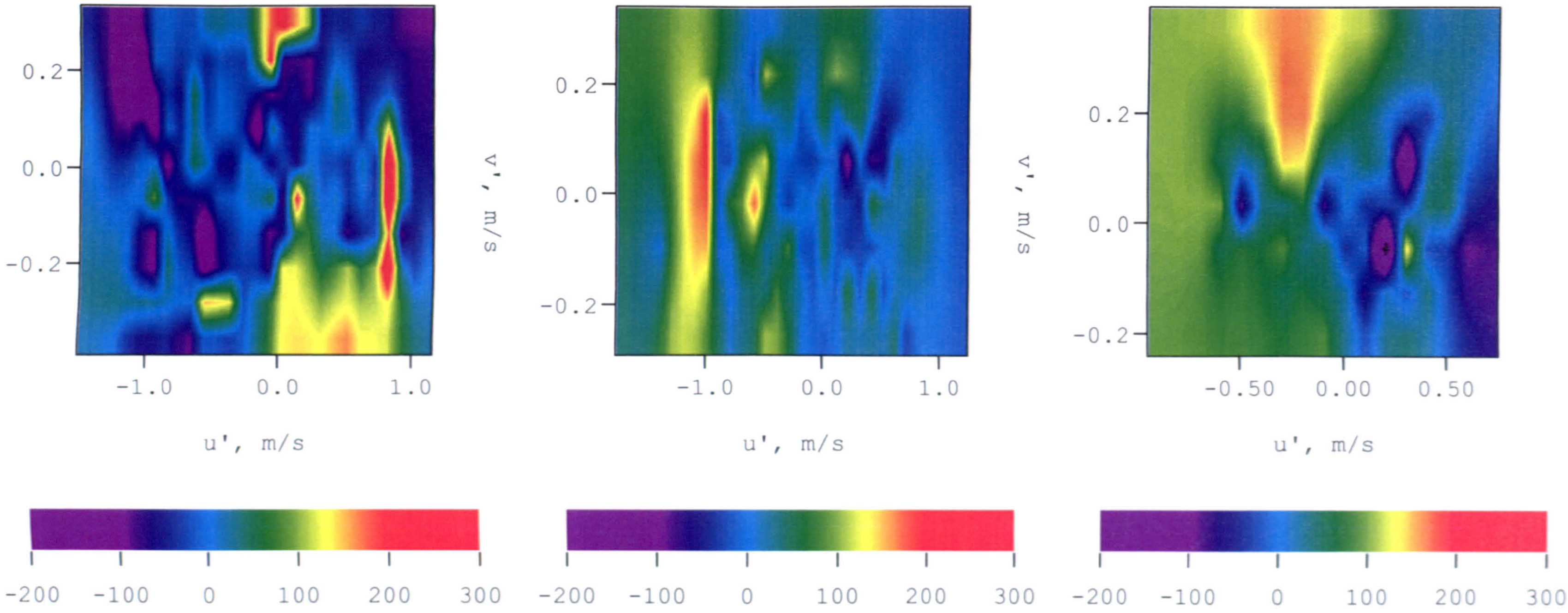

Figure 6.8, for caption see over

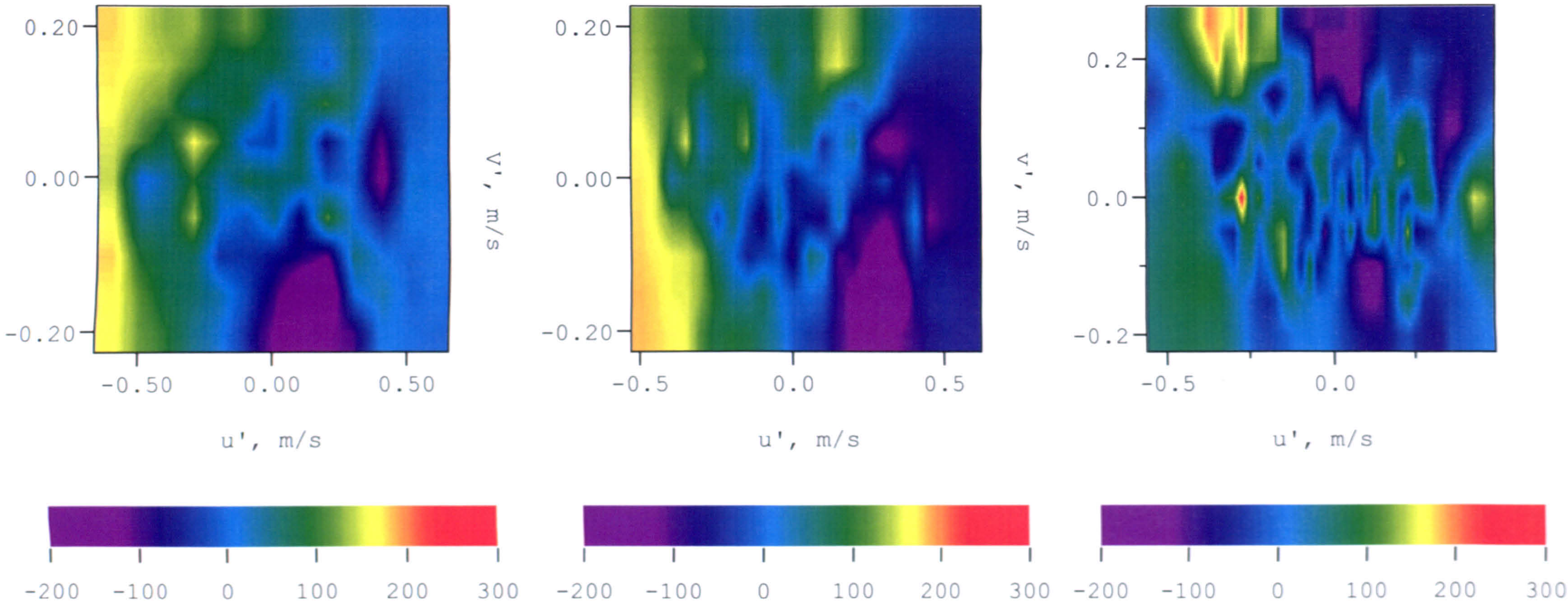

Suspended sediment fluctuation, mg/l

(d) depth = 7.7 m

(e) depth = 5.7 m

(f) depth = 3.7 m

Figure 6.8, for caption see over

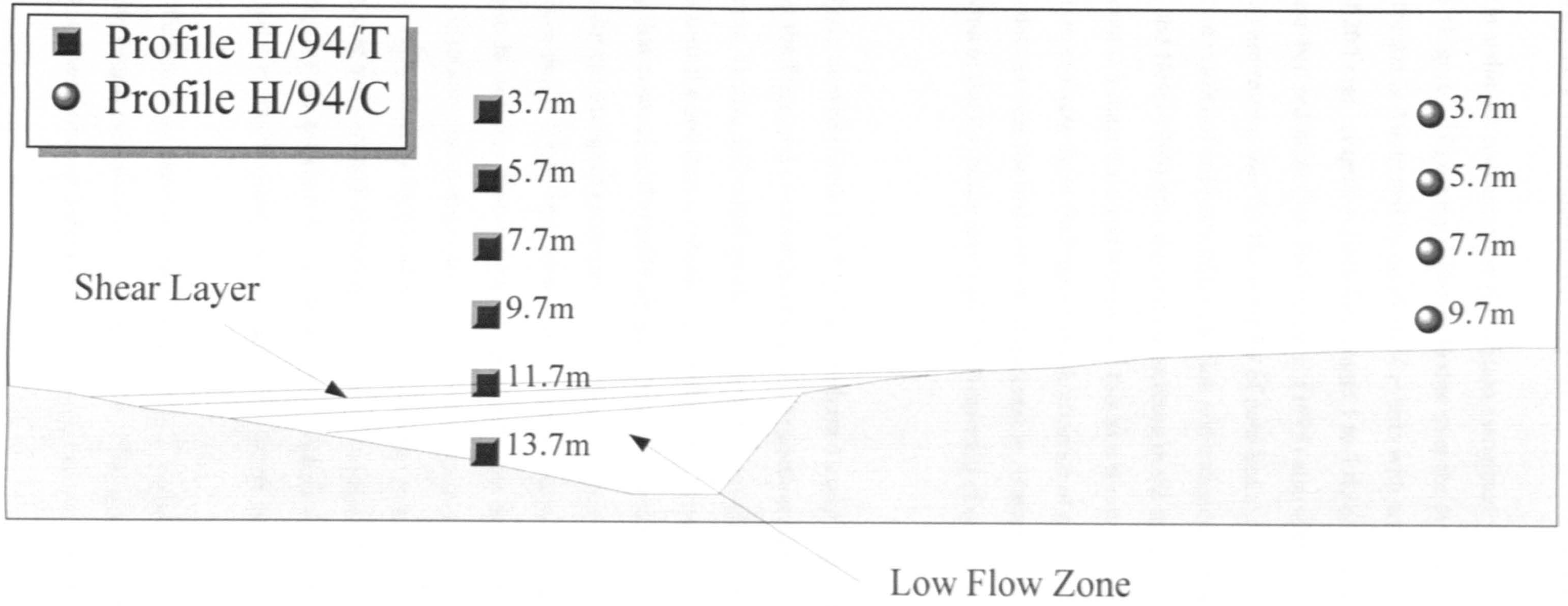

Figure 6.9, vertically exaggerated dune profile showing location of profiles used in Figures 6.8 (H/94/T)and 6.9 (H/94/C).

6.4.2.2 Turbulence-related sediment transport over a dune crest

The variation in sediment concentration fluctuation associated with turbulent events over the dune crest (Figure 6.10) is very different to that over the dune trough. Near-bed sediment fluctuation is dominated by quadrant 4 events with maximum concentration fluctuations of 200 mgl^{-1} (Figure 6.10d). Quadrants 1 to 3 do not contribute significantly to the positive near-bed sediment flux. Nelson *et al.* (1995) also illustrated that quadrant 4 events (sweeps) are responsible for the majority of near-bed sediment transport, so giving credence to these results of sediment concentration and turbulence structure at the dune crest. Bennett and Best (1995) also showed an increase in the relative importance of quadrant 4 events at a dune crest and interpreted this as a result of flow convergence. It is also important to evaluate these findings of the dominance of quadrant 4 events in transporting sediment near the bed over the dune crest in relation to the contribution of quadrant 4 events to the Reynolds stress and the frequency of quadrant 4 events occurrence (Section 5.5.7).

Quadrant analysis showed (Section 5.5.7) that quadrant 4 event occurrence increases near the bed but that the fractional contribution to -u'v' of quadrant 4 events is less than for quadrant 2 events. Hence, individual quadrant 4 or sweep events transport higher sediment concentrations near the bed than quadrant 2 ejections even though they contribute less to -u'v', showing that examining Reynolds stress or momentum fluxes is an inaccurate method of analysing sediment transport processes over dunes (Nelson *et al.*, 1995). Consequently, these results show that it is very important not to examine turbulence structure using quadrant analysis in isolation from the processes of sediment transport, since the at-a-point contribution of ejections and sweeps may not give an accurate assessment of the amount of sediment being transported by individual events. This may be a consequence of the frequency structure and duration of events as it has been suggested by Nelson *et al.* (1995) that a single long lasting quadrant 4 event will move much more sediment than several separate quadrant 4 events of equal intensity but with shorter durations.

In the outer flow column the dominance of quadrant 4 events on high positive sediment fluctuation is no longer evident (Figure 6.10a). Most of the sediment fluctuations are small, with only localised points of sediment fluctuation greater than 150 mgl^{-1} (Figure 6.10 (a,b,c)).

Figure 6.10, (right), Fluctuations in suspended sediment concentration in relation to turbulent fluctuations in the instantaneous deviations from the downstream and vertical velocity above a dune crest , at a depth of (a) 3.7 m, (b) 5.7 m, (c) 7.7 m, and (d) 9.7 m.

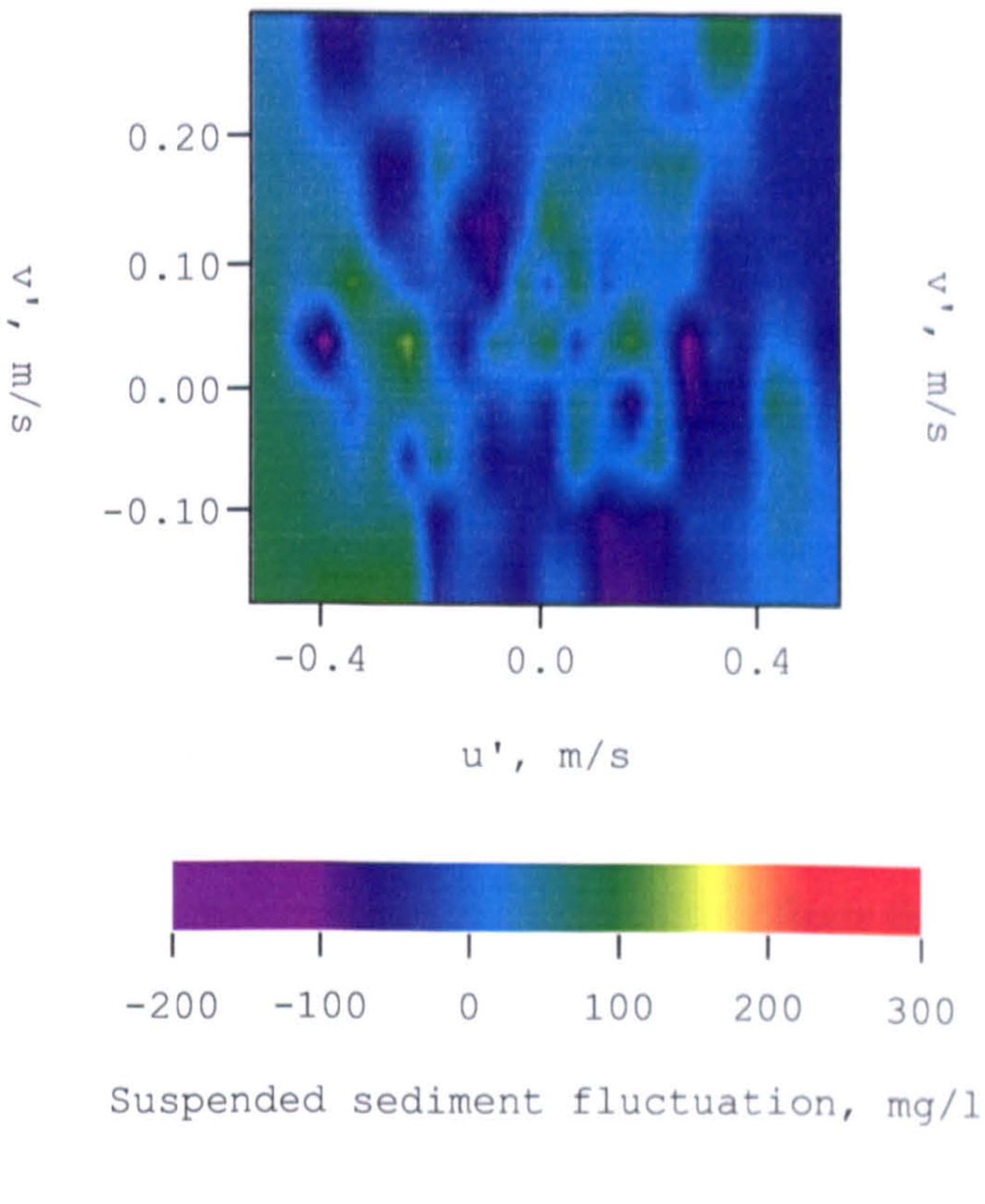

(a) depth = 3.7 m

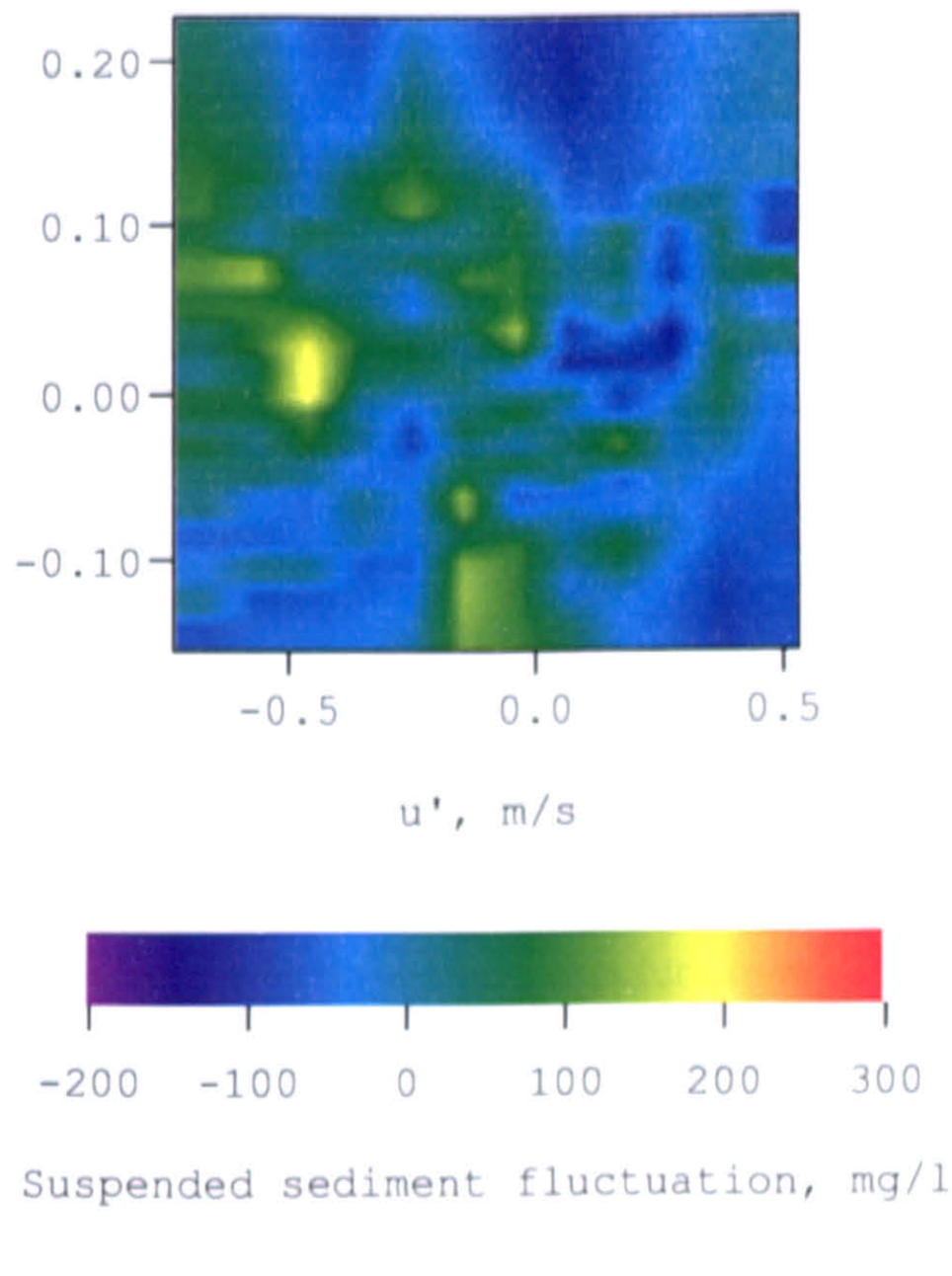

(b) depth = 5.7 m

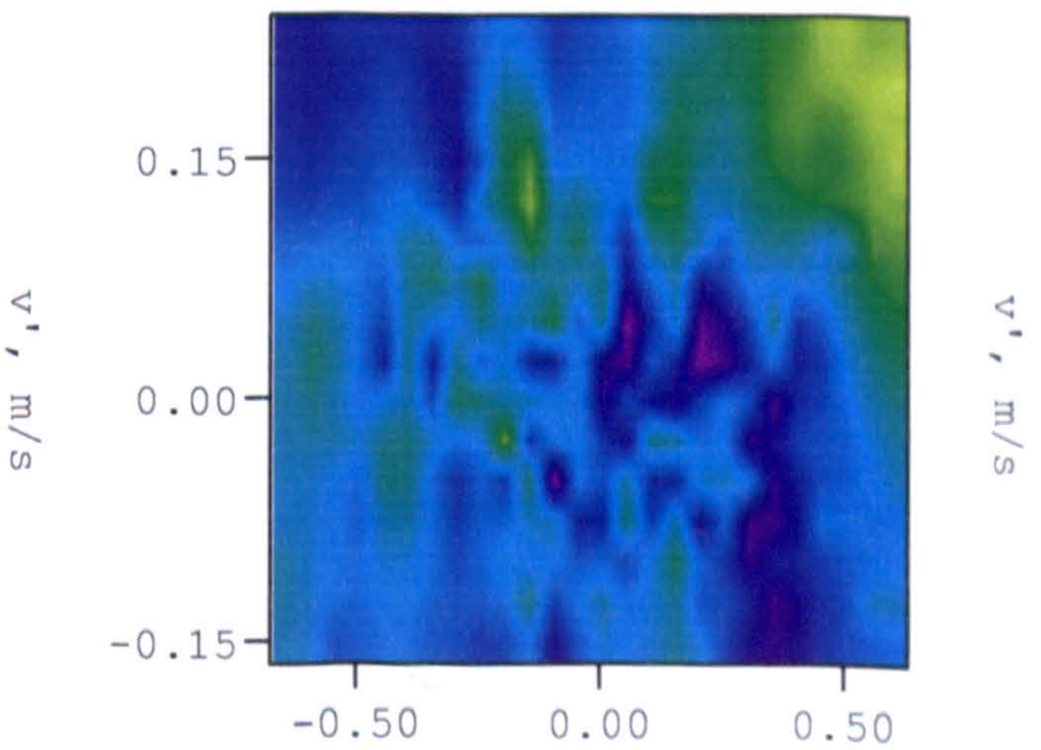

(c) depth = 7.7 m

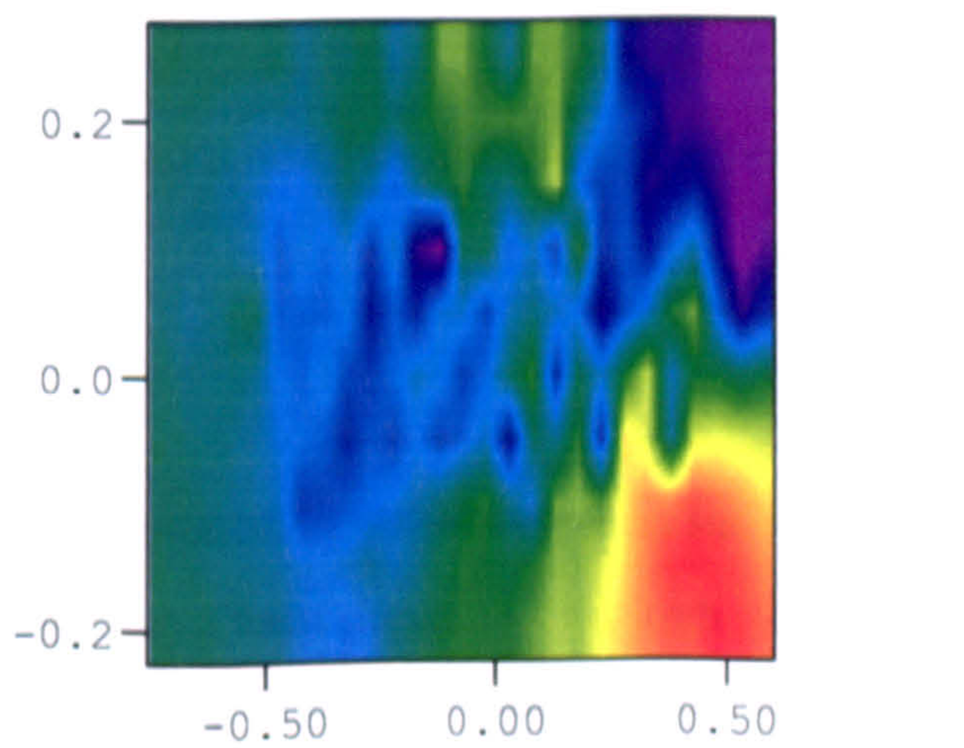

(d) depth = 9.7 m

272

6.5 Conclusions

This study has shown that suspended sediment transport over a dune varies both temporally and spatially. Mean profiles of suspended sediment concentration over high angled dunes under low and high hydraulic regimes have been shown to vary spatially along dunes indicating that flow separation plays an important role in sediment transport over the bedform. Dunes have also been shown to affect suspended sediment concentrations over larger spatial scales (Figure 6.5) with individual bedforms influencing sediment transport within the entire vertical flow column. Dunes may therefore have a significant role on total sediment flux in such large sand bed rivers as the Jamuna.

The differential in suspended sediment concentration between the u'v' quadrants at different locations and heights over the dune has been shown to be great (Figure 6.11). The variation in sediment transport characteristics reflects the spatial changes in turbulence structure over dunes, with quadrant 4 events (fluid inrushes or sweeps directed towards the bed) being responsible for the majority of high positive sediment concentrations over the dune crest, and quadrant 2 (ejections away from the shear layer) being much more important through the free shear layer.

Turbulence production on the lee side of high angled dunes, which is caused by the process of flow separation and the formation of a separation zone free shear layer, is dominated by the frequent ejection of quadrant 2, Kelvin-Helmholtz instabilities. These quadrant 2 vortices are responsible for transporting suspended sediment upwards into the water column and such ejections with high suspended sediment concentrations are intermittently apparent on the water surface.

Quadrant 3 type events may also be important in sediment transport processes as such low downstream and negative vertical velocity packages have been shown to bear high suspended sediment concentrations within the lower part of the free shear layer (Figure 6.11). Such quadrant 3 events may therefore be indicative of entrained of low-velocity, high sediment concentration fluid that has moved from the low flow zone into the shear layer due to flow reversals (Section 5.5.5), thereby increasing suspended sediment concentration in the shear layer.

In the reattachment zone, quadrant 4 events dominate; these vortices are extremely important as they may be responsible for eroding sediment from the dune trough and lower stoss side, and increasing sediment suspension into the wake zone and along the lower dune back. Quadrant 1 events, which also contribute a positive fluctuation in the downstream velocity may also be important for sediment transport in the flow reattachment zone.

Quadrant 4 events are also very significant near-bed over the dune crest where sweeps of fluid with high suspended sediment concentrations increase the downstream sediment flux. In the upper flow region above the crest occasional quadrant 2 events occur with substantially higher suspended sediment concentrations than the ambient fluid. These quadrant 2 events may be the result of vortex shedding from the upstream dunes which are manifest on the water surface as boils.

The spatial pattern of sediment entrainment, transport, suspension and deposition is controlled by the formation and downstream extent of the separation zone shear layer for high slip faced angled dunes (see Figure 6.11). Turbulence structures significantly affect the sediment transport field not only near the bed (as shown by Nelson et al., 1995) but also higher in the water column, specifically within the separation zone shear layer where the ejection of Kelvin-Helmholtz instabilities is associated with high suspended sediment concentrations. The spatial variation in the turbulence field therefore induces spatial modification in the sediment transport characteristics, so indicating that flow separation governs the development and stability of dunes (Raudkivi, 1963; Nelson *et al.*, 1993; Bennett and Best, 1995; Nelson *et al.*, 1995).

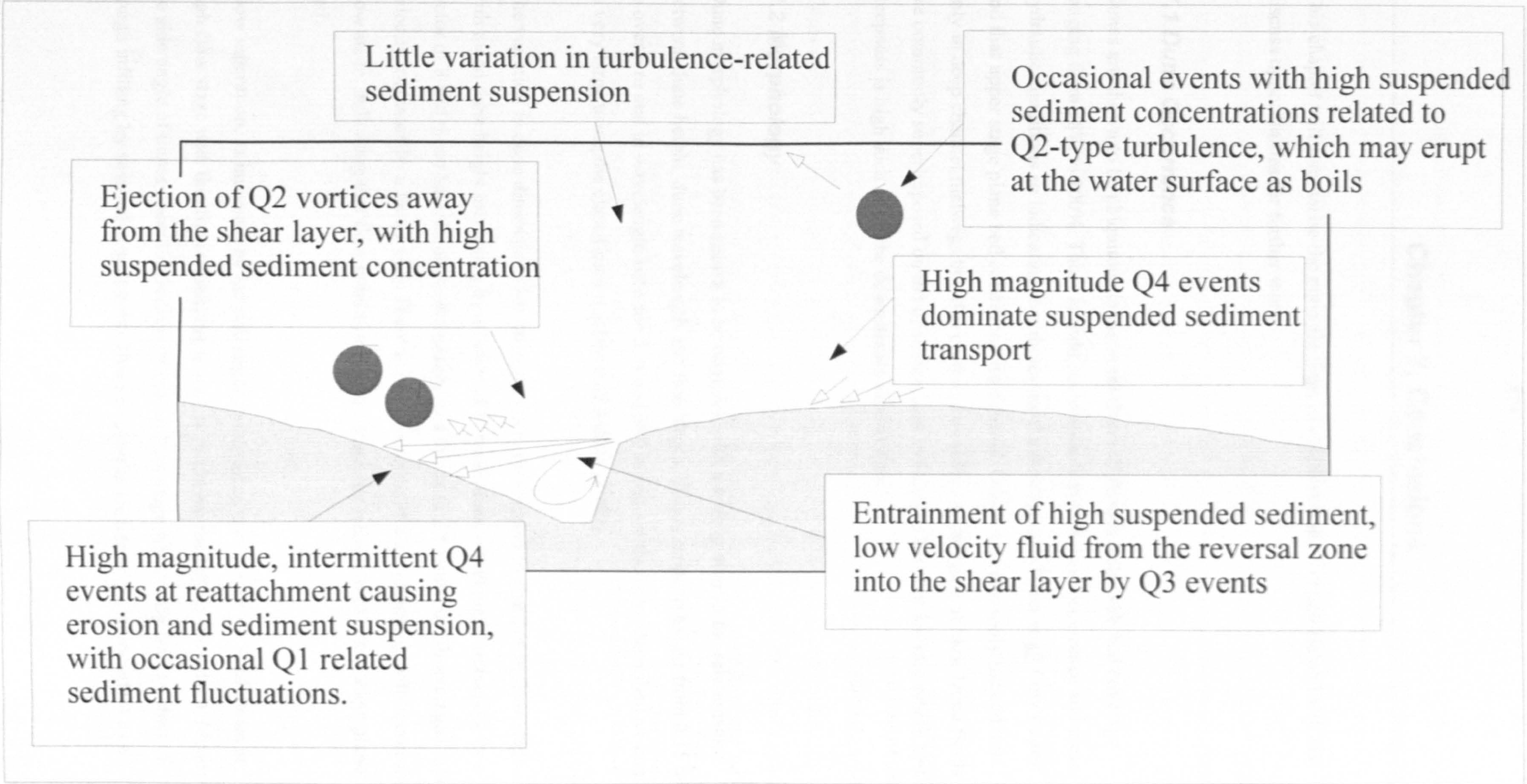

Figure 6.11, Schematic summarising main points of Chapter 6

Chapter 7. Conclusions

This chapter will summarise the main findings of chapters four, five and six and will also discuss opportunities for further work.

7.1 Dune Occurrence

Dunes are shown to be ubiquitous in the main rivers of Bangladesh, with bed coverage ranging from 38% to 100%. There is little correlation between dune occurrence and mean hydraulic conditions so indicating that dunes are the dominant bedform at all flow stages and that upper stage plane bed conditions are unusual. Dunes are commonly located not only in deep channel thalwegs but also on the stoss sides and margins of bars. Dune fields are commonly superimposed on the upstream face and tops of bars but are rare where bed steepness is high such as on the downstream face of bars

7.2 Morphology

Dune morphology has been shown to be complex with a wide scatter in the relationships between dune height, dune wavelength and flow depth. Dunes range in height from 0.15 m to over 6 m and in wavelength between 3 m and 300 m and are therefore described as small to very large using the classification scheme of Ashley (1990).

The variation in dune dimensions has been shown to correspond to changes in flow stage, with mean dune height increasing by a factor of 6, mean dune wavelength increasing by a factor of 8 and mean lee side angle increasing by a factor of 2.5 whilst depth-averaged mean velocity increases by a factor of 5. There is little evidence of dune flattening with increasing flow stage, indicating that flow conditions do not reach the transition to upper stage plane bed.

Flow separation, as indicated by lee side angle, is expected to occur for 45 % of dunes at high flow stage with this figure lowering to just 10 % during the falling flow stage. Mean lee side angle of dunes decreases rapidly at falling flow stage which may be a product of trough infilling by suspended sediment. This variation in leeside angle is important as it

indicates that an increase in turbulence production and sediment suspension will occur with increasing flow stage as flow separation becomes more prevalent. Dune lee side slopes are often complex with several local changes in slope occurring downstream of the dune crest. The break in slope at the dune crest has been shown to commonly dip gently downstream (4.1°) before a sharp break in slope at the brink point (mean angle 11.7°). The effects of compound breaks in slope may induce further complexities in turbulence production for the separation zone free shear layer.

The dune shape factor, which is a measure of the fullness of a bedform, has also been shown to alter with flow stage with a maximum mean value (0.71) occurring under high flow conditions. Under low flow conditions, the mean shape factor decreases to less than 0.5. Bedload sediment transport, which is frequently calculated using dune migration rates, would be underestimated by up to 30% at high flow stage if an estimation of the shape factor is used. Models used to estimate flow resistance using bedform parameters have been shown to be imprecise at high and rising flow stages, this may be partially a factor of estimating the value of the dune shape factor.

In planform, dunes have been shown to be three-dimensional at both high and low flow stages. Dunes exposed on bar tops at low flow stage after water levels have declined vary in height from 0.15 m to over 2 m and have well developed lee faces and troughs. Side scan sonar surveys have shown that dune crestlines are laterally continuous under both high and low flow conditions, even where there is great variation in crestline morphology, although secondary, superimposed dunes are often discontinuous.

The Jamuna data set is used to test van Rijn's (1985, 1993) model which proposes that dune morphology varies as a function of the excess bed shear stress (T). Dunes exist at a much wider range of T values (up to 58) than proposed by van Rijn, who speculated that upper stage plane beds should ensue at T values greater than 25. Only a small fraction of the dunes measured in the present study begin to flatten at high T values and this flattening occurs at T greater than 40, indicating that dunes are the dominant bedform even at high flow stage. It seems likely that van Rijn's model underpredicts dune occurrence because of the very low Froude numbers occurring in the deep, wide alluvial channels that are found in the Jamuna river (Julien and Klaassen, 1995). The important corollary of this is that dunes are the dominant bedform in such alluvial channels at all flow stages and hence will dominate the preserved sediments of such alluvial channels.

7.3 Mean Flow

7.3.1 Steep Lee Face Angled Dunes

There is great spatial variation in profiles of temporal mean downstream and vertical velocity over dunes. Maximum mean downstream velocities (up to 2.5 ms^{-1}) were measured in the upper flow column above a dune crest. The vertical flow column above a dune trough may be divided into three sections: a near-bed low flow zone overlain by a region exhibiting high shear which is followed by an outer flow region. Contrary to studies of dunes conducted in flumes, the mean downstream velocity within the low flow zone is positive, although small (0.2 ms^{-1}), over the entire survey period, indicating that a permanent separation cell may not exist. However, over shorter periods of up to five minutes, negative mean downstream velocities do occur and a more permanent flow separation zone may exist closer to the dune crest. The formation of a flow separation zone above the dune trough and the resulting free shear layer dominates the mean flow field with the highest downstream velocity gradients (of 0.14 m^{-1} under both low and high flow conditions) situated across the shear zone, which is a consequence of rapid flow deceleration and expansion downstream of the dune crest.

7.3.2 Low Lee Face Angled Dunes

Flow expansion downstream of the dune crest over low lee face angled dunes is much smaller than over high slip faced angle bedforms. Maximum, time-averaged, downstream velocity gradients are 50% of those forming over high lee face angled dunes and no shear zone is identifiable from mean velocity profiles. Spatial variation in mean velocity profiles is therefore much smaller over low lee face angled dunes although in general flow is accelerating up the dune stoss face due to topographic forcing and then expands downstream from the lee face.

7.4 Turbulence

Although there is little evidence of turbulence production over low-lee face angled dunes, the turbulence structure over steeply dipping lee face dunes has been quantified. The root-mean-square of the downstream and vertical velocity components is greatest over steeply-dipping lee face dune troughs at the height of the separation zone shear layer which is

denoted by the mean velocity profiles. Positive vertical RMS values have previously been shown to indicate fluid ejection from the free shear layer (Itakura and Kishi, 1980). The Reynolds stress has been shown to increase with depth over dune troughs contrary to earlier flume studies, this increase in Reynolds stress is indicative of motion or flapping of the shear layer and hence the flow reattachment location is variable. Turbulence over steeply dipping lee faced dunes has also been quantified using quadrant analysis. Over dune troughs, high magnitude quadrant 2 type events have been shown to dominate turbulence production through the separation zone free shear layer, in terms of contribution to the total Reynolds stress and frequency of occurrence. These quadrant 2 'ejection' events are Kelvin Helmholtz instabilities that are intermittently shed off the unstable shear layer. In the near bed zone close to flow reattachment, quadrant 4 sweep type events dominate contributions to the Reynolds stress therefore indicating a change in the turbulence production between the shear layer and the reattachment zone. Higher in the flow above the shear layer, the Reynolds stress much smaller, but is still dominated by quadrant 2 and 4 events. Over the dune crest the total Reynolds stress is much lower than over the dune trough shear and separation zones, and is dominated by quadrant 2 type events.

Examination of the temporal variation in the velocity gradient over the dune trough has shown that the separation zone shear layer is temporally unstable. The growth and decay of high magnitude velocity gradients has been linked with the production of turbulence, with 98% of quadrant 4 events and 71 % of quadrant 2 events occurring at a velocity gradient magnitude greater than 1. This study therefore confirms the earlier untested hypothesis (e.g. Bennett and Best, 1995) that the magnitude and frequency of ejection events is determined by the velocity gradients acting across the separation zone shear layer. In addition to fluctuations in the shear layer due to eddy shedding, the location of the shear layer has also been shown to move or flap within the flow column, hence confirming that the instantaneous impingement location of the shear layer is variable as was indicated by vertical profiles of Reynolds stress.

Spectral analysis of velocity time series through the separation zone shear layer proved inconclusive in determining dominant eddy shedding frequencies. A mean eddy shedding period of approximately 20 to 25 seconds is inferred from a combination of visual observation of boil eruption at the flow surface and statistically insignificant spectral analysis results.

7.5 Sediment Transport

This study has shown that suspended sediment transport over a dune varies both temporally and spatially. Mean profiles of suspended sediment concentration over high angled bedforms under low and high hydraulic regimes have been shown to vary spatially along dunes indicating that flow separation plays an important role in sediment transport over dune. Dunes have also been shown to affect suspended sediment concentrations over larger spatial scales with individual bedforms influencing sediment transport within the entire vertical flow column. Dunes may therefore have a significant role on total sediment flux in such large sand bed rivers as the Jamuna.

The differential in suspended sediment concentration between the -u'v' quadrants at different locations and heights over the dune has been shown to be great. The variation in sediment transport characteristics reflects the spatial changes in turbulence structure over dunes, with quadrant 4 events (fluid inrushes or sweeps directed towards the bed) being responsible for the majority of positive sediment fluctuation concentrations over the dune crest, and quadrant 2 (ejections away from the shear layer) being much more important through the free shear layer. Near the flow reattachment zone, quadrant 4 events are again associated with high suspended sediment concentrations and are therefore responsible for scour in the dune trough.

7.6 Dune Stability

The spatial pattern of sediment entrainment, transport, suspension and deposition is controlled by the formation and downstream extent of the separation zone shear layer for high slip faced angled dunes. Turbulence structures significantly affect the sediment transport field not only near the bed (as shown by Nelson *et al.*, 1995) but also higher in the water column. Within the separation zone shear layer the frequent and high magnitude ejections of Kelvin-Helmholtz instabilities are associated with high suspended sediment concentrations, and are the source of dune-related macro-turbulence. The spatial variation in the turbulence field therefore induces spatial modification in the sediment transport characteristics so indicating that flow separation governs the development and stability of

dunes as also found by Raudkivi, (1963), Nelson et al., (1993), Bennett and Best, (1995) and Nelson et al., (1995).

7.7 Suggestions for Further Work

1. This study has highlighted the requirement for a detailed flume study to model mean flow and turbulence over low lee face angled dunes. The stability of dunes with low lee face angles is still an area of controversy, primarily due to the lack of reliable data detailing mean flow and turbulence fields and hence the controls on the stability of low lee face angled dunes.

2. Dune morphology in this study has been shown to be extremely complex, contrary to many flume and numerical studies which assume a more simplistic dune shape. Much further study of the variation in mean flow and turbulence over dunes with compound breaks in leeside slope and the effect of increased complexity of dune shape (as found in the field) on flow is required to improve prediction models of dune morphology and flow resistance.

3. This study has emphasised the importance of velocity gradients on eddy shedding and shear layer flapping of the separation zone shear layer. Further experimental work on the variation in velocity gradient and the linkages of these variations with crestal velocity, the eddy shedding frequency and rotational velocity of Kelvin Helmholtz instabilities is required to elucidate dune-related macro-turbulent structures such as the boils seen at the flow surface in this study.

4. The results from this thesis have indicated that flow reversals in the dune trough may be linked with ejections of fluid away from the shear layer, continuing the work of Müller and Gyr (1986) who suggested that strong negative velocities in the dune troughs are linked with ejection of turbulent fluid which reaches the flow surface. There remains much uncertainty into the cause of this process but it may again be linked with variations in velocity gradients within the shear layer which may be controlled by the distribution of vorticity in the flow upstream of the separation point. Further investigation between

the variation in shear zone magnitude with variation in the velocity and turbulence structure prior to flow separation at the dune brink point is necessary.

5. The links between turbulence structure and sediment transport characteristics is of great importance when investigating dune bedforms. The complex interactions and feedbacks within the bedform 'trinity' is still an area of much uncertainty. The temporal variations in bedload sediment transport downstream of flow reattachment have been investigated by Nelson et al. (1995). However, to date, no studies have examined or quantified the linkages between dune related turbulence and bedload sediment transport within the separation zone or sediment suspension from the shear zone into the outer flow. Although this study has endeavoured to connect spatial variations in turbulence and sediment transport there undoubtedly remains much scope for further work to investigate these complex interactions. Detailed flume studies of the spatial variation in flow and sediment transport over bedforms are therefore a necessity as they are of fundamental importance to bedform mechanics.

References

Allen, J.R.L., 1964. Primary current lineations in the lower old red sandstone (Devonaian) Anglo Welsh Basin. Sedimentology, **3**, 163-198.

Allen, J.R.L., 1968. Current Ripples. North Holland Publishing Company, Amsterdam, 433pp.

Allen, J.R.L.,1970. Physical Processes of Sedimentation. George Allen and Unwin, London, 275pp.

Allen, J.R.L, 1976. Conceptual models for dune time-lag: general ideas, difficulties and results. Sedimentary Geology, **15**, 1-53.

Allen, J.R.L., 1977. The plan shape of current ripples in relation to flow conditions. Sedimentology, **24**, 53-62.

Allen, J.R.L., 1980. Sandwaves, a model of origin and internal structure. Sedimentary Geology, **26**, 281-328.

Allen, J.R.L. and Leeder, M.R., 1980. Criteria for the instability of upper stage plane bed. Sedimentology, **27**, 209-217.

Allen, J.R.L., 1982. Sedimentary structures: their character and physical basis. Elsevier, Amsterdam, 539 pp.

Allen, J.R.L.,1983. River Bedforms: progress and problems. In: Modern and Ancient Fluvial Systems, Collinson, J.D. and Lewin, J. (Eds.). Special Publication International Association of Sedimentologists, **6**, 19-33.

Allen, J.R.L., 1985. The Principles of Physical Sedimentology. Allen and Unwin, London, 272pp.

Aliotta, S. and Perillo, G.M.E, 1987. A sand wave field in the entrance to Bahia Blanca estuary, Argentina. Marine Geology, **76**, 1-14.

Amsler, M.L. and Garcia, M.H., 1997. Sand dune geometry of large rivers during floods, discussion. Journal of Hydraulic Engineering, **123**, 582-584.

Ashley, G.M., 1990. Classification of large-scale subaqueous bedforms: a new look at an old problem. Journal of Sedimentary Petrology, **60**, 160-172.

Ashworth, P.J., Best, J.L., Roden, J.E., Bristow, C.S. and Klaassen, G.J., in review. Morphological evolution and dynamics of a large, sand braid-bar, Jamuna River, Bangladesh. Sedimentology.

Baas, J.H., 1994. A flume study on the development and equlibrium morphology of small scale bedforms in very fine sand. Sedimentology, **41**, 185-209.

Babakaif, C.S. and Hickin, E.J., 1996. Coherent flow structures in Squamish River estuary, British Colombia, Canada. In: Coherent Flow Structures in Open Channels, Ashworth, P.J., Bennett, S.J., Best, J.L and McLelland, S.J (eds), Wiley 1996, pp 321-342.

Barlow, R.S. and Johnston, J.P., 1988(a). Structure of a turbulent boundary layer on a concave surface. Journal of Fluid Mechanics, **191**, 137-176.

Barlow, R.S. and Johnston, J.P., 1988(b). Local effects of large-scale eddies on bursting in a concave boundary layer. Journal of Fluid Mech., **191**, 177-195.

Barr, I.H., Jopling, A.V., Senturk, F., White, C.M., MacMahon, B., Nordin, C.F. and Algert, H., 1965. Geometrical properties of sand waves, discussion. ASCE, Journal of Hydraulics Division, **91**, HY3, 343-374.

Bennett, S.J. and Best, J.L., 1995. Mean flow and turbulence structure over fixed, two-dimensional dunes: implications for sediment transport and bedform stability. Sedimentology, **42**, 491-513.

Bennett, S.J. and Best, J.L., 1996. Mean flow and turbulence structure over fixed ripples and the ripple-dune transition. In: Coherent Flow Structures in Open Channels, Ashworth, P.J., Bennett, S.J., Best, J.L and McLelland, S.J (eds), Wiley 1996, pp 281-304.

Best, J.L. and Leeder, M.R., Drag reduction in turbulent muddy seawater flows and some sedimentary consequences. Sedimentology, **40**, 1129-1137.

Best, J.L., 1993. On the interactions between turbulent flow structure, sediment transport and bedform development: some considerations from recent experimental research. Turbulence: perspectives on flow and sediment transport. Clifford N.J., French, J.R. and Hardisty J. (eds).

Best, J.L., 1996. The fluvial dynamics of small-scale alluvial bedforms. In: Advances in Fluvial Dynamics and Stratigraphy, Carling, P.A. and Dawson, M.R. (eds), Wiley and sons, pp 1-32.

Best, J.L and Ashworth, P.J., 1997. Scour in large braided rivers and the recognition of sequence stratigraphic boundaries. Nature, **387**, 275-277.

Best. J.L., Ashworth, P.J., Bristow, C.S. and Roden, J.E., (in review). Three-dimensional sediemtnary architecture of a large mid-channel sand braid bar, Jamuna River, Bangladesh. Journal of Sedimentary Research.

Bogard, D.G. and Tiederman, W.G., 1986. Burst detection with single point velocity measurements. Journal of Fluid Mechanics, **162**, 389-413.

Boguchwal, L.A. and Southard, J.B., 1990. Bed configurations in steady unidirectional water flows. Part 1: Scale model study using fine sands. Journal of Sedimentary Petrology, **60**, no. 5. 649-657.

Boguchwal, L.A. and Southard, J.B., 1990. Bed configurations in steady unidirectional water flows. Part 2 Synthesis of flume data. Journal of Sedimentary Petrology, **60**, no. 5., 658-679

Boguchwal, L.A. and Southard, J.B., 1990. Bed configurations in steady unidirectional water flows. Part 1Effects of temperature and gravity. Journal of Sedimentary Petrology, **60**, no. 5, 680-692.

Boothroyd, J.C. and Hubbard, D.K., 1975. Genesis of bedforms in mesotidal estuaries. In: L.E. Cronin (ed), Estuarine Research, Vol 2, Geology and Engineering. Academic Press, New York, pp. 217-234.

Bouma, A.H., Rappeport, M.L., Orlando, R.C. and Hampton, M.A., 1980. Identification of bedforms in the lower Cool Inlet, Alaska. Sedimeantary Geolology, **26**, 625-648.

Bridge, J.S. and Best, J.L., 1988. Flow, sediment transport and bedform dynamics over the transition from dunes to upper-stage plane beds: implcations for the formation of planar laminae. Sedimentology, **35**, 753-763.

Bristow, C.S., 1993. Sedimentary structures exposed on bartops in the Brahmauptra River, Bangladesh. In: Braided Rivers, J.L. Best and C.S. Bristow (eds) , Geological Society Special Publication, **75**, 277-290.

Bristow, C.S., 1993. Sedimentology of the Rough Rock: a Carboniferous braided river sheet sandstone in norther England. in Braided Rivers, J.L. Best and C.S. Bristow (eds) , Geological Society Special Publication, **75**, 291-304.

Bristow, C.S., 1987. Brahmaputra River: Channel migration and deposition, In: Etheridge, F.G., Flores, R.M. and Harvey, M.D. (eds.), Recent Developments in Fluvial Sedimentology, Society of Economic Paleontologists and Mineralogists, Special Publication, **39**, 63-74.

Bradshaw, P. and Wong, F.Y.F., 1972. The reattachment and relaxation of a turbulent shear layer. Journal of Fluid Mechanics, **52**(1), 113-135.

Brownlie, W.R., 1983. Flow depth in sand bed channels. ASCE, Journal of Hydraulics Division, **109**, no. 7, 959-990.

Burger, J.W., Klaassen, G.J. and Prins, A., 1988. Bank erosion and channel processes in the Jamuna river, Bangladesh. International symposium on the impact of river bank erosion, flood hazard and the problem of population deplacement, Bangladesh, 1-17.

Cant, D.J. and Walker, R.G., 1978. Fluvial processes and facies sequences in the sandy braided South Saskatchewan River, Canada. Sedimentology, **25**, 625-648.

Campbell Scientific Instruments Canada Corperation, 1993. UDG01, UDG User guide, 34pp.

Carey, W.C. and Keller, M.D., 1957. Systematic changes in the beds of alluvial rivers. ASCE, Journal of Hydraulics Division, 83(4), 1331-1 - 1331-24.

Carling, P.A., 1998. Gravel Dunes. Sedimentology, 1998, in press.

Caston, V.N.D, 1965. Localised sediment transport and submarine erosion in Tremadoc Bay, Northern Wales. Marine Geology, **3**, 401-410.

Clifford, N.J. and French, J.R., (1993). Monitoring and analysis of turbulence in geophysical boundaries: some analytical and conceptual issues. In: Turbulence: Perspectives on Flow and Sediment Transport, N.J. Clifford, J.R. French and J. Hardisty (eds), Wiley , Chichester, pp 39-120.

Coleman, J.M., 1969. Brahmaputra river: channel processes and sedimentation. Sedimentary Geology, **3**, 129-239.

Coleman, S.E. and Melville, B.W., 1994. Bed form development. Journal of Hydraulic Engineering, vol 120, no 4, 544-562.

Collinson, J.D., 1970. Bedforms of the Tana River, Norway. Geogr. Annlr., **52A**, 31-56.

Corino, E.R. and Brodkey, R.S., 1969. A visual investigation of the wall region in turbulent flow. Journal of Fluid Mechanics, **37**, 1, 1-30.

Costello, W.R., 1974. Development of bed configurations in coarse sands. Unpublished Ph.D. thesis, Massachusetts Institute of Technology, 120pp.

Costello, W.R. and Southard, J.B., 1981. Flume experiments on lower regime bedforms in coarse sand. Journal of Sedimentary Petrology, **51**, 849-864.

Crickmore, M.J., 1970. Effect of flume width on bedform characteristics. ASCE, Journal of Hydraulics Division, **96**, 473-422.

Curray, F, and Moore, A., 1971. Growth of the Bengal deep sea fan and denudation of the Himalayas. Geolological Society of America, Bulletin, **82**, 563-572.

Dalrymple, R.W., Knight, R.J. and Lambiase, J.J., 1978. Bedfroms and their hydraulic stability relationships ina tidal environment, Bay of Fundy, Canada. Nature, **275**, 100-104.

Dalrymple, R.W., 1984. Morphology and internal structure of sandwaves in the Bay of Fundy. Sedimentology, **31**, 365-382.

Dalrymple, R.W. and Rhodes, R.N., 1995. Estuarine dunes and bars. in Geomorphology and sedimentology of estuaries. In: Developments in Sedimentology, **53**, G.M.E. Perillo (ed), Elsevier Science.

Delft Hydraulics, 1990. Electromagnetic Flow Meter, User's Manual, Delft Hydraulics, NL, 16pp.

Delft Hydraulics, 1992. Water level logger level log manual, version 1.08, Delft Hydraulics, NL, 23pp.

Delft Hydraulics and DHI, 1995. FAP24 River Survey Project, Special Report 2, Water level Gauging Stations (prepared for FPCO), Dhaka, Bangladesh, 65pp.

Delft Hydraulics and DHI, 1996a. FAP24 River Survey Project, Final Report, Main Volume (prepared for FPCO), Dhaka, Bangladesh, 280 pp.

Delft Hydraulics and DHI, 1996b. FAP24 River Survey Project, Special Report 6, Floodplan levels and abnkfull discharge (prepared for FPCO), Dhaka, Bangladesh, 20pp.

Delft Hydraulics and DHI, 1996c. FAP24 River Survey Project, Special Report 14, Physical properties of river sediments (prepared for FPCO), Dhaka, Bangladesh, 36pp.

Delft Hydraulics, DHI and Leeds University, 1996. FAP24 River Survey Project, Special Report 9, Bedform and bar dynamics in the main rivers of Bangladesh (prepared for FPCO), Dhaka, Bangladesh, 107pp.

Dinehart, R. L., 1989. Dune migration in a steep, coarse-bedded stream. Water Resources Research, **25**, 911-923.

Dinehart, R. L., 1992. Evolution of coarse gravel bed forms: field measurements at flood stage. Water Resources Research, **28**, 2667-2689.

Dingham, S.L., 1984. Fluvial Hydrology. W.H. Freeman and company, New York.

Ditchfield, R. and Best, J.L., 1992. Development of bed features: discussion. ASCE , Journal of Hydraulic Engineering , **118**, 647-650.

Drazin, P.G. and Reid, W.H., 1981. Hydrodynamic stability. Cambridge University Press. New York, 213pp.

Driver, D.M., Seegmiller, H.L and Marvin, J., 1987. Time dependant behaviour of a reattaching shear layer. American Institute of Aeronautics and Astronautics, **25**, 914-919.

Engel, P., 1981. Length of flow separation over dunes. ASCE, Journal of Hydraulic Engineering, **107**, no. HY10.

Engel, P., and Lau, Y.L., 1980. Computation of bedload using bathymetric data. ASCE , Journal of the Hydraulics Division, **106**, 369-380.

Engelund, F., 1966. Hydraulic resistance of alluvial streams. ASCE, Journal of Hydraulics Division, **92**, HY2, 315-326.

Engelund and Hansen, 1967. A monograph on sediment transport in alluvial streams. Teknisk Forlag, Copenhagen, Denmark.

Engelund, F., 1970. Instability of erodible beds. Journal of Fluid Mechanics, **42**, 225-244.

Engelund, F., 1977. Hydraulic resistance for flow over dunes. Progress Report 44, Institute of Hydraulics and Hydraulic Engineering, Technical University of Denmark, Denmark, 29pp.

Engelund, F. and Fredsøe, J., 1982. Sediment ripples and dunes. Annual Reviews in Fluid Mechanics, 14, 13-37.

FAP24 River Survey Project Report, 1993. Selection of Survey Techniques, 300pp.

Fenster, M.S., Fitzgerald, D.M., Bohlen, W.F., Lewis, R.S. amd Baldwin, C.T., 1990. Stability of giant sandwaves in eastern Long Island Sound, U.S.A. Marine Geololgy, 91, 207-225.

Ferguson, R.I., Kirkbride, A.D. and Roy, A.G., 1996. Markov analysis of velocity fluctuations in gravel-bed rivers. In: Coherent Flow Structures in Open Channels, Ashworth, P.J., Bennett, S.J., Best, J.L and McLelland, S.J (eds), Wiley 1996, pp 165-184.

Flemming, B.W., 1980. Sand transport and bedform patterns on the continental shelf between Durban and Port Elizabeth (southeastern Afircan continental margin). Sedimentary Geology, 26, 179-205.

Fredsoe, J., 1974. On the developemnt of dunes in erodible channels. Journal of Fluid Mechanics, 64, part 1, 1-16.

Fredsøe , J., 1980. The Formation of Dunes. Int. Symp. on River Sedimentation, Beijing, China.

Fredsoe, J., 1982. The shape and dimensions of stationary dunes in rivers. ASCE, Journal of Hydraulic Engineering, 8, 932-947.

Fukuoka, S. And Fukushima, Y., 1989. Characteristics of ascending currencts and boils inducded by large-scale eddies. In: H. Kikkawa and Y. Iwasa (eds), Proceedins of the third International Symposium on Stochastic Hydraulics, Tokyo, pp. 609-619.

Gabel, S.R., 1993. Geometry and kinematics of dunes during steady and unsteady flows in the Calamus River, Nebraska, U.S.A. Sedimentology, 40, 237-269.

Gill, M.A., 1971. Height of sand dunes in open channel flows. ASCE , Journal of Hydraulic Engineering, vol 97, no HY12, 2067-2074.

Gomez, B and Naff, R.L., 1989. Temporal variations in bedload trasnport rates associated with the migration of bedforms. Earth Surface Processes and Landforms, 14, 135-156.

Gordon, R.L., 1989. Acoustic measurement of river discharge. Journal of Hydraulic Engineering, 115, no. 7, 925-936.

Grass, A.J., 1974. Transport of fine sand on a flat bed: turbulence and suspension mechanics. In: Transport, Erosion and Deposition of Sediment in Turbulent Streams, Proc. Euromech 48, pp 33-34. Tech. Univ. of Denmark.

Guy, H.P., Simons, D.B and Richardson, E.V., 1966. Summary of channel data from flume experiments, 1956-61. United States Geological Survey professional paper 462-I.

Gyr, A. and Muller, A., 1982. Visualisation of the mixing layer behind dunes. Euromech 156: Mechanics of sediment transport, Istanbul, 12-14 July.

Gyr, A. and Muller, A., 1996. The role of coherent structures in developing bedforms during sediment transport. In: Coherent Flow Structures in Open Channels, Ashworth, P.J., Bennett, S.J., Best, J.L and McLelland, S.J (eds), Wiley 1996, pp 227-236.

Hand, B.M. and Bartberger, C.E., 1988. Leeside sediment fallout patterns and the stability of angular bedforms. Journal of Sedimentary Petrology, **58**, 1, 33-43.

Haque, M.I. and Mahmood, K., 1986. Analytical study on steepness of ripples and dunes. Journal of Hydraulic Engineering, vol.**112**, no.3.PP

Harris, P.T. and Collins, M.B., 1985. bedform distributions and sediment transport paths in the Bristol Channel and Severn Estuary, U.K., Marine Geology, **62**, 153-166.

Heathershaw, A.D., 1974. 'Bursting' phenomena in the sea. Nature, **248**, 394-395.

Hossain, M.M., 1993. Economic effects of riverbank erosion: some evidence from Bangladesh. Disasters, **17**, 25-32.

INTERCONSULT (Norway), 1991. Determination of standard low water and standard high water-levels in Bangladesh (Vol. II, Technical Report). Bangladesh Inland Water Transport Authority, Dhaka, 89pp.

InterOcean Systems inc., 1990. S4 Current Meter, User's Manual. San Diego, USA.

Itakura, T. and Kishi, T., 1980. Open channel flow with suspended sediment on sand waves. In: Proc. 3rd International Symposium on Stochastic Hydraulics (eds H. Kikkawa and Y. Iwasa), International Association of Hydraulic Research, Tokyo, pp 599-609.

Jackson, R.G., 1976. Sedimentological and fluid dynamic implications of the turbulent bursting phenomemon in geophysical flows. Journal of Fluid Mechanics, 77, 531-560.

Jones, N.S., Kain, J.M. and Stride, A.H., 1965. The movement of sand waves on Warts Bank, Isle of Man. Marine Geology, 3, 329-336

Jordan, P.R., 1965. Fluvial sediment of the Mississippi River at St. Louis, Missouri. Paper 1802, U.S. Geological Survey, Washington D.C..

Julien, P.Y., 1992. Study of bedform geometry in large rivers. Report Q1386, Delfy Hydrulics, Emmeloord, The Netherlands.

Julien, P.Y. and Klaassen, G.J., 1995. Sand dune geometry of large rivers during floods. Journal of Hydraulic Engineering, **121**, 657-663.

Karim, F.K., 1995. Bed configurations and hydraulic resistance in alluvial-channel flows. ASCE, Journal of Hydraulic Engineering, **121**, 1, 15-25.

Karim, F.K. and Kennedy, J.F., 1990. Menu of coupled velocity and sediment discharge relations for rivers. ASCE, Journal of Hydraulic Engineering, **116**, 8, 978-996.

Karahan, M.E. and Peterson, A.W., 1981. Visualisation of separation over sand waves. Journal of Hydraulic Engineering, **106**, no. HY8, 1345-1352.

Kennedy, J.F.,1961. Stationary waves and antidunes in alluvial channels. Rep. W.M.Keck Lab., Hydraulics and Water Resources KH-R-2 (Cal. Inst. Tech., Pasadena, Cal.)

Kennedy, J.F., 1969. The formation of sediment ripples, dunes and anti-sunes. Annual Reviews in Fluid Mechanics, 1, 147-168.

Kim, H.T.M, Kline, S.J. and Reynolds, W.C., 1971. The production of turbulence near a smooth wall in a turbulent boundary layer. Journal of Fluid Mechanics, 50, 133-160.

Klaassen, G.J. and Vermeer, K., 1988. Sedimentological processes in the Jamuna (Lower Brahmaputra) River, Bangladesh, In: Proceedings International Conference on Fluvial Hydraulics, Budapest, Hungary, 381-394.

Kline, S.J. and Robinson, S.K., 1989. Turbulent boundary layer structure: progress, status and challenges. In: Structure of Turbulence and Drag Reduction, A. Gyr (ed), Hemisphere, New York, 3-22.

Kline, S.J. and Robinson, S.K., 1990. Quasi-coherent structures in the turbulent boundary layer. Part 1: status report on a community-wide summary of the data. In: Near Wall Turbulence, Proceedings of the 1988 Zoran Zaric Memorial Conference, S.J. Kline and N.H. Agfan (eds), Hemisphere, New York, 200-217.

Kornman, B.A., 1995. The effect of changes in the leeside shape of dunes on the flow field, turbulence and roughness, report on measurements. Institute of Marine and Atmospheric Research, University of Utrecht, Report R 95-1.

Kostaschuk, R.A and Church, M.A., 1993. Macroturbulence generated by dunes: Fraser River, Canada. Sedimentary Geology, 85, 25-37.

Kostaschuk, R.A., Church, M.A., and Luternauer, J.L., 1989. Bedofrms, bed material and bed load transport in a slat wedge estuary - Fraser River, British Colombia. Canadian Journal of Earth Science, 26, 1440-1452.

Kostaschuk, R.A and Ilersich, S.A., 1995. Dune geometry and sediment transport: Fraser River, British Columbia. in River Geomorphology, E.J. Hickin (ed), Wiley and sons ltd., pp 19-36.

Kostaschuk, R.A and Villard, P., 1996. Flow and sediment transport over large subaqueos dunes: Fraser River, Canada. Sedimentology, 43, 849-863.

Kostaschuk, R.A. and MacDonald, G.M., 1989. Multi-track surveying of large bedforms. Geo-Marine Letters, 8, 57-62.

Langhorne, D.N., 1973. A sandwave field in the outer Thames estuary, Great Britain. Marine Geology, 14, 129-143.

Lapointe, M., 1992. Burst-like sediment suspension events in a sand bed river. Earth Surface Processes and Landforms, 17, 253-270.

Lapointe M., 1993. Monitoring alluvial sand suspension by eddy correlation. Earth Surface Processes and Landforms, 18, 157-175

Lapointe, M.F., 1996. Frequency spectra and intermittency of the turbulent suspension process in a sand bed river. Sedimentology, **43**, 439-449.

Leclair, S.F. and Bridge, J.S., 1997. Preservation of cross-strats due to migration of subaqueous dunes over aggrading and non-aggrading beds: comparison of experimental data with theory. Gescience Canada, **24**, 1, 55-66.

Leeder, M.R., 1983. On the interacions between turbulent flow, sediment transport and bedform mechanics in channelised flows. In: Modern and Ancient Fluvial Systems, Collinson, J.D. and Lewin, J. (Eds.). Special Publication International Association of Sedimentologists, **6**, 19-33.

Levi, E., 1983. A universal Strouhal law. Journal of Engineering Mechanics, **109**, 718-727.

Levi, E., 1991. Vortices in hydraulics. Journal of Hydraulic Engineering, **117**, 399-413.

Lu, S.S. and Willmarth, W.W., 1973. Measurements of the structure of the Reynolds stress in a turbulent boundary layer. Journal of Fluid Mechanics, **60**, 481-511.

Lucanda, M., Peters, J.J., Swartenbroeckx, P. and Cornet, P., 1992. Applicaability of sediment transport theories to large sand bed rivers, In: Proceedings 5th international symposium on river sediemntation, Karlsruhe, Germany, 327-337.

Luchik, T.S. and Tiederman, W.G., 1987. Timescale and structure of ejections and bursts in turbulent channel flows. Journal of Fluid Mechanics, **174**, 529-552

Lyn, D.A., 1992. Turbulence measurements in open channel flows over artificial bed forms. Journal of Hydraulic Engineering, **119**, no. 3, 306-326.

Maniruzzaman-Miah, M, 1988. Flood in Bangladesh: A Hydromorphological study of the 1987 Flood. Academic Publishers, Dhaka, Bangladesh, 94pp.

Matthes, G.H., 1947. Macroturbulence in natural stream flow. Transactions of American Geophyics Union, **28**, 255-262.

McLean, S.R., 1990. The stability of ripples and dunes. Earth Science Reviews, **29**, 131-144.

McLean, S.R. and Smith, J.D., 1979. Turbulence measurements in the boundary layer over a sand wave field. Journal of Geophysics Research, **84**, no C12, 7791-7808.

McLean, S.R. and Smith, J.D., 1986. A model for flow over two-dimensional bedforms: implication for sediment transport. Journal of Geophysics Research, **99**, 12729-12747.

McLean, S.R. and Wolfe, S.R, 1993. Mean flow and turbulence over two-dimensional bedforms. Water Resources Research, **29**, no. 12, 3935-3953.

McLean, S.R., Nelson, J.M. and Wolfe, S.R., 1994. Turbulence structure over two-dimensional bedforms: imlpications for sediment transport. Journal of Geophysics Research, **99**, 12729-12747.

McLean, S.R., Nelson, M.N. and Sherve, R.L., 1996. Flow-sediment interactions in separating flows over bedforms. In: Coherent Flow Structures in Open Channels, Ashworth, P.J., Bennett, S.J., Best, J.L and McLelland, S.J (eds), Wiley 1996, pp 203-226.

McLelland, S.J., Ashworth, P.J., Best, J.L., Roden, J.E. and Klaassen, G.J., 1998. Flow structure and transport of sand-grade suspended sediment around an evolving braid bar, Jamina River, Bangladesh, in press.

Mendoza, C. and Shen, H.W., 1990. Investigation of turbulent flow over dunes. Journal of Hydraulic Engineering, **116**, no.4., 459-477.

Metcalfe, R.W, Orsag, S.A., Brachet, M.E., Menon, S. And Riley, J.J., 1987. Secondary instability of a temporally growing mixing layer. Journal of Fluid Mechanics, **184**, 207-243.

Middleton, G.V. and Southard, J.B., 1986. Mechanics of sediment movement, 2nd edition. SEPM short course, 3, 246pp.

Mohrig, D. and Dungan-Smith, J., 1996. predicting the migration rates of subaqueous dunes. Water Resources Res., vol. 32, no. 10.

Müller, A. and Gyr, A., 1982. Visualisation of the mixing layer behind dunes. Euromech 156, Istanbul, July 1982, 41-45.

Müller, A. and Gyr, A., 1986. On the vortex formation in the mixing layer behind dunes. Journal of Hydraulics Research, **24**, 359-375.

Nakagawa, H. and Nezu, I., 1981. Structure of space-time correlations of bursting phenomena in an open channel flow. Journal of Fluid Mechanics, **104**, 1-43.

NEDECO (Netherlands Engineering Consultants), 1967. Surveys of inland waterways and ports, East Pakistan Inland Water Transport Authority.

Neill, C.R., 1965. Bed forms in the lower Red Deer River, Alberta. Journal of Hydrology, 7, 58-85.

Nelson, J.M. and Smith, J.D., 1989. Mechanics of flow over ripples and dunes. Journal of Geophysics Research, 94, no. C6, 8146-8162.

Nelson, J.M., McLean, S.R. and Wolfe, S.R., 1993. Mean flow and turbulence fields over two-dimensional bedforms. Water Resources Research, 29, 3935-3953.

Nelson, J.M., Shreve, R.L., McLean, S.R. and Drake, T.G., 1995. Role of near-bed turbulence structure in bed load transport and bed form mechanics. Water Resources Research, 31, 8, 2071-2086.

Nezu, I. and Nakagawa, H., 1987. Experimental investigation of turbulent structure of backward-facing step flow in an open channel. Journal of Hydraulics Research, 25, 67-89.

Nordin, C.F. and Algert, H., 1965. Geometrical properties of sand waves, discussion. ASCE, Journal of Hydraulic Engineering, 91, HY3, 367-374.

Ogink, H.J.M., 1988. Hydraulic roughness of bedforms. Delft Hydraulics Report M2017.

Onslow, R.J., Thomas, N.H and Whitehouse, R.J.S, 1993. Vorticity and sandwaves: the dynamics of ripples and dunes. In: Turbulence: Perspectives on Flow and Sediment Transport. (eds) Clifford, N.J., French, J.R. and Hardisty, J., John Wiley and sons ltd.

Osborne, P.D. and Vincent, C.E., 1996. Vertical and horizontal structure in suspended sand concentrations and wave induced fluxes over bedforms. Marine Geology, **131**, 195-208.

Parsons, J.D., 1998. Mixinf mechanisms in density intrusions. Unpublished Ph.D. thesis, Univeristy of Illinois, U.S.A., 238pp.

Peters, J.J., 1993. Morphological studeis and data needs, Proceedings international workshop on morphological behaviour of major rivers in Bangladesh, FAP-24 Dhaka, 12pp.

Prandtl, L., 1927. Journal of the Royal Aeronautical Society, 31, 720-741.

Radio Technical Commission for Maritime Services, 1990. RTCM Paper 134-89/SC 104-68, Recommended Standards for Differential NAVSTAR GPS Service, version 2.0. PO Box 19087, Washington DC 20036, USA.

Rao, K.N., Narasimha, R. and Badri Narayanan, M.A., 1971. The 'bursting' phenonemon in a turbulent boundary layer. Journal of Fluid Mechanics, **48**, 339-352.

Raslan, Y., 1991. Geometrical properties of dunes. Unpublished Msc. thesis, Colarado State University. Fort Collins, U.S.A.

Raudkivi, A.J., 1963. Study of sediment ripple formation. ASCE, Journal of Hydraulic Engineering, **89**, 15-33.

Raudkivi, A.J., 1966. Bed forms in alluvial channels. Journal of Fluid Mechanics, **26**, 507-514.

RD Instruments, 1989. Acoustic Doppler Current Profilers, Principles of Operation: A Practical Primer. San Diego, USA.

Reichel, G. and Nachtnebel, H.P., 1994. Suspended sediment monitoring in a fluvial environment: advantages and limitations applying an acoustic Doppler current profiler. Water Resources Reseacrh, Vol. 28, no. 4.

Richards, K.J., 1980. The formation of ripples and dunes on an erodible bed. Journal Fluid Mechanics, 99, 597-618.

Rifai, M.F. and Smith, K.V.H., 1971. Flow over triangular elements simulating dunes. ASCE, Journal of Hydraulic Engineering, 97, 963-975.

Robinson, A.H.W., 1961. Ebb-flood channel systems in sandy bays and estuaries. Geography Journal, 127, 63-77

Robinson, S.K., 1990a. Coherent motions in the turbulent boundary layers. Annual Reviews in Fluid Mechanics, 23, 601-639.

Robinson, S.K., 1990b. A review of vortex structures and associated coherent motions in turbulent boundary layers. In: Structure of Turbulence and Drag Reduction, A. Gyr (ed), Hemisphere, New York, 23-50.

Rood, K.M. and Hickin, E.J., 1989. Suspended sediment concentration in relation to surface-flow structure in the Squamish River estuary, southwestern British Columbia. Canadian Journal of Earth Sciance, 26, 2172-2176.

Roshko, A., 1976. Structure of turbulent shear flows: a new look. American Institute of Aeronautics and Astronautics, **14**, 1349-1357.

Rubin, D.M. and McCulloch, D.S., 1979. Single and superimposed beforms: a synthesis of San Fransisco Bay and flume observations. Sedimentary Geology, **26**, 207-231.

Rubin, D.M. and Ikeda, 1990. Flume experiments on the alihnment of transverse, oblique and longitudinal dunes indirectionally varying flows. Sedimentology, **37**, 673-684.

Sandborn, V.A. and Kline, S.J., 1961. Flow models in boundary layer stall inception.Transactions of the American Society of Mechanical Egineers, D, **83**, 317-327.

Sandborn, V.A. and Liu, C.Y., 1968. On turbulent boundary layer separation. Journal of Fluid Mechanics, **32**, 293-304.

Sarker, M.H., 1996. Morphological processes in the Jamuna river. Unpublished M.Sc. thesis, International Institute for Infrastructure, Hydraulic and Environmental Engineering, Delft, Netherlands, August 1996, 175pp.

Saunderson, H.C. and Lockett, F.P.J., 1983. Flume experiments on bedforms and structures at the dune-plane bed transition. In: Collinson, J.D. and Lewin, J. (Eds.). Special Publication International Association of Sedimentologists, **6**, 19-33.

Schumm, S.A. and Winkley, B.R., 1994. The character of large alluvial rivers. In: The Variability of Large Alluvial Rivers, Schumm and Winkley (eds), pp 1-13, ASCE.

Simons, D.B., Richardson, E.V. and Nordin, C.F., 1965. Bedload equations for ripples and dunes. United states geological survey professional paper, 462-H.

Simpson, R.L., 1976. Interpreting laser and hot-film ananmometry signals in a separation boundary layer. American Institute of Aeronautics and Astronautics, 124-126.

Simpson, R.L., Chew, Y.T and Shivaprasad, B.G, 1981. The structure of a separating turbulent boundary layer. Part 1. Mean flow and Reynolds stresses. Journal of Fluid Mechanics, vol. **113**, 23-51

Simpson, R.L. and Shivaprasad, B.G, 1983. The sturcture of a separating turbulent boundary layer. Part 5. Frequncy effects on periodic unsteady free-stream flows. Journal of Fluid Mechanics, **131**, 319-339.

Simpson, R.L., 1989. Turbulent boundary layer separation. Annual Reviews in Fluid Mechanics, **21**, 205-234.

SIMRAD, 1988. Hydrograhic Echo Sounder, Instruction Manual.

Smith, J.D., 1970. Stability of a sand bed subjected to a shear flow of low Froude number. Journal of Geophysics Research, **74**, 5928-5939.

Smith, J.D. and McLean, S.R., 1977. Spatially averaged flow over a wavy surface. Journal of Geophysics Research, **82**, 12, 1735-1746.

Smith, C.R. and Metzler, S.P., 1983. The characteristics of low speed streaks in the near wall region of a turbulent boundary layer. Journal of Fluid Mechanics, **129**, 27-54.

Sorby, H.C., 1859. On the structures produced by the currents present during the deposition of stratified rocks. The Geologist, **2**, 137-147.

Soulsby, R.L., Atkins, R., Waters, C.B. and Oliver, N., 1991. Field measurements of suspended sediment over sandwaves. Euromech 262- Sand transport in rivers, estuaries and the sea, Soulsby and Bettess (eds), Balkema, Rotterdam, 155-162.

Southard, J.B. and Boguchwal, L.A., 1990. Bed configuration in steady unidirectional water flows, part3: effects of temperature and gravity. Journal of Sedimentary Petrology, **60**, 680-686.

Stride, A.H., 1963. Current swept sea floors near the southern half of Great Britain. Quarterly Journal of the Geolological Society of London, **119**, 175-199

Sumer, B.M and Oguz, B., 1978. Particle motions near the bottom in turbulent flow in an open channel. Journal of Fluid Mechanics, **86**, 109-127.

Swan, A.R.H. and Sandilands, M., 1995. Introduction to geological data analysis. Blackwell Science Ltd., Oxford, U.K, 312 pp.

Tennekes, H. and Lumley, J.L., 1994. A First Course in Turbulence. The MIT Press, Cambridge, Massachusetts and London, 300pp.

Termes, P.P., 1986. Dimensions of bed forms under steady flow at high sediment trasnport rates (in Dutch). Report M2130, Delft Hydraulics, Delft, The Netherlands.

Terwindt, J.H.J. and Brouwer, M.J.H.M., 1986. The behaviour of intertidal sandwaves during neap-spring tide cycles and the relevance for palaeoflow reconstructions. Sedimentology, **33**, 1-31.

Thorne, C.R., Russel, A.P.G. and Alam, M.K., 1993. Planform pattern and channel evolution of the Brahmaputra river, Bangladesh. In: Bradied Rivers, Best and Bristow (eds), pp. 257-276, Special Publication of Geological Society, **75**.

Thorne, P.D., Williams, J.J. and Heathershaw, A.D., 1989. In situ acoustic measurments of marine gravle threshold and entrainment. Sedimentology, **36**, 61-74.

Thorne, P.D., Hardcastle, P.J. and Hogg, A., 1996. Observations of near-bed suspended sediment turbulence structures using multifrequency acoustic backscattering. In: Coherent Flow Structures in Open Channels, Ashworth, P.J., Bennett, S.J., Best, J.L and McLelland, S.J (eds), Wiley 1996, pp 343-358.

Thorne, P.D., Hardcastle, P.J., Flatt, D. and Humphery, J.D., 1994. On the use of acoustics for measuring shallow water suspended sediment processes. IEEE Journal of Oceanic Engineering, Vol **19**, no. 1.

Tritton, D.J., 1988. Physical Fluid Dynamics, 2nd edition, Clarendon Press, Oxford, 519pp.

Van der Knaap, F.C.M, van Mierlo, M.C.L.M. and Officier, M.J., 1990. Measurements and computations of the turbulent flow field above fixed bedforms. Delft Hydraulics publication number 437, Delft, NL.

Van Essen, B.V.. Delft Bottle DF 12 Suspended Load Sampler Instruction Manual.

Van Rijn, L.C., 1982. Equivalent roughness of alluvial bed. Journal of the Hydraulics Division, ASCE, 108, HY 10.

Van Rijn, L, 1984b. Sediment transport, part 2: bedforms and alluvial roughness. ASCE, Journal of Hydraulic Engineering, 110, no 11, 1613-1641.

Van Rijn, L.,1993. Principles of sediment transport in rivers, estuaries and coastal seas. Aqua publications, Amsterdam, Netherlands.

Weiergang, J., 1995. Estimation of suspended sediment concentration based on a single frequency Acoustic Doppler profiler. Proc. 14th world Dredging Congress, Amsterdam.

Williams, G.P., 1967. Flume experiments on the transport of coarse sand. United States Geological Survey Professional Paper, 562-B

Williams, J.J., 1996. Turbulent flow in rivers. In: Advances in Fluvial Dynamics and Stratigraphy, Carling, P.A. and Dawson, M.R. (eds), Wiley and sons, 1-32.

Wilock, P.R., 1992. Experimental invetsiagtion of the effects of mixture properties on transport dynamics. In: Dynamics of Gravel-bed Rivers, P. Billi, R.D. Hey, C.R. Thorne and P. Taconni (eds), Wiley, Chichester, 109-139.

Wilock, P.R. and Southard, J.B., 1989. Bed load transport of mixed size sediment: fractional transport rates, bed forms and the development of a coarse bed surface layer. Water Resources Research, 25, 7, 1629-1641.

Yalin, M.S., 1964. Geometric properties of sand waves. ASCE, Journal of Hydraulics Division, 90, 105-119.

Yalin, M.S., 1977. Mechanics of sediment transport, 2nd edition, pergamon Press, Oxford, 219 pp.

Yalin, M.S., 1992. River Mechanics. Pergamon Press, Oxford, 219 pp.

Yoon, J.Y. and Patel, V.C., 1996. Numerical model of turbulent flow over sand dune. Journal of Hydraulic Engineering, **122**, 10-18.

Znamenskaya, N.S., 1964. Soviet Hydology Selected papers, no 3, 253-275.

Zyserman, J.A. and Fredsoe, J., 1994. Data analysis of bed concentration of suspended sediment. Journal of Hydraulic Engineering, **120**, 1021-1042.

Appendix A. Results of Quadrant Analysis from Low Flow Surveying

Results of quadrant analysis using velocity time series data collected by at-a-point profiling during the low flow survey (February 1996) proved inconclusive with no apparanet trends. An example of percentage occurrence of quadrant 1,2,3 and 4 events is given in Figure A.1. The inconclusive results may be due to the resolution of the vertical velocity component of the ADCP during low flow surveying, as vertical velocities are very small.

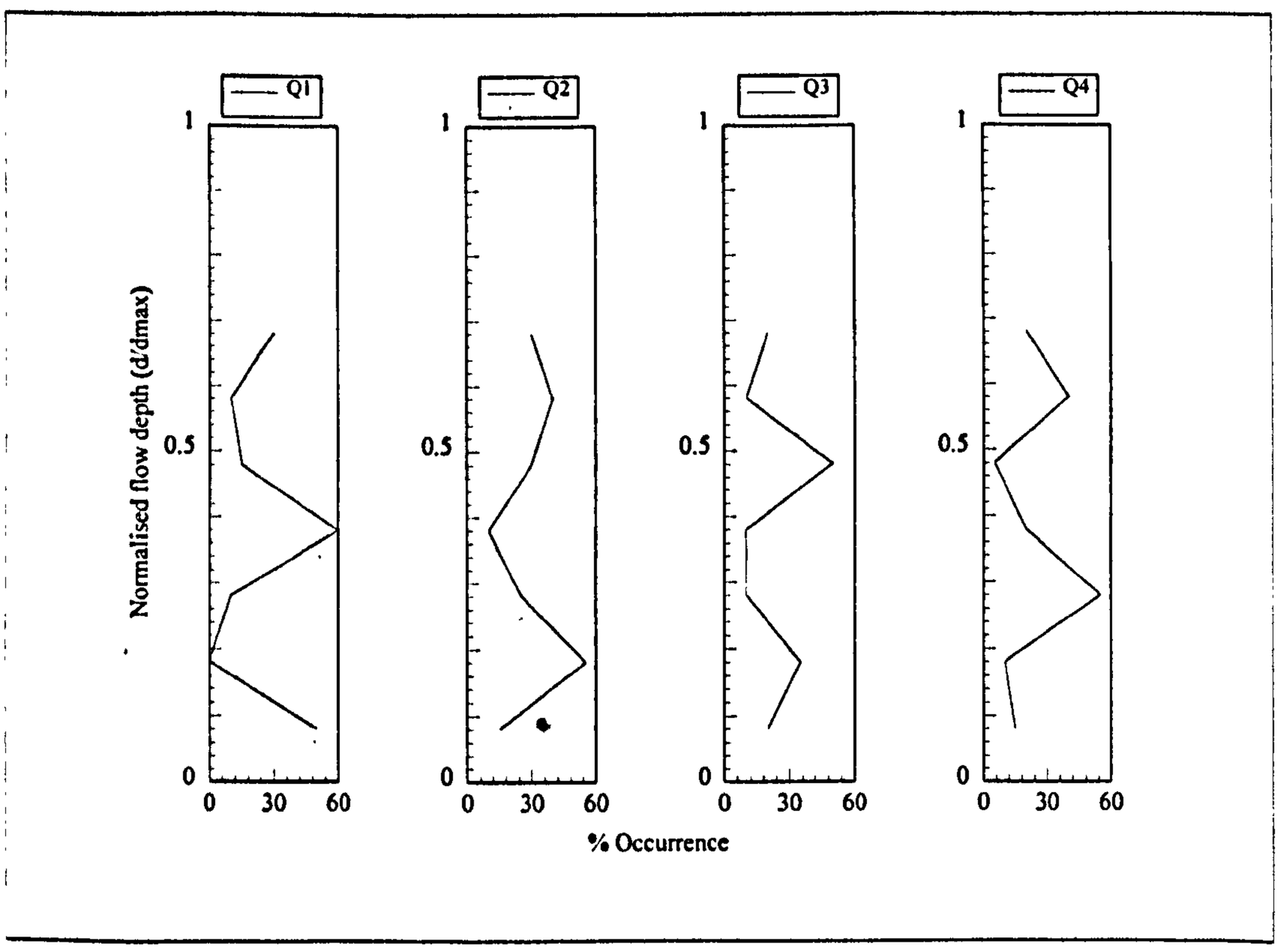

Figure A.1, Percentage occurrence of quadrant events from at-a-point profiling over a dune trough (L/96/T)